Volume 186 Supplement 1 September 2023 ISSN 0167-8140

ELSEVIER

Radiotherapy & Oncology

Journal of the European SocieTy for Radiotherapy and Oncology

CARO-COMP Joint Scientific Meeting

September 20-23, 2023

Hôtel Le Centre Sheraton Montréal

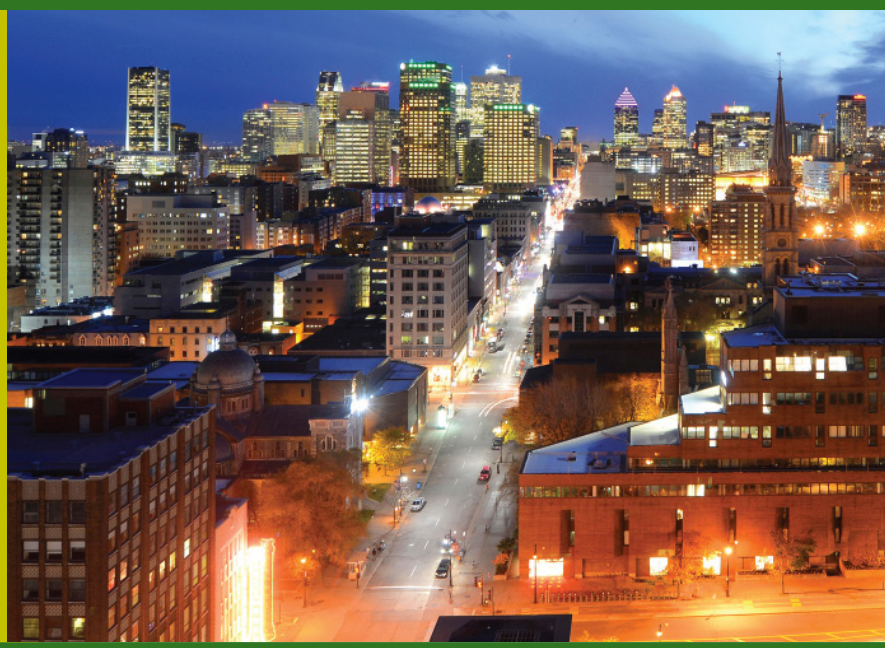

ESTRO

Radiotherapy &Oncology

Journal of the European SocieTy for Radiotherapy and Oncology

Volume 186 Supplement 1 (2023)

Radiotherapy & Oncology is available online:
For ESTRO members: http://www.thegreenjournal.com
For institutional libraries: http://www.sciencedirect.com

ELSEVIER

Amsterdam • Boston • London • New York • Oxford • Paris • Philadelphia • San Diego • St. Louis

International Standard Serial Number 0167-8140

Orders, claims, and journal inquiries: Please visit our Support Hub page https://service.elsevier.com for assistance.

Funding Body Agreements and Policies

Elsevier has established agreements and developed policies to allow authors whose articles appear in journals published by Elsevier, to comply with potential manuscript archiving requirements as specified as conditions of their grant awards. To learn more about existing agreements and policies please visit https://www.elsevier.com/fundingbodies

0167-8140(202309)186:S1;1-M

Available online at www.sciencedirect.com

ScienceDirect

1

ANALYSIS OF HODGKIN'S LYMPHOMA PATIENTS WITH INCOMPLETE METABOLIC RESPONSE AFTER FIRST-LINE SYSTEMIC THERAPY

Donna (MengWen) Liao[1], Mahmood Aminilari[3], May Tsao[2], Sameera Ahmed[3], Xiang Y. Ye[3], Anca Prica[3], Ur Metser[3], Amit Singnurkar[2], David Hodgson[3]
[1]*University of Toronto, Toronto, ON*
[2]*Sunnybrook Health Sciences Centre, Toronto, ON*
[3]*Princess Margaret Cancer Centre, Toronto, ON*

Purpose: Optimal management of patients with Hodgkin's Lymphoma (HL) who do not achieve complete metabolic response on Positron Emission Tomography (PET) after primary systemic therapy is unclear. Options vary significantly and include radiation therapy (RT) to sites of PET avid disease, salvage chemotherapy followed by autologous stem-cell transplant (ASCT), or observation with serial imaging. This multi-centre study sought to investigate the management approaches and outcomes for HL patients who achieved partial metabolic response after primary systemic therapy.

Materials and Methods: In this retrospective study, patients diagnosed with HL were identified from the electronic medical records of two large academic centres in Toronto between January 2009 and September 2021. PET scan results following initial systemic therapy were reviewed and responses were categorized using International Working Group (IWG) criteria, with the initial staging imaging being used as the reference against which response was evaluated. We performed descriptive analysis of demographic and clinical characteristics of the population and determined progression-free survival (PFS) using the Kaplan-Meier method.

Results: The charts of 1,093 HL patients were reviewed. A total of 765 patients had a post chemotherapy PET scan and 57 of those showed partial metabolic response. Of these 57 patients included for analysis, 31 (54%) were male, the median age at diagnosis was 31 (range: 18-74) and the median length of follow up was 1.6 years (average 2.9 years). Three (5%) were Stage I, 18(32%) Stage II, 13(23%) Stage III, and 23(40%) Stage IV. Typical initial systemic therapy included ABVD, ABVD switched to BEACOPP due to abnormal interim PET, and AVD with Brentuximab.

Among all patients with partial metabolic response to initial systemic therapy, the two-year PFS was 72.8% (95% CI = 60.9-87%). Thirty-three (58%) of these patients were treated with planned radiation therapy alone, and their two-year PFS was 80.7% (95% CI: 66.6-97.9%). For those who did not receive radiation as part of their treatment, two-year PFS was 62% (95% CI: 44-87.3%). Eight of these patients underwent repeat imaging without immediate further treatment; in four of these cases (50%), the patient remained free of recurrence without additional treatment.

Conclusions: To our knowledge, this is the largest study of HL patients with partial metabolic response following primary systemic therapy. Our preliminary analysis showed that treatment with radiation was associated with good PFS at two years and many of those treated with radiation alone were cured.

2

IMPROVING VISUALIZATION AND GUIDANCE FOR BREAST BRACHYTHERAPY: DEVELOPING, COMMISSIONING, AND IMPLEMENTING A HIGH-RESOLUTION ROBOTIC 3D ULTRASOUND SYSTEM

Claire Zhang[1,2], Shuwei Xing[3], Lori Gardi[3], Aaron Fenster[3], Juanita Crook[1], Deidre Batchelar[1,2], Michelle Hilts[1,2]
[1]*British Columbia Cancer, Kelowna, BC*
[2]*The University of British Columbia, Okanagan, BC*
[3]*Western University, London, ON*

Purpose: To develop, commission, and implement a high-resolution robotic 3D ultrasound system for improved target visualization and imaging guidance in breast brachytherapy.

Materials and Methods: The robotic 3DUS system consists of a 3D printed probe holder customizable for any commercial ultrasound transducer (BM Medical 8811 used in our system), a motor that drives the transducer through a hybrid translation-rotation motion for image acquisition, an ultrasound transparent TPX plate to support probe motion, and an encoder-based counterbalanced arm, which allows tracking of the transducer location. The tracking arm consists of five joints, which allow the transducer position to be tracked in a 3D space with accuracy sufficient for clinical use. Linear and volumetric imaging accuracies were quantified using phantoms with targets separated by known distances and of known volumes. The tracking arm was calibrated and tracking accuracy was quantified using an optical tracking device (Polaris Spectra, Northern Digital Inc., Canada). The feasibility to use this system to acquire 3DUS images, achieve registration to CT, visualize the implant template for needle insertion guidance in breast brachytherapy, and visualize and identify metal markers on 3DUS images are evaluated qualitatively and discussed.

Results: The robotic 3DUS system provides 3D images with small voxel sizes (0.075mm, 0.082mm, and 0.33mm in lateral, axial, and elevational directions, respectively). The 3D imaging error of this system was less than 2% and 3% for linear volume measurements, respectively, both below TG128 action levels. The arm tracking error was 1.0±0.5mm. The tracking arm provided an approximately 110×100×10cm^3 moving range and covered a sufficient 3D tracking space relative to a CT couch. Our preliminary tests on using this system for image registration, implant visual guidance, and metal marker identification demonstrated good feasibility.

Conclusions: We have developed and calibrated a high-resolution robotic 3DUS system for breast brachytherapy. The system provides excellent imaging and tracking accuracies for clinical use. The spatial tracking arm has sufficient movement range for clinical settings. We also showed huge potential in using this system to acquire registered 3DUS-CT images, guide template-based needle insertion procedures, and identify surgical clips or implanted seeds in breast brachytherapy.

3

PLASMA EBV DNA IN NASOPHARYNGEAL CANCER (NPC) TREATED WITH DEFINITIVE RADIOTHERAPY (RT)

Eric Stutheit-Zhao, Ian King, Shao Hui Huang, Katrina Rey-McIntyre, John Cho, Lawson Eng, Ezra Hahn, Ali Abdalaty Hosni, John Kim, Tony Tadic, Andrea McNiven, Andrew McPartlin, Jolie Ringash, Brian O'Sullivan, Lillian Siu, Anna Spreafico, C. Jillian Tsai, John N. Waldron, Andrew Hope, Scott V. Bratman
Princess Margaret Cancer Centre, Toronto, ON

Purpose: EBV DNA has well-studied roles in NPC including early detection, molecular residual disease (MRD), and surveillance. There are limited Canadian data on EBV DNA testing, and clinical thresholds are unclear. Our centre has routinely tested EBV DNA since 2010. We hypothesized (1) first post-RT EBV DNA clearance is associated with favourable prognosis, and (2) EBV DNA is highly specific at a low detection threshold.

Materials and Methods: We retrospectively reviewed all patients with non-metastatic (TNM-7 Stage I-IVB) NPC treated with definitive RT/chemoRT (CRT) ± adjuvant chemotherapy (AC) between 2010-2017. EBV DNA was assayed by quantitative PCR in a CAP/CLIA-certified laboratory and reported in copies/mL of plasma. Pre-RT is defined as 0-90 days before the first RT fraction and post-RT within one year after RT completion. We report log odds

ratios (LOR) from a linear model of T- and N-category with log-adjusted EBV DNA as the response variable. Survival outcomes were analyzed with log-rank tests and Cox multivariate analyses (MVA) adjusted for age, stage, and treatment, reporting adjusted hazard ratios (HR). 95% confidence intervals of LOR and HR are reported. The detection threshold that maximized the F1 accuracy score was considered optimal.

Results: Of 271 patients in the study window, 179 had pre-RT +/- post-RT EBV DNA testing. Six received RT, 43 CRT, and 130 CRT+AC. With seven-year median follow-up, 37 recurred and 37 died. Detectable pre-RT EBV DNA was found in 154 (86%) with a median of 928 copies/mL (range: 1-239214). EBV DNA level correlated with higher N category (LOR: 0.28, 0.15-0.42, p<0.001), but not T category (0.04, -0.06-0.13, p=0.5). Above-median pre-RT EBV DNA was associated with worse recurrence-free survival (RFS) by log-rank test (p=0.016) and Cox MVA (HR: 2.2, 1.1-4.8, p=0.03) along with N category, age, and no AC. Post-RT EBV DNA was available in 99 patients, a median of 54 days after completing RT. Patients with undetectable versus detectable post-RT EBV DNA had three-year RFS of 81% versus 48% (p=0.0005, negative predictive value/NPV=81%), PFS of 80% versus 43% (p=0.0003, NPV=80%), and OS of 94% versus 57% (p<0.0001, NPV=95%). If EBV DNA was detectable after the full treatment (RT±AC), three-year RFS and PFS each dropped further to 20%. In Cox MVA, post-RT EBV DNA was independently prognostic of RFS (HR: 1.25, 1.11-1.40, p<0.001), PFS (1.24, 1.10-1.39, p<0.001), and OS (1.34, 1.20-1.49, p<0.001). EBV DNA was performed within 30 days of recurrence in 30 patients, and 24 were detectable (80% sensitivity). Conversely, of 152 patients without recurrence and at least three-year follow-up, 95 had post-RT EBV DNA testing and 84 were undetectable (88% specificity). An EBV DNA threshold of 31 copies maximized F1 accuracy metric, yielding 74% sensitivity and 97% specificity.

Conclusions: Post-RT EBV DNA is a strong, independent predictor of RFS, PFS, and OS. Pre-RT EBV DNA is prognostic and associated with N-category. An optimized threshold of 31 copies/mL was 97% specific for detecting recurrence.

4

ASSOCIATION OF ARTIFICIAL INTELLIGENCE-SCREENED INTERSTITIAL LUNG DISEASE WITH RADIATION PNEUMONITIS AND MORTALITY IN LOCALLY ADVANCED NON-SMALL CELL LUNG CANCER

Hannah Bacon[1], Nicholas McNeil[1], Tirth Patel[2], Mattea Welch[3], Xiang Y. Ye[3], Andrea Bezjak[1], Benjamin H. Lok[1], Srinivas Raman[1], Meredith Giuliani[1], John Cho[1], Alexander Sun[1], Patricia Lindsay[1], Geoffrey Liu[3], Sonja Kandel[2], Chris McIntosh[2], Tony Tadic[1], Andrew Hope[1]
[1]*University of Toronto, Toronto, ON*
[2]*University Health Network, Toronto, ON*
[3]*Princess Margaret Cancer Centre, Toronto, ON*

Purpose: Radiation pneumonitis (RP) is a common and dose-limiting toxicity following radiotherapy for non-small cell lung cancer (NSCLC). Patients with interstitial lung disease (ILD) are believed to be at increased risk of developing complications including RP, ILD progression, or death. An automated method to identify patients prior to radiotherapy at high risk of developing toxicities or death may allow clinicians to mitigate risk through informed treatment planning and careful patient monitoring.

Materials and Methods: All locally advanced NSCLC patients treated with definitive radiation at our institution from 2006-2021 with a minimum of one year of follow-up were assessed. RP and mortality data were prospectively collected and retrospectively reviewed. A convolutional neural network (CNN) was previously developed and validated to identify patients with radiographic ILD using planning computed tomography (CT) images, with an accuracy of 0.82. Planning CT scans for the retrospective cohort were used as input to the CNN, with artificial intelligence-screened ILD (AI-ILD) score as an output. AI-ILD scores above our established threshold were labeled as AI-ILD+. The association between AI-ILD score, AI-ILD+/−, mean lung dose (MLD), and the primary outcome of Grade ≥2 (G2+) RP or mortality, as well as the secondary outcomes of G2+ RP and mortality were assessed using Wilcoxon rank sum test, univariate and multivariable logistic regression, and Kaplan-Meier survival analysis.

Results: Of 799 patients reviewed, 745 eligible patients were included in the analysis; Grade 0-5 RP was reported in 51.3%, 27.1%, 16.9%, 4.0%, 0.1%, and 0.5% of patients respectively. Overall, 22.9% of patients were AI-ILD+, and therefore at high risk (>20% chance) of having true ILD. On UVA, AI-ILD score, AI-ILD+ and MLD were significantly associated with the primary outcome of G2+ RP or mortality, as well as the secondary outcome of mortality. However, only MLD was significantly associated with the secondary outcome of G2+ RP. On MVA, both AI-ILD+ (OR 1.42, 95% CI 1.02-1.97, p=0.04) and MLD (OR 1.13, 95% 1.05-1.21, p=0.008) were significantly associated with the primary outcome of G2+ RP or mortality. On Kaplan-Meier analysis, the median toxicity-free survival (TFS) time for AI-ILD+ and AI-ILD− patients were 1.7 and 3.4 years respectively, with a two-year TFS of 48.3% versus 59.3% (log-rank test: p=0.02). There was no significant difference in rates of G2+ RP.

Conclusions: The AI-ILD algorithm can detect high risk patients with significantly decreased TFS following definitive treatment for NSCLC. AI-ILD classification was not associated with a significant difference in rates of G2+ RP when accounting for MLD. Future work will focus on improving the classification algorithm, expert radiologist validation of this dataset, and exploring reasons for the mortality difference in AI-ILD+ patients.

5

NON-COPLANAR, ADAPTIVE, LUNG PATIENT TREATMENT PLANNING ON A LOW-COST, KILOVOLTAGE, ISOCENTRIC RADIOTHERAPY (KVIRT) SYSTEM

Jericho O'Connell[1], Magdalena Bazalova-Carter[1], Michael Weil[2]
[1]*University of Victoria, Victoria, BC*
[2]*N/A, Half Moon Bay, CA*

Purpose: To plan, optimize, and benchmark two adaptive, non-coplanar, stereotactic ablative radiotherapy (SABR) lung patient treatment plans on a very low-cost, kilovoltage, isocentric, treatment (kVIRT) machine for deployment to underserved populations globally.

Materials and Methods: A novel, robust, low-cost treatment machine design has been proposed featuring a 320 kVp x-ray tube with the intent of delivering non-coplanar, isocentric treatments at a fraction of the cost of conventional radiotherapy. A deep learning cone-beam CT (CBCT) to synthetic CT (sCT) method is employed to avoid the additional cost of acquiring planning CTs in low-income countries. A novel inverse treatment planning approach using GPU backprojection is used to create a highly non-coplanar treatment plan with circular beams generated by an iris collimator. Treatments were planned and simulated using the TOPAS Monte Carlo (MC) code on two anonymized lung patients, dose volume histograms (DVHs) and dose distributions were compared to 6 MV VMAT treatments planned in Eclipse for a Truebeam linac.

Results: kVIRT treatment doses were uniform in the planning target volume (PTV) with minimum- maximum doses of 50.1-60.6 and 50.3-61.2 Gy as opposed to 48.8-63.8 and 49.1-62.3 Gy for VMAT. The non-coplanar kVIRT treatment plans showed mean doses in all soft tissue organs at risk (OARs) within 2 Gy of the

VMAT plans. Compared to the 6 MV VMAT doses, the maximum kVIRT doses were reduced in all soft tissue OARs except for the skin, where it increased by less than 1.5 Gy. The mean and maximum doses for the ribs were higher in the kVIRT plans due to the photoelectric interactions of kV photons. Overall, a radiation oncologist deemed the treatment plans acceptable for delivery.

Conclusions: We demonstrated a novel, low-cost, kilovoltage, isocentric radiotherapy system meeting our initial clinical treatment targets for two lung cases. Design optimisation will need to be followed by manufacturing and experimental characterization ahead of utilisation of the system in low-income countries.

6

TRAJECTORY VMAT OPTIMIZATION USING A 4PI INTENSITY MAP

Jakob Marshall[1], Marie-Pierre Milette[2], Benjamin Mou[2], Andrew Jirasek[3], Tony Teke[2]
[1]University of British Columbia, Okanagan, BC
[2]British Columbia Cancer, Kelowna, BC
[3]University of British Columbia, Kelowna, BC

Purpose: To develop and assess a framework capable of optimizing the dynamic motion of the treatment couch and linear accelerator gantry for trajectory Volumetric Modulated Arc Therapy (VMAT) treatment.

Materials and Methods: A dosimetric beam scoring map, termed the "4Pi intensity map", is generated by optimizing the field weights of conformal radiation beams distributed on the 4Pi sphere, an arbitrary sphere surrounding the patient. Each field weight characterizes the utility of the beam orientation. Large field weights indicate the ability to treat the planning target volume (PTV) while sparing organs at risk (OAR) and healthy tissue. Conversely, small field weights indicate excessive OAR or healthy tissue exposure. These field weights, or 4Pi intensities, are used to generate a map in couch-gantry coordinate space. Dijkstra's shortest path algorithm is used to find paths through the 4Pi intensity map which includes high intensity regions while avoiding low intensity regions. In total, 3700 different trajectories are generated each with a different starting and ending couch and gantry angle. For all 3700 trajectories, the field weights are re-optimized while only considering the subset of beam orientations along the trajectory and the corresponding dosimetric objective function is assessed. The trajectory with the lowest dosimetric objective function is taken as optimal. Finally, VMAT optimization is used to optimize the MLC motion and dose rate modulation. The developed framework was used to create trajectory VMAT treatment plans for six patients with single brain lesions. The trajectory VMAT treatment plans were optimized using in-house software before importing them to the Eclipse treatment planning system for final dose calculation and comparison with coplanar treatment plans that were optimized in Eclipse.

Results: The 4Pi intensity map was found to rank beam orientations based on their potential to irradiate the PTV while sparing OAR and healthy tissue. By using Dijkstra's algorithm and the Fast Inverse Dose Optimization (FIDO) algorithm trajectories were generated and assessed on their dosimetric quality. In all cases, the trajectory with the lowest dosimetric objective function (OF) was superior to the OF from a full coplanar arc. In total, the trajectory optimization framework presents a pre-processing step to VMAT optimization that takes <15 minutes to find the optimal trajectory. The benefits of trajectory VMAT was most pronounced for brain lesions nearby OAR. This is due to the ability to select beam orientations in the trajectory which spare the nearby OAR structures. For all 6 patients with single brain lesions, the trajectory VMAT treatment plans were comparable, or superior, to the coplanar VMAT treatment plans.

Conclusions: A method for trajectory VMAT optimization that relies on a "4Pi intensity map" was presented. The method is a pre-processing step to conventional VMAT treatment planning that selects the best trajectory based on dosimetry.

7

PREDICTING THE NEED FOR A REPLAN IN OROPHARYNGEAL CANCER: A RADIOMIC, CLINICAL, AND DOSIMETRIC MODEL

Tricia Chinnery, Pencilla Lang, Anthony Nichols, Sarah Mattonen
Western University, London, ON

Purpose: Patients with oropharyngeal cancer (OPC) treated with chemoradiation experience weight loss and tumour shrinkage. Treatment replanning ensures patients do not receive excessive doses to normal tissue. However, it takes one to two weeks to acquire a new treatment plan, and during this time, overtreatment of normal tissues could lead to increased toxicities. Additionally, there are limited prognostic factors to determine which patients will require a replan. We aimed to develop and evaluate a CT-based radiomic model, integrating clinical and dose information, to predict the need for a replan prior to treatment.

Materials and Methods: A dataset of patients (n=315) with OPC treated with chemoradiation was used for this study. The dataset was split into independent training (n=220) and testing (n=95) datasets. Tumour volumes and organs at risk (OARs) were contoured on planning CT images prior to treatment. PyRadiomics was used to compute radiomic image features (n=1218) on the original, wavelet, and Laplacian of Gaussian filtered images from each of the primary tumour, nodal volumes, and ipsilateral and contralateral parotid glands. Nine clinical features and eight dose features extracted from the OARs were collected and those significantly ($p<0.05$) associated with the need for a replan in the training dataset were used in a baseline model. Random forest feature selection was applied to select the optimal radiomic features to predict replanning. Logistic regression, Naïve Bayes, support vector machine, and random forest classifiers were built using the non-correlated selected radiomic, clinical, and dose features on the training dataset and performance was assessed in the testing dataset. The area under the curve (AUC) was used to assess the prognostic value.

Results: A total of 78 patients (25%) required a replan. Smoking status, nodal stage, tumour subsite, and larynx mean dose were found to be significantly associated with the need for a replan in the training dataset and incorporated into the baseline model, as well as into the combined models. Seven predictive radiomic features were selected (three nodal volume, two primary tumour, and two ipsilateral parotid gland). The baseline model comprised of clinical and dose features alone achieved an AUC of 0.66 [95% CI: 0.51-0.79] in the testing dataset. The Naïve Bayes was the top-performing radiomics model and achieved an AUC of 0.80 [95% CI: 0.69-0.90] in the testing dataset, significantly outperforming the baseline model ($p=0.003$).

Conclusions: This is the first study to use radiomics from the primary tumour, nodal volumes, and parotid glands for the prediction of replanning for patients with OPC. Radiomic features augmented clinical and dose features for predicting the need for a replan in our testing dataset. Once validated, this model has the potential to assist physicians in identifying patients that may benefit from a replan, allowing for better resource allocation, patient management, and reduced toxicities.

8

STEREOTACTIC BODY RADIOTHERAPY FOR BREAST CANCER SPINAL METASTASES IS ASSOCIATED WITH LOW

RATES OF LONG-TERM LOCAL FAILURE AND VERTEBRAL COMPRESSION FRACTURE INDEPENDENT OF MOLECULAR STATUS

Bryce Thomsen, Danny Vesprini, Liang Zeng, Sten Myrehaug, Chai-lin Tseng, Jay Detsky, Hanbo Chen, Beibei Zhang, Katarzyna Jerzak, Eshetu Atenafu, Pejman Maralani, Hany Soliman, Arjun Sahgal
University of Toronto, Toronto, ON

Purpose: There is limited outcome data specific to breast cancer spinal metastases following spine SBRT. This study aims to report outcomes specific to breast cancer spinal metastases receiving spine SBRT and determine the implication of biomarker status.

Materials and Methods: We have been maintaining a prospective database since the inception of the spine SBRT program. A retrospective review identified 168 breast cancer patients with 409 spinal segments treated with spine SBRT between January 2008 and January 2023. Molecular subtypes were grouped based on luminal A, luminal B, basal, and HER2 enriched. Patients were followed with q3-monthly full-spine MRI and a clinical assessment. The primary endpoint was MRI-based local failure (LF), and secondary endpoints were overall survival (OS) and vertebral compression fracture (VCF).

Results: The median follow-up was 33 months (range, 3.3-123 months). Amongst the 168 patients, the majority were ECOG 0 or 1 (95%), neurologically intact (94%), polymetastatic (74%), and either luminal A (71%) or luminal B (8%). A total of 17% of patients were HER2+ve versus 83% HER2-ve. Of 409 treated segments the majority (76%) had no prior radiation or surgery (denovo), were SINS stable (60%), had either no or low-grade epidural disease (86%) and treated with 24-28 Gy in 2 fractions (73%). The LF and OS rates at one, three, and five years were 5%, 11%, and 14%, respectively, and 91%, 65%, and 45%, respectively, independent of molecular subtype on univariate analyses. The cumulative risk of VCF at two and five years was 7% and 10%, respectively.

Conclusions: We observe, in the largest breast cancer spine cohort to date, excellent long-term local control rates independent of molecular sub-group, and acceptable VCF rates.

9

MACHINE LEARNING PLAN ADAPTATION IMPROVES QUALITY OF ULTRA-HYPOFRACTIONATED ADAPTIVE RADIATION THERAPY FOR PROSTATE CANCER ON A 1.5T MR-LINEAR ACCELERATOR

Aly Khalifa[1], Jeff Winter[2], Tony Tadic[2], Chris McIntosh[1], Thomas G Purdie[2]
[1]*University of Toronto, Toronto, ON*
[2]*Princess Margaret Cancer Centre, Toronto, ON*

Purpose: Online radiation therapy (RT) plan adaptation strategies are critical for the safe delivery of ultra-hypofractionated adaptive radiation therapy (ART) treatments in prostate cancer. The purpose of this study was to assess the dosimetric advantages of machine learning (ML) automated treatment planning as an adaptation strategy compared to the standard manual optimization and objective adjustment in the current adapt-to-shape (ATS) clinical workflow.

Materials and Methods: A clinically validated atlas regression forest method for automated treatment planning was used to simulate ML plan adaptation in the ART setting. The ML model was trained using data from 46 consecutive prostate cancer patients who received intensity modulated RT (IMRT) on the Unity magnetic resonance (MR) linear accelerator (linac) with a prescription dose of 4270 cGy in 7 fractions. Training data consisted of reference MR imaging, segmented targets and organs, and the dose distribution from the clinical reference RT plans. The model was validated on a held-out test set of 12 patients by comparing ML plans generated on reference MR imaging to clinical reference plans using institutional dose-volume evaluation criteria and one-sided t-tests with false discovery rate (FDR) correction ($p<0.05$). To simulate ML plan adaptation in the ART context, the validated model was used to generate ML plans for all 7 fractions of ART for patients in the test set (a total of 84 plans) and compared to the respective ATS plans. Statistically significant differences in dose-volume metrics between ML and human-driven ATS plans were compared using two-sided t-tests with FDR correction ($p<0.05$).

Results: The trained ML model produced high-quality RT plans on the reference imaging of the 12 patient held-out test set. ML plans showed statistically significant decreases to PTV D1cc, Rectum D20, Bladder D40 and D5cc, Large Bowel D1cc, penile bulb D50 and D1cc, and increases to CTV D99. Applying the validated model to generate adaptive RT plans at each fraction also demonstrated significant dose improvements. Compared to ATS adapted plans, ML adaptation on average reduced the dose to several organs at risk including the rectum (D20: -306 cGy, D50: -93 cGy, D1cc: -53 cGy), bladder (D40: -465cGy, D5cc: -203 cGy), large bowel (D1cc: -177 cGy), and small bowel (D1cc: -212 cGy). However, ML plans had increased organ doses to the right femur (D5: +317 cGy) and Urethra (D50: +31 cGy). ML plans also showed an increase in CTV coverage (D99: +65 cGy) and small decreases in PTV coverage (D99: -20 cGy).

Conclusions: ML plan adaptation provides significant dosimetric advantages over the current standard ATS method. The ML plan adaptation approach is more robust to anatomical changes as it creates a new treatment plan at each fraction based on daily anatomy, while the ATS approach requires time-constrained adjustment by a human planner of optimization objectives from a reference RT plan. These findings suggest that ML plan adaptation may improve the effectiveness of ART treatments on MR-linacs for prostate cancer.

10

LONG-TERM OUTCOMES FOLLOWING FAIRLY BRIEF ANDROGEN SUPPRESSION AND STEREOTACTIC RADIOTHERAPY IN HIGH-RISK PROSTATE CANCER: UPDATE FROM THE FASTR/FASTR-2 TRIALS

Terence Tang[1], George Rodrigues[1,2], Glenn Bauman[1,2]
[1]*Western University, London, ON*
[2]*London Health Sciences Centre, London, ON*

Purpose: There has been emerging interest in the role of ultra-hypofractionated radiotherapy for high-risk prostate cancer, especially given its low α/β ratio. However, there is limited data on the long-term outcomes of this treatment strategy. The FASTR and FASTR-2 clinical trials were designed to assess the tolerability of stereotactic ablative body radiotherapy (SABR) in high-risk prostate cancer. FASTR was discontinued early due to unacceptable acute toxicity, whereas the acute toxicities in FASTR-2 were minimal. Herein, the long-term results from these trials are reported.

Materials and Methods: Eligible patients had at least 1 high-risk feature as per the National Comprehensive Cancer Network criteria for high-risk prostate cancer, no evidence of metastatic disease, and either a score of 3+ on the Vulnerable Elderly Scale or declined standard therapy. A total of 19 patients from a single institution were enrolled on FASTR between 2011 and 2015. They received 40 Gy to the prostate and 25 Gy to the pelvic lymph nodes in 5 fractions delivered once weekly for 5 weeks, along with 1 year of androgen deprivation therapy (ADT). The excessive acute toxicity in FASTR prompted several modifications in FASTR-2, including the omission of nodal irradiation. A total of 30 patients from the

same institution were enrolled on FASTR-2 between 2015 and 2017. They received 35 Gy to the prostate alone in 5 fractions delivered once weekly for 5 weeks, along with 18 months of ADT.

Results: A total of 44 patients were eligible for analysis, 16 from FASTR and 28 from FASTR-2. Most patients were >70 years old (77%). High-risk features included Gleason score ≤8 (46%), T3-T4 disease (27%) and baseline PSA >20 (50%). With a median follow-up of 6.4 years, the cumulative incidence of grade ≤3 genitourinary/gastrointestinal toxicity was 50% among FASTR patients and 7% among FASTR-2 patients. At five years, the combined rates of biochemical failure-free survival, freedom from distant metastases, prostate cancer-specific survival and overall survival were 72%, 90%, 92% and 83%, respectively. A total of 12 patients (27%) required further treatment. No significant differences in clinical outcomes were noted between the FASTR and FASTR-2 cohorts.

Conclusions: SABR for high-risk prostate cancer is an attractive option for reducing treatment burden. Clinical outcomes and toxicity with the FASTR-2 protocol were comparable to conventionally fractionated radiotherapy plus ADT. Larger prospective, randomized trials exploring the role of SABR with ADT in high-risk disease are necessary to better understand the efficacy and tolerability of this approach.

11

CLINICAL UTILITY OF 3D TRANSVAGINAL ULTRASOUND IN GYNECOLOGIC PERINEAL TEMPLATE INTERSTITIAL HIGH-DOSE-RATE BRACHYTHERAPY

Devin Van Elburg[1], Tyler Meyer[1,2], Kevin Martell[2], Robyn Banerjee[2], Tien Phan[2], Sarah Quirk[3,4], Aaron Fenster[5], Michael Roumeliotis[6]
[1]*University of Calgary, Calgary, AB*
[2]*Tom Baker Cancer Centre, Calgary AB*
[3]*Brigham & Women's Hospital, Boston, MA*
[4]*Harvard Medical School, Boston, MA*
[5]*Western University, London, ON*
[6]*Johns Hopkins University, Baltimore, MD*

Purpose: To demonstrate the clinical utility of 3D transvaginal ultrasound (3DTVUS) for intraoperative needle insertion guidance in gynecologic template interstitial high-dose-rate brachytherapy (HDRBT).

Materials and Methods: Perineal template (Syed/Neblett) interstitial HDRBT patients treated between November 2021 and October 2022 with gross residual tumours at the top of the vagina or inferior were included in this study. All patients received EBRT (45 Gy in 25 fractions) followed by either 3 fractions of 6.5 – 7 Gy (n=6) or 6 fractions of 6.5 Gy (n=1) of HDRBT. Pre-brachytherapy MRI images were obtained to assess tumour response to EBRT and to strategize the implant. A pre-insertion 3DTVUS was obtained to visualize the anatomy including the tumour and vaginal wall. Target coverage needles were inserted using 2D live ultrasound based on 3DTVUS positioning. Intermittent 3DTVUS images visualized inserted needle position relative to the target and anatomy. The standard clinical workflow continued once the clinician was satisfied with the implant. Qualitative assessment includes visualization of implant anatomy (tumour, needles, organs) and identification of cases where 3DTVUS is beneficial. Quantitative assessment includes dosimetry, calculation of relative importance of 3DTVUS-guided needles, and survey responses by 3DTVUS users (radiation oncologists).

Results: Seven patients were included in this study. Disease sites were primary vaginal (n=2) and vulvar (n=1) cancers and vaginal recurrences (n=4). In total, 20 3DTVUS-guided needles were implanted. The needles, vaginal wall, bladder, and rectum were well visualized. In four of seven patients the tumour was directly visible in 3DTVUS. Mid-implant 3DTVUS identified deflected needles were adjusted and assessed with subsequent 3DTVUS imaging. Five patients met all target planning constraints, while one exceeded the bladder D2cc and one exceeded the rectum D2cc. For three patients, 3DTVUS-guided needles contributed over 50% of the total needle dwell time, and in five patients the 3DTVUS-guided needles alone contributed over 20% of D90 target doses, highlighting the importance of these needles. Four radiation oncologists from three different centres with 3DTVUS experience responded to the survey. All indicated substantial improvement in visualization of the tumour, vaginal wall, and interstitial needles compared to 2D ultrasound techniques. There is consensus 3DTVUS improves implant quality and is preferred over 2D ultrasound alone, and that 3DTVUS is practical considering implant time, system bulkiness, and patient safety, though one expressed sterility concerns.

Conclusions: 3DTVUS provides improved visualization of tumours, vaginal wall, and interstitial needles during implant, and impacts the needles most important to target coverage. Radiation oncologist feedback was positive and indicated that 3DTVUS guidance improves implants and is preferred over 2D ultrasound methods.

12

SAFETY AND EFFICACY OF STEREOTACTIC BODY RADIOTHERAPY FOR ULTRA-CENTRAL THORACIC TUMOURS

George Li, Hendrick Tan, Humza Nusrat, Hanbo Chen Joe Chang, Jeevin Shahi, Ian Poo, May Tsao, Yee Yung, Patrick Cheung, Alexander V. Louie
Sunnybrook-Odette Cancer Centre, Toronto, ON

Purpose: Stereotactic body radiotherapy (SBRT) is increasingly utilized in the management of ultra-central thoracic tumours, although concerns regarding significant toxicity remain. We sought to evaluate the toxicity and efficacy of SBRT to these tumours at our institution.

Materials and Methods: Patients with ultra-central lung tumours or nodes treated at our institution with SBRT between 2009 and 2019 were retrospectively reviewed. Ultra-central was defined as having the planning target volume (PTV) overlapping or abutting the central bronchial tree and/or esophagus. All SBRT plans were generated with homogenous dose distributions using target coverage objectives of ITV V100% >99%, PTV V95% >99%, and an ideal PTV Dmax <105% (strict <120%). All plans were reviewed in quality assurance rounds by a team of dosimetrists, physicists, and radiation oncologists. The primary endpoint was incidence of severe toxicity (ST), defined as SBRT-related Grade ≥3 toxicities, graded using the Common Terminology Criteria for Adverse Events V5.0. Secondary endpoints included local failure (LF), progression-free survival (PFS) and overall survival (OS). Competing risk analysis was used to estimate incidence and predictors of ST and LF, with death as a competing risk. Kaplan-Meier method was used to estimate PFS and OS.

Results: A total of 154 patients who received 162 ultra-central courses of SBRT were included, with a median follow-up of 21.5 months. Treatment intent was most commonly for oligoprogression (46%), oligometastasis (30%), followed by curative (20%). The most frequent tumour histologies were NSCLC (41%) and RCC (26%). SBRT prescription doses ranged from 30-55Gy in 5 fractions (BED_{10} range 48-115Gy). The most common prescription was 50Gy in 5 fractions (42%). The cumulative incidence of ST was 8.9% at 3-years. The most common ST was pneumonitis (n=4). Notable toxicities included bronchopleural fistula (n=2, Grade 3 and 4), bronchial stricture (n=1, Grade 3), and esophagitis leading to bleeding (n=1, Grade 4). There were no esophageal strictures or perforations, and no bronchial bleeds. There was one possible treatment related death from pneumonitis/pneumonia. Predictors

of any ST included increased lung V5Gy, decreased PTV V95%, and not having prior radiation therapy to the chest. The cumulative incidence of LF was 4.8%, 11% and 14% at one-, two-, and three-years respectively. Predictors of LF included younger age, and greater volume of overlap between the PTV and esophagus. Median PFS was 8.4 months, while median OS was 3.7 years.

Conclusions: In one of the largest case series of ultra-central thoracic SBRT reported to date, homogenously prescribed SBRT plans were associated with relatively low rates of ST and LF across a variety of treatment indications. Predictors of ST should be interpreted recognizing the heterogeneity in toxicities observed. Identified predictors of both ST and LF can contribute to future work to optimize the therapeutic ratio in treatment of ultra-central thoracic tumours.

13

IMPACT OF NATIONAL CONFERENCE-ASSOCIATED MEDICAL STUDENT RESEARCH AND MENTORSHIP AWARD IN RADIATION ONCOLOGY ON MEDICAL STUDENTS, RESIDENT MENTORS, AND RESEARCH PROJECT SUPERVISORS

Ruijia (Rachel) Jin[1], Che Hsuan (David) Wu[2], Meredith Giuliani[3], Corinne M. Doll[4], Jolie Ringash[3], Danny Lavigne[5], Paris-Ann Ingledew[1]

[1]University of British Columbia, Vancouver, BC
[2]McMaster University, Hamilton, ON
[3]University of Toronto, Toronto, ON
[4]University of Calgary, Calgary, AB
[5]Université de Montréal, Montréal, QC

Purpose: The Canadian Association of Radiation Oncology (CARO) Medical Student Research and Mentorship Award (CARO MSRMA) was established in 2020 to support medical students pursuing radiation oncology (RO) research and RO as a career. Initial evaluations of the program have shown positive impact. This study aims to update the impact of three consecutive years of this award on medical students, RO resident mentors and research supervisors.

Materials and Methods: Medical student mentees, resident mentors, and staff RO research supervisors who participated in one of three cycles of CARO MSRMA (2020-2022 inclusive) were identified. Three separate surveys were developed for these groups using best practice strategies for medical education surveys and circulated for peer-review amongst experts in oncology medical education. The surveys were sent to 52 individuals: 18 medical students (Group 1), 18 RO resident mentors (Group 2), and 16 supervisors (Group 3). After anonymization, quantitative answers were analyzed using descriptive statistics and narrative responses were evaluated using a grounded theory approach.

Results: Survey response rate was 92% (48/52). For Group 1, the award maintained (71%) or increased interest in pursuing an RO career (24%). The aspects of the research award rated as most important were financial support through registration cost coverage and travel accommodations to attend the CARO Annual Scientific Meeting (mean rating 4.8/5) and mentorship with an RO resident (mean rating 4.6/5). Through mentorship, 60% of students attained valuable information about a career in RO, 60% received helpful residency matching (CaRMS) advice, and another 60% gained insight into RO residency. For Group 2 respondents, 100% felt the program either maintained or increased their motivation to mentor students in RO. Mentors and mentees met an average of two times; the most popular medium was video call, with more in-person meetings during the most recent iteration. For Group 3, 100% agreed or strongly agreed that they enjoyed being a supervisor in the CARO MSRMA program and would participate again, as well as recommend it to others. All three Groups agreed or strongly agreed that it would be useful for CARO to create a virtual network of mentors/mentees/supervisors to share shadowing and research opportunities to encourage cross-Canada collaboration. The first cohort of medical student awardees has CaRMS matching results, with approximately 50% matching to RO.

Conclusions: CARO MRSMA has had a positive impact on all three groups of participants: medical students in motivation to continue pursuing RO research and career opportunities, RO resident mentors in enhancing mentorship skills, and supervisors in inspiring the next generation of prospective RO colleagues. Further research is recommended to determine the impact of the award on subsequent CaRMS matching, and whether expansion of this award to other opportunities may be beneficial.

14

CANADIAN NATIONAL SURVEY OF CONTINUING PROFESSIONAL DEVELOPMENT FOR RADIATION ONCOLOGISTS: WHERE ARE THE GAPS AND BARRIERS?

Sympascho Young[1], Gurjit Parmar[2], Nicolas Siriani-Ayoub[2], Timothy Nguyen[1]

[1]Western University, London, ON
[2]University of British Columbia, Vancouver, BC

Purpose: Continuing professional development (CPD) is a fundamental aspect of the practice of medicine and a Royal College requirement for practising physicians in Canada. CPD consists of a range of activities undertaken to maintain competency in clinical and interprofessional skills, including continuing medical education (CME), research, teaching and administration. Although CPD has been well explored in other specialties, the literature specific to radiation oncology is lacking. We sought to evaluate current CPD practices of radiation oncologists in Canada and identify unmet needs and barriers.

Materials and Methods: An online survey on CPD was developed in both English and French and emailed to all Radiation Oncology (RO) departments across Canada as well as to all members of the Canadian Association of RO (CARO). Respondents' current practices, preferences, barriers and needs were explored across the CPD domains of CME, research, teaching and administrative skills.

Results: One-hundred twenty-four radiation oncologists completed the survey with representation across all listed disease sites and provinces. Respondents had an average 13.6 years of experience as staff (6 months to 38 years) and 96% were affiliated with a university. ROs indicated the most helpful resources for CME were reading journal articles (27%), attending tumour boards (25%), conferences (19%), informal discussion with colleagues (11%), free online websites (e.g. NCCN) (4%) and Twitter (3.5%). Lack of time was unanimously regarded as a barrier for CME. Other barriers included growing clinical workloads, expanding literature, and a lack of renumeration for CME. The mean score was 3.5/5, between "neutral" and "satisfied" for "satisfaction that CME needs are met" on a 5-point Likert scale. Seventy-six percent of respondents are currently engaged in research, with 48% involved as a research supervisor. However, only 35% had protected time for research (ranging from 10-80% FTE). Time (89%), funding (63%) and human resources (63%) were cited as barriers. Respondents wanted to improve skills in statistical analysis, clinical trial design and grant writing. Most researchers (78%) were comfortable with quantitative methodologies. Conversely, only 35% were comfortable with qualitative methods. Nearly all respondents (98%) were involved with clinical teaching. While the majority of respondents were satisfied with their teaching ability, many wanted to improve skills in coaching, providing feedback and delivering lectures. The preferred learning formats for improving these skills were either workshops at conferences or online. Half of the respondents are currently in an administrative/leadership role,

and of those that are not, only 30% were interested in pursuing future leadership positions. The main barriers cited were time and the experience required.

Conclusions: Overall satisfaction scores for current CME practices were mediocre amongst Canadian ROs, with lack of time consistently mentioned as a barrier. There were notable unmet needs in research, teaching and administration – highlighting potential areas for future CPD initiatives.

15

PATIENT EDUCATION PRACTICES AND PREFERENCES OF INTERPROFESSIONAL RADIATION ONCOLOGY PROVIDERS

Jie Jane Chen[1], Anna M. Brown[2], Allison E. Garda[3], Ellen Kim[3], Sarah A. McAvoy[3], Subha Perni Subha Perni[3], Michael K. Rooney Michael K. Rooney[2], Kevin Shiu, MD Kevin Shiu, MD[3], Kristi L. Tonning[3], Laura Warren[3], Daniel W. Golden[3], Jennifer Croke[4], Radiation Oncology Education Collaborative Study Group (ROECSG) Patient Education Working Group N/A[2]
[1]University of California, San Francisco, CA
[2]N/A, Wausau, WI
[3]N/A, Rochester, MN
[4]Princess Margaret Cancer Centre, Toronto, ON

Purpose: Patient understanding of radiotherapy (RT) processes and data regarding optimal approaches to patient education (PE) within radiation oncology (RO) are limited. Our objective was to evaluate PE practices and preferences of interprofessional RO providers to inform recommendations for delivering inclusive, accessible, and patient-centred education.

Materials and Methods: An anonymous 17-item online survey, approved by an ethics review board, was administered to all members of the Radiation Oncology Education Collaborative Study Group (ROECSG) between October 5, 2022 and November 23, 2022. Respondent demographics, provider PE practices and preferences, and institutional assessment practices were collected. Qualitative items explored key strategies, challenges and desired resources for PE. Descriptive statistics summarized survey responses. Fisher's exact test compared PE practices by provider role and PE timing. Thematic analysis was used for qualitative responses.

Results: One hundred and twenty-three ROECSG members completed the survey (31% response rate). Respondents consisted primarily of RO attendings (64%), followed by RO trainees (21%), medical physicists (7%), physician assistants/nurses (2%), radiation therapists (2%), and "other" (4%). Most practiced in an academic setting (86%) within North America (82%). The most common PE resources used were custom created institution-specific (61%) and electronic health system generated materials (38%). PE was delivered primarily by one-on-one teaching (72%), paper handouts (69%), and organizational websites (21%) (e.g., RTanswers.org). Almost half (41%) reported that their PE practices differed based on type of clinical encounter, for example paper handouts for in-person visits and multimedia resources for virtual visits. The majority (86%) stated that their institution has access to disease site-specific PE materials, with nearly all having breast (91%) and/or head and neck cancer materials (89%). Only 58% reported access to non-English PE materials, most commonly in Spanish (68%) or Chinese (18%). The most common institutional assessment method of PE materials was staff review (53%), with 19% reporting no formal assessment. Among institutions with an assessment process, respondents were mostly "unsure" (56%) of frequency, whereas 20% conducted assessments at least annually. RO attendings/trainees were more likely than other team members to deliver PE at consultation (98% versus 71%, p=0.03). PE practices amongst ROs differed according to the timing along the RT care path (consultation versus simulation versus first fraction, respectively): one-on-one teaching: 89% versus 49% versus 56%, p<0.01 and paper handouts: 69% versus 28% versus 16%, p<0.01. Key PE strategies included incorporating multimedia resources, personalizing delivery, and repetition at multiple time points by the interprofessional team. Limited time, inadequate administrative support, and lack of customized resources were identified as challenges in PE delivery.

Conclusions: Interprofessional RO providers engage in PE, with most utilizing custom created institution-specific materials. PE practices differ according to the type of clinical encounter and timing in the RT care path. Increased adoption of multimedia materials and partnerships with patients to tailor PE resources based on learning styles and to include underrepresented populations are needed to foster high-quality, patient-centred PE delivery.

16

EXPLORING TRENDS IN WORK SATISFACTION, STRESS AND BURNOUT AMONG ONCOLOGISTS AND ONCOLOGY TRAINEES

Selena Laprade[1,2], Ege Babadagli[1,2], Gordon Locke[1,2], Joanne Meng[1,2], Angela McNeil[1], Julie Renaud[1], Elisabeth Cisa-Paré[3], Jessica Chan[4], Jiheon Song[5], Rajiv Samant[1,2]
[1]The Ottawa Hospital Cancer Centre, Ottawa, ON
[2]University of Ottawa, Ottawa, ON
[3]Northern Ontario School of Medicine, Sudbury, ON
[4]University of British Columbia, Vancouver, BC
[5]University of Toronto, Toronto, ON

Purpose: As burnout becomes a common subject of discussion, oncologists remain a group of physicians at increased risk due to the high stakes and emotional burden that is associated with their work. We sought to explore the levels of satisfaction, stress and burnout of trainees and attending physicians working in radiation and medical oncology to examine these trends.

Materials and Methods: An ethics approved survey exploring staff satisfaction, stress, and burnout was sent to all staff working in oncology at The Ottawa Hospital, including attending and resident physicians. This survey methodology included multiple choice questions and free text questions. Only the multiple-choice section was analyzed for the purposes of this study.

Results: A total of 56 oncologists and oncology trainees answered the survey, including 10 medical oncologist residents/fellows, 13 radiation oncology residents/fellows, 14 staff medical oncologist and 19 staff radiation oncologists. 66% of respondents were males, 27% female, 7% preferred not to say, and 64% are between the ages of 31-50. For years of experience, 52% have 0-5 years, 32% have 5-20 years, and 16% have over 20 years. The group with the highest level of satisfaction were medical oncology residents, with 50% reported being "very satisfied" with their work. In terms of enjoying their work, radiation oncology staff had the highest proportion answering "yes, very much" with 65%, and the radiation oncology residents/fellows had the smallest proportion with 38.5%. Oncologists and trainees identified the same aspects of work they found enjoyable: interactions with patients, interactions with colleagues, and learning new things. When asked if they found their work stressful, 50% of medical oncology trainees, 28.5% of medical oncology staff, 15.4% of radiation oncology trainees and 15% of radiation oncology staff answered "yes, very stressful". Above 80% in all groups have never called in sick due to stress. 72% of oncologists and oncology trainees report that they often or sometimes experience burnout. However, only 9% feel that there is enough support when they are stressed or burnt out.

Conclusions: We identified variations in stress levels and work enjoyment which differed depending on the specialty and level

of training. Oncologists are overall experiencing high levels of burnout and stress, and there is a clear need for additional support for physicians.

17
CHALLENGES IN DEFINING OLIGOMETASTATIC DISEASE IN CLINICAL PRACTICE
Inmaculada Navarro-Domenech, Aisling Barry, Jane Tsai, Grace Ma, Philip Wong
University of Toronto, Toronto, ON

Purpose: There is little data understanding the multi-disciplinary application of oligo-metastatic disease (OMD) treatment and decision-making. Through an anonymous survey, we sought to understand the knowledge gaps and challenges faced by physicians caring for cancer patients in deciphering and delivering treatments for patients with OMD.

Materials and Methods: This was an IRB approved single institution quality improvement study conducted via an anonymous electronic survey. Three clinical cases of OMD that ranged from de-novo OMD to oligo-progressive disease were presented to check participants' comprehension of OMD. Descriptive statistics were used to summarize quantifiable information obtained from the survey. A qualitative approach was taken for the open-ended questions, in which the answers were reviewed by two independent readers and grouped together into common themes, and analyzed using sector and bar diagram, decision-tree method and sorted by prevalence.

Results: The survey was answered by 70 clinicians (39 (56%) medical oncologists, 17 (24%) radiation oncologists, five (7%) surgeons, nine (13%) from anatomical pathology/radiology/palliative care). The three clinical cases were correctly answered in 63%, 94% and 76%, respectively; of these, 76% to 84% would offer local treatment for each OMD scenario. Most (79%) perceived differences between local therapies (surgery, SBRT and RFA). Surgery was preferred to improve local control and overall survival, while SBRT was considered as being less invasive and more beneficial to patient quality of life. The definition of OMD was perceived by 94% as patients harboring 1-5 metastases. The main perceived challenges consist of lack of evidence in clinical and prospective trial data. Referrals are hindered as the goals and approach of OMD care are unclear. The most important determinant in deciding whether patients may benefit from OMD treatment is tumour histology and molecular profile.

Conclusions: SBRT as a treatment of OMD emerged during an era of rapid expansion in systemic treatments and improvements in imaging techniques. Positive and negative trials in various histologies of cancer further added uncertainty on who would best benefit from OMD SBRT. As more radiation centres offer SBRT, the discordance in the outcome expectations from referring physicians, radiation oncologists and patients will need to be addressed to ensure that patients' goals of care are met.

18
SUCCESSFUL IMPLEMENTATION OF A RADIATION THERAPIST-LED INTERDISCIPLINARY COURSE FOR LEARNING MALIGNANT SPINAL CORD COMPRESSION MANAGEMENT
Yiming Michael Zhu, Brian Chwyl, Susan Fawcett, Fan Yang, Heather Warkentin, Sunita Ghosh, Brock Debenham, Adele Duimering, Mustafa Al Balushi
University of Alberta, Edmonton, AB

Purpose: Malignant spinal cord compression (MSCC) is an emergent presentation and requires timely action by an interdisciplinary treatment team. High fidelity simulation (HFS) training is particularly suited to high-stakes, uncommon situations such as MSCC, allowing for otherwise rare hands-on practice. Traditionally, interdisciplinary medical simulation courses have been physician-led, potentially to the detriment of radiation therapy (RTT) and medical physics (MP) learner needs. This pilot study aims to characterize and evaluate a first of its kind course to examine the educational outcomes of an RTT designed and led interdisciplinary radiation oncology (RO) emergency simulation course.

Materials and Methods: An interdisciplinary course design team comprised of RO residents, RO faculty, RTT course instructors, and MPs created a HFS course using collaboratively developed learning goals, with RTT instructors providing final input on learning objectives. 15 learners including RO residents (n=9), senior RTT students (n=5) and an MP resident (n=1) participated in a live, RTT led HFS involving a sample clinical case, patient model, and a "cold" linear accelerator. Learners were assigned roles according to their educational background and worked collaboratively to complete the case. Participants were asked to complete anonymized pre and post simulation validated interdisciplinary education perception (IPE) scales and a course evaluation assessing educational outcomes before and after the HFS. Paired t-tests were used for the assessment of pre and post course evaluation scores.

Results: Fifteen participants completed their course educational evaluation and 14 completed their IPE questionnaire. Standard IPE questionnaire results showed highly favourable perceptions of respondents' own specialty and other allied specialties, with no change in these perceptions seen before and after the HFS in any domain. The course evaluation assessed 10 learning objectives, with significant improvements seen in self-rated post-course knowledge related to identifying MSCC symptoms (p=0.027); appropriate work-up (p=0.005); treatment decision making (p=0.001); treatment sequencing (p=0.003); dosing (p=0.022); simulation set-up (p=0.007); plan review (p=0.023); post treatment toxicities (p=0.017); and side effect management (p=0.001). Pre-course evaluations showed that six of 15 participants agreed or strongly agreed that they felt comfortable in their knowledge of all included domains, after course completion 14/15 participants agreed or strongly agreed they felt comfortable in all domains.

Conclusions: This first of its kind pilot study demonstrates that RTT led HFS courses are not only viable but can be an effective means of improving learning outcomes for RO residents, RTT students and MP residents. Collaboration is essential in radiation oncology and curriculum design should be shifted towards an interdisciplinary model which allows all allied disciplines to meet their educational goals and work towards a shared purpose of improving patient care.

19
PREDICTING ESOPHAGITIS: A SECONDARY ANALYSIS OF THE PALLIATIVE RADIATION FOR ADVANCED CENTRAL LUNG TUMOURS WITH INTENTIONAL AVOIDANCE OF THE ESOPHAGUS (PROACTIVE) PHASE III RANDOMIZED TRIAL
Muhammad I. Karamat[1], Douglas A. Hoover[1], Patrick V. Granton[2], Alysa Fairchild[3], Andrea Bezjak[4,5], Darin Gopaul[6], Liam Mulroy[7], Anthony Brade[4,8], Andrew Warner[9,1], Brock Debenham[3], David Bowes[7], Joda Kuk[6], Alexander Sun[3], George B. Rodrigues[9,1], David Palma[9,1], Alexander V. Louie[10,11]
[1]*London Health Sciences Centre, London, ON*
[2]*Erasmus Medical Center, Rotterdam, NL*
[3]*University of Alberta, Edmonton, AB*
[4]*University of Toronto, Toronto, ON*
[5]*Princess Margaret Cancer Centre, Toronto, ON*
[6]*Grand River Regional Cancer Centre, Kitchener, ON*
[7]*Dalhousie University, Halifax, NS*

[8]Credit Valley Cancer Centre, Toronto, ON
[9]Western University, London, ON
[10]Carleton University, Ottawa, ON
[11]Sunnybrook Health Sciences Centre, Toronto, ON

Purpose: In the phase III PROACTIVE randomized trial (NCT02752126), esophageal-sparing intensity modulated radiotherapy (ES-IMRT) reduced symptomatic Grade ³2 esophagitis, when compared to standard thoracic radiotherapy (RT). The purpose of this secondary analysis was to determine dosimetric predictors of esophagitis in PROACTIVE trial patients.

Materials and Methods: Ninety Stage III/IV NSCLC patients receiving either 20 Gy in 5 fractions or 30 Gy in 10 fractions were randomized to ES-IMRT or standard thoracic RT. Doses were converted to EQD2 using an alpha/beta of 3 (Gy_3). Clinical esophagus contours were subdivided into three categories: 1) entire esophagus (EE), 2) contralateral esophagus (CE), defined as the bisection of the esophagus along the esophagus centre of mass contralateral to the PTV, extended 2 cm inferior and superior to the PTV, and 3) the esophagus extended 2 cm inferior and superior to the PTV (E2SI). Volumetric ($V10Gy_3$, $V15Gy_3$, $V20Gy_3$, $V25Gy_3$, $V30Gy_3$), length ($L10Gy_3$, $L15Gy_3$, $L2Gy_3$, $L25Gy_3$, $L30Gy_3$), mean dose, and maximum dose parameters were calculated for these structures. Univariable logistic regression modelling was performed on EE, CE, and E2SI volume, length, mean and maximum dose parameters to determine predictors of symptomatic esophagitis. Factors with $p < 0.05$ on univariable modeling, in addition to treatment arm and prior systemic therapy (previously identified in primary trial multivariable analysis) were then evaluated through stepwise multi-variable logistic regression modelling. Factors entered into the model and maintaining $p<0.10$ remained, otherwise were removed. Predictive factors with $p<0.05$ were considered to be significant in the final model.

Results: Between June 2016 and March 2019, 90 patients were randomized at six Canadian centres. Thirty-six patients (40%) received 20 Gy in 5 fractions (28 Gy_3) and 54 (60%) received 30 Gy in 10 fractions (36 Gy_3). Twelve patients developed symptomatic RT-related esophagitis, 11 (24.4%) in the control arm and 1 (2.2%) in the ES-IMRT arm (p=0.002). The median mean EE dose was 8.3 Gy_3 (interquartile range [IQR]: 5.9-11.9) and the median maximum EE dose was 26.5 Gy_3 (IQR: 21.9-34.7). The median mean CE dose was 11.0 Gy_3 (IQR: 7.7-15.8) and the median maximum CE dose was 25.4 Gy_3 (IQR: 19.7-32.6). The median mean E2SI dose was 12.8 Gy_3 (IQR: 9.4-18.3) and the median maximum E2SI dose was 26.5 Gy_3 (IQR: 21.9-34.7). On multivariable stepwise logistic regression modelling, prior chemotherapy (odds ratio [OR]: 11.53, p=0.02) and maximum EE dose (OR per 1 Gy: 1.32, p=0.01) were significant predictors of symptomatic esophagitis, and CE $V10Gy_3$ (OR per 1 cc: 1.23, p=0.07) trended towards significance.

Conclusions: ES-IMRT reduced the incidence of symptomatic esophagitis. We propose prior chemotherapy, maximum esophagus dose and potentially CE $V10Gy_3$ as predictors of symptomatic esophagitis, which will inform the design of a dose escalation PROACTIVE2 clinical trial.

20

PNEUMONITIS RISK FOLLOWING COMBINED OSIMERTINIB AND THORACIC RADIOTHERAPY IN EGFR-MUTATED NON-SMALL CELL LUNG CANCER

David Y. Mak[1], Humza Nusrat[2], Michael Yan[2], Ambika Parmar[2], Ian Poon[2], Yee Ung[2], May Tsao[2], Andrew Warner[3], Patrick Cheung[2], Alexander V. Louie[2]
[1]University of Toronto, Toronto, ON
[2]Sunnybrook-Odette Cancer Centre, Toronto, ON
[3]London Health Sciences Centre, London, ON

Purpose: In epidermal growth factor receptor mutated (EGFR+) metastatic non-small cell lung cancer (mNSCLC), pneumonitis is a known side effect independently associated with Osimertinib and thoracic radiotherapy (TRT). The objective of this study was to examine the risk of pneumonitis with concurrent Osimertinib and TRT, and to observe patterns of practice regarding the cessation of Osimertinib during TRT.

Materials and Methods: In this single institution retrospective cohort study between 2016 and 2020, patients with EGFR+ mNSCLC who received both Osimertinib and TRT were included. TRT was defined as any course of radiotherapy that involved lung parenchyma within the treated field. The primary endpoint was the incidence of symptomatic (CTCAE Grade ≥ 2) pneumonitis. Comparisons were made with multivariable Cox proportional hazards regression for both Grade ≥ 2 and any grade pneumonitis.

Results: Out of 151 patients receiving Osimertinib during the study period, 41 underwent 147 courses of radiation either during or within six months of Osimertinib initiation. Sixty-eight (46.3%) treated lesions met our definition of TRT. In total, five patients developed symptomatic pneumonitis (12.2%), of which one was Grade 4 and another Grade 5. Mean (±SD) age at TRT was 65.5 (±12.0) years. Most patients had de novo metastatic disease (n=31; 75.6%), adenocarcinoma histology (n=38; 92.7%), and 16 (39%) were on Osimertinib as first line systemic therapy. The mean (±SD) number of cycles of Osimertinib was 9.6 (±4.3). Median total dose and fractionations were 20 Gy (interquartile range [IQR]: 20-30 Gy) and 5 (IQR: 1-5), respectively. During TRT, Osimertinib was knowingly held in 12 patients (29.3%), most commonly for 1-2 days before and after (n=7; 17.1%). Osimertinib was knowingly continued during TRT for five patients (12.2%), and undocumented in eight patients (19.5%). Multivariable analysis identified that each additional cycle of Osimertinib was associated with an increased incidence of Grade ≥ 2 pneumonitis (hazard ratio [HR]: 1.54, 95% confidence interval [CI]: 1.15-2.07, p=0.004). Total radiation dose was also associated with increased incidence of any grade of pneumonitis (HR per 5 Gy: 1.38, 95% CI: 1.03-1.86, p=0.031). There was no association with incidence of pneumonitis (any grade) if Osimertinib was continued during TRT (HR: 3.36, 95% CI: 0.13-86.56, p=0.47) or if TRT was given within six months of Osimertinib initiation (HR: 0.20, 95% CI: 0.02-2.21, p=0.19).

Conclusions: Our study did not identify any association of increased incidence or severity of pneumonitis in patients receiving concurrent Osimertinib and TRT. Patterns on whether to hold Osimertinib during TRT, and for how long, were variable. Symptomatic pneumonitis was associated with increasing doses of TRT, and further analysis to identify any significant dosimetric parameters are underway.

21

NUTRITIONAL INTERVENTIONS TO SUPPORT LUNG CANCER PATIENTS UNDERGOING THORACIC RADIATION: A SYSTEMATIC REVIEW

Lise Wolyniuk[2], Andrew N. Youssef[2], Alexander V. Louie[1], Adam Mutsaers[1]
[1]University of Toronto, Toronto, ON
[2]Western University, London, ON

Purpose: Patients undergoing thoracic radiation (TRT) for lung cancer can face serious nutritional challenges from their cancer symptoms, including obstruction, cachexia and fatigue. Combined with the toxic effects of therapy, including esophagitis, patients are at risk for malnutrition which is linked to poorer oncologic outcomes and quality of life. Standard interventions and supports vary widely prompting a systematic review of randomized nutritional interventions for patients undergoing TRT for lung cancers.

Materials and Methods: A systematic review was performed to PRISMA guidelines. Medline, Embase and Cochrane databases were queried from inception for English language, randomized trials investigating supportive nutritional supplements, counselling, and alternative feeding routes and for patients receiving TRT +/- systemic therapy for lung cancer, with clinical endpoints. Independent reviewers screened abstracts, and full texts, with a third author settling discrepancies. Reviews, non-randomized studies, and those investigating chemoprevention or anti-cancer effects were excluded. Relevant data were abstracted and synthesized qualitatively.

Results: 2,003 unique studies were screened, with 215 undergoing full-text review; 12 distinct cohorts met criteria, representing 850 lung cancer patients. Studies were published between 1985 and 2021 with a median of 60 patients. Six studies were completed in North America and five in Asia. Half of the studies were double-blinded, and half non-blinded. Intent of treatment was curative in seven cohorts, two palliative and three mixed. TRT dose ranged from 25Gy/10 fractions to 70Gy/35 fraction. Common primary endpoints included esophagitis Grade (n=4) and change in weight of lean body mass (n=4). Risk of bias was low in five cohorts, moderate in four, and high in three. Efficacy of oral nutrition supplements and additives was evaluated in seven trials. Both omega-3 and epigallocatechin-3-gallate enriched oral supplements demonstrated clinical benefit through significantly improving weight and reducing esophagitis, respectively. Manuka honey, sodium alginate and cysteine-rich protein supplements showed no clinical benefits over controls. Glutamine supplementation showed conflicting results in two trials. Role of intensive dietary counselling was explored in two studies of patients undergoing curative therapy. In the inpatient setting, patients receiving specialized nutrition-team management had significantly improved nutritional indices. In the outpatient setting, patients reported higher nutritional satisfaction, but no significant improvements in clinical endpoints. Two large trials evaluated anamorelin supplementation as an appetite stimulant in palliative patients, demonstrating significantly improved lean body mass over 12 weeks, with minimal toxicity. Inpatient total parenteral nutrition over 30 days was compared to standard care in 119 patients, improving mean weight in the short term, but without durable impact.

Conclusions: Various nutrition interventions have demonstrated benefit for lung cancer patients undergoing TRT. Quality randomized data are limited, and significant heterogeneity precluded metanalysis. There is no clear evidence to recommend a specific nutritional intervention approach and more, rigorous RCTs are needed.

22

DOSE ESCALATED RADIOTHERAPY IS ASSOCIATED WITH IMPROVED OUTCOMES FOR HIGH GRADE MENINGIOMA

Arjun Sahgal[1], Sten Myrehaug[1], Hany Soliman[1], Chia-Lin Tseng[1], Jay Detsky[1], Hanbo Chen[1], Mary-Jane Lim-Fat[1], Mark Ruschin[1], Eshetu Atenafu[2], Julia Keith[1], Nir Lipsman[1], Chris Heyn[1], Pejman Maralani[1], Sunit Das[1], Farhad Pirouzmand[1], K. Liang Zeng[1]
[1]University of Toronto, Toronto, ON
[2]University Health Network, Toronto, ON

Purpose: Conventionally fractionated radiotherapy (RT) is a defined treatment following surgery for atypical and malignant meningioma. However, the optimal radiotherapeutic approach is unclear. We present the results of our dose-escalation strategy.

Materials and Methods: Consecutive patients with histopathologic Grade 2 or 3 meningioma treated with RT were retrospectively reviewed. The primary outcome was progression-free survival (PFS), and secondary outcomes included cause-specific survival (CSS), overall survival (OS), local failure and incidence of radiation necrosis. We specifically compared the dose-escalation cohort, defined as those treated with ≥66Gy EQD2 (equivalent dose in 2 Gy fractions, a/b=10), to the standard dose cohort receiving <66Gy EQD2. We defined adjuvant as RT delivered within six months of surgery otherwise the treatment was salvage.

Results: A total of 118 patients with Grade 2 (111/118) or 3 (7/118) meningioma were identified. 54/118 (45.8%) received dose-escalation and 64/118 (54.2%) standard dosing. 34/54 (63.0%) dose-escalated and 45/64 (70.3%) standardly dosed were treated adjuvantly. The median follow-up was 45.4 months (IQR: 24.0-80.0 months) and median OS was 9.7 years. Post-operative residual disease was present in all dose-escalated patients, as compared to 65.6% in the standard dose cohort. PFS at three-, four- and five-years in the dose-escalated versus standard dose cohort were 78.9%, 72.2% and 64.6% versus 57.2%, 49.1% and 40.8%, respectively, (p=0.030). On multivariable (MVA) analysis, dose-escalation (HR: 0.544, 95%CI: 0.303-0.977, p=0.042) was associated with improved PFS, whereas ≥2 surgeries (HR: 1.989, 95%CI: 1.049-3.773, p=0.035) and older age (HR: 1.035, 95%CI:1.015-1.056, p<0.001) associated with worse PFS. The cumulative risk of local failure at three-, four- and five-years in the dose-escalated versus standard dose cohort were 16.9%, 23.8% and 31.8% versus 39.6%, 45.6% and 53.9%, respectively, favouring dose-escalation (p=0.016). MVA confirmed dose-escalation as predictive of a lower risk of LF (HR: 0.483, 95%CI: 0.263-0.887, p=0.019), while ≥2 surgeries prior to RT predicted for greater LF rates (HR:2.145, 95%CI:1.220-3.771, p=0.008). A trend was observed for prolonged CSS and OS in the dose escalation cohort (p=<0.1). Seven patients (5.9%) developed symptomatic radiation necrosis (RN) with no significant difference between the two cohorts.

Conclusions: Dose-escalated radiotherapy for high grade meningioma to ≥66Gy is associated with significantly improved rates of local control and PFS with an acceptable risk of RN.

23

A RETROSPECTIVE STUDY COMPARING OUTCOMES IN MATCHED PATIENTS WITH POOR PROGNOSIS TREATED WITH TARGETED CONVENTIONAL VOLUMETRIC MODULATED ARC RADIOTHERAPY VERSUS WHOLE BRAIN RADIOTHERAPY FOR BRAIN METASTASES

Gurjit Parmar, Timothy Kong, Jeremy Hamm, Mitchell Liu, Shilo Lefresne, Hannah Carolan, Eric Berthelet, Jessica Chan, Alan Nichol
University of British Columbia, Vancouver, BC

Purpose: Patients with brain metastases and poor prognosis are often treated with whole brain radiotherapy (WBRT) which can cause a variety of side effects. Our institution devised a new RAPid simPLE (RAPPLE) brain-sparing radiotherapy technique to treat multiple brain metastasis for patients whose poor prognosis does not warrant SRS. This study compares the oncologic outcomes of matched patients treated with RAPPLE and WBRT.

Materials and Methods: RAPPLE uses single-isocentre, coplanar volumetric modulated arc therapy and a non-stereotactic head-shell with IntegraBite™. Brain metastasis were contoured in a single gross tumour volume and expanded by 3 mm to create a planning target volume, of which 99.5% was covered with 95-110% of 20 Gy in 5 fractions. Patients treated with a first course of RAPPLE from January 2017 to December 2021 were identified in an institutional database. Using age, cancer diagnosis, and treatment date, we identified a matched cohort of patients receiving a first course of WBRT with 20 Gy in 5 fractions. Overall survival (OS) was calculated using the Kaplan-Meier method, and intracranial progression was calculated using cumulative incidence with a competing risk of death. Log-rank, Cox regression and Fine-Gray

analyses were used for comparisons. Paired t-tests were used to compare patient-reported fatigue measured using 5-level Likert scales before and 2-6 weeks after radiotherapy.

Results: The RAPPLE and WBRT cohorts each had 137 patients. The matched median age was 69 years. Primary diagnoses were lung cancer (72%) and other cancers (28%). The minimum, median, and maximum numbers of metastases treated with RAPPLE were 1, 3, and 18, respectively. The median Karnofsky Performance Score (KPS) was 70 in both cohorts. The median survival was 4.1 months for RAPPLE and 4.2 months for WBRT, and the 18-month OS was 11% for RAPPLE and 12% for WBRT (log-rank p 0.8). On multivariable analysis, KPS, diagnosis, extracranial disease, and use of systemic therapy before and after RT were predictive of OS, but use of RAPPLE versus WBRT was not (HR = 0.97, 95%CI: 0.75-1.25, p=0.8). The 18-month cumulative incidence of intracranial progression was 0.49 for RAPPLE and 0.37 for WBRT (p=0.04). After RAPPLE, 17% required more focal RT and 4% required salvage WBRT, while after WBRT, 3% required focal RT and 4% required repeat WBRT. After RAPPLE, mean patient-reported fatigue remained stable from baseline to first follow-up (2.18 versus 2.27, p=0.9), but, after WBRT, it worsened from baseline to first follow-up (1.95 versus 2.63, p=0.002).

Conclusions: As expected, after RAPPLE, more targeted radiotherapy was required for intracranial progression, but there was no difference in OS between the RAPPLE and WBRT cohorts. Patients reported significantly worse fatigue after WBRT. Almost all patients (96%) treated with RAPPLE avoided WBRT.

24

STEREOTACTIC BODY RADIOTHERAPY FOR POSTERIOR ELEMENT ONLY SPINAL METASTASES: OUTCOMES AND VALIDATION OF RECOMMENDED CLINICAL TARGET VOLUME DELINEATION PRACTICE

Laura Burgess[1,2], K. Liang Zeng[1,2], Sten Myrehaug[1,2], Hany Soliman[1,2], Chia-Lin Tseng[1,2], Jay Detsky[1,2], Hanbo Chen[1,2], Daniel Moore-Palhares[1,2], Christopher D. Witiw[1,3], Beibei Zhang[1,2], Pejman Maralani[1,4], Arjun Sahgal[1,2]
[1]University of Toronto, Toronto, ON
[2]Sunnybrook-Odette Cancer Centre, Toronto, ON
[3]St. Michael's Hospital, Toronto, ON
[4]Sunnybrook Health Sciences Centre, Toronto, ON

Purpose: Spine stereotactic body radiotherapy (SBRT) results in improved local control and pain response compared to conventional external beam radiotherapy. Consensus stipulates MRI-based delineation of the clinical target volume (CTV) is critical and is based on spine segment sector involvement. The applicability of these contouring guidelines to metastases confined to the posterior elements is unknown. The purpose of this study was to determine the patterns of failure, as well as the safety of treating posterior element metastases when the vertebral body was intentionally excluded from the CTV.

Materials and Methods: A retrospective review of a prospectively maintained database of 605 patients and 1412 spine segments treated with spine SBRT was performed. Only treated segments involving the posterior elements alone were included for the analyses. Patients were followed per institutional protocol with a clinical assessment and full spine MRI every 2–3 months or sooner, as clinically indicated. The primary outcome was local failure, as per SPINO recommendations, and secondary outcomes included patterns of failure, toxicities. Clinical and tumour factors were reported with descriptive statistics. The cumulative risk of local failure was estimated using the Fine-Gray method, accounting for death before local failure as a competing risk.

Results: Between January 2008 to December 2021, 24/605 patients and 31/1412 segments within the database were treated to the posterior elements only. Of the 24 patients, the most common primary malignancies was renal cell carcinoma (11/24, 45.8%). 87.5% were treated in the de novo setting, 8.3% were post-operative and 4.2% re-irradiation. The majority were within the thoracic (15/31, 48.4%) and lumbar (13/31, 41.9%) spine. While the majority had paraspinal extension (20/31, 64.5%), most did not have any epidural disease (22/31, 71.0%). Local failure occurred in 11/31 segments. The cumulative rate of local recurrence was 9.7% at 12 months and 30.8% at 24 months. Amongst local failures, the most common histologies were renal cell carcinoma (36.4%) and non-small cell lung cancer (36.4%). At baseline, four of 11 (36.4%) segments with local failure (36.4%) had epidural disease and eight of 11 (72.7%) had paraspinal disease. Most local failures were treated in the de novo setting (8/11, 72.7%). Six of 11 (54.5%) failed exclusively within treated CTV sectors and 5/11 (45.5%) with both treated and adjacent untreated sectors. Of these five, four had disease progression within the untreated vertebral body. No failures occurred exclusively within the untreated vertebral body. One patient (4.2%) experienced a Grade 4 skin toxicity and one patient (4.2%) developed an iatrogenic Grade 1 vertebral compression fracture.

Conclusions: Posterior element alone metastases are rare. Our analyses support SBRT consensus contouring guidelines such that the vertebral body can be excluded from CTV in spinal metastases confined to the posterior elements.

25

DUAL ENHANCEMENT IN THE RADIOSENSITIVITY OF PROSTATE CANCER THROUGH NANOTECHNOLOHY AND CHEMOTHERAPEUTICS

Nolan Jackson[1], Abdulaziz Alhussan[1], Iona Hill[2], Kyle Bromma[1], Belal Abousaida[2], Jessica Morgan[1], Yuri Mackeyev[2], Wayne Beckham[3], Sunil Krishnan[2], Devika Chithrani[1]
[1]University of Victoria, Victoria, BC
[2]University of Texas Health Science Center, Houston, TX
[3]British Columbia Cancer, Victoria, BC

Purpose: The efficacy of current radiotherapy (RT) techniques is limited due to normal tissue toxicity that is induced during treatment. Therefore, the introduction of radiosensitizers to radiotherapy (RT) treatment can improve curative rates by increasing the local tumour control. Incorporating gold nanoparticles (GNPs) into RT results in the enhancement of reactive oxygen species, and by combining GNPs with clinically used docetaxel (DTX), which traps cells in the G2/M phase, the most radiosensitive phase, there is potential to create a synergistic radiosensitization effect. The purpose of this study is to elucidate the further enhancement in radiosensitivity of prostate cancer cells due to the incorporation of DTX to GNP enhanced RT.

Materials and Methods: For in vitro study, PC-3 prostate cancer cell cultures were dosed with GNPs and DTX at a concentration of 1 nM and 2 nM, respectively. Monolayer cell cultures were irradiated 24 h post dosing, with a dose of 2 Gy or 5 Gy. DNA double-strand breaks (DSBs) in cells were probed and cell proliferation was monitored to examine the efficacy of treatment. For in vivo assays, a mouse xenograft model was used. Mice were treated at concentrations of 2 μg/g and 6 μg/g of GNPs and DTX, respectively, 24 h prior to 5 Gy irradiation. Tumour volume measurements and mice survival rates were used to determine treatment efficacy.

Results: A radiation dose of 2 Gy resulted in a 38% increase in DNA DSBs in PC-3 cells treated with the combination of GNP/DTX versus cells treated with GNPs (p=0.003). There was also a significant reduction in the relative growth of cells treated with both GNPs/DTX after being irradiated with 5 Gy. In vivo

results displayed significant reduction in tumour growth with the treatment of GNP/DTX/RT when compared to RT (p=0.02) as well as 100% mice survival.

Conclusions: Increasing local tumour control through the enhancement of tumour radiosensitivity can substantially impact clinical outcomes. Our study suggests that chemotherapeutic DTX can be used in combination with GNPs, which have been well tolerated in phase I trials, to create a synergistic radiosensitization effect increasing local tumour control. The concentrations used in this study are clinically feasible, and therefore, there is potential for this strategy to be translated into clinical settings.

26

CLINICAL IMPLEMENTATION OF VMAT BASED TOTAL BODY IRRADIATION

Dan Morton, Laura Drever, Cody Crewson, Chantal Perry, Philip Wright
Saskatchewan Cancer Agency, Saskatoon, SK

Purpose: Total body irradiation (TBI) is an established technique used with systemic chemotherapy to increase effectiveness in bone marrow transplantation. Methods of delivering homogeneous dose to the entire body vary widely. Locally, an extended field lateral parallel opposed pair was used. Linac replacement with more restrictive bunker dimensions instigated the need to implement a technique to deliver TBI in a less restrictive manner. The aim of this work was to develop and implement a robust VMAT based TBI planning and delivery workflow to efficiently create high quality treatments that can be delivered on and TrueBeam linac.

Materials and Methods: Treatment planning was performed in Varian Eclipse using scripts developed to automate the planning process (Simiele, PRO, 2021). 10MV arc fields are placed in three upper and two lower body isocenter groups, with beam arrangements set to cover the entire body. Planning target volume (PTV) is defined as the entire body, 3mm from skin surface, and is generated automatically along with optimization structures, including a flash target. Successive optimizations of the full plan are performed using Eclipse scripting API. Following successful optimization, isocentre groups are broken into individual plans; the lower body plans mirrored to be delivered feet-first. Plan quality was evaluated based on PTV coverage, max dose, and lung dose. Planning was assessed using CT datasets from previously treated TBI patients and phantoms. A delivery workflow was designed to image orthogonal upper body kv-pairs at each isocentre, apply mean shifts, deliver the three plans sequentially, then rotate the patient to feet-first and repeat. Verification of delivery was performed with ArcCheck, an ion chamber in a block phantom, and OSLDs inside an anthropomorphic phantom. In-vivo dosimetry was performed during patient treatments using OSLDs on the thigh and in the naval.

Results: The VMAT TBI process was able to generate clinically acceptable treatment plans in approximately four hours. Treatment plans with 12-15 arcs provide full PTV coverage, with hotspots up to 130% of prescription, and lung V100<20%, in comparison to previous extended field plans goals of 115% hotspot and lung V100 of 40%. Total set up and delivery time for patients was approximately one hour. Mean gamma (3%/2mm) passing rate on ArcCheck was 98.5% ± 2.2%, and ion chamber measurements were a mean -0.2% ± 2.7% difference to Eclipse calculated values for all arcs. OSLDs in the anthropomorphic phantom were 3.6% ± 1.9% difference from calculated values for OSLDs distributed within the phantom, and 3.7% ± 1.1% on the surface. The first three patient plans had mean PTV coverage of 105% ± 2% of the prescription dose and V90>99% with hotspots D1cc = 127.7% ± 12.4%. Lung mean doses were spared to 91.0% ± 3.3% of prescription, with V100 = 18.1 % ± 0.7%. In-vivo measurements for treatments were 4.3% ± 3.3% of calculated values.

Conclusions: Performing TBI using VMAT allowed for treatments to be delivered at any TrueBeam linac, while providing the benefit of satisfactory dose coverage and ability to control lung dose. Planning time can be reduced with the automation of additional steps in the script. Improved setup and immobilization are being explored to increase treatment delivery efficiency.

27

A NOVEL APPROACH TO LONGITUDINAL BEAM STABILITY IN A COMPACT DIELECTRIC WALL ACCELERATOR FOR PROTON THERAPY

Christopher Lund[1,2], Paul Jung[3,4], Morgan Maher[1,2], Julien Bancheri[1,2], Thomas Planche[4,3], Rick Baartman[3,4], Jan Seuntjens[5,6,7]
[1]*McGill University Health Centre, Montréal, QC*
[2]*McGill University, Montréal, QC*
[3]*TRIUMF, University of Victoria, BC*
[4]*University of Victoria, Victoria, BC*
[5]*Princess Margaret Cancer Centre, Toronto, ON*
[6]*University Health Network, Toronto, ON*
[7]*University of Toronto, Toronto, ON*

Purpose: Maintaining stable longitudinal particle motion (described by energy and time deviations) within proton bunches during acceleration is important for Bragg peak sharpness, maximum dose rate, and other proton therapy (PT) dose characteristics. However, a suitable mechanism does not exist for the dielectric wall accelerator (DWA), a compact accelerator under consideration for low-cost PT. This is a major barrier to the development of such a device. We propose a new approach to field generation in a DWA which allows for time-varying accelerating fields. In this work, we test whether linear time variations are sufficient to maintain longitudinal stability.

Materials and Methods: A novel numerical model of a DWA was developed and integrated into the particle-in-cell code Warp. The accelerating fields were treated analytically, with a multipole expansion describing the spatial distribution and a 1 ns FWHM profile with linear gradient Γ′ describing the time variation. A set of differential equations describing the dynamics of a single (fictitious) particle along the centre of the DWA, termed the reference particle, were derived and used to coordinate the timing of each accelerating field. The particle phase space distributions of a 1 μA peak current, 0.5 ns, 25 keV proton bunch (focused to beam waist at entrance by a magnetic solenoid) were tracked through a 15 cm (150 x 1 mm modules, 1 cm aperture), 10 MV/m DWA segment and compared for Γ′ in [-1,5] MV/m/ns.

Results: The data indicate that positive Γ›s produce a region of stability around the reference particle, which is consistent with a linear optics interpretation. Particles in this region experience a restorative force that maintains beam quality throughout acceleration. Γ′, analogous to the spring force in a harmonic oscillator, drives a rotation in phase space about the reference particle. This results in an inverse relationship between the temporal width and energy spread of the bunch during acceleration. A maximum bunch charge was observed for Γ′=2 MV/m/ns, which can be explained by considering two competing trends. As Γ′ is increased to 2 MV/m/ns, the region of stability encompasses an increasing number of particles. However, the time variation in the field also produces transverse forces that result in the final beam width increasing with Γ′. At Γ′=5 MV/m/ns, approximately 3% of the beam is lost to wall collisions, from <<1% for Γ′=2 MV/m/ns. The amount of beam loss and its relationship to Γ′ will change with gradient strength, segment length, and aperture radius. Further, the length of the segment will also affect the degree of rotation caused by Γ′, and thus the final temporal width and energy spread.

Conclusions: A positive linear time variation in the accelerating fields of a DWA may be sufficient for providing longitudinal stability in proton bunches during acceleration. The choice of Γ' will vary with the specifics of the system and represents an important design decision.

28

MEASUREMENT OF NEUTRON DOSE FOR VMAT AND SRS TREATMENT AT ENERGIES BETWEEN 6 AND 10 MV

Marco Carlone, Ray Yang, Derek Hyde, Nathan Becker, John Cocarell
British Columbia Cancer, Kelowna, BC

Purpose: Volumetric radiotherapy is usually done at 6 or 10 MV. At higher doses, neutron body dose increases which creates unwanted total body dose. Below 10 MV, photoneutron production drops off non-linearly. Understanding dose due to photoneutrons below 10 MV may help choose a more optimal treatment energy for volumetric radiotherapy. The purpose of this study is to measure photoneutron yields in a medical linac over a continuum between 6 and 12 MV, which may offer an improved trade-off between beam penetration and dose rate as compared to 6 MV while reducing photoneutron production which is present at 10 MV.

Materials and Methods: A Varian iX linear accelerator undergoing decommissioning at our clinic was made to operate over a range of photon energies between 6 and 15 MV by calibrating the bending magnet and adjusting other beam generation parameters. Neutron exposure within the treatment room was measured using an Anderson-Braun type detector over a continuum of intermediate energies.

Results: The photoneutron production for energies below 10 MV was measured, adding to data that is otherwise scarce in literature. Our results are consistent with previously published results for neutron yield. We found that the photoneutron production at 8 MV was about 1/10 of the value at 10 MV, and about 10 times higher than detector background at 6 MV.

Conclusions: Photoneutron production drops off below 10 MV, but is still present at 8 MV. An 8 MV beam is more penetrating than a 6 MV beam, and may offer a suitable tradeoff for modern radiotherapy techniques such as VMAT, SRS and SABR. Further studies are needed to better understand the impact on treatment plan quality between 8 and 10 MV beams considering the benefits to facility requirements and non-therapeutic patient dose.

29

POTENTIAL OF GOLD NANOPARTICLES IN CURRENT RADIOTHERAPY USING A CO-CULTURE MODEL OF CANCER CELLS AND CANCER ASSOCIATED FIBROBLASTS

Abdulaziz Alhussan[1], Nicholas Palmerely[1], Julian Smazynski[2], Joanna Karasinska [3], Daniel J. Renouf [3], David Scaheffer[4], Wayne Beckham[2], Abraham Alexander[2], Devika Chithrani[1]
[1]*University of Victoria, Victoria, BC*
[2]*British Columbia Cancer, Victoria, BC*
[3]*British Columbia Cancer, Vancouver, BC*
[4]*University of British Columbia, Vancouver, BC*

Purpose: One reason experimental therapeutics fail in clinical trials relates to limitations in the pre-clinical models that lack a true representation of the tumour microenvironment (TME). The tumour promoting effect of cancer associated fibroblasts (CAFs) within the TME is thought to reduce cancer therapeutics' efficacy. Our goal is to create a co-culture of CAFs and tumour cells to model the interaction between cancer and stromal cells in the TME and allow for better testing of therapeutic combinations.

Materials and Methods: To test the proposed co-culture model, a gold nanoparticle (GNP) mediated-radiation response was used on a pancreatic ductal adenocarcinoma (PDAC) as the tumour model due to its very low survival rates. Cells were grown in co-culture with different ratios of CAFs to cancer cells. MIA PaCa-2 was used as our PDAC cancer cell line. Co-cultured cells were treated with 2 Gy of radiation following GNP incubation. DNA damage and cell proliferation were examined to assess the combined effect of radiation and GNPs.

Results: Cancer cells in co-culture exhibited up to a 23% decrease in DNA double strand breaks (DSB) and up to a 35% increase in proliferation compared to monocultures. GNP/Radiotherapy (RT) induced up to a 25% increase in DNA DSBs and up to a 15% decrease in proliferation compared to RT alone in both monocultured and co-cultured cells.

Conclusions: The observed resistance in the co-culture system may be attributed to the role of CAFs in supporting cancer cells. Moreover, we were able to reduce the activity of CAFs using GNPs during radiation treatment. Indeed, CAFs internalize a significantly higher number of GNPs, which may have led to the reduction in their activity. We have demonstrated a co-culture platform to test GNP/RT in a clinically relevant environment.

30

CHARACTERIZING A NOVEL 4 MV FFF BEAM FOR CLINICAL APPLICATION

Isabelle St-Martin[1], Ermias Gete[2], Carrie-Lynne Swift[2], Cheryl Duzenli[1,2]
[1]*University of British Columbia, Vancouver, BC*
[2]*British Columbia Cancer, Vancouver, BC*

Purpose: The purpose of this research is to characterize a 4 MV flattening filter free (FFF) photon beam with the goal of comparing it to other photon energies in current clinical use, and to explore the clinical applications of this new energy.

Materials and Methods: A 4 MV FFF photon beam was created on a Varian TrueBeam linear accelerator (linac) that was configured to deliver a 4 MV flat photon beam. Since Varian does not provide a 4 MV FFF beam to date, this energy was achieved by retracting the flattening filter during 4 MV beam delivery. Beam data was acquired using a scanning water tank. Measurements included percent depth doses (PDDs), inline, crossline, and diagonal profiles, tissue maximum ratios (TMRs), and relative dose factors (RDFs). PDDs and profiles were measured with a MicroDiamond detector for small field sizes (≤ 5 cm x 5 cm), and a CC13 ion chamber was used for all other field sizes. Surface doses were measured using an Advanced Markus chamber. TG-51 protocol was followed for reference dosimetry using a PTW 30013 ion chamber. Configuration of the 4 MV FFF beam in the Eclipse treatment planning system is being investigated.

Results: The 4 MV FFF beam was tuned to achieve a maximum dose rate of 700 cGy/min under reference conditions, which is 2.8 times the dose rate of the 4 MV flat beam. For the 10 cm x 10 cm open field, 4 MV FFF PDD parameters were d_{max} = 0.9 cm, PDD(d_{10cm}) = 59.9%, and PDD(d_{20cm}) = 31.0%. Comparing to clinical beams, 6 MV PDD parameters were d_{max} = 1.4 cm, PDD(d_{10cm}) = 66.4%, and PDD(d_{20cm}) = 38.0%; 6 MV FFF PDD parameters were d_{max} = 1.3 cm, PDD(d_{10cm}) = 63.3%, and PDD(d_{20cm}) = 34.5%. The beam flatness for the 10 cm x 10 cm open field was 3.2% at d_{max} and 4.1% at d_{10cm}. Comparing to a 6 MV FFF beam, flatness values at d_{max} and d_{10cm} were 4.6% and 6.2%, respectively. Open field transverse beam profiles for the FFF beam demonstrated little difference compared to the flat beam at small field sizes. For example, the FFF flatness was within 0.5% of the flat beam for the 3 cm x 3 cm field at a depth of 10 cm. A peak at the central beam

axis in the FFF beam became more pronounced with increasing field size, as demonstrated by the 10 cm x 10 cm values above.

Conclusions: A 4 MV FFF beam was successfully delivered and the beam properties were characterized for treatment planning. Applications for treating shallow tumours are under investigation.

31

PROSPECTIVE LONGITUDINAL ASSESSMENT OF QUALITY OF LIFE AFTER STEREOTACTIC ABLATIVE RADIOTHERAPY FOR OLIGOMETASTASES: ANALYSIS OF THE POPULATION-BASED SABR-5 PHASE II TRIAL

Ella Mae Cruz-Lim[1,2], Benjamin Mou, [1,2], Sarah Baker[1,3], Gregory Arbour[1], Kelsey Stefanyk[1], Will Jiang[1,3], Mitchell Liu[1,4], Alanah Bergman[1,4], Devin Schellenberg[1,3], Abraham Alexander[1,6], Tanya Berrang[1,6], Andrew Bang[1,4], Nick Chng[5], Quinn Matthews[5], Hannah Carolan[1,4], Fred Hsu[1,7], Stacy Miller[1,5], Siavash Atrchian[1,2], Elisa Chan[1,4], Clement Ho[1,3], Islam Mohamed[1,2], Angela Lin[1,2], Vicky Huang[3], Ante Mestrovic[6], Derek Hyde[1,2], Chad Lund[1,3], Howard Pai[1,6], Boris Valev[1,6], Shilo Lefresne[1,4], Scott Tyldesley[1,4], Robert Olson[1,5]
[1]University of British Columbia, Vancouver, BC
[2]British Columbia Cancer, Kelowna, BC
[3]British Columbia Cancer, Surrey, BC
[4]British Columbia Cancer, Vancouver, BC
[5]British Columbia Cancer, Prince George, BC
[6]British Columbia Cancer, Victoria, BC
[7]British Columbia Cancer, Abbotsford, BC

Purpose: To evaluate longitudinal patient-reported quality of life (QoL) in patients treated with stereotactic ablative radiotherapy (SABR) for oligometastases.

Materials and Methods: The SABR-5 trial was a population-based single-arm phase II study of SABR to up to five sites of oligometastases, conducted in six regional cancer centres in British Columbia from 2016 to 2020. Prospective QoL was measured using treatment site-specific QoL questionnaires at pre-treatment baseline and three, six, nine, 12, 15, 18, 21, 24, 30, and 36 months after treatment. Patients with bone metastases were assessed with the Brief Pain Inventory (BPI). Patients with liver, adrenal, and abdominopelvic lymph node metastases were assessed with the Functional Assessment of Chronic Illness Therapy-Abdominal Discomfort (FACIT-AD). Patients with lung and intrathoracic lymph node metastases were assessed with the Prospective Outcomes and Support Initiative (POSI) lung questionnaire. The two one-sided test procedure was used to assess equivalence between the worst QoL score and baseline score of individual patients. Mean QoL at all time points was used to determine the trajectory of QoL response after SABR. The proportion of patients with "stable," "improved," or "worsened" QoL was determined for all time points based on standard minimal clinically important differences (MCID; BPI worst pain = 2, BPI Functional Interference Score [FIS] = 0.5, FACIT-AD Trial Outcome Index [TOI]= 8, POSI= 3).

Results: All enrolled patients with baseline QoL assessment and at least one follow-up assessment were analyzed (n=135). On equivalence testing, patients' worst QoL scores were clinically different from baseline scores and met MCID (BPI worst pain mean difference: 1.8, 90% CI [1.19 to 2.42]; BPI FIS mean difference: 1.68, 90% CI [1.15 to 2.21]; FACIT-AD TOI mean difference: -8.76, 90% CI [-11.29 to -6.24]; POSI mean difference: -4.61, 90% CI [-6.09 to -3.14]). However, the mean FIS transiently worsened at nine, 18 and 21 months but eventually returned to stable levels. The mean FACIT and POSI scores also worsened at 36 months, albeit with a limited number of responses (n=4 and 8, respectively). The majority of patients reported stable QoL at all time points (range: BPI worst pain 71-82%, BPI FIS 45-78%, FACIT-AD TOI 50-100%, POSI 25-73%). Clinically significant stability, worsening, and improvement were seen in 70%/13%/18% of patients at three months, 53%/28%/19% at 18 months and 63%/25%/13% at 36 months.

Conclusions: SABR in the oligometastatic setting can lead to transient decreases in QoL. However, most patients experienced stable QoL relative to pre-treatment levels on long-term follow-up. Further studies are needed to characterize patients at greatest risk for decreased QoL.

32

RATE OF PACHYMENINGEAL FAILURE FOLLOWING ADJUVANT WBRT VERSUS SRS IN PATIENTS WITH BRAIN METASTASES

Enrique Gutierrez Valencia[1], Aristotelis Kalyvas[2], Kaiyun Yang[2], Ruth Lau[2], Benazir Khan[1], Barbara-Ann Millar[1], Normand Laperriere[1], Tatiana Conrad[1], Alejandro Berlin[1], Jessica Weiss[1], Xuan Li[1], Gelareh Zadeh[2], Mark Bernstein[2], Paul Kongkham[2], David B. Shultz[1]
[1]Princess Margaret Cancer Centre, Toronto, ON
[2]University of Toronto, Toronto, ON

Purpose: Stereotactic radiosurgery (SRS) has supplanted whole brain radiotherapy (WBRT) as standard-of-care adjuvant treatment following surgery for brain metastasis (BrM). Concomitant with the adoption of adjuvant SRS, a new pattern of failure termed "Pachymeningeal failure" (PMF) has emerged.

Materials and Methods: A prospective registry of 279 BrM patients; 145 and 134 were treated adjuvantly with WBRT and SRS, respectively. The Cox proportional hazards model was used to identify variables correlating to outcomes. Outcomes were calculated using the cumulative incidence (CI) method. Univariate (UVA) and multivariate analyses (MVA) were done to identify factors associated with PMF.

Results: CI of PMF was 2% and 16% at 12 months, and 2% and 20% at 24 months for WRBT and SRS, respectively (p<0.001). The CI of classic leptomeningeal disease (LMD) was 3% and 4% at 12 months, and 6% and 6% at 24 months for WBRT and SRS, respectively (P=0.862). On UVA, adjuvant SRS [HR 8.46 (2.98-23.97) (P<0.001)]; Preoperative dural contact (PDC) [HR 4.40 (1.36-14.23) (P<0.013)]; and GPA score [HR 1.66 (1.12-2.46) (P<0.012)]; were associated with PMF risk. On MVA, adjuvant SRS [HR 8.14 (2.54-26.05) (P<0.001)] and PDC [HR 3.70 (1.14- 12.01) (P<0.029)] remained associated with PMF.

Conclusions: Combined with the observations that PDC is a consistent risk factor and PMF is specific to the adjuvant setting, and assuming that the reduced incidence of PMF associated with WBRT results from comprehensive pachymeningeal radiation coverage, strategies that can be combined with SRS to reduce surgical seeding or provide improved pachymeningeal sterilization should be considered.

33

EFFICACY OF ULTRA HYPOFRATIONED RADIOTHERAPY COMBINED WITH HDR BRACHYTHERAPY

Ingrid Sidibé, Marie-Michèle Beaudry, Damien Carignan, Marie-Anne Froment, William Foster, Eric Vigneault, Sindy Magnan, Sylviane Aubin, Janelle Morrier, Eric Poulin, Frédéric Lacroix, Marie-Claude Lavallée, Luc Beaulieu, André-Guy Martin
CHU de Québec-Université Laval, Quebec City, QC

Purpose: To evaluate the biochemical cure proportion at four years or more (defined by PSA<0.2ng/ml) and efficacy of ultra hypofractionated radiotherapy (UHF) combined with high dose rate (HDR) brachytherapy boost (BB) in comparison to a

moderately hypofractionated (MHF) regimen, in patients treated for intermediate risk prostate cancer according to National Comprehensive Cancer Network (NCCN) guidelines.

Materials and Methods: In this prospective single institution study, 28 patients with intermediate risk prostate cancer were recruited to the experimental treatment of 25 Gy in 5 fractions using image guided radiation therapy (IGRT) plus a 15 Gy HDR BB. They were compared to two historical control groups, treated with either 36 Gy in 12 fractions or 37.5 Gy in 15 fractions with an identical HDR BB. The control groups included 151 and 311 patients respectively. Patients in the experimental cohort for UHF treatment regimen were enrolled between July 2015 and November 2016. Follow up visits and PSA testing were scheduled six weeks after the implant and every four months for the first year, then every six months for years 2 to 5 and yearly thereafter. The biochemical cure after brachytherapy (PSA <0.2ng/ml) > 4 years was defined according to the criteria defined by Crook et al [1], based on biochemical failure after radical prostatectomy. Biochemical relapse-free survival (bRFS) according to the Phoenix definition (PSA> nadir+2ng/ml) was also reported

Results: Of the 28 patients recruited, four died free of prostate cancer. At the time of analysis, median follow up was 81 months for the 25 Gy group, 47 months for the 36 Gy group and 60 months for the 37.5 Gy group. 85.7%, 78.8% and 67.8% of patients had a PSA <= 0.2ng/ml after 4 years in the UHF and both MHF groups, respectively. This difference was statistically significant (Chi-Square p-value = 0.012). The ISUP grade was not statistically different between the three groups p=0.64. However, in the 36 Gy group more patients with a PSA > 0.2ng/ml at four years had received short term androgen deprivation therapy (STADT) (p=0.0056). There was no siginificant relation between total dose of radiotherapy, ISUP and STADT and a PSA level > 0.2ng/ml at 4 years (p=0.74, p=0.65 and p=0.12 respectively). Estimated bRFS at 76 months was 90.9% for the UHF group, 97.3% for the 36 Gy arm and 88.5% for the 37.5 Gy arm. The difference was statistically significant between the 36 Gy group and 37.5 Gy group (p=0.017) but no difference was found between UHF and both MHF group (p=0.49 and 0.166 respectively). There was no statistically significant difference in overall survival (OS) between the three groups at 76 months.

Conclusions: BRFS and OS are similar between UHF and MHF. Our results also show that UHF might be associated with an improved biochemical cure rate suggested by PSA<0.2ng/ml after four years.

Reference:

[1] Crook JM, Tang C, Thames H, Blanchard P, Sanders J, Ciezki J, et al. A biochemical definition of cure after brachytherapy for prostate cancer. Radiother Oncol 2020;149:64–9. https://doi.org/10.1016/j.radonc.2020.04.038

34

TESTOSTERONE RECOVERY FOLLOWING ANDROGEN SUPPRESSION AND PROSTATE RADIOTHERAPY (TRANSPORT) - UPDATED ANALYSES FROM THE MARCAP CONSORTIUM

Wee Loon Ong[1,2], Holly Wilhalme[3], Jeremy Millar[4,5], Allison Steigler[6], James Denham[6], David Joseph[7], Soumyajit Roy[8], Shawn Malone[9], Nicholas Nickols[3], Matthew Rettig[3], Luca Valle[3], Michael Steinberg[3], Yilun Sun[10,11], Nicholas Zaorsky[10,11], Daniel Spratt[10,11], Luis Souhami[12], Nathalie Carrier[13], Abdenour Nabid[13], Amar U. Kishan[3]

[1]*University of Toronto, Toronto, ON*
[2]*Sunnybrook-Odette Cancer Centre, Toronto, ON*
[3]*University of California Los Angeles, CA*
[4]*Alfred Health, Melbourne, AU*
[5]*Monash University, Melbourne, AU*
[6]*University of Newcastle, Newcastle, AU*
[7]*University of Western Australia, Perth, AU*
[8]*Rush University Medical Center, Chicago, IL*
[9]*The Ottawa Hospital, Ottawa, ON*
[10]*University Hospitals Seidman Cancer Center, Cleveland, OH*
[11]*Case Western Reserve University, Cleveland, OH*
[12]*McGill University Health Centre, Montréal, QC*
[13]*Centre hospitalier Universitaire de Sherbrooke, Sherbrooke, QC*

Purpose: Time to testosterone recovery (TR) following androgen deprivation therapy (ADT) and radiotherapy for prostate cancer varies following cessation of ADT. We aimed to quantify the association between time to TR and duration of ADT and patient age.

Materials and Methods: We identified prospective randomized trials of prostate radiotherapy and ADT in the Meta-Analysis of Randomized trials in Cancer of the Prostate (MARCAP) consortium for which prospectively collected serial testosterone values were available. The time to non-castrate TR (NCTR) (>1.7ng/mL), non-hypogonadal TR (NHTR) (>8.0ng/mL) and full TR (FTR) (>10.5ng/mL) were estimated from the end date of prescribed ADT using the Kaplan Meier method. Cox regression was used to evaluate the differences in time to TR for men aged <65 years and ≥65 years for each duration of ADT. Interaction effects between ADT duration and patient age on TR were evaluated.

Results: 2,628 men from five trials (TROG 9601, TROG 0304, PCSIII, PCSIV, and Ottawa-01) met the inclusion criteria for analysis. Of these, 236, 1485, 731, and 176 men had three-, six-, 18-, and 36-months of ADT respectively. 1,502 (57%) men had baseline (pre-ADT) testosterone data available, of which 99% (1494/1502) had non-castrate testosterone (>1.7ng/mL), and 78% (1178/1502) had normal testosterone (>10.5ng/mL) at baseline. At last follow-up, there were 96% (2522/2628), 77% (2035/2628) and 65% (1700/2628) of men who had NCTR, NHTR and FTR respectively. The median time (range) to NCTR was 1.9 (0.2-60), 6.2 (0.0-92), 6.3 (0.0-92), and 15.7 (0.1-75) months for men who had three-, six-, 18- and 36-months of ADT, respectively. The median time (range) to NHTR was 2.5 (0.4-73), 11.2 (0.1-93), 17.7 (0.2-92), and 53.4 (5.3-76) months for men who had three-, six-, 18- and 36-months of ADT, respectively. The median time (range) to FTR was 5.8 (0.4-72), 16.7 (0.3-95), and 26.0 (0.2-90) for men who had three-, six-, and 18-months of ADT, respectively, while the median time to FTR was not reached in men who had 36-months of ADT. In men who had six months of ADT, men aged ≥65 years were 35% (95%CI=26-43%) less likely to have FTR compared to men aged <65 years, while for those who had 18-months of ADT, men aged ≥ 65 years were 52% (95%CI=41-60%) less likely to have FTR compared to men aged < 65 years. There was no statistically significant interaction between the effect of ADT duration and age on the time to FTR (interaction p=0.07 for the entire cohort).

Conclusions: In this updated individual patient-data meta-analysis of prospectively collected serial testosterone data from five randomized trials, substantial delay in FTR in men who had longer duration of ADT was observed, consistent with prior analyses. Approximately one in three men did not have FTR, which may have life-long impacts on their quality of life.

35

OUTCOMES FOLLOWING ALTERED FRACTIONATED RADIOTHERAPY ALONE IN PATIENTS WITH TNM-7 STAGE III/IV HEAD AND NECK SQUAMOUS CELL CARCINOMA (HNSCC)

Marc Vincent Barcelona[1,2], Shao Hui Huang[1,2], Jie Su[2], Li Tong[1,2], Scott Bratman[1,2], John Cho[1,2], Ezra Hahn[1,2], Andrew Hope[1,2], Ali Hosni Abdalaty[1,2], John Kim[1,2], Andrew McPartlin[1,2], Brian O'Sullivan[1,2], Jolie Ringash[1,2], Lillian Siu[1,2], Anna Spreafico[1,2], Lawson Eng[1,2], Christopher MKL Yao[1,2], Wei Xu[1,2], John

Waldron[1,2], Chiaojung Jillian Tsai[1,2]
[1]*University of Toronto, Toronto, ON*
[2]*Princess Margaret Cancer Centre, Toronto, ON*

Purpose: This study was undertaken to determine outcomes and prognostic factors of definitive intensity-modulated radiotherapy (IMRT) alone for patients with TNM-7 Stage III/IV HNSCC who did not receive concurrent chemotherapy.

Materials and Methods: We evaluated TNM-7 Stage III/IV HNSCC patients treated with definitive IMRT alone in our institution from 2004-2019. Patients were reclassified according to TNM-8 staging. Stage II HPV+ oropharyngeal cancers (OPC) were subdivided into T1-2N2 and T3N0-2 for analysis. The rationale for chemotherapy omission was obtained retrospectively from clinical documentation. Recurrence-free survival (RFS) and overall survival (OS) were estimated, stratified by HPV status (determined by p16 staining, sometimes supplemented by HPV DNA testing). Multivariable analysis (MVA) identified prognostic factors for RFS and OS, taking into account stage and IMRT regimen. Age, performance status, and smoking were also examined for OS.

Results: A total of 1,083 patients were included (460 HPV+ and 623 HPV-). Reasons for omission of chemotherapy included: age >70 years or frailty (n=551, 51%), cisplatin contraindication (n=241, 22%), patient refusal (n=106, 10%), and clinician's decision (n=185, 17%). Median age was 67 years for HPV+ and 70 years for HPV- cohorts. IMRT mostly utilized altered fractionation regimens (n=1016, 94%): moderately accelerated (70 Gy/35 fractions [f]/6 weeks [w], 55%), hypofractionated (60 Gy/25f/5w, 14%), and hyperfractionated-accelerated (64 Gy/40f/4w, 25%). Median follow-up was five years. Five-year RFS and OS were 89%/86%/76%/52% and 83%/80%/64%/33% for HPV+ TNM-8 Stage I/T1-2N2/T3N0-N2/III were and 58%/52%/39% and 47%/27%/13% for HPV- TNM-8 stage III/IVA/IVB, respectively (all p<0.01). MVA confirmed that HPV+ T3N0-2 subset within Stage II and Stage III had lower RFS and OS while T1-2N2 did not differ versus Stage I: RFS (T1-2N2/T3N0-N2/III versus Stage I): hazard ratio [HR] 1.13 (p=.81)/1.88 (p=.04)/5.98 (p<.01); OS 1.39 (p=.40)/2.22 (p<.01)/4.09 (p<.01). MVA also showed that HPV- Stage IVA and IVB (versus Stage III) carried worse RFS versus Stage III: RFS (Stage IVA/IVB versus Stage III: HR 1.31 (p<.04)/2.25 (p<.01); and worse OS: 1.69 (p<.01)/2.62 (p<.01). Moderately accelerated IMRT patients had better OS compared to standard fractionation (70 Gy/35f/7w) for both HPV+ (HR 0.44, p<.01) and HPV- (HR 0.46, p<0.01) cohorts.

Conclusions: Despite the retrospective nature and inherent selection bias, this large single institutional study shows that altered fractionated IMRT alone is an acceptable alternative for elderly, frail or cisplatin ineligible patients with HPV+ Stage I/IIA (T1-2N2) OPC. Patients with HPV+ T3N0-2/Stage III OPC and HPV-Stage III/IV HNSCC have worse outcomes and may benefit from alternative strategies.

36

DAWN OF STAGING FOR HEAD AND NECK SOFT TISSUE SARCOMA: VALIDATION OF THE NOVEL 8TH EDITION AJCC T CLASSIFICATION AND PROPOSED STAGE GROUPINGS

Rohan Salunkhe[1], Shao Hui Huang[1], Brian O`Sullivan[1], Susie Su[1], Wei Xu[1], Ali Hosni[1], John Waldron[1], Jonathan Irish[1], John deAlmeida[1], Ian Witterick[1], Eric Monteiro[1], Ralph Gilbert[1], Albiruni Razak[1], Lingxin Zhang[2], Dale Brown[1], David Goldstein[1], Patrick Gullane[1], Li Tong[1], Ezra Hahn[1]
[1]*Princess Margaret Cancer Centre, Toronto, ON*
[2]*Mount Sinai Hospital, Toronto, ON*

Purpose: After decades of stagnation, the 8th edition TNM (TNM8) introduced a new T classification for head and neck (HN) soft tissue sarcomas (STS). New size cutoffs of 2 and 4 cm define T1-3, and a novel T4 category is defined by local invasion of adjoining structures. These size cutoffs had been chosen arbitrarily to advance data collection in this unique disease site since literature showed approximately 70% of HN STS did not reach the previous size threshold (5 cm) for the existing T1 category. The definition of the TNM8 T categories also align with mucosal HN cancers. No stage grouping for HN STS was defined since this new classification required more data collection to derive stage groups. This study aims to validate the TNM8 T classification and to propose stage groupings.

Materials and Methods: Clinical data of all adult (>16 years) HN STS patients treated from 1988 – 2019 with curative intent in our tertiary cancer centre were retrieved from a prospective database, and supplemented with chart review. As per TNM8, cutaneous angiosarcoma, embryonal and alveolar rhabdomyosarcoma, Kaposi sarcoma, and dermatofibrosarcoma protuberans were excluded due to their different behavior. Multivariate analysis (MVA) identified prognostic factors for overall survival (OS). Adjusted hazard ratios (AHR) and recursive partitioning analysis (RPA) were used to derive stage groupings. Stage grouping performance for OS was assessed and also compared against the existing TNM8 groups for non-HN STS.

Results: A total of 221 patients (N1: 2; M1: 2) were included. Of the 219 M0 patients, 63% were males; median tumour size was 3.0 cm (range: 0.3-14.0); the proportion of TNM8 T1-T4 were 35%, 34%, 26%, and 5%, respectively. Median follow up was 5.9 years. Five-year OS was 79%. MVA confirmed the prognostic value of T category (T4 HR 7.73, 95% CI 3.62-16.5) and Grade (G2/3 versus G1 HR 3.7, 95% CI 1.82-7.53), in addition to age (HR 1.03, 95% CI 1.01-1.04) (all p<0.001) for OS. AHR model derived T1-3_Grade 1 as Stage 1; T1-3_Grade 2/3 as Stage II; and T4_any Grade or any T_N1 as Stage III (Table 1); the corresponding five-year OS was 93%, 73%, and 38%, respectively. Both patients with M1 died within 1.5 years after diagnosis and M1 disease was designated Stage IV. The AHR-grouping outperformed the RPA and non-HN TNM8 stage grouping for hazard consistency, hazard discrimination, percent variance explained, hazard difference, and sample size balance.

Conclusions: The novel T4 category introduced in TNM8 is associated with a >7 fold increased risk of death. Grade continues to be a critical prognostic factor in HN STS. The TNM8 HN STS T classifications have been validated, and the proposed new stage groupings with TNM8 incorporating grade have excellent performance for OS.

Table 1. Proposed Stage Grouping

T	N	M	Grade	Stage
T1, T2, T3	N0	M0	G1	I
T1, T2, T3	N0	M0	G2, G3	II
T4	N0	M0	Any G	III
Any T	N1	M0	Any G	III
Any T	Any N	M1	Any G	IV

37

DIRECT VALIDATION OF ACUROS XB FOR DOSE-TO-MEDIUM CALCULATIONS IN BONE-SURROGATE USING CALORIMETRY MEASUREMENTS

Stanislaw Szpala[1], James Renaud[2], Bryan Muir[2], Alexandra Bourgouin[2], Kirpal Kohli[1], Malcolm McEwen[2]
[1]*British Columbia Cancer, Surrey, BC*
[2]*National Research Council of Canada, Ottawa, ON*

Purpose: Acuros XB (AXB) from Varian is a treatment planning system intended to calculate dose distributions rivaling the accuracy

of Monte Carlo simulations, but with shorter computational time. The accuracy of AXB has been extensively studied for calculations in water, but little experimental validation has been reported for calculations in higher density media such as bone. This is in part due to unavailability of medium-specific corrections for commonly used detectors (ionization chambers, radiochromic film) to compensate for changes to the spectra of photons and secondary electrons. A calorimeter, in contrast, can be used to measure the absolute dose directly in the medium of interest. The requirement for a medium-specific correction can be eliminated by matching the material the calorimeter and the phantom are constructed from.

Materials and Methods: There has been no reports of a calorimeter made of bone-like material. Aluminum has been selected for the calorimeter in this work as a close to bone material (albeit higher density and atomic number) that is also available for calculations in AXB (only a selected number of materials are available in AXB). Great care was taken to match the experimental and calculated geometries, taking into account accurate measurements based on a CT scan. The sensitivity of the comparison was investigated by varying the energy (6X and 10X) and the radial beam profile (WFF and FFF) of the delivered and simulated beam (Varian TrueBeam). The structures mimicking the calorimeter were contoured in Eclipse to facilitate dose calculation using AXB. Both dose-to-medium (DTM) and dose to water (DTW) were calculated.

Results: Calculations of the DTM using AXB agreed with the DTM measured directly using the calorimeter within -3.5%, -3.5%, -3.2% and -2.8% for the 6X, 10X, 6FFF and 10FFF beams, respectively. While the agreement is fair from clinical perspective, it is above the uncertainty of the measurement of about 0.5%. The discrepancy is believed to be due to limited accuracy of AXB calculations in media more dense than water. Use of DTW instead would have overestimated the calculated dose by almost 40%.

Conclusions: For the first time the DTM calculated with AXB in aluminum, a bone surrogate, was experimentally validated directly without applying computed medium corrections. The comparison differences are viewed as an upper limit on the accuracy of AXB in clinically relevant situations in the presence of bone. These results also confirm previous work that using DTW would lead to a significant dosimetric error in estimating the dose deposited in bone.

38

PLASTIC SCINTILLATOR DOSIMETRY OF ULTRAHIGH DOSE-RATE 200 MEV ELECTRONS AT CLEAR

Alexander Hart[1], Cloé Giguère[2], Nolan Esplen[1], Joseph Bateman[3], Pierre Korysko[3], Wilfrid Farabolini[4], Roberto Corsini[4], Manjit Dosanjh[3], Luc Beaulieu[2], Magdalena Bazalova-Carter[1]
[1]University of Victoria, Victoria, BC
[2]Université Laval, Quebec City, QC
[3]University of Oxford, Geneva, CH
[4]CERN, Geneva, CH

Purpose: To test the ability of plastic scintillator dosimeters (PSDs) optically coupled to a hyperspectral dosimetry system to measure dose delivered by very high energy electron (VHEE) beams at the CERN Linear Electron Accelerator for Research (CLEAR). VHEE beams with energies greater than 60 MeV may be a good candidate for FLASH radiotherapy due to their favourable dose distributions and ability to achieve ultrahigh dose-rates (UHDR). We investigated the ability of PSDs to respond linearly to dose under UHDR VHEE conditions, up to 2.4× 10^9 Gy/s, and examined the radiation hardness of two scintillator compositions.

Materials and Methods: PSDs connected to a Hyperscint RP-100 spectrometer system (Medscint, Quebec) were used to measure 200 MeV electrons. Two scintillator compositions were investigated: the polystyrene-based BCF-12 and a proprietary polyvinyltoluene-based Medscint material. Output linearity measurements were conducted by scaling the dose/train between ~4 and 160 Gy, (up to 2.4× 10^9 Gy/s for a 66 ns train/pulse). The radiation hardness of the probes was assessed by tracking the delivered dose to each of the probes during all measurements up to total doses of 26.2 and 13.8 kGy for the BCF-12 and Medscint probes. Output linearity measurements were conducted periodically to monitor changes in the performance of the probes due to radiation damage.

Results: The BCF-12 probe exhibited linear light output with dose per train from 4.9 to 125.2 Gy, at dose rates up to 1.9× 10^9 Gy/s. At higher doses/train the probe failed to respond linearly, eventually emitting even less scintillation light than at lower doses/train. The Medscint probe saturated at lower doses, showing linearity from 3.9 to 59.5 Gy per train, and dose rates up to 9.0× 10^8 Gy/s. Review of the spectra before and after saturation allows elimination of the spectrometer as the limiting factor. While output linearity was retained (R^2>0.999) after delivering 26.2 and 13.8 kGy to the BCF-12 and Medscint probes, respectively, the light output was reduced in both cases.

Conclusions: PSDs can be used for real-time dosimetry of UHDR VHEE beams. In this work we have demonstrated that the polystyrene based BCF-12 PSD has a linear response with dose per pulse up to 125.2 Gy at a dose rate of 1.9× 10^9 Gy/s. Further, PSDs retain output linearity after receiving damaging doses of radiation, allowing them to be recalibrated for further use.

39

EVALUATION OF ORGAN ABSORBED DOSES IN INTRAOPERATIVE RADIOTHERAPY OF GLIOBLASTOMA

David Santiago Ayala Alvarez[1], Peter G F Watson[2], Marija Popovic[2], Veng Jean Heng[1], Michael D C Evans[2], Valerie Panet-Raymond[2], Jan Seuntjens[3]
[1]McGill University, Montréal, QC
[2]McGill University Health Centre, Montréal, QC
[3]University Health Network, Toronto, ON

Purpose: The INTRAGO clinical trial assesses survival in glioblastoma patients treated with intraoperative radiotherapy (IORT) using the INTRABEAM. Treatment planning for INTRABEAM relies on vendor-provided in-water depth dose curves obtained according to the TARGIT dosimetry protocol. However, recent studies have shown discrepancies between the estimated TARGIT dose from the delivered dose. This work evaluates the effect of the choice of INTRABEAM dosimetry formalism on the doses to organs at risk (OARs) in INTRAGO patients.

Materials and Methods: A treatment planning framework for INTRABEAM was developed to retrospectively calculate the IORT dose in eight INTRAGO patients. These patients received an IORT prescription dose of 20 to 30 Gy to the surface of the INTRABEAM applicator, in addition to EBRT. The OAR doses from IORT were obtained from: (a) the TARGIT method; (b) the V4.0 method recommended by the manufacturer; (c) the C_Q method, which uses an ionization chamber Monte Carlo (MC) calculated factor; (d) MC dose-to-water; and (e) MC dose-to-tissue. The combined OAR doses from IORT and EBRT were determined by converting IORT dose to EQD2.

Results: According to the TARGIT method, the OAR dose constraints were respected in all cases. However, the other formalisms estimated a higher mean dose to OARs and revealed one case where the constraint for brainstem was exceeded. The addition of the EBRT and TARGIT IORT doses resulted in 10 cases of OARs exceeding the dose constraints. The more accurate MC calculation of dose-to-tissue led to the highest dosimetric differences, with

three, three, two, two, two, and two cases (out of 8) exceeding the dose constraint to the brainstem, optic chiasm, optic nerves, and lenses, respectively. Moreover, the mean cumulative dose to brainstem exceeded its constraint of 66 Gy with the MC to tissue method, which was not evident with the current INTRAGO clinical practice.

Conclusions: The current clinical approach of calculating the IORT dose with the TARGIT method may considerably underestimate doses to nearby OARs. In practice, OAR dose constraints may have been exceeded, as revealed by more accurate methods.

40

PROTON THERAPY MEDIATES DOSE REDUCTIONS TO CRITICAL BRAIN ORGANS AT RISK WHICH ARE ASSOCIATED WITH BETTER COGNITION IN CHILDREN WITH MEDULLOBLASTOMA

Julianna Sienna[1], Lisa Kahalley[2], Donald Mabbott[3], David Grosshans[4], Anna Theresa Santiago[5], Arnold Paulino[4], Gohar Shahwar Manzar[4], Hitesh Dama[5], Murali Chintagumpala[6], Mehmet Fatih Okcu[6], William Whitehead[6], Vijay Ramaswamy[7], Normand Laperriere[5], Thomas Merchant[8], Tim Craig[5], Derek Tsang[5]
[1]McMaster University, Hamilton, ON
[2]Baylor College of Medicine, Houston, TX
[3]University of Toronto, Toronto, ON
[4]The University of Texas MD Anderson Cancer Center, Houston, TX
[5]Princess Margaret Cancer Centre, Toronto, ON
[6]Texas Children's Cancer Center, Houston, TX
[7]Hospital for Sick Children, Toronto, ON
[8]St. Jude Children's Research Hospital, Memphis, TN

Purpose: Our group previously demonstrated an improvement in cognition among children with medulloblastoma treated with proton therapy, as compared to photon therapy (https://doi.org/10.1200/jco.19.01706). However, the reason for this cognitive improvement was unclear. In this study, our aim was to determine whether dose to critical brain structures acted as a mediator of improved cognition in patients treated with proton therapy.

Materials and Methods: In this retrospective study, a cohort of 75 children with medulloblastoma from two institutions was assembled (39 photon, 36 proton). Included patients were treated with similar radiation and cognitive follow-up protocols. Study endpoints were verbal comprehension (VCI), perceptual reasoning (PRI), working memory (WMI), processing speed (PSI) indices and full scale IQ (FSIQ). Brain structures were segmented and dose comparisons by RT modality were compared using independent t-tests. Linear mixed effects models with random intercepts were created to evaluate cognitive endpoints using R version 4.2.2.

Results: Median follow-up from RT to last cognitive assessment was 4.8 years. Total dose, including RT boost, was slightly lower in the proton cohort than the photon cohort (mean, 54.6 Gy versus 56.1 Gy, respectively, $p<0.001$). Eleven children (31%) treated with proton therapy received 36 Gy CSI, while six children (15%) treated with photon therapy received 36 Gy CSI ($p=0.07$). Children treated with proton therapy had reduced composite doses to brain structures as compared to photon therapy, including the brain (mean $p=0.03$, D40 $p=0.007$), left and right temporal lobes (mean and D50, $p<0.001$ for both), and left and right hippocampi (mean, $p<0.001$ for both). Mean dose reductions with proton therapy ranged from 2.7 Gy (mean brain dose) to 11.2 Gy (mean right hippcampus). After adjustment for age at RT and posterior fossa syndrome, higher whole brain mean dose and time since RT were associated with greater decrease in VCI ($p=0.033$), higher left temporal D50 and time since RT with greater decrease in PRI ($p=0.031$), higher whole brain D40 and time since RT with greater decrease in PSI ($p<0.001$) and FSIQ ($p=0.030$).

Conclusions: Our study demonstrates that proton therapy for patients with medulloblastoma reduces dose to normal brain tissues, which is associated with better intellectual outcomes. Children with medulloblastoma who undergo RT should be treated with proton therapy, if available.

41

CALORIMETRIC VERIFICATION OF ELECTRON ULTRA-HIGH DOSE RATE (E-FLASH) DOSIMETRY ON A TRUEBEAM LINAC

Cheryl Duzenli[1], Tania Karan[2], James Renaud[3], Bryan Muir[3], M. Peter Petric[2], Don TA[1], Claudia Mendez[4], Malcolm McEwen[3]
[1]University of British Columbia, Vancouver, BC
[2]British Columbia Cancer, Vancouver, BC
[3]National Research Council of Canada, Ottawa, ON
[4]British Columbia Cancer, Abbotsford, BC

Purpose: To establish absolute dose per pulse and average dose rate in an ultra-high dose rate (UHDR) electron beam using calorimetry measurements on a reversibly modified medical linac. Calorimetry provides an absolute reference dose for cross calibration of a range of other dosimeters and does not suffer from saturation effects which limit ionization methods.

Materials and Methods: A portable aluminum calorimeter was positioned on a Varian TrueBeam linac couch at SSD 100 cm under a 10 cm x10 cm electron cone with jaws set to 20 cm x 20 cm. The linac delivered an electron beam following retraction of the x-ray target, flattening filter and monitor unit chamber and addition of a scattering foil, using the 10 MV beam current. An Arduino pulse counting circuit using a plastic scintillator positioned outside the primary beam enabled 5 to 100 pulses to be systematically and reproducibility delivered. Linearity of response with increasing pulse count and pulse repetition rates of 180 s^{-1} and 360 s^{-1} were examined. The gun pulse width was 4.5 μs. A CC01 ion chamber at depth 2 cm in solid water phantom was irradiated under the same UHDR conditions to confirm the dose response relative to its response under standard dose rate conditions (600 cGy/min). The dose response of EBT3™ radiochromic film and optically stimulated luminescent dosimeters (OSLDS) under UHDR conditions were also assessed relative to their standard dose rate response.

Results: Using a Monte Carlo generated dose conversion factor to account for the geometry and materials in the calorimeter, dose per pulse of 0.152 ± 0.002 Gy and average dose rate of 59.1 ±0.5 Gy/s were established for a 10 pulse beam delivery at water equivalent d_{max} of 2 cm. The CC01 ion chamber dose response under this UHDR condition agreed to within 1.5 % of it's dose response under standard dose rate conditions. Film and OSLD responses at UHDR agreed with their standard dose rate response within 2%.

Conclusions: A portable aluminum calorimeter provides a feasible method to establish absolute dose rate in eFLASH conditions on a reversibly modified standard medical linac. Absolute dose rate and dose per pulse calorimetric measurements confirm the relative dose response of the CC01 ionization chamber, radiochromic film and OSLD under UHDR conditions. Further refinement and testing of the calorimeter is ongoing.

42

RADIATION SURVEY OF A TRUEBEAM LINAC OPERATING IN ELECTRON FLASH-RT MODE

Andrew K. H. Robertson, Amy Frederick, Sheila MacMahon, M. Peter Petric
British Columbia Cancer, Vancouver, BC

Purpose: Recent studies indicating that ultra high dose rate radiotherapy (FLASH-RT) may improve normal tissue sparing

have increased interest in conducting pre-clinical FLASH-RT experiments. To support our institution's FLASH-RT research program, the modified operation of a TrueBeam linac is used to generate electron fields with FLASH-RT dose rates (>40 Gy/s). This work reports on the resulting radiation levels outside the linac vault and provides a comparison with dose rates observed during unmodified TrueBeam operation.

Materials and Methods: A TrueBeam linac located in a typical clinical vault was used for FLASH-RT experiments. The radiation shielding included a maze with a neutron door (0.95 cm steel, 0.95 cm lead, 5.1 cm borated polyethylene), and primary shielding of 46 cm steel and 102 cm concrete at the console area and 37 cm steel and 111 cm concrete at the building exterior. FLASH-RT dose rates were produced by running the linac in photon mode with a high repetition rate and with the target, flattening filter, and monitor unit chamber retracted from the beam and with the electron scattering foil inside the beam. This results in a high flux electron field capable of delivering a dose rate at depth of maximum dose (D_{max}') of 46.9 Gy/s and 25.4 Gy/s at isocentre in solid water for a 10 MeV and 15 MeV beams, respectively. During continuous 15 MeV FLASH-RT delivery, a radiation survey was conducted using a Victoreen 451P survey meter and a Berthold 6411 neutron meter. Dose rates were measured at multiple locations outside the vault with the linac gantry rotated towards the point of measurement and both with and without scattering material in the field. FLASH-RT survey measurements were compared with results acquired during continuous delivery of the highest energy 15 MV clinical photon beam (D_{max}' of 0.1 Gy/s at isocentre in solid water).

Results: Maximum observed gamma radiation dose rates during FLASH-RT (clinical beam) delivery were 10 (3.2) µSv/h at the vault door, 7.6 (0.8) µSv/h at the linac console, 5.6 (0.5) µSv/h through primary shielding adjacent to the vault door, 22 (2.5) µSv/h at a physics cable port in the shielding, and 27 (2.8) µSv/h through primary shielding on the building exterior. Background readings were below 0.1 µSv/h. Maximum observed neutron dose rates were 0.1 µSv/h above background (0.1 µSv/h) at the vault door during FLASH-RT delivery and background during clinical beam delivery. The high (>25 µSv/h) field measured outside the building during FLASH-RT resulted in the decision to restrict the gantry angle used in FLASH-RT experiments to 0º only.

Conclusions: While TrueBeam linacs are capable of producing radiation fields suitable for electron FLASH-RT experiments, the ability to operate in FLASH-RT mode while complying with radiation safety regulations may depend on the existing vault shielding design.

43

BRACHYTHERAPY-ON-CHIP: A MICROFLUIDIC SETUP FOR IN VITRO INTERROGATION OF HYPOXIC SPHEROIDS

Rodin Chermat[1,2], Elena Refet-Mollof[1,2], Jean-François Carrier[1,3], Philip Wong[1,4], Thomas Gervais[1,2], Yuji Kamio[3]
[1]*Centre de Recherche du Centre Hospitalier de l'Université de Montréal (crCHUM), Montréal, QC*
[2]*Polytechnique Montréal, Montréal, QC*
[3]*Centre Hospitalier de l'Université de Montréal, Montréal, QC*
[4]*Princess Margaret Cancer Centre, Toronto, ON*

Purpose: Despite evidence of its advantages in many cancers, brachytherapy (BT) remains clinically underused and understudied in the pre-clinical setting due to a lack of versatile RT-compatible in vitro tools that can emulate the tumour microenvironment and radiobiology of various cancers. Microfluidic devices use conventional cell culture methods in 3D-tumour models, are radiocompatible and can integrate radiobioassays. However, they are seldom used in pre-clinical BT research. This project engineered the first microfluidic tool for in vitro testing of BT, with applications in translational radiobiology.

Materials and Methods: PDMS microfluidic devices were engineered to grow and culture concentric rows of hypoxic spheroids, and to allow the insertion of a clinical iodine-125 BT seed at the centre of the device. FaDu (hypopharyngeal squamous cell carcinoma), SK-LMS-1 (leiomyosarcoma) and HCT116 (colorectal carcinoma) cell lines were selected for their clinical relevance and ability to form spheroids. Presence of hypoxia in spheroids was assessed by immunofluorescence (IF) staining for hypoxic protein Carbonic Anhydrase IX (CAIX). On-chip dose distribution was calculated using clinical TG-43 parameters and compared to EBT-XD Gafchromic film analysis. Target dose criteria was fixed at 8 Gy in the centre of the first row of spheroids. Treatment response was quantified by DNA damages (γH2AX IF, comet assay) and cell survival (clonogenic assay). Response of hypoxic and normoxic regions of spheroids will be compared in IF.

Results: Fifteen spheroids that are 750µm or larger can be cultured in our device, arranged as five rows of three spread from 1.5 mm to 7.5 mm away from a central iodine-125 seed. Forty-eight hours after cell seeding, hypoxic cores were observed in spheroids derived from FaDu (50 ± 4% of cross-section, N=3) and SK-LMS-1 (46 ± 4% of cross-section, N=3) cells, results are pending for HCT116. TG-43 formula predicts that the centre of each row receives 8 Gy, 2.6 Gy, 1.2 Gy, 0.7 Gy and 0.4 Gy respectively. Gafchromic film analysis confirms on-chip TG-43 calculated doses (N=5, R^2 = 0.999). Similarly, tail moment (a measure of DNA damages) from comet assays follows predicted dose trends (n>60, N=3). There was no statistical difference between 8 Gy BT and 8 Gy GammaCell (8 Gy BT versus 8 Gy GammaCell, p=0.8758), with a statistical difference between 8 Gy BT (8 Gy BT versus 2.6 Gy BT,1.2 Gy BT,0.7 Gy BT,0.4 Gy BT,0 Gy, p<0.0001), 2.6 Gy BT (2.6 Gy BT versus 1.2 Gy BT,0.7 Gy BT,0.4 Gy BT,0 Gy, p<0.05) or 8 Gy GammaCell (8 Gy GammaCell versus 2.6 Gy BT,1.2 Gy BT,0.7 Gy BT,0.4 Gy BT,0 Gy, p<0.0001) and other lower BT doses.

Conclusions: For the first time, brachytherapy can be easily integrated on-chip and its effects evaluated on relevant 3D-tumour models. Our system allows simultaneous quantification of BT efficacy on normoxic and hypoxic cells treated at various BT doses. On-chip combination of BT with antitumour drug will be explored in future work. We hope this device will serve as further proof of the potential of BT/RT-on-chip systems for better drug development, treatment planification and theranostics.

44

DOSIMETRIC PARAMETERS PREDICTIVE OF TREATMENT-RELATED TOXICITY IN HIGH DOSE-RATE BRACHYTHERAPY AS MONOTHERAPY FOR PROSTATE CANCER

Jiheon Song, Mark Corkum, Andrew Loblaw, Hans Chung, Chia-Lin Tseng, Patrick Cheung, Ewa Szumacher, Stanley Liu, William Chu, Melanie Davidson, Matt Wronski, Liying Zhang, Alexandre Mamedov, Gerard Morton
University of Toronto, Toronto, ON

Purpose: High dose-rate (HDR) brachytherapy as monotherapy is an effective treatment for patients with low- and intermediate-risk prostate cancer and is increasingly being offered as a 2-fraction protocol. There is a lack of consensus on the optimal dosimetric planning parameters to use, or whether there is any benefit summating dosimetric parameters from more than one implant. Our goal is to determine planning parameters associated with disease control, toxicity and health-related quality of life (HRQOL).

Materials and Methods: Data were collected on 83 patients with low- and intermediate-risk prostate cancer who received 2 fractions of 13.5 Gy HDR brachytherapy without androgen-deprivation

therapy as part of a randomized phase II clinical trial. An in-house deformable, registration algorithm was used to co-register and dose-summate the plans from both implants for each patient. Acute and late genitourinary (GU) and gastrointestinal (GI) toxicities were measured using Common Toxicity Criteria for Adverse Events (CTCAE) 4.0 and HRQOL was measured in urinary, bowel, sexual and hormonal domains using the expanded prostate cancer index composite (EPIC) scores. Treatment efficacy was assessed through PSA measurement and imaging with or without biopsy where indicated. Covariates included baseline clinical factors, disease characteristics and treatment dosimetric parameters. Cox proportional hazards was performed to evaluate covariates impact on treatment toxicity and efficacy, and logistic regression analysis evaluated covariates impact on HRQOL.

Results: Among the 83 patients, median prostate volume was 46.7cm3. Median summated planning target volume receiving 100% prescription dose (PTV V100%) was 97.4%, median PTV V150% 42.4% and median PTV V200% 15.5%. Median highest dose to the 1cm3 rectum (D1cc) was 66.9% of the prescription dose and median rectum V80% was 0.008cm3. Median urethral D1cc was 99.0% of the prescription dose, median urethral Dmax 121.7% and median urethral D10% 116.2%. Grade ≥2 GI toxicity was uncommon (3.7% acute and 8.5% late), but Grade ≥2 GU toxicity was reported in 73.2% (acute) and 46.3% (late) patients. Rectum D1cc and V80% were found to be significantly associated with Grade 2 or higher acute GI toxicity, while use of a-blocker at baseline was associated with Grade ≥2 acute GU toxicity. Similarly, use of a-blocker were associated with late Grade ≥2 GU toxicity, but with no dosimetric associations. No other variables were associated with treatment-related toxicities. Only rectum D1cc was significantly associated with changes in bowel EPIC scores. Dosimetric parameters did not predict disease recurrence. Estimated five-year biochemical disease-free survival was 93.9% and five-year cumulative incidence of local failure was 3.8%.

Conclusions: HDR monotherapy with 27 Gy delivered in two fractions in treatment of prostate cancer is well tolerated with high rates of disease control and minimal toxicity. Dose summation between two fractions of HDR brachytherapy is feasible, with rectal dose predicting acute GI toxicity. The lack of association between dose metrics and urinary toxicity raises the potential for further dose escalation.

45

HEALTH-RELATED QUALITY OF LIFE AFTER COMBINED EXTERNAL BEAM AND EITHER HIGH DOSE RATE (HDR) OR LOW DOSE RATE (LDR) BRACHYTHERAPY: DID THE RECTAL DOSE FROM THE LDR BRACHYTHERAPY MAKE A DIFFERENCE?

Felipe Castro-Canovas[1,2], Cynthia Araujo[1,2], Juanita Crook[1,2], Gregory Arbour[2], Deidre Batchelar[1,2], Nikitha Moideen[1,2], Michelle Hilts[1,2], Ross Halperin[1], David Kim[1], David Petrik[1], Jim Rose[1], Francois Bachand[1,2]
[1]*British Columbia Cancer, Kelowna, BC*
[2]*University of British Columbia, Vancouver, BC*

Purpose: The recently reported randomized Phase III trial comparing health related quality of life (HRQOL) after combined external beam radiation therapy (EBRT) and either HDR or LDR brachytherapy (BT) found a significant decline in the EPIC Bowel domain HRQOL score at 24- 48 months after treatment in the LDR arm of the trial. As all patients in the trial received the same EBRT dose, and HDR rectal dose was strictly controlled to be <9.5 Gy to 1cc of rectal wall (RD1cc), we investigated whether the variable rectal dose from the LDR component of treatment was related to the decline in Bowel HRQOL for these patients.

Materials and Methods: One hundred and ninety-five men with upper tier intermediate or high-risk prostate cancer were assigned by a random number generator to receive either an HDR (15 Gy, n=108) or LDR (110Gy, n=87) brachytherapy boost combined with 46Gy/23 fractions EBRT. All LDR patients had one month post implant quality assurance using CT-MRI fusion. The Expanded Prostate Cancer Composite (EPIC) questionnaire was used to evaluate HRQOL at baseline, q3 mo. for one year, q6mo for three year and then annually. A multivariate linear regression model was used to investigate the dose-response relationship between EPIC bowel domain score at 24- 48 months and RD1cc.

Results: With a median follow up of 48 months, the previous analysis confirmed the expected time course of acute bowel/ urinary symptoms, with LDR showing more prolonged decline in HRQOL bowel domain at three and six months, but equivalence to HDR by 12 months. HRQOL urinary domain remained equivalent from 12-60 months. The decline in the HRQOL bowel domain observed for LDR patients from 24-48 months was analyzed for the 79 patients with sufficient data. The mean baseline HRQOL bowel domain score was 92 and fell to 85 at 24-48 months. Mean RD1cc for the LDR patients was 82 Gy (SD 22 Gy). In terms of RV100 (rectal volume receiving 100% of prescribed dose), the rectal doses are within the recommended limit of < 1.3 cc at one month, with the mean RV100 being 0.4cc, (SD 0.5). In this range of rectal doses, a 20Gy increase in RD1cc, was associated with a non-significant 1.5-point decrease in EPIC HRQOL bowel domain score (p=0.21).

Conclusions: The rectal dose received by the LDR patients showed a non-significant dose-response with the EPIC Bowel domain HRQOL score. This confirms the accepted rectal dose constraints for LDR brachytherapy but does not explain the observed decline in bowel scores from 24-48 months.

46

PATTERNS OF RELAPSE AND BIOCHEMICAL CONTROL IN INTERMEDIATE RISK PROSTATE CANCER TREATED WITH HIGH DOSE RATE BRACHYTHERAPY (HDRB) MONOTHERAPY

Jayson Paragas[1], Luis Souhami[1], Simon Gauvin[1], Leticia Alvaredo[1], Richard Sioufi[2], Gabriela Stroian[1], Doris Marti[1], Marie Duclos[1]
[1]*McGill University, Montréal, QC*
[2]*Centre Hospitalier Anna Laberge, Chateauguay, QC*

Purpose: HDRB boost has been used with excellent results in low and intermediate risk prostate cancer (IRPC). The aim of this study is to report our experience with single fraction HDRB in selected patients with IRPC.

Materials and Methods: Eligible patients had a biopsy-proven IRPC, a prostate volume ≤ 60cc, clinical Stage T1-2, PSA < 20 ng/ml and grade group 1-3. We excluded patients with poor urinary function, previous TURP, and patients receiving hormonal therapy. All patients underwent outpatient monotherapy HDRB to a single dose of 21Gy delivered under spinal anesthesia and ultrasound guidance. The dose was prescribed as per the CCTG PR15 protocol. The PTV was the prostate with no added margin. Planning was performed using CT scan in all patients, and MRI in 51% of them.

Results: From January 2016 to November 2020, we treated 91 patients with IRPC. Median age was 74 years (range: 48-87). Thirty-nine patients (42.8%) had a favourable IRPC and 52 patients (57.2%), unfavourable. Pre-treatment median PSA was 7.2 ng/ml (range:0.59-18). Grade group was as follows: group 1, 15 patients, group 2, 65 patients and group 3, 11 patients. The median prostate volume was 36 cc. Acute genitourinary (GU) and gastrointestinal (GI) toxicities were 5.6 and 0%, respectively. With a median follow-up of 55 months (range: 21-72), median PSA nadir was 0.77 ng/ml (range: 0.08-5.47) and the median time to PSA nadir was 24 months (range: 4-56). Grade ≥ 2 late GU or GI toxicity was seen in 5.5 and 0%, respectively. Biochemical failure occurred

in 19 patients (20.8%). Of these, nine patients were favourable IRPC and 10 patients, unfavourable. MRI/PET PSMA and biopsy confirmed local recurrence/persistent disease in 14 patients. Loco-regional disease was seen in two and negative staging in three others. V100% was 95.1%. One of our GU radiologists, blinded to the outcome, contoured all potential recurrent sites. We reviewed dosimetric parameters in all patients with local recurrence. Dosimetric evaluation of the recurrent site showed that D98%, D90% and Dmean values were 21.6Gy, 23.7Gy and 30.6Gy, respectively. On multivariable analysis, pre-treatment PSA [HR 1.4(95% CI 1.34-1.73), p=0.02], group grade [HR 5.13(CI 1.14-23.1), p=0.033] and V100% [HR 0.85(CI 0.73-0.1),p =0.043] were statistically significant predictors of local relapse.

Conclusions: HDRB monotherapy delivering a dose of 21Gy in patients with IRPC is safe. However, despite adequate dose coverage, the local relapse was higher than expected. We do not recommend this approach as a routine treatment.

47

LONG-TERM DISEASE-FREE SURVIVAL AND HEALTH-RELATED QUALITY OF LIFE RESULTS OF HIGH-DOSE-RATE BRACHYTHERAPY AS MONOTHERAPY FOR LOW AND INTERMEDIATE-RISK PROSTATE CANCER TREATED IN A COMMUNITY CANCER CENTRE

Raphael Rezkallah[1], Pierre-Yves McLaughlin[1], Alain Haddad[2], Mathieu Pharand-Charbonneau[3], Debbie Wright[3], Marc Gaudet[2]
[1]McGill University, Montréal, QC
[2]University of Ottawa, Ottawa, ON
[3]Hôpital de Gatineau, Gatineau, QC

Purpose: To determine the long-term disease-free survival, long-term toxicity, and effect on health-related quality of life of a two-fraction regimen of high-dose-rate (HDR) prostate brachytherapy.

Materials and Methods: Patients with low- or intermediate-risk prostate cancer were treated with CT-planned HDR brachytherapy as monotherapy in two implants of 13.5 Gy spaced 7-14 days apart in one community cancer centre in a prospective study. Prostate-specific antigen (PSA), International Prostate Symptom Score (IPSS) and Expanded Prostate Index Composite (EPIC) questionnaires were evaluated at baseline, 1, 3, 6, 9, 12, 16, 20, 24, 30, 36, 48, 60 and 72 months after brachytherapy. Mortality and biochemical recurrence (Phoenix definition) were evaluated to determine disease-free survival at each of the intervals above. Proportion of patients in each IPSS category (mild = 0-7, moderate = 8-18, severe = 19+) was evaluated at each of the intervals above.

Results: Thirty patients were accrued to the study between 2014 and 2016. Median prostate-specific antigen was 8,7 (range 4.1-17.5). T stages were T1c = 65%, T2a = 21%, and T2b = 14%. Twenty-seven percent of patients had a Gleason score of 6 and 73% had a Gleason score of 7. 13% were in low-risk category and 87% in intermediate risk category. Median follow-up was 84 months. There were no deaths at 72 months after brachytherapy. Disease-free survival was 90% at 72 months after brachytherapy. IPSS categories at one, three, six, 12, 24, and 60 months were mild (43%, 48%, 60%, 75%, 57%, 79%), moderate (36%, 41%, 32%, 21%, 35%, 14%), and severe (21%, 10%, 8%, 4%, 9%, 7%), respectively.

Conclusions: This study serves as proof of concept that HDR monotherapy can be performed successfully with excellent long-term outcomes in a community cancer centre. The long-term disease-free survival rate and the health-related quality of life appear acceptable as compared to other treatment modalities. Further study is ongoing with regard to the optimal dosing regimen for HDR monotherapy.

48

FOCAL BRACHYTHERAPY FOR LOCALIZED PROSTATE CANCER: SYSTEMATIC REVIEW AND META-ANALYSIS

Enrique Gutierrez Valencia[1], Inmaculada Navarro[1], Ronald Chow[1], Kailee Zhou[1], Rouhi Fazelzad[1], Matthew Ramotar[1], Irving Sanchez[2], Victor Ruiz[2], Robert Weersink[1], Rachel Glicksman[1], Alejandro Berlin[1], Peter Chung[1], Srinivas Raman[1]
[1]Princess Margaret Cancer Centre, Toronto, ON
[2]University of Guadalajara, Guadalajara, MX

Purpose: Advances in image-guided brachytherapy have increased the interest in focal brachytherapy (F-BT) approaches to optimize disease control while reducing the toxicities associated whole gland treatments for prostate cancer (PCa). In this study, we performed a systematic review to report biochemical control (BC), and genitourinary (GU) and gastrointestinal (GI) toxicity rates in patients with localized prostate cancer treated with F-BT as a definitive or salvage modality.

Materials and Methods: This project was registered in the PROSPERO database (ID CRD42022320921). A comprehensive literature search was conducted in Cochrane Central databases, Cochrane Database of Systematic Reviews, Embase Classic +Embase, and Medline ALL, all from the OvidSP platform and Web of Science from Clarivate, from each database's inception to July 2022. Search was restricted to English and included terms: focal brachytherapy/prostate cancer, partial brachytherapy/prostate cancer. In total, 14862 articles were identified. Manuscripts that not related to focal or partial prostate brachytherapy, review papers and studies not reporting BC were excluded. After eliminating duplicates, and studies deemed irrelevant by consensus among three independent reviewers, 44 articles remained for in-depth review and data extraction.

Results: Thirty studies that included BC outcomes were included for this analysis, comprising 1556 patients treated with F-BT for PCa. Of these, 1094 (70%) and 462 (30%) underwent F-BT as definitive monotherapy or salvage, respectively; while 585 (38%) and 971 (62%) received HDR or LDR, respectively. For F-BT as monotherapy, the most commonly prescribed dose for HDR was 19 Gy in 1 fraction (range 19-24 Gy), and for LDR, 145 Gy (90-160Gy). Whereas for salvage F-BT, the most common dose schedule of HDR was 19Gy in 1 fraction (19-27GY) and LDR 145Gy (144-145Gy). BC random effects estimate for F-BT monotherapy at one-, two-, three-, and five-years were 100% (p=1.0), 96% (p=0.45), 91%(p=0.45) and 87% (p<0.01), respectively. Whereas BC random effects estimate for salvage at one-, two-, three-, and five-years were 91% (p=0.86), 68% (0.17), and 57% (p=0.20), respectively. GI and GU Grade 3-4 crude toxicity rates for monotherapy and salvage ranged from 0-3.33% and 0-17%, respectively.

Conclusions: Over the last decade, there has been increasing interest in F-BT approaches, both as monotherapy and in the salvage setting. BC and toxicity profiles of F-BT appear favourable, and future studies directly comparing with whole-gland treatments are warranted.

49

NOPAUSE: DEVELOPMENT AND VALIDATION OF CLINICAL PROTOCOLS FOR A NOVEL VMAT PLAN AUTOMATION SYSTEM

Nick Chng[1], Stacy Miller[2], Robert Olson[2]
[1]British Columbia Cancer, Prince George, BC
[2]University of British Columbia, Vancouver, BC

Purpose: To describe the process of developing and validating automatic planning protocols for H&N, prostate and rectum sites by retrospectively comparison to manual clinical plans.

Materials and Methods: The Northern Plan Automation Services project is a collection of in-house applications and scripts designed to improve efficiency and quality in radiotherapy treatment planning. The core platform is the Treatment Planning Automation System (TPAS) that enables VMAT plans to be produced within our Eclipse/ARIA environment in as little as one click. TPAS determines optimization objectives from an Eclipse clinical protocol and/or RapidPlan model. Although many clinics will already have these developed and TPAS will support them as-is, specific customizations may be useful. With automation, it is feasible to subdivide OARs into more segments than is practical to do manually, potentially improving the robustness of the system to more challenging cases. TPAS also supports automatic priority re-scaling and re-optimization if clinical goals are not met during the first run, potentially allowing greater focus on initial OAR sparing than a more balanced protocol designed to be run once. Seventy-five clinical plans were retrospectively identified from three sites (H&N, Prostate, and Rectum) at one centre. Twenty plans for each site were used to develop new protocol objective templates, created using OARs divided into regions of PTV overlap and volumes cropped back by a variety of distances (e.g. 1 mm, 5 mm, 10 mm) from the PTV. For the H&N site, our local RapidPlan model was also utilized. The templates were validated by auto-planning the remaining five cases for each site.

Results: All plans in the validation-sets were considered clinically acceptable based on constraints, with minor variations in coverage between clinical and automatically planned cases. The average target coverage (V95%) for automated [manual] plans for each site was HN: 98.7% [99.1%], Prostate: 98.8% [98.9%], Rectum: 99.6% [99.1%]. High priority OAR doses were also comparable, although they trended lower for second-tier constraint doses where the TPAS protocol pushed harder than may have been deemed necessary in the clinical setting. For example, the average rectal D0.035% for prostate was 99.3% [99.5%], whereas the rectal V83% was 9% [13.4%]. In the H&N, minimizing salivary gland dose is usually a focus, and this was reflected by comparable results. Mean doses for combined parotids were 28.1 Gy [29.6 Gy]. As cord doses are not typically at constraint, these were lower with average PRV D0.035cc doses of 41.5 Gy [47.1 Gy], with true cord D0.035cc at 35.7 Gy [42.0 Gy].

Conclusions: This study suggests that with appropriate protocols, TPAS can produce clinically acceptable plans for a variety of sites. If the benefit of automated planning is confirmed in prospective studies, there could be benefits to planning throughput in resource-challenged environments.

50
IN-HOUSE SCRIPTING AND 3D PRINTING PROCESS FOR CUSTOM FLEXIBLE SILICONE BOLUS CREATION

Quinn Matthews, Nathan Smela, Kim Lawyer, Nick Chng
British Columbia Cancer, Prince George, BC

Purpose: To describe our six-year experience and current process for in-house scripting and 3D printing for accurate, efficient, reliable, and cost-effective creation of custom flexible silicone bolus.

Materials and Methods: An in-house ESAPI script generates a structure to guide bolus contouring according to departmental standards (CTV intersection with 6 mm skin rind, plus PTV margin and 1 cm lateral margin for placement uncertainty). A second script exports the bolus structure as an STL file. An in-house open-source program (Fabolus v16, https://github.com/nsmela/Fabolus-v16) loads the STL file, applies smoothing, and creates a 3D-printable mold to house the silicone during curing. Fabolus allows the user to modify the mold orientation and customize placement of holes for silicone injection and air displacement. The final mold is saved as an STL file and loaded into open-source slicing software (PrusaSlicer, https://www.prusa3d.com/page/prusaslicer_424/), where mold break-points (for eventual silicone bolus extraction) are added by reducing the flow rate to 50% for several layers every 2 to 4 cm. The mold is printed on a consumer grade 3D printer (Prusa i3 MK3) with a 0.6mm nozzle, 2 wall layers, 0.4mm layer height, and 8% infill (to support the mold), using polylactic acid (PLA) filament (DigitMakers.ca). After printing, 2-part silicone (Smooth-On EcoFlex 00-30) is mixed, placed in a vacuum chamber for ~1 minute to remove trapped air, and injected into the mold. Once cured (~4 hours) the mold is CT scanned, and data is imported into the treatment planning system for homogeneity QA and registration with the original bolus structure to verify geometric accuracy. The mold is then split apart at the break-points and the silicone is removed. The excess silicone from the air holes is cut off and the final bolus is labelled with permanent marker and delivered to treatment staff.

Results: Our clinic has used the above methods (or their predecessors) to create on average one silicone bolus per week since 2017 (~50 per year). With our latest processes, we estimate the failure rate of manufacturing (printing, filling, or extraction) to be less than 1%. Treatment therapists report excellent efficiency and accuracy of bolus placement, and excellent adaptability to changes in patient contour with minimal skin gaps under bolus through the treatment course (via routine CBCT monitoring). Our average soft bolus volume is ~70 mL, which costs ~$8.50 CAN in raw materials (PLA and silicone) and takes ~4 hours to print the mold. Our largest bolus was ~500 mL, costing ~$52 and ~21 hours to print the mold. Our clinical experience has demonstrated that our process is robust to urgent planning timelines, re-plans, and expansion to novice staff with minimal training.

Conclusions: Our streamlined and clinically validated methods may be adopted by others interested in a cost-effective in-house option for using 3D printing for creation of custom flexible silicone bolus.

51
DOSIMETRIC AND QUALITATIVE EVALUATION OF MAGNETIC RESONANCE FOR CALCULATING ATTENUATION (MRCAT) FOR HEAD AND NECK RADIOTHERAPY

Allan Hupman, Lee Chin, Melanie Davidson
University of Toronto, Toronto, ON

Purpose: To compare the quality of head and neck (HN) synthetic CT (sCT) images generated using Philips' MRCAT package compared to CT, and assess impact of image differences on dosimetry.

Materials and Methods: Nine HN patients underwent CT and MRI simulation. CT and sCT images were compared qualitatively in terms of features, and quantitatively in terms of Hounsfield Units (HU). The clinical CT plans were recalculated on the sCT and dosimetry compared using DVH metrics and gamma analysis.

Results: Qualitatively, sCT images did not include accessories commonly used for HN treatments like the couch, headrest, bolus, mask, or mouth-bites. Artifacts from dental fillings, however, were significantly reduced on sCT. The appearance of mastoids and cartilage (cricoid) differed on sCT, which could impact daily image guidance for some HN cancers. Quantitatively, there was a mean absolute error of 81 HU between sCT and CT compared in a voxel-wise fashion, with the mean sCT value being 26 HU lower than the CT (sCT on average was less dense). This is comparable to published works on MRCAT for other anatomical sites. This difference in image content translated to modest dose differences, whereby dosimetry on sCT was generally hotter than on CT for the target. For example, mean dose to the high-dose target was 0.8 ± 0.4% greater on average in plans recalculated on sCT (range of 0.3-1.1%). The max dose to the spinal canal was greater by 0.5

± 0.8% on average (range of -0.7-1.4%). The mean dose to the parotids and eyes were less by -0.6 ± 0.7 % (range of -1.4-0.7%) for the parotids and -0.4 ± 0.5% (range -1.1-0.3%) for the eyes. On gamma analysis, the dosimetric agreement using 2%/2mm pass criteria was 96 ± 2% with a dose threshold of 10% and 97 ± 3% with a threshold of 90%. Using 1%/1mm pass criteria the pass rates dropped to 88 ± 3% with 10% threshold and 82 ± 14% with 90% threshold. The higher standard deviation when using a higher threshold indicates that the high dose regions exhibited greater variability than the lower dose regions.

Conclusions: Commercial packages deriving sCT from MRI are starting to be used clinically, particularly for pelvic sites. Very little has been reported on the suitability of MRCAT for HN. Though differences in image content between CT and sCT could pose a challenge for image guidance, they may not result in clinically unacceptable dosimetric differences. A more thorough evaluation with additional patients will be required to establish the clinical suitability of sCT for various HN malignancies.

52
AUTOMATED TANGENTS-ONLY TREATMENT PLANNING FOR BREAST CANCER RADIOTHERAPY USING THE ECLIPSE SCRIPTING APPLICATION PROGRAMMING INTERFACE (ESAPI)

Muhammad I. Karamat[1], Owen T. Karnas[2], Jamiel Nasser[3], Jason Vickress[2,1], Scott Karnas[2,1], Jonatan Snir[2,1], Jeff Kempe[1], Jennifer Neeb[1], Wendy Wells[1], Diana SlegersKrekewich[1], Stewart Gaede[2,1]
[1]London Health Sciences Centre, London, ON
[2]Western University, London, ON
[3]University of Waterloo, Waterloo, ON

Purpose: Treatment planning for breast cancer radiotherapy attributed to 23% of dosimetry workload in 2021-2022 at our centre. Typically, it requires 30-120 minutes for a dosimetrist to optimize a plan using a manual forward planned IMRT technique. The purpose of this work was to develop and test an automation script to create tangent-only clinically acceptable treatment plans requiring minimal effort within a few minutes.

Materials and Methods: A sliding window based IMRT technique was developed using ESAPI v15.6 (Varian Medical Systems, Palo Alto, USA). The script was provided the planning CT, the treatment isocentre location, normal tissue contours (lungs and heart), and physician defined treatment open-fields. The script then enables an initial dose calculation, where the 50% isodose line is converted to a contour. The script then creates a CTV by cropping the contour to exclude areas within 5 mm of the ipsilateral lung (iLung) and heart. The PTV was defined as a 25 mm expansion of the outer margin of the CTV in both anterior and lateral dimensions. Optimization objectives and constraints are automatically populated and enabled. Once a set of iterations is completed, the script automatically defines hot and cold spots and re-optimizes until treatment goals become acceptable. The script was evaluated using 25 clinically treated plans (12 left sided, 11 right sided and 1one bilateral breast patient). A comparison between clinical and script generated plans was performed using absolute percent difference between volumes of 90, 95 and 99% isodose curves, and dose metrics for the heart and iLung. The script generated plans were also validated for accuracy and deliverability using portal dosimetry (PD) and Mobius3D (M3D). The gamma pass rate (GPR) was calculated using 2% dose difference at 2 mm distance to agreement i.e., (2%, 2 mm) and (3%, 3 mm) for PD and at (3%, 3 mm) and (5%, 3 mm) for M3D.

Results: All treatment plans were optimized in 2-3 minutes and satisfied all treatment goals. The absolute percent difference for volume of 90, 95 and 99% isodose were (3.5 ± 4.2)%, (3.6 ± 3.5)% and (4.9 ± 4.2)% respectively. The heart and iLung received doses well below our local tolerance limits in all the cases. For heart, V5%, V10% and V15% the absolute difference between script and clinical plans was (0.5 ± 1.1)%, (0.3 ± 0.8)% and (0.2 ± 0.7)% respectively. Similarly, for iLung V10% and V30% the difference was (0.4 ± 1.5)%. The outliers in the data were related mainly to the quality of the auto-generated CTV. The GPR for PD were (98.3 ± 1.8)% and (100 ± 0.2)% for (2%, 2 mm) and (3%, 3 mm) respectively. Respective GPR for M3D validation at (3%, 3 mm) and (5%, 3 mm) were (94 ± 4.5)% and (98.3 ± 1.9)%, confirming deliverability of all plans.

Conclusions: Our automated script can create clinically acceptable treatment plans within 2-3 minutes with minimal effort. The validation results showed excellent feasibility for clinical implementation. Future work includes allowing user generated CTVs, implementation of 4-field breast and planning with simultaneous in-field boost (SIB).

53
AUTOPLANNING SOFTWARE FOR 3D PRINTABLE INTERSTITIAL GYNECOLOGICAL BRACHYTHERAPY TEMPLATES

Michael Kudla[1], Francois Bachand[2], Deidre Batchelar[2], Tony Teke[2]
[1]University of British Columbia, Vancouver, BC
[2]British Columbia Cancer, Kelowna, BC

Purpose: Pre-planning of needle trajectories for the design of patient-specific 3D printed templates for interstitial gynaecological (GYN) high dose rate (HDR) brachytherapy (BT) is currently a time-consuming manual process, taking even experienced planners between three and six hours. A novel automated planning algorithm, which generates candidate needle trajectory sets for patient-specific cylinder templates (PSCTs) in approximately 10 minutes, is presented. Treatment plans generated using autoplanned needle trajectories are evaluated in a retrospective patient cohort.

Materials and Methods: The algorithm begins by creating interstitial line segment candidates progressively through the target volume. The remaining intracavitary section of each needle is then generated by placing a smooth curve from the segment to the base of the cylinder. Intersections between needles or at the wall of the cylinder are corrected. Straight needle paths are then added to the template where possible, extending through the top of the cylinder through the target. The user may search over a range of interstitial needles and any number of iterations to generate a library of independent candidate plans. A 3D plot and ordered list of each needle trajectory set is presented to the user for review. Once the selected plan is imported back into the planning system, dwell time optimization can be performed, and the plan can be exported for printing. The in-house developed autoplanning software was used to generate a library of treatment pre-plan needle trajectory sets for nine clinical cases of patients who have been treated for GYN malignancies using PSCTs. For each patient, an experienced planner selected the best trajectory set from a generated library and optimized pre-plan dwell times to generate a simulated preplan. Autoplanned preplan dosimetric indices were calculated and compared to the patient's original PSCT treatment preplan. Dose-volume histograms (DVHs) and autoplanning times were calculated for each set.

Results: The median time to optimize 25 sets of needle trajectories for each patient was 9min55s. Autoplanner-based preplans met or exceeded most institutional targets and GEC-ESTRO recommendations. Median autoplan versus manual pre-plan dosimetric differences (%) for HRCTV D90 V100, V125, V150, V200, and D2cm^3 for Bladder, Rectum, Sigmoid, Small Bowel D2m^3 were 1.0, 0.0, 3.0, 1.4, -0.2, 0.1, 0.0, 0.0, and 0.1, respectively.

Conclusions: We have developed a simple and fast algorithm to generate high-quality candidate needle trajectories for PSCTs for HDR GYN BT. The resultant library of plans allows the clinician to evaluate multiple candidate needle sets at once, and select the best option for their patient, permitting the creation of a dosimetrically equivalent pre-plan in significantly less time. Current investigations are extending this work to include in-the-loop dwell time optimization and Pareto-front-generation.

54

FEASIBILITY STUDY AND DOSIMETRIC EVALUATION OF A VMAT TECHNIQUE FOR PARTIAL BREAST IRRADIATION

Hedi Mohseni, Michelle Chan, Alana Pellizzari, Teodor Stanescu
Princess Margaret Cancer Centre, Toronto, ON

Purpose: There have been growing discussions regarding concerns about over-treating early-stage breast cancer patients who receive whole-breast radiotherapy. Partial Breast Irradiation (PBI) is an alternative treatment option for this group of patients where only the surgical cavity plus a margin is treated. The purpose of this study is to investigate the feasibility and potential dosimetric trade-offs of a partial arc volumetric modulated arc therapy (VMAT) technique compared to our current institutional 3- to 5-field non-coplanar IMRT technique (maximum of two couch kicks) for partial breast irradiation.

Materials and Methods: This retrospective dosimetric study involved 20 early-stage breast cancer patients originally treated with partial breast IMRT technique (ten left- and ten right-sided, including medial and lateral cavities). The prescription was 26 Gy in 5 fractions. All left-sided cases were treated with activated breathing control (ABC). Institutional clinical goals were used for plan quality assessment. To arrive at a class solution, all cases were planned with the same beam arrangement with two coplanar partial arcs with rotations of 210 degrees.

Results: To date, 10 cases have been completed, including five left- and five right-sided cases (five medial and five lateral cavities). All VMAT plans met our institutional clinical goals. The conformity was superior in VMAT plans compared to IMRT plans. Conformity index and conformation number improved by mean values of 18.0% (range: -2.4% to 31.1%) and 22.7% (range: -3.8% to 42.5%), respectively. The mean reduction in the volume of the ipsilateral lung receiving 30% of the prescription was 51.3% (range: -30.3% to 82.2%), and the mean heart dose was, on average, increased by 4.9 cGy (range: -1 to 26 cGy). The mean dose to the contralateral breast dose was also increased in VMAT plans relative to IMRT by 28.9 cGy on average (range: 3 to 75 cGy).

Conclusions: The coplanar partial arc VMAT plans met all the institutional clinical goals and improved the dose conformity and ipsilateral lung dose. However, the mean doses to the contralateral breast and heart were slightly increased. Additionally, the coplanar VMAT technique has the advantage of faster treatment time compared to the non-coplanar IMRT technique due to no couch kicks or collision risk.

55

PREDICTING DOSIMETRY OF STEREOTACTIC ABLATIVE RADIOTHERAPY FOR THE TREATMENT OF MULTIPLE LUNG LESIONS

Edward Wang[1], Hassan Abdallah[1], Jonatan Snir[2], Jaron Chong[1], David Palma[1], Sarah Mattonen[1], Pencilla Lang[1]
[1]*Western University, London, ON*
[2]*London Health Sciences Centre, London, ON*

Purpose: Stereotactic ablative radiotherapy (SABR) has recently been used to treat increasing numbers of lung metastases, either synchronously or over multiple courses of treatment. Selecting the optimal dose and fractionation to balance risk of local failure and treatment toxicity is challenging. This project uses machine learning to provide rapid dosimetry predictions of SABR to multiple lung lesions, allowing exploration of different dose prescription options prior to the radiation (RT) planning process.

Materials and Methods: A generative adversarial network (GAN) was trained to predict the dosimetry of multi-lesion thoracic SABR treatment from the planning CT scan, target and organ at risk contours, and the prescribed dose-fractionation without the need to carry out treatment planning. RT plans of patients who received at least one SABR treatment for ≥2 lung lesions between 2014-2020 at a single tertiary centre were included in the analysis. All prescriptions were converted to their equivalent doses in two Gray fractions (EQD2). SABR treatments received at different timepoints were registered, and EQD2 doses were accumulated with no repair. Model performance was assessed using 5-fold cross validation. Plans were randomly divided into 5 folds, stratified by the number of lesions (no patients crossed folds). Each fold served as the testing set once, with the model trained on the other 4 folds. The model was evaluated on the difference in the volume of lung receiving above 20 Gray (V20) of the predicted dosimetry compared to the true dosimetry.

Results: Treatment plans (n=103) were included from 81 patients with 280 lesions (62, 23, 8, and 10 plans had 2, 3, 4, and ≥5 lesions respectively). Fifty-five, 18, and four patients had a single, two and three courses of RT respectively. Fifty-two patients were treated for primary lung cancer, 28 patients treated for metastases from other sites, and one patient for both. Seven patients (8.6%) developed ≥ Grade 2 pneumonitis. Doses prescribed were 60/8 (n=136), 55/5 (n=49), 54/3 (n=27), 24/1 (n=21), 35/5 (n=13), 30/5 (n=9), and other (n= 25). The mean lung V20 for all patients was 11.3% [1.5%-29.6%]; the mean lung V20 was 9.3%, 12.2%, 13.5% and 20.4% for plans with 2, 3, 4, ≥ 5 lesions respectively. The mean absolute difference (MAD) in lung V20 between the predicted dosimetry and true dosimetry over all 5-folds was 1.9% [0.0%-13.4%]; the MAD in lung V20 between the predicted and actual dosimetry was 1.6%, 2.1%, 2.9% and 2.6% for plans with 2, 3, 4, ≥ 5 lesions respectively.

Conclusions: The GAN-based model created in this study can predict the dosimetry of any number of lesions in the thorax treated with SABR. The model can be used to quickly determine the feasibility of SABR treatment for multiple synchronous lesions, or in the retreatment setting. The ability to explore the dosimetry of different prescription options for a given patient prior to RT planning may allow for personalized risk-adapted treatment if combined with local control and toxicity modelling.

56

STEREOTACTIC ABLATIVE RADIOTHERAPY FOR OLIGO-PROGRESSIVE CANCERS: RESULTS OF THE RANDOMIZED PHASE II STOP TRIAL

Devin Schellenberg[1], Zsolt Gabos[2], Adele Duimering[2], Brock Debenham[2], Alysa Fairchild[2], Fleur Huang[2], Lindsay Rowe[2], Diane Severin[2], Meredith Giuliani[3], Andrea Bezjak[3], Benjamin Lok[3], Srinivas Raman[3], Peter Chung[3], Yizhou Zhao[1], Clement Ho[1], Michael Lock[4], Alexander Louie[3], Shilo Lefresne[5], Hannah Carolan[5], Mitchell Liu[5], Vivian Yau[6], Allison Ye[6], Rob Olson[6], Benjamin Mou[7], Islam Mohamed[7], David Petrik[7], Maryam Dosani[8], Howard Pai[8], Boris Valev[8], Stewart Gaede[9], Andrew Warner[4], David Palma[4]
[1]*British Columbia Cancer, Surrey, BC*
[2]*University of Alberta, Edmonton, AB*
[3]*University of Toronto, Toronto, ON*
[4]*London Health Sciences Centre, London, ON*
[5]*British Columbia Cancer, Vancouver, BC*

[6]British Columbia Cancer, Prince George, BC
[7]British Columbia Cancer, Kelowna, BC
[8]British Columbia Cancer, Victoria, BC
[9]Western University, London, ON

Purpose: In the metastatic setting, there is uncertain benefit to localized eradication of one or more lesions that are progressing despite systemic therapy. This randomized phase II trial examined if patients with ≤5 sites of oligoprogression benefited from the addition of stereotactic ablative radiotherapy (SABR) to standard of care (SOC) systemic therapy.

Materials and Methods: Eligibility criteria included age ≥18 years, ECOG performance status 0-2, and oligoprogressive disease, defined as 1-5 lesions actively progressing while on systemic therapy. Patients were required to have at least three months of disease stability/response on systemic therapy prior to oligoprogression. After stratifying by type of systemic therapy (cytotoxic versus non-cytotoxic), patients were randomized 2:1 to SABR to all progressing lesions plus SOC (SABR arm) versus SOC alone (SOC arm). The trial began exclusive to non-small cell lung cancer but did not meet accrual goals and was expanded in 2019 to include all non-hematologic malignancies. The primary endpoint was progression-free survival (PFS). Secondary endpoints included overall survival (OS), lesional control, quality of life (QOL), toxicity, and duration of current systemic agent post-SABR.

Results: Between February 2017 and June 2021, 90 patients with 125 oligoprogressive metastases were enrolled across eight Canadian institutions, with 59 patients randomized to SABR and 31 to SOC. Median age was 67 years (IQR: 61-73 years) and 39 (43%) were female. The most common primary sites were lung (44% of patients), genitourinary (23%) and breast (13%), with the most common oligo-progressive locations being lung (43%), bone (19%), lymph nodes (14%), and liver (13%). In the SABR arm, the most common fractionations were 35Gy/5 (38% of lesions) and 50Gy/5 (18%). Protocol adherence in the SOC arm was suboptimal: three patients (10%) withdrew immediately after randomization, and seven additional patients (23%) received high-dose or ablative therapies. Median follow-up was 31 months. There was no difference in PFS between arms (median PFS 8.4 months in the SABR arm versus 4.3 months in the SOC arm; however the curves cross and two-year PFS was 9% versus 24% respectively, p=0.91). Median OS was 31.2 months versus 27.4 months, respectively (p=0.22). Lesional control with SABR was 71% versus 39% with SOC (p=0.002). Median duration of post-randomization first-line systemic therapy was 10.3 months versus 7.6 months, respectively (p=0.71). Treatment was well-tolerated with two (3.4%) Grade 3 treatment-related toxicities in the SABR arm and no Grade 4/5 events attributable to SABR. QOL did not differ between arms.

Conclusions: Despite being a well-tolerated treatment providing superior lesional control, SABR for oligoprogression did not improve PFS or OS. Results may have been impacted by withdrawals and desire for ablative treatments on the SOC arm, and this lack of equipoise may make accrual to phase III trials difficult, although larger studies in select sub-populations are desired. (NCT02756793)

57
ABLATIVE RADIATION THERAPY TO RESTRAIN EVERYTHING SAFELY TREATABLE (ARREST) - A PHASE 1 STUDY OF SABR FOR POLY-METASTATIC DISEASE

Timothy Nguyen[1], Sherif Ramadan[1], Abhirami Hallock[2], David Palma[1], Mark Corkum[3], Melissa O'Neil[1], Anders Celinski[1], Hatim Fakir[1], Michael Lock[1], Pencilla Lang[1], Vikram Velker[1], Glenn Bauman[1]
[1]Western University, London, ON
[2]N/A, Niagara, ON
[3]University of Ottawa, Ottawa, ON

Purpose: Polymetastatic disease is a state where patients have widespread dissemination of their cancer beyond oligometastatic disease. Currently, these patients are treated with systemic therapy, but there are a finite number of treatment lines available. For these patient's palliative radiotherapy is typically directed at symptomatic sites, and its role beyond that is unclear. In this phase 1 study, we aimed to determine the feasibility and safety of delivering SABR to all polymetastases in patients where further lines of systemic therapy have been exhausted.

Materials and Methods: Full details of this Phase I protocol (NCT04530513) have been published in BMC Cancer 21, 405 (2021). Inclusion criteria include ECOG 0-2, estimated life expectancy >3 months, >10 metastases, and no standard of care systemic therapy options available. The 3+3 design includes four dose levels from 12Gy (6Gy weekly x 2) to 30Gy (6Gy weekly x 5) with dose de-escalation mandated if OAR constraints cannot be met at a given dose level for a given patient. Dose limiting toxicity (DLT) was defined a priori as any Grade 4 or 5 events, or more than three separate Grade three toxicity events within 6 weeks of treatment (CTCAE v5.0). The maximal tolerated dose (MTD) is declared if 1/3 or 2/6 patients experience DLT or if a dosimetrically acceptable plan is achieved in fewer than half of patients at a given dose level. Secondary endpoints include quality of life (FACT G and EQ5D5L) at six weeks post treatment and progression-free survival (PFS).

Results: To date 11 patients have been enrolled in the study: six male and five female patients with a median age of 67 (range= 55-83). A total of 178 lesions have been treated, with a median of n=16 lesions per patient (range= 10-27) to treat on average two organ systems (range= 1-5). The median lesion size treated was 1.68 cm^3 (range= 0.07 – 106.09). Patients were treated from one to three treatment sessions per fraction and required a median of three isocentres (range= 2-8). At six week follow up six patients had no acute toxicity (55%) and five patients had acute toxicities: (n=2,18%) Grade 1 nausea and vomiting, (n=2, 18%) Grade 2 radiation pneumonitis and cutaneous rash, (n=1, 9%) Grade 3 neutropenia. There were no Grade 4 or 5 acute toxicities. When assessing QoL the EQ5D5L had a pretreatment median score of 75% and a six-week follow up median of 70%. At a median follow-up of six months post treatment, eight of 11 patients have had disease progression with a median time to progression of 88 days.

Conclusions: Interim analysis of this Phase I study found SABR treatment for patients with more than 10 metastases to be technically feasible with acceptable acute toxicity at dose levels up to 24Gy (6Gy weekly x 4). Dose limiting toxicity has not been observed to date. Accrual at the final dose level 4 (30Gy, 6Gy weekly x 5) is underway, with completion expected in early 2023.

58
SHOULD ORGANS AT RISK (OARS) BE PRIORITIZED OVER TARGET VOLUME COVERAGE IN STEREOTACTIC ABLATIVE RADIOTHERAPY (SABR) FOR OLIGOMETASTASES? A SECONDARY ANALYSIS OF THE POPULATION-BASED PHASE II SABR-5 TRIAL

Reno Eufemon Cereno[1,2], Benjamin Mou[1,2], Sarah Baker[1,3], Nick Chng[4], Gregory Arbour[1], Alanah Bergman[1,5], Mitchell Liu[1,5], Devin Schellenberg[1,3], Quinn Matthews[4], Vicky Huang[3], Ante Mestrovic[6], Derek Hyde[2], Abraham Alexander[1,6], Hannah Carolan[1,5], Fred Hsu[1,7], Stacy Miller[1,4], Siavash Atrchian[1,2], Elisa Chan[1,5], Clement Ho[1,3], Islam Mohamed[1,2], Angela Lin[1,2], Tanya Berrang[1,6], Andrew Bang[1,5], Will Jiang[1,4], Chad Lund[1,3], Howard Pai[1,6], Boris Valev[1,6], Shilo Lefresne[1,5], Scott Tyldesley[1,5], Robert Olson[1,4]
[1]University of British Columbia,
[2]British Columbia Cancer, Kelowna, BC
[3]British Columbia Cancer, Surrey, BC

[4]*British Columbia Cancer, Prince George, BC*
[5]*British Columbia Cancer, Vancouver, BC*
[6]*British Columbia Cancer, Victoria, BC*
[7]*British Columbia Cancer, Abbottsford, BC*

Purpose: Stereotactic ablative radiotherapy (SABR) for oligometastases may improve survival, however concerns about safety remain. To mitigate risk of toxicity, target coverage was sacrificed to prioritize organs at risk (OARs) during SABR planning in the population-based SABR-5 trial. This study evaluated the effect of this practice on dosimetry, local recurrence (LR), and progression-free survival (PFS).

Materials and Methods: This single-arm phase II trial included patients with up to five oligometastases between November 2016 and July 2020. The protocol-specified planning objective was to cover 95% of the planning target volume (PTV) with 100% of the prescribed dose, however PTV coverage was reduced as needed to meet OAR constraints. This trade-off was measured using the coverage compromise index (CCI), computed as minimum dose received by the hottest 99% of the PTV (D99) divided by the prescription dose. Under-coverage was defined as CCI <0.90. The potential association between CCI and outcomes was evaluated.

Results: Five hundred forty-nine lesions from 381 patients were assessed. Mean CCI was 0.88 (95% confidence interval [CI], 0.86-0.89), and 196 (36%) lesions were under-covered. The highest mean CCI (0.95; 95%CI, 0.93-0.97) was in non-spine bone lesions (n=116), while the lowest mean CCI (0.71; 95% CI, 0.69-0.73) was in spine lesions (n=104). On multivariable analysis, under-coverage did not predict for worse LR (HR 0.48, p=0.37) or PFS (HR 1.24, p=0.38). Largest lesion diameter, colorectal and 'other' (non-prostate, breast, or lung) primary predicted for worse LR. Largest lesion diameter, synchronous tumour treatment, short disease free interval, state of oligoprogression, initiation or change in systemic treatment, and a high PTV Dmax were significantly associated with PFS.

Conclusions: PTV under-coverage was not associated with worse LR or PFS in this large, population-based phase II trial. Combined with low toxicity rates, this study supports the practice of prioritizing OAR constraints during oligometastatic SABR planning.

59

POLYMETASTATIC RECURRENCE-FREE SURVIVAL IN PATIENTS WITH REPEAT OLIGOMETASTASES ON THE SABR-5 TRIAL

Wei Liu[1], Subhadip Das[2], Robert Anton Olson[3], Sarah Baker[4], Emma Dunne[1], Jee Suk Chang[1], Devin Schellenberg[4], Tanya Berrang[2], Fred Hsu[5], Will Jiang[4], Benjamin Mou[6], Shilo Lefresne[1], Scott Tyldesley[1], Mitchell Liu[1]
[1]*British Columbia Cancer, Vancouver, BC*
[2]*British Columbia Cancer, Victoria, BC*
[3]*British Columbia Cancer, Prince George, BC*
[4]*British Columbia Cancer, Surrey, BC*
[5]*British Columbia Cancer, Abbotsford, BC*
[6]*British Columbia Cancer, Kelowna, BC*

Purpose: To determine polymetastatic recurrence-free survival (PMRFS) in patients with repeat oligometastases (OM) on the SABR-5 trial.

Materials and Methods: SABR-5 is a prospective, multi-centre trial that evaluated the safety of stereotactic ablative radiotherapy (SABR) in patients with 1-5 OM or oligoprogressive lesions. On SABR-5, patients were followed post-SABR according to standardized protocols. Patients with repeat extra-cranial OM after metastasis-directed therapy (MDT; SABR, surgery, or thermoablation) to all initial OM (including those treated before enrolment on SABR-5) were identified. Exclusion criteria included history of multiple primary malignancies and incomplete re-staging. PMRFS was defined as time from presentation of repeat oligometastases to death or presentation of 6 or more progressing metastases, leptomeningeal metastases, lymphangitic carcinomatosis, malignant ascites, or malignant pleural effusion. PMRFS, overall survival (OS), and progression-free survival (PFS) were calculated using the Kaplan-Meier method.

Results: Seventy-six patients with repeat OM were included, of which 44 (58%) received second MDT to all OM. The most common histology in patients who received second MDT was colorectal cancer (10/44 [23%]) and in those who did not was prostate cancer (17/32 [53%]). Patients who did versus did not receive second MDT had fewer metastases at repeat OM (mean 1.3 versus 2.2; p<0.001) and no difference in time between initial OM and repeat OM (16 versus 17 months; p=0.74). For patients who received second MDT, median follow-up from presentation of repeat OM was 2.6 years. Median PFS after first and second MDT were 15 months (95% CI 11-18) and 11 months (95% CI 7-17), respectively. At last follow-up, 22/44 patients (50%) were alive without polymetastatic recurrence. Three-year PMRFS and OS from presentation of repeat OM were 51% (95% CI 33-66%) and 66% (95% CI 47-79%), respectively.

Conclusions: Patients presenting with repeat OM after MDT may still have favourable three-year PMRFS and OS, which may justify exploring aggressive local treatments in this subpopulation. Further randomized trials in this space are needed.

60

STEREOTACTIC BODY RADIOTHERAPY (SBRT) FOR SACRAL METASTASES: DEVIATION FROM RECOMMENDED TARGET VOLUME DELINEATION PREDICTS HIGHER RISK OF LOCAL FAILURE

Daniel Palhares, Kang Liang Zeng, Sten Myrehaug, Hanbo Chen, Hany Soliman, Chia-Lin (Eric) Tseng, Jeremie Larouche, Pejman Maralani, Jeff Wilson, Mark Ruschin, Beibei Zhang, Eshetu Atenafu, Arjun Sahgal, Jay Detsky
University of Toronto, Toronto, ON

Purpose: An international consensus recommendation was published to guide target volume delineation specific to sacral stereotactic body radiotherapy (SBRT). We report outcomes after sacrum SBRT, focusing on the impact of contouring deviation on local failure (LF) risk, with an aim to validate this guideline.

Materials and Methods: All patients who underwent sacral SBRT from 2010 to 2021 were identified from a prospectively maintained institutional database. Primary outcome was magnetic resonance-based LF. Secondary outcomes included vertebral compression fracture (VCF) and overall survival (OS). Cumulative LF and VCF rates were calculated per segment using the competing risk analysis method. Kaplan Meier analysis was used to estimate OS per patient. Cox proportional hazards model was used to assess predictive factors of LF, VCF, and OS.

Results: A total of 215 treated sacral segments in 112 patients were retrospectively reviewed. The median follow-up was 13 months (range, 0.4-116.9). The median age was 64 years (range, 18-86). Most patients (52%) had treatment to a single segment. The median clinical target volume (CTV) was 129.2 cc (range, 5.8-753.5). Most segments were treated with 30 Gy/4 fractions (51%), 24 Gy/2 fractions (31%), or 30 Gy/5 fractions (10%). Thirty-one percent of segments were of radioresistant histology (gastrointestinal, kidney, melanoma, sarcoma, or thyroid primary), and 51% had extraosseous disease. Sixteen percent of segments were under-contoured per consensus guidelines, with incomplete coverage of the involved sector (71%), omission of the adjacent

uninvolved sector (17%), or both (11%) as the causes for deviation. The cumulative incidence of LF was 18.4% (95% CI 13.5-24.0) at 12-months and 23.1% (95% CI 17.6-29.0) at 24-months. On multivariate analysis (MVA), under-contouring (HR 2.4, 95% CI 1.3-4.7, p=0.008), radioresistant histology (HR 2.4, 95% CI 1,4-4.1, p=0.001), and extraosseous extension (HR 2.5, 95% CI 1.3-4.7, p=0.005) were predictors of increased risk of LF. The LF rates at 12/24-months were 15.1%/18.8% for segments contoured per guideline versus 31.4%/40.0% for those under-contoured. The cumulative incidence of VCF was 7.1% (95% CI 4.1-11.1) at 12-months and 12.3% (95% CI 8.2-17.2) at 24-months. On MVA, female gender was the only risk factor for VCF (HR 2.3, 95% CI 1.1-5.2, p=0.04). The median OS was 29.5 months (95% CI 17.5-59.2). On MVA, primary kidney (HR 4.7, 95% CI 1.7-12.5, p=0.002) or lung histology (HR 3.4, 95% CI 1.3-8.5, p=0.010), the presence of liver (HR 2.8, 95% CI 1.2-6.4, p=0.016) or lung (HR 2.5, 95% CI 1.3-5.1, p=0.008) metastases, ECOG performance status 2 or 3 (HR 3.3, 95% CI 1.2-8.2, p=0.013), and the presence of sensory or motor deficit (HR 2.6, 95% CI 1.2-5.4, p=0.012) were prognostic for worse OS.

Conclusions: Sacral SBRT is associated with high rates of efficacy and an acceptable VCF risk. Adherence to target volume delineation consensus guidelines reduces the risk of LF.

61

DEVELOPMENT OF BIG DATA HEALTH CARE FRAMEWORK IN ONCOLOGY WITH DYNAMIC INTEGRATION OF MULTIMODAL HEALTH INFORMATION

Jee Suk Chang[1], Eun Sil Baek[2], Jin Sung Kim[2], Robert Olson[3], Sang Joon Shin[2]
[1]*British Columbia Cancer, Vancouver, BC*
[2]*Yonsei University College of Medicine, Seoul, KR*
[3]*British Columbia Cancer, Prince George, BC*

Purpose: Medical data contain an enormous volume, and newer data sources are likely to create a tsunami of additional health information. The oncology profession has already experienced unprecedented levels of burnout, as shown in a previous study which revealed that physicians spent almost double the amount of time engaging with the electronic medical record (EMR) compared to direct patient face time. Here, we report on our collaborative, cross-departmental effort to construct a comprehensive, continuous, dynamic, and expandable data framework in oncology that links clinical, genomic, and imaging data.

Materials and Methods: To ensure high data quality with minimized risks of false and missing data, we developed different approaches for each cancer type to select individuals. Then, we developed a patient-centred data model to process the data through an Extract-Transform-Load (ETL) on a daily basis using SQL queries, Python code, and natural language processing. Data quality control (QC) was continuously iterated automatically and manually in closed-loop systems to ensure the cleansed target data was optimally accurate. As proof of concept, we demonstrate how the navigation of processed data could be used to provide detailed EMR summarization in one click to mitigate the mindless hours spent navigating the EMR. Finally, we show how this framework could be used to collect big data instantly for conducting retrospective research.

Results: The final database contains data from 178,620 individuals with a history of 11 cancers (breast, colorectal, lung, gastric, liver, melanoma, kidney, prostate, thyroid, pancreatic, and bile duct cancers) at a single institution from 2006 to 2021. Throughout the developed framework, individual profiles of the database were continuously generated and updated from electronic health records to contain a comprehensive representation of essential oncologic elements across a timeline. We successfully developed a system that automatically displays succinct summaries of an individual's medical history and treatment course in one click. We also answer a clinical question: whether radiotherapy-related neutrophilia and lymphopenia would have prognostic significance in more than 1000 cases of locally advanced rectal cancer within the data framework context without a heavy workload on data collection.

Conclusions: We report the development of a data framework in oncology for the longitudinal, continuous capture of comprehensive data. We also demonstrate its possible utility for mitigating physicians' cognitive burden and for the quick generation and testing of clinical hypotheses. The development of a deep learning-based auto-segmentation of gross tumour volumes within this data framework is currently underway to timely identify oligometastatic disease states, which may escalate the chance of them being discussed for local therapy in multidisciplinary tumour boards.

62

OPERATIONAL ONTOLOGY FOR RADIATION ONCOLOGY (OORO) - A PROFESSIONAL SOCIETY-BASED, MULTI-STAKEHOLDER CONSENSUS DRIVEN INFORMATICS STANDARD SUPPORTING CLINICAL AND RESEARCH USE OF REAL-WORLD DATA

Charles Mayo[1], Clifton David Fuller[2], Mary Feng[3], Kristy Brock[2], Randi Kudner[4], Peter Balter[2], Jeffrey Buchsbaum[5], Amanda Caissie[6], Elizabeth Covington[1], Emily Daugherty[7], David Sup Hong Jr[8], Andra Krauze[9], Jon Kruse[10], Todd McNutt[11], Richard Popple[12], Susan Richardson[13], Jatinder Palta[14], Thomas Purdie[15], Lawrence Tarbox[16], Ying Xiao[17]
[1]*University of Michigan, Ann Arbor, MI*
[2]*The University of Texas MD Anderson Cancer Center, Houston, TX*
[3]*University of California San Francisco, CA*
[4]*ASTRO, Arlington, VA*
[5]*National Cancer Institute, Bethesda, MD*
[6]*Dalhousie University, Halifax, NS*
[7]*University of Cincinnati, Cincinnati, OH*
[8]*University of Southern California, Los Angeles, CA*
[9]*National Institute of Health, Washington, DC*
[10]*Mayo Clinic, Rochester, MN*
[11]*Johns Hopkins University, Baltimore, MD*
[12]*University of Alabama, Birmingham, AL*
[13]*Washington University, Springfield, MO*
[14]*Virginia Commonwealth University, Richmond, VI*
[15]*Princess Margaret Cancer Centre, Toronto, ON*
[16]*University of Arkansas for Medical Sciences, Little Rock, AR*
[17]*University of Pennsylvania, Philadelphia, PA*

Purpose: There is a critical need for large-scale, multi-institutional "real-world" data to evaluate patient, diagnosis and treatment factors affecting oncology patient outcomes. However, lack of data standardization undermines the potential for automated learning from the vast amount of information routinely archived in electronic health records (EHRs), Radiation Oncology Information Systems and other cancer care databases. As next step to promote data standardization beyond the American Association of Physicists in Medicine (AAPM)'s TG-263 guidance for radiotherapy (RT) nomenclature, the AAPM's Big Data Subcommittee (BDSC) has led an international RT professional society collaboration to develop the Operational Ontology for Radiation Oncology (OORO).

Materials and Methods: Initiated July 2019 to explore issues that typically compromise formation of large inter- and intra-institutional databases from EHRs, the AAPM's BDSC membership includes representatives from the AAPM, American Society of Radiation Oncology (ASTRO), Canadian Organization of Medical Physicists (COMP), Canadian Association of Radiation Oncology (CARO), European Society of Therapeutic Radiation Oncology (ESTRO) and clinical trials experts from NRG Oncology. Multiple

external stakeholders were engaged, including government agencies, vendors and RT community members through the iterative and consensus-driven approach to OORO development.

Results: The OORO includes 42 key elements, 359 attributes, 144 value sets, and 155 relationships, ranked for priority of implementation based on clinical significance, likelihood of availability in EHRs, or ability to modify routine clinical processes to permit aggregation. The initial version of OORO includes many disease-site independent concepts common for all cancer patients and a smaller set specific for prostate cancer. The OORO development methodology is currently being applied/adapted to include additional disease site-specific concepts beginning with head and neck cancers.

Conclusions: The first of its kind in radiation oncology, the OORO is a professional society-based, multi-stakeholder, consensus driven informatics standard. The iterative and collaborative approach to ontology development and refinement aims to ensure that OORO serves as a « living » guidance document, facilitating incremental expansion of data elements over time, as disease site-specific standards are set and RT concepts evolve. Supporting construction of comprehensive "real-world" datasets and application of advanced analytic techniques, including artificial intelligence (AI), OORO holds the potential to revolutionize patient management and improve outcomes.

63

CLINICAL ACCEPTABILITY OF ARTIFICIAL INTELLIGENCE-SCREENED INTERSTITIAL LUNG DISEASE (AI-ILD) IN LUNG CANCER PATIENTS TREATED WITH RADIOTHERAPY

Nicholas McNeil[1], Hannah Bacon[1], Sonja Kandel[1,2], Tirth Patel[2], Mattea Welch[3], Xiang Y. Ye[3], Chris McIntosh[1], Andrea Bezjak[3], Benjamin H. Lok[3], Srinivas Raman[3], Meredith Giuliani[3], John Cho[3], Alexander Sun[3], Patricia Lindsay[1], Geoffrey Liu[3], Tony Tadic[1], Andrew Hope[3]
[1]University of Toronto, Toronto, ON
[2]University Health Network, Toronto, ON
[3]Princess Margaret Cancer Centre, Toronto, ON

Purpose: Patients with interstitial lung disease (ILD) treated with thoracic radiotherapy (RT) are at greater risk of pulmonary toxicity. Automatic universal screening for ILD allows radiation oncologists (ROs) to risk stratify patients and implement necessary modifications to their respiratory monitoring or treatment. Automatic screening however may affect RO workload and so it is imperative to assess the clinical acceptability of this tool.

Materials and Methods: We have developed a machine learning algorithm to identify patients who are at high risk of having ILD based on RT planning computed tomography (CT) images. A quality improvement (QI) project was initiated to test feasibility and acceptability of the machine learning algorithm. If positive, the results of the machine learning algorithm were made available to ROs via structured electronic reporting. ROs were prompted to review the patient and consider expert radiologist consultation if thought appropriate. All electronic surveys and qualitative comments were summarised to describe clinical acceptability. Expert radiologist established gold standard ILD status of all patients on the study. A formal review of RO feedback was collected for all screen-positive, true-positive cases.

Results: Two hundred-forty cases were screened of which 45 were flagged as AI-ILD positive and the responsible RO notified. Of these 45 screen-positive cases, all continued on to RT except for three patients with tumour progression. From these 45, 24 surveys were completed, 21 had no prior suspicion of ILD. There were seven true-positives, of which one had a survey response. Based on the survey responses, 88% of cases underwent review by the responsible RO. In 16 cases this automatic notification prompted case consultation with an expert radiologist. Expert review was performed from 10 minutes up to 53 hours after the email prompt to the radiologist, with median response time of 1.5 hours. In the seven screen-positive, true-positive cases, only two were not previously known to the responsible RO. In the two cases where true-positive ILD status was previously unknown, one was a mild case of ILD and the other had previously received thoracic RT at this institution without ILD being identified, in both cases the ROs were grateful that this diagnosis was identified prior to treatment. RO confidence in the machine learning prediction was moderate due to the high proportion of false positives.

Conclusions: Based on available survey results, more than 75% of the screen-positive cases were reviewed by the responsible RO and two-thirds of these involved expert radiology input. RO feedback was generally positive and this tool was rated as a net benefit despite the high rate of false positives and the need for clarification.

64

A PROSPECTIVE STUDY OF MACHINE LEARNING-ASSISTED RADIOTHERAPY PLANNING FOR PATIENTS RECEIVING 54 GY TO THE BRAIN

Derek Tsang[1], Grace Tsui[2], Anna Santiago[3], Harald Keller[2], Thomas Purdie[2], Chris McIntosh[2], Nancy La Macchia[2], Amy Parent[2], Hitesh Dama[2], Sameera Ahmed[2], Tim Craig[2], Normand Laperriere[1], Barbara-Ann Millar[1], David Hodgson[1]
[1]University of Toronto, Toronto, ON
[2]Princess Margaret Cancer Centre, Toronto, ON
[3]University Health Network, Toronto, ON

Purpose: Radiotherapy (RT) planning is presently a semi-manual, iterative, labour-intensive process which may result in unnecessary variation in plan quality. We previously piloted a machine learning (ML) platform in our treatment planning system for patients receiving 54 Gy in 30 fractions for a primary brain tumour. We conducted a prospective, blinded study to compare ML-assisted planning with conventional VMAT/IMRT planning.

Materials and Methods: From January 31, 2022 – January 10, 2023, 40 patients receiving 54 Gy for primary CNS tumours were prospectively enrolled (median age 50 years, range 4-78 years). Patients underwent standard CT/MR simulation and target/OAR delineation by the treating radiation oncologist. Each patient had one ML plan and 1-2 manual RT plans created by different planners. The reviewing oncologist was blinded to planning method by removing optimization and beam arrangement details from all plans, which were then rated based on clinical acceptability, target coverage, OAR sparing, conformity, and dose-fall off. One preferred plan was chosen and used for clinical treatment.

Results: A total of 115 plans for 40 patients were evaluated: 40 ML plans (35% of all plans), and 75 manual plans (65% of all plans; five and 35 patients had one and two manual plans created, respectively). ML plans required a mean planning time of 65 minutes as compared to 107 minutes for manual plans, with a mean time savings of 41 min per patient (paired t-test p=0.002). 97% of ML plans (95% confidence interval [CI] 85-100) and 96% of manual plans (95% CI 87-99) were designated clinically acceptable by the treating radiation oncologist. While ML-assisted plans represented 35% of plans evaluated, they were chosen as preferred for clinical treatment in 43% of cases (17/40, 95% CI 29-58, p=0.32). Median doses to the brain (10.8 Gy versus 11.3 Gy, Wilcoxon rank-sum p=0.012) and brain minus PTV (9.2 Gy versus 10.0 Gy, Wilcoxon rank-sum p=0.009) were lower with ML planning versus manual planning, respectively. Doses to other structures, including hippocampi, cochlea, pituitary and hypothalamus were not statistically different.

Conclusions: In this prospective study with blinded oncologist evaluation, ML-assisted RT planning for primary CNS tumours was faster than manual planning, and produced a very high rate of acceptable plans with similar or superior OAR sparing. Future work will be undertaken to iteratively refine the ML model using the preferred cases from this study.

65

PRELIMINARY VALIDATION OF SYNTHETIC CT FROM CBCT IMAGES FOR DOSE RECONSTRUCTION IN LUNG CANCER RADIOTHERAPY

Dipal Patel[1], Teodor Stanescu[1,2], Jean-Pierre Bissonnette[1,2]
[1]University of Toronto, Toronto, ON
[2]Princess Margaret Cancer Centre, Toronto, ON

Purpose: Daily dose reconstruction on cone-beam CT (CBCT) imaging may lead to dosimetric errors of ±15% due to degradations in image quality that misrepresent the physical density of tissues. Synthetic CT (sCT) images derived from CBCT images using a Deep Learning methodology may enable accurate dose recalculations for each treatment by accurately restoring physical tissue densities. We aim to validate this approach in patients with lung cancer by assessing image similarity and comparing doses calculated on CBCT and sCT images with the clinical plan. Our approach may reveal dosimetric or geometric reasons for treatment failure or excessive toxicity due to deformations occurring during long treatment courses.

Materials and Methods: Planning CTs, treatment plans, and CBCTs at all fractions of delivered radiotherapy were collected from a retrospective cohort of patients (n=30) with locally-advanced non-small cell lung cancer. Twenty-five datasets, consisting of the planning CT and first fraction CBCT, were used to train a CycleGAN model. Synthetic CTs for five datasets were used for preliminary model validation. Hounsfield unit histograms, mean absolute error (MAE) and complex-wavelet structural similarity (CW-SSIM) indices were analyzed to compare sCT, CBCT and CT images. Treatment plans were recalculated on sCT and clinically-relevant dose-volume parameters were compared for tumour and mediastinal structures.

Results: Hounsfield unit histograms show strong overlap between sCT and CT for each patient. The mean MAE and CW-SSIM for sCT were 23.06±7.38 HU and 0.9047±0.0291, respectively; for CBCT, corresponding values were 58.27±17.08 HU and 0.8759±0.0268. Relative dose differences between the clinical plan and those recalculated on sCT and CBCT were $D_{95}(PTV_p)_{sCT}$=0.9 ± 0.9% and $D_{95}(PTV_p)_{CBCT}$=0±3%, respectively. Sample dose differences for organs at risk include $V30(Heart)_{sCT}$=1±3% versus $V30(Heart)_{CBCT}$=1±6%, $D_{max}(Cord)_{sCT}$=0±0% versus $D_{max}(Cord)_{CBCT}$=2±5%, and $D_{mean}(Esophagus)_{sCT}$=1±1% versus $D_{mean}(Esophagus)_{CBCT}$=1±3%. The lower standard deviations observed for doses calculated on sCT may indicate that this approach is more consistent than dose calculation on CBCT images. Metrics for lung doses are not shown since the field of view of the original CBCT did not span the entire lung volume.

Conclusions: Compared to CBCT, derived synthetic CT images show significant reduction of image artifacts and yield CT numbers much closer to those of a conventional CT from CBCTs while retaining geometric accuracy. Therefore, sCT reproduce more faithfully lung and soft tissue densities, and resulting dose calculations are more consistent. Therefore, accurate dose reconstruction is achievable by substituting sCT for CBCT for patients with lung cancer. Future work aims to improve the CycleGAN model by increasing training dataset size, further optimizing training parameters, and perform dose reconstruction over entire courses of lung radiotherapy.

66

DUAL-CENTRE VALIDATION OF USING MRI RADIOMICS AND MACHINE LEARNING TO PREDICT STEREOTACTIC RADIOSURGERY OUTCOMES

David DeVries[1], Terence Tang[2], Ghada Alqaidy[3], Ali Albweady[4], Andrew Leung[1], Joanna Laba[1], Frank Lagerwaard[5], Jaap Zindler[6], George Hajdok[1], Aaron Ward[1]
[1]Western University, London, ON
[2]London Health Sciences Centre, London, ON
[3]King Fahad Armed Forces Hospital, Jeddah, SA
[4]Unaizah College of Medicine and Medical Sciences, Unaizah, SA
[5]Amsterdam UMC - Vrije University Medical Center, Amsterdam, NL
[6]Haaglanden Medical Centre, Den Haag, NL

Purpose: Stereotactic radiosurgery (SRS) is an established treatment for brain metastases (BMs), but treatment failures can occur. A predictive model of SRS outcomes could aid clinicians in treatment selection, prescribing SRS dose, and accounting for possible re-treatment for the organs at risk within the SRS treatment plan. Previous studies have shown the ability of magnetic resonance imaging (MRI) radiomics and machine learning to predict SRS outcomes, but these methods have never been externally validated at another institution/centre, which is a crucial step towards clinical translation. We report the results of the first dual-centre validation of a system using MRI radiomics to predict SRS outcomes.

Materials and Methods: We acquired two retrospective BM datasets from patients treated with first-line SRS at the Amsterdam University Medical Centre ("Centre A"; n=123 BMs) and the London Regional Cancer Program ("Centre B"; n=117 BMs). For each dataset, pre-treatment T1w contrast-enhanced MRI, BM SRS planning contours, and the BM progression/no progression post-SRS status were collected. After applying MRI resolution and intensity normalization pre-processing, 107 radiomic features were extracted per BM. Random decision forest machine learning models trained to predict progression post-SRS using the radiomic features were then evaluated in three validation scenarios.

Results: First, a model was trained using Centre A's dataset, locked, and then tested using Centre B's dataset. The inverse was also performed. Each model achieved an area-under-the-receiver-operating-characteristic curve (AUC) value of 0.61. By restricting the use of features only to a harmonized set that was mutually important across both centres (according to the random forest), the AUC values in this scenario rose to 0.70. Second, the scenario of training a model using a locked methodology developed at an external centre was investigated. A model training methodology was developed using Centre A's dataset and locked. This methodology achieved an AUC of 0.74 when tested on Centre A's dataset using bootstrap resampling. When externally validated by retraining on Centre B's dataset, the methodology achieved an AUC of 0.80. Lastly, Centres A and B's datasets were pooled and the same methodology was evaluated using bootstrap resampling. An AUC of 0.78 was achieved, with balanced accuracy for samples from either centre.

Conclusions: A radiomics-based SRS outcome predictive model can be trained at one centre and used at another, but at the cost of model accuracy. Harmonization of radiomic features can reduce this effect by compensating for the MRI scanner heterogeneity between centres. An external centre could alternatively train their own more accurate model by using this study's methodology with a local dataset. The balanced performance from the pooled datasets results demonstrates the possibility of producing a more generalizable model trained with multi-centre data, though external validation of this result is required.

67

DOSE VERIFICATION OF MRI-GUIDED ONLINE ADAPTIVE TREATMENT DELIVERY FOR UGI SITES

Oleksii Semeniuk, Andrea Shessel, Michael Velec, Cathy Carpino-Rocca, Jelena Lukovic, Ali Hosni, Laura Dawson, Teodor Stanescu
University of Toronto, Toronto, ON

Purpose: To investigate an automated pipeline for rapid dosimetric assessment of online adaptive treatments using 3D imaging data acquired during beam delivery on the Unity MR-Linac platform.

Materials and Methods: The MRI-guided online adaptive workflow is complex and resource-intensive. The dose-of-the-day (DOTD) procedure was developed to enhance the Unity system's ability to monitor target position in real-time with an on-demand comprehensive dosimetric assessment. The automated DOTD pipeline was integrated within the scripting environment in RayStation. Input data included adapt-to-shape (ATS) planning data from Online Monaco (3D MR images, contours, dose cloud) and 3D MR images acquired during beam-on (BON) exported from MR console. The analysis sequence relied on a) data import, b) intensity-based deformable image registration (DIR) between ATS and BON image series, b) deformable contour mapping from ATS to BON, c) rigid contour transfer from BON to ATS, d) derivation of dosimetric analytics, and e) generate pdf summary report highlighting clinical goal difference specific to each clinical protocol (1, 3 and 5-fraction SBRT).

Results: The retrospective analysis was performed for 18 liver and pancreas patients and a total 75 treatment fractions. Two expert reviewers evaluated 499 structures to validate the accuracy of DIR process, which was found clinically acceptable. Twenty-four ATS plans were recomputed on BON data in Offline Monaco and the max discrepancy in the dose clouds was found to be within 1% of prescription dose. For the majority of luminal structures, DOTD reported ATS-BON clinical goal values of up to ±50 cGy. The DOTD analysis also detected larger outliers which were not apparent at the time of treatment. Outliers were not found to be correlated with a given fractionation regiment or anatomical structure.

Conclusions: The DOTD pipeline is expected to become an important tool to augment the RT online adaptive workflow. It can also be used to verify pre-treatment setups and inform decision to pass/fail the ATS plan. Furthermore, the dosimetric intra-fraction differences derived by DOTD can be used to develop dose accumulation processes with prospective adaptation of clinical goals prior to each treatment fraction.

68

SEMI-AUTOMATED METHODS FOR ROUTINE QUALITY ASSURANCE FOR OPTICAL SURFACE IMAGING SYSTEMS

Eric Wright, Kaleigh Young
University of British Columbia, Kelowna, BC

Purpose: The American Association of Physicists in Medicine recently released new guidelines for routine quality assurance (QA) of optical surface imaging systems used for surface-guided radiation therapy (SGRT). The purpose of this work was to develop semi-automated methods for performing routine QA for SGRT systems.

WITHDRAWN

Materials and Methods: A styrafoam anthropomorphic head phantom embedded with a 5 mm diameter high density sphere was rigidly affixed onto the 6-dof couch of a linac equipped with an SGRT system. The centre of the embedded sphere was set up at the MV isocentre using portal imaging. Two developer mode scripts were created, one for monthly assessment of dynamic localization accuracy, and one for assessing accuracy of the SGRT system at non-zero couch rotations (yaw) with and without camera blockage from the gantry head. Matlab scripts were created to automatically synchronize and assess trajectory log files and SGRT log files to determine results of the QA tests. The dynamic localization accuracy script took an MV image in the starting position before translating the couch laterally, longitudinally, and vertically by ±1cm and ±5cm, and taking an MV image after each translation, then yaw, roll, and pitch were varied by ±3° in 0.5° increments. Translations reported by trajectory log files and SGRT were compared against translations measured by finding the difference in the position of the centre of the embedded sphere in MV images. Rotations were compared between trajectory log files and SGRT. The script for assessing accuracy at non-zero couch angles with and without camera blockage took an MV image in the starting position, then rotated the couch to ±45° and 90°, took an MV image, and then rotated the gantry to block one of the SGRT camera pods. Couch walkout was estimated from MV images at each couch angle. The difference between SGRT-reported translations and couch walkout was recorded, both with and without the linac head blocking one of the SGRT camera pods.

Results: Dynamic localization accuracy was found to be within ±1mm in three experiments. Maximum deviations from the expected translations in MV images and SGRT log files were -0.9mm and -0.8mm respectively. Maximum deviations from expected rotations in identify log files were 0.2°. SGRT system error at non-zero couch angles was found to be within ±0.5mm in three experiments. Without blockage of SGRT cameras by the linac head, average SGRT error was between 0.2mm and 0.3mm depending on couch angle. With camera blockage, average SGRT error ranged between 0.1mm and 0.5mm depending on the couch angle.

Conclusions: Semi-automated methods have been developed for routine quality assurance assessing dynamic localization accuracy of SGRT systems, and SGRT system accuracy at non-zero couch angles with and without camera blockage. With further improvement these methods could be an efficient and standardized way of performing routine QA on these systems.

69

EXPERIMENTAL VALIDATION OF A NOVEL METHOD OF DOSE ACCUMULATION FOR THE RECTUM

Haley Patrick, Emily Poon, Kayla O'Sullivan-Steben, John Kildea
McGill University, Montréal, QC

Purpose: To experimentally validate the use of dose-surface maps (DSMs) as an alternate means of performing dose accumulation for the rectum.

Materials and Methods: A custom PVC rectum phantom capable of representing typical rectum interfraction motion and filling variations was constructed for this project. The phantom allowed for the placement of EBT3 film sheets on the representative rectum surface to measure rectum surface dose. A multi-fraction prostate VMAT treatment was designed and delivered to the phantom in a water tank for a variety of interfraction motion scenarios. DSMs for each fraction were calculated using CBCT images acquired during delivery and summed to produce accumulated DSMs. Accumulated DSMs were then compared to film measurements using gamma analysis with a criteria of 3% global dose, 2 mm, and a 10% dose threshold. Film measurements were also compared to DSMs produced by deformable image registration (DIR) based dose accumulation (MIM Maestro) to allow for a comparison of our DSM-based dose accumulation to the conventional approach.

Results: Baseline agreement between film measurements and accumulated DSMs for a stationary rectum was 95.6%.

Agreement between film and accumulated DSMs in the presence of interfraction motion and filling variations were 94.9% and 98.1%, respectively. In comparison, DIR-based DSM agreement with film measurements for these scenarios were 38.9% and 75.5%, respectively.

Conclusions: To the best of our knowledge, this is the first time that the validity of DSM-based dose accumulation has been tested experimentally. DSM-based dose accumulation has very good agreement with physical measurements and is a viable means of accumulating rectum dose that may outperform conventional DIR-based dose accumulation for rectum structures.

70

ACTIVE SURFACE MONITORING FOR REAL-TIME CLINICAL GUIDANCE DURING PELVIC ADAPTIVE RADIOTHERAPY

Timothy Keiper[1], Grace Gwe-Ya Kim[1]
University of California San Diego, La Jolla, CA

Purpose: Active surface monitoring (ASM) facilitates real-time observation of the patient providing fidelity in treatment delivery during adaptation. Correlation between intrafraction motion determined by ASM and verification cone-beam CT (CBCT) is investigated to develop decision criteria to reduce patient imaging dose and treatment time.

Materials and Methods: The ring-mounted surface monitoring system was commissioned on a closed-bore linac capable of CBCT-driven adaptive radiotherapy. A clinical workflow was developed to include ASM during adaptation, and six degree-of-freedom monitoring was implemented for nine patients undergoing adaptive radiotherapy of the pelvis over 104 total fractions. Every fraction consisted of an initial CBCT for adaptation and a verification CBCT before treatment delivery. For ASM, a region of interest was selected on the lower abdomen by the radiation therapists. To determine the underlying drift of the surface for comparison to the intrafraction shifts observed after verification CBCT, adjacent averaging using a 20 s window was applied to the motion curves. Receiver operating characteristic (ROC) curves and the corresponding area-under-the-curve (AUC) values are used to propose clinical thresholds where ASM drift is indicative of patient motion.

Results: The in-bore system performed as expected using the clinical workflow for ASM for pelvic adaptive radiotherapy lasting on average 18 minutes. ROC analysis revealed that drift of the translational 3D magnitude motion was indicative of patient motion using a CBCT threshold of 1.5 mm (AUC = 0.59) and non-sensitive to patient motion when 1 mm (AUC = 0.50) or 2 mm (AUC = 0.45) thresholds were used. A threshold of 1.5 mm magnitude shift on verification CBCT showed that specific motion axes yielded AUC > 0.50 for longitudinal (0.53) motion while all others showed AUC < 0.50. The Euclidean minimum distance from the top left of the ROC curve corresponds to an ASM threshold value of 4.75 mm.

Conclusions: The relationship between ASM data and patient motion for pelvic adaptive radiotherapy is complicated by breathing motion, organ filling, and large relative distances from the surface to the internal targets. Using a limited initial dataset and ROC analysis, we propose that monitoring the translational magnitude motion could be used to indicate cases where patient motion requires the acquisition of a verification CBCT during adaptive radiotherapy of the pelvis. Site-specific guidelines for ASM could support the reduction of margins and normal tissue sparing by identifying patient motion during adaptation after thorough analysis.

71

MODELLING THE 6-DOF RESPIRATORY MOTION OF THE HEART IN CARDIAC RADIOSURGERY USING MULTI-LEAD TRACKING

Jakob Marshall[1], Alanah Bergman[2], Tania Karan[2], Marc Deyell[3], Devin Schellenberg[2], Richard Thompson[4], Justin Poon[1], Steven Thomas[2]
[1]*University of British Columbia, Vancouver, BC*
[2]*British Columbia Cancer, Vancouver, BC*
[3]*University of British Columbia, Vancouver, BC*
[4]*University of Alberta, Edmonton, AB*

Purpose: To evaluate the utility of tracking multiple cardiac leads for developing a respiratory motion model of the heart for application in respiratory tracking in Cardiac Radiosurgery (CaRS).

Materials and Methods: Bi-planar fluoroscopy, acquired at 5 Hz, was used to image the position of cardiac leads under free breathing conditions for 15-20 seconds. Data was acquired for two patients considered for CaRS. A number of points on the cardiac leads was tracked in 3D using an in-house program. The points were divided into two categories: (i) motion model creation points, and (ii) evaluation points. The motion model creation points were the leads from the cardiac resynchronization device in the right atrium, right ventricle, and on the left ventricle. The evaluation points were two additional electrodes along the left ventricular lead. Additionally, patient 1 had two extra evaluation points on the left ventricular lead and one on an independent right ventricular lead. The respiratory component of the lead motion was extracted using a low-pass filter with a cut-off frequency determined using the patient's heart rate and respiratory rate during image acquisition. Using the motion model creation points two models were created: (i) a model accounting for translations only and (ii) a model accounting for translations and rotations. Translations were computed based on the centre of mass displacement and rotations were determined using singular value decomposition (SVD). The error in each model was calculated as the magnitude of the 3D vector displacement between the predicted position from the model and the actual position. For comparison, the error in using no model was calculated as the magnitude of the 3D displacement for each lead.

Results: The average error between the predicted and actual position of the evaluation leads under free breathing conditions was 3.31±0.08 mm with no motion model, 2.6±0.6 mm with a model considering translations only, and 1.1±0.3 mm with a model considering both translations and rotations. Furthermore, the maximum positional error was 10.5±1.4 mm with no motion model, 6.1±1.1 mm with a model considering translation, and 2.3±0.5 mm with a model considering translations and rotations. These results suggest that accounting for rotational movement is required to accurately model the motion of the heart through respiration.

Conclusions: Based on the analysis of two patients, our results suggest that multi-lead tracking can be used to create a 6-DoF respiratory motion model of the heart. This information can be used to reduce planning margins for potential dynamic target tracking applications in CaRS. Further analysis on a larger dataset is warranted to validate the results of this study.

72

A DEEP LEARNING APPROACH TO TUMOUR MOTION FORECASTING FOR SURFACE GUIDED RADIATION THERAPY BASED ON VOLUMETRIC 4D-CT

Timothy Yau, Ting-Yim Lee, Stewart Gaede
Western University, London, ON

Purpose: During real-time tumour tracking, high accuracy and precision is required to ensure the tumour does not move outside the field of radiation. However, prediction algorithms must incorporate the machine's inherent latency to prevent the radiation beam from lagging behind the true tumour position. Our aim was to investigate the feasibility of a deep learning workflow based on volumetric 4D-CT (v4D-CT) for generating patient-specific tumour prediction models for implementation of non-invasive dynamic tumour tracking with surface guided radiation therapy (SGRT).

Materials and Methods: Time series v4D-CT images were acquired for four patients with a 1 6cm axial field of view and 280ms temporal resolution for 35 to 45 seconds at a single table position. Each voxel along the chest surface was tracked overtime along the anterior-posterior axis to generate a surface breathing curve. The chest respiratory trace was divided into a 70%-30% train-test split and trained using a combination of recurrent neural network (RNN) layers and fully connected layers to predict the centroid of the gross tumour volume (GTV) 280ms ahead. Chest position and velocity were used as model inputs, with the model hyperparameters optimized per patient using the hyperband algorithm for fast convergence and evaluated using root mean squared error (RMSE). Multiple instances of the model were trained simultaneously and the averaged response of the ensemble was taken for evaluation.

Results: RMSE values for forecasted GTV centroids from the ensemble were 0.37-0.80 mm, 0.67-0.78 mm, and 0.25-0.60 mm in the left-right, anterior-posterior, and superior-inferior direction respectively. Averaged ensemble predictions decreased RMSE values by 0.05-0.8 mm in each direction over individual models.

Conclusions: v4D-CT combined with deep learning algorithms is capable of generating accurate, patient-specific tumour motion prediction models from a limited sample of time points for markerless tumour tracking with SGRT.

73

HYPOFRACTIONATED RADIOTHERAPY FOR HEMATOLOGICAL MALIGNANCIES DURING COVID-19 PANDEMIC AND BEYOND

Febin Antony[1,2], Arbind Dubey[2,1], Pascal Lambert[1], Pamela Skrabek[1,2], Naseer Ahmed[1,2]
[1]*CancerCare Manitoba, Winnipeg, MB*
[2]*University of Manitoba, Winnipeg, MB*

Purpose: Conventionally fractionated radiotherapy (RT) has shown to have excellent local control in hematological malignancies (HM). Up to date there is none or scant literature about the use of hypofractionated radiotherapy (HFRT) for the treatment of HM, this single institution study analyzed the efficacy of HFRT in HM. We hypothesized that HFRT in HM will result in a similar local tumour control that has been reported with standard fractionated RT.

Materials and Methods: In this retrospective study, we analyzed the data from patients within the provincial cancer registry diagnosed with HM treated with a curative intent using HFRT regimens suggested by International Lymphoma Radiation Oncology Group between 2020-2022 during the COVID-19 pandemic. Primary outcome of the study was overall response rate (ORR), measured as complete response (CR), partial response (PR) or stable disease (SD) within the irradiated field determined radiologically or clinically post completion of RT. Secondary end point was freedom from local progression (FFLP), calculated from the date of initiation of RT to the first date among in-field progression, death, and last follow-up. Summary statistics were used to describe cohort and treatment characteristics. FFLP was calculated by 1 minus cumulative incidence accounting for competing risk (i.e., death).

Results: Of the 36 patients included for analysis, 18 were aggressive non-Hodgkin lymphoma (NHL), nine were indolent NHL, six were Hodgkin lymphoma (HL) and three were other HM. Among them 25 had consolidation RT and 11 had definitive RT. HFRT daily dose per fraction ranged from 2.67 Gy to 5 Gy and total dose regimens ranged from 18 Gy to 42.5 Gy in 6 - 17 fractions and median equivalent dose in 2 Gy fractions (EQD2) for alpha/beta = 10Gy was 36 Gy (±7.5). ORR for the entire cohort was 94.4%. With a median follow up of 13.2 months, FFLP at one year for the entire cohort was 91.5% and death without infield progression was 8.7%. Among the four patients who had in radiation field recurrence, two had aggressive NHL and two had HL. No Grade 3 or 4 acute toxicities were reported.

Conclusions: This retrospective study using HFRT showed an ORR and FFLP comparable to historical studies using standard fractionation. Further long-term follow-up is warranted to confirm these findings.

74

HYPOFRACTIONATED PREOPERATIVE RADIOTHERAPY 30GY IN 5 FRACTIONS FOR SOFT TISSUE SARCOMA OF THE EXTREMITY

Rie Asso[1], Fabio Cury[1] , Constanza Martinez[1], Neelabh Rastogi[2] , Paul Ramia[1], Carolyn Freeman[1]
[1]*McGill University Health Centre, Montréal, QC*
[2]*McGill University, Montréal, QC*

Purpose: Hypofractionated preoperative radiotherapy (HypoRT) is being used with increasing frequency for soft tissue sarcomas (STS) of the extremities. Besides the social and economic advantages, HypoRT has a theoretical advantage in STS because of their low α/β ratio. The objective of this study is to review our experience using HypoRT to a dose of 30Gy in 5 fractions in STS of the extremities.

Materials and Methods: This study is a retrospective review of patients with extremity STS treated at our centre with preoperative HypoRT to a dose of 30Gy in 5 fractions given on alternate days over two weeks. Inclusion criteria were age ≥18 years, biopsy-proven primary STS in an extremity, and fitness for surgery. The primary endpoint was major wound complications (MWC) defined as the need for wound management or secondary operation under general or regional anesthesia within 120 days from surgery. Secondary objectives were: early toxicity Grade ≥ 2 and clinical outcomes, including local control (LC), and metastasis-free survival (MFS). Descriptive statistics were used to evaluate patient and treatment characteristics. The Kaplan-Meier method was used to estimate survival.

Results: A total of 40 patients received preoperative HypoRT at our centre between 2016 and 2022. The median age was 70 years (30 - 91). Males accounted for 57.5% of the patients. The most common primary site was the lower extremity (62.5%). The most prevalent histologic type was myxofibrosarcoma (27.5%), followed by pleomorphic spindle cell sarcoma (20%). All patients were treated with image-guided intensity modulated radiotherapy with margins for the CTV as tested in the RTOG 0630 study. Median follow-up was 14.8 months (5 - 86). Acute side effects were seen in 80% of the patients, all Grade <3. The most common toxicity was dermatitis (37.5%), the second was fatigue (20%), and the third was pain (15%). Surgery was performed in all cases after a median interval from completion of HypoRT of 34 days (16-59). Amputation was performed in one patient with a fungating tumour, HypoRT having been aborted at only 24Gy because of worsening symptoms. On pathologic examination, positive margins were found in four cases (10%). The percentage of necrosis was ≥ 90% in seven patients and 50%-90% in 10. MWC occurred in 13

patients (32.5%), including 10 who underwent a procedure with anesthesia. Sixteen patients were treated for a wound infection. Only one patient recurred locally. Two-year LC was 91.7%. MFS was 87.4% at six months and 60.8% at two years**.** DFS was 84.9% at six months and 64.8% at two years.

Conclusions: The preoperative HypoRT regimen of 30Gy in 5 fractions given on alternate days for extremity STS is safe. Acute toxicity was not different from our previous experience using the conventional regimen of 50Gy in 25 fractions over five weeks and the MWC rate was comparable to that reported for the conventional regimen. Local control was excellent.

75

HEATMAPS TO ASSESS TUMOUR MOTION PROBABILITY WITH MRCINE IN HEAD AND NECK CANCER

Adam Mutsaers, Yonatan Weiss, Lee Chin, Ian Poon, Andrew Bayley, Geordi Pang, Angus Lau, Irene Karam
University of Toronto, Toronto, ON

Purpose: Intrafraction motion affects, including respiration and deglutition, can affect tumour position during radiation for head and neck cancers (HNC) and can be assessed using magnetic resonance cine (MR-cine). Heatmaps – a visual representation of patient specific temporal tumour location akin to internal target volume (ITV) from a 4DCT- were analyzed to demonstrate the variation in motion between primary oropharyngeal (OP) and laryngeal/hypopharyngeal (LH) sites and provide insight towards the need for personalized margins.

Materials and Methods: MR-cine patient (900-1500 slices, sagittal orientation, 2x2x7 mm^3 resolution, across 3-5 minutes per patient) were acquired for LH and OP HNC patients as part of simulation protocol. Gross target volumes (GTVs) were contoured for each frame then integrated over the entire scan to create a heatmap displaying the most probable GTV location in time. Next, a baseline contour representing the average tumour rest position was expanded both isotropically and directionally in 1 mm increments in a novel analysis to define the contribution of each margin increment on target coverage. Histograms demonstrating the proportion of scan time the tumour was within each target expansion were generated for each patient to determine required motion margins for 25% - 95% target coverage. To assess directional dependence, displacements from rest position were evaluated in 4 planes from centroid: (A) 12 o'clock (OC) to 6OC (capturing volumetric shift in a portion of superior, posterior and inferior directions), B) 3OC-9OC, C) 6OC-12OC, D) 9OC-3OC. Wilcoxon-rank-sum test was performed to compare motion by site.

Results: Motion was evaluated in 66 patients (LH n=27, OP n=39). In LH, a median (med) isotropic expansion of 8.5 mm was required to achieve 95% target coverage. This group exhibited a large variation in motion margins with a minimum (min) of 2.8mm and maximum (max) of 23.5mm. Smaller differences were observed for OP with med: 5.3mm, min:1.9mm and max: 14.6mm. At 75%, 50% and 25% coverage, expansions for LH (med:4.8 min: 1.9 max: 17.3; med: 3.8 min: 1.2 max: 12.9; med: 3.3, min: 0.6, max: 9.3, respectively) were not significantly different than OP (med: 3.8, min: 1.7, max: 10.9; med: 3.1 min: 1.3, max: 9.4; med: 2.1, min: 0.7, max: 8.4), suggesting larger but infrequent shifts in LH. Directional tumour displacement varied widely further indicating a need for patient specific assessment of motion. Significant differences ($p<0.05$) were noted between LH and OP in median displacement in C and D planes to achieve 95% coverage temporally.

Conclusions: This study indicates a wide range of GTV motion between and within HN sub-sites that is not captured on CT simulation. Moving forward, motion based heatmaps derived from MR-cine may serve as a visualization tool for ITV contouring or analyzed to derive personalized motion margins.

76

A NOVEL STRATEGY TO ENHANCE RADIOTHERAPY EFFICACY: RESULTS FROM THE PROSPECTIVE PHASE I CLINICAL TRIAL OF MR-GUIDED FOCUSED ULTRASOUND-STIMULATED MICROBUBBLES (MRgFUS+MB) TREATMENT FOR BREAST CANCER

Daniel Palhares, Archya Dasgupta, Murtuza Saifuddin, Ling Ho, Lin Lu, Maria Lourdes Anzola Pena, Shopnil Prasla, Ewa Szumacher, Edward Chow, Danny Vesprini, Irene Karam, Hany Soliman, Arjun Sahgal, Gregory Czarnota
University of Toronto, Toronto, ON

Purpose: Preclinical studies have demonstrated that tumour cell death can be enhanced 10- to 40-fold when radiotherapy (RT) is combined with focused-ultrasound (FUS)-stimulated microbubbles (MB) treatment. MBs are gas microspheres used as intravascular contrast agents. The acoustic exposure of MBs within the target volume causes bubbles cavitation that induces perturbation of tumour vasculature. This activates apoptotic pathways responsible for the ablative effect of stereotactic body radiotherapy, which would otherwise require high-dose radiotherapy (>8-10 Gy/fraction) to be activated. Subsequent irradiation of MB-sensitized tumour causes increased anoxic tumour killing, which occurs in addition to canonical RT-induced DNA damage. Given the compelling results of preclinical data, we conducted a phase I clinical trial of magnetic resonance (MR)-guided FUS-stimulated MBs (MRgFUS+MB) treatment for breast cancer. We report the safety and efficacy results of this new radioenhancement treatment.

Materials and Methods: This is a single-centre, single-arm, investigator-initiated phase 1 clinical trial (NCT04431674). We included patients with Stage I-IV breast cancer with tumour in situ for whom breast/chest wall RT was deemed adequate by a multidisciplinary team. Patients were excluded if they had contraindications for contrast-enhanced MR or MB administration. Patients underwent 2-3 MRgFUS+MB treatments throughout the RT course. We used an MR-coupled FUS-device operating at 500 KHz and 540 kPa peak negative pressure to deliver the treatment. The FUS sonicated intravenously administrated MB within the MR-guided target volume. Pts were monitored for 30-min post-procedure and subsequently treated with RT. The primary outcome was acute toxicity per CTCAEv5.0. Secondary outcomes were radiological response at three months and local control (LC) at one year. Kaplan-Meier method was used to estimate local control. All patients signed a written consent form before study participation.

Results: We enrolled 18 female patients with 20 primary breast cancer treated with MRgFUS+MB therapy. Median age was 60 years (range, 44-90). Molecular subtypes consisted of basal-like (15%, n=3/20), luminal (55%, n=11/20), and HER2-enriched (30%, n=6/20). Prescribed dose was 20 Gy/5 fractions (40%, n=8/20), 30-35 Gy/5 fractions (35%, n=7/20), 30-40 Gy/10 fractions (15%, n=3/20), and 66 Gy/33 fractions (10%, n=2/20). The median follow-up was nine months (range, 0.3-29). All patients completed the planned MRgFUS+MB treatments. The only MRgFUS+MB treatment-related toxicity consisted of Grade 1 allergic reaction (mild cough) 30 minutes after the last MB injection. Radiation dermatitis was the most comom toxicity, being Grade 1 in 70% (n=14/20), Grade 2 in 10% (n=2/20), and Grade 3 in 10% (n=2/20) of patients. At three months, 75% had partial (n=6/20) or complete (n=9/20) response, with a single progression. The one-year LC rate was 86%.

Conclusions: MRgFUS+MB was a safe and efficient treatment that provided durable responses.

77

SINGLE PRE-OPERATIVE RADIATION THERAPY (SPORT-CK) TRIAL FOR LOW-RISK BREAST CANCER: EARLY RESULTS OF A PHASE 2 STUDY

Dima Mahmoud[1], Leticia Alvarado[1], Christine Lambert[1], Sarkis Meterissian[1], Michael Yassa[2], Francine Tremblay[1], Naim Otaky[1], John Keyeserlingk[1], Valerie Panet-Raymond[1], Neil Kopek[1], Marc David[1], Marie Duclos[1], David Fleischer[1], Ari Meguerditchian[2], Antoine Loutfi[1], Tarek Hijal[1]
[1]McGill University, Montréal, QC
[2]University of Montréal, Montréal, QC

Purpose: Pre-operative partial breast irradiation (PBI) is a novel technique that can be used in patients with early-stage breast cancer with the goal of limiting the irradiated breast volume, toxicity and number of treatment sessions. The aim trial is to assess the toxicity, surgical complications, and oncologic and cosmetic outcomes of pre-operative PBI.

Materials and Methods: In this single-centre phase II, single-arm trial, we enrolled elderly women (age ≥ 60), with unifocal low-risk, early-stage breast invasive ductal carcinoma (cT1N0, grade 1 and 2, ER positive, Her2 negative, without LVI on biopsy). Patients were treated with 20 Gy in single fraction of pre-operative PBI using volumetric modulated arc therapy (VMAT). Patients then underwent breast-conserving surgery (BCS) +/- sentinel lymph node biopsy within 72h from radiation. Patients with positive surgical margins underwent margin re-excision. Adjuvant whole breast or locoregional irradiation was indicated for several unexpected pathologic findings such as tumour > 3cm, Grade 3 disease, positive lymph nodes or if final pathological margins were < 1mm. Patients were assessed for surgical complications, cosmetic outcome, and local recurrence on post-operative days 7-8, 14, and then at three, six, and 12 months for the first year and then annually for 10 years. Primary outcomes were rate of surgical complications and early toxicity. Secondary outcomes were cosmesis at 12 months, chronic toxicity and ipsilateral breast tumour recurrence.

Results: Twenty-five patients were recruited with a median age of 67 (range 60-81), and a median follow-up of 40 months (6-72). Mean size of the lesions was 10.6 mm. Sentinel LN biopsy was done for 24 patients (96%) and only one was positive (4%). On final pathology 15 patients had Grade 1 (60%) and 10 had Grade 2 (40%) disease. Nineteen patients had negative margins of at least 1 mm (76%), four patients had close margins of <1 mm (16%), one had positive margins for invasive disease (4%) and another positive for DCIS (4%). Surgical margin revision was done for five patients (20%). Two patients received adjuvant radiation therapy (one loco-regional, and one breast only). Within the first 90 days, none of the patients had surgical complications such as wound infections or healing delays and almost all had G0-1 acute toxicity. There were no local, regional or distant recurrences. All patients had Grade 0 to 1 late RTOG skin toxicity except for one with G2 telangiectasia seen on the five-year follow-up, one with induration and fibrosis at the surgical bed seen at two and three years, and one patient with breast edema seen in the first three years only.

Conclusions: Pre-operative PBI is a safe and feasible treatment for elderly patients with low-risk early-stage breast cancer, with no surgical complication and very low rates of acute and late radiation toxicity. Randomized controlled trials are needed to compare pre-operative to adjuvant PBI in this patient population.

78
CARDIAC SBRT FOR THE TREATMENT OF VENTRICULAR TACHYCARDIA

Matthew Volpini, Katie Lekx-Toniolo, Calum Redpath, Andrew Crean, David Tiberi, Graham Cook
The Ottawa Hospital, Ottawa, ON

Purpose: Ventricular tachycardia (VT) is commonly treated with antiarrhythmic medications and invasive cardiac ablation procedures to reduce the risk of recurrence and sudden cardiac death. Despite these therapies, however, some patients sustain recurrence of their VT. Advances in non-invasive cardiac arrhythmia mapping have allowed for the delivery of stereotactic body radiotherapy (SBRT) as a means for cardiac radioablation in the treatment of patients with treatment-refractory VT.

Materials and Methods: In this retrospective study, we report on thirteen patients with treatment refractory VT treated with SBRT—25 gray in a single fraction while awake. Treatment volumes were defined by arrhythmogenic scar regions identified on electocardiographic studies, which were subsequently visualized on treatment planning computed tomography (CT) imaging. SBRT simulation, planning, and treatment delivery were completed in accordance with our centre's standard techniques. Efficacy was assessed by totalling the number of VT episodes as recorded by implantable cardioverter-defibrillator (ICD) device. Adverse events were assessed based on clinical follow up with serial cardiac and thoracic imaging.

Results: From March 2020 to January 2023, 13 patients underwent treatment. In the three months prior to treatment patients sustained an average of 19.2 episodes of VT per month. During the six-week post-ablation "blanking period" (time during which arrhythmias can occur due to post-treatment myocarditis) patients sustained an average of 6.7 episodes of VT per month. Following the six-week blanking period, patients sustained an average of just 1.4 episodes of VT per month, a reduction of 92% from pre-treatment baseline. All patients achieved a reduction in their rate of VT episodes. One patient (8%) with history of amiodarone-related pulmonary fibrosis sustained radiation pneumonitis and was successfully treated with a tapering course of oral steroids. Subsequent CT thorax imaging confirmed resolution of this adverse event. The mean ejection fraction was unchanged post treatment for our cohort. There were no deaths due to treatment.

Conclusions: Thirteen patients with treatment refractory VT experienced a marked reduction in the number of VT episodes following SBRT treatment. The safety profile was acceptable, with a single case of radiation pneumonitis.

79
VIRTUAL MENTORING FOR MEDICAL PHYSICISTS: GUIDANCE PROVIDED BY A GLOBAL ONLINE PERCEPTIONS SURVEY

Jacob Van Dyk[1], Matt Jalink[2], John Schreiner[2], Robert Jeraj[3]
[1]Western University, London, ON
[2]Queen's University, Kingston, ON
[3]University of Wisconsin, Madison, WI

Purpose: Medical physics education, training, and continuing professional development are restricted in some parts of the globe, especially under conditions of limited resources, and where availability of experienced medical physicists is sparse. Support organizations might enhance training by developing virtual mentoring programs aimed at assisting clinical physicists or trainees seeking to improve their competences. To optimize such virtual mentoring programs, a survey was developed to address questions related to the best approach to virtual mentoring, methods of matching mentors and mentees, and challenges and successes affecting the mentoring process.

Materials and Methods: The survey was approved by a university research ethics board. It was established using the general concepts of survey design including literature review, focus groups, employing validated questions, and pilot testing. The survey was designed to establish feedback on mentorship issues such as: factors and barriers influencing successful mentoring; preferences for matching mentors/mentees; frequency and length of meetings; the importance of defining clear expectations; having

a formal agreement; and for ongoing assessment of the success of the mentoring process. The survey invitations were sent out to multiple national and international medical physics organizations, medical physics list servers, and professional contacts.

Results: There were 396 responders (68% male and 32% female) from 76 countries [65% from high-income countries (HICs) and 35% from low-and-middle income countries (LMICs)]. Forty-three percent of responders reported little experience and 38% reported a lot of experience as mentors, while 53% had a little experience as a mentee and 23% a lot. Eighty-three percent were interested in participating as mentor, or mentee, or both. Responses from HICs were compared to those from LMICs. LMIC responders were generally younger with less work experience. Differences between LMIC and HIC responses occurred when looking at the perceived limitations and barriers to virtual mentoring. Regarding virtual mentoring specifics, preferences were given to meeting once every 2-4 weeks for 30-60 minutes to discuss and help solve specific problems, to address clinical questions, and to address specific clinical implementation procedures. Ninety-seven percent felt it was important to have clear expectations formalized at the initiation of the mentoring process.

Conclusions: The survey provides significant assistance in optimizing the global virtual mentoring process, especially for volunteer organizations seeking to advance medical physics education and training in environments with limited resources. The results are applicable to both HIC and LMIC contexts. The survey results may also have relevance to the radiation oncology and radiation therapy communities.

80

VIRTUAL REALITY SIMULATOR FOR LINAC SAFETY TRAINING

Varlukhin Anton[1], Geordi Pang[2,3], Syed Bilal Ahmad[4], Humza Nusrat[2]
[1]*Toronto Metropolitan University, Toronto, ON*
[2]*Sunnybrook Health Sciences Centre, Toronto, ON*
[3]*University of Toronto, Toronto, ON*
[4]*Thunder Bay Regional Health Sciences Centre, Thunder Bay, ON*

Purpose: Training new staff on safe linear accelerator (linac) operation can be time consuming and lead to significant strain on staff. Increased teaching workload can potentially lead to poor training, which can result in unsafe linac operation. The goal of this work is to develop a virtual reality (VR) simulator that will aid in new staff teaching. Once new staff pass through the VR simulator, their in-person training can be streamlined to reduce training time and workload demands on staff.

Materials and Methods: The VR simulator was developed in Unreal Engine 5.0 (Epic Games; Maryland, USA), utilizing the Oculus Quest 2 headset (Meta; Cambridge, USA). In addition to the linac model and treatment bunker, the simulator models important linac safety features including interlocks, beam on/off signage, last-person out (LPO) buttons, emergency beam-off buttons, and audio/visual equipment. The modeling was done by conducting a detailed survey of a treatment room at the Odette Cancer Centre, Sunnybrook Hospital (Toronto, Canada) and replicating it into a 3D model using Blender (Blender; Netherlands). The simulator was evaluated by 13 staff volunteers who were surveyed with Likert scale questions before and after using the simulator. Participants were given a task to complete in the simulator: conducting six safety tests and turning the beam on.

Results: The mean time required to complete the task was 5.5 minutes. After going through the simulator, users felt strongly that VR training could be used to reduce staff training burden (Likert scale increase of 3.0 to 3.5). Additionally, the majority of users felt that it was a realistic representation of a treatment bunker.

Conclusions: VR has the potential to augment new staff training on the safe operation of linacs. In this work, a VR simulator was developed and evaluated. Future work involves improving the accuracy of the simulator with respect to sound and user movement.

81

THE DEVELOPMENT AND IMPLEMENTATION OF SIMULATION-BASED INTER-PROFESSIONAL EDUCATION FOR RADIATION ONCOLOGY AND MEDICAL PHYSICS RESIDENTS IN RADIATION THERAPY SAFETY EVENTS

Michelle Nielsen[1], Andrew Bayley[1], Jay Detsky[1], Nicole Harnett[2], Andrea McNiven[2]
[1]*Odette Cancer Centre, Toronto, ON*
[2]*Princess Margaret Cancer Centre, Toronto, ON*

Purpose: The aim of this work was to develop a multi-disciplinary education module for medical physics (MP) and radiation oncology (RO) residents. Incidents and disclosure experience can be difficult to integrate into clinical training logistically due to the sporadic timing and variable severity, and the sensitivity and potential urgency is not well-suited for incorporating learners at the time of occurrence. The module combines didactic teaching and a simulation-based learning activity to help the residents gain clinical competencies related to incident investigation in the multi-disciplinary radiotherapy environment. Specifically for the RO residents, the module was also designed to allow for the assessment of the entrustable professional act (EPA) on managing medical errors and adverse events.

Materials and Methods: A two-day module (two half days and a full day simulation) was developed to immerse residents in incident investigation. The inter-professional component of this module is intended to provide the residents with a greater appreciation of roles and expertise in the clinical environment and their respective responsibilities for incident analysis as they completed the investigation in small inter-professional groups. A survey was designed, adapted from previously validated tools, to query the learners' perceptions of their own understanding of 12 concepts and their ability to apply them in practice on a scale of 1-10 (e.g. incident reporting, incident analysis, error mitigation). This was administered pre- and post- activity to assess the efficacy of this learning activity, and to inform future quality improvement.

Results: Didactic components of the course, as implemented, included incident investigation frameworks, patient disclosure, quality tools and just culture. The incident in the simulation was adapted from multiple actual reported events and scenario material was developed to mimic clinical information or resources that would be available to an investigation team. The simulation activity included staff interviews, chronology creation, dosimetric impact assessment (MP resident), disclosure of the incident to a standardized patient (RO resident), and identification of contributing factors and generation of possible recommendations. Twelve second year residents (four MP and eight RO) participated in the full activity, 13 pre- and seven post-activity surveys were completed. There was an improvement in average score reported by the learners for each item in the survey, with average scores improving by 1.5-3.5 marks. This indicates that the activity did improve the learners understanding or gave them more confidence that they would be able to apply this knowledge in practice. Free-form comments indicated appreciation of the ability to observe and learn from the other discipline.

Conclusions: A novel simulation-based learning activity has been successfully developed and implemented to support the competency based education of RO and MP residents. Early results indicate that the simulation improved the learners' confidence and that they valued the interprofessional nature of the activity.

Future work will explore the incorporation of radiation therapy trainees and assessment of competencies for the MP residents. EDI related competencies could also be incorporated in the simulation framework.

82

FUTURE-PROOFING THE RADIATION THERAPY WORKFORCE: THE PROMISE OF AN MR-INTEGRATED RADIATION THERAPY TRAINING PROGRAM

Darby Erler[1,2], Nicole Harnett[2,3], Ruby Bola[1], Mikki Campbell[2], Laura D'Alimonte[2,4]
[1]*Sunnybrook Health Sciences Centre, Toronto, ON*
[2]*University of Toronto, Toronto, ON*
[3]*Princess Margaret Cancer Centre, Toronto, ON*
[4]*Windsor Regional Hospital, Windsor, ON*

Purpose: Due to the superior soft-tissue contrast of Magnetic Resonance Imaging (MRI), Radiation Therapy (RT) departments across the globe continue to invest in MRI simulators and integrated MRI-guided treatment delivery systems. The adoption of MRI into the RT workflow is not trivial as significant challenges exist extending beyond MRI safety requirements including the imaging literacy of Radiation Therapists (RTTs). As technology advances, there is a need for RTTs to increase their expertise and for departments to "future proof" their workforce. Initially, MRI training for RTTs was limited to two-year diagnostic certificate programs, which require excessive time commitment and lack an RT focus. The purpose of this work was to design an education program specifically for RTTs to acquire the knowledge, skills and judgement to safely operate MRI within a therapeutic oncology context and rigorously evaluate the beta cohort.

Materials and Methods: Curriculum design was informed by the findings of a modified Delphi study that identified the core competencies required to safely operate MRI in the RT setting. Once program goals were articulated, an international, interprofessional advisory group undertook a curriculum mapping exercise. The inaugural cohort of seven practicing RTTs started the program in May 2022. Course and program evaluations were executed using a mixed methods approach. Formative evaluations were conducted after each live-session and summative course evaluations were administered post-course to identify areas of successful curriculum design and improvement. Learners were asked to complete a pre- and post-program assessment of their understanding of the core competencies of the program based on a 1 (novice) - 5 (expert) Likert scale to evaluate if the program was successful in supporting the integration of MRI into their practice.

Results: A unique 31-week hybrid program was developed that combined didactic with clinical consolidation through virtual labs and an intensive hospital experience. Course evaluations indicated learners valued instruction from interprofessional, practicing clinicians and that examples from RT practice increased applicability of the learning. The learners revealed they are thinking more critically about the integration of MRI into their practice such as, the direct application of MRI safety and appreciating the trade-offs of MRI. The learners felt they acquired a deeper understanding of MRI language and its' application within RT. The opportunity to practice activities such as screening and managing safety incidents was highly regarded as well as participation in end-to-end workflows. The pre-program assessment was completed by 5/7 learners and post-program assessment by 6/7 learners. Results demonstrated an increase in confidence and experience in integrating safe MRI principles into practice $Mean_{pre}$= 2.2 (SD 1.6), $Mean_{post}$= 3.8 (SD 0.9) and applying safe screening principles $Mean_{pre}$= 1.8 (SD 0.9), $Mean_{post}$ = 4.0 (SD 0.6) as well as their understanding of analyzing MRI image quality $Mean_{pre}$= 2.4 (SD 1.7), $Mean_{post}$ = 3.5 (SD 0.5). All learners will be working with MRI technology at their respective centres as a result of completing this program.

Conclusions: A comprehensive, learner-centred curriculum was designed for RTTs to acquire the confidence and competence to integrate MR-technology into RT practice. Preliminary data suggests this was achieved as the first cohort of learners reported a greater understanding of the core competencies required to safely operate MRI in RT.

83

IMPACT OF THE COVID-19 PANDEMIC ON ACADEMIC PRODUCTIVITY IN ONCOLOGY: A JOURNAL-, CONFERENCE- AND AUTHOR-LEVEL ANALYSIS

Vivian Tan, Andrew Warner, Anthony Nichols, Eric Winquist, David Palma
Western University, London, ON

Purpose: The objective of this study was to determine the impact of the COVID-19 pandemic on academic productivity in oncology as measured by conference abstracts, journal publications and individual authorship trends.

Materials and Methods: Using a reference time frame of 2018 to 2022, we obtained data on the number of abstracts and articles submitted and published from a selection of oncology conferences and journals. To assess individual authorship patterns, we randomly selected 200 articles from 2018 papers (i.e. the 'index paper') and tracked publications over subsequent years for the first or last authors from that paper. Linear time-trend analyses and independent two-sample t-tests were used to assess changes in academic productivity over time, and univariable and multivariable linear regression were used to analyze individual factors predictive of publication rates, including gender, continent, specialty, MD versus non-MD, and career status (early if within five years of training completion versus late for all others).

Results: Data on submitted and published abstracts were available from five and seven conferences, respectively. Both abstract categories demonstrated decreasing values over time but not reaching statistical significance: conference submissions decreased from 15,308 in 2018 to 13,623 in 2022, (p=0.11), and published abstracts decreased from 13,111 to 11,848, respectively (p=0.16). Journal submissions were available from six journals and increased from 14,142 in 2018 to a peak of 20,241 in 2020 (2018 versus 2020: p<0.001), and then declined to 15,650 in 2021. Journal publications (from 10 journals) showed no clear trends over time (p=0.64). For the author-level analysis, of the 200 authors randomly selected, the majority were male (66.5%, n=133), from North America (55.5%, n=111), with an MD degree (80.9%, 131/162) and late career (86.6%, 129/149). The most common specialties included surgery (29%, n=58), radiation oncology (18.5%, n=37), epidemiology/public health (11%, n=22) and medical oncology (10%, n=20). In terms of articles authored per year, there was no linear trend detected (p=0.51), although the mean number of publications per author peaked in 2020/2021 (papers/year for 2018-2022: 18.1, 18.1, 20.1, 21.2, 19.6). On univariable analysis, factors significantly associated with increasing publication rates were male gender, last author position on index paper, late career status, MDs, speciality of surgery or public/health epidemiology, and authors from Asia (all p<0.01). On multivariable analysis, factors remaining significantly predictive were late career status, MDs, surgeons and public health/epidemiologists, and authors from Asia (all p<0.01).

Conclusions: The number of conference submissions/ acceptances trended downward from 2018 to 2022. Journal submissions peaked overall in 2020, but this did not translate to increases in journal publication rates. Disparities in publication trends were found, based on speciality and geographic regions, including a negative impact on early-career researchers. Further research is needed to ameliorate disparities from those disproportionately affected.

84

REMOTE DELIVERY OF A MINDFULNESS-BASED INTERVENTION TO DECREASE STRESS LEVELS AND PROMOTE COPING AMONG HEALTH-CARE WORKERS DURING THE COVID-19 PANDEMIC

Joelle Helou[1], Aisling Barry[2], Philip Ye[3], Fei-fei Liu[3], Colleen Dickie[3], Anet Julius[3], Daniel Letourneau[3], Philip Wong[3], Laura Dawson[3], Mary Elliott[3]
[1]Western University, London, ON
[2]University of Cork College, Cork, IE
[3]University of Toronto, Toronto, ON

Purpose: The COVID-19 pandemic has caused significant stress amongst everyone. Healthcare workers (HCW) in particular, experience substantial stress in these challenging environments. In an effort to find supportive interventions for radiation oncology providers, while respecting the requirements of physical distancing, we proposed the remote delivery of a mindfulness-based intervention (MBI). The primary aim of this study is to determine the association of this intervention with a reduction of perceived stress. Secondary aims are to evaluate the impact on coping and burnout amongst HCW in the Radiation Program (RP).

Materials and Methods: This is a single-centre, single-arm, pilot study. All HCW associated with the RP were eligible. This was a voluntary effort. The intervention - manualized, mindfulness-based group for HCW, entitled Mindfulness-Based Resilience and Well-Being Training, consisted of four one-hour sessions per week for four weeks. From November 2020 to December 2021, six consecutive closed groups MBI were delivered remotely using Zoom. Each group consisted of 5-12 participants and one professional with a background in mindfulness facilitation. The Perceived Stress Scale (PSS), the BriefCOPE questionnaire and the Maslach Burnout Inventory (MBI-HSS) were collected pre-intervention, and at one, four and 12 weeks post-intervention. The PSS is a 10-item scale with scores from 0 to 40: 0-13=low stress, 14-26=moderate stress and 27-40 = high. The Brief-COPE is a 28-item questionnaire designed to determine someone's primary coping styles on the following three subscales: Problem-Focussed Coping, Emotion-Focussed Coping, and Avoidant Coping. The MBI-HSS comprises 22 items pertaining to occupational burnout, and addresses three scales: Emotional exhaustion (EE), depersonalization (DP) and personal accomplishment (PA). Linear mixed effect models with a random intercept to account for the repeated measures were used to assess the change of outcomes over time.

Results: Amongst 43 HCW who expressed initial interest, 33 completed the study. At one-, four- and 12-weeks post-intervention 25, 24 and 21 participants provided completed questionnaires respectively. Time constraint was the main reason for withdrawal and missing data. There was a significant decrease in perceived stress at week one, four and 12 when compared to baseline [mean baseline PSS score: 22.5 ± 4.6, week 1: 18.4 ± 4.9, p=0.002, week 4: 16.8 ± 6.5, p<0.001, week 12: 16.3 ± 6.8, p<0.001]. Overall, seven (21%) participants reported high PSS (27-40) at baseline while none reported high levels at 1 and 12 weeks. Problem focused coping (p=0.02), and active coping (p=0.009) were significantly higher at one week but not at four and 12 weeks. High levels of EE were reported by 45 % of HCW at baseline and 33 % at week 12. The majority of HCW reported low PA levels, suggesting that they did not feel successful with no significant change post intervention.

Conclusions: The remote delivery of a MBI is effective to reduce perceived stress levels and to promote coping across HCWs. Time was a major constraint preventing the participation of HCWs and occupational burnout remain a significant concern. These findings need to be validated in a larger cohort. Meanwhile, it would be valuable for departments to support interventions to help HCWs cultivate skills to meet the demands related to working in healthcare environments beyond the pandemic and develop programs and strategies to prevent occupational burnout.

85

MR DISTORTION ARTIFACT CORRECTION FOR SPINE SABR PATIENTS WITH PEDICLE SCREWS

Andrew K. H. Robertson[1], Keith Wachowicz[2], Teo Stanescu[3], Emma Dunne[1], Mitchell Liu[1], Monty Martin[1], Hannah Carolan[1], Steven Thomas[1]
[1]British Columbia Cancer, Vancouver, BC
[2]University of Alberta, Edmonton, AB
[3]Princess Margaret Cancer Centre, Toronto, ON

Purpose: Stereotactic body radiation therapy (SBRT) delivers high biologically effective radiation doses to metastatic disease with single-millimeter spatial precision that limits dose to nearby OARs such as the spinal cord. Planning of spine SBRT treatments relies on thin-sliced MRI scans registered to the treatment planning CT to accurately delineate within the spinal segment both the tumour to target and the spinal cord to avoid. However, for patients with metal pedicle screws implanted within spinal segments for spine stabilization, the presence of this metal corrupts the MR images and compromises their ability to guide precise SBRT delivery. These MRI metal artifacts arise due to the substantial difference between the magnetic susceptibilities of metal and tissues, creating bends within the magnetic field that result in dark signal loss and bright signal pileup regions near the implants. Geometric distortion artifacts also occur further from the screw, often within the vicinity of the spinal cord. Previous simulations estimated these distortions to be up to 4 mm in spinal cord regions. This reduced reliability in spinal cord localization requires increased margins around the spinal cord and reduces the quality of the SBRT plan. This work describes a post-processing method to correct spatial distortions that can be applied to MRI scans containing pedicle screws.

Materials and Methods: A MATLAB script was created to perform spatial distortion correction of MRI scans containing pedicle screws. MRI image sets, co-registered CT images, and the associated registration file were exported from Eclipse and used as inputs to the MATLAB script. Metal regions were identified using a CT-value threshold (>3071 HU) and known spatial properties of the pedicle screws were used to identify the separate titanium and cobalt-chromium components. A magnetic susceptibility map containing water, titanium, and cobalt-chromium was then created using values of -9, 199.5, and 1003.7 ppm, respectively. This map was then used to calculate the resulting spatial distortions, which were then used to correct the MR images. This MATLAB code was tested on a single set of images of a Lego phantom containing two pedicle screws.

Results: Phantom images show that the corrected MR images exhibit structures that better agree with contours made in the registered CT. At the approximate centre of the pair of pedicle screws, an initial spatial distortion of 3.5 mm (5 pixels) in the horizontal plane of the image is reduced to <0.7 mm (<1 pixel).

Conclusions: Initial work demonstrates the potential of the MR artifact correction method to improve the accuracy of spinal cord contouring in the vicinity of pedicle screws. Future work will focus on translation to patient image sets and a more detailed assessment of the algorithms performance.

86

HIGH-RESOLUTION DEDICATED 3D AUTOMATED BREAST ULTRASOUND WITH COMPLEMENTARY IMAGING FOR POINT-OF-CARE BREAST CANCER SCREENING

Claire Park[1,2], Tiana Trumpour[1,2], Jeffrey Bax[2], Igor Gyacskov[2],

David Tessier[2], Lori Gardi[2], Aaron Fenster[1,2]
[1]*Western University, London, ON*
[2]*Robarts Research Institute, London, ON*

Purpose: Breast cancer screening has reduced mortality through early detection, but there exists a need for more robust, cost-effective, and high-resolution imaging approaches for increased-risk and diverse patient populations, including those with dense breasts. We developed a portable, cost-effective, dedicated 3D automated breast ultrasound (ABUS) system for point-of-care breast cancer screening. Since the 3D ABUS system integrates any commercially available US transducer, the 3D image resolution is limited due to the poor elevational resolution of the transducer. This work describes the dedicated 3D ABUS system and a novel complementary breast ultrasound (CBUS) approach to improve whole-breast image resolution. We evaluated the reconstruction accuracy and resolution in various phantom experiments, then demonstrated its utility in healthy volunteer studies.

Materials and Methods: The dedicated 3D ABUS system contains a rapid-prototype 3D-printed dam assembly that conforms to the patient, an adjustable compression assembly, and a motorized computer-driven 3DUS scanner, adaptable to any commerically available US transducer. The acquisition involves collecting 2D US images at a fixed spatial interval and reconstructing them into a 3DUS image in real-time. To improve resolution, 3D ABUS images are acquired in orthogonal craniocaudal and mediolateral orientations, then combined into a single CBUS image with a spherical-weighted function. The geometric reconstruction accuracy of a single ABUS image was evaluated with linear and volumetric measurements in a 3D grid and tissue-mimicking breast phantom. To evaluate the 3D CBUS approach, resolution analysis was performed with an angular wire phantom and the full width at half maximum (FWHM) resolution was calculated. Dedicated 3D ABUS images were acquired in proof-of-concept healthy female volunteer studies.

Results: Dedicated 3D ABUS imaging was performed in phantoms; and linear measurement errors were 0.06±0.09, 0.05±0.06, 0.15±0.07 mm (N=22 each) in lateral, elevational, and axial US directions, respectively. Volumetric reconstruction error was 1.98±1.34% (N=10) in spherical inclusions of known volumes. FWHM measurements in the 3D CBUS image resulted in increased resolution uniformity, compared with original orthogonal ABUS images. Dedicated 3D ABUS images of healthy female volunteers demonstrate whole-breast 3DUS imaging with clear anatomical structures and details.

Conclusions: The proposed dedicated 3D ABUS system and the CBUS approach show potential as an alternative, accurate, and high-resolution approach for whole-breast 3DUS imaging. These results demonstrate potential utility toward breast cancer screening in increased-risk populations and cost-constrained settings, independent of breast density.

87

ACCURATE VISUALIZATION OF STENTS THROUGH ARTIFACT REDUCTION WITH PHOTON-COUNTING DETECTOR CT

Devon Richtsmeier[1], Pierre-Antoine Rodesch[1], Kris Iniewski[2], William Siu[3], Magdalena Bazalova-Carter[1]
[1]*University of Victoria, Victoria, BC*
[2]*Redlen Technologies, Saanichton, BC*
[3]*Fraser Health Authority, New Westminster, BC*

Purpose: Computed tomography (CT) imaging of stents is often impacted by blooming and metal artifacts, which reduce the diagnostic quality of images as they obscure areas surrounding, and especially within, the stent. Photon-counting detector CT (PCD-CT) offers higher spatial resolution than current energy-integrating detector (EID) scanners, as well separating the incident spectrum into multiple energy bins. These benefits have been shown to reduce the artifacts that plague stent imaging. This study compared the diagnostic quality of stent images between two clinical CT scanners and a prototype bench-top PCD-CT system. The comparison was done by determining the accuracy of stent strut width, which would appear larger due to blooming and metal artifacts, lumen diameter, which would appear smaller, as well as the image signal within the stent lumen, which would be affected by said artifacts.

Materials and Methods: Three stents were studied: Medtronic Protégé, Cordis Precise, and Cordis S.M.A.R.T. Control. Strut thicknesses of the stents were measured at 0.186 mm, 0.238 mm, and 0.177 mm and lumen diameters at 5.82 mm, 5.71 mm, and 5.84 mm, respectively. Each stent was placed in water, into a custom 10-cm diameter high-density polyethylene phantom and CT images were acquired on two clinical EID-CT scanners and an in-house prototype PCD-CT system. The stents were imaged on the EID-CT scanners with a reconstructed pixel size of 0.248 mm and a slice thickness of 0.625 mm, and PCD-CT images were first reconstructed with the same parameters and then at the highest spatial resolution with a pixel size of 0.205 mm and a slice thickness of 0.208 mm, referred to as HR PCD-CT. The apparent strut thickness, lumen diameter, and lumen attenuation were evaluated, and K-edge images were reconstructed to demonstrate more accurate delineation of the Ta radiopaque markers.

Results: The prototype system (both HR and PCD-CT) demonstrated significantly lower percent differences for strut thickness compared to the physical measurements for all stents ($p < 0.001$) and for lumen diameter for the Protégé and Precise stents ($p < 0.01$). The lumen attenuation was more accurate with both PCD-CT modes ($p < 0.01$), though the differences between the Optima 580 and non-HR PCD-CT for the Protégé and Precise stents was not significant. The stents were all more accurately delineated in both PCD-CT modality images and 3D volume renderings, and the radiopaque markers were seen with no metal artifacts in K-edge specific images.

Conclusions: The PCD-CT system provided better stent visualization and diagnostic quality compared to the EID-CT scanners in terms of strut thickness, lumen diameter, and lumen attenuation. The results suggest that PCD-CT may be a promising alternative for stent imaging and overcome the challenges posed by blooming and metal artifacts. This, along with K-edge imaging, would allow iodine contrast to be more accurately measured and distinguished from calcifications.

88

SODIUM CONCENTRATION MEASUREMENTS IN PROSTATE CANCER AND NORMAL TISSUE USING AN EXTERNAL SODIUM MRI BUTTERFLY COIL

Josephine Tan[1,2,3], Vibhuti Kalia[1], Jonathan Thiessen[1,2], Timothy Scholl[1,3,4], Alireza Akbari[1,3]
[1]*Western University, London, ON*
[2]*Lawson Health Research Institute, London, ON*
[3]*Robarts Research Institute, London, ON*
[4]*Ontario Institute for Cancer Research, Toronto, ON*

Purpose: Sodium (^{23}Na) MRI is a molecular imaging technique that can detect the increased tissue sodium concentration (TSC) exhibited in several tumour types. For prostate cancer (PCa) imaging, ^{23}Na MRI is conventionally performed using an endorectal coil which is associated with a nonuniform sensitivity profile and limited field of view, constraining its clinical utility. To address these challenges, we have developed a completely external, non-invasive 'butterfly' coil for ^{23}Na MRI of the prostate. In this abstract, we investigate the ability of this coil to measure TSC differences between normal prostate tissue and PCa lesions.

Materials and Methods: All MR images were acquired at 3 T (Siemens Biograph mMR). ^{23}Na MRI was performed with an external, PET-compatible, flexible transmit/receive butterfly coil built in-house (diameter=18cm, tuning=32.6MHz) using a 3D density-adapted radial projection sequence (TR=50ms; TE=0.8ms; nominal isotropic resolution=5mm; FOV=36×36×10cm^3). ^{23}Na MRI was acquired in six male volunteers (age=51.3±16.2 years) and three patients with biopsy-proven PCa (age=65.3±2.5 years). Clinical multiparametric MRI, which included T_2-weighted and diffusion-weighted imaging (b-values=0,100,800s/mm^2) was evaluated by a radiologist (V.K.) to delineate the normal peripheral zone (PZ), transition zone (TZ), and PCa lesions. TSC was quantified in the PZ, TZ, and tumours using the iliac arteries as internal references of 80 mM. TSC was compared between the regions using a one-way analysis of variance and Tukey test.

Results: In all volunteers and patients, ^{23}Na MR images acquired using the butterfly coil exhibited sodium signal throughout the whole prostate and pelvic region in contrast to those acquired using an endorectal coil. Overall, mean TSC in PZ was higher than in TZ (PZ=52.0+-11.0mM; TZ=45.2+-8.2mM, p>0.05) but the difference was not statistically significant. There was also no significant difference between the mean TSC in the five tumours identified (tumour=38.7+-9.6mM, p>0.05) and surrounding normal PZ and TZ tissue. However, lower tumour TSC may reflect the high cellularity characteristic of many tumour types including PCa. Other ^{23}Na MRI studies have reported mean increased TSC in PCa relative to normal tissue, suggesting that (1) changes in tumour TSC cannot solely be attributed to differences in cellular density and (2) there is intra- and intertumour heterogeneity in TSC. Future work will aim to characterize the imaging sensitivity of this coil to tumours with Gleason grade defined by histopathology as the ground truth.

Conclusions: Our butterfly coil achieved a uniform sensitivity profile and a larger field of view for ^{23}Na MRI of the prostate. Lower TSC was measured in PCa lesions relative to normal prostate tissue in the PZ and TZ, though this difference was not statistically significant. This work aims to enhance the workflow of ^{23}Na MRI in future PCa studies compared to conventional endorectal coils.

89
INTEGRATION OF IMAGING PHYSICISTS IN RADIATION ONCOLOGY

David Hintenlang, Kathleen Hintenlang, Michael Weldon, Nilendu Gupta, Xiangyu Yang, Xia Jiang, Jun Zhang, Nathan Quails
The Ohio State University, Columbus, OH

Purpose: Imaging plays an increasingly important role in radiation oncology practice. Imaging physics expertise lies largely in the realm of medical physicists certified and practicing in the area of diagnostic imaging and MR science. Advances in radiation oncology are reliant on a variety of advanced imaging modalities, which are also utilized in radiology. The expertise of imaging physicists can be of equal value to both disciplines, although these physicists most commonly hold positions in radiology. It is important to explore innovative methods to integrate this expertise with the imaging needs of radiation oncology. Our purpose is to improve operational workflows in radiation oncology and radiology through improved integration of imaging physics expertise in radiation oncology.

Materials and Methods: Our institution has utilized a formalized integration of imaging physicists in support of radiation oncology-based imaging platforms. Imaging physicists in the Department of Radiology provide services supporting the imaging needs of the Department of Radiation Oncology through formal hospital agreements. Services include periodic evaluations of imaging systems, consultation regarding the implementation of new image-based technologies, accreditation support, and integration with many of the quality improvement and assurance programs associated with radiology, such as protocol and dose review.

Results: By sharing responsibility for oversight of imaging system quality assurance with imaging physicists based in radiology, the institution has gleaned improved efficiency of physics workflow. The existing skillsets and expertise of the imaging physicists can be seamlessly applied to the imaging systems utilized in radiation oncology to ensure that these systems meet appropriate quality assurance, accreditation and regulatory standards. This permits the radiation oncology physicists to focus on treatment related workflow and minimizing the need to develop additional areas of expertise in imaging physics. The arrangement also provides quality improvements through the independent oversight provided by imaging physics. Some examples where improved efficiency have been obtained include the implementation, evaluation and reviews of CT protocols, development of specialized MR pulse sequences for specific cases, technical evaluation of MR systems for radiation oncology specific applications, input on the selection and acquisition of new imaging systems, and optimization of imaging protocols for tumour visualization, fusion and contouring. Examples of improved collaborative experience for both physics groups have also been realized through close cooperation through applications involving new technologies such as integration of Dual Energy and Photon Counting CT, AI, cardiac radiation ablation, theranostics and synthetic CT images from MR. By integrating patient doses from the treatment simulation CT systems the imaging physics group is also able to enhance patient safety by identifying pediatric simulations or unusually large doses often associated with 4D simulations.

Conclusions: The integration has benefited physicians and physicists in both Radiation Oncology and Radiology and contributed to a culture of collaboration between the two departments. Radiation Oncology physicists and residents comfortably call on their colleagues in Radiology for insights into novel imaging applications, and imaging physicists gain an expanded perspective of imaging applications, imaging system requirements, regulatory requirements, and practice guidelines which can be further extended to a broader of set of medical imaging applications.

90
ROLE OF MRI-BASED RADIOMIC SIGNATURES IN PREDICTING LOCAL CONTROL AFTER STEREOTACTIC BODY RADIOTHERAPY FOR MALIGNANT LIVER TUMOURS

Arun Elangovan[1], Keith Wachowicz[1], Terence Riauka[1], Sunita Ghosh[1], Jihyun Yun[1], Aswin Abraham[1], Asmara Waheed[1], Helene Daly[2], Heather Warkentin[1], Diane Severin[1], Kurian Joseph[1]
[1]*University of Alberta, Edmonton, AB*
[2]*Alberta Health Services, Edmonton, AB*

Purpose: We routinely deliver Stereotactic Body Radiotherapy (SBRT) for malignant liver tumours using planning computed tomography (CT) and Magnetic Resonance Images (MRI) to aid target definition. In this study, we extracted radiomic features from the MR images to predict local control (LC) post-SBRT.

Materials and Methods: We retrospectively analyzed patients with either hepatocellular cancers (HCCs) or liver metastases (Mets) treated with SBRT between August 2014 and August 2020. All patients had CT simulation followed by 1.5 Tesla planning MRI in treatment position. Contrast enhanced T1 VIBE and T2 Haste MR Sequences were registered with planning CT for target definition. Radiomic features were extracted from Gross Tumour Volumes (GTV) masked out of 60 seconds post contrast T1 VIBE MR images

using the Radiomics calculator tool RaCaT. The output included 480 (408 textural, 50 intensity and 22 morphological) features for each target. Principal Component Analysis of the outputs obtained from all the targets yielded 20 radiomic feature clusters after computational prioritization. These clusters were correlated to LC outcomes at various time points post-SBRT. LC was defined as non-progressive disease. Accuracy of predictions was measured by area under (AUC) receiver operating characteristic curve. Cox regression analysis was done to find univariate and multivariate clinical [HCCs versus Mets, single versus multiple lesions, previous local therapy (yes versus no), GTV volume (≤40 versus >40 cc)], radiomic and dosimetric predictors (continuous) of LC.

Results: In total, 97 patients received SBRT to 122 lesions. The median dose prescribed was 45 Gy (range, 30-50 Gy). Median age was 69 years (interquartile range, IQR 61-73 yrs.). Fifty-nine patients had HCCs and 38 had Mets. Twenty-four lesions had prior ablative therapy. Seventy-five patients had one target, and 22 had multiple targets. Median GTV was 43.5 cc (IQR 23.4-78.6 cc). Median follow up was 16.6 months (IQR 9.7-27.2 mths). Median LC was 13.6 months (IQR 8.0-23.5 mths). On univariate analysis, histology (HCCs versus Mets; Hazard ratio (HR) 2.9, 95% CI 1.4-6.4; $p < 0.006$), radiomic clusters ($p<0.006$) and the max., mean, and min. doses to GTV and Planning Target Volumes correlated with improved LC (all p-values < 0.05). On multivariate analysis, histology (HCCs versus Mets; HR 4.4, 95% CI 1.6-12.3; p=0.004), radiomic clusters (p=0.034) and prescription dose (p=0.048) were significant covariates. Specifically, the 20 radiomic clusters were predictive of LC, and the accuracy of predictions showed promise with AUC values of 0.74, 0.80, and 0.81 at 12, 24, and 36 months post-SBRT, respectively. AUC values for LC in HCCs versus Mets at 12, 24, and 36 months were 0.83, 0.77, and 0.70, and 0.66, 0.77, and 0.88, respectively.

Conclusions: MR-based radiomics predict LC post-SBRT in patients with malignant liver tumours. Further research focused on independent validation of the model is required to explore its clinical use.

91

PATIENT SELF-REPORTED OVERALL WELL-BEING CORRELATES WITH CONCURRENT CANCER-RELATED SYMPTOMS?

Catherine McKenna[1,3], Brook-Lynn Fleury[1,2], Ernest Osei[1,3], Johnson Darko[1,3]
[1]*Grand River Regional Cancer Centre, Kitchener, ON*
[2]*Wilfred Laurier University, Waterloo, ON*
[3]*University of Waterloo, Waterloo, ON*

Purpose: Systematic self-reporting of patients' symptoms is important to improve symptom management in oncologic care. Consequently, several different tools such as the Edmonton Symptom Assessment System (ESAS) have been designed to collect patient self-reported outcomes to enable clear and timely communication of patients' symptoms to their clinicians and other healthcare providers. The purpose of this study is to investigate the relationship between patients reported overall well-being and concurrent symptoms experienced by cancer patients.

Materials and Methods: In this study, we analyzed ESAS questionnaire responses from 2014 to 2020 completed by 17,818 cancer patients at our centre as part of their routine care and considered part of patients' standard of care. The ESAS symptoms consist of nine cancer-related symptoms that are scored on an 11-point scale of 0 to 10, where 0 indicates the absence of a symptom or best well-being, and 10 indicates severe symptoms. Descriptive statistics are used to summarize patient demographics, disease characteristics and patient-reported symptom severity and prevalence. Statistical analyses were performed using IBM SPSS Statistics Version 28.0.

Results: Multivariate binary logistic regression analysis for odd ratios (OR) showed that patients self-reported severe scores (7-10) for tiredness (OR=3.93), pain (OR=3.63), lack of appetite (OR=3.39) and depression (OR=2.81) are associated with higher odds of self-reporting severe (7-10) overall well-being. Moreover, patients self-reported severe tiredness (OR=6.66), pain (OR=4.34), lack of appetite (OR=3.84), anxiety (OR=3.51) and depression (OR=3.47) correlated with higher odds of self-reporting moderate-to-severe (4-10) overall well-being. For self-reported mild (1-3) symptoms, we observed no impact on the odds of scoring severe well-being except lack of appetite which had an odd ratio of 1.13. Principal component analysis (PCA), exploratory factor analysis (EFA), and hierarchical clustering analysis (HCA) of the symptoms show well-being was always clustered with tiredness and drowsiness (Cronbach's alpha: 0.845).

Conclusions: Integration of patient-reported symptom outcome measures in routine oncologic care is useful to determine patterns of symptom burden and the design of patient-centred supportive care needs. The co-relationship between self-reported overall well-being and other concurrent cancer symptoms experienced by patients shows the need for the development of comprehensive symptom assessments incorporating the utilization of multimodal management approaches that consider concurrent symptoms.

92

HYPOFRACTIONATED DOSE-INTENSIFIED PALLIATIVE RADIOTHERAPY: 25 GY IN 5 FRACTIONS FOR ENHANCED SYMPTOM CONTROL

Jayson Paragas, Vanessa Di Lalla, Leticia Alvarado, Tanner Connell, Sonia Skamene, Marc David
McGill University, Montréal, QC

Purpose: Selection between standard palliative dose schedules versus more aggressive palliative approaches is an ongoing dilemma, with recent shift towards the latter to provide improved symptom relief and local control, especially among patients with longer life expectancy. Stereotactic approaches show promise in these respects; however, these techniques are highly resource-intensive and may not be widely available. We assessed the tolerance and efficacy of non-stereotactically planned 25 Gy in 5 fractions to strike a balance between higher biologically effective dose (BED) with acceptable side effect profile and shorter treatment duration.

Materials and Methods: Our local radiotherapy database was retrospectively reviewed over a 10-year period (September 2011 to August 2021) for patients receiving 25 Gy in 5 fractions treated with palliative intent. Patients who received stereotactic ablative treatment techniques, curative-intent therapy, and patients who were asymptomatic at the treated sites were excluded.

Results: A total of 127 patients corresponding to 136 treated sites were included in this analysis. The median age was 70 years (range 35-98 years), 51% were ECOG ≥ 2, 66% had Charlson comorbidity index ≥8 and 77% were metastatic at time of treatment. Treated sites were rectum (20%), non-spine bone (18%), spine (12%), lymph node (12%) and esophagus (8%), and 88% had no previous RT at the same site. Median GTV 110.1cc (range 4-2940.8cc) and median PTV 321.8cc (range 14.7-3991cc). Treatment was delivered using VMAT (74.5%), IMRT (10.9%) 3DCRT (10.2%), or 2D (4.4%). At a median follow-up of 20 weeks (1-308 weeks), the overall response rate was 96% for pain control, 93% for obstruction relief, 100% for bleeding control and 69% for improvement of neurologic deficits. Toxicities ≥ Grade 3 occurred in 3.6% of the cohort (odynophagia, dyspnea, progression of intestinal obstruction and wound infection progression). Median OS was 9 months. Fifty (37%) patients survived more than one year. Only one patient died within 30 days from cause unrelated to palliative radiotherapy meeting the quality indicator for radiation futility. On multivariate analysis,

only ECOG score was significantly associated with treatment response (OR 0.40, p=0.036).

Conclusions: To our knowledge, this is the largest study reporting on the use of non-stereotactically delivered 25 Gy in 5 fractions palliative radiotherapy. Our data suggests that this dose fractionation is tolerable and effective for symptom control, even among elderly frail symptomatic patients when compared to historical data using alternative palliative dose fractionation schemes. Further exploration of non-stereotactic moderate hypofractionation for palliation is needed to optimize palliation in patients without access to or those ineligible for stereotactic approaches.

93

RISK FACTORS FOR UNSCHEDULED ACUTE CARE VISITS FOR GYNECOLOGIC ONCOLOGY PATIENTS RECEIVING RADIOTHERAPY

Aaron Dou[1], Mary Doherty[2], Xuan Li[2], Kathy Han[1], Stephanie L'heureux[2], Jelena Lukovic[1], Mike Milosevic[1], Genevieve Bouchard-Fortier[2], Jennifer Croke[1]
[1]*University of Toronto, Toronto, ON*
[2]*N/A, Toronto, ON*

Purpose: Unscheduled acute care utilization during cancer treatment negatively impacts patient quality of life, clinical outcomes, and results in increased healthcare resources and costs. Our objective was to evaluate risk factors for unscheduled acute care utilization in gynecological oncology patients receiving radiotherapy (RT).

Materials and Methods: This was a retrospective review of gynecological cancer patients treated with RT at an academic cancer centre between August 1, 2021 and January 31, 2022. Patients were divided into two cohorts: those receiving concurrent chemoradiation regimens (CCR) and those receiving RT alone. Baseline socio-demographic data, as well as clinical and treatment characteristics, were extracted from medical records. Acute care utilization was defined as any unscheduled visit to our Radiation Nursing Clinic (RNC), a drop-in nurse-led ambulatory care clinic for patients during RT and up to two weeks post-treatment. Data pertaining to RNC visits were collected, including number of visits during treatment, chief complaint, and interventions performed. Results were summarized by descriptive statistics. Wilcoxon rank sum test and chi-squared test/Fisher exact test were used for comparisons of continuous and categorical variables, respectively.

Results: RT was delivered to 181 gynecological cancer patients within the time period, of which 42 received CCR (23.2%) and 139 (76.8%) received RT alone. The most common CCR regimen was PORTEC-3 for endometrial cancer (59.5%), followed by weekly cisplatin/RT for cervix cancer (33.3%). Patients receiving CCR had higher rates of unscheduled acute care utilization (RNC visits) compared to those receiving RT alone (54.8% versus 18.8%, p<0.001), and presented more frequently during treatment (CRT: 71 visits, average 3.1 visits/patient versus RT: 27 visits, average 1.04 visits/patient; p=0.005). Patients undergoing CCR most commonly presented with dehydration requiring intervention (e.g. IV fluids) (33.6% of visits), whereas RT only patients presented with questions surrounding symptom management requiring patient education (21.4% of visits). Within the CCR cohort, patients who required acute care utilization were less likely to be married/in a relationship (57% versus 89%, p=0.02), were more likely to be referred to Psychosocial Oncology (39% versus 5.3%; p=0.01) and were more likely to experience treatment interruptions (52% versus 16%, p=0.014; 52% versus 8%, p<0.001). There were no associations between unscheduled acute care utilization and age, disease site, or distance to the cancer centre.

Conclusions: Gynecological oncology patients undergoing CCR are at increased risk for unscheduled acute care utilization compared to patients receiving RT alone. Psychosocial referrals, being single and treatment interruptions were significantly higher in CCR patients utilizing acute care. Targeted strategies to better meet the supportive care and psychosocial needs of this population are required.

94

EVALUATING GEOGRAPHIC ACCESS TO RADIOTHERAPY SERVICES IN CANADA

Oluwaseun Davies, Yang Xu, Shaun Loewen
[1]*University of Calgary, Calgary, AB*

Purpose: To identify jurisdictions and demographic factors associated with increased driving times to the nearest radiotherapy (RT) facility in Canada.

Materials and Methods: RT facilities in Canada were identified using information obtained from the Canadian Association of Radiation Oncology and the IAEA Directory of Radiotherapy Centres. The 2021 Canadian census was used to determine demographic profiles for each dissemination area, the smallest geographic unit (target size 400-700 people) on which all census data is reported. Poor geographic access was defined as a driving time between a dissemination area and the closest RT facility exceeding 90 minutes as computed using the OpenStreetMap database. The association between province and poor geographic access was assessed using multivariable logistic regression adjusting for population density by decile. Demographic characteristics were subsequently introduced into the logistic regression to identify factors associated with poor access.

Results: A total of 51 radiotherapy centres and 57,937 dissemination areas were mapped. Median driving time to the closest RT facility was 23 minutes, and 13% of the population had poor access to RT. RT was least accessible in the three territories, whose residents had a median driving time of 1096 minutes. Among the provinces, Newfoundland had the longest median driving time of 91 minutes while Manitoba had the shortest median driving time of 20 minutes. On logistic regression with population density as a covariate, dissemination areas in Newfoundland (OR, 9.64 compared to Ontario; 95% CI, 8.3 to 11.2) and British Columbia (OR, 5.46; 95% CI, 5.03 to 5.93) had the highest odds of poor geographic access, whereas Ontario (reference) and PEI (OR, 0.49; 95% CI, 0.34 to 0.69) had the lowest odds. Inclusion of demographic variables in the logistic regression revealed that dissemination areas with higher median age (OR, 1.035 per year; 95% CI, 1.030 to 1.039), more males (OR, 1.033 per %; 95% CI, 1.021 to 1.045), lower income (OR, 1.030 per % low income status; 95% CI, 1.024 to 1.035), increased aboriginal representation (OR, 1.050 per %; 95% CI, 1.045 to 1.054), fewer visible minorities (OR, 0.979 per %; 95% CI, 0.973 to 0.985), fewer immigrants (OR, 0.934 per %; 95% CI, 0.927 to 0.941), and lower attainment of postsecondary education (OR, 0.976 per %; 95% CI, 0.972 to 0.979) were associated with poorer access to RT.

Conclusions: Approximately 13% of Canadians have a driving time exceeding 90 minutes to the closest RT facility. Geographic access to RT varied by province and dissemination areas with higher median age, low socioeconomic status, a greater proportion of males, and higher aboriginal populations were associated with poorer access. Our study identified deficiencies in access to existing RT facilities and may inform planning efforts for locations of new facilities in Canada.

95

USE OF RADIATION THERAPY AMONG PATIENTS WITH EXTENSIVE-STAGE SMALL-CELL LUNG CANCER RECEIVING IMMUNOTHERAPY: CANADIAN CONSENSUS RECOMMENDATIONS

Alexander Sun[1], Barbara Melosky[2], Devin Schellenberg[3], Bassam Abdulkarim[4], Normand Blais[5], Jonathan Greenland[6], Alexander Louie[1], Stephanie Snow[7], Geoffrey Liu[1]
[1]*University of Toronto, Toronto, ON*
[2]*University of British Columbia, Vancouver, BC*
[3]*British Columbia Cancer, Surrey, BC*
[4]*McGill University, Montréal, QC*
[5]*University of Montréal, Montréal, QC*
[6]*Eastern Health, St. John's, NL*
[7]*Dalhousie University, Halifax, NS*

Purpose: Thoracic radiation therapy (TRT) and prophylactic cranial irradiation (PCI) are commonly used in the management of extensive-stage small-cell lung cancer (ES-SCLC); however, Phase III trials of first-line immunotherapy often excluded these options. Guidance is needed regarding appropriate use of TRT, PCI, and magnetic resonance imaging (MRI) surveillance while new data are awaited.

Materials and Methods: In two web-based meetings, a pan-Canadian expert working group of five radiation oncologists and four medical oncologists addressed eight clinical questions regarding use of radiation therapy (RT) and MRI surveillance among patients with ES-SCLC receiving immunotherapy. A targeted literature review was conducted using PubMed and conference proceedings to identify recent (January 2019–April 2022) publications in this setting. Fifteen recommendations were developed; online voting was conducted to gauge agreement with each recommendation.

Results: After considering recently available evidence across lung cancer populations and clinical experience, the experts recommended that all patients with a response to chemo-immunotherapy, good performance status (PS), and limited extra-thoracic disease be considered for consolidation TRT (e.g., 30 Gy in 10 fractions). When considered appropriate after multidisciplinary team discussion, TRT can be initiated after completion of initial chemo-immunotherapy, during maintenance immunotherapy. All patients who respond to concurrent chemo-immunotherapy should undergo restaging with brain MRI to guide decision-making regarding PCI versus MRI surveillance alone. MRI surveillance should be conducted for two years after response to initial therapy. PCI (e.g., 25 Gy in 10 fractions or 20 Gy in 5 fractions) can be considered for patients without central nervous system involvement who have a response to chemo-immunotherapy and good PS. Concurrent treatment with PCI (+/- TRT) and immunotherapy is appropriate after completion of initial therapy. All recommendations were agreed upon unanimously.

Conclusions: These consensus recommendations provide practical guidance regarding appropriate use of RT and immunotherapy in ES-SCLC while additional clinical data are awaited.

96

BREAST CANCER OUTCOMES OF PATIENTS WITH T4b DISEASE: A POPULATION-BASED RETROSPECTIVE ANALYSIS

Nicolas Siriani-Ayoub, Theodora Koulis, Lovedeep Gondara, Caroline Speers, Rekha Diocee, Caroline Lohrisch, Alan Nichol, Pauline Truong
University of British Columbia, Vancouver, BC

Purpose: Breast cancers with non-inflammatory skin involvement are classified as T4b in the TNM staging system. With wide variations in tumour size and clinical characteristics among the T4a-d subgroups, optimal treatment and outcomes in patients with T4b disease is controversial. This study evaluates recurrence and survival outcomes in patients with T4b tumours compared to other T4 subgroups.

Materials and Methods: Subjects were 680 patients referred to a Canadian institution with newly diagnised pT4 or cT4, any N, M0 breast cancer between 2005-2015. Clinicopathologic and treatment characteristics, locoregional recurrence-free survival (LRRFS) and breast cancer-specific survival (BCSS) were compared between patients with T4b (n=354, 52%) to T4a (n=78, 11.5%) and T4d (n=248, 36.5%) disease. T4c tumours (T4a + b) were excluded to minimize confounding. Multivariable analysis was used to identify variables significantly associated with LRRFS and BCSS.

Results: Median age of T4a, T4b and T4d patients were 63, 63, and 56.5 years, respectively (p<0.001). Among T4b patients, subtypes were luminal A (24.9%), luminal B (32.5%), HER2-positive (25.7%), and triple negative (12.4%). Corresponding rates were 41.0%, 23.1%, 29.9%, and 15.3% among T4a patients and 10.9%, 21.8%, 38.7%, and 23.4% among T4d patients. Patients with T4a disease had smaller tumours 2.1-5cm (56.4%), while patients with T4b and T4d disease had larger tumours >5cm, 55.6% and 43.5%, respectively (p<0.001). Mastectomy was the most common surgical treatment: 69.2% in T4a, 76.3% in T4b, and 85.1% in T4d (p<0.001), with clear margins in 61.5%, 66.4% and 77% of T4a, b and d cases, respectively (p=0.003). The majority of T4a, b and d subgroups received chemotherapy and hormone therapy (39.7%, 28.5%, and 25%, p<0.001). Adjuvant radiotherapy was most commonly used in T4a and b (56.3% and 50.2%), while neoadjuvant radiotherapy was more commonly used in T4d disease (42.7%); (p<0.001). In T4a, T4b and T4d subgroups, 10-year LRRFS were 85.4%, 85.1% and 82.8%, (p=0.40) and 10-year BCSS were 55.5%, 50.4%, and 47.9%, respectively (p=0.04). Locoregional recurrence was more common with >=4 positive nodes (p=0.025), positive margins (p=0.005), luminal B (p=0.008), and triple negative subtypes (p=0.003). LRRFS and BCSS were improved with hormone therapy with or without chemotherapy and with adjuvant or neoadjuvant RT (all p<0.05). On multivariable analysis, factors associated with lower LRRFS and BCSS were >= 4 positive nodes, luminal B, and triple negative subtypes, while positive margin was associated with lower LRRFS (all p<0.05).

Conclusions: No significant difference in 10-year LRRFS was observed between T4b compared to T4a and T4d breast cancer. Ten-year BCSS was significantly better with T4a disease. Advanced nodal stage, luminal B and triple negative disease were associated with worse LRRFS and BCSS. Systemic therapy and locoregional RT were significantly associated with better LRRFS and BCSS.

97

PROBING MICROSTRUCTURAL CHANGES IN A MOUSE MODEL OF MILD TRAUMATIC BRAIN INJURY USING DIFFUSION MRI TECHNIQUES

Naila Rahman, Kathy Xu, Arthur Brown, Corey Baron
Western University, London, ON

Purpose: Imaging markers of mild to moderate concussion are notoriously difficult to detect in vivo. Advanced diffusion MRI (dMRI) techniques have shown increased sensitivity and specificity to microstructural changes in various disease and injury models. Oscillating gradient spin echo (OGSE) diffusion MRI (dMRI) and microscopic fractional anisotropy (μFA) dMRI may provide additional insight by increasing sensitivity to smaller spatial scales and disentangling fiber orientation dispersion from true microstructural changes, respectively, compared to conventional diffusion MRI. Here, we evaluate mean diffusivity difference between OGSE frequencies (ΔMD), microscopic fractional anisotropy (μFA), and traditional dMRI metrics (mean diffusivity

(MD) and fractional anisotropy (FA)) longitudinally in vivo in sham and injured mice, following a single mild traumatic brain injury (mTBI).

Materials and Methods: The sham and concussed cohort each consisted of six female and six male C57Bl/6 mice, aged 10-12 weeks at the start of the study. Longitudinal imaging was performed on the sham and concussed cohorts at baseline (BL), and two days, one week, four weeks, eight weeks, and 20 weeks post-injury (D2, W1, W4, W8, W20 respectively). Imaging was performed at 9.4T with a 1 T/m gradient insert using single-shot EPI with an in-plane resolution of 0.175mm x 0.2mm, 0.5mm slice thickness, and a total scan time of two hours. The OGSE sequence was implemented with b=800s/mm, TE=37ms, 10 directions and OGSE frequencies of 0, 50, 100, 145, and 190 Hz. The μA sequence was implemented using a single diffusion encoding (SDE) scheme with linear and spherical tensor encodings at b=2000s/mm (30 directions) and b=1000s/mm (12 directions). Post processing included denoising and eddy current correction with FSL. The protocols have been described in detail in earlier work (Rahman et al., Scientific Data, 2023). Parameters were measured in the corpus callosum (CC), prefrontal cortex (PFC), and fornix (FX). The mean values in each ROI were averaged across all subjects in each cohort, and the change in the averages between each timepoint and the baseline was calculated. A repeated measures ANOVA was used for each metric to determine if there were statistically significant interaction effects ($p<0.05$) between sham and concussed mice over time, and post-hoc analysis (with Tukey-Kramer multiple comparison correction) was used to determine if the groups differed within each timepoint post-mTBI.

Results: Notably, the single mild impact resulted in no observable symptoms or qualitative MRI differences. ΔMD (PFC) showed a net increase from baseline in concussed mice, compared to shams ($p<0.05$) at D2, W8, and W20 post-mTBI (7%, 8%, and 11% increases respectively). A similar trend was found in ΔMD (FX) with increases at D2 and W8 (11% and 13% respectively). MD only showed net decreases at D2 (FX) and 8W (PFC). μFA and FA showed net increases at 8W (CC).

Conclusions: In the concussed cohort, the trend of acute net increased ΔMD (related to axon beading (Baron et al., Stroke, 2015)), pseudo-normalization of ΔMD, and chronic net increased ΔMD, is consistent with the notion of multi-phase concussion recovery. The decreases in MD are consistent with axon degeneration and increases in FA are consistent with astrogliosis. Overall, our data shows that the advanced dMRI metrics (ΔMD and μFA) provide greater sensitivity to changes post-mTBI at both acute and chronic stages, than the conventional dMRI metrics (MD and FA). This work highlights the promise of advanced dMRI techniques in detecting evolving microstructural changes throughout the course of disease progression and injury recovery.

98

RADIOSENSITIZATION OF GLIOBLASTOMA USING TARGETED INHIBITION OF N-MYRISTOYLATION

Deepak Dinakaran, Evan Wilson, Nicholas Rydzewski, Kevin Camphausen
National Institute of Health, Bethesda, MD

Purpose: Treating Glioblastoma remains a major challenge. Radiotherapy has a long-standing role in extending survival, but almost all tumours are expected to recur and be fatal. Historic dose-escalation studies do not yield additional benefit beyond the current 60 Gy dose. Further therapeutic improvement can be gained with radiosensitizers. An undiscovered potential radiosensitization approach may exist in inhibiting the N-myristoylation pathways upregulated in malignant cells. Inhibiting this pathway has been shown to have pleotropic effects including decreasing PARP-1 activity and other cancer-driving pathways that may synergize with radiotherapy. This is a first report in using a targeted N-myristoyltransferase (NMT) inhibitor as a radiosensitizer in glioblastoma.

Materials and Methods: Immortalized glioma cell lines (U87 and U251) and patient-derived de novo (ED501) and post-chemoradiation recurrent (ED512) cell lines were used to a NMT1/2 inhibitor with radiotherapy. Cell surface expression levels for NMT1 and NMT2 were established using immunofluorescence microscopy. In vitro cell viability studies via mitochondrial reduction of resazurin dye and clonogenic assays were done with single fraction 2 & 4 Gy irradiation with five days of drug exposure (5-150 nM 3 days prior to irradiation and two days post) to account for drug pharmacodynamics. PARP-1 expression by western blot was tested with exposure to drug and/or radiation. Whole exome sequencing and methylation profiling were done to find predictive markers of radiosensitization.

Results: Preliminary results show significant radiosensitization effect with a dose enhancement factor ranging from 1.33 to 2.71x higher than radiation alone. The amount of radiosensitization varied per cell line, with U251 and ED512 being more sensitive. The cell line sensitivity was not reliably predicted by the NMT cell surface receptor expression. PARP-1 activity increased with radiotherapy but was inhibited with drug exposure. Exome sequencing showed the radiosensitizing effect correlated with mutations in DNA damage repair and myristoylation pathways.

Conclusions: N-myristoylation inhibition appears to be a novel method of radiosensitization for glioblastoma. N-myristoylation affects multiple oncogenic pathways including PARP-1 downregulation, which impedes DNA damage repair and may be what leads to radiosensitization. Future studies are aimed at further predictive markers and in vivo efficacy.

99

CHARACTERIZATION OF THE RADIATION RESPONSE AND PREVENTION OF RADIATION-INDUCED MALIGNANCIES IN LI-FRAUMENI SYNDROME

Pamela Psarianos, Katherine Sauberli-Stewart, Nicholas Fischer, David Malkin
University of Toronto, Toronto, ON

Purpose: Li-Fraumeni Syndrome (LFS) is a genetic disorder associated with a significant risk of early-onset cancer. This condition is driven by germline mutations in the TP53 gene which plays a primary role in the regulation of the radiation response. Aberrant TP53 function contributes to radiation vulnerability and a greater risk of secondary, radiation-induced malignancies. As a result, therapeutic options for LFS patients are often limited to exclude radiotherapy (RT), which may otherwise be beneficial for the treatment of primary tumours. Corroborating transcriptomic data from our lab show that DNA repair is significantly altered in mutant p53 patient skin fibroblasts following irradiation (IR); however, it is unknown whether reprogramming this radiation response can decrease the risk of radiation-induced malignancy in LFS. Metformin, a commonly prescribed anti-diabetic drug, is associated with lower cancer incidence and may decrease cancer-related mortality in murine LFS models. In addition to its potential anti-tumourigenicity, recent studies have shed light on the ability of metformin to protect against radiation injury in normal tissue via the augmentation of DNA damage repair; hence, we hypothesized that metformin can reprogram the radiation response and delay the onset of radiation-induced tumours in LFS.

Materials and Methods: To establish a murine model of radiation-induced tumours in LFS, and to investigate whether metformin can delay tumour onset in this model, whole-body or localized

IR were administered to mice harboring a hotspot $TP53^{R172H/+}$ mutation in the presence and absence of metformin. Serial MRI was conducted to monitor for tumour development. To understand the temporal evolution of the mutant p53 radiation response, and whether metformin can reprogram this response in vivo, IR was administered to $TP53^{R172H/+}$ mice. Normal and irradiated skin were collected longitudinally from untreated and metformin-treated cohorts for whole transcriptome sequencing. In parallel, we have begun to characterize the effect of metformin on the human radiation response in vitro. Briefly, Western blotting and immunofluorescence assays were conducted to investigate levels of DNA damage in patient skin fibroblasts following IR and metformin treatment.

Results: We demonstrate that IR decreases tumour latency in $TP53^{R172H/+}$ mice, and that metformin may delay tumour onset within the radiation field. Moreover, we show that metformin rescues the expression of radiation response proteins while decreasing the frequency of DNA damage following IR in mutant p53 fibroblasts in vitro. Transcriptome analyses will be presented.

Conclusions: Overall, we show that metformin may delay radiation-induced tumour onset in LFS mice, and have begun to characterize the biology underpinning this reprogrammed response to IR. This study is the first to highlight metformin as a radioprotective agent in the context of germline mutant p53, with the potential to broaden RT treatment options for LFS patients.

100

PROGNOSTIC ASSOCIATIONS OF THE NEUTROPHIL-TO-LYMPHOCYTE AND PLATELET-TO-LYMPHOCYTE RATIO IN PATIENTS TREATED WITH SURGERY FOR PLEURAL MESOTHELIOMA AFTER RADIOTHERAPY

Enrique Gutierrez Valencia, Nicholas McNeil, Rohan Salunkhe, Avipsa Das, Jessica Weiss, Natasha Leighl, Shaf Keshavjee, Marc de Perrot, Andrea Bezjak, Alexander Sun, John Cho
Princess Margaret Cancer Centre, Toronto, ON

Purpose: Immunity profile have had prognostic implications in some thoracic malignancies. We examine the prognostic significance of neutrophil-to-lymphocyte ratios (NLR) and platelet-to-lymphocyte ratios (PLR) at different time points for patients with malignant pleural mesothelioma (MPM) treated with Surgery for Mesothelioma After Radiation Therapy (SMART).

Materials and Methods: From a prospective study database, we identified all patients with histologically proven MPM treated with Surgery for Mesothelioma After Radiation Therapy (SMART). Complete blood count (CBC) values were collected, and the NLR, and PLR immune profiles were calculated at four time points: pre-RT (before radiation), pre-op (after radiation/before surgery), one month post-op (30-60 days after surgery) and three month post-op (60-180 days after surgery). The endpoints of interest were: overall survival (OS), disease-free survival (DFS), and time to distant recurrence (DR). Each was measured in months from the date of starting treatment. OS and DFS were assessed using the Cox Proportional-Hazards Model, and distant recurrence (contralateral chest, pericardium, abdomen, liver, bone or other distant) was compared using the Fine-Gray sub-distribution hazard model to account for competing risks from local/mediastinum recurrence and death.

Results: Between 2008 to 2020, 123 MPM patients were treated on the SMART protocol. Patient demographics were: median age 66 (range: 33-82) years, epithelial histology 94 (76%), biphasic histology 29 (24%). On univariate analysis (UVA) epithelial histology was significantly associated to improved OS hazard ratio (HR) 0.5029 (0.3150-0.8027) P= 0.0040, $NLR_{3m\text{-}post\text{-}op}$ HR 1.0504 (1.0121-1.0900) P= 0.0094 and $PLR_{3m\text{-}post\text{-}op}$ HR 1.0035 (1.0006-1.0064) p-value = 0.0181. On multivariate analysis (MVA) for OS epithelial histology HR 0.5597 (0.3302-0.9487) P=0.0311, $NLR_{3m\text{-}post\text{-}op}$ 1.0635 (1.0228-1.1058) P= 0.0020 and $PLR_{3m\text{-}post\text{-}op}$ 1.0042 (1.0014-1.0071) P=0.0037. On MVA for DFS epithelial histology HR 0.4573 (0.2721-0.7684) P=0.0031 and $NLR_{3m\text{-}post\text{-}op}$ HR 1.0587 (1.0188-1.1002) P=0.0036. On UVA and MVA NtoL and $PLR_{3m\text{-}post\text{-}op}$ were not significantly correlated to DR HR 1.0251 (0.9771,1.0754) P= 0.3100 and HR 0.9997 (0.9992,1.0003) P= 0.3700, respectively. Epithelial histology was significantly associated with DR on UVA HR 0.4459 (0.2657,0.7481) P=0.0022 but not on MVA HR 0.6182 (0.3401,1.1240) P= 0.1100.

Conclusions: In this study, we found that the three-month post-operative NLR and PLR, as well as epithelial histology were significantly associated with DFS and OS but not DR.

101

RADIOTHERAPY UTILIZATION BASED ON MOLECULAR MARKER STATUS IN TREATMENT OF EARLY-STAGE ENDOMETRIAL CANCER

Jiheon Song, Amandeep Taggar, Elizabeth (Toni) Barnes, Hanbo Chen, Eric Leung
University of Toronto, Toronto, ON

WITHDRAWN

classification system that incorporates molecular marker status significantly differ from the system that relies on traditional risk factors. Treatment intensification may be considered particularly in patients whose molecular marker predicts higher risk of disease recurrence.

102
A FULL BODY BLOOD FLOW MODEL FOR APPLICATIONS IN TBI DOSIMETRY

Cassidy Northway[1], Ingrid Spadinger[2]
[1]*University of British Columbia, Vancouver, BC*
[2]*British Columbia Cancer, Vancouver, BC*

Purpose: Total body irradiation (TBI) is a form of radiation therapy during which the entirety of the patient's body is irradiated to eliminate residual cancer cells. It is unknown how the multitude of TBI delivery techniques compare regarding the heterogeneity in dose to the circulating blood, which has implications for both eradication of circulating cancer cells and the risk of lymphopenia as a side-effect of treatment. To help address this question, a real-time four-dimensional (4D) blood flow model that tracks sub-volumes of blood through the Extended Cardiac-Torso (XCAT) Phantom has been created, with the eventual aim being to incorporate it into a Monte Carlo dose calculation algorithm that determines the dose accumulated in blood sub-volumes by various TBI techniques.

Materials and Methods: The 4D XCAT Phantom is a full body virtual research phantom that includes models of the major vessels. Random sample consensus fitting and principal component analysis were used to extract the length and radius of the vessels in the phantom. Next, a one- to zero-dimensional paired blood flow model was computed, determining the flow rate and splitting ratios for all the vessels. By sampling the computed flow rates at various locations within the anatomy and comparing them to clinical data, the validity of the model was tested. Finally, the model was converted from a continuous to a discrete format.

Results: Blood flow rates at various points in the model have been compared to clinical data reported in the literature and shown to demonstrate results comparable those seen in other modelling studies. Successful discretization will allow the model to be meaningfully utilized in combination with 4D Monte Carlo Dose calculations.

Conclusions: The completion, validation, and discretization of the 4D blood flow model will enable calculation of dose to circulating blood components during TBI in future research.

103
PREDICTING LUNG DOSE FOR RIGHT-SIDED BREAST CANCER PATIENTS WITH TRADITIONAL MACHINE LEARNING AND NEURAL NETWORKS

Fletcher Barrett[1], Sarah Quirk[2,3], Owen Paetkau[1], Sangjune Lee[1], Philip McGeachy[1]
[1]*University of Calgary, Calgary, AB*
[2]*Harvard Medical School, Boston, MA*
[3]*Brigham & Women's Hospital, Boston, MA*

Purpose: To compare the performance of traditional machine learning and neural network-based models that predict lung dose for right-sided breast cancer patients at the time of CT-sim to determine if deep inspiration breath hold is needed.

Materials and Methods: All patients treated between 2015 and 2020 with adjuvant right-sided breast/chest wall and regional nodal irradiation were included in the cohort. Treatment plans delivered 42.5Gy in 16 fractions using the mono-isocentric 4-field technique with wide tangents to include the internal mammary lymph nodes. Measurements of lung anatomy relative to radiation field boundaries and bony anatomy were obtained from free-breathing patient CT-sim images and lung doses were extracted from clinical plans. Anatomic measurements were used as input to train models to predict lung dose. The lung metric of interest was the volume of lung receiving 20Gy, V20Gy(%). Model performance was evaluated with the root mean squared error (RMSE) between predicted and actual V20Gy(%). Models were developed using two methods, traditional machine learning (TML) and neural networks (NN). Models were tuned with a training/validation dataset (85% of cohort) via grid search using 5-fold cross validation to minimize the RMSE. Models were categorized into 'measurement groups' defined by the number of anatomic measurements used for training, ranging from one to ten. The optimal models in each measurement group were those with the lowest RMSE, resulting in ten optimized models for TML and NN. Optimized model performance was assessed with a testing dataset (15% of cohort). Optimized models using TML and NN were compared based on RMSE and anatomic measurement selection. RMSE for three ranges in V20Gy(%) (low: 19% to 27%, intermediate: 27% to 33%, and high: 33% to 45%) were compared to identify which optimized model could differentiate low versus high lung dose (i.e., RMSE < 3%) using the fewest measurements.

Results: The cohort consisted of 238 patients. Training/testing datasets included n=58/9 low, n=83/16 intermediate, and n=61/11 high dose patients. Optimized models using TML and NN had an average difference in RMSE of 0.1% across all measurement groups and selected the same anatomic measurements 97% of the time. Optimized models improved more per measurement in the first 5 measurement groups (TML: Δ0.35%, NN: Δ0.34%) than the last 5 (TML: Δ0.07%, NN Δ0.04%). Using TML, the five-measurement optimized model used the fewest measurements to achieve an average RMSE < 3% (low: 2.4±0.5%, intermediate: 2.4±0.2%, and high: 2.3±0.2%).

Conclusions: TML and NN-based models are comparable in performance and achieve better accuracy with more measurements. Given the increased hardware cost associated with NN, TML offers a more accessible alternative. The five-measurement optimized model using TML successfully differentiates low and high lung dose with the fewest measurements. This model could be implemented at the time of CT-sim to determine which patients need deep inspiration breath hold.

104
AUTOMATIC TREATMENT PLAN GENERATION FOR PROSTATE RADIOTHERAPY USING DEEP LEARNING

Cody Church[1], Michelle Yap[1], Dal Granville[2]
[1]*N/A, Ottawa, ON*
[2]*Ottawa Hospital Research Institute, Ottawa, ON*

Purpose: To automatically generate deliverable treatment plans for prostate radiotherapy patients using deep learning (DL) dose prediction and an automated optimization workflow.

Materials and Methods: A neural network based on a residual UNET architecture was trained using previously treated prostate patient datasets (n = 100). All treatment plans delivered 60 Gy to the prostate and 54 Gy to the proximal seminal vesicles in 20 fractions. The DL model used 3D structure sets (PTV60, PTV54, bladder, rectum, femoral heads, and external) as input and predicted 3D dose distributions. The model was trained using a loss function based on mean absolute error (pixel-weighted by isodose and structure priority) and various DVH metrics. A separate validation dataset (n = 20) was used to evaluate the model hyperparameters and to develop an automated optimization workflow that converted the predicted dose distributions first into optimization objectives

and then into deliverable VMAT plans within the RayStation TPS (RayStation v11B, RaySearch Laboratories AB, Stockholm, Sweden). An independent test dataset (n = 20) was used to evaluate the similarity between automatically and manually generated plans. For comparison, all plans were normalized such that $D_{95\%}$ of the PTV60 was 60 Gy.

Results: For the two PTVs (prostate and seminal vesicles) the automatically generated plans resulted in a $V_{100\%}$ $D_{99\%}$ and $D_{95\%}$ within an average of 0.51 ± 0.45 %, 0.84 ± 0.97 % and 0.27 ± 0.37 % of the manually created plans, respectively. Bladder and rectum volume-at-dose objectives agreed within an average of 0.89 ± 3.74 % of the OAR volumes, with 52.5% of the metrics being lower in the automatically generated plans.

Conclusions: The automatic generation of clinically deliverable prostate plans was achieved using predictions from a DL model. Automatically generated plans closely matched manually created plans, demonstrating the potential of this approach for autoplanning.

105
IMPROVED DOSE PREDICTION FOR BREAST RADIOTHERAPY USING NOVEL ANATOMICAL MASK INPUTS FOR 3D DEEP LEARNING MODELS
Lance Moore, Fatemeh Nematollahi, Sandra Meyers, Kevin Moore, Kelly Kisling
University of California San Diego, CA

Purpose: Dose prediction for breast radiotherapy has the potential to facilitate automated planning and clinical decision support. This work compares the performance of four 3D U-net deep learning models for dose prediction trained with different, innovative loss functions and inputs. Specifically, we assess the performance of a model trained with a traditional mean squared error (MSE) loss function, a novel gradient weighted mean squared error (GW-MSE) loss function, and the performance of both loss functions used in conjunction with standard binary anatomical masks or a novel 'glowing' mask input type.

Materials and Methods: The dataset consisted of 311 (216 train/45 validation/46 test) treatment plans for patients treated for left-sided, intact breast cancer using tangential fields from 2012-2018. Prescription dose ranged from 40.05 to 50.40 Gy. The inputs for all models included a CT image and masks for the tumour bed, heart, and lung left contours. The standard contour inputs were represented as binary masks. For the novel 'glowing' masks, the goal was to encode proximity to the contoured structure into every voxel in the mask images. To accomplish this, voxels outside the binary mask were calculated to represent the inverse square fall-off outside the contour mask and normalized to ensure continuity at the edge of the contours. For the models using a standard MSE loss, the error was computed per voxel between the predicted dose and the clinical dose values and averaged over all voxels. We also tested a GW-MSE loss to emphasize the regions of the dose distribution that define the field borders. For the GW-MSE models, the gradient (G) of the clinical dose was first calculated with a 3D Sobel filter convolution, then the values of the gradient were normalized between 0 and 1 using a tanh function to produce the weighting matrix. Finally, the weighted squared error between predicted and clinical dose was added to the non-weighted squared error (SE) before an average was computed, resulting in the following loss function: Loss=Mean (SE+ tanh (G) *SE). Model performance was evaluated by comparing predicted to clinical dose using the following metrics: mean absolute error (MAE) and standard deviation (STD) over all voxels, tumour bed, heart, and lung. We also assessed the overlap of the 50% and 95% isodose volumes using the Dice Similarity Coefficient (DSC) as a surrogate for treated volume and breast tissue coverage.

Results: All doses are represented as percent of prescription. The MAE (STD) over all voxels for the test set was 2.64 (7.37) / 2.52 (7.56) / 2.84 (7.54) / 2.64 (7.28) for MSE loss + binary masks/ MSE + glowing masks/GW-MSE loss + binary masks/GW-MSE + glowing masks. The MAE to tumour bed was 6.48 / 2.19 / 11.31 / 4.04, heart 1.54 / 0.69 / 1.73 / 1.29, and lung 2.62 / 2.44 / 3.15 / 2.63. The mean DSC for 50% isodose was 0.92 / 0.93 / 0.92/ 0.91 and for 95% isodose was 0.85 / 0.87 / 0.87 / 0.79.

Conclusions: The combination of standard MSE loss with glowing masks shows superior performance across all assessed metrics. We speculate that the reason for this is that the network is able to learn the general locations of the masks earlier in the encoding layers, and is thus better able to distinguish more holistic features related to these locations. This model shows very high accuracy and will be used as an input to a new framework for automated planning for breast radiotherapy.

106
AN EFFICIENT PATIENT SELECTION METHOD FOR RAPIDPLAN MODEL DEVELOPMENT
Matthew Mouawad, David Sasaki
CancerCare Manitoba, Winnipeg, MB

Purpose: RapidPlan (RP) is a knowledge-based modelling algorithm that uses previous patient and planning data to estimate dose to new patients. A critical aspect in training a RP model is that the training (and validation) data set must include the same anatomical diversity as the set of patients on which it will be used. Identifying patients and that fit this criterion can be time consuming. To our knowledge, no systematic way of selecting such patients exists. In this work, we present an approach to select patients systematically and efficiently with diverse anatomies.

Materials and Methods: This work was done as part of development of a Pelvis/Prostate model at our institution. Included were patients from the last two years with single phase, two dose level plans and no hip prostheses. The following features were extracted for each patient: (1) target volume (CTVs/PTVs, both dose levels) and (2) organ-at-risk (OAR) volume for each OAR in the RP model. For each target and OAR combination, the (3) centroid distance, and (4) overlap volume of each OAR with each target was calculated. The following analysis was performed in python: each feature was normalized using the standard scalar technique, and principal component analysis was used for dimensionality reduction, selecting features such that 95% of the variance was explained. Iterative KMeans clustering was used to yield clusters with at least two patients per cluster. Two patients were selected from each group and this subsampled population was compared to the total population for each feature separately by: (1) visually inspecting pairs of histograms, (2) descriptive statistics compared for each feature, including the absolute value of the Z-Score (indicating the number of standard deviations (std) the sampled mean is away from the original dataset), and (3) a Kolmogorov-Smirnov test to determine if the subsampled population was representative ($\alpha<0.05$) of the total population.

Results: With four target structures, and eight OARs, there were 54 non-zero features in 204 patients. Eleven KMeans groups were used, and with two patients sampled per group there were 22 patients in the subsample. Visual inspection of the histograms for each feature exhibited similar distributions between sampled data and patient population features (mean/std), and this observation was supported by descriptive statistics for all features. The mean±std Z-score across features was 0.16±0.12 (max=0.4), indicating the sampled feature means were well within the original data standard deviation. The Kolmogorov-Smirnov test for each feature showed non-significance ($p<0.05$), indicating a representative.

Conclusions: We proposed an efficient way of sampling a diverse set of patients in training and validation of a RP model. We will use this method to derive the validation data set and apply this to more complex sites such as head and neck. Further work will look to compare this method to other methods of sampling.

107

CRANIAL METASTASIS DETECTION USING LONGITUDINAL VOXEL-WISE RADIOMICS AND DIFFUSION WEIGHTED IMAGING-BASED MACHINE LEARNING

Joseph Madamesila[1], Nicolas Ploquin[1], Salman Faruqi[1], Subhadip Das[2], Ekaterina Tchistiakova[1]
[1]University of Calgary, Calgary, AB
[2]University of British Columbia, Victoria, BC

Purpose: To develop a machine learning (ML) model for early detection of brain metastases using longitudinal diffusion weighted imaging (DWI) and voxel-wise radiomics.

Materials and Methods: We examined 116 patients who had undergone multiple DWI sessions prior to metastasis treatment via stereotactic radiosurgery. For each patient we co-registered longitudinal CT, contrast-enhanced T1 MRI, and apparent diffusion coefficient (ADC) maps. Voxel-based extraction was used to create radiomic maps from ADC maps. Additional difference maps were created by comparing images at different time points. Cubic masks measuring 1 cm^3 (125 voxels) were generated from all 186 radiomic and difference maps to extract the final dataset inputs. Clinical features (age, sex, primary cancer, and time between imaging sessions) were included in the dataset. Output labels were based on whether a metastasis would present within the local region on future imaging sessions. The classification ML training pipeline consists of splitting training examples using 5-fold cross validation and 80/20 training-to-test with stratification, selecting features based on the Boruta algorithm, and tuning each classifier's hyperparameters towards macro-averaged recall. Three classification models (XGBoost, CatBoost, and LightGBM) were trained. Standard classification metrics were calculated on the unseen test set to assess model performance.

Results: CatBoost displayed an early metastasis detection accuracy of 86.3±0.8% and a recall of 84.9±0.7%. Both XGBoost (accuracy: 86.0±0.9%, recall: 81.1±0.6%) and LightGBM (accuracy: 82.6±0.8%, recall: 84.4±0.8%) performed slightly worse in detecting metastases but showed similar overall performance across both prediction classes. The features chosen by Boruta primarily represented mean changes in radiomic values and primary cancer diagnosis.

Conclusions: The models trained using longitudinal radiomic maps demonstrated predictive power in detecting metastases forming within the brain. Implementation as a decision tool would help clinicians determine whether further monitoring via increased imaging is recommended. Future work includes improving classification metrics and deployment for prospective testing on patients with high metastatic recurrence rates.

108

CLINICAL APPLICATION OF AI-GENERATED CONTOURS IN PROSTATE ULTRASOUND BRACHYTHERAPY

Mathieu Goulet[1], Laurie Pilote[1], Émilie Brouillard[1], Dany Thériault[1,2], James Tsui[3]
[1]Centre régional intégré de cancérologie, Lévis, QC
[2]Université Laval, Quebec City, QC
[3]McGill University Health Centre, Montréal, QC

Purpose: High dose rate (HDR) prostate brachytherapy is a highly effective treatment for localized prostate cancer. The planning process requires imaging of the prostate to guide transperineal needle insertion, either with CT, MR, or ultrasound (US) imaging. The latter modality is sometimes preferred for workflow efficiency (as a single-step procedure) and/or when faced with limited access to other imaging alternatives. As the patient is often kept under general anesthesia from implantation to treatment, keeping the total planning time as low as possible could limit possible complications due to anesthesia and allow for better management of operating room time. In this study, we explore the accuracy and time-saving potential of AI-driven auto-segmentation of organs at risk in the context of US-guided prostate brachytherapy planning.

Materials and Methods: A 3D-UNet convolutional machine learning network was implemented to automatically segment the anterior rectal wall and the prostatic urethra on prostate 3D-US DICOM images. A set of 35 3D-US images acquired using a BK3000 ultrasound after transperineal needle implantation was used for training. The ultrasound system was equipped with a E14CL4b endocavity biplane transducer and 3D DICOM volume reconstruction was obtained with the treatment planning software Oncentra Prostate from Elekta. Model design and training were performed using the PyTorch library version 1.8.2 on a CUDA-capable GPU (NVIDIA Quadro RTX 6000). Clinical urethra and rectum reference contours were used as training baseline using a Dice similarity coefficient loss and AdamW optimizer. Segmentation accuracy was evaluated using a 10-fold cross-validation on the 3D-US dataset. Time savings were quantified on routine clinical cases, which served as the test dataset; these 3D-US images were never seen by the networks during the training/validation phase.

Results: A mean Dice similarity coefficient (DSC) of 0.885 and 0.777 was obtained for the AI-generated rectum and urethra contours from the validation data, respectively. The mean surface DSC on the same dataset was 0.810 and 0.884 for rectum and urethra contours, respectively, using a clinical tolerance of 1 mm. Since the introduction of the automatically segmented urethra and rectum contours, (66±18)% (average + standard deviation) of the contour slices generated using the proposed approach were used clinically without modifications. When more than 50% of either the rectum or the urethra was used without modification, there was a mean gain of 9.6 minutes on the overall planning time (which represents around 17% of the total planning time, which included fusion, contours, and dosimetry).

Conclusions: This study demonstrates the feasibility of integrating auto-segmentation into the clinical workflow and shows the time-saving potential of AI-generated contours from 3D-US images acquired during HDR prostate brachytherapy.

109

CLINICAL VALIDATION OF HPV CTDNA FOR EARLY DETECTION OF RESIDUAL DISEASE FOLLOWING CHEMORADIATION IN CERVICAL CANCER

Kathy Han[1], Jinfeng Zou[2], Zhen Zhao[2], Zeynep Baskurt[2], Yangqiao Zheng[2], Elizabeth Barnes[1], Jennifer Croke[1], Anthony Fyles[1], Adam Gladwish[1], Magali Lecavalier-Barsoum[3], Jelena Lukovic[1], Eve-Lyne Marchand[4], Michael Milosevic[1], Amandeep Taggar[1],Scott Bratman[1], Eric Leung[1]
[1]University of Toronto, Toronto, ON
[2]University Health Network, Toronto, ON
[3]Jewish General Hospital, Montréal, QC
[4]University of Montréal, Montréal, QC

Purpose: Despite chemoradiation (CRT), 30-40% of patients with locally advanced cervical cancer relapse. Most cases are caused by human papilloma virus (HPV), and HPV circulating tumour DNA (ctDNA) may identify patients at highest risk of relapse. Our previous pilot study showed that detectable HPV ctDNA at the end of CRT is associated with inferior progression-free survival (PFS) using digital polymerase chain reaction (dPCR), and that a

next generation sequencing approach (HPV-seq) may outperform dPCR. We hypothesized that HPV ctDNA may identify cervical cancer patients at increased risk of relapse following CRT and aimed to prospectively validate HPV ctDNA as a tool for early detection of residual disease.

Materials and Methods: This prospective, multi centre validation study accrued 70 patients with HPV+ Stage IB-IVA cervical cancer treated with CRT between 2017-2022. Patients underwent phlebotomy at baseline, end of, 4-6 weeks and three months post CRT for HPV ctDNA levels. HPV genotyping was performed on the baseline plasma sample using HPV-seq. HPV genotype-specific DNA levels in plasma were quantified using both dPCR and HPV-seq. PFS was estimated using the Kaplan-Meier method and compared using the log rank test. Multivariable Cox regression analyses incorporating stage and HPV ctDNA detectability assessed independent prognostic factors associated with PFS.

Results: At the time of abstract, results for 67 patients were available. The majority had squamous histology (84%) and Stage IIB (36%) or IIIC1 (25%) disease. HPV genotyping using HPV-seq revealed 54% (36/67) of cases harboring HPV-16, and 46% harboring other HPV types: 15 HPV-18; five HPV-59; two HPV-31; two HPV-33; two HPV-52; one each HPV-39, HPV-45, HPV-53, HPV-58, and HPV-82.With a median follow up of 2.2 (range 0.4 - 5.2) years, there were 21 PFS events. Most recurrences (14/21) were distant and/or paraaortic; four local and nodal/distant; two pelvic nodal; and one local. Patients with detectable HPV ctDNA on dPCR at the end of, 4-6 weeks and three months post CRT had significantly worse two-year PFS compared to those with undetectable HPV ctDNA (78 versus 52%, p=0.04; 82 versus 26%, p<0.001; and 80 versus 23%, p=<0.001, respectively). HPV-seq showed similar results (87 versus 55%, p=0.02; 81 versus 45%, p=0.003; and 84 versus 31%, p=< 0.001, respectively). On multivariable analyses, detectable HPV ctDNA on dPCR and HPV-seq remained independently associated with inferior PFS.

Conclusions: HPV-seq enables HPV genotyping directly from plasma. Persistent HPV ctDNA following CRT is independently associated with inferior PFS in this prospective validation study. HPV ctDNA testing can be used to identify patients at high risk of recurrence in future treatment intensification trials.

110
HYPOMAGNESEMIA AND SURVIVAL IN PATIENTS WITH CERVICAL CANCER TREATED WITH DEFINITIVE CHEMORADIOTHERAPY

Ruth Fullerton[1], Kevin Martell[1], Rutvij A. Khanolkar[1], Tien Phan[1], Robyn Banerjee[1], Tyler Meyer[1], Laurel Traptow[2], Martin Köbel[1], Prafull Ghatage[1], Corinne M. Doll[1]
[1]*University of Calgary, Calgary, AB*
[2]*Tom Baker Cancer Centre, Calgary, AB*

Purpose: Hypomagnesemia is a common side effect of platinum-based chemotherapy regimens. Although there are data reporting that hypomagnesemia is associated with worse survival in patients receiving platinum-based chemotherapy or chemoradiotherapy (CRT), this has not been documented in patients with cervical cancer treated with definitive CRT. We hypothesized that in patients with cervical cancer undergoing definitive CRT, on-treatment hypomagnesemia would be associated with longer treatment duration and worse cancer-specific survival (CSS).

Materials and Methods: Patients with cervical cancer treated with definitive CRT from 1999 to 2015 were identified from a single cancer centre's clinicopathologic database. Lowest on-treatment magnesium value was recorded and categorized as per Common Terminology Criteria for Adverse Events (CTCAE) v5.0 grading (Grade 1: <0.7 - 0.5 mmol/L, Grade 2: <0.5 - 0.4 mmol/L, Grade 3: <0.4-0.3 mmol/L, and Grade 4 <0.3 mmol/L). Grade 0 was defined as ≥ 0.7 mmol/L. Treatment duration was defined as the number of days between the first day of radiotherapy until the last day of pelvic treatment (either brachytherapy or pelvic external beam radiotherapy boost). Prolonged treatment was considered as any treatment duration greater than 63 days. CSS for patients with either Grade 0-1 or Grade ≥ 2 CTCAE v5.0 magnesium toxicity was estimated using the Kaplan-Meier method, and the Peto & Peto modification to the generalized Gehan-Wilcoxon was used to determine statistical significance between groups. Associations with prolonged treatment duration was explored using logistic regression. P-values of <0.05 were considered statistically significant.

Results: One hundred eighty-six patients were identified; median follow-up was seven (IQR 2-11) years. One hundred twenty-five (67%) had Stage I-II disease and 61 (33%) Stage III-IV. Median treatment duration was 51 (IQR 48-57) days. All patients received concurrent weekly cisplatin-based chemotherapy with RT: the majority (n=133; 72%) received 5 or 6 cycles. 147 (79%) patients received routine IV magnesium infusion with their chemotherapy and 173 (93%) received routine IV mannitol. During treatment the highest CTCAE v5.0 magnesium toxicity score was Grade 0-1 in 158 (85%) and Grade ≥ 2 in 28 (15%). Magnesium Grade ≥ 2 was associated with worse 5-year CSS [Grade 0-1: 5yr CSS 67.2%, (95% CI 60.1-75.1); Grade ≥ 2: 5yr CSS 50%, (95% CI 34.5-72.4); p=0.039]. Magnesium status was not associated with an increase in treatment duration [OR 1.465 (95% CI 0.3177 – 6.753); p=0.625].

Conclusions: On-treatment hypomagnesemia ≥ Grade 2 (CTCAE v5.0) was associated with worse CSS but did not predict longer treatment duration. This is the first study that shows a detrimental survival impact of on-treatment hypomagnesemia in this patient population. These findings highlight the need to ensure adequate monitoring, support and correction of magnesium during definitive CRT.

111
RADIATION THERAPY IN RECURRENT ENDOMETRIAL CANCER POST ROBOTIC HYSTERECTOMY; AN INSTITUTIONAL REVIEW

Zainab Al Habsi, Ericka Wiebe, Ananya Beruar, Sean Zhu, Sunita Ghosh, Jasmine Gill, Sophia Pin
University of Alberta, Edmonton, AB

Purpose: Endometrial cancer is the most common gynecologic malignancy and standard of care involves surgery, followed by observation or adjuvant treatment. Despite optimal treatment there continues to be a number of recurrences, which are associated with a poor prognosis. Our aim was to review radiation use at our institution among patients who had an endometrial cancer recurrence.

Materials and Methods: A retrospective chart review of patients treated in a Canadian tertiary cancer centre between January 2012 to December 2019 was performed from a pre-established endometrial cancer database consisting of 1247 patients. One hundred and foryt-three recurrence cases and 147 controls were ultimately included in the analysis after individual selection.

Results: Of the 143 recurrence cases, 26% had received adjuvant EBRT and 39% received adjuvant vaginal vault brachytherapy. When adjusted for age, stage, histology and BMI, the odds of recurrence was lower by 13% after adjuvant EBRT, adjusted OR=0.87 (95% CI: 0.41 - 1.85) p=0.714, and lower by 60% after adjuvant brachytherapy, adjusted OR=0.40 (95% CI: 0.22 – 0.71) p=0.002. Median RFS was 60.8 months (95% CI: 39.5 – 82.1). 56% received radiation for treatment of recurrence, 51% with curative intent. Most common sites of recurrences were the abdomen

(37%), vagina (36%), lung (28%), para-aortics (15%), and pelvis (13%). The most common histology of recurrence was serous for which 8% had complete response to treatment, followed by Grade 1 endometrioid, with 46% complete response to treatment.

Conclusions: Serous histology was the most common pathology in patients with a recurrence and had poor response to treatment, followed by Grade 1 endometrioid, with the best response to treatment. The most common sites of recurrences were the abdomen, vagina and regional nodes. Vaginal vault brachytherapy was associated with a statistically significant reduction in recurrence cases. Grade 1 histology is a low risk feature, and in early stage disease would not warrant adjuvant therapy. Further analysis is ongoing to characterize risk factors associated with recurrences, and refine adjuvant therapy strategies.

112

IS HYPOFRACTIONATED WHOLE-PELVIS RADIOTHERAPY (WPRT) AS WELL TOLERATED AS CONVENTIONALLY FRACTIONATED WPRT IN PROSTATE CANCER PATIENTS? AN EARLY ANALYSIS OF THE HOPE-TRIAL

Lucas C. Mendez[1,2], Glenn Bauman[1,2], Ross Halperin[3], Kevin Martell[4], Vikram Velker[1,2], Belal Ahmad[1,2], Michael Lock[1,2], Aneesh Dhar[1,2], Bryan Schaly[2], Douglas Hoover[2], Andrew Warner[2], Juanita Crook[3], David D'Souza[1,2]
[1]Western University, London, ON
[2]London Health Sciences Centre, London, ON
[3]British Columbia Cancer, Kelowna, BC
[4]University of Calgary, Calgary, AB

Purpose: Stereotactic ablative radiotherapy is a standard of care option for men with a high probability of prostate cancer confined to the prostate. However, the role of extreme hypofractionated radiotherapy for pelvic nodal radiotherapy is not well defined. This trial investigates the role of hypofractionated WPRT combined with a high-dose rate (HDR) brachytherapy boost.

Materials and Methods: HOPE-trial is a phase 2, multi-institutional, randomized clinical trial for unfavourable intermediate (UIR) or high-risk (HR) prostate cancer. The trial enrolled patients from February 2020 to December 2022. All patients received androgen deprivation and 15 Gy HDR brachytherapy boost to the prostate. Patients were randomized in a 1:1 ratio prior to any radiotherapy to either Arm 1, conventionally fractionated WPRT (45-46 Gy in 23-25 daily fractions), or Arm 2, experimental WPRT (25 Gy in 5 fractions on alternate days). Toxicity, patient-reported outcomes (EPIC-50 and IPSS), PSA, and survival data were collected. In this submission, we present data on early QOL endpoints (up to 6 weeks post-WPRT) for these two RT regimens.

Results: Eighty patients (39 in Arm 1 and 41 in Arm 2) participated in this trial. Median follow-up was 10.4 months, with 70 patients currently followed six weeks or more post radiotherapy completion. Baseline clinical characteristics were not statistically different between arms. The two arms were not different in risk group balance with Arm 1 having 28% UIR and 72% HR while Arm 2 had 44% UIR and 56% HR. (p=0.144). All patients received WPRT regimen delivered in accordance to randomization. Planning target volumes between treatment arms were not statistically different. IPSS and EPIC scores at the first WPRT day (post HDR brachytherapy) were not statistically different between Arms 1 and 2. EPIC bowel domain (p=0.015), bowel function subdomain (p=0.009), and bowel bother subdomain (p=0.043) scores were significantly higher (better) in the experimental arm on the last day of WPRT, but not at six weeks post-WBRT. With exception of EPIC urinary irritation score being significantly higher (better) in Arm 1 at 6 weeks post-WBRT (p=0.043), no differences in IPSS, EPIC urinary, and sexual domains were observed between arms at any time point.

Conclusions: Hypofractionated WPRT is well tolerated acutely with comparable urinary and sexual QOL scores to conventionally fractionated RT. Bowel QOL scores were less impacted by hypofractionated WPRT at the end of treatment than with conventionally fractionated WPRT, although this difference lost significance at six weeks.

113

FINAL RESULTS FROM A PROSPECTIVE RANDOMIZED PILOT TRIAL OF STEREOTACTIC BODY RADIATION THERAPY VERSUS RADIOFREQUENCY ABLATION FOR THE MANAGEMENT OF SMALL RENAL MASSES (RADSTER)

Anand Swaminath[1], Raees Cassim[1], Braden Millan[1], Oleg Mironov[1], Priya Ahir[2], Camilla Tajzler[3], Jen Hoogenes[1], Kimmen Quan[1], Edward Matsumoto[1], Anil Kapoor[1]
[1]McMaster University, Hamilton, ON
[2]St. Joseph's Health Care, Hamilton, ON
[3]N/A, Toronto, ON

Purpose: The benefits of stereotactic body radiation therapy (SBRT) as a primary treatment modality for small renal masses (SRMs) ≤4cm are unclear. Our objective was to evaluate both SBRT and radiofrequency ablation (RFA) for SRMs to determine the utility of a future Phase III randomized controlled trial (RCT).

Materials and Methods: Patients with SRMs who declined active surveillance, surgery or were deemed inoperable were recruited at a single tertiary academic centre. After meeting inclusion/exclusion criteria, participants were assigned 1:1 to SBRT or RFA, with crossover allowed if technical or patient factors precluded either treatment. SBRT included an initial simulation and a single delivered fraction of 25 Gy to the planning target volume. RFA was conducted percutaneously with two cycles of up to eight minutes each upon reaching target temperature. Renal protocol imaging (CT or MRI) was completed q3 months (up to one year) post-procedure. Diagnostic and one-year renal biopsies were also required. The objective of this trial was feasibility of randomization, with the aim of recruiting 24 patients based on this assumption.

Results: From January 2020 to June 2021, 33 patients were screened, with 24 recruited and initially randomized (SBRT=12; RFA=12). Median age was 67 years (53-85) and 17/24 were male. Seventeen patients had clear cell renal cell carcinoma (RCC), six had papillary RCC, and one had chromophobe RCC. Following randomization, a total of 14 patients had SBRT, seven had RFA, and three declined treatments. Crossover mainly occurred from RFA to SBRT due to technical inability to perform RFA. One Grade 2 acute pain flare occurred in the SBRT group (none in the RFA group). No late toxicity up to one year was reported in either group. At one year, no radiographic local failure (RECIST) was observed, although RFA patients were more likely to have loss of arterial enhancement (83.3% versus 23%, p=0.041). Mean reduction of estimated glomerular filtration rate was similar at one year (RFA -3 mL/min, SBRT -5.3 mL/min, p=0.7). Biopsies were performed in 23/24 patients at one year, on per-protocol analysis 7/7 (100%) of RFA patients had no evidence of residual RCC, whereas with SBRT 5/14 (36%) patients had no evidence of residual RCC, 2/14 (14%) had scant/minimal residual disease, and 7/14 (50%) had evidence of RCC. No patients developed distant failure or death from RCC during follow-up.

Conclusions: Recruitment, randomization and follow-up of patients with SRMs was feasible in this study. More patients received SBRT compared to RFA, highlighting the need for thorough multidisciplinary evaluation prior to randomization. Both treatments have excellent safety profiles, with RFA demonstrating initial higher rates of pathological/radiologic response, however long-term follow-up is required. This trial supports the need for a large scale RCT with appropriate radiographic and pathological endpoints built in.

114

STEREOTACTIC BODY RADIATION THERAPY (SBRT) AND HYPO-FRACTIONATED RADIATION THERAPY (HFRT) OUTCOMES FOR LOW AND INTERMEDIATE-RISK PROSTATE CANCER (PRCA): EXPERIENCE AT TWO ONTARIO CENTRES

Hsin-pei (Spencer) Hu[1,2], Gregory Anagnostopoulos[2,1], Mohammad Gouran-Savadkoohi[1,2], Ian Dayes[1,2], Adrian Ishkanian[3], Abhirami Hallock[3], Himanshu Lukka[1,2], Kimmen Quan[1,2], Kara Schnarr[1,2], David Cuthbert[3], Mira Goldberg[1,2], Theodoros Tsakiridis[1,3,2]
[1]Hamilton Health Sciences, Hamilton, ON
[2]McMaster University, Hamilton, ON
[3]Niagara Health, St. Catharines, ON

Purpose: Several studies suggest biochemical progression-free survival (bFFS) rates after SBRT compare favourably with other definitive RT treatments for low and intermediate-risk PrCa. Randomized trial outcomes of 7-fraction SBRT have been reported, but results of randomized studies that compare 5-fraction SBRT with conventional and hypo-fractionated radiotherapy (HFRT) are pending or ongoing. The objective of this study was to assess regional outcomes following definitive SBRT and HFRT in patients with localized low or intermediate-risk PrCa treated at two institutions in Ontario.

Materials and Methods: We reviewed patients with low or intermittent-risk PrCa treated with SBRT or HFRT alone in the period of July 2010 and February 2022. Database search criteria included treatments with SBRT 35-40Gy in 5 fractions and HFRT 60-62Gy in 20 fractions. Overall survival (OS), time to biochemical failure (per Phoenix criteria: i.e. 2ng/mL above PSA nadir) and bFFS were reviewed. Kaplan-Meier curves were used to assess OS and bFFS. Propensity matching were used to match HFRT-treated patients to SBRT-treated patients based on baseline characteristics, including patient age, Gleason grade, clinical T-stage, and PSA at treatment. Hazard ratios were obtained with Cox Proportional Hazards models to assess the effects of treatment with SBRT versus HFRT. Further, in the SBRT-treated patients with biochemical failure, we reviewed their restaging CT scans, bone scans, and PSMA-PET scans (if available) for the patterns and specific sites of recurrence.

Results: We identified 314 patients with low or intermediate risk PrCa who were treated with SBRT and 639 patients who were treated with HFRT. Median follow-up was 32.8 months for the SBRT cohort and 31.8 months for the HFRT cohort. Intermediate risk category composed 86% and 95% of the SBRT and HFRT cohorts, respectively. Mean time to biochemical failure was 33.0 months after SBRT versus 30.1 months after HFRT. After propensity matching, the five-year OS and bFFS rates were 96.6% [93.8-99.4%] and 92.3% [88.2-96.5%] for SBRT-treated patients, respectively, versus 95.8% [92.9-98.7%] and 92.9% [87.6-98.5%] for HFRT-treated patients, respectively. SBRT and HFRT treatments produced similar OS or bFFS rates [hazard ratios of 0.962 (p=0.94) and 1.118 (p=0.67), respectively].

Conclusions: SBRT is an effective treatment option for low to intermediate-risk PrCa with encouraging OS and bFFS rates comparable with HFRT. Pending randomized trial results will determine whether SBRT is the new standard of care for this population.

115

PREDICTORS OF TUMOUR DYNAMICS DURING A SIX-WEEK COURSE OF CHEMORADIOTHERAPY FOR GLIOBLASTOMA

Wee Loon Ong[1,2], James Stewart[1], Arjun Sahgal[1,2], Hany Soliman[1,2], Chia-Lin Tseng[1,2], Jay Detsky[1,2], Ling Ho[1,2], Sunit Das[1], Pejman Maralani[3], Nir Lipsman[1], Greg Stanisz[4], James Perry[1,2], Hanbo Chen[1,2], Eshetu Atenafu[5,1], Angus Lau[4], Mark Ruschin[4,1], Sten Myrehaug[1,2]
[1]University of Toronto, Toronto, ON
[2]Sunnybrook-Odette Cancer Centre, Toronto, ON
[3]Sunnybrook Health Sciences Centre, Toronto, ON
[4]Sunnybrook Research Institute, Toronto, ON
[5]University Health Network, Toronto, ON

Purpose: Our prior imaging studies have shown geometrically meaningful inter-fraction tumour dynamics specific to glioblastoma (GBM). We aim to identify predictors associated with tumour dynamics during a six-week course of concurrent chemoradiotherapy (CRT) for GBM.

Materials and Methods: Patients enrolled in a prospective serial magnetic resonance imaging (MRI) study were reviewed. All patients were treated with 54-60Gy in 30 fractions. The gross tumour volume (GTV) included the surgical cavity and T1c enhanced residual tumour; clinical tumour volume (CTV) included GTV with a 15 mm isotropic expansion, respecting anatomical boundaries; planning target volume (PTV) was 4 mm expansion. MRIs were obtained at RT planning (F0), fraction 10 (F10), and fraction 20 (F20). Tumour dynamic metrics (relative to F0) assessed included the GTV volume (Vrel), Hausdorff distance (dH) and migration distance (dM). dH is the average distance between two datasets in metric space. dM is the maximum linear displacement of the GTV in any direction. Factors to be determined associated with tumour dynamics included: age, sex, corpus callosum (CC) involvement, extent of surgery (gross total resection (GTR), subtotal resection (STR) or biopsy alone (Bx)), MGMT methylation and IDH mutation status.

Results: One hundred twenty-nine patients were reviewed. Median GTV was 20.9cc at F0, 17.6cc at F10 (Vrel 0.85), and 16.1cc at F20 (Vrel 0.78). Patients without CC involvement had more marked GTV volume reduction: Vrel 0.82 versus 1.02 with CC involvement at F10 (P=0.05), and Vrel 0.77 versus 0.88 with CC involvement at F20 (P=0.03). Patients with GTR (versus STR versus Bx) had more marked GTV volume reduction across all time points: Vrel 0.78, 0.85 and 1.07 respectively at F10 (P=0.001), and Vrel 0.69, 0.80, 1.04 respectively at F20 (P=0.001). The median dH was 8.1 mm at F10 and 9.2 mm at F20. Patients with CC involvement (versus without CC involvement) had a larger dH: 54% versus 25% had dH>10mm respectively at F10 (P=0.03), and 73% versus 28% had dH>10mm respectively at F20 (P<0.005). Patients with a GTR had smaller dH at both F10 (P=0.02) and F20 (P=0.006). At F20, 20%, 47% and 37% of patients with GTR, STR and Bx had dH>10mm (P=0.04). The median dM were 4.7mm at F10 and 4.7mm at F20. Patients with CC involvement (versus without CC involvement) had larger dM: 41% versus 12% had dM >10mm respectively at F10 (P=0.01), and 45% versus 9% had dM >10mm respectively at F20 (P<0.001). Patients with GTR had smaller dM at F10 (P=0.03) and F20 (P0.002). At F20, 0%, 25% and 19% of patients with GTR, STR and Bx had dM>10mm (P=0.002). Age, sex, MGMT methylation and IDH mutation status were not associated with Vrel, dH and dM at F10 and F20.

Conclusions: We identified CC involvement and extent of surgery to be associated with tumour dynamics at F10 and F20 over the course of CRT for GBM. This offers opportunities to better select patients who may benefit from earlier/ more frequent RT replan/ adaptation to ensure adequate tumour coverage, or to reduce RT toxicities.

116

A CHARGED DEBATE: PHOTON VERSUS PROTON SBRT FOR HEAD AND NECK MUCOSAL PRIMARIES ACROSS TWO INSTITUTIONS

Adam Mutsaers[1], Lee Chin[1], He Catherine Wang[2], Mohammed Aldohan[1], Christopher Goodman[3], Xiaodong Zhang[2], Madette

Galapin[1], Anna Lee[2], G. Brandon Gunn[2], Andrew Bayley[1], Ian Poon[1], Jack Phan[2], Irene Karam[1]
[1]*University of Toronto, Toronto, ON*
[2]*The University of Texas MD Anderson Cancer Center, Houston, TX*
[3]*Western University, London, ON*

Purpose: Stereotactic body radiotherapy (SBRT) for Head and Neck mucosal tumours is increasingly used in patients unfit for conventional therapy. Plans require vigorous optimization to protect organs at risks (OARs) while delivering high biologically effective doses (BED) to maximize tumour control. A dosimetric comparison of SBRT plans using photon-based volumetric modulated arc therapy (VMAT) and intensity-modulated proton therapy (IMPT) was completed.

Materials and Methods: With ethics approval, a multi-institutional planning study compared 13 treated plans from Centre 1 (C1), with IMPT plans from Centre 2 (C2) generated on identical data sets. Patients were treated with photon SBRT (BED_{10}>=59.5Gy) at C1 from 2014-2022, and included de novo mucosal targets in the oropharynx (OP) or oral cavity (OC), limited/contiguous nodes, and were ineligible for conventional therapy. Gross tumour volumes (GTV) were defined at C1 on CT/MRI with 3mm planning target volume (PTV) expansion. Dose objectives (PTV V40>95%) and OAR limits from C1 were utilized. Photon plans were generated in Pinnacle, primarily with VMAT (1-2 arcs) using SmartArc optimization and a collapsed cone convolution superposition dose algorithm. IMPT plans generated by C2 were created in Raystation using Monte Carlo algorithm for small spot size (3-6 mm sigma in air) Hitachi proton therapy unit. IMPT plans used 4-5 non-coplanar fields with robust optimization (±2.5% range, 2mm setup uncertainties). Coverage, R50, R25, conformity index (CI=100% isodose/PTV), heterogeneity index (HI=D2%/D98%) and OAR mean and maximum doses (dmax) were compared using descriptive statistics and Wilcoxon signed-rank test.

Results: Thirteen cases (5OP, 8OC) of T2-T4, N0-1 squamous cell carcinomas that received a median dose of 40Gy in 5 fractions (range: 35-48Gy) to the PTV (8 planned with integrated boost of 45Gy to GTV) were analyzed. Mean GTV (primary+node) was 40cc (range: 3.8-157.2cc).
IMPT performed significantly better on most metrics. Protons significantly improved PTV V40 coverage (mean 98.1% versus 95.69%, p=0.0196). Despite no additional optimization, IMPT achieved significantly greater sparing of brain/spinal cord and parotids (dmax decrease=7.4Gy, p<0.05; 6.7Gy, p=0.03). For adjacent mandible and uninvolved mucosa, dmax was similar, while mean dose was significantly improved (mean 8.3Gy versus 16.0Gy, p=0.03; mean 4.9Gy versus 12.9Gy, p=0.008). CI was similar between modalities (mean 1.12 versus 1.14, p=0.61). However, R50 and R25 significantly improved with IMPT (mean: 2.72 versus 3.99, p=0.008; 5.26 versus 8.17, p=0.008). IMPT delivered a more homogenous dose within GTV and PTV (mean HI:1.04 versus 1.08 p=0.013; 1.17 versus 1.22, p=0.04).

Conclusions: In this dosimetric analysis, IMPT significantly improved target coverage, homogeneity, low/intermediate dose wash and sparing of OARs for mucosal HN targets treated with SBRT. Prospective data is required to determine clinical benefits and cost-effectiveness analysis will be vital to evaluate feasibility.

117
EVALUATION OF PLANNING TARGET VOLUME (PTV) IN THE OUTCOMES OF PROSTATE CANCER PATIENTS TREATED WITH MODERATE HYPOFRACTIONATED RADIOTHERAPY

Rania Soliman[1], Luis Souhami[2], Marie Duclos[2], Fabio Cury[2], Horacio Patrocinio[2], Sergio Faria[2]
[1]*McGill University, Montréal, QC*
[2]*McGill University Health Centre, Montréal, QC*

Purpose: In our institution, moderate hypofractionated radiotherapy has been offered for any patient with prostate cancer, independently of the size of the prostate. However, there is an understandable concern that patients with large prostate volumes may not respond as well to this approach. In this study, we aimed to compare the outcomes of patients with two different prostate volumes.

Materials and Methods: We reviewed prostate cancer patients treated in our institution between April-2010 and January-2017, with a dose of 60Gy in 20 daily fractions and a minimum follow-up of 24 months. Typically, the PTV was the prostate volume with a 7 mm margin. Patients were divided into two groups depending on the volume of the PTV. A large PTV volume (L-PTV) was defined as the volume of PTV at the highest quartile. We compared acute/late genitourinary (GU) and gastrointestinal (GI) toxicity, prospectively scored on each follow-up according to CTCv3.0, and survival without events (events defined as any type of relapse or death for any cause) among patients with and without L-PTV.

Results: We reviewed 306 patients. Of these, 77 (last quartile) had L-PTV (PTV ≥ 154 cm^3), with a median PTV of 195 cm^3 (range: 154-289), and the remaining 229 patients had a median PTV of 110 cm^3 (range: 55.3-153.7 cm^3). The median age was 70 years in both groups. Median follow-up was 70 months (range: 26-143), similar to both groups. Hormonal therapy was given to 38% versus 71% of L-PTV versus non L-PTV patients, respectively. Acute Grade 2/3 GU toxicity was 31% versus 19% (p=0.03), whereas acute Grade 2/3 GI toxicity was 14% versus 11% (p=0.42) for the L-PTV versus non-L-PTV patients, respectively. Late Grade 2/3 GU toxicity was 2.6% versus 5.7% (p=0.27), whereas late Grade 2/3 GI toxicity was 7.8% versus 4.4% (p=0.24) for the L-PTV versus non L-PTV patients, respectively. At the last follow-up, more patients were alive and with no evidence of prostate cancer (90% versus 78%, p=0.026) in the L-PTV group.

Conclusions: In this cohort of prostate cancer patients treated with 60Gy in 20 fractions, a large PTV (≥ 154 cm^3) was not associated with poorer tumour control compared with patients with PTV < 154 cm^3, recognizing that are many other factors related to tumour control. In terms of toxicity, L-PTV patients had higher acute Grade 2/3 GU toxicity but not late GU toxicity compared to patients with smaller prostate volume. Acute and late Grade 2/3 GI toxicity looked similar in both groups.

118
CODE GREY IS STILL IN EFFECT: LESSONS LEARNED FROM A CYBERATTACK

Teri Stuckless[1,2], Donia MacDonald[1], Suzanne Drodge[1,2], Maria Corsten[1], Susan Costello[1], Astrid Billfalk-Kelly[1,2]
[1]*Cancer Care Program, Eastern Health, NL*
[2]*Memorial University of Newfoundland and Labrador, NL*

Purpose: On October 29, 2021, Newfoundland and Labrador's health care system fell victim to a cyber attack resulting in a province-wide code grey, paralyzing our health information systems and networks. The highly complex technology of radiotherapy makes it one of the most computer- and-network-dependent areas of healthcare. With cyber-attacks increasing in frequency, departmental emergency planning needs to cover all scenarios up to and including a complete loss of access to internal and external networks and shared software.

Materials and Methods: We will discuss experiences from radiation oncology, therapy, physics and administration during a total loss of network functionality. We will describe the event, the impact on clinical operations, contingency planning during the event and after, lessons learned and future directions to mitigate risk in the future.

Results: We identified four key problems: (1) inability to access patient information and identify those patients currently receiving treatment or awaiting treatment, (2) loss of access to radiation planning and treatment information, (3) loss of access to all information stored on network drives, including quality assurance procedures, and (4) risks associated with paper documentation of encounters in the electronic era. This will include a description of struggles associated with lack of access to the EMR and all health information systems. We will also present some of the measures that have been put in place as a result, including a procedure we developed and tested for treating on a C-Series Linac with no network access.

Conclusions: A machine downtime policy is not adequate to cover loss of network access. Every department should examine their day-to-day processes and be aware that something as simple as accessing patient contact information may not be possible during network downtime.

119

AN MRI-BASED CONVOLUTIONAL NEURAL NETWORK TO PREDICT BIOCHEMICAL RECURRENCE FOLLOWING RADIOTHERAPY FOR INTERMEDIATE AND HIGH RISK LOCALIZED PROSTATE CANCER

Negin Piran Nanekaran[1], Tony Felefly[2], Eranga Ukwatta[1], Nicola Schieda[2], Scott Morgan[2]
[1]*University of Guelph, Guelph, ON*
[2]*The Ottawa Hospital, University of Ottawa, Ottawa, ON*

Purpose: The risk of biochemical recurrence (BCR) following radiotherapy (RT) for localized prostate cancer (LPCa) varies considerably within risk stratification groups defined by classic clinical and pathologic variables; there is an unmet need for low-cost tools that more robustly predict BCR and allow for individualized therapy. Published imaging-based algorithms for BCR prediction after RT are limited to hand-crafted radiomics and/or small cohorts. We aimed to develop a deep learning model to predict BCR at five years after RT for intermediate and high risk LPCa using pre-treatment T2-weighted (T2W) MRI.

Materials and Methods: Patients with intermediate and high risk LPCa treated with radical RT at our institution between 2010 and 2015 were included. We excluded those who did not have a pre-treatment T2W-MRI and those with less than five years of follow-up. The Phoenix definition for BCR was used. The dataset (DS1) was split into training (70%), validation (20%), and test (10%) sets using a stratified technique. A U-Net model for prostate segmentation was trained and tested on a separate annotated prostate T2W-MRI dataset (DS2) of 225 patients from our institution. The U-Net model was then used to segment the whole prostate gland on the MRI images of DS1, and the segmented images were fed into four 2D convolutional neural networks (CNNs) using different network architectures and regularization techniques (VGG blocks with batch normalization, dropout, and max pooling layers) to predict BCR at 5 years. The CNNs were evaluated using the area under the receiver operating characteristic curve (AUC) on the test set. For benchmarking, three machine learning classifiers (Random Forest, Logistic Regression, and Support Vector Machines) were developed using the five most important features selected by Mean Decrease in Impurity from a set of 18 clinical variables.

Results: A total of 189 patients were included in DS1. Androgen deprivation therapy (ADT) was received by 83.6% of patients. BCR was identified in 26% of the cases. The Dice score for the U-Net segmentation model was 78% on the test set of DS2. The AUC achieved by the different CNNs for predicting BCR ranged between 0.53 and 0.75. The best performing CNN consisted of 3 convolutional layers, the first two followed by max-pooling layers, a flattening layer, a dense layer, and an output layer with softmax activation function. The best clinical model was a Random Forest algorithm with an AUC of 0.70. The selected clinical variables by decreasing feature importances were: age, time to nadir PSA, pre-treatment PSA, percentage of positive biopsy cores at diagnosis, and nadir PSA.

Conclusions: We developed a deep learning model based on pre-treatment T2W-MRI to predict BCR at five years following radical RT for intermediate and high-risk LPCa. This CNN outperformed a model based on clinical variables and warrants further validation in external cohorts.

120

DESIGN OF PATIENT SPECIFIC MULTI-CATHETER GYNECOLOGICAL BRACHYTHERAPY APPLICATORS WITH CUSTOMIZABLE CATHETER POSITIONS

Jasmine Penney[1,2], Dr. Krista Chytyk-Praznik[2,1], Dr. Amanda Cherpak[2,1]
[1]*Dalhousie University, Halifax, NS*
[2]*Nova Scotia Health Authority, Halifax, NS*

Purpose: Brachytherapy patients are often planned with vendor supplied applicators; for asymmetric gynecological targets, the applicator of choice is often the MIAMI. These applicators have different diameters; however, they do not have individualized catheter locations, which could result in higher doses delivered to organs at risk (OARs) and normal tissues. This research designed patient specific multi-catheter applicators with the potential for customizable catheter positions and applicator shape, which could be produced with a 3D printer. Adjusting the size and shape of the applicator, along with determining catheter locations based on the patient's specific anatomy, will allow asymmetric cases to be treated more effectively with brachytherapy.

Materials and Methods: This study used anonymized planning data from past brachytherapy patients treated at the QEII Cancer Centre. The tumour volume and OARs were contoured, as was an applicator based on patient anatomy, and general shape of the original treatment applicator. Catheter positions were placed based on tumour location. DVH parameters from the patient specific applicator(s) were then compared to the original treatment plan.

Results: When comparing the patient specific plans with the original treatment plans, clinical target volume (CTV) coverage was better in the patient specific plans (for example, V_{100} was 88.52% versus 97.92% in one patient). D_{98} also showed similar results (86.24% versus 99.63%). Evaluating dose to surrounding tissues, the patient specific plans showed less unwanted dose to the surrounding tissues than the original plan. Quality indices and OAR doses were also superior in the patient specific plans over the original treatment plans.

Conclusions: Patient specific applicators with customizable shape and catheter locations showed a more homogeneous and conformal target coverage when compared to the original treatment plan. A patient specific, 3D-printed applicator could result in better coverage of the CTV, while also better sparing the OARs, when comparing the plans created with standardized applicators.

121

NEURAL NETWORK DOSE PREDICTION FOR CERVICAL BRACHYTHERAPY: OVERCOMING DATA SCARCITY FOR APPLICATOR-SPECIFIC MODELS

Lance Moore, Karoline Kallis, Nuno Vasconcelos, Kelly Kisling, Dominique Rash, Catheryn Yashar, Jyoti Mayadev, Kevin Moore, Sandra Meyers
University of California San Diego, CA

Purpose: 3D neural network dose predictions have been shown to be useful for automating tandem-and-ovoid (TO) brachytherapy treatment planning for cervical cancer. However, cervical brachytherapy can be delivered with numerous applicators, which necessitates development of models that can generalize to other applicator types. This variability and scarcity of data for any given applicator type poses challenges for deep learning. The goal of this work was to compare three methods of neural network training: (1) a single model trained on all applicator data, (2) transfer learning (TL) of the combined model to each applicator, and (3) individual applicator models - in order to determine the optimal method for accurate dose prediction.

Materials and Methods: Neural network models were produced for four applicator types - TO, TO with 1-7 needles (TON), tandem-and-ring (TR) and TR with 1-4 needles (TRN). First, a single model was trained on all applicator data using 907 treatment plans from 273 cervical cancer patients treated from 2010 onwards. The train/validation/test split was 70%/15%/15%, with approximately 49%/11%/18%/21% TO/TON/TR/TRN in each dataset. The inputs included four channels for binary anatomical masks (high-risk CTV (HRCTV), bladder, rectum and sigmoid), a binary mask representing the location of dwell positions, and dose kernel channels for each dwell position. The dose kernel channels were created by mapping a 3D dose kernel to each dwell position in the plan, with uniform dwell time weight. A 3D Cascade U-Net with a mean squared error (MSE) loss function was used. Then we applied TL in an attempt to further improve applicator-specific performance. The encoding layers of the combined model were frozen and decoding layers were updated with further training on applicator-specific data. Finally, single applicator models were trained using only data from a specific applicator type. Performance of these three model types, evaluated for each applicator type separately, were compared using the following metrics: mean error (ME, representing model bias) and mean absolute error (MAE) over all dose voxels and ME of clinical metrics (high-risk CTV (HRCTV) D90% and D2cc of bladder, rectum and sigmoid), averaged over all patients. A positive ME indicates the predicted dose was lower than clinical.

Results: The combined model generally provided the most accurate dose predictions, with ME=2.0/0.9/0.1/1.8% (TO/TON/TR/TRN), MAE=5.3/5.8/3.9/5.2%, range of ME D2cc across organs=1.3-2.9/(-1.9)-3/(-1.3)-0.5/1.5-3.6%, and ME D90=2.6/-4.4/4.8/0.0%. The only exception was TO, where TL improved ME by 0.6%, MAE by 0.2% and clinical metrics by 1.2% on average.

Conclusions: 3D brachytherapy dose was predicted accurately for all applicator types, as indicated by low voxel-based ME and MAE and <5% ME in clinical metrics. Training on all treatment data overcomes challenges with data scarcity in each applicator type, resulting in superior performance than can be achieved with TL or training on individual applicators alone. We believe the larger, more diverse dataset allows the neural network to learn underlying trends and characteristics in dose that are common to all treatment types. The fact that TO performance improved with TL indicates that TL may be beneficial when there is sufficient data to prevent overfitting. Accurate, applicator-specific dose predictions could enable automated, knowledge-based planning for any cervical brachytherapy treatment.

122
IS SELENIUM-75 A FEASIBLE HDR BRACHYTHERAPY SOURCE?

Jake Reid[1], Shirin A. Enger[1], Jonathan Kalinowski[1], Andrea Armstrong[2], John Munro III[3]
[1]*Lady Davis Institute for Medical Research, Jewish General Hospital, Montréal, QC*
[2]*McMaster University, Hamilton, ON*
[3]*N/A, MA*

Purpose: Selenium-75 (^{75}Se, $t_{1/2}$ = 118 days, Eγ,avg = 210 keV) is a radioisotope that is widely used in industrial gamma radiography. Its lower photon energy and longer half-life compared to Iridium-192 (^{192}Ir, $t_{1/2}$ = 74 days, Eγ,avg = 380 keV) make it a viable candidate for use as a brachytherapy source. The goal of this study was to investigate the feasibility of using a ^{75}Se source for brachytherapy applications and investigate its shielding properties combined with a novel rectal applicator developed for intensity-modulated brachytherapy.

Materials and Methods: An active core (0.65 mm diameter, 7 mm length, 3.7 g/cm^3 packed density) of a ^{75}Se source was encapsulated in a titanium (4.5 g/cm^3, 0.90 mm outer diameter, 0.25 mm wall thickness) capsule. The length of the active core was chosen to hold 23 Ci of ^{75}Se, providing a dose rate equivalent to 10 Ci of ^{192}Ir. The American Association of Physicists in Medicine TG-43U1 brachytherapy dosimetry parameters were determined for the ^{75}Se source using the Monte Carlo-based treatment planning system, RapidBrachyMCTPS. Dose distributions were acquired in a water phantom for two tungsten shields: a static shield used in conventional brachytherapy with a shield diameter of 8 mm and a rigid intensity-modulated brachytherapy shield with an emission window of 180° and a thickness of 7.5 mm. The resulting data were used to calculate the transmission factors for the different shield models and compared with simulations performed using an ^{192}Ir source. One of the rigid shield designs was retrospectively tested on CT images for a rectal cancer patient treated with high dose rate brachytherapy to calculate the absorbed dose to the tumour and surrounding healthy tissues for both the ^{75}Se and ^{192}Ir sources. The treatment optimization was completed identically for both sources, with the prescribed dose to 90% of the tumour volume being 10 Gy and the dwell positions created along the source channel having a step size of 5 mm with a 15° increment shield rotation.

Results: The radial dose function and 2D anisotropy function were calculated and plotted in comparison with ^{192}Ir. The air kerma strength per unit activity and dose rate constant for ^{75}Se were 4.751 +/- 0.005 x 10^{-8} U/Bq and 1.116 +/- 0.001 cm^{-2} respectively and for ^{192}Ir 9.79 +/- 0.01 x 10^{-8} U/Bq and 1.110 +/- 0.001 cm^{-2} respectively. Dose distributions in a water phantom were calculated and the dose colour maps for all scenarios were plotted. For the conventional brachytherapy shield the TF values were 20.0 +/- 0.1 % and 4.12 +/- 0.06 % for ^{192}Ir and ^{75}Se, respectively. For the rigid IMBT shield the TF values were 17.1 +/- 0.1 % and 3.18 +/- 0.06 % for ^{192}Ir and ^{75}Se, respectively. This displayed that ^{75}Se had 4.85 and 5.38 times better attenuation than ^{192}Ir for the shields analyzed. For the calculated absorbed doses on the patient data, with both treatment plans achieving a prescribed dose of 10 Gy to 90% of the tumour volume, all dose indices were improved when using the ^{75}Se source. The most noticeable improvements were that the D_{2cc} of the contralateral rectum was decreased by 1 Gy and the D_{50} for the rectum was decreased by 1.2 Gy when using the ^{75}Se source. The type A uncertainty for these values were <1%.

Conclusions: The designed ^{75}Se source was found to be better at attenuating through tungsten shields than ^{192}Ir due to its lower energy while still producing an equivalent dose rate. This allows for improved treatment plans that deliver the same absorbed dose to tumours as ^{192}Ir, with similar treatment times, while reducing the dose to surrounding organs at risk. These results justify further analysis of this source for use in conventional brachytherapy and intensity-modulated brachytherapy.

123
COMMISSIONING OF AN OPEN-SOURCE MONTE CARLO CODE FOR LOW DOSE RATE BRACHYTHERAPY DOSE EVALUATION

Narjes Moghadam[1], Claire Zhang[2,3], Samuel Ouellet[4], Dakota

Mckeown[2,5], Joanna Cygler[6], Michelle Hilts[2,5], Luc Beaulieu[4], Rowan Thomson[1]
[1]*Carleton University, Ottawa, ON*
[2]*British Columbia Cancer, Kelowna, BC*
[3]*University of British Columbia, Kelowna, BC*
[4]*Université Laval, Quebec City, QC*
[5]*University of British Columbia, Kelowna, BC*
[6]*The Ottawa Hospital, Ottawa, ON*

Purpose: To clinically implement the egs_brachy graphical user interface (eb_gui) for low-dose-rate (LDR) prostate and breast brachytherapy, and to commission eb_gui MC simulations by comparing to treatment planning system (TPS) calculations for a series of test cases.

Materials and Methods: A series of test cases for both breast and prostate was developed: (I) one-seed; (II) 3x3 seed grid; (III) 3x3x3 seed grid; (IV) clinical case. Breast cases were generated using ^{103}Pd (TheraSeed200, 2.5U, 90 Gy prescription dose) and clinical TG43 dosimetry calculated in MIM Symphony (V6.9.5). The prostate cases were generated using ^{125}I (SelectSeed, 0.76212U, 144 Gy prescription dose) and TG43 dose calculated in Oncentra Prostate (V4.2.2; Elekta). For each case, two MC simulations were performed using eb_gui: (i) TG43MC (water phantom, no interseed attenuation), and (ii) TG186MC (realistic tissue assignment with interseed attenuation). Voxel-based dose comparisons were performed between MC and TPS results evaluating local and global differences, as well as considering dose metrics and dose-volume histograms.

Results: Dose distributions for all cases were evaluated using eb_gui. The level I validation of TG186 was accomplished by comparing TG43MC dose distributions with TPS data and good agreement was found for both breast and prostate cases. Dose differences between TPS and TG43MC doses were less than 0.2 Gy (one seed) and 2 Gy (clinical cases) for 90% of dose voxels. For the clinical test cases, the maximum local and global relative dose differences were less than ±10% and ±2%, respectively. The TG186 dose comparisons with TG43MC or TPS show an overestimation of dose indices, up to 27% (D90 prostate), using water approximation confirming the need for a model-based dose calculation algorithm (MBDCA).

Conclusions: A clinical implementation of the eb_gui workflow along with various test cases for LDR breast and prostate were developed. This is one step further in the implementation of TG186 model-based dose calculation methods for LDR brachytherapy in a clinical setting to ensure dosimetric accuracy and clinical safety and efficiency. Our results show substantial dose differences between MBDCA (TG186MC) and clinical TPSs; egs_brachy and eb_gui address an important need for improved dosimetric accuracy in clinical LDR brachytherapy. In the next step, egs_brachy-based TG186 MC simulation results will be compared with other MBDCAs to accomplish the level II validation of TG186.

124
DEVELOPMENT OF A NOVEL DOSIMETRY SOFTWARE FOR PATIENT-SPECIFIC INTRAVASCULAR BRACHYTHERAPY TREATMENT PLANNING ON OPTICAL COHERENCE TOMOGRAPHY IMAGES

Maryam Rahbaran[1], Jonathan Kalinowski[1], James Man Git Tsui[2,3,4], Joseph DeCunha[5], Kevin Croce[3,4], Brian Bergmark[3,4], Philip Devlin[3,4], Shirin A. Enger[1]
[1]*McGill University, Montréal, QC*
[2]*McGill University Health Centre, Montréal, QC*
[3]*Brigham & Women's Hospital, Boston, MA*
[4]*Harvard Medical School, Boston, MA*
[5]*The University of Texas MD Anderson Cancer Center, Houston, TX*

Purpose: Intravascular brachytherapy (IVBT) is a modality of radiation therapy used to treat in-stent restenosis. Drug-eluting stents are the primary therapy for the treatment of in-stent restenosis, but IVBT remains critical for treatment if they fail. However, current clinical dosimetry for IVBT is water-based, ignoring the patient's artery, calcified plaques, metallic stents, and guidewire from the IVBT delivery system. We have previously shown with Monte Carlo simulations, in an artery model, that target dose due to these heterogeneities could be as low as 60% of the planned dose. Vascular optical coherence tomography (OCT) is currently the only clinically available imaging modality which can detect calcification, stents, and the guidewire prior to treatment. The purpose of this study was to continue to investigate the uncertainties in water-based IVBT dosimetry by extending our previous software to account for patient-specific geometry from OCT images.

Materials and Methods: Monte Carlo treatment planning software based on the Geant4 toolkit v. 10.02.p02 was developed. A Novoste Beta-Cath 3.5F IVBT device with a Sr-90/Y-90 source train was simulated. OCT images for two patients at Brigham and Women's Hospital in Boston, Massachusetts were used to calculate the absorbed dose with the developed software taking all heterogeneities into account compared to dose calculated in water. One patient (Patient 1) had a larger surface area of stenting and the other (Patient 2) had a smaller lumen in certain areas due to a higher degree of calcification. The patient arteries were segmented as water (lumen), calcified plaque (around the lumen), smooth muscle (tunica media) and stainless steel (guidewire and stents). Simulations were performed on the Digital Research Alliance of Canada Narval computing cluster with 1 billion decay events to yield less than 1% uncertainty on absorbed dose in the target volume. The absorbed dose was scored in rectangular voxels of 0.05 mm by 0.05 mm in the axial plane of the artery and 4.2 mm thickness along the 42 mm length including the stents, source train and an additional 2 mm margin. The prescribed dose was 23 Gy to the target volume, at 2.0 mm from the source centre for both patients.

Results: There was severe under-dosing of radiation behind the guidewire and stents (up to 62% for Patient 1 and up to 56% for Patient 2). The dose distributions around the source in the patient-specific simulations were non-homogenous due to the guidewire, the stents and calcification.

Conclusions: Monte Carlo dose calculation software for IVBT was developed, where accurate attenuation of the dose by heterogeneities is considered. Patient treatments based on water dosimetry is inaccurate, and model-based dose calculation methods should be considered.

125
TOWARD THE TRANSLATION OF RECTAL INTENSITY MODULATED BRACHYTHERAPY FOR FEASIBILITY AND SAFETY STUDIES

Jonathan Kalinowski[1], Shirin Enger[2]
[1]*McGill University, Montréal, QC*
[2]*Jewish General Hospital, Montréal, QC*

Purpose: Intensity modulated brachytherapy (IMBT) is a proposed modality of brachytherapy which employs dynamically rotating metallic shields to deliver conformal dose distributions to tumours while sparing surrounding healthy tissue. We have previously showcased a novel applicator designed for intracavitary rectal cancer IMBT featuring a tungsten shield with an 180° emission window. Using the Monte Carlo (MC)-based treatment planning system, RapidBrachyMCTPS, a rectal cancer IMBT treatment was planned and optimized with clinical optimization objectives on a retrospective rectal brachytherapy patient. The IMBT plan

resulted in better sparing of organs at risk than the conventional static-shielded applicator currently used at our centre for an equivalent CTV dose. This work encapsulates the translational steps to develop and manufacture a prototype IMBT system, moving the technology toward a feasibility and safety study.

Materials and Methods: Components of the prototype rectal IMBT system were manufactured, including a 3D-printed flexible mold applicator, a 3D-printed gearbox driven by a stepper motor, and the 180° tungsten shield with a disposable 180° 3D-printed plastic cover. This will be used as a modular add on to our existing clinical brachytherapy setup. Software was also developed to facilitate the delivery of a rectal IMBT plan.

Results: We have developed a functional prototype system for rectal IMBT delivery that can be employed as a modular addition to a clinical rectal brachytherapy setup. A software package complete with a GUI was created to ensure precise and fast rotation of the shield to the planned angles; this also interfaces directly with RapidBrachyMCTPS for treatment plan exporting and with the Elekta Flexitron afterloader for precise synchronization of source translation and shield rotation.

Conclusions: With a functional IMBT delivery system prototype, we will shortly begin measurements to verify dose distributions computed in RapidBrachyMCTPS. A protocol will be developed for quality assurance of rectal IMBT plan delivery, including dose verification in patient-specific 3D-printed phantoms. Additionally, we will investigate rectal IMBT dose optimization objectives beyond existing clinical practice to ensure planned doses that are maximally conformal to targets and will examine the applicability of rectal IMBT to larger and thicker rectal tumours than are currently treatable in current clinical practice.

126
INVESTIGATION OF A MONTE CARLO MODEL BASED DOSE CALCULATION FOR ^{103}Pd LOW DOSE RATE BREAST BRACHYTHERAPY

Dakota McKeown[1], Samuel Ouellet[2], Claire Zhang[1], Narjes Moghadam[3], Eric Wright[4], Felipe Castro Cánovas[1], Juanita Crook[1], Deidre Batchelar[4], Joanna Cygler[5], Luc Beaulieu[2], Rowan Thomson[3], Michelle Hilts[4]
[1]University of British Columbia, Kelowna, BC
[2]Université Laval, Quebec City, QC
[3]Carleton University, Ottawa, ON
[4]British Columbia Cancer, Kelowna, BC
[5]The Ottawa Hospital Cancer Centre, Ottawa, ON

Purpose: Clinical brachytherapy is typically performed using TG43 formalism, which assumes a homogeneous water medium and does not account for factors such as interseed attenuation or tissue inhomogeneities. Monte Carlo (MC) model-based dose calculation algorithms (MBDCA) provide improved dosimetric accuracy. The purpose of this work is to quantify the impact of eb_gui, a Canadian developed, user-friendly MC MBDCA, on plan evaluation with 80 low dose rate (LDR) brachytherapy patients.

Materials and Methods: Dosimetry of 80 breast brachytherapy cases treated with ^{103}Pd seeds (TheraSeed200, 2.3-2.8 U, 90 Gy prescription dose) were simulated using the MC program and doses were calculated using two methods: 1) TG43 (assuming an infinite water medium) and 2) MC-based (with tissue heterogeneity and interseed attenuation). The clinical dose-volume histogram (DVH) metrics of V100 for the target and D1cm² for the skin for both simulations are extracted and compared across the patient cohort.

Results: The clinical treatment volume (CTV, defined as seroma) had an average V100 2.4% lower in the MBDCA compared to the TG43 simulations and 6.1% lower for the evaluated treatment volume (ETV, seroma +0.5cm margin). For skin the average D1cm² was 22.7±3.4% higher in the MDBCA compared to TG43.

Conclusions: MC simulation of 80 breast LDR patients were performed. Slight overestimation of dose in target volumes (CTV & ETV) and potentially clinically significant underestimation of dose in skin were seen using the standard TG43 calculations when compared to the more accurate MBDCA. These differences motivate the future adoption of eb_gui as a valuable tool for LDR breast treatments in clinical practices.

127
IMPACT OF BRACHYTHERAPY APPLICATOR ON CLINICAL OUTCOMES IN CERVIX CANCER: AN EMBRACE-I STUDY ANALYSIS

Monica Serban[1,2], Sofia Spampinato[2], Astrid de Leeuw[3], Israel Fortin[4], Nicole Nesvacil[5], Christian Kirisits[5], Maximilian Schmid[5], Umesh Mahantshetty [6], Peter Hoskin[7], Barbara Segedin[8], Kjersti Bruheim[9], Fleur Huang[10], Bradley Pieters[11], Remi Nout[12], Richard Pötter[5], Kathrin Kirchheiner[5], Ina Jürgenliemk-Schulz[3], Kari Tanderup[2]
[1]Princess Margaret Cancer Centre, Toronto, ON
[2]Aarhus University Hospital, Aarhus, DK
[3]University Medical Centre Utrecht, Utrecht, NL
[4]University of Montreal, Maisonneuve-Rosemont Hospital, Montréal, QC
[5]Comprehensive Cancer Center, Medical University of Vienna, Vienna, AT
[6]Tata Memorial Hospital, Mumbai, IN
[7]Cancer Centre, Mount Vernon Hospital, London, UK
[8]Institute of Oncology Ljubljana, University of Ljubljana, Ljubljana, SI
[9]The Norwegian Radium Hospital, Oslo University Hospital, Oslo, NO
[10]Cross Cancer Institute, University of Alberta, Edmonton, AB
[11]University of Amsterdam, Amsterdam, NL
[12]Erasmus MC Cancer Institute, University Medical Center Rotterdam, Rotterdam, NL

Purpose: To investigate the effect of brachytherapy (BT) applicator and implant type on morbidity and local control in locally advanced cervix cancer treated on the EMBRACE I study.

Materials and Methods: 1071 patients treated with tandem&ring (T&R) (n=725) and tandem&ovoids (T&O) (n=346) from 19 EMBRACE-I centres were analyzed. After receiving EBRT (45-50 Gy in 25-30fx) and MR-guided BT (IGBT) using intracavitary (IC) (n=559) or intracavitary/interstitial (IC/IS) (n=512) implants, patients were prospectively followed (in median 48 months). Local control (LC) and physician-assessed (CTCAE v.3) late morbidity were compared based on (1) applicator type: T&R versus T&O, and (2) implant type: IC versus IC/IS. Moderate-to-severe (G≥2) genito-urinary (GU: cystitis, frequency), gastro-intestinal (GI: proctitis, bleeding, diarrhea) and vaginal (stenosis, mucositis) symptoms were analysed separately. Severe-to-life-threatening events (G≥3) were pooled for evaluation of GU, GI and vaginal morbidity. Comparisons between applicator and implant types were evaluated by Cox proportional hazard multiple regression model, adjusting for: patient (baseline morbidity, age, body mass index), disease (local FIGO stage, organ involvement, tumour dimensions, histology, tumour necrosis), and treatment-related confounders (CTV-HR D90%, EBRT dose) (Table 1), which were included in the multivariable analysis (MVA) if significant in the univariate analysis (p≤0.15).

Results: OAR doses (bladder and rectum D2cc; ICRU points) for T&O versus T&R were higher by 5-7Gy in IC implants and by 1-5Gy in IC/IS implants, while target dose (CTV_{HR} D90%) was lower by

on average 2.5Gy in T&O compared to T&R applicators. Patients treated with the T&O applicator were at higher risk of developing individual G≥2 symptoms and pooled G≥3 GU/GI/vaginal/fistula morbidity compared to those treated with the T&R applicator. Hazard ratios (HRs) for individual G≥2 symptoms were ranging between 1.35 – 2.73 for IC applicators (T&O IC versus T&R IC) and between 2.04 – 5.14 for IC/IS applicators (T&O IC/IS versus T&R IC/IS). In 3/7 and 6/7 evaluated individual symptoms (IC and IC/IS implants, respectively), the T&O showed a statistically significant ($p<0.05$) higher risk for G≥2 morbidity compared to T&R. Crude incidence of local failure was 7.3% (25/343) and 6.6% (47/712) in patients treated with T&O and T&R, respectively. In MVA, local control did not statistically differ between the two groups ($p>0.1$).

Conclusions: In this patient cohort treated between 2008-2015, T&O applicators were associated with higher OAR and lower target doses as compared to T&R. The risk for G≥2 and G≥3 morbidity was higher for patients treated with T&O, while local control was similar. For IC/IS-treated large CTV volumes >35cm^3, target doses were higher by 3.5 Gy compared to IC applicators. Nevertheless, combined IC/IS applicators did not increase the risk of morbidity compared to IC applicators.

128

LONG-TERM TOXICITY IN PATIENTS RECEIVING RADIOTHERAPY FOR ULTRACENTRAL STAGE I NON-SMALL CELL LUNG CANCER - A SECONDARY ANALYSIS OF THE LUSTRE RANDOMIZED TRIAL

Che Hsuan David Wu[1], Marcin Wierzbicki[2], Sameer Parpia[3], Vijayananda Kundapur[4], Alexis Bujold[5], Edith Filion[5], Harold Lau[6], Sergio Faria[7], Naseer Ahmed[8], Nelson Leong[4], Gordon Okawara[3], Khalid Hirmiz[9], Timothy Owen[10], Alexander Louie[11], James Wright[3], Timothy Whelan[3], Anand Swaminath[3]
[1]British Columbia Cancer, Victoria, BC
[2]Juravinski Cancer Centre, Hamilton, ON
[3]McMaster University, Hamilton, ON
[4]University of Saskatchewan, Saskatoon, SK
[5]Université de Montréal, Montréal, QC
[6]University of Calgary, Calgary, AB
[7]McGill University, Montréal, QC
[8]University of Manitoba, Winnipeg, MB
[9]Western University, London, ON
[10]Queen's University, Kingston, ON
[11]University of Toronto, Toronto, ON

Purpose: Hypofractionated and stereotactic body radiotherapy (SBRT) are increasingly used in the treatment of centrally located, early-stage non-small cell lung cancer (NSCLC), though there are concerns of increased morbidity and mortality in patients with ultracentral tumours (UC). We report on the long-term toxicity of patients with UC lung cancer treated on a prospective randomized clinical trial of SBRT versus conventionally hypofractionated radiotherapy (CRT) for Stage I NSCLC (NCT01968941).

Materials and Methods: Patients with UC tumours, defined as those where the planning target volume directly overlaps with the proximal bronchial tree (PBT), were identified from the larger cohort of patients treated on the trial. These patients received either SBRT with 60Gy in 8 fractions or CRT with 60Gy in 15 fractions. The primary endpoint of this secondary analysis was development of any Grade 3 or higher toxicity defined using CTCAE version 3.0. Secondary endpoints included local control, as well as dosimetric analysis of the PBT, using EQD2 with α/β ratio of 3 to assess the relationship between dose to the PBT and toxicity.

Results: Twenty-nine patients were identified with UC tumours; 21 received SBRT and 8 received CRT. Median age was 72 years (range 55-88 years) and 59% were female. Median FEV1 was 1.46L (range 0.64-2.37L). Patients had either T1 (59%) or T2 (41%) lesions, with median tumour size 2.5cm (range 1.1-4.9cm). Most patients had histologically confirmed disease (squamous cell, n=10; adenocarcinoma, n=8; radiographically suspicious, n=11). The median follow-up was 2.9 years (range 0.7-5.2 years). The 3-year local control rate of all patients was 88.3% (95% confidence interval: 75.7-100%). There were 3 patients with late (>3 months) Grade 3 toxicity (bronchial stricture, chest pain, and atelectasis) and 1 patient with late Grade 5 toxicity (bleeding/hemorrhage), all treated in the SBRT arm. Median EQD2 dose to PBT in patients with Grade ≥3 late toxicity compared to the rest of the cohort was: Dmax, 132 versus 129Gy; D0.1cc, 129 versus 119Gy; D1cc, 124 versus 80Gy; and D5cc, 83 versus 41Gy. Median EQD2 volumetric doses in Grade ≥3 patients (compared to the rest) to PBT were: V65Gy, 9.7 versus 2.2cc; V80Gy, 7.9 versus 1.1cc; V90Gy, 6.2 versus 0.4cc; and V100Gy, 4.8 versus 0.3cc. The single patient with Grade 5 toxicity had the highest D5cc (116Gy) and V100Gy (7cc) among all patients.

Conclusions: Stereotactic radiation with 60Gy in 8 fractions for UC lung cancer provides good local control but carries an approximately 15-20% rate of late Grade ≥3 toxicity. There appears to be a dosimetric association between toxicity and dose to the PBT. It may be more important to minimize volumetric PBT dose rather than maximum point dose to reduce risk of severe late toxicity.

129

ASSESSMENT OF PRECISION IRRADIATION IN EARLY NON-SMALL CELL LUNG CANCER AND INTERSTITIAL LUNG DISEASE (ASPIRE-ILD): PRIMARY ANALYSIS OF A PHASE II TRIAL

David Palma[1], Houda Bahig[2], Andrew Hope[3], Stephen Harrow[4], Brock Debenham[5], Alexander Louie[6], Toni Vu[2], Edith Filion[2], Andrea Bezjak[6], Marie-Pierre Campeau[2], Adele Duimering[5], Meredith Giuiliani[6], Joanna Laba[1], Benjamin Lok[6], Pencilla Lang[1], X. Melody Qu[1], Srinivas Raman[6], George Rodrigues[1], Christopher Goodman[1], Stewart Gaede[7], Julie Morisset[2], Andrew Warner[1], Inderdeep Dhaliwal[1], Christopher Ryerson[8]
[1]London Health Sciences Centre, London, ON
[2]Centre Hospitalier de l'Université de Montréal, Montréal, QC
[3]University of Toronto, Toronto, ON
[4]Beatson West of Scotland Cancer Centre, Edinburgh, SC
[5]University of Alberta, Edmonton, AB
[6]University of Toronto, Toronto, ON
[7]Western University, London, ON
[8]University of British Columbia, Vancouver, BC

Purpose: The use of stereotactic ablative radiotherapy (SABR) in patients with fibrotic interstitial lung disease (ILD) has been associated with an increased risk of toxicity, but patients with ILD and lung cancer may have no other options for curative-intent treatment. The goal of the ASPIRE-ILD trial was to assess the benefits and toxicities of SABR in patients with fibrotic ILD.

Materials and Methods: We enrolled patients with fibrotic ILD and a diagnosis of T1-2N0 NSCLC who were not candidates for surgery. All patients were centrally reviewed prior to enrollment to confirm the presence and subtype of ILD. After stratification by the ILD-GAP score (a measure of ILD severity and prognosis), patients were treated with SABR to a dose of 50 Gy in 5 fractions EOD (BED=100 Gy_{10}), with a built-in de-escalation protocol in case of unacceptable toxicity. The primary endpoint was overall survival (OS), powered to distinguish one-year OS >70% versus an unacceptable rate of ≤50%. Secondary endpoints included toxicity (CTC-AE version 4.0), progression-free survival (PFS), local control (LC), patient-reported outcomes (FACT-L quality of life and cough severity), and changes in pulmonary function tests (PFTs). The study pre-specified that SABR would be considered worthwhile if median OS was >1 year, with a Grade 3-4 toxicity

risk <35% and a Grade 5 toxicity risk <15%. Target accrual was 39 treated patients.

Results: Thirty-nine patients were enrolled and treated with SABR between March 2019 and January 2022, all to a dose of 50 Gy in 5 fractions, at five institutions in Canada and 1 in Scotland. Median age was 78 years (interquartile range: 67-83), 59% were male, and 92% had a history of smoking (median 43 pack-years). At baseline, 70% reported dyspnea, median FEV_1 was 80% predicted and median DLCO was 49% predicted. ILD-GAP scores were as follows: ≤2 (i.e. best ILD status): n=14; 3-5: n=23; ≥6 (i.e. worst ILD status): n=2. Median follow-up was 19 months. OS at one-year was 78.9% (p<0.001 by binomal test versus the unacceptable rate). Median OS was 25 months, median PFS was 19 months, and two-year LC was 92%. AE rates (possibly, probably or definitely related) were as follows (highest grade per patient): Grade 1-2: n=12 (31%); Grade 3: n=4 (10%); Grade 4; n=0; Grade 5 n=3 (7.7%, all due to respiratory deterioration). AE rates did not differ by ILD-GAP category or ILD subtype. FACT-L scores trended downward over time (p=0.07), and cough severity scale scores worsened over time (p=0.02). Comparing last-available PFTs with baseline, DLCO declined (median: -4%; p=0.046), FVC trended downward (median: -2.5%; p=0.11), and FEV1 remained stable (median change: 0%).

Conclusions: The use of SABR in patients with ILD met the pre-specified acceptability thresholds for both toxicity and efficacy, supporting the use of SABR for curative-intent treatment after a careful discussion of risks and benefits. Further studies exploring pharmacologic options to reduce toxicity may be beneficial in this population. (NCT03485378)

130
DEVELOPMENT OF A PRIMARY STANDARD OF ABSORBED DOSE TO WATER FOR PROTON BEAMS

Claudiu Cojocaru[1], James Renaud[1], Cornelia Hoehr[2], Camille Belanger-Champagne[2], Michael Trinczek[2], Malcolm McEwen[1]
[1]*National Research Council, Ottawa, ON*
[2]*TRIUMF, Vancouver, BC*

Purpose: It is anticipated that proton beam radiotherapy will become available in Canada in the near future, and so it is a priority to establish a primary standard for measuring the absorbed dose to water in these beams.

Materials and Methods: A water calorimeter system measures the absorbed dose by measuring the increase in temperature of water when radiation passes through it. Building on our experience of water calorimetry in photon and electron beams, we adapted, transported and tested for the first time a system to measure absorbed dose to water in clinically relevant proton beams at the TRIUMF facility in Vancouver. The proton beam line is referred to as BL2C and was previously used for ocular cancer therapy treatments. It has an energy of 68 MeV at a nominal beam intensity of 5 nA and over a period of several days, a total 14 sets of calorimeter runs were collected. The dose was measured with a passively-scattered beam, both energy-modulated and pristine distributions, and the effects of distance from the source and field size were investigated. All measurements were carried out at 4 °C to eliminate convection.

Results: The standard deviation of the raw dose measurement for a set of ten runs was between 0.5 % and 0.9 %. The relative variation for a group of seven sets obtained for the scattered beam setup over multiple days was at the +/- 1 % level. Field size impacted radial heat flow as expected.

Conclusions: The feasibility of operating a water calorimeter system in a low-energy proton beam was successfully demonstrated at the TRIUMF facility. Once correction factors for heat flow and radiochemistry have been evaluated, it is estimated that that the standard uncertainty in the determination of absorbed dose to water should be around 1%.

131
A PROSPECTIVE STUDY OF MR-ASSISTED SALVAGE HDR PROSTATE BRACHYTHERAPY WITH INTRA-PROSTATIC BOOST

Hans Chung[1,2], Andrew Loblaw[1,2], Chia-Lin Tseng[1,2], Jure Murgic[3], Ananth Ravi[2], Melanie Davidson[1,2], Matt Wronski[1,2], Moti Paudel[1,2], Masoom Haider[2], Andrea Deabreu[1], Gerard Morton[1,2]
[1]*Sunnybrook-Odette Cancer Centre, Toronto, ON*
[2]*University of Toronto, Toronto, ON*
[3]*University Hospital Center Sestre Milosrdnice, Zagreb, HR*

Purpose: Because multiparametric MRI can generate detailed images of the anatomic extent of cancer within the prostate, its integration in salvage therapies such as brachytherapy has been widely embraced. It has enabled focal therapies and whole-gland therapies with intra-prostatic boost. The objectives of our prospective study is to investigate the efficacy and toxicities of MR-assisted whole-gland salvage HDR prostate brachytherapy with intra-prostatic boost in patients with local recurrent prostate cancer.

Materials and Methods: Eligible patients included: multiparametric 3T MRI (mpMRI) visible biopsy confirmed local recurrence >30 months after XRT, negative metastatic workup, and IPSS <15. Ultrasound-based HDR brachytherapy with intraoperative contour-based deformable registration between the mpMRI and ultrasound images were done in 28 of 30 patients, and cognitive fusion in the remaining two patients. The prescription dose was 21 Gy to the entire prostate and 27 Gy to the MR-defined intraprostatic target volume (TV) divided over two implants separated by 1-2 weeks with dose constraints to the urethra and rectum. Adjuvant androgen deprivation therapy (ADT) was not used. Post-treatment response was evaluated using mpMRI 1-2 years after salvage. Follow-up PSA, IPSS and CTCAE v4.0 toxicities were collected.

Results: Thirty patients (median age 74 years) were enrolled in the study. Median follow up from salvage HDR was 33 months (12-60). At initial presentation, there were three, 18 and nine low-, intermediate- and high-risk disease. The initial XRT dose was 70-78Gy with conventional fractionation in 28 patients and alternate fractionation in two patients (35Gy/5F and 50Gy/15F). Median time from initial treatment to biopsy-confirmed local recurrence was 9.3 years (2.4-17.6). The Gleason score of the local recurrence was six, seven and 8-10 in 2, 19 and 9, respectively. The pre-HDR median PSA was 3.67ng/mL (0.63–11.01). The median size of the prostate was 33.8 mL (15.9-86.0) and TV was 4.7mL (1.5-15.5). The median dosimetric endpoints per implant were: prostate V10.5Gy 96.5% (94.1-98.7), prostate D90 11.4Gy (10.9-12.0), TV V13.5Gy 94.2% (63.3-100), TV D90 18.1Gy (15.0-22.2), urethral D10% 12.0Gy (11.5-12.6), urethral Dmax 12.6Gy (12.2-13.5) and rectal V8.4Gy 0mL (0-0.8). Four patients (13%) required temporary urinary catheterization. There were no acute/late GU/GI Grade 3-5 toxicities. The most common acute toxicity was frequency, dysuria and urgency. Mean IPSS at baseline, 1.5-, 3-, 6-, 9-, 12-, 18-, 24-, 30- and 36-months was 6, 15, 10, 11, 10, 12, 10, 10, 9 and 7, respectively (p=0.03). Three-year PSA progression-free survival and freedom from ADT rate was 67% and 93%, respectively. Of the 26 patients who had a post-HDR MRI (median 415 days), 18 (69%) patients had a complete response and eight had persistent disease in the TV. No patients recurred elsewhere in the prostate.

Conclusions: Our toxicity, IPSS and PSA failure-free results suggests that whole gland salvage HDR brachytherapy with intra-prostatic boost is well tolerated and effective.

132

HYPOXIA ON A CHIP

Elena Refet-Mollof[1,2], Rodin Chermat[1,2], Thomas Gervais[1,2], Philip Wong[2,3,4,5]
[1]*Polytechnique Montréal, Montreal, QC*
[2]*Centre de Recherche du Centre Hospitalier de l'Université de Montréal (crCHUM), Montreal, QC*
[3]*University Health Network, Toronto, ON*
[4]*University of Toronto, Toronto, ON*
[5]*Princess Margaret Cancer Centre, Toronto, ON*

Purpose: Tumour hypoxia is found in ~50% of solid tumours and is associated with radiation therapy (RT) resistance, metastasis progression and overall poor prognosis in patients. Nevertheless, hypoxia is seldom considered during treatment development due to the lack of a user-friendly way to culture hypoxic 3D tumour models such as spheroids. Microfluidic devices have previously been used to generate precise conditions for growing spheroids and to study the effects of different therapies on tumour spheroids. Therefore, we developed a user-friendly in vitro microfluidic preclinical tool allowing the study of natural chronic hypoxia and its effects on treatment response in 3D tumour model.

Materials and Methods: Microfabrication was used to design a microfluidic chip allowing culture, treatment, and analysis of 240 sarcoma jumbo spheroids. PDMS, a biocompatible silicone, was used to manufacture the microfluidic chip. Sarcoma cell lines SK-LMS-1 (leiomyosarcoma), SW872 (liposarcoma), SW684 (fibrosarcoma), STS93 (soft-tissue-sarcoma), STS117 (soft-tissue-sarcoma) were selected for their clinical relevance regarding hypoxia, as sarcomas tend to form very large hypoxic tumours. Both soft-tissue-sarcomas (STSs) cell lines were derived from patients' primary extremity STS diagnosed as an undifferentiated pleomorphic sarcoma and were kindly provided by Dr. Gladdy from University of Toronto. Presence of hypoxia was assessed by immunofluorescence (IF) staining of carbonic anhydrase IX (CAIX). To assess hypoxia-related radioresistance, spheroids were irradiated on chip at 8 Gy of external beam radiotherapy (Gammacell) and DNA-damages were quantified at 0 min, 30 min, 4 h and 24 h using yH2AX by IF staining. RNA expression of hypoxia associated genes HIF1a, CAIX, VEGFA, SLC2A1 (GLUT1), CD47, CD73, LOX, Vimentin is being assessed by RTqPCR. Metastatic potential of hypoxic spheroids will be assessed by monitoring invasion in Matrigel using live microscopy (Incucyte).

Results: For all cell lines, spheroids were formed 48 to 96 hours after cell suspension was seeded inside the chip. These large spheroids on a chip are the largest to date, with a diameter exceeding 750 µm. They express gold-standard hypoxic protein CAIX in their core only, contrary to smaller spheroids (< 450 µm) of the same cell lines. 45% ± 8.9% of SK-LMS-1, 49% ± 11.4% of STS117, 43% ± 7.2% of STS93, 43% ± 9% of SW684 cross section areas express CAIX, results are pending for SW872. Normoxic cells (outer region of large spheroids) harbour significantly more DNA damages than hypoxic region 30 minutes after irradiation in SK-LMS-1 (0 Gy versus 8 Gy, $p<0.05$). Results for STS117 are pending. RNA hypoxic signature is currently being assessed to provide insight in genes expression related to hypoxia.

Conclusions: Our device allows the easy culture of spheroids harbouring both normoxic and hypoxic regions without the use of chemicals or hypoxic chambers. Additionally, our microfluidic chip is fully compatible with RT. Using our microfluidic device and our naturally hypoxic spheroids to explore the biology of hypoxia and its implications on treatment resistance on a variety of cancer types would provide a useful preclinical tool for drug screening and treatment combinations.

133

PREDICTORS OF STAFF SATISFACTION, STRESS, AND BURNOUT AT A CANADIAN CANCER CENTRE

Ege Babadagli[1], Selena Laprade[1], Gordon Locke[1], Angela McNeil[1], Joanne Meng[1], Julie Renaud[1], Elisabeth Cisa-Pare[2], Jessica Chan[3], Jiheon Song[4], Rajiv Samant[1]
[1]*University of Ottawa, Ottawa, ON*
[2]*Northern Ontario School of Medicine, Thunder Bay, ON*
[3]*University of British Columbia, Vancouver, BC*
[4]*University of Toronto, Toronto, ON*

Purpose: Oncology health care professionals (HCPs) generally find their work rewarding, however are at risk of severe workplace stress and burnout. This study investigated predictors of workplace satisfaction, stress, and burnout amongst staff at The Ottawa Hospital Cancer Centre.

Materials and Methods: A 61-item ethics approved staff satisfaction survey was developed at our cancer centre to evaluate factors contributing to workplace satisfaction, stress, and burnout. The online survey was distributed to staff via email for self-completion in 2020 and inferential statistics were used to evaluate the responses.

Results: A total of 478 individuals completed the online survey, out of which there were 89 resident, fellow and staff physicians, 102 nurses, and 95 radiation therapists. Other respondents included secretaries, administrative clerks, managers, clinical trials staff, pharmacists, psychosocial oncology staff, and physicists. Managers reported the highest level of workplace satisfaction, whereas pharmacists reported the lowest. Level of satisfaction in general was correlated with age, with those aged 60 or older demonstrating higher levels of satisfaction ($p=0.038$). Additionally, satisfaction was correlated with years worked, with employees having worked 0-2 years demonstrating the highest level of satisfaction, and those having worked over 20 years demonstrating the lowest level of satisfaction ($p=0.002$). Level of satisfaction was not correlated with workload. Resident and fellow physicians reported the highest levels of stress, while secretaries reported the lowest levels of stress. Levels of stress was not correlated with perceived quality of care provided by healthcare professionals. Consideration of a career change was correlated with years worked, with those having worked more than 20 years more likely to have considered changing careers ($p=0.041$). Radiation therapists reported the highest perceived levels of burnout, while secretaries reported the lowest perceived levels. Perceived burnout was correlated with lower level of job satisfaction ($p<0.001$), higher levels of stress ($p<0.001$), higher workload ($p<0.001$), and calling in sick due to stress more frequently ($p<0.001$).

Conclusions: Although the majority of oncology staff members find their work satisfying, stress is common and certain groups of staff admit to having high degrees of stress and/or symptoms of burnout. Age and years worked interestingly present as common themes, however predictors of satisfaction, stress, and burnout remain multifactorial. As such, strategies to address these issues also necessitate a multifactorial approach tailored towards the varying groups of oncology healthcare professionals.

134

A QUALITATIVE ANALYSIS OF MEDICAL STUDENT REFLECTIONS FOLLOWING PARTICIPATION IN A CANADIAN RADIATION ONCOLOGY STUDENTSHIP

Brandon Chai[1], Meredith Giuliani[2], Joanne Alfieri[3], Jeffery Cao[4,9], Andrea Bezjak[2], Michael Kim[5], Che Hsuan David Wu[6], Nauman Malik[7], David Mak[2], Paris-Ann Ingledew[1,8]
[1]*University of British Columbia, Vancouver, BC*
[2]*Princess Margaret Cancer Centre, Toronto, ON*
[3]*McGill University, Montréal, QC*

[4]*University of Calgary, Calgary, AB*
[5]*Dalhousie University, Halifax, NS*
[6]*British Columbia Cancer, Victoria, BC*
[7]*University of California, San Francisco, CA*
[8]*British Columbia Cancer, Vancouver, BC*
[9]*Tom Baker Cancer Centre, Calgary, AB*

Purpose: Radiotherapy is a key cancer treatment modality that will continually be required with the predicted rise in cancer incidence. However, recent workforce projections predict a shortage of Canadian Medical Graduate-trained radiation oncologists. Exposure to radiation oncology in the Canadian medical school curricula is limited, and thus mentorship and research opportunities like the Canadian Association of Radiation Oncology (CARO)-Canadian Radiation Oncology Foundation (CROF) Dr. Pamela Catton Summer Studentship program attempt to bridge this gap and stimulate interest in the specialty. In 2020, due to the COVID-19 pandemic, the studentship pivoted to incorporate virtual research mentorship and case-based discussions. This study explores the impact of COVID-19 on the studentship, the students' perceptions of the program, and its impact on the students' medical training and career choice.

Materials and Methods: All 15 studentship participants during 2020-2022 submitted program completion essays reflecting upon their experiences. These essays were obtained from the CARO Education Committee and anonymized. Thematic analysis was carried out to interpret the anonymized essays systematically with Nvivo. Two independent reviewers coded the essays. Themes and sub-themes were established by identifying connections between coded excerpts. Consensus was achieved through multiple rounds of discussion by iteratively reviewing each theme and sub-theme with respect to the coded excerpts. Representative quotes were used to illustrate the themes and sub-themes.

Results: The themes elucidated confirmed that the studentship was feasible during the pandemic and that the students perceived it to be beneficial. Students participated in case-based discussions and research, with participation in clinical experiences as permitted by public health restrictions. Perceived benefits of the program included mentorship and networking opportunities; gaining practical and fundamental knowledge in radiation oncology; developing clinical and research skills; and creating positive attitudes towards radiation oncology and the humanistic aspect of the field. The studentship supported medical specialty selection by helping define student values, shaping perceptions of the specialty characteristics, and promoting self-reflection upon students' personal needs.

Conclusions: This study informs future iterations of the studentship to promote radiation oncology in Canadian medical school curricula. It may serve as a model for studentships in other specialties that have limited exposure and similar challenges with medical student recruitment.

135
EXPLORING FAMILY PHYSICIAN TRAINING NEEDS TO IMPROVE CANCER PATIENT CARE

Marissa Sherwood[1], Janet Papadakos[1], Kulamahan Kulasegaram[1], Maria A. Martimianakis[1], Edward Kucharski[2], Meredith Giuliani[1]
[1]*University of Toronto, Toronto, ON*
[2]*Casey House Hospital, Toronto, ON*

Purpose: Family physicians have multifaceted roles in cancer patient care and oncology education among this group is unfortunately inadequate. This study explored the needs and perspectives of family physicians regarding their oncology training and experiences.

Materials and Methods: The authors employed a qualitative approach with family physicians participating in semi-structured interviews. General practitioners in oncology were excluded. Purposeful sampling was used, with recruitment through Ontario regional primary cancer care leads and social media. Interviews were transcribed and thematic analysis conducted.

Results: Thirteen participants were interviewed - 1.6:1 female: male, ages 30-39, practicing for an average of nine years (0.5-30 years), with urban and suburban practices. Most trained in Canada as undergraduates and completed their residency in Ontario; 62% had participated in at least one oncology continuing medical education session. Three major themes emerged: Delineation of roles, Oncology knowledge and education, and Palliative care. Participants reported role uncertainty after cancer diagnosis, with oncology teaching at all levels described as lacking relevance. Palliative care rotations were an avenue for oncology education and where participants returned to cancer care.

Conclusions: Changing existing teaching, information access and avenues of oncology experiences may be the next step to supporting successful cancer care by family physicians.

136
INVESTIGATING A RESIDUAL NEURAL NETWORK TO GENERATE CUSTOMIZABLE RADIOFREQUENCY PULSES FOR MAGNETIC RESONANCE IMAGING

Seger Nelson, Rebecca Feldman
University of British Columbia, Kelowna, BC

Purpose: Magnetic resonance imaging (MRI) uses carefully designed radiofrequency (RF) electromagnetic pulses to excite protons in the human body in order to acquire signal from specific slices from which images are formed. Simultaneous multi-slice (SMS) imaging accelerates image acquisition time with minimal impact on signal-to-noise ratio by acquiring images of multiple slices of the patient simultaneously. Power-independent-of-number-of-slices (PINS) RF pulses enable SMS excitation, with power deposition comparable to single-slice excitation. However, the development of custom-designed RF pulses that yield desirable slice profiles requires time-consuming iterative tuning. We explore simplifying the design process by training a deep learning model to generate an RF pulse given a custom slice profile.

Materials and Methods: The training dataset consisted of 92,610 generated 180° refocusing RF pulse and gradient/spatial profile pairs. Each RF pulse was labeled with its corresponding slice profile, then the dataset was shuffled, batched, and separated into training (67%) and test (33%) sets. An 18-layer Residual Neural Network (ResNet) was trained on the dataset from which loss and validation accuracy were recorded over epoch. The output RF pulse of the model was interpolated to its original size, then slice profiles were simulated and validated against their respective slice profiles from the model input.

Results: The model loss converged at 30 epochs, and the accuracy converged at 50 epochs, peaking at approximately 73%. Results were visually investigated by simulating the outputs and comparing them to the spatial profiles from the training data. The model performed reasonably well when a clean gradient was used for the spatial simulation. However, it was less accurate when simulated with the generated gradient.

Conclusions: The model serves as a proof of concept. Further investigation will include the exploration of different models, the generation of larger and more diverse training datasets, and the optimization of the training dataset to reduce the complexity of the classification task.

137

STEREOTACTIC BOOST AND SHORT-COURSE RADIOTHERAPY FOR P16-ASSOCIATED OROPHARYNX CANCER (SHORT-OPC): FIRST PLANNED INTERIM SAFETY ANALYSIS FROM A RANDOMIZED PHASE II TRIAL

Sweet Ping Ng[1], David C. Fuller[2], Adam S. Garden[2], David I. Rosenthal[2], Jack Phan[2], Phuc Felix Nguyen-Tan[3], Ying Yuan[2], Edith Filion[3], Denis Soulieres[3], Apostolos Christopoulos[3], Katherine Hutcheson[2], Anna Lee[2], Houda Bahig[1]
[1]*Austin Health, Austin, TX*
[2]*The University of Texas MD Anderson Cancer Center, Houston, TX*
[3]*Centre Hospitalier de l'Universite de Montréal, Montréal, QC*

Purpose: There is a need for safe treatment de-intensification in p16+ oropharynx cancer (OPC). The standard of care (SOC) radiotherapy (RT) regimen is cumbersome and associated with high toxicity. Stereotactic radiotherapy (SBRT) and multimodality image guidance is an opportunity to precisely target the gross tumour while safely reducing elective irradiation dose. We aim to assess the safety and efficacy of a short course RT for p16+ OPC, consisting of an SBRT boost to the gross tumour volume (GTV) followed by de-escalated elective irradiation.

Materials and Methods: In this randomized Phase II trial, patients with p16-positive, Stage I-II OPSCC with primary tumour <30 cc (8th Ed AJCC) are planned with combined CT, MRI and FDG-PET, and randomized to 1) SBRT boost (14 Gy in 2 fractions) to the GTV followed with de-escalated RT (+/- Cisplatin) to a dose of 40 Gy in 20 fractions, or 2) SOC RT (+/- Cisplatin) to a dose of 70 Gy in 33 fractions to the GTV and 59.4-54Gy (or equivalent) to the intermediate-to-low dose elective region. Patients are stratified by Stage (I versus II) and use of chemotherapy. The primary endpoint of the trial is locoregional control at two years, powered for a sample size of 100 patients. A Bayesian adaptive design includes two planned safety interim analysis using Grade ≥ 3 subacute toxicity >40% as a stopping criterion, and one planned futility analysis. Acute adverse events (AE) are defined as those occurring ≤ 60 days from RT, subacute AE between 60-180 days after RT, and late AE >180 days from RT. This is the first planned toxicity analysis.

Results: Twenty-one patients were randomly assigned and eligible (11 in SOC and 10 in experimental arm). Median age was 69 years (range 49-84); 29% and 71% had Stage T1 and T2, while 10%, 85% and one patient had N0, N1 and N2 disease, respectively. RT alone and chemoradiation was administered in 67% and 33% of patients, respectively. At a median follow-up of 11 months (range 1.7-17.6), there was one local recurrence at the primary tumour site in the SOC arm (at 10 months) and no recurrence in the experimental arm. All enrolled patients remain alive at the time of analysis. There was a 54.5% rate of Grade 3 acute AE in the SOC arm and 30.0% rate of Grade 3 acute AE in the experimental arm. More specifically, one, five (45%), two (18%), and two (18%) versus 0, one, one and one patient developed acute Grade 3 dysphagia, mucositis, pain and dermatitis in the SOC and experimental arm, respectively. There was no acute Grade 4 or 5 toxicity. There was no Grade ≥ 3 subacute toxicity or late toxicity in both arms.

Conclusions: This primary safety analysis showed that SBRT boost followed by a short course of de-escalated elective irradiation in p16+ OPC has limited early toxicity and meets criteria for study continuation.

138

FIVE-YEAR FEASIBILITY STUDY OF A THREE-DAY RAPID ACCESS PALLIATIVE VMAT PROGRAM IN A TWO LINAC CENTRE

Quinn Matthews[1], Kim Lawyer[1], Evan Maynard[1], Robert Olson[1], Allison Ye[1], Vivian Yau[1], Stacy Miller[1], Boris Valev[2], Nick Chng[1]
[1]*British Columbia Cancer, Prince George, BC*
[2]*British Columbia Cancer, Victoria, BC*

Purpose: To report the five-year experience of implementing and evolving Rapid Access Palliative VMAT (RAP-VMAT) in a two linac cancer centre with no dedicated resources.

Materials and Methods: A three-day turnaround RAP-VMAT program in our two-linac centre was launched in 2018 with eligibility criteria of: expected clinical benefit versus CT sim-and-treat, sufficient pain control for VMAT delivery, excluded sites of soft-tissue neck, head, skin, extremities and bilateral whole pelvis, and allowed prescriptions of up to 8 Gy/1#, 20 Gy/5# (25 Gy for pelvis), and 30 Gy/10#. Additional criteria for CT and dosimetry were implemented to ensure patients could be planned with VMAT with minimal complexity and obviate the need for patient-specific measurement QA. Physics monitor unit verification was performed with IMSure v3.7+ (Standard Imaging). A predefined list of optional organs at risk (OARs) with dose constraints was created by our interdisciplinary team, with a limit of two OARs per plan chosen by the radiation oncologist (RO) at contouring. Specialized communication workflows were implemented to minimize hand-off and ensure team awareness of the patient's progress. Pre-defined breakpoints in planning timelines were enforced if critical tasks were not completed by specified times, resulting in the patient's start date moved back by one day. From 2019-2022 eligibility was expanded to allow up to 40 Gy/15# for lung and pelvis sites, include brain and skull sites with up to 25 Gy/5#, 34 Gy/10# or 40 Gy/15#, and to introduce a five-day workflow option to accommodate diagnostic image fusion for planning. For timing analysis, task durations were tracked using ARIA task creation times, as part of a continuous quality monitoring and improvement initiative.

Results: Since launch, 240 patients have been requisitioned for RAP-VMAT. Of these, 150 (63%) were fully eligible for three-day RAP-VMAT throughout the planning process, and 10 were eligible for five-day RAP-VMAT with image fusion. The remaining 80 patients were recorded as "off-protocol", with reason(s) recorded (plan complexity requiring measurement QA, clinical trial, planned delay to start time, linac unavailability, or change in prescription / intent during planning). Of the 150 patients eligible for three-day RAP-VMAT, five did not make planning timelines due to delays in RO contouring, resulting in a one day delay to patient RT start. No patients were delayed for any other reason. Task timing analysis of the 145 "on-time" patients revealed that the majority of time between tasks was spent in the dosimetry plan and check process (median 8.9 working hours) followed by RO contouring and plan evaluation (3.7 hours), physics plan checks (2.6 hours), and CT staff duties (0.2 hours). Median time from first to last task in the planning process was 16.8 working hours.

Conclusions: RAP-VMAT allows an accelerated path to VMAT for many patients that otherwise would be treated with either a CT sim-and-treat or standard two-week planning workflow.

139

EFFECT OF COBALT-60 CALIBRATION DOSE-RATE ON ARTERIOVENOUS MALFORMATION OBLITERATION AFTER STEREOTACTIC RADIOSURGERY

Victoria Anthes[1], Michael Schwartz[2], Michael Cusimano [3], Ivan Radovanovic[4], Abhaya Kulkarni[5], Normand Laperriere [6], David Payne[6], Robert Heaton[6], Monique van Prooijen[6], Sunit Das[3], Derek Tsang[6]
[1]*University of Toronto, Toronto, ON*
[2]*Sunnybrook Health Sciences Centre, Toronto, ON*
[3]*St. Michael's Hospital, Toronto, ON*
[4]*University Health Network, Toronto, ON*
[5]*Hospital for Sick Children, Toronto, ON*
[6]*Princess Margaret Cancer Centre, Toronto, ON*

Purpose: Stereotactic radiosurgery (SRS) marginal dose is associated with successful obliteration of cerebral arteriovenous malformations (AVM). Calibration SRS dose rate – how old the cobalt-60 sources are – is known to influence outcomes for some neurologic conditions and benign tumours. It is not known if SRS dose rate influences AVM obliteration. The objective of this study was to determine the association between cobalt-60 calibration dose rate and cerebral AVM obliteration in patients treated with SRS.

Materials and Methods: We performed a retrospective study of 361 patients undergoing 411 AVM-directed SRS treatments between 2005 and 2019 at a single institution. Lesion characteristics, SRS details, and post-treatment obliteration and toxicities were recorded. Univariate and multivariate regression analyses of AVM outcomes with regard to SRS dose rate were performed.

Results: At 10 years post-SRS, 68% of AVMs were obliterated on follow-up cerebral angiography or MRI (if angiogram was not done). Dose rates >2.9 Gy/min were found to be significantly associated with AVM obliteration compared to those <2.1 Gy/min ($p = 0.034$). AVM size was also associated with obliteration, with obliteration more likely for smaller lesions. Higher dose rates were not associated with development of post-SRS radiologic or symptomatic edema, though larger AVM volume was associated with both types of edema.

Conclusions: Patients with cerebral AVMs treated with higher SRS dose rates (from fresh cobalt-60 sources) experience higher incidences of obliteration without a significant change in the risk of post-treatment edema.

140

ADAPTIVE STAGED STEREOTACTIC RADIOSURGERY TO SALVAGE PREVIOUSLY IRRADIATED BRAIN METASTASES

Dana Shor, Kang Liang Zeng, Lori Holden, Hanbo Chen, Pejman Maralani, Chris Heyn, Beibei Zhang, Sten Myrehaug, Chia-Lin (Eric) Tseng, Jay Detsky, Hany Soliman, Arjun Sahgal
University of Toronto, Toronto, ON

Purpose: We report outcomes specific to a novel 3 fraction staged stereotactic radiosurgery (St-SRS) regimen designed to salvage metastases previously irradiated and considered to be at high risk of radiation necrosis (RN).

Materials and Methods: Twenty-four patients with 55 metastases treated with our three fraction St-SRS approach were reviewed. Prior to each fraction, patients were re-simulated and planned with a new MRI to allow for treatment adaption. The primary endpoint was the cumulative incidence of local failure (LF) and secondary endpoints included tumour dynamics and RN rates.

Results: The median follow up was 9.0 months (range: 2.7-40.1 months) and median age was 59-years (range: 32-84). Primary cancers were of breast (44%), lung (33%), melanoma (22%), and gastro-intestinal (1%) origin. Individual metastases treated with St-SRS had initially failed surgery and post-op cavity hypofractionated SRS (HSRS) for 2/55 (4%), SRS alone for 19/55 (34%), whole brain radiation (WBRT) alone for six out of 55 (11%), HSRS for two out of 55 (4%), and prior SRS and WBRT exposure for 28/55 (51%). 46/55 (84%) were prescribed 8 Gy, 8 Gy, 4 Gy; 8/55 (14%) had 6 Gy, 6 Gy, 4 Gy and 1/55 (2%) had 8 Gy, 8 Gy, 6 Gy. The median number of weeks between fractions was 2.6 (range: 1.0-6.8). The median of the mean and maximum target doses were 9.7 Gy (range: 5.4-11.7 Gy) and 12.4 Gy (range, 7.5-16.0 Gy) respectively. The median prescription isodose line was 62% (range: 50-85%). The mean lesion volume and diameter was 3.8cc (range: 0.05-24.8 cc) and 1.6 cm (range: 0.2-4.4 cm), respectively. The mean percent target volume coverage, Paddick Conformality Index and Gradient Index were 100% (range: 97-100%), 0.7 (range: 0.1-0.9), and 3.2 (range: 2.5-6.7), respectively. The mean volume change between staged fractions was -4.2% (range: -69.3 to +63.1%), and based on the first and last St-SRS MRI was -10.8% (range: -86.6% to +68.7%). The crude LF rate was 27%. The median time to LF was 3.4 months (range: 1.2-7.4 months). Amongst those with a LF, seven out of 15 (46%) were melanoma, six out of 15 (40%) HER2 positive breast cancer, one out of 15 (7%) gastrointestinal and one out of 15 (7%) non-small cell lung carcinoma. Eight out of 15 (53%) had prior WBRT and SRS exposure, one out of of 16 (7%) surgery and cavity HSRS, five out of 15 (33%) SRS alone and one out of 15 (7%) WBRT alone. Only asymptomatic RN events were observed in four out of 55 (7%).

Conclusions: St-SRS is a promising approach to salvage previously irradiated brain metastases, including prior SRS, with a favourable rate of RN. Tumour volume dynamics between stages can be significant warranting adaptive replanning.

141

TOXICITY AND ONE YEAR OUTCOMES IN A SERIES OF SIX PATIENTS RECEIVING STEREOTACTIC ARRHYTHMIA RADIOABLATION FOR VENTRICULAR TACHYCARDIA

Ian J. Gerard, Alfieri Joanne, Gabriela Stroian, Valeria Anglesio, Martin Bernier, Tarek Hijal, Sarah Konermann, Neil Kopek, Piotr Pater, Bruno Toscani Gomes da Silveira
McGill University, Montréal, QC

Purpose: Stereotactic body radiation therapy (SBRT) to the arrhythmogenic scar regions defined by noninvasive cardiac mapping has been described for patients with standard-of-care refractory ventricular tachycardia (VT). Long-term outcomes and toxicities are not well described in this patient population. We report the one-year outcomes along with radiation toxicity for six patients treated with this technique at our institution.

Materials and Methods: Six patients treated between 2019 and 2022 with refractory VT with previously failed ablations and at least one anti-arrhythmic drug were treated at our institution. All were treated with 25 Gy in a single fraction to the suspected arrhythmogenic scar. Cardiac microstructure contouring was done following the atlas by Duane et al. 2017. Implantable cardioverter defibrillator (ICD) interrogation was performed regularly by the treating cardiologist to assess the number of VT and ICD events, and, patients were seen immediately following SBRT, and at three, six, and 12 months respectively. Computed tomography of the chest was done at three months to assess for radiation induced pneumonitis and transthoracic echocardiograms were done as per the cardiologist's discretion. Radiation toxicity was evaluated using CTCAE v5.0.

Results: The median follow-up time for the six evaluated patients is 24 months. Three patients (50%) remained VT free during the one year period post-SBRT. Two of these patients remain VT free and are either on reduced or discontinued anti-arrhythmic drugs, while another failed at 24 months in an area of the arrhythmogenic substrate that was intentionally not irradiated due to organ at risk safety concerns. Among the three patients who failed in the first year, the median time to failure was four months (range 3-5 months). All six patients tolerated treatment with no immediate acute side effects. Three (50%) of the patients had no acute clinical or radiographic side effects. Grade 1 esophagitis, Grade 1 fatigue, and Grade 1 cough was reported in one (17%) patient each (all different patients), and one patient required hospitalization four months after SBRT for a heart failure exacerbation (potentially SBRT-related). One patient (17%) died within three months following treatment but their death was not attributed to radiation treatment. No cardiac microstructure toxicity has been reported to date.

Conclusions: Despite increasing reports in the literature, there are no established criteria to predict success for SBRT in the context of treatment-refractory VT, or the best treatment dose for success, making it difficult to identify optimal patients. Current limited evidence suggests that this technique may be a relatively safe approach to provide an acute reduction in VT burden for those refractory to standard of care and has an acceptable acute toxicity profile however longer term follow-up is required. Long term toxicity, specifically to cardiac microstructures, and dose optimization is currently are the focus of ongoing study.

142

PATIENT-REPORTED DISTRESS AND ACUTE CARE UTILIZATION FOR CERVICAL CANCER PATIENTS UNDERGOING CONCURRENT CHEMO-RADIATION AND BRACHYTHERAPY

Areeb Hassan[1], Alyssa Macedo[1], Genevieve Bouchard-Fortier[1], Stephanie L'heureux[2], Manjula Mangati[1], Kathy Han[2], Candice Yu[1], Madeline Li[2], Jennifer Croke[2]
[1]Princess Margaret Cancer Centre, Toronto, ON
[2]University of Toronto, Toronto, ON

Purpose: Although concurrent chemo-radiation (CRT) and brachytherapy (BT) is curative for locally advanced cervical cancer (LACC), it requires complex coordination of care and is associated with treatment-related toxicity. Our objective was to evaluate patient-reported symptoms and social distress in LACC patients undergoing concurrent CRT and BT to determine whether they are predictive of acute care utilization.

Materials and Methods: Patients with LACC treated with concurrent CRT and BT between 2013-2020 completed the Edmonton Symptom Assessment Scale-revised (ESAS-r; nine cancer-related symptoms ranked 0-10) and the Social Difficulties Inventory-21 (SDI-21; 21 social issues ranked 0-3) at every ambulatory care visit as part of routine distress screening. Socio-demographic, clinical and treatment characteristics and ESAS-r/SDI-21 scores were extracted from medical records. Acute care utilization was defined as any unscheduled visit to the radiation nursing clinic, urgent care clinic, emergency department or hospitalization within one year from starting treatment, and data was identified from an administrative database. Descriptive statistics summarized patient, clinical and treatment characteristics, ESAS-r/SDI scores and acute care visits. A logistic regression model will be used to evaluate associations between ESAS-r and SDI-21 scores and acute care utilization.

Results: Among the 256 LACC patients treated with concurrent CRT and BT from 20130-2020, 151 patients completed a total of 354 ESAS-r and SDI questionnaires longitudinally. Mean age at diagnosis was 49.9 years (30-90), 44% were FIGO 2B and overall treatment time was 53.6 days (32-135). At baseline, the most prevalent moderate to severe symptoms (ESAS-r score $\geq$4) were well-being (50%), anxiety (44%), tiredness (43%) and pain (36%). At one-year post-treatment, these persisted in 29%, 18%, 34%, and 25%, respectively. The most common social distress at baseline was financial (33%). Financial distress post-treatment was significantly predictive of worse well-being (OR=5.80, p<0.006), anxiety (OR=3.33, p=0.04) and depression (OR=4.76, p=0.01). Use of acute care within one year after starting treatment occurred in 99 patients (66%) for a total of 613 visits: radiation nursing clinic 71.3%, urgent care clinic 4.4%, emergency department 8.3%, hospitalization 16%. On average there were 6.1 unscheduled acute care visits/patient (0-31), with the average number of days between treatment start and first acute care visit being 17.9 days (0-74).

Conclusions: Cervical cancer patients treated with concurrent CRT and BT report prevalent financial distress and moderate to severe symptoms that persist post-treatment. Acute care utilization commonly occurred during treatment, highlighting a time when additional support is needed. Predictive modelling for distress factors resulting in acute care utilization is now underway.

143

NOPAUSE: INITIAL EXPERIENCE DEPLOYING A NOVEL MULTI-CENTRE VMAT PLAN AUTOMATION SYSTEM

Nick Chng[1], Fred Cao[1], Michael Lamey[2], Sergei Zavgorodni[3], Quinn Matthews[1], Parmveer Atwal[4], Robert Olson[1]
[1]British Columbia Cancer, Prince George, BC
[2]British Columbia Cancer, Kelowna, BC
[3]British Columbia Cancer, Victoria BC
[4]British Columbia Cancer, Abbotsford, BC

Purpose: To provide an update on the development of our generalized automatic planning framework, the techniques and protocols being targeted, and the different workflow models being implemented by the participating centres.

Materials and Methods: The Northern Plan Automation Services (NoPAUSE) project is a collection of in-house applications and scripts designed to improve efficiency and quality in radiotherapy treatment planning. The core platform is the Treatment Planning Automation System (TPAS) that enables fully automatic VMAT plans to be produced within our Eclipse/ARIA environment. The TPAS front-end is a simple app that prompts the user to select a protocol and confirm the prescription, targets, and organs at risk (OAR). A request is then sent to a distributor service that manages the planning queue and email notifications. The submission process is asynchronous; the user may perform other clinical tasks or submit other requests while waiting. Field geometries are determined based on detected target location and distribution, and iterative re-optimization conditions can be configured based on clinical goal conditions. On completion, the user is sent a plan report summarizing dosimetric quality relative to protocol constraints. TPAS was developed to support the SUPR-3D trial for bone mets, but has a relatively low barrier to broader application because it operates by automating existing objective templates and/or RapidPlan models, which makes the results transparent and easy to adjust.

Results: The TPAS system has been installed at five centres within our organization, and is in clinical use at three. Approximately 115 clinical cases have been planned using the system. The clinical setting of most interest (four centres) is rapid-access palliative VMAT, due to the urgency, volume and relatively simple planning needs of this patient population. It is also utilized for more challenging techniques, such as prostate, gyne, and anal canal, and in tandem with the opening of new clinical trials (PR-22). At one site, it is available as a quality control tool for H&N, GU and GI sites, for comparison with the manually optimized plan at the time of physics review. TPAS is also enabling new efficiencies in planning workflows. Two centres are piloting processes in which the radiation oncologists are submit plan requests themselves, so contouring, optimization and plan review can occur in one encounter.

Conclusions: Our early experience suggests the automation framework is robust to differences in planning practices and local workflows between centres. Work is underway to develop and validate pre-packaged auto-planning protocols as an option for TPAS users to improve the accessibility of the system.

144

VALIDATION OF GPU-ACCELERATED MONTE CARLO SIMULATIONS FOR PATIENT-SPECIFIC CT DOSE CALCULATIONS

Ronan Lefol[1], Yannick Lemaréchal[1], Jonathan Boivin[2], Philippe Després[1]

[1]*Université Laval, Quebec City, QC*
[2]*CHU de Québec-Université Laval, Quebec City, QC*

Purpose: A limitation to patient-specific Computed Tomography (CT) dose profiling has been the prohibitive computational cost involved in moving from generic dose indices to a dose-to-organ approach on a large scale. The continuous development of GPU-enabled algorithms opens the door to personalized dose calculations on a massive scale in diagnostic imaging. This study aims to validate an extension of an existing GPU Monte-Carlo code (GPUMCD) for CT dose estimations.

Materials and Methods: An extension to GPUMCD was developed for the CT modality, where all the simulation parameters such as direction, pitch, and current of the X-ray source were retrieved from information found in the DICOM CT-examination files. This source and its trajectory were used to simulate energy deposition in a voxelized numerical phantom corresponding to the geometry (the patient) being scanned. Material and density were assigned from CT images following a standard calibration procedure. The GPUMCD extension was validated by experimental measurements under known conditions. Specifically, weighted CT Dose Index ($CTDI_w$) and in-air ($CTDI_{100,air}$) measurements were performed and compared to simulation results. Measurements were taken with various pitch factor values and volume sizes. In addition, a full scanning procedure was also performed to calibrate the simulated dose. Measurements on an anthropomorphic head volume were also performed in order to compare dose deposition values in more complex geometries.

Results: Simulated dose in the centre of a PMMA CTDI body phantom agreed within 5% to experimental values measured in different CT examinations. The simulated values of $CTDI_w$ for a standard PMMA body phantom agreed within 4% of the measured $CTDI_w$ value. On an NVIDIA RTX 2070, the simulation of a typical chest CT reached a 2% mean uncertainty, with 6.7×10^8 emitted photons, in under 8 minutes.

Conclusions: This work demonstrates the capacity for the new CT extension of GPUMCD to produce fast and accurate three-dimensional dose distributions for CT examinations. These simulations, driven by the unique CT study details and volume, allow the generation of patient-specific dose-to-organ profiles. The existing development of an automatic segmentation pipeline alongside this project allows massive dose-to-organ recalculations on a scale compatible with epidemiological studies.

145

QUANTIFICATION OF RADIOMIC FEATURE VARIABILITY ACROSS PROVINCIAL COMPUTED TOMOGRAPHY SCANNERS

Lorna Tu[1,2], Herve Choi[2], Haley Clark[1,3], Bradford Gill[2], Scott Young[2], Samantha Lloyd[1,2]
[1]*University of British Columbia, Vancouver, BC*
[2]*British Columbia Cancer, Vancouver BC*
[3]*British Columbia Cancer, Surrey, BC*

Purpose: Radiomics involves extracting quantitative features from medical images and is increasingly used to improve diagnosis, prognosis, and predict treatment response. Studies have shown that radiomic features may be sensitive to computed tomography (CT) acquisition parameters such as tube current and noise index. The potential inconsistency of radiomic features may be an issue in multi-centre radiomic collaborations, as combined data may be too heterogeneous for robust analysis. Our aim is to compare radiomic features from radiotherapy planning CTs obtained using provincial CT scanner hardware and protocols.

Materials and Methods: A novel, three-dimensional phantom with a water insert was designed and created using a plastic test tube and lung-equivalent foam. The phantom was scanned with three GE version 7 CT scanners at different provincial treatment centres using four respective routine lung stereotactic ablative radiotherapy planning acquisition protocols and manufacturer-defined image reconstruction methods. Sixty-one radiomic features were extracted from contours using Imaging Biomarker Explorer (IBEX) software. Features across scanners were compared using Kruskal-Wallis H tests.

Results: Centre-specific routine protocols contained similar acquisition parameters, apart from generator power (ranging from 4800 to 52800 kW) and tube current (ranging from 10 to 100 mA). Any variations in radiomic features may be attributed to these differences, although they do not reach the level of significance in our preliminary findings (Bonferroni-corrected $p>0.05$). Minimal variance within most features was observed, with shape features found to be especially stable. Some statistical-based texture features had a higher variance. Additional scans may be required to determine if the higher variance is statistically significant.

Conclusions: Our analysis does not find inconsistent radiomic features in the routine lung CT scans acquired at these provincial centres. Further study can determine if certain radiomic features or data originating from other centres can be included in a harmonized dataset.

146

FIVE-YEAR RENAL FUNCTION OUTCOMES AFTER SABR FOR PRIMARY RENAL CELL CARCINOMA: A REPORT FROM THE INTERNATIONAL RADIOSURGERY ONCOLOGY CONSORTIUM OF THE KIDNEY (IROCK)

Vivian Tan[1], Alexander Louie[2], Andrew Warner[1], Muhammad Ali[3], Alexander Muacevic[4], Lee Ponsky[5], Rodney Ellis[6], Simon Lo[7], Hiroshi Onishi[8], Anand Swaminath[9], Young Suk Kwon[10], Scott Morgan[11], Fabio Cury[12], Bin Teh[13], Anand Mahadevan[14], Irving Kaplan[15], William Chu[2], Raquibul Hannan[10], Michael Staehler[4], William Grubb[16], Shankar Siva[3], Rohann Correa[1]
[1]*Western University, London, ON*
[2]*University of Toronto, Toronto, ON*
[3]*Peter MacCallum Cancer Centre, Melbourne, AU*
[4]*University of Munich Hospitals, Munich, DE*
[5]*Case Western Reserve University, Cleveland, OH*
[6]*GenesisCare, Cape Coral, FL*
[7]*University of Washington School of Medicine, Seattle, WA*
[8]*University of Yamanashi, Yamanashi, JP*
[9]*McMaster University, Hamilton, ON*
[10]*University of Texas Southwestern Medical Center, Dallas, TX*
[11]*University of Ottawa, Ottawa, ON*
[12]*McGill University, Montréal, QC*
[13]*Houston Methodist Hospital Cancer Center and Research Institute, Houston, TX*
[14]*NYU Langone Health, New York, NY*
[15]*Beth Israel Deaconess Medical Center, Boston, MA*
[16]*Augusta University, Augusta, GA*

Purpose: Renal cell carcinoma (RCC) presents uncommonly in patients with a congenital solitary kidney or prior contralateral nephrectomy. The objective of this study was to compare renal function outcomes of stereotactic ablative body radiotherapy (SABR) in patients with solitary versus bilateral kidneys.

Materials and Methods: Patients with primary RCC with ≥2 years of follow-up at 12 participating International Radiosurgery Consortium for Kidney (IROCK) institutions were included. Patients with upper tract urothelial carcinoma or metastatic disease were excluded. Renal function was measured by estimated glomerular filtration rate (eGFR). For patients where eGFR was not recorded, Chronic Kidney Disease Epidemiology Collaboration (CKD-EPI) equation was used to estimate eGFR based on known creatinine.

Baseline characteristics and renal function outcomes were compared between solitary versus bilateral kidneys. Multivariable logistic regression was used to identify factors predictive of eGFR decline ≥ 15 mL/min and any eGFR increase evaluated at one-year post-SABR.

Results: One hundred and ninety patients with solitary (n=56) or bilateral kidneys (n=134) underwent SABR and were followed for a median of 5.0 years (IQR: 3.4-6.8). Pre-SABR eGFR (mean ± SD) was similar in patients with solitary (61.1 ± 23.2 mL/min) versus bilateral kidneys (58.0 ± 22.3 mL/min, p=0.324). Mean tumour size was 3.70 ± 1.40 cm in solitary and 4.35 ± 2.50 cm in bilateral kidneys (p=0.026). After SABR, an initial compensatory increase in eGFR was observed in both cohorts (22.7% solitary and 17.7% bilateral at 1 year). This compensatory increase persisted in patients with bilateral but not a solitary kidney (10.3% versus 0% at three years and 21.1% versus 0% at five years, respectively). At five years post-SABR, eGFR decreased by -14.5 ± 7.6 in solitary and -13.3 ± 15.9 mL/min in bilateral kidneys (p=0.665). At all timepoints assessed, there were no significant differences in eGFR decline between solitary versus bilateral cohorts (all p>0.05). There were also no significant differences in post-SABR end-stage renal disease (7.1% versus 6.7%) or dialysis (3.6% versus 3.7%) in solitary versus bilateral, respectively. Multivariable analysis demonstrated that increasing tumour size (OR per 1 cm: 1.57; 95% CI: 1.14-2.16, p=0.006) and baseline eGFR (OR per 10 mL/min: 1.30; 95% CI: 1.02-1.66, p=0.034) was more likely to be associated with eGFR decline ≥ 15 mL/min. There was no significant association between solitary versus bilateral kidney and eGFR decline (OR: 1.22; 95% CI: 0.45-3.34, p=0.693).

Conclusions: There was no observed difference between renal function outcomes in patients with a solitary versus bilateral kidneys. While larger tumour size may increase the risk of eGFR decline post-SABR, treatment of a solitary kidney does not appear to increase the risk of renal dysfunction long-term.

147

EVALUATION OF VOLUMETRIC RESPONSE ASSESSMENT FROM STEREOTACTIC ABLATIVE RADIOTHERAPY (SABR) FOR RENAL CELL CARCINOMA (RCC)

Daniel Schep[1,2], Ian Dayes[1,2], Himanshu Lukka[1,2], Kimmen Quan[1,2], Anil Kapoor[2,3], Jasmin Vansantvoort[1], Tom Chow[1], Anand Swaminath[1,2]
[1]Juravinski Cancer Centre, Hamilton, ON
[2]McMaster University, Hamilton, ON
[3]St. Joseph's Health Care, Hamilton, ON

Purpose: SABR has recently been proven to be a safe, effective treatment for RCC. However, long term follow-up assessment can be challenging as traditional methods of assessment such as RECIST may not identify tumour response, and delayed responses to SABR are common. The purpose of this study was to quantify SABR response using volumetric changes from baseline throughout follow-up.

Materials and Methods: We conducted a single-centre retrospective study including all patients treated with SABR for RCC from 2013 to 2020. Patients were included if they had no metastatic disease, no resection after SABR, and had follow-up imaging available for at least 12 months following SABR. All available follow-up CT scans were collected and aligned, and tumours were contoured on all follow-up scans to measure volume and maximum linear dimension. Response to SABR was assessed by comparing tumour volume at follow-up to the initial tumour volume at the time of CT simulation.

Results: Twenty-four patients with 25 tumours were included. The dose was between 25Gy and 42Gy in 1-5 fractions; 64% of tumours received 35Gy in 5 fractions. Follow-up time was between 16 and 67 months; median follow-up was 32 months. A total of 164 follow-up scans were contoured. The relative volume and standard deviation (compared to baseline) at three, six, nine, 12, 24, 36, and 48 months was 0.76 (SD 0.22), 0.80 (SD 0.27), 0.76 (SD 0.32), 0.75 (SD 0.26), 0.61 (SD 0.33), 0.53 (SD 0.41), and 0.34 (SD 0.22) respectively. One tumour (4%) showed continued growth after SABR, while 24 of 25 tumours (96%) had durable volumetric response after SABR. Eighteen of 25 tumours (72%) decreased in volume on first follow-up scan and continued to shrink, while six of 25 tumours (24%) displayed growth after SABR (average 33% increase in volume) before shrinking below their initial volume. The median time to any volumetric response was 3.5 months (range 2-19 months). Nineteen tumours (76%) had 30% volumetric response. Median time to 30% volumetric response was seven months (range 3-55 months). In contrast, 12 tumours (48%) had 30% decrease in maximum linear size, with median time to 30% linear response of 16 months (range 4-42 months). Thirteen tumours (52%) had 50% volumetric response; median time to 50% volumetric response was 11 months (range 4-37 months). Among tumours for which contrast-enhanced scans were available, 15 of 22 tumours (68%) displayed arterial enhancement at their most recent follow-up scan, at a median time of 24 months after SABR.

Conclusions: SABR is a highly effective treatment for RCC, achieving durable local control in 96% of cases. Initial growth after SABR is common before volumetric response occurs. Volumetric response is more frequent and occurs earlier than decrease in maximum linear dimension, even with persistent arterial contrast enhancement following SABR.

148

IMPACT OF STATIN USE ON BIOCHEMICAL RECURRENCE IN PROSTATE CANCER PATIENTS TREATED WITH RADIATION THERAPY

Danny Lavigne[1], Kevin Kaulanjan[2], Benedikt Hoeh[3], Fred Saad[1], Pierre I. Karakiewicz[1], Rocco Simone Flammia[4], Luis Alex Kluth[3], Philipp Mandel[3], Felix K.H. Chun[3], Daniel Taussky[1]
[1]Université de Montréal, Montréal, QC
[2]Université des Antilles, Pointe-à-Pitres, FR
[3]Goethe University Frankfurt am Main, Frankfurt am Main, FFM
[4]Sapienza Rome University, Rome, IT

Purpose: In vitro experimental data suggest that statins may harbor antitumoural and radiosensitizing properties, but several clinical studies showed mixed results regarding statin use to prevent prostate cancer (PCa) progression. Due to the radiobiological differences of low dose-rate brachytherapy (LDR), high dose-rate brachytherapy (HDR), and external beam radiotherapy (EBRT), we sought to investigate the impact of statin use on biochemical recurrence (BCR) in prostate cancer patients undergoing these different treatment modalities.

Materials and Methods: Patients treated with curative-intent primary radiation therapy for localized PCa between January 2001 and January 2022 were included in this retrospective analysis and stratified according to statin use. All data were collected from the prospectively maintained institutional database. Patients were treated with one of three modalities: EBRT, LDR, or EBRT plus HDR. Kaplan-Meier plots and multivariable Cox regression models tested five- and ten-year BCR-free survival and its association with statin use after adjustment for D'Amico risk, treatment modality, age, PSA at diagnosis, and androgen-deprivation therapy. Statistical analyses were repeated separately for low- and intermediate-risk LDR-treated patients as well as for intermediate- and high-risk EBRT-treated patients.

Results: Median follow-up was 52 months for a total of 3555 patients, of which 43% were taking statins, while 1208 were treated with EBRT, 1679 with LDR, and 599 with EBRT plus HDR. Overall,

BCR-free survival at five and 10 years were 95% and 83% versus 93% and 80% for patients receiving statins versus patients not receiving statins, respectively (log-rank=0.1). Only intermediate-risk patients treated with LDR fared better with statin use in univariate analysis (HR 0.38, 95% CI 0.16-0.92, p=0.03), but this association was not significant in multivariate analysis (HR 0.44, 95% CI 0.18–1.10, p=0.06).

Conclusions: Based on a large prospectively maintained database, statin use is not associated with a reduced risk of BCR in patients treated with EBRT, LDR, or EBRT plus HDR after adjusting for potential confounders.

149

ACCUMULATED KIDNEY DOSE IN RENAL STEREOTACTIC BODY RADIOTHERAPY: ANALYSIS FROM A PROSPECTIVE PHASE II TRIAL

Joelle Helou[1], Jeff Winter[2], Jerusha Padayache[2], Inmaculada Navarro[2], Tony Tadic[2], Srinivas Raman[2], Peter Chung[2], Padraig Warde[2], Antonio Finelli[2], Rob Hamilton[2], Tony Lam[2], Charles Catton[2], Alejandro Berlin[2], Jennifer Dang[2], Andrew McPartlin[2], Philip Ye[2], Laura Dawson[2] Rachel Glicksman[2]
[1]Western University, London, ON
[2]University of Toronto, Toronto, ON

Purpose: Stereotactic body radiotherapy (SBRT) for renal tumours is associated with promising outcomes and is gaining acceptance as a treatment option in poor surgical candidates. The aim of this analysis is to estimate the accumulated delivered dose to the kidney using image guided radiotherapy in a prospective phase II trial and to evaluate its impact on the primary outcome.

Materials and Methods: This was a prospective single-centre phase II study of renal SBRT in patients with a solid kidney mass (primary RCC or metastasis). The primary outcome was nephron toxicity measured by the change in glomerular filtration rate (GFR) using Modified Diet in Renal over two years. The controlled exhale breath-hold (EBH) feasibility and tolerance relative to the free-breathing range was used to determine the planning and treatment technique: free breathing 4DCT with an ITV-based approach or controlled EBH. The choice of prescribed dose (27.5-40 Gy) in 5 fractions was based on the volume of uninvolved renal cortex and proximity of gastrointestinal luminal structures. Uninvolved renal cortex volume (cc) was defined as the combined renal cortex-17.5 Gy isodose line. Dosimetric analysis with accumulated dose based on 4D cone beam CTs (CBCT) prior to each fraction was performed, using a hybrid intensity/structure-based algorithm for CT-to-CBCT deformable image registration. Univariate and multivariable linear regression were performed to determine the association of parameters with the primary outcome.

Results: Twenty patients were included in this analysis: 11 free breathing and nine controlled EBH. The mean (±SD) age at time of treatment was 73 (±12) years, 95% of treated lesions were primary kidney cancer and the median (range) tumour size was 4.4 cm (2.1-8). 80% of treated patients had CKD Stage 3 at baseline. 80% of patients were prescribed ≥35 Gy. Median (range) follow up was 21.6 months (7.4-29.8). At last follow-up none of the patients had a local recurrence or cancer-related death. The mean GFR (mL/min) decline was four (±15) at 12 months and nine (±16) at 24 months. The volume of uninvolved renal cortex was an independent predictor of GFR change at last follow-up [B=0.05, 95%CI (0.02-0.09),p=0.006]. The planned uninvolved renal cortex volume [(median (range): 192.8 cc (113.5-311.4)] was highly correlated to the accumulated volume [197.7 cc (119.2-312.9)]. (R-square 0.99, p<0.001). The accumulated (versus planned) uninvolved kidney cortex was a stronger predictor for GFR decrease [B=0.06, 95% CI (0.02-0.11), p=0.003].

Conclusions: Uninvolved renal cortex is an independent predictor of renal toxicity. Ensuring the reproducibility of kidney dose-volume metrics over the treatment course is key to ensure optimal nephron-sparing.

150

SUCCESS IS BEST WHEN IT IS SHARED: ONE DEPARTMENT'S INTERPROFESSIONAL TEAM EFFORT TO REDUCE WAIT TIME FOR HEAD AND NECK RADIATION THERAPY PATIENTS

Marc LeBlanc, Jenna Clayfield, Murali Rajaraman, Nathan Lamond, Monique Ashe, Peilong Zhang, Leah Hensel, Steven Burrell, Carol-Anne Davis
Dalhousie University, Halifax, NS

Purpose: Studies have shown that delays in Radiation Therapy (RT) treatment can result in decreased locoregional control and overall survival in Head and Neck squamous cell cancer patients (HNSCC). Between referral and start of treatment, many inter-professionals (IP) are involved in the patient management. Authors identified the need to bring together an IP project team, review care paths, guidelines and establish changes in practice to reduce wait times to start RT. Project goal is to establish a HNSCC Pre-booking program where patients start treatments within three weeks of Request of Radiation Services (RFRS) and two weeks from CT simulation.

Materials and Methods: Over a period of five months, co-authors consisting of various IP departments identified challenges in the booking process for HNSCC patients. IP project leads developed a system for prioritizing bookings for HNSCC patients with relevant IP professionals. A designated head and neck cancer referral officer was established along with the creation of clear booking guidelines to aid in efficiently scheduling diagnostic imaging, dental and Medical and Radiation Oncology appointments. Commitment was made from Medical Oncologists to pre-book chemotherapy to allow them to hold coordinated earlier start dates for our concurrent Chemo-Radiation patient population. Online patient booking care paths were modified to pre-book start dates for these patients within our targeted time frames.

Results: Prior to the IP team approach, the average time between RFRS to start date was ~27 days (range: 20 - 36 days, mode: 27 days) and the average time from CT simulation to start date was ~19 days (range: 12 - 32 days, mode: 20 days. Preliminary results suggest these times have been decreased to ~21 days (range:15 - 28 days, mode: 21) and ~14 days (range: 10 - 20, mode: 14 days) respectively.

Conclusions: Our initial findings show a trend of starting the treatments within the proposed timelines, which is on average about one week sooner than before implementing our new guidelines. In addition, these patients received notification of their targeted date much earlier. Further studies will be needed to determine correlation with overall survival and decreased locoregional control.

151

SURGEON, PATHOLOGIST AND PATHOLOGY TECHNICIAN EFFECTS ON NODAL YIELD AFTER A NECK DISSECTION

Veeral Desai[1], Adam Mutsaers[2], Rui Fu[2], Mark Khoury[2], Carlos Khalil[2], Peter Leventis[2], Antoine Eskander[2], Zain Husain[2]
[1]Queen's University, Kingston, ON
[2]University of Toronto, Toronto, ON

Purpose: A minimum nodal count of 18 lymph nodes has been associated with improved survival after neck dissection and has been suggested as a head and neck cancer quality metric. Despite its critical importance, factors affecting nodal yield are

poorly studied. In particular, the relative contribution of surgeons, pathologists, and pathology technicians has not been evaluated. The purpose of this study was to understand both patient and provider related factors that affect nodal yield after neck dissection for patients with oral cavity squamous cell carcinoma (OCSCC).

Materials and Methods: This retrospective cohort study involved review of all adult patients with OCSCC undergoing primary neck dissection between 2000-2020 at an academic medical centre. The outcome of interest was a continuous variable denoting the number of nodes removed per side during neck surgery. Surgeon and pathologist year of experience were calculated and represented in quartiles. A multilevel multivariable linear regression model was used to assess the association of surgeon/pathologist experience quartiles with nodal yield, controlling for patient age, comorbidity index, previous cancer, tumour grade, and clinical nodal status.

Results: The 508 patients included in our cohort were treated by five surgeons and six pathologists and involved 44 pathology technicians. Of these patients, 310 (61.0%) were male with a mean age of 63. Oral tongue primary tumours were 46.7% of the cohort, while 64.4% of patients had cT1-T2 tumours, and 65.2% were cN0. The mean nodal yield was 24.2 nodes. The ANOVA analysis revealed significant difference in mean nodal yield by surgeon (p-value=0.03), pathologist (p-value<0.01) and pathology technician (p-value=0.037). After accounting for patient-level characteristics and patient clustering by surgeon, increasing surgeon experience was found to be significantly associated with a higher nodal yield (joint significance of surgeon years of experience quartiles <0.01). Specifically, when compared to surgeons with the least experience (first quartile), those whose years of experience fell into the second, third, and fourth quartile removed 4.69 (95% CI: 0.97 to 7.92), 4.47 (95% CI: 0.33 to 7.87), and 7.37 (95% CI: 0.73 to 11.27) more lymph nodes. Meanwhile, there was no association between pathologist experience and nodal yield (joint significance of pathologist years of experience quartiles = 0.27). Additionally, previous cancer diagnosis and cN0 disease were significantly associated with lower nodal yield (all p-values=0.02).

Conclusions: This study demonstrates an independent association between increasing surgeon experience and higher nodal yields. Importantly, it also demonstrates that pathologists and pathology technicians contribute to the variation in nodal yield, and their contribution should not be overlooked in the implementation of a lymph node yield-based quality metric.

152

AN UPDATE OF STEREOTACTIC BODY RADIOTHERAPY (SBRT) FOR THE PALLIATION OF UNIRRADIATED MUCOSAL HEAD AND NECK SQUAMOUS CELL CARCINOMA (SCC)

Mohammed Aldohan, Elwyn Zhang, Irene Karam, Andrew Bayley, Madette Galapin, Antoine Eskander, Kevin Higgins, Liying Zhang, Lee Chin[1], Ian Poon
[1]*University of Toronto, Toronto, ON*

Purpose: We report the treatment outcomes of palliative Stereotactic Body Radiation Therapy (SBRT) in patients with primary mucosal head and neck cancer (HNC) who were not eligible to receive conventional radiation therapy (RT).

Materials and Methods: This is a retrospective study that reviewed the medical records of patients with primary SCC mucosal HNC who were treated with SBRT between 2011 and 2022. Patients with other histologies, skin cancer, parotid tumours, or recurrent previously irradiated tumours were excluded from the study.

Results: Seventy-four patients and 77 tumours were treated with SBRT in this cohort. The median age in the study was 81(52-97) years and the median follow-up was 7.2 months. The most common site of HNC was the oral cavity (62%), followed by the oropharynx (18%), hypopharynx (8%), larynx (5%), nasal cavity/sinonasal cancer (3%), and unknown primary (1%). T3-4 lesions were found in most patients (76%). SBRT doses ranged from 35-50 Gy in 5 fractions, and the most common prescription dose was ≥45 Gy in 5 fractions (60%) for the GTV prescription. An elective nodal volume of 25 Gy in 5 fractions was infrequently (17%) used. Most patients (81%) who were treated twice a week completed in ≤14 days. The predominant symptoms at presentation were: pain (41%), mass effect (39%), dysphagia/odynophagia (14%), headache/nasal obstruction (1.4%), bleeding (1.4%), stridor (1.4%), asymptomatic (1.4%), and unknown (1.4%). Eighty-four percent of patients had symptomatic response to treatment with 24% of them having complete symptom response. Cumulative incidence of local failure (LF) was 6.7% and at six months and 17.9% at 12 months, respectively. Cumulative incidence of distant metastasis was 7.3% and 10.5% at six and 12 months. Cancer was the most common cause of death in 29 patients (51%). The median overall survival (OS) was eight months with six- and 12-month OS rates of 67% and 36%, respectively. Thirty-nine percent of patients developed acute G3 toxicity, including 30% with G3 mucositis, 5% with G3 dysphagia, and 4% with G3 dermatitis. A crude rate of late G ≥3 toxicity was observed in 11% of patients including (5%, n=4) with osteoradionecrosis, and a single case of dysphagia, soft tissue necrosis, supraglottic ulceration, and mucosal necrosis.

Conclusions: This study highlights the feasibility of SBRT as a treatment option for primary mucosal head and neck cancer patients who are not eligible for conventional radiation therapy. The results indicate that SBRT was effective in achieving local control and symptom relief, but larger prospective studies are needed to confirm the findings. The Canadian Cancer Trials Group has endorsed HN-13, a randomized control trial comparing HN SBRT to palliative RT.

153

BIOMARKER STATUS PREDICTS FOR LOCAL CONTROL FOLLOWING SPINE STEREOTACTIC BODY RADIOTHERAPY IN NON-SMALL CELL LUNG CANCER PATIENTS WITH SPINAL METASTASES

Dana Shor, Kang Liang Zeng, Hanbo Chen, Ines Menjak, Eshetu Atenafu, Chia-Lin (Eric) Tseng, Jay Detsky, Jeremie Larouche, Beibei Zhang, Hany Soliman, Pejman Maralani, Sten Myrehaug, Alexander V. Louie, Arjun Sahgal
University of Toronto, Toronto, ON

Purpose: We report outcomes after spine stereotactic body radiotherapy (SBRT) in patients with metastatic non-small cell lung cancer (NSCLC), to determine the significance of programmed death-ligand 1 (PD-L1) status and epidermal growth factor (EGFR) mutation on local failure (LF) rate.

Materials and Methods: One hundred sixty-five patients and 389 spinal segments were retrospectively reviewed from 2009 to 2021. Baseline patient characteristics, treatment and outcomes were abstracted. Primary endpoint was LF and secondary outcomes included overall survival (OS) and vertebral compression fracture (VCF) rates. OS was estimated using the Kaplan-Meier method. Cumulative LF and VCF rates were calculated using competing risk analysis method. Multivariable analysis (MVA) evaluated factors predictive of LF and VCF.

Results: Median follow-up, OS and age was 13 months (range, 0.5-95 months), 18.4 months (95% CI 11.4-24.6), and 67 years (range, 28.2-89.9) respectively. Fifty-two percent were female, 76% had an adenocarcinoma histology and 61% had a smoking history. 49/165 (29%) had an EGFR mutation. PD-L1 status was analysed in 109/165 (66%) patients with 16% PD-L1 ≥ 50%, 20%

PD-L1 1-49% and 35% PD-L1 <1%. Of 389 segments, 79% were denovo and 21% were previously radiated. At baseline, 35% had a VCF, 27% had epidural disease, 27% had paraspinal extension, and 49% were Spinal Instability in Neoplasia Score (SINS) stable. 239/389 (61%) were treated with either 24 or 28 Gy in 2 SBRT fractions. Within one month of SBRT, 39/165 (24%) had a tyrosine kinase inhibitor, 27/165 (16%) immunotherapy (IO) with or without chemotherapy, and 31/165 (19%) chemotherapy alone. LF cumulative incidence at one- and two-years was 16.3% (95% CI 12.8-20.3%) and 25.4% (95% CI 20.9%-30%), respectively. EGFR positivity (p<0.0001), PD-L1≥50% (p=0.013) and treatment with IO within one month of SBRT (p=0.004) predicted for improved local control on MVA. The one- and two-year LF rate in EGFR-positive versus negative patients were 12.9% versus 16.6% and 17.7% versus 28.8%, respectively, and in those PD-L1 ≥50% versus PD-L1<50% were 7.8% versus 19.6% and 7.8% versus 38.1% respectively. Cumulative incidence of VCF at one- and two-years were 6.6% (95% CI 4.4-9.4%) and 8.8% (95% CI 6.1-12.0%). MVA identified prior SBRT to the same treated segment (p<0.0001) and a baseline VCF (p<0.0001) as significant predictors. Eighteen of 389 (4.6%) had radiation-induced radiculopathy and no radiation myelopathy events detected.

Conclusions: We identify the predictive utility of EGFR mutation and PD-L1 ≥50% status on local control in NSCLC patients with spinal metastases treated with spine SBRT, and a therapeutic benefit with peri-SBRT IO.

154
PROSTATE STEREOTACTIC RADIOTHERAPY WITH AND WITHOUT A RECTAL SPACER: EFFECTS ON DOSIMETRY AND EARLY ACUTE TOXICITY

Subhadip Das, Dominique Fortin, Isabelle Gagne, Winkle Kwan, Abraham Alexander
University of British Columbia, Victoria, BC

Purpose: The use of a rectal spacer hydrogel has been shown to help reduce bowel toxicities for prostate cancer patients treated with intensity modulated radiotherapy. This study aims to determine the effect of the spacer on rectal dose and early toxicity in the setting of prostate stereotactic ablative radiotherapy (SABR).

Materials and Methods: Patients enrolled on a prospective, province-wide prostate SABR registry, who had completed their first (six to eight weeks) post-treatment follow-up, were included in the analysis (n=157). Dosimetric data was extracted from the treatment plans. Baseline parameters, dosimetry and toxicity at six to eight weeks were compared between those with (n=68) and without (n=89) a rectal spacer. Dose metrics considered included rectum V36Gy, V18Gy and bladder V36Gy, V18Gy. These metrics were ranked to determine percentile values. RTOG/SOMA Genitourinary (GU) and Gastro-intestinal (GI) toxicities at baseline and at six to eight weeks (post-SABR) were analyzed. Statistical significance was determined using Student's t or Fisher's exact test where appropriate.

Results: The two groups were comparable with respect to age, Gleason score, diabetes, hypertension, prior TURP, pre-treatment PSA, risk group, treatment schedule, and use of androgen deprivation therapy. There was a significant difference between the two groups with respect to prescribed dose to the prostate, with 98.5% of rectal spacer patients receiving 40Gy in 5 fractions and 61.8% of non-spacer patients receiving 36.25Gy in 5 fractions. Groups also differed in bowel preparation: All (100%) of spacer patients and 34.8% of non-spacer patients used fleet enema; and 43.8% of non-spacer patients used glycerin suppositories. The rectal spacer group had significantly lower rectal V36Gy and V18Gy. In the non-spacer group, the mean (median) V36Gy was 0.93 cc (0.84 cc), while it was 0.16 cc (0.07 cc) in the spacer group. The difference in rectal V18Gy was also significant, with a mean (median) of 32% (37%) in the non-spacer group, compared to 14% (11%) in the spacer group. The bladder V36Gy and V18Gy also showed significant differences between the two groups favouring the rectal spacer. No significant differences were observed in rectal toxicity at 6-8 weeks post-RT.

Conclusions: The use of a rectal spacer with prostate SABR significantly reduces rectal dose. Despite a much greater proportion of patients with higher prescribed prostate dose in the spacer group, no difference in early post-SABR toxicity at six to eight weeks was observed. Results from on-going multivariate analysis and longer follow-up time are needed to fully evaluate the impact on the toxicity profile.

155
OUTCOMES OF HEAD AND NECK CUTANEOUS ANGIOSARCOMA TREATED IN THE IMRT ERA

Saheli Saha, Shao Hui Huang, Brian O'Sullivan, Jie Su, Wei Xu, Ali Hosni Abdalaty, John Waldron, Jonathan Irish, John de Almeida, Ian Witterick, Eric Monteiro, Ralph Gilbert, Charles Catton, Peter Chung[1], Dale Brown, David Goldstein, Albiruni Abdul Razak, Patrick Gullane, Ezra Hahn
University of Toronto, Toronto, ON

Purpose: Clinical behavior, natural history, and varied presentations of cutaneous angiosarcomas of the head and neck region (HN), in conjunction with its rarity, have rendered standardization of treatment elusive. We aimed to assess outcomes and patterns of failure for patients treated with surgery and radiation (Sx+RT) and radiation alone (RT).

Materials and Methods: A retrospective review of all HN angiosarcoma patients amenable to upfront Sx or RT in our institution between 2004-2018 was completed. Generally, treatment included Sx when feasible and RT for large or extensive/ill-defined tumours. Demographic, tumour characteristics, local (LC), regional (RC), distant control (DC), and overall survival (OS), as well as patterns (in-field, marginal, out-of-field) of local failure at five-year were estimated. Univariate analysis (UVA) was conducted to assess association with outcomes.

Results: Thirty-three patients were eligible (14 Sx+RT and 19 RT). Tumour locations were: scalp (16, 48%), face (n=12, 36%), and overlapping (five, 15%). Lesion types were: nodular (n=23, 70%), flat (n=4, 12%) and mixed (n=6, 18%). Tumour size was larger in the RT group (median: 10.00 versus 2.85 cm, p<0.01). RT and Sx+RT patients had otherwise similar baseline characteristics: median age 74.3; male 70%; and ECOG performance status ≤1 85%. RT dose fractionations ranged from 50-70 Gy in 25-35 fractions in the RT group and 50-66 Gy in 25-33 fractions in the Sx+RT group. Four (12%) patients received neoadjuvant chemotherapy. Median follow-up was 5.5 years. Five-year LC, RC, DC, and OS for RT versus Sx+RT groups were 68% versus 85% (p=0.28); 95% versus 86% (p=0.89); 79% versus 86% (p=0.39); and 45% versus 55% (p=0.71), respectively. The in-field/marginal/out-of-field local failure rate at five years were 16% versus 7% (p=0.46), 26% versus 15% (p=0.41), and 13% versus 0% (p=0.24) for the RT versus Sx+RT groups, respectively. UVA for OS showed the following factors associated with worse survival: performance status (ECOG 2-3 versus 0-1, HR 4.74, 95% CI 1.43, 15.75, p=0.01); scalp versus face location (HR 5.15, 95% CI 1.43, 18.5, p=0.01); ulceration/bleeding (HR 8.09, 95% CI 2.74, 23.9, p=<0.001); and smoking (HR 1.02, 95% CI 1, 1.05, p=0.02). UVA for DC showed the following factors associated with worse distant control: bone invasion (HR 4.82, 95% CI 1.13, 20.59, p=0.03) and ulceration/bleeding (HR 4.6, 95% CI 1.04, 20.31, p=0.04). Lesion type (nodular/flat/mixed), tumour size, and treatment type (Sx+RT versus RT), were not significantly associated with LC or pattern of local failure.

Conclusions: Scalp tumours, as compared to face, portended poorer prognosis, and ulceration/bleeding and bone invasion were associated with increased distant metastases. Sx+RT was the preferred treatment modality when possible and typically used for smaller and better-defined tumours. RT was reserved for larger and extensive/ill-defined disease; despite this, in the IMRT era, RT achieves reasonable rates of control, markedly superior to historical series.

156

IMPACT OF IMMUNE, INFLAMMATORY, AND NUTRITIONAL INDICES ON OUTCOME IN PATIENTS WITH CERVICAL CANCER TREATED WITH DEFINITIVE (CHEMO) RADIOTHERAPY

Ruth Fullerton[1], Kevin Martell[1], Rutvij A. Khanolkar[1], Tien Phan[1], Robyn Banerjee[1], Tyler Meyer[1], Laurel Traptow[2], Martin Köbel[1], Prafull Ghatage[1], Corinne M. Doll[1]
[1]*University of Calgary, Calgary, AB*
[2]*Tom Baker Cancer Centre, Calgary, AB*

Purpose: Systemic immune, inflammatory, and nutritional indices have been shown to be prognostic for outcome across a range of tumour sites. However, a comprehensive analysis of these markers in patients with cervical cancer treated with definitive (chemo) radiotherapy [(C)RT] has not been performed. We hypothesized that systemic immune, inflammatory, and nutritional indices may be associated with progression-free survival (PFS) and overall survival (OS) in patients undergoing definitive (C)RT for cervical cancer.

Materials and Methods: Patients with cervical cancer treated with definitive (C)RT from 1999-2015 were identified from a single cancer institution's retrospective clinicopathological database. Pre-treatment immune, inflammatory, and nutritional parameters were collected, and indices derived. Systemic immune-inflammation index (SII) = neutrophil count x platelet count / lymphocyte count(10^9/L); PLR = platelet count / lymphocyte count(10^9/L), NLR =neutrophil count / lymphocyte count (10^9/L); MLR =monocyte count / lymphocyte count (10^9/L); albumin to alkaline phosphatase ratio (AAPR) = serum albumin level (g/L)/alkaline phosphatase level (U/L) and prognostic nutritional index (PNI) = serum albumin (g/L) + 5 x lymphocyte count (10^9/L). Univariate analysis was first performed on each parameter as continuous variables for PFS and OS. For variables with statistically significant associations, ROC curves were analyzed to determine if an optimal cut point could be established for each outcome. Common cut points were then defined for each variable. PFS and OS were analyzed by the Kaplan-Meier method and the Log-Rank test. Multivariate analysis was performed using Cox regression with covariates of tumour stage, histology, and age. P-values of <0.05 were considered statistically significant.

Results: One hundred and ninety-six patients were identified; median follow-up seven years. 131 (67%) had Stage I-II and 65 (33%) Stage III-IV disease. One hundred and eighty-seven (95%) received CRT and 9 (5%) RT alone. Higher SII (≤700 versus >700; p=0.01), higher PLR (≤ 250 versus >250; p<0.001) and higher NLR (≤ 5 versus >5; p=0.003) were associated with worse PFS. Higher SII [≤700 versus >700: 5y OS 74.9 versus 55.8; p=0.02], higher PLR [≤ 250 versus >250: 5y OS 69.9% versus 42.0%; p<0.001] and higher NLR [≤ 5 versus >5: 5y OS 65.3% versus 51.0%; p=0.01] were associated with worse OS. MLR, AAPR and PNI were not associated with outcome on univariate analysis. On multivariate analysis, SII and PLR were independently associated with both PFS [SII: HR 1.647 (CI 1.029-2.639), p=0.038; PLR: HR 2.301 (95% CI 1.507 - 3.512), p=<0.001], and OS [SII: HR 1.649 (95% CI 1.009-2.696), p=0.046; PLR: HR 2.212 (95% CI 1.416-3.455), p<0.001]; NLR did not remain statistically significant.

Conclusions: SII and PLR, but not nutritional indices, were independently associated with PFS and OS in patients with cervical cancer treated with definitive (C)RT. Further evaluation of these systemic immune and inflammatory indices in a validation set will be required to better define their clinical utility.

157

RECURRENCE RATES AND PATTERNS IN LOCALLY ADVANCED CERVICAL CANCER IN THE IMRT ERA: A SINGLE INSTITUTION EXPERIENCE

Bayan Malakouti-Nejad, Ege Babadagli, Krystine Lupe, Tien Le, Rajiv Samant
University of Ottawa, Ottawa, ON

Purpose: Locally advanced cervical cancer is treated with concurrent chemoradiotherapy with combined external beam radiotherapy (EBRT) and brachytherapy. Since 2015, our institution has been using intensity-modulated radiotherapy (IMRT) for EBRT treatments in addition to HDR intracavitary brachytherapy for these patients. We conducted a review of patients treated since this implementation in order to assess rates and patterns of recurrence and determine whether these differ from prior cohorts.

Materials and Methods: A retrospective chart review was conducted of patients with locally advanced (FIGO Stage IB-IVA) cervical cancer treated with curative-intent concurrent chemotherapy (weekly cisplatin) and radiotherapy (external beam and brachytherapy) at our centre between 2015 and 2019. Recurrences were analyzed and rates and patterns were reported. These were compared to recurrences from the cohort of patients treated between 2008 and 2014, predominantly with 3-dimensional conformal radiotherapy (3D-CRT).

Results: Between 2015 and 2019, 89 patients with locally advanced cervical cancer were treated at our institution. The median age was 50 years and breakdown according to stage was as follows: 12% Stage I, 64% Stage II, and 24% Stage III/IV. Based on CT imaging, 47% had lymph node involvement. With median follow-up of 3.9 years, 26 patients (29.2%) developed recurrences. Of these, 12 (13.5%) had locoregional/in-field recurrence and 18 (20.2%) had distant recurrence, with four patients presenting with both locoregional and distant recurrence. Recurrences were more common among patients with lymph node involvement (33% versus 25%). Local failure occurred in 11% of patients, and none among Stage I patients. These results compare favourably to our cohort of patients treated between 2008 and 2014, in which there was locoregional and distant recurrence rates of 17.1% and 30.3% respectively with median follow-up of 5.2 years.

Conclusions: Our study confirms that that the routine use of IMRT in the primary treatment of cervix cancer appears very effective, with relatively low rates of locoregional relapses and outcomes comparable to the published literature using larger treatment targets. Distant relapses now predominate, and this requires better systemic treatment approaches.

158

PATTERNS OF TREATMENT AND OUTCOMES OF PATIENTS WITH BRAIN-ONLY METASTATIC BREAST CANCER

Badr Id Said, Ellen Warner, Hany Soliman, Veronika Moravan, Sten Myrehaug, Chia-Lin Tseng, Jay Detsky, Arjun Sahgal, Katarzyna Jerzak
University of Toronto, Toronto, ON

Purpose: Data regarding the epidemiology of brain-only metastatic breast cancer (MBC) is limited. We characterized the incidence, risk factors and survival of MBC patients with brain metastases (BrM) as the first and only site of metastatic disease in a large, retrospective institutional cohort.

Materials and Methods: MBC patients treated for BrM at a quaternary institution with SRS and/or WBRT between 2005 and 2019 were identified. MBC patients with BrM but without extracranial metastases (ECM) or leptomeningeal involvement were classified as brain-only MBC based on review of available imaging. Clinical/pathologic features associated with brain-only MBC, brain specific progression-free survival (bsPFS) and overall survival (OS) were investigated with univariable (UVA) and multivariable analyses (MVA).

Results: Overall, 691 MBC patients with BrM were analyzed. 40 patients (5.8%, n=40/691) were classified as having brain-only MBC; 40% (n=16) had TNBC, 37.5% (n=15) had HER2+, and 17.5% (n=7) had HR+/HER2- subtypes. 37.5% of brain-only MBC patients (n=15) had a single BrM. On MVA, patients with brain-only MBC were more likely to have a single BrM (OR 3.45 [1.61-7.14], p=0.001) along with either HER2+ (OR 3.3 [1.32-9.65], p=0.03) or TNBC (OR 4.09 [1.42-11.74], p=0.009) subtypes as compared to those with concurrent extra-cranial metastatic disease. Compared to the whole cohort, patients with brain-only MBC had longer bsPFS (HR 0.45 [0.24-0.86], p=0.006) and OS (HR 0.35 [0.13-0.96], p=0.02). With a median follow-up of eight months (IQR 2-35), the median bsPFS and OS of patients with brain-only MBC was 6.5 months and eight months as compared to four months and five months among patients with extracranial metastases.

Conclusions: In our cohort, patients with brain-only MBC had a longer bsPFS and OS than those with concurrent extra-cranial metastatic disease. Patients with HER2+ and TNBC subtypes were more likely to have brain-only disease compared to those with HR+/HER2- MBC.

159

SBRT FOR EXTRACRANIAL OLIGOMETASTATIC HEAD AND NECK CANCER: A META-ANALYSIS

Adam Mutsaers[1], Aquila Akingbade[2], Liying Zhang[1], Ian Poon[1], Alexander V Louie[1], Antoine Eskander[1], Irene Karam[1]
[1]*University of Toronto, Toronto, ON*
[2]*Western University, London, ON*

Purpose: Stereotactic body radiotherapy (SBRT) is increasingly used to treat disease in the oligometastatic (OM) setting due to mounting evidence demonstrating efficacy and safety. However, OM head and neck cancers (HNC) are under-represented in present prospective studies. The purpose of this study was to perform a systematic review and meta-analysis of outcomes of HNC patients with extracranial OM disease treated with SBRT.

Materials and Methods: A systematic review was conducted, with Cochrane, Medline and Embase databases queried from inception to August 2022, for studies with extracranial OM HNC treated with stereotactic radiotherapy. Polymetastatic patients (>5 lesions), mixed-primary cohorts failing to report HNC separately, lack of treatment to all lesions, non-quantitative endpoints, and other definitive treatments (surgery, conventional radiotherapy, radio-ablation) were excluded. Meta-analysis was performed to examine pooled effects of 12 and 24 month local control (LC) per lesion, progression-free survival (PFS) and overall survival (OS). Statistical analyses were conducted using Meta-Analysis Package for R (version 4.2.1). Weighted random-effects were assessed using DerSimonian and Laird method, with heterogeneity evaluated using the I^2 statistic and Cochran Qtest. Forest plots were generated for each endpoint.

Results: Fifteen studies met inclusion criteria (639 patients, 831 lesions), with 12 eligible for quantitative synthesis with common endpoints and sufficient reporting. Fourteen studies were retrospective, with a single prospective trial. Studies were small with a median of 32 patients (Range:6-81) and 63 lesions (Range:6-126). OM definition varied with an upper limit from 2-5 metastasis, mixed synchronous and metachronous lesions, and few studies including oligoprogressive lesions. Most common site of metastasis was lung. Radiation was delivered in 1-10 fractions (20-70 Gy). One-year LC (LC1), reported in 12 studies, was 86.9% (95% confidence interval [CI]: 79.3-91.9%). LC2 was 77.9% (95% CI: 66.4-86.3%), with heterogeneity across studies. PFS was reported in 5 studies, with a PFS1 of 43.0% (95% CI: 35.0-51.4%) and PFS2 of 23.9% (95% CI: 17.8-31.2%), with homogeneity across studies. OS was analyzed in 9 studies, demonstrating an OS1 of 80.1% (95% CI: 74.2-85.0%) and OS2 of 60.7% (95% CI: 51.3-69.4%). Treatment was well tolerated with no reported Grade 4 or 5 toxicities. Grade 3 toxicity rates were uniformly below 5%, when reported.

Conclusions: SBRT offers excellent LC, and promising OS with acceptable toxicities in OM HNC. Durable PFS remains rare, highlighting the need for effective local or systemic therapies in this population. Further investigation on concurrent and adjuvant therapies are warranted.

160

OVOID APPLICATOR COMMISSIONING USING 2D OPTICAL SCINTILLATING IMAGING

Robert Weersink, Hedi Mohseni, Jette Borg, Maryam Golshan, Akbar Beiki-Ardakani, Alexandra Rink
University of Toronto, Toronto, ON

Purpose: Commissioning of gynecological applicators used in high dose rate brachytherapy requires a comparison of the actual dwell positions when the remote afterloader is delivering a plan, and the corresponding dwell positions as noted in the treatment planning system (TPS). For lunar ovoids and rings, the path of the source is affected by the channel's curvature and width, causing disagreement with x-ray markers. Furthermore, the height of these applicators causes substantial blurring on the film, making traditional double exposure methods difficult. We propose a new method for applicator commissioning, demonstrated here for lunar ovoids, based on 2D optical scintillating imaging of the applicators.

Materials and Methods: Treatment plans were generated for 22 mm and 26 mm diameter Venezia applicators, using 4-7 dwell positions in each ovoid based on the TPS source path model. To provide ground truth registration between the treatment plan and optical imaging system, catheters were placed in each applicator with only tip dwell positions activated in order to define the fixed geometry of the applicator catheter holes. Images of the applicator dwell positions were acquired using a pinhole apparatus combined with scintillating material and optical camera. Multiple image frames were captured in a single acquisition, with each frame imaging an individual dwell position. Images were processed to identify pixel locations with peak signal intensity. Images of the catheter dwell positions were used to calculate the registration transform between the pixel locations in the optical imaging and absolute coordinates of the dwell positions in the treatment planning coordinate system. This registration was used to convert the measured ovoid dwell positions into the treatment planning coordinate system for comparison with the theoretical plan positions. Errors were calculated using the standard deviation in the Euclidean distance between measured and expected ovoid dwell positions. Measurements were repeated three times for each ovoid, including repositioning the applicator on the measurement system.

Results: Imaging of each applicator was completed in ~20 minutes for all dwell positions. Catheter registration errors were 0.15 ± 0.03 mm and 0.26 ± 0.01 mm for the 26 and 22 mm applicators, respectively, demonstrating that the system can perform repeatable, high-resolution images of the dwell

positions. Differences between the imaged and planned ovoid dwell positions for the 22 mm applicator were 0.66 ± 0.05 mm for Ovoid 1 and 1.00 ± 0.16 mm for Ovoid 2. For the 26 mm applicator, these measurements were 0.96 ± 0.15 mm for Ovoid 1 and 0.78 ± 0.06 mm for Ovoid 2. All differences in dwell position locations between the expected values in the TPS and those measured were within tolerance of 2.0 mm.

Conclusions: 2D-Scintillating imaging of lunar ovoid applicator dwell positions is feasible, accurate and faster than previous methods used at our centre. For the applicators tested in this study, any differences between the measured dwell positions and those used in the TPS were within 2.0 mm tolerance.

161
REAL-TIME RADIOBIOLOGICAL MODELLING: THE DEVELOPMENT OF A TOOL FOR ON-THE-FLY BED ASSESSMENT FOR HDR BRACHYTHERAPY

Matthew Mouawad[1], Niranjan Venugopal[1,2]
[1]*CancerCare Manitoba, Winnipeg, MB*
[2]*University of Manitoba, Winnipeg, MB*

Purpose: To develop an on-line tool for real-time radiobiological assessment for HDR Brachytherapy, that is automated, visually intuitive, and integrated into the treatment planning software.

Materials and Methods: A crucial step in planning HDR brachytherapy for cervix, is the calculation and assessment of biologically equivalent dose (BED), to ensure target coverage and optimal sparing of organs at risk (OAR). This has historically been calculated manually or using spreadsheets, both of which require manual data entry which can be error prone and time consuming. In addition, due to the large amount of information (~18 structure metrics reporting physical dose, EQD2, different fractions etc. for each structure), visualization and interpretation can be difficult. We have developed an application that works within the Eclipse/ARIA framework, that was written in C# and composed of two parts. The first is the main GUI interface that was designed to simplify the presentation of data, but also still allowing the user to selectively see any dose calculation information they may need. It also allows the user input/modifications to physical dose for external beam or brachytherapy fractions so that potential trade-offs in planning aims can be explored. In addition, a stoplight system has been used to indicate when a particular structure is meeting the planning aims or not. The second part involved automatically grabbing the relevant dosimetric information from the external beam and previous/current brachytherapy fractions. This was done using the eclipse scripting API (ESAPI) which allows programmatic access to Eclipse/Brachyvision. An "ESAPI adaptor" was developed which automatically populates the relevant aspects of the GUI with the data provided by the treatment planning system. This involved rules for automatically identifying external beam and previous brachy plans, as well as reference points and structures to extract dose-volume data. In addition, manual selection fallback tools were generated in the case that these rules were not followed at the time of plan creation. The current version of the software in currently undergoing both calculation-based, and user-based validation for clinical readiness.

Results: Initial verification was done with three patients. Dose metrics for all targets, and OARs were verified to against manual calculations (using EMBRACE metrics) to be within rounding error. Qualitative feedback from our brachytherapy team (five Medical Physicists, and two Radiation Oncologists) demonstrated that the software is easy to use, functional, and without software errors. The software is currently being prepared for clinical rollout.

Conclusions: We have developed a novel real-time BED calculator that works directly in the Eclipse/ARIA ecosystem and can be used in real-time to simplify the viewing of dosimetric data associated with the treatment.

162
THE DEVELOPMENT AND ASSESSMENT OF A CORE-NEEDLE BIOPSY LOCALIZATION METHODOLOGY IMPLEMENTED DURING PROSTATE HIGH DOSE-RATE BRACHYTHERAPY TREATMENTS

Matthew Muscat[1], Jeff Andrews[1], Felipe Castro Canovas[2], Juanita Crook[1], Andrew Jirasek[1], Nathan Becker[1]
[1]*University of British Columbia, Kelowna, BC*
[2]*British Columbia Cancer, Kelowna, BC*

Purpose: Clinicians who perform prostate high dose-rate (HDR) brachytherapy are increasingly utilizing multiparametric magnetic resonance (MR) to identify and target dominant intraprostatic lesions (DILs). Prostate HDR also offers a unique opportunity for the acquisition of tissue samples via core-needle biopsy, and Raman spectroscopy may provide an observational window for which to monitor radiation treatment. In this work, we localize the core-needle biopsy within the patient to assess tissue type (DIL versus normal prostate), and radiation dose variation across the core. We further assess the impacts of the biopsy localization uncertainty on dose and tissue classification variation.

Materials and Methods: Ultrasound imaging was acquired during the core needle biopsy procedure, and the biopsy position identified through ultrasound and MR fusion. To estimate the dose and tissue classification across the biopsy core, and to assess the localization uncertainty, two methods were employed to simulate both systematic and random uncertainty. The first is a Monte-Carlo based method, where uncertainties are randomly sampled. The second is through the use of a non- parametric constant Gaussian kernel regression (convolution) of the background dosimetric and tissue classification lattice. The degree of uncertainty in these methods are controlled by the sampling distribution parameters and kernel parameters respectively. The magnitude of localization uncertainty was varied in both methods to determine the most significant directions of uncertainty, as well as to determine upper bounds on the localization uncertainty vectors to achieve discernible variation across the biopsy tissue core.

Results: Preliminary analysis was performed using constant 1, 3, and 5 mm uncertainty (σ_1, σ_3, σ_5) in each of the orthogonal directions of the patient coordinate system for all structures. The analysis was performed on biopsy core tissue samples of lengths (15.2 ± 0.1) mm (A) and (17.0 ± 0.1) mm (B). The biopsy tissue cores were voxelized in 1 mm × 0.6 mm (length and radius) cylindrical volumes, with approximately 10000 samples per voxel. This provided dosimetry profiles ranging from (σ_1: (16 ± 1) Gy, σ_5: (15 ± 4) Gy) (A) and (σ_1: (22 ± 2) Gy, σ_5: (22 ± 14) Gy) (B) at the inferior voxel, to (σ_1: (57 ± 29) Gy, σ_5: (23 ± 14) Gy) (A) and (σ_1: (34 ± 12) Gy, σ_5: (28 ± 16) Gy) (B) at the superior voxel after the first treatment fraction. The probability of the core tissue classification varied from σ_1 : (100 ± 0)% (A and B) prostate and (0 ± 0)% (A and B) DIL at the inferior voxel; to σ_1 : (95 ± 2)% (A) and σ_1 : (98 ± 1)% (B) DIL at the superior voxel.

Conclusions: Preliminary results suggest that localization uncertainties on the order of a millimeter allow for statistically discernible variation in both the dosimetry and tissue classification within the biopsy core tissue sample. Future work will look to assess and identify specific sources of uncertainty such as deformable registration, and provide patient specific estimates from our outcome assessment models.

163

EVALUATING THE INTER-OBSERVER VARIABILITY IN THE DELINEATION OF RECTAL LESIONS IN ENDOSCOPY IMAGES

Alana Thibodeau-Antonacci[1], Corey Miller[2], Luca Weishaupt[3], Aurélie Garant[4], Te Vuong[2], Philippe Nicolaï[5], Shirin Enger[1,3]
[1]*McGill University, Montréal, QC*
[2]*Jewish General Hospital, Montréal, QC*
[3]*Lady Davis Institute for Medical Research, Jewish General Hospital, Montréal, QC*
[4]*University of Texas Southwestern Medical Center, Dallas, TX*
[5]*Université de Bordeaux, Bordeaux, FR*

Purpose: Accurate contouring of rectal tumours in planning images is essential to deliver precise radiation treatments. To facilitate tumour localization, MRI-compatible metallic clips can be placed around the lesion during an endoscopy exam before the first treatment. However, the borders of the tumour are generally determined by eye, and this is prone to errors. The goal of this study was to quantify the inter-observer variability associated with the task of identifying and delineating rectal lesions in endoscopy images.

Materials and Methods: Two radiation oncologists and one gastroenterologist identified tumours and treatment change (i.e., radiation proctitis, ulcers and tumour bed scars) in 801 endoscopy images from 24 rectal cancer patients undergoing radiotherapy. In cases where the image quality was too low to confidently classify the tissues, the image was labeled as "poor quality". Whole image classification was compared between annotators. Four classes were identified: poor quality, tumour, treatment change and unclassified (i.e., no contour). In cases where an image contained both tumour and treatment change contours, it was classified as "tumour" as this was considered more clinically relevant. For the tumour and treatment change classes, the F1-score was computed to quantitatively determine the agreement between annotators. Inter-observer variability was also assessed on a contour level for tumour and treatment change. If any two annotators agreed that a class was present in an image, the Dice score between the contours was calculated.

Results: Significant inter-observer variability was reported both for whole image classification and on a contour level. There was a greater disagreement between annotators for the treatment change class than for the tumour class. The average F1-score was 0.60 and 0.75 for treatment change and tumour, respectively, while the average Dice score was 0.58 and 0.83 for these classes. Some of the differences may have been caused by the limitations of the method used. In particular, the labeling software did not permit scrolling through a series of images such that the annotators could not examine endoscopy pictures taken directly before or after a given image. These often contain useful information that can guide the physician when contouring lesions.

Conclusions: Automated methods, such as deep learning-based models, can help standardize and accelerate the practice of contouring rectal lesions in endoscopy images. However, the high inter-observer variability observed in this study indicates that caution must be taken when creating ground-truth data. Our results suggest that it should be composed of labels from multiple annotators to avoid the model learning a single person's bias.

164

DYNAMIC PREDICTION OF TOXICITIES IN HEAD AND NECK CANCER RADIOTHERAPY BY 3D CONVOLUTIONAL NEURAL NETWORK USING DAILY CONE-BEAM CTS

Charmin (Chulmin) Bang[1], Willam Trung Le [2], Phuc Felix Nguyen-Tan[1], Édith Filion [1], Denis Soulières [1], Brian O'Sullivan[1], Apostolos Christopoulos[1], Éric Bissada [1], Tareck Ayad[1], Louis Guertin [1], Arthur Lalonde [1], Daniel Markel[1], Samuel Kadoury [2], Houda Bahig[1]
[1]*Centre Hospitalier de l'Université de Montréal, Montréal, QC*
[2]*Polytechnique Montréal, Montréal, QC*

Purpose: Radiotherapy (RT) is essential in head and neck cancer (HNC) treatments, but often causes significant toxicity. Different machine learning models have shown promise in predicting RT-induced toxicity, but none have yet integrated the fluctuating anatomical changes. By integrating daily cone-beam CTs (CBCT) allowing sequential anatomical views, our aim is to build a dynamic predictive model for three major HNC RT toxicities: reactive feeding tube placement, hospitalization and radionecrosis (RN).

Materials and Methods: Two hundred and ninety-two HNC cases treated with curative RT between 2017-2019 at our institution were retrospectively analyzed for clinical and radiological data. VoxelMorph, a deep deformable registration model, integrated the daily anatomical deformations between each CBCT and the planning CT, then converted them to Jacobian determinant matrix (J_f). Resnet, a convolutional neural network with multiple layers was trained using a 5 fold cross validation to integrate both radiological and clinical data. Each toxicity was classified as a binary decision using the cross-entropy loss to account for a class imbalance. Its predictive performance was compared to the baseline model using only clinical data.

Results: The cohort included 78% men and 22% women, with a median age of 63 years (range 35-84). Primary cancer sites were 46% oropharynx, 19% larynx, 14% oral cavity, 7.5% nasopharynx, 5% hypopharynx, 4% unknown primary and 5% others; and stage ranged between Tx-4b N0-3b M0 (AJCC 8th Ed). Induction chemotherapy, concurrent chemotherapy, and adjuvant RT was used in 9%, 57% and 20% of patients, respectively. The incidence of feeding tube, hospitalization and RN was 19.9%, 7.2%, and 3.8%, respectively. Integrating Jf from the 10th RT CBCT showed better accuracy for each toxicity prediction: feeding tube (69.1% > 57.2%), hospitalization (75.3% > 63.1%) and RN (85.8% > 75.7%). Integrating both the raw CBCT and Jf improved hospitalization prediction (79.0% > 73.6%). Substituting Jf for the raw CBCT improved the prediction for RN (79.7% > 74.7%) and hospitalization (73.6% > 64.4%). For feeding tube, predictive performance of the Jf model trained against deformations showed a positive correlation between its performance and the RT received (r^2 > 0.9) with increasing RT fractions, with a maximum accuracy of 83.1% at the 25th fraction. No such correlation was found for RN or hospitalization prediction.

Conclusions: To our knowledge, this is the first study showing promising results to predict HNC RT toxicities using daily per-treatment CBCT. Next steps involve integrating both the radiomic and the dosimetric inputs to build a more powerful model. This could expand to predict therapeutic outcomes and, ultimately, could guide decisions in individualized RT.

165

DOSIMETRIC IMPACT OF USING MACHINE LEARNING-PREDICTED HYBRID INTERSTITIAL NEEDLE ARRANGEMENTS FOR HIGH-DOSE-RATE CERVICAL BRACHYTHERAPY

Kailyn Stenhouse[1], Sarah Quirk[2], Michael Roumeliotis[3], Kevin Martell[1], Robyn Banerjee[1], Tien Phan[1], Corinne Doll[1], Philip Ciunkiewicz[1], Svetlana Yanushkevich[1], Philip McGeachy[1]
[1]*University of Calgary, Calgary, AB*
[2]*Brigham & Women's Hospital, Boston, MA*
[3]*Johns Hopkins University, Baltimore, MD*

Purpose: To quantify the dosimetric impact of machine learning (ML) predicted needle arrangements compared to clinical needle arrangements and assess model performance in a prospective study for hybrid interstitial needle cervical brachytherapy (BT).

Materials and Methods: Cervical cancer patients scheduled for high-dose-rate BT using intracavitary ring/semi-lunar ovoid and tandem (IC) or hybrid interstitial ring/semi-lunar ovoid and tandem (IC/IS) applicators were eligible for enrollment in this prospective study. An ML model first predicted the need for an IC or IC/IS implant based on target volume geometry from the pre-BT diagnostic MR. If an IC/IS implant was predicted, the arrangement of hybrid interstitial needles was also predicted. In cases where the ML model predicted an IC/IS implant and agreed with the consensus treatment applicator, dosimetric differences between the ML-predicted needle arrangement and the clinical needle arrangement were compared for the three scheduled treatment fractions. Precision, recall, and accuracy were used to assess model performance and were calculated based on agreement with the needles loaded for a majority of the treatment fractions (consensus needles).

Results: Ten patients were accrued from December 2020-October 2022. In five cases, the ML-predicted IC/IS applicator agreed with the consensus treatment applicator. For these cases, the average accuracy, precision, and recall of the ML model when using the consensus needle arrangement as ground truth was 82.3%, 85.3%, and 83.3%. When investigating the dosimetric impact of differing ML and clinical needle arrangements, significant changes existed for the first treatment fraction. The largest dosimetric changes occurred in patients where needles were not used clinically until the second and third fractions after plan quality was observed through adherence to clinical planning aims, or in cases where fewer needles were used for the first fraction. When replanning using the ML-predicted needles and matching tumour coverage metrics from the clinical plans, average improvements in bladder D2cc, rectum D2cc, and sigmoid D2cc of 40.5 cGy, 25.9 cGy, and 40 cGy were achieved. This was compared to smaller average changes when replanning for second and third fractions, with a bladder D2cc reduction of 11.1 cGy and rectum and sigmoid D2cc increases of 1.1 cGy and 1.7 cGy. Results indicate that the use of hybrid interstitial needles has the greatest impact on dosimetry, with the number of needles being secondary, and the arrangement being tertiary.

Conclusions: The ML-based decision support tool shows strong predictive capabilities in a prospective setting, with the greatest dosimetric benefit on the first fraction of treatment. For the following two fractions, differences between the ML-predicted and clinical needle arrangements had minimal impact on plan quality, leading to comparable plans when using ML. Further work assessing model performance across a large cohort of patients in a multi-centre setting is required.

166

DEEP LEARNING-BASED TRANSFER OF TG-43 BASED DOSE TO WATER TO DOSE TO MEDIUM IN MEDIUM IN HIGH DOSE RATE BRACHYTHERAPY

Sébastien Quetin[1], Boris Bahoric[1,2], Farhad Maleki[3], Shirin Abbasinejad Enger[1]
[1]*McGill University, Montréal, QC*
[2]*Jewish General Hospital, Montréal, QC*
[3]*University of Calgary, Calgary, AB*

Purpose: RapidBrachyDL, a rapid and accurate radiation dose prediction model for high dose rate (HDR) brachytherapy applications via deep learning (DL) was previously developed by our group. Doses predicted with RapidBrachyDL on prostate cases showed excellent agreement with ground truth Monte Carlo (MC) simulations on a coarse dose scoring grid (3*3*3 mm^3). This model was then improved to predict dose in a finer voxel size (1*1*1 mm^3) but that required dose to water in water ($D_{w,w}$) calculated with the MC method. In this study, the model was further developed to use TG-43 $D_{w,w}$ and patient geometry as input, and predict accurate patient specific absorbed dose to medium in medium ($D_{m,m}$) for HDR brachytherapy without need for time consuming MC simulations.

Materials and Methods: In this retrospective study, CT images of breast cancer patients treated with HDR brachytherapy were used. RapidBrachyMCTPS treatment planning software was used to generate both TG-43 $D_{w,w}$ and MC $D_{m,m}$ 3D dose maps, which were used as input and outputs respectively, in the DL model training. Each MC $D_{m,m}$ dose map took on average 15 minutes to simulate on 64 CPU core nodes with 10^7 ^{192}Ir decay events simulated for every single dwell position. The voxel size was 1*1*1 mm^3. For the DL training, the obtained TG-43 $D_{w,w}$ maps and patient geometries were cropped such that only the part of the organs at risk relevant to the dosimetric indice computations were considered. That allowed for easier training of DL models on large volumes. The computed $D_{w,w}$ maps were fed into a "combining Unet" model along with the patient geometries to predict the $D_{m,m}$ maps. The architecture of the model was designed to handle the training with these two input volumes ($D_{w,w}$ maps and patient geometry) while focusing on the necessary combination of features between the heterogeneous patient geometry and homogenous water dose. Data from 70 breast cancer patients were used for the training of the model, 14 for validation and 14 for the test.

Results: Training took 27 hours on a A100 GPU. Once trained, the performance of the model was tested on 14 patients never seen by the model. On average, the test patients had 147 dwell positions per patient and the model predicted dwell position dose maps in 0.07 second. This represents dose maps for the entire plans predicted on average in 10 seconds. The proposed 3D DL regression demonstrated excellent agreement with the MC $D_{m,m}$ regarding dosimetric indice comparison. Mean percent error for dosimetric indices between the DL model and MC $D_{m,m}$ does not exceed 0.1% for any of the organs at risk and CTV.

Conclusions: DL can be used to efficiently transform rapidly computed TG-43 $D_{w,w}$ into accurate $D_{m,m}$ in the patient geometry without adding much computation time. This will allow for accurate dose calculations in a clinical workflow without need for time consuming calculations required by more traditional model based dose calculations algorithms.

167

MULTI-TIMEPOINT DOSIOMIC MODELING OF PATIENT-REPORTED DYSPHAGIA

Owen Paetkau[1], Sarah Weppler[2], Andrea Seibel[2], Ekaterina Tchistiakova[1], Charles Kirkby[1]
[1]*University of Calgary, Calgary, AB*
[2]*Tom Baker Cancer Centre, Calgary, AB*

Purpose: The goal of this study is to use dosiomic features from multiple radiotherapy timepoints to predict late patient-reported dysphagia for head and neck cancer patients.

Materials and Methods: A retrospective cohort of head and neck patients (n=64) exhibited oropharyngeal or nasopharyngeal cancer and were treated with concurrent chemo-radiotherapy (70Gy in 33 fractions or 66Gy in 30 fractions). A chart review determined no patients included in the cohort exhibited baseline dysphagia. After more than one-year post-radiotherapy, patients completed the MD Anderson Dysphagia Inventory patient-reported outcome measure. Patient-reported dysphagia was defined as patients reporting a <60 composite score. According to this patient-reported outcome measure, half of the cohort reported dysphagia and half were asymptomatic post-radiotherapy. Weekly cone-beam CTs were taken throughout the course of patient treatment. A validated deformable image registration algorithm was used to create synthetic CTs from cone-beam CTs. Planning CT organ-at-risk

contours, such as the pharyngeal constrictors, were propagated to the synthetic CT using the same deformation vector field. The original treatment plan was applied to the synthetic CTs to evaluate the delivered dose distribution at each cone-beam CT timepoint. Dosiomic features were extracted using a contour-based method with original and wavelet image filters available in the PyRadiomics package. The pharyngeal constrictor contours and the 80% and 95% isodose line masks were used to extract dosiomic features. These features were pulled from the planning CT, defined as 'planned' features, and the first and last synthetic CTs. The difference in the first and last synthetic CT features were defined as 'delta' features. Feature reduction was performed using a filter method to reduce collinearity and a K-Best wrapper method to identify relevant variables. Random forest classification models were developed using 5-fold cross-validation and evaluated using patient-reported dysphagia classification accuracy. The collinearity threshold, number of features in the K-Best wrapper method, and random forest hyperparameters were tuned using grid search. The best models for each timepoint were identified using the validation accuracy, reporting the mean and standard deviation.

Results: Initial results indicate the planned dosiomic features predict patient-reported dysphagia to a 95±2% training accuracy and 80±10% validation accuracy. Delta features alone offered a 93±3% training accuracy and 53±15% validation accuracy. The delta features combined with the planned features resulted in a 95±2% training accuracy and 81±8% validation accuracy.

Conclusions: The planned dosiomic features developed a successful patient-reported dysphagia model, while delta features provide a near random guess. Delta features do not add any significant predictive power when creating models with features from all timepoints.

168

LEARNING-EMPOWERED REAL-TIME NEEDLE IDENTIFICATION FOR ULTRASOUND-GUIDED PERCUTANEOUS LIVER TUMOUR ABLATIONS

Shuwei Xing[1], Ningtao Liu[1,3], Derek W. Cool[1], Elvis C.S. Chen[1,2], Terry M. Peters[1], Aaron Fenster[1]
[1]Western University, London, ON
[2]Lawson Health Research Institute, London, ON
[3]School of Artificial Intelligence, Xidian University, CN

Purpose: Ultrasound (US)-guided percutaneous thermal ablation is a promising curative treatment technique for focal liver tumours. To eradicate the entire cancerous cells, accurately inserting the needle (i.e., ablation applicator) into the tumour as planned is a crucial step during real-time US guidance. However, due to complex US artifacts and indistinguishable image contrast between the needle and adjacent tissues, identifying the needle, particularly the needle tip, has been considered as a difficult problem. Therefore, our work aims to develop a deep learning-based approach using acquired sequential US frames for real-time needle identification.

Materials and Methods: We first developed a patch scale self-supervised pre-training model for visual representations. Then, a needle detection-segmentation model was developed based on the SELSA (sequence level semantics aggregation) module. To train our model, 62 US video clips from 13 consecutive cases with focal liver tumours were collected. On average, each video clip lasts for 81.4 seconds and includes 651 US frames. These data were divided into training and validation partitions with 50 and 12 US videos, respectively.

Results: Our proposed needle identification approach achieved an average needle tip distance error of 9.71±5.66 mm, and a needle shaft average angle error of 5.80±4.15°. The runtime for each US frame on NVIDIA V100 takes approximately 0.15 seconds.

Conclusions: Preliminary results demonstrated that our proposed deep learning approach can successfully identify the needle in real-time US videos. The segmentation accuracy shows the potential for assisting the needle guidance during the ablation procedure. Our future work is to further improve the accuracy of the needle identification and expand our training dataset.

169

QUALITATIVE EVALUATION OF AI CONTOURS

Radim Barta[1], Charles Kirkby[2,3], Conor Shaw[2,3], Samuel See[4], Ian Nygren[1,5]
[1]Central Alberta Cancer Centre, Alberta Health Services, Red Deer, AB
[2]Jack Ady Cancer Centre, Alberta Health Services, Lethbridge, AB
[3]University of Calgary, Calgary, AB
[4]Grande Prairie Cancer Centre, Alberta Health Services, Grand Prairie, AB
[5]University of Alberta, Edmonton, AB

Purpose: The differences between prostate CT contours generated by artificial intelligence (Limbus Contour, Limbus AI, Regina, SK, Canada) and those expertly drawn are characterized qualitatively.

Materials and Methods: Patient CT scans imaged at three Alberta sites were contoured with Limbus Contour and independently by dosimetrists. For a minority of patients, the Limbus Contours were available to dosimetrists during the contouring step, allowing editing or re-contouring as deemed appropriate. The clinical contours were compared to the Limbus contour using Dice-coefficient (DC) and distance-to-agreement (DT) metrics. Further the contours were qualitatively reviewed to identify volumes of disagreement, and the potential for downstream clinical impact.

Results: Quantitative measurements are in line with past studies of U-Net algorithm-based auto-segmentation. Qualitatively, auto-segmentation contours differ from the clinical contours for different reasons. The agreement for bladder (DC=97%, DT=4.3 mm) speaks to its relatively consistent shape and position in the pelvic region, as well as soft tissue contrast. Auto-segmentation generates overlapping bladder and prostate, and this may contribute to disagreement in prostate contours (90%, 7.7 mm) when clinically mutual exclusivity is enforced. Disagreement for the high-contrast femurs (83%, 12.1 mm) results from variation in the number of slices contoured. While auto-segmentation tends to contour the full extent of the femoral heads, expert-generated contours may truncate to only the relevant slices, i.e. those likely to receive doses relevant for plan optimization or assessment. This was also seen in the rectum (80%, 14 mm) and bowel bag (56%, 33 mm). Penile bulb (59%, 6 mm) highlights a common evaluation challenge with small structures. Even single slice differences in contours lead to significant DC differences, the 6 mm DT better captures the variation seen.

Conclusions: This study suggests auto segmentation can be used effectively to begin the contouring process. It allows trained experts to focus more time on difficult contours and defining problem areas.

170

TOWARDS AI-BASED DOSE PREDICTION OF DAILY DELIVERED DOSE DURING LUNG CANCER RADIOTHERAPY

Matthieu Chenier[1], Marcin Wierzbicki[2]
[1]McMaster University, Hamilton, ON
[2]Juravinski Cancer Centre, Hamilton, ON

Purpose: Anatomical changes between radiotherapy planning and delivery reduce treatment accuracy. It is not currently practical to develop new plans for every fraction. However, a method that

quantifies the daily dose would aid therapists in deciding if the treatment is safe. This would also enable cumulative tracking to allow comprehensive documentation and to inform decisions that affect the overall treatment quality.

Materials and Methods: A convolutional neural network was trained to update the planned dose distribution according to anatomical changes that occur between fractions. Fan beam CT (FBCT), planned dose distributions, and cone beam CT (CBCT) images across 30 fractions were anonymized for 13 patients treated for advanced stage lung cancer. The CBCT images were rigidly registered to the corresponding patient's FBCT image and used to re-compute dose in the treatment planning system. These CBCT-based distributions were assumed to represent the gold standard, daily treated dose under six degree-of-freedom couch corrections for patient positioning. All data were fed into the U-Net architecture neural network with the goal of predicting the daily delivered dose given the patient's FBCT, original dose distribution, and current CBCT. A total of 13 separate models were created, where each model was trained with 12 of the 13 sets of patient data. The remaining set was used for validation.

Results: Gamma index maps with 3%/3mm tolerance and a 20% max dose threshold were calculated by comparing the predicted and gold standard dose distributions. The models yielded a mean gamma pass rate of 86.9 ± 13.8% with a median of 93.1%.

Conclusions: Although model predictions do not yet sufficiently match the delivered dose distributions we did see promising trends. Further work is needed with additional patient cases and strategies to reduce the dimensionality of the fitted models.

171
EVALUATING THE PERFORMANCE OF CHATGPT AT BREAST TUMOUR BOARD

Yang Xu, Natalie Logie, Tien Phan, Lisa Barbera, Robert Nordal, Jordan Stosky, Sangjune Lee
University of Calgary, Calgary, AB

Purpose: Chat Generative Pre-trained Transformer (ChatGPT) is a chatbot built on the GPT-3 language model. We sought to determine whether it can contribute to tumour board discussions by comparing the accuracy and clarity of its answers to challenging breast radiation oncology questions with that of human specialists.

Materials and Methods: Twenty consecutive breast radiation oncology questions between January and February 2023 that received at least one human answer were curated from theMedNet, a physician-only Q&A platform for expert answers to real-world clinical situations. These questions were posed to ChatGPT, and its answers were paired with the first chronological human response. Breast radiation oncologists at one academic institution were asked to rate from 1 (strongly disagree) to 5 (strongly agree) the extent to which they agreed with each answer (accuracy score) and whether they felt the response provided clear and specific guidance relevant to the original question (clarity score). Reviewers were blinded to whether each answer was provided by ChatGPT or a human responder. Wilson score intervals with continuity correction were used to estimate the proportion of answers on which ChatGPT received a higher median accuracy or clarity score than human responders. The Wilcoxon signed-rank test was used to compare median accuracy and clarity scores across all 20 questions.

Results: Six board-certified breast radiation oncologists evaluated answers to the 20 questions, resulting in 120 distinct assessments of each ChatGPT and human responders. The evaluators agreed or strongly agreed with ChatGPT responses on 49 (41%) of assessments and human responders on 66 (55%) of assessments. ChatGPT achieved a higher median accuracy score than human responders on 7 (35%; 95% Wilson score CI, 16-59%) questions whereas humans outperformed ChatGPT on 8 (40%) questions; there was no significant difference in median scores (Wilcoxon signed-rank p=0.3). There was agreement or strong agreement that ChatGPT provided clear and specific guidance on 38 (32%) of assessments compared to 45 (38%) assessments of human answers. No differences were detected in median clarity score across all of the questions (Wilcoxon signed-rank p=0.8). On 3 questions (15%; 95% Wilson score CI, 4-39%), ChatGPT surpassed human responders on both median accuracy score and median clarity score. Human responders similarly outperformed ChatGPT in both metrics on 3 (15%) questions.

Conclusions: There was no detectable difference in the accuracy and clarity of answers provided by ChatGPT and human responders in this sample of 20 challenging breast radiation oncology questions. ChatGPT outperformed human responders in the accuracy and clarity of its answers to some questions, suggesting that it has the potential to contribute meaningfully to discussions about real-world clinical problems.

172
THE IMPACT OF ANDROGEN-DEPRIVATION THERAPY ON CERAMIDES, A POTENTIAL BIOMARKER OF OUTCOMES OF PROSTATE CANCER FOR PATIENTS TREATED WITH EBRT AND HDR BRACHYTHERAPY BOOST

Damien Carignan[1], Marine Bourgeois[2], William Foster[3], André-Guy Martin[3], François Paris[2], Eric Vigneault[1]
[1]*Université Laval, Quebec City, QC*
[2]*Université de Nantes, Nantes, FR*
[3]*CHU de Québec-Université Laval, Quebec City, QC*

Purpose: Negative outcomes of prostate cancer (PCa) can take years to occur after the initial treatment. Having a biomarker that could predict early treatment success or failure would therefore be valuable. Increased levels of plasma ceramides after radiation therapy have been previously correlated with tumour response. Some in vitro studies also suggest that androgen-deprivation could alter the sphingolipid composition of PCa cells. The primary objective of this pilot study was to examine the impact of androgen deprivation therapy (ADT) on ceramide subspecies plasmatic levels before, during and after EBRT + HDR treatment.

Materials and Methods: Thirty intermediate- to high-risk PCa patients were recruited between 2018 and 2020. Blood samples were taken at the time of consent, after the last EBRT fraction, after the HDR-BT treatment, and then at three, six, 1- and 18 months post-treatment. Lipids were extracted and purified from plasma samples, and sphingolipid content analyzed by liquid chromatography-electrospray ionization-tandem mass spectrometry. Patients were categorized based on whether they received ADT or not. Tumour control was estimated by the last PSA value obtained as of January 2023.

Results: The 30 patients had a mean age of 70.8 ± 7.7 years and the median follow-up was 31.0 months (range 20-37 months). Seventeen patients (56.7%) had an intermediate-risk disease according to the NCCN classification and thirteen (43.3%) a high-risk disease. Nineteen (63.3%) patients received androgen deprivation therapy as part of their treatment regimen. Contingency tables analysis revealed that patients not receiving ADT were more likely to have decreased levels of total ceramides, as well as C16, C20, C22 and C24 in the follow-up period (OR 3.49 to 7.65, p=0.007 to 0.049). Their level of C22 (OR=5.0, p=0.049) and C24:1 (OR 3.94, p=0.026) were also at greater risk of being diminished during treatments. Nevertheless, multivariate generalized linear modeling showed that only increased levels of C24:1 during and after treatments were significantly associated with tumour control

(p<0.001), as assessed by the last available PSA value, and ADT was not (p=0.351).

Conclusions: This study showed that ADT seems to impact plasmatic ceramides concentration changes in PCa patients undergoing EBRT + HDR treatment. One ceramide subspecies was significantly associated with higher PSA values during follow-up (C24:1), independently of the ADT status of the patients. Because of the small sample size and unconventional outcome assessment, these results are hypothesis generating and can serve as a cornerstone from which to plan a larger study.

173

PLASMA COLLECTED DURING RADIOTHERAPY IN TRIPLE-NEGATIVE BREAST CANCER PATIENT STIMULATES DEVELOPMENT OF LUNG METASTASES IN A MOUSE MODEL

Benoit Paquette[1], Hélène Therriault[1], Isabelle Gauthier[2], Sawyna Provencher[2]
[1]*Université de Sherbrooke, Sherbrooke, QC*
[2]*Centre hospitalier Universitaire de Sherbrooke, Sherbrooke, QC*

Purpose: Recurrence within the first three years after treatment occurs in ~30% of patients with early stages triple-negative breast cancer (TNBC). However, there is no biomarker to identify them. Radiotherapy (RT) triggers an inflammation in all patients. Some of these inflammatory cytokines promote cancer cell invasion, increase the number of circulating tumour cells and stimulates metastasis development. The purpose of this study is to determine if plasma collected during RT could be used to identify TNBC patients at high risk of recurrence.
Materials and Methods

Materials and Methods: Plasmas were collected in TNBC patients before RT and after the 4th radiation fraction (plasma during RT). The increase in inflammatory cytokines was analyzed by ELISA type test. The plasmas were incubated with TNBC MDA-MB-231 (human) and D2A1 (mouse) cells in order to determine which plasmas collected during RT increase their invasion capacity in vitro, as well as the formation of metastases in mice.

Results: Our preliminary results obtained from fiveTNBC patients demonstrated that RT increased the plasma level of the cytokines IL-1β, IL-5 and IL-6 only in the patient whose cancer recurred within the first nine months following treatment. Only plasma from this patient collected during RT increased the invasiveness of TNBC cells in vitro and the formation of metastases in an animal model. The formation of metastasis was completely blocked by adding the cyclooxygenase-2 (COX-2) inhibitor Celecoxib to this plasma collected during RT.

Conclusions: We would like to continue recruiting TNBC patients in order to confirm that plasma collected during RT could identify patients at high risk for recurrence.

174

NEUTROPHIL-TO-LYMPHOCYTE RATIO POST-HYPOFRACTIONATED RADIATION THERAPY IN SOFT TISSUE SARCOMAS IS A PROGNOSTIC BIOMARKER FOR RECURRENCE AND METASTASES

Constanza Martinez, Rie Asso, Neelabh Rastogi, Carolyn Freeman, Fabio Cury
[1]*McGill University, Montréal, QC*

Purpose: The neutrophil-to-lymphocyte ratio (NLR) is a measure of systemic inflammation. In different cancer types, NLR has shown to be a prognostic marker for outcomes and treatment response, including soft tissue sarcomas (STS). We aim to determine if in STS patients treated with hypofractionated radiotherapy (HFRT) BEFORE surgery, NLR is a prognostic biomarker of recurrence, metastasis, and overall survival (OS).

Materials and Methods: We performed a single-centre retrospective analysis of patients treated pre-operatively with HFRT (30 Gy in 5 fractions) between 2016 and 2023. Clinical, demographic, and complete blood count (CBC) data were collected from medical records. The NLR calculation was done by dividing the absolute neutrophil count by the absolute lymphocyte count. We dichotomized the variable into ≤4 and >4. Only patients with CBCs within £ six months post-RT were included in the analyses. We used univariable and multivariable logistic regression analyses to assess the impact of NLR on outcomes, adjusting for age, gender, tumour size, and histology. For continuous variables, we used mean ± standard deviation. Analyses were done with SPSS. A p-value <0.05 was considered significant.

Results: In total, 40 patients received HFRT and had a CBC £ 6 months after RT. The mean age was 66 ± 17.5 years. There were 17 (42.5%) females and 23 (57.5%) males. The mean tumour size was 7.1cm (± 6.4) and the mean NLR was 5.3 ± 0.6. The histologies were myxofibrosarcoma (17.5%), leiomyosarcoma (7.5%), pleomorphic spindle cell sarcoma (10%), and myxoid liposarcoma (5%). Other histologies with n<2 accounted for 65%. The median follow-up was 15.4 ±2.2 months. Overall, 3 patients died of disease, and the same 13 (32.5%) patients presented recurrence and metastatic disease. Univariable analyses for NLR >4 showed an increased recurrence and metastases (Odds ratio (OR): 8, CI 95% = {1.48 – 43.4}, p=0.016). The multivariable analyses also showed that post-RT NLR >4, was associated with increased recurrence and metastases (OR: 7.73, CI 95%= {1.17- 50.9}, p-value=0.034). In both univariable and multivariable analyses NLR>4 was not associated with decreased overall survival (p=0.998). Age, gender, histology, and tumour size were not significant variables.

Conclusions: This is the first study assessing neutrophil-to-lymphocyte ratio as a prognostic biomarker in STS treated with pre-operative hypofractionated radiotherapy. In this population, an NLR >4 was prognostic for recurrence and distant metastasis, but not for overall survival. There is an unmet clinical need to deepen knowledge of the immuno-biological effects of RT. This should be further addressed in the context of clinical trials due to its simplicity and potential prognostic value.

175

ELIMINATE CANCER CELLS INFILTRATED IN THE BRAIN BY ATTRACTING THEM INTO A MACROPOROUS HYDROGEL TRAP

Benoit Paquette[1], Caroline Safi[2], Sahar Naasri[1], Angela Giraldo Solano[1], Hélène Therriault[1], Benoît Liberelle[2], Nathalie Faucheux[1], Marc-Antoine Lauzon[1], Nick Virgilio[2]
[1]*Université de Sherbrooke, Sherbrooke, QC*
[2]*Polytechnique Montréal, Montréal, QC*

Purpose: Glioblastoma cells (GBM) that leave the tumour to infiltrate the brain cannot be removed by surgery, and they are frequently more resistant to chemo- and radiotherapy than healthy brain tissue. We are developing a trap in the form of a macroporous hydrogel that will be implanted in the surgical cavity after tumour removal. This gel will release a chemoattractant, CXCL12, in order to attract GBM cells which will enter the pores of the hydrogel. Once trapped, the GBM cells will be irradiated by stereotaxic radiosurgery. A higher dose of radiation can thus be delivered to the GBM cells, while preserving the brain cells at the periphery of the trap.

Materials and Methods: Hydrogels grafted with the cell adhesion peptide RGD (CGRGDS) were synthesized with different percentages of alginate and chitosan. These gels contained pores whose mean

diameter was adjusted between 50 and 500 µm. The accumulation, retention and distribution of the GBM cells F98 were determined.

Results: The accumulation and retention of GBM cells (5 x 10^5) in the hydrogel were improved by grafting the cell adhesion peptide RGD to the surface of the pores at a density of 3.5 x 10^{-7} mol/400 mg of alginate. Addition of chitosan to an alginate hydrogel improved its structural stability in biological medium, and further increased the accumulation of GBM cells. The best distribution and accumulation of GBM cells in the hydrogels were obtained in those having pores with a diameter of 200 µm. A 3D migration system has demonstrated that GBM cells can migrate over a distance of 5 mm in 14 h and then accumulate in a hydrogel that releases the chemoattractant CXCL12 encapsulated in nanoparticles.

Conclusions: These results support testing this GBM cell trap in an animal model.

176
COMBINED EFFECTS OF ARSENIC AND RADIATION
Connie Le, Shengwen Shen, Michael Weinfeld, Chris Le
University of Alberta, Edmonton, AB

Purpose: Arsenic has been used successfully to treat several diseases and is approved by the U.S. Food and Drug Administration for the treatment of acute promyelocytic leukemia (APL). The mechanism(s) of arsenic therapeutic effects are not fully understood. However, arsenic has been shown to inhibit cellular repair of DNA damage. Radiation therapy induces cancer killing by causing DNA damage. We aim to study the combined effects of arsenic and radiation, with the long-term objective of using arsenic for potential radiosensitization of cancer therapy.

Materials and Methods: We reviewed published studies on the combined treatment of human cancer cells with arsenic and radiation. We also treated a panel of normal and cancer cells with arsenic, radiation, and genotoxic agents, either alone or in combination; and examine the combined effects. We focused on mechanistic understanding of the observed effects, including cell-killing, induction of cell autophagy and apoptosis, DNA damage, and effects on DNA repair and cell cycle signaling.

Results: Studies have shown that inorganic arsenite (As^{III}) enhanced the radiation sensitivity of human prostate cancer cells, including LNCaP (androgen-sensitive human prostate cancer cells) and PC-3 cells (androgen-independent human prostate cancer cells). Combination treatment with As^{III} and ionizing radiation induced both autophagy and apoptosis and enhanced cell-killing effects in human fibrosarcoma cells in vitro. The combination of ionizing radiation and As^{III} significantly reduced the volume of xenograft tumours in severe combined immunodeficient (SCID) mice. The observed synergistic effects of As^{III} and ionizing radiation in osteosarcoma cells were also through the induction of both autophagy and apoptosis. The combined carcinogenic effects of arsenic and radiation have been studied using lower concentrations of arsenic than those for studying the therapeutic effects. Others have reported that As^{III} is a cocarcinogen with solar ultraviolet radiation and that arsenic compounds interfered with DNA repair processes and cell cycle control. Our research team have shown that arsenic compounds in its trivalent oxidation state, such as As^{III} and its trivalent methylation metabolites (MMA^{III}), inhibited cellular repair of DNA damage. MMA^{III} impaired the p53 induction in response to treatment with benzo(a)pyrene, a common chemical carcinogen found in cigarette smoke. The attenuated p53 expression translated into reduced p53 DNA binding activity. A p53-null cell line failed to exhibit the inhibitory effect of MMA^{III} on DNA repair. MMA^{III} dramatically inhibited p53 phosphorylation at Ser15 suggesting that one mechanism by which MMA^{III} destabilizes p53 is by inhibiting its phosphorylation.

Conclusions: Arsenic is the most effective treatment of relapsed acute promyelocytic leukemia. Arsenic could potentially sensitize cancer cells for radiation therapy. Understanding of the combined effects of arsenic and radiation could lead to potential therapeutic strategy for various cancers.

177
SINGLE CELL RNA SEQUENCING CHARACTERIZATION OF AN IN VITRO MODEL FOR STUDIES OF HEPATITIS B VIRUS
Connie Le[1], Reshma Sirajee[2], Rineke Steenbergen[1], Michael Joyce[1], William Addison[1], D. Lorne Tyrrell[1]
[1]*University of Alberta, Edmonton, AB*
[2]*University of Calgary, Calgary, AB*

Purpose: Two billion individuals have been infected with hepatitis B virus (HBV) globally, resulting in 400 million chronically infected carriers. Unfortunately, chronic carriers can develop complications in spite of available treatments, culminating in approximately 1 million deaths annually. HBV chronic infection represents the leading cause of hepatocellular carcinoma worldwide. Although infectious in vivo, there is a lack of convenient and efficient HBV infectable in vitro models. The purpose of this study is to establish and characterize an easily infectable in vitro hepatoma cell culture systems for studying HBV.

Materials and Methods: We overexpressed sodium taurocholate co-transporting polypeptide (NTCP) in a liver cell line (Huh7.5 cells) and subsequently supplemented with human serum (HS). We characterized Huh7.5-NTCP cells differentiated in HS-supplemented culture using single-cell RNA sequencing (scRNA-seq). Single-cell RNA sequencing is a state-of-the-art technique that generates big data depicting RNA expression profiles of individual cells. Analysis of generated data was conducted using R programming language and the Seurat analysis package.

Results: In human serum cultures, HBV infection was enhanced by as much as 20-fold in comparison with conventional cultures supplemented with fetal bovine serum (FBS) and dimethyl sulfoxide (DMSO). HS culture increased levels of hepatocyte differentiation markers in Huh7.5-NTCP cells to similar levels found in primary human hepatocytes. Furthermore, N-glycosylation of NTCP induced by culture in human serum may contribute to enhanced viral entry. scRNA-seq analysis of 3119 Huh7.5-NTCP cells at the single cell resolution revealed heterogeneity within the cell culture system. Most HS-cultured Huh7.5-NTCP cells had similar gene expression profiles to those of primary hepatocytes isolated from human liver. Importantly, a subgroup of cells expressed cholangiocyte-like phenotype.

Conclusions: The Huh7.5-NTCP hepatoma cells differentiated in human serum is a useful alternative to primary human hepatocytes for studying HBV.

178
PRELIMINARY INVESTIGATION OF PLACENTAL [1-13C] PYRUVATE METABOLISM CORRELATED WITH PLACENTAL EFFICIENCY IN GUINEA PIGS
Lindsay E. Morris[1], Lanette J. Friesen-Waldner[1], Timothy RH. Regnault[1,2], Charles A. McKenzie[1,2]
[1]*Western University, London, ON*
[2]*Children's Health Research Institute, London, ON*

Purpose: Placental efficiency (PE) is often defined as the ratio of fetal volume to placental volume. A low PE indicates poor placental function, or placental insufficiency, and is associated with immediate and long-term adverse effects for the fetus. We hypothesize that inefficient placental function may be associated with altered placental metabolism. Hyperpolarzied ^{13}C-pyruvate MRI is a metabolic imaging method that enables the visualization

of substrates during key reactions in vivo. This preliminary work aimed to correlate placental [1-^{13}C]pyruvate metabolism with PE in a guinea pig model near-term.

Materials and Methods: Five pregnant sows in an ongoing study underwent an MRI exam (~60 ± 1 days gestation, full term ~ 68 days) that acquired T1-weighted (T1-w) and hyperpolarized [1-13C]pyruvate metabolic images. T1-w images were manually segmented in 3D Slicer to obtain 14 fetal and placental volumes (8 males, 6 females). The mean signal intensities of [1-13C]pyruvate and its metabolites (lactate (LAC), alanine (ALA), and bicarbonate (BIC)) were measured in the placental volumes as a function of time. The metabolic conversion rates were estimated using the area under the curve (AUC) method. The PE data were correlated with the metabolic conversion rates using a linear mixed model (LMM) controlled by the maternal sow.

Results: There were no significant correlations ($p>0.05$) between the PE data and the AUC ratios for LAC, ALA, or BIC. However, there was a weak positive correlation between the PE and AUC ratios for LAC and BIC.

Conclusions: We did not observe a significant correlation between PE and the rates of conversion of pyruvate to its metabolites; however, there appear to be trends. We will work towards acquiring and analyzing additional data to see if a larger sample confirms these trends.

179

VALIDATION OF THE MONTREAL SPLIT-RING APPLICATOR IN A GYNECOLOGICAL PHANTOM SIMULATING CLINICAL IMPLANTS CONDITIONS IN INTRACAVITARY/INTERSTITIAL BRACHYTHERAPY

Marie-Ève Roy[1,2], Maroie Barkati[2], Marie-Claude Beauchemin[2], Yuji Kamio[2,3], Stéphane Bedwani[1,2,3]
[1]*Université de Montréal, Montréal, QC*
[2]*Centre Hospitalier de l'Université de Montréal, Montréal, QC*
[3]*Centre de Recherche du Centre Hospitalier de l'Université de Montréal (crCHUM), Montréal, QC*

Purpose: This work presents an improved design for the Montreal split-ring applicator making it compatible with smaller patient anatomies for combined intracavitary/interstitial (IC/IS) brachytherapy (BT). An evaluation of needle positioning errors during implant was done in a gynecological (GYN) phantom developed to simulate clinical conditions.

Materials and Methods: Models of the Montreal applicator's Adaptiiv caps were redesigned using Fusion 360™. Three models were created to reduce each cap's outer radius and increase their inner radius, reposition their IS guiding tube notches under the printed split-ring canal and increase their thicknesses allowing the possibility for IS needles to exit through the vaginal wall. All caps were 3D printed with a Form 3B SLA printer using biocompatible and sterilisable BioMed Clear resin. The GYN phantom's implantable structures were produced using different silicone recipes developed based on feedback from two radiation oncologists. These structures were then assembled in an educational phantom (3B Scientific). Plastic radiopaque markers were integrated to the Adaptiiv caps and to the phantom's cervix. The phantom with the Montreal split-ring applicator in place was imaged by computed tomography and IS needle trajectories were reconstructed in Oncentra Brachy TPS. Deviations in trajectories' pitch and yaw angles as well as distance-to-agreement (DTA) relative to their designed reference values at the level of the cervix and a depth of 3 cm were determined.

Results: The improved Adaptiiv caps allow a maximum of five IS needles on the outer radius of each split-rings and two on each inner radius. The outer radius was reduced by up to 8.4 mm compared to the original design for patients with smaller anatomies. Variable cap thicknesses allowing IS needles to exit through the vaginal wall were tested from 18 to 30 mm. Adaptiiv caps are interchangeable allowing better optimization of dose distributions. Needle trajectories in the phantom were successfully reconstructed in Oncentra Brachy TPS. With 10 needles implanted with six different angles, the mean DTA at the level of the cervix is (0.4 ± 0.2) mm and (1.2 ± 0.6) mm at a depth of 3 cm. The mean pitch angle deviation is (0.9 ± 0.6)° and the mean yaw angle deviation is (1.3 ± 0.8)°.

Conclusions: Three new 3D-printed Adaptiiv caps were developed to reduce the overall size of the Montreal split-ring applicator and allow new IS needle trajectories. Implant positioning errors were evaluated in a GYN phantom simulating clinical conditions by analyzing needle trajectories relative to their designed positional and angular reference values.

180

LARGE-SCALE RETROSPECTIVE MC DOSE RECALCULATION FOR PERMANENT IMPLANT PROSTATE BRACHYTHERAPY

Samuel Ouellet[1], Éric Vigneault[1], André-Guy Martin[1], Yannick Lemaréchal[1], Francisco Berumen[1], Marie-Claude Lavallée[1], William Foster[1], Rowan Thomson[2], Philippe Després[1], Luc Beaulieu[1]
[1]*Université Laval, Quebec City, QC*
[2]*Carleton University, Ottawa, ON*

Purpose: Although MC simulations are the gold standard when it comes to dosimetry, their computational time limits the production of large datasets valuable to validate current radiobiological models, to accurately quantify TPS weaknesses, or to train dose predicting deep learning models. In this work, a fully automated systematic TG186 MC dose recalculation pipeline is validated and applied to a dataset composed of 1500 permanent implant prostate brachytherapy patients.

Materials and Methods: To benchmark the pipeline for permanent implant brachytherapy using the Nucletron SelectSeed, MC simulations in TG43 conditions (TG43MC) for 10^9 photons scored using a track length estimator (TLE) were validated against standard TG43 calculations for a single seed and a full treatment plan with both TOPAS and egs_brachy MC codes. For TG186 dose distributions, the validation was made by assessing the differences in dosimetric indices when comparing the simulation results from both MC codes. Finally, the post-implant dosimetry DICOMs of 1500 patients were stored and automatically fed to the recalculation pipeline by the analysis platform (PARADIM). The MC simulation was launched with the same treatment context, based on the contours from the RTSTRUCT, on the plan configuration from the RTPLAN, and on the segmented calcifications, if applicable. The calculated dose maps, the standard deviation and DVHs, were then automatically pushed back to the platform as DICOM RTDOSE objects. A TG43MC and a TG186 simulation were done for all patients within the database. A dosimetric comparison using the entire database was made between the clinical data and both the MC TG43 and MC TG186 dose distributions (10^8 photons scored with TLE).

Results: When comparing the TG43MC simulations to the TG43 calculations, the $\%\Delta D_{local}$ values for egs_brachy and TOPAS are within ±3% and [-5, 3]% for the single seed and the full plan simulations respectively, showing good agreement. Comparing dosimetric indices for TG186 simulations between TOPAS and egs_brachy, all clinically relevant indices have absolute differences under 2%. Only D0.1cc for the urethra and the rectum still has differences over 2%, which are associated to the shortcoming of the grid-based DVH algorithm for small volume indices. The

results of the dosimetric comparison on the first 262 (17%) patients show the expected mean overestimation of 2% on PTV coverage indices from the TPS compared to the TG43MC simulations due to the point source approximation used in the clinic. Additionally, the considerable overestimations of the TG43MC simulations on the dose received by organs at risk, reaching more than 20% compared to the TG186, is due to the innacuracy of considering all organs as water.

Conclusions: In this work, a systematic MC dose recalculation pipeline for permanent implant brachytherapy was built and validated to be launched on a large-scale patient cohort. The generated dataset, agreeing with previously published results, is a valuable tool for future studies.

181

RapidBrachyTG43: A TG-43 PARAMETER AND DOSE CALCULATION MODULE FOR RapidBrachyMCTPs

Jonathan Kalinowski[1], Shirin Enger[2]
[1]*McGill University, Montréal, QC*
[2]*Jewish General Hospital, Montréal, QC*

Purpose: Clinical dose calculations in brachytherapy are performed according to the AAPM TG-43 formalism, where dose to water in water (D_{ww}) from a photon-emitting source is calculated as a product of source-specific 'TG-43 parameters.' RapidBrachyMCTPS is a brachytherapy treatment planning system (TPS) built upon a Monte Carlo (MC) dose calculation engine, instead calculating dose to patient medium (D_{mm}) from photon transport simulations inside a reconstruction of the patient geometry. However, computation of TG-43 based D_{ww} for a treatment plan is often still desirable for its reproducibility and relevance to clinical dosimetry. RapidBrachyMCTPS presently requires users to run full MC simulations to compute D_{ww} maps. This work aims to optimize D_{ww} calculation in RapidBrachyMCTPS by implementing dose calculation based on the TG-43 formalism. It also encapsulates the development of a specialized MC usercode needed to determine the D_{ww} necessary for accurate calculations of TG-43 parameters for sources available in RapidBrachyMCTPS.

Materials and Methods: TG-43 D_{ww} calculations were implemented in RapidBrachyMCTPS. To obtain TG-43 parameters for sources, D_{ww} are calculated from a MC usercode based on Geant4 v. 10.02.p02, with all necessary input files automatically generated from RapidBrachyMCTPS. TG-43 parameter calculations were benchmarked for the SelectSeed (I-125), microSelectron-v2 (Ir-192), and Bebig A86 (Co-60) sources. TG-43 D_{ww} calculation performed by this module was compared to MC D_{ww} from RapidBrachyMCTPS; planned dose for an Ir-192 breast brachytherapy case was calculated for both methods for a 1x1x1 mm^3 dose grid. 10^7 Ir-192 decays were simulated to obtain MC D_{ww}, resulting in a mean uncertainty of <1% on the 100% isodose line.

Results: Computed TG-43 parameters for the three sources generally agreed within 1% to published data, with >1% differences arising near the source central axis only. DVH metrics for the PTV and OARs for this plan agreed within 1% for MC and TG-43 D_{ww}. A gamma index comparison between the two dose distributions yielded a pass rate of 99.3% with a 1%/1 mm criterion. The TG-43-based calculation was able to calculate high-resolution D_{ww} in 47 seconds, 180 times faster than the comparable MC D_{ww} map.

Conclusions: Fast D_{ww} calculations are now possible in RapidBrachyMCTPS via the TG-43 formalism in lieu of MC simulations. These TG-43 parameters and dose calculations will be used in dose optimization, source design, and as ground truth for AI dose calculation investigations.

182

ACUTE TOXICITY OUTCOMES FROM SALVAGE HIGH-DOSE-RATE BRACHYTHERAPY FOR LOCALLY RECURRENT PROSTATE CANCER AFTER PRIOR RADIOTHERAPY

Breanna Fang[1], Phillip McGeachy[1], Siraj Husain[1], Tyler Meyer[1], Kundan Thind[2], Kevin Martell[1]
[1]*University of Calgary, Calgary, AB*
[2]*Henry Ford Health System, Detroit, MI*

Purpose: Recurrence of prostate adenocarcinoma within the prostate after radiotherapy is challenging as the cure options pose significant risks of harm. Brachytherapy may be an option, but supportive data are limited. This study aims to present the acute toxicity results from using salvage high-dose-rate brachytherapy (sHDR-BT) as a treatment in these cases.

Materials and Methods: Fourteen consecutive patients treated with sHDR-BT salvage between 2019 and 2022 were prospectively evaluated. Eligible patients for sHDR-BT had to have received curative intent prostate radiotherapy previously and show evidence of new biochemical failure. Patients were evaluated for confirmation of intraprostatic recurrence of disease. For patients receiving prior BT, sHDR-BT was standardized with prescribed dose of 27Gy in 2 fractions to prostatic regions with confirmed disease on MR or biopsy. For patients not receiving prior BT, sHDR-BT included a prescribed dose of 21Gy in 2 fractions to the entire prostate with integrated boost irradiation of 27Gy in 2 fractions to the prostatic zones with confirmed disease on MR or biopsy. All plans were designed using trans-rectally acquired ultrasound image sets in Oncentra Prostate®. Evaluation with AUA and CTCAE symptom assessments were performed one, three and 12 months post treatment and yearly thereafter.

Results: Median (inter-quartile-range) age prior to salvage treatment was 72 (67-76) years. Seven (50%) patients received external beam radiotherapy (EBRT) monotherapy (74-78Gy) as initial treatment. One (7%) received EBRT (46Gy) + low-dose-rate BT (LDR-BT) (110Gy) and six (43%) received LDR-BT (144Gy) monotherapy as initial treatment for prostate cancer. Four (29%) had received elective nodal irradiation (46Gy) with EBRT. At baseline prior to sHDR-BT, 7 (50%) patient had significant lower urinary tract symptoms. Median AUA score was 8 (3-20) prior to sHDR-BT. 3 (21%) patients reported irregular bowel function and 2 (14%) reported hematochezia prior to sHDR-BT. At first fraction of sHDR-BT rectal D100cc was 8 (6-9)Gy, urethra D10% was 12 (11-15)Gy, urethra Dmax was 15 (13-16)Gy. At second fraction of sHDR-BT rectal D100cc was 8 (7-9)Gy, urethra D10% was 12 (12-14)Gy and urethra Dmax was 13 (12-16)Gy. One month post-treatment the median AUA score was 13 (18-21; p=0.48), and using CTCAE scoring, there were no cases of Grade 2+ bowel or rectal toxicity and no cases of Grade 3+ urinary toxicity. Reported Grade 2 urinary toxicities included eight (57%) cases of bladder spasms, two (14%) cases of incontinence, one (7%) urinary obstruction and two (14%) reports of urinary urgency.

Conclusions: This study adds to the existing literature by confirming the acute toxicity profile of sHDR-BT is acceptable even without intraoperative MR guidance or image registration. Further study is ongoing to determine long-term efficacy and toxicity of treatment.

183

MONTE CARLO INVESTIGATION OF DOSE DISTRIBUTION OF UNIFORMLY AND NON-UNIFORMLY LOADED STANDARD AND NOTCHED EYE PLAQUES

Robert Weersink[1], Oleksii Semeniuk[1], Victor Malkov[1], Marc Chamberland[2]
[1]*University of Toronto, Toronto, ON*
[2]*University of Vermont, Burlington, VT*

Purpose: Currently, low dose rate (LDR) brachytherapy with uniformly loaded COMS eye plaques is the most common treatment option for a number of eye cancers. Using Monte Carlo simulations, we investigate the effect of non-uniform loading on dose distribution for standard and notched eye plaques.

Materials and Methods: Using EGSnrc Monte Carlo (MC) simulations, we investigate eye plaque dose distributions in water and in an anatomically representative eye phantom. Simulations were performed in accordance with TG-43 formalism and compared against full MC simulations which account for inter-seed and inhomogeneity effects.

Results: For standard plaque configurations, uniformly and non-uniformly loaded plaque dose distributions in water showed virtually no difference between each other. For both standard and notched plaque scenarios, TG43 calculations overestimate the absolute dose. For standard plaque, the MC calculated dose distribution in planes parallel to the plaque are narrower than the TG43 calculation due to attenuation at the periphery of the plaque by the modulay. MC calculated dose behind the plaque is fully attenuated. Similar results were found for the notched plaque, with asymmetric attenuation along the plane of the notch. Calculations in the eye model were used to calculate doses to the target volume and organs at risk. Cumulative dose volume histograms showed significant reductions in the calculated MC dose to the lens and optic nerve compared to TG43 calculations. The effect was most pronounced for the notch plaque where MC dose to the optic nerve was greatly attenuated by the modulay surrounding the optic nerve compared to the TG43.

Conclusions: TG43 calculations overestimate the absolute dose and the lateral dose distribution of both standard and notched eye plaques, leading to the dose overestimation for the organs at risk (optic nerve, iris, lens, etc.) and underestimation of target coverage. The dose matching along the central axis for the non-uniformly loaded plaques to that of uniformly loaded ones was found to be sufficient for providing a comparable coverage and can be clinically used in eye-cancer-busy centres. The developed eye and notched plaques models might be used to facilitate the development of the MC-based treatments for patient-specific eye lesions with both uniformly and non-uniformly loaded plaques.

184

AUTOMATED HDR QA TESTS USING AN ORGANIC PLASTIC SCINTILLATOR WITH OPENCV

Richard Lee[1], David Sasaki[1,2], Niranjan Venugopal[1,2], Swapanpreet Kaur[1], JORGE ALPUCHE AVILES[1,2]
[1]CancerCare Manitoba, Winnipeg, MB
[2]University of Manitoba, Winnipeg, MB

Purpose: To automate a series of quality assurance tests used in HDR Brachytherapy, using a novel organic scintillator camera apparatus supported by OpenCV.

Materials and Methods: A 15 mm thick organic plastic scintillator (OPS) (Eljen Technology, TX, USA) was used in combination with our Perma-Doc Phantom (RPD Inc., MN, USA) to verify source positional accuracy. The OPS was sufficiently thick, to release enough visible light when irradiated by a 5-10 Ci Ir-192 source, yet thin enough to visualize the graticule built into the Perma-Doc. A novel apparatus which combines a miniature camera and computer (https://www.raspberrypi.com) was constructed to minimize ambient light, and rigidly mounted to remove systematic offsets between independent measurements. Continuous video was recorded using a framerate = 32 fps, with a resolution of 1280 pixels by 720 pixels. This resulted in a spatial resolution of 0.23 mm/pixel and 31 ms/frame. We recorded approximately 90 seconds of video with zero frame-loss. The optimization of lighting and acquisition parameters was needed to assist our technique for automatic localization. Each frame was corrected for lens distortion, however, the optical effects of the scintillator itself was corrected by applying an empirical calibration curve measured at large distances (10 cm) using a linear regression fit model. The system was tested by having the HDR source remain stationary at 130, 125 and 129 cm for 15 seconds at each dwell position. Further the position resolution was evaluated by introducing a positional deviation of -2, -1, 0, +1 and +2 mm for each of the dwell positions except for 130 where only the retracted deviations could be applied. Similarly, deviations were introduced to the dwell time by -0.3 (-2%), -0.1(-0.7%), 0.0, +0.1(+0.7%) and +0.3 (+2%) s.

Results: The calibration correction was applied and resulted in source positions corrections of 0.81 mm at 130 cm and 0.32 mm at 120 cm. The mean correction was 0.55 mm. The mean agreement between the known source positions and those calculated was 0.2 mm with a standard deviation of 0.3 mm. The disagreement exceeded 0.5 mm twice and the maximum was 0.8 mm. In terms of timer accuracy, the average deviation between calculated and programmed dwell time was 0.4 % (of the programmed dwell time) with a standard deviation of 0.44 %. The maximum timer disagreement was less than 1%.

Conclusions: Our novel system has demonstrated that we can automatically determine source location using light generated from OPS materials. The system can automatically calculate source dwell positions within 0.8 mm and dwell time within 1%. Furthermore, we can detect deviations exceeding action levels based on current quality assurance recommendations, making it a viable solution for routine QA tests. In conclusion, we have presented a completely automated method that can be easily adopted by brachytherapy clinics.

185

DEVELOPMENT OF TEST CASES FOR COMPARISON OF MODEL-BASED DOSE CALCULATIONS IN LOW-ENERGY BRACHYTHERAPY

Elizabeth Fletcher[1], Facundo Ballester[2,3], Luc Beaulieu[4,5], Hali Morrison[6,7], Audran Poher[5,4], Mark Rivard[8], Ron Sloboda[9,10], Javier Vijande[2,3], Rowan Thomson[1]
[1]Carleton University, Ottawa, ON
[2]Universitat de Valencia, Valencia, ES
[3]Instituto de Investigación Sanitaria La Fe-Universitat de Valencia, Valencia, ES
[4]Université Laval, Quebec City, QC
[5]CHU de Québec-Université Laval, Quebec City, QC
[6]University of Calgary, Calgary, AB
[7]Tom Baker Cancer Centre, Calgary, AB
[8]Warren Alpert Medical School of Brown University, Providence, RI
[9]Cross Cancer Institute, Edmonton, AB
[10]University of Alberta, Edmonton, AB

Purpose: To outline a systematic framework for developing low-energy brachytherapy test cases to assist in comparing and benchmarking model-based dose calculation algorithms (MBDCAs) and implement it for the case of eye plaque brachytherapy.

Materials and Methods: Low-energy brachytherapy presents unique challenges stemming from the dominance of photoelectric interactions and their dependence on material cross-sections, which results in dose distributions being highly sensitive to patient geometry and elemental compositions of the materials involved in the treatment (tissues, applicators, seeds, etc.). As MBDCAs and Monte Carlo (MC) codes in particular are adopted and used for more accurate dose calculations, it is important to benchmark them relative to one another in order to validate calculations. We have developed a framework for systematically evaluating low-energy MBDCA dose calculation results, with the

specific application to I-125 eye plaque brachytherapy where a 16 mm COMS plaque is loaded with 13 model 6711 seeds. For this scenario, five test cases were developed, ranging from simple to complex: (1) modelling a single seed in water, the 13 seeds (2) individually and (3) in combination in water, (4) the full plaque in water, and (5) the full plaque in a realistic eye phantom. The progression of the test cases allowed for troubleshooting of differences between the four MC codes being benchmarked.

Results: Doses were compared between codes across the five test cases. Differences in dose distributions seen in the simplest test cases (single seed dose distributions) can be used to explain differences seen in more complex test cases whose origins may not otherwise have been obvious. The simplicity of the initial test case allowed initial troubleshooting of differences like seed and phantom geometry before more complex elements such as the eye plaque were introduced to the simulations. For the eye plaque example shown here, agreement for all test cases was within ~2.5% for the four MC codes studied, which is compatible with the expected combined Type A and B uncertainties of ~2%. Comparing agreement across the test cases, agreement was best in the single seed in water case; disagreement increased with the presence of the plaque and heterogeneous phantom media. The progression of the test cases enables the identification of the origins of differences between MBDCAs, whether they come from differences in user implementations such as differently modeled geometries or material compositions, or from factors within the codes such as the cross-section libraries or radiation transport algorithms used.

Conclusions: The framework outlined here allows for systematic comparison of low-energy brachytherapy dose distributions between different MBDCAs, shown here with the example of I-125 eye plaque brachytherapy. This framework can be readily extended from the eye plaque scenario presented here to other low-energy brachytherapy scenarios such as breast or prostate brachytherapy, where published benchmarked data are still lacking.

186
DIFFUSION OF 220RN AND 212PB IN DIFFUSING ALPHA-EMITTER RADIATION THERAPY DOSIMETRY WITH GEANT4
Victor Daniel Díaz Martínez, Shirin Enger
McGill University, Montréal, QC

Purpose: Diffusing alpha-emitter radiation therapy (DaRT) is a novel brachytherapy treatment modality that uses short-lived alpha-emitting atoms generated from ^{224}Ra decaying. From this decay, ^{220}Rn and ^{212}Pb atoms are of interest due to their ability to diffuse among the tumour cells alpha-decaying or decaying into other alpha-emitter daughters, respectively. This diffusion will contribute to a high-dose region up to few mm around the source overcoming the short range of alpha particles in tissue. The diffusion length of the alpha-emitting atoms varies for different types of tumours, producing a non-homogeneous dose distribution. The aim of this study was to investigate the dosimetry of DaRT with the Geant4 Monte Carlo (MC) toolkit. However, Geant4 does not simulate the diffusion of these daughters, hence, another aim of this study was to implement their diffusion to later use this data for MC-based dosimetry in Geant4.

Materials and Methods: The diffusion equations of the two diffusing daughters (^{220}Rn and ^{212}Pb) were solved using an in-house Matlab script. The results were used as input to an in-house MC-based Geant4 user-code developed for DaRT dosimetry. This Geant4 user-code simulates a 10 mm length DaRT seed with an inner diameter of 0.4 mm, outer diameter of 0.7 mm, and stainless steel as its material with a mass density of 7.92 g/cm^3. The user-code also simulates the radioactive decay of ^{224}Ra and retrieves information of all the decay products such as the total number of decay products generated, their position and energy. From this simulation, the emitted spectra from the source were obtained and compared to previously reported data. To assess the diffusion and the contribution of the alpha-particles to the dose, a dose map around the seed was obtained.

Results: The results obtained from these simulations include a visualization of the distribution of the radioactive daughters and alpha-particles around the seed up to few mm. The spectra emitted from the DaRT seed were also obtained which include the alpha, beta, and gamma radiation. These results were in good agreement with reported data from the IAEA having a percentage difference in the range of 0.006-0.015%, 0.18-4.81%, and 0-0.0.081%, respectively for alpha, beta, and gamma radiation. Finally, a dose map with the implemented diffusion was obtained showing an extension of the high-dose region around the seed due to the diffusing alpha-emitting atoms.

Conclusions: In this work the diffusion of the diffusing alpha-emitting daughters (^{220}Rn and ^{212}Pb) from the ^{224}Ra decay chain was implemented in the simulations, extending the distance at which alpha particles can deposit their energy. The MC-based user-code simulates the entire decay chain of ^{224}Ra retrieving useful information, such as the emitted spectra and position of every daughter, which can be modified according to the solution of their respective diffusion equation. The results show that the developed user-code can be used to investigate the DaRT dosimetry.

187
COST OF HIGH-DOSE RATE ENDOBRONCHIAL BRACHYTHERAPY FOR AIRWAY MALIGNANCY
Ethan Kutanzi[1], Nicole O'Callaghan[2], Zain Siddiqui[1], Conrad Falkson[1], Aamer Mahmud[1]
[1]*Queen's University, Kingston, ON*
[2]*Kingston Health Sciences Centre, Kingston, ON*

Purpose: Patients with malignant airway disease require in-patient and/or Intensive Care Unit (ICU) care. High-dose rate endobronchial brachytherapy (HDREB) has been shown to be an effective treatment for malignant airway disease, leading to a significant symptom improvement among these patients. The cost of HDREB is poorly documented in the literature. This study evaluates the cost of HDREB in treating malignant endobronchial disease and compares it with cost of stay in the ICU or a step-down unit. The average length of stay in hospital for respiratory failure as per Canadian Institute for Health Information is 12.7 days.

Materials and Methods: A retrospective chart review was completed for a cohort of patients at our institution who received HDREB between 2010 and 2019. Costs were calculated for treating patients with 2 fractions of HDREB using Cancer Care Ontario funding and Ontario Ministry of Health billing codes. The cost for the ICU included the cost of one day spent with a ventilator in the ICU, as per the fee guide from Queensway Carleton Hospital and Ontario Ministry of Health billing codes. The cost of one day in a step-down unit was calculated using the fee guide from Queensway Carleton Hospital and Ontario Ministry of Health billing codes.

Results: Fifty-eight patients received HDREB at our institution between 2010 and 2019, 52% among these had prior external beam radiation therapy (EBRT), where further EBRT administration was challenging or not possible. A total of eight (14%) were treated while admitted to the ICU, with seven of these patients being discharged from hospital following treatment. Total cost of HDREB for 2 fractions was calculated to be $3,415. Cost of one day in the ICU was calculated to be at least $4,287, where the cost of one day in a step-down unit per day was at least $1,025.

Conclusions: HDREB increases the likelihood of an earlier discharge from hospital as well as decreases financial burden to the healthcare system for patients with endobronchial malignancy, indicating a need to increase awareness and availability of HDREB.

188

DEVELOPMENT AND EVALUATION OF A GUI USING AI-ASSISTED ALGORITHM FOR CATHETER RECONSTRUCTION IN MR-ONLY GYNECOLOGICAL INTERSTITIAL HDR BRACHYTHERAPY

Kaiming Guo[1,2], Moti Raj Paudel[1,2]
[1]*Sunnybrook-Odette Cancer Centre, Toronto, ON*
[2]*Princess Margaret Cancer Centre, Toronto, ON*

Purpose: During MRI-guided HDR gynecological brachytherapy, several catheters are inserted through a standard template. Current approach, manual reconstruction of the implanted catheters, is time-consuming. We developed a novel deep-learning-assisted-semi-automatic (DLASA) algorithm and a Graphical-User-Interface (GUI) for catheter reconstruction. We present the GUI and robustness study of DLASA algorithm.

Materials and Methods: A GUI was built using open source Python libraries. All catheters are localized at a reference image slice which is the slice just before the catheters enter into the template. Information in the input file is passed to U-Net model to identify all possible catheter positions in a given image slice. Then, the true location of each catheter is tracked by finding the extrema in T1- and T2-weighted MR images. Once reconstruction is completed, catheter positions are saved to xls file. Modified Napari 3D orthogonal viewer is used to view and edit reconstructed catheter position on image slices on three cardinal planes. To evaluate the algorithm's catheter tracking performance, the construction of a catheter is compared with a manual reconstruction for 25 patients.

Results: Amongst 15/25 patients, the catheters reconstruction agreed with the manual reconstruction (mean error=0.4 mm, SD=0.7 mm. Among them, slightly over 97% of reconstruction positions had error <2 mm. The AI-assisted reconstruction shows great deviations from manual reconstruction for rest of the patients. In term of speed, more than 50% time was saved compared to manual reconstruction. This speed can potentially be increased with newer computing hardware.

Conclusions: The adoption of GUI has potential to improve treatment planning efficiency by reducing catheter reconstruction time. In future the training model in DLASA needs to be updated to obtain robustness of the catheter reconstruction. Also, we need to collaborate with the vendor to implement this solution to the treatment planning system for further evaluation.

189

ESTABLISHING A LOW DOSE RATE (LDR) BRACHYTHERAPY TREATMENT IN PROSTATE CANCER PROGRAM IN AN EMERGING ECONOMY

Nadeem Pervez, Tauseef Ali, Zahid Almandhari, Agha Khan, Jamsari Khalid, Nirmal Babu, Muhammad Ali Gurmani, Iqbal Al Amri, Abdullah Alshaikh, Mulham Alyahmadi, Mukaram Said, Sercan Yilmaz
Sultan Qaboos Comprehensive Cancer Care and Research Centre (SQCCCRC), Muscat, OM

Purpose: Prostate cancer accounts for about 5% of new cancer diagnosed in Oman. This is in absence of the prostate cancer screening program. LDR prostate brachytherapy alone or in combination with External Beam Radiotherapy (EBRT) is a standard curative treatment option for localized prostate cancer patients. It is also used for salvage treatment option for local failure after EBRT. Our institute successfully launched the first LDR brachytherapy program in the Middle East and Region.

Materials and Methods: Establishing a new service in countries with minimal experience and exposure is challenging. The following requirements and steps to acquire them was identified to initiate the program:

- Equipments: Operating room and Anaesthesia equipments were already in place. Other requirements were acquired through the Biomedical Engineering department including VariSeed software, BK ultrasound system with trans-rectal probe, CIVCO stepper and table mount, penile clamp and other disposable items. Due to the process: requesting approval from the Executive Committee, a tender to be floated and have to purchase through a third party (not directly from companies) which was costly, complicated and was time consuming. However this process was completed by team work.
- Personnel: Qualified and experienced staffs were already hired. Further in-house training was provided by internal and external expertise.
- Regulatory requirements: There is a regulatory requirement to import radioactive material in country, which was fulfilled by obtaining required license from Government officials.
- Quality assurance (QA) is important in radiotherapy treatment delivery. All equipments QA, radioactive seeds calibrations and brachytherapy plans were performed by Medical Physics.
- Timeline: About 15 months consumed from concept to start the program was due to the above mentioned challenges.
- Seed delivery: Seed was ordered and supplied from USA through protected item shipment and cleared by customs in Oman. On time seeds delivery was challenging in the first few cases due to this new process. After collaborating with stakeholders, transport and shipment is now delivered in a timely manner with minimal complications.

Results: Program function was successful after challenges were met. Five patients were treated so far including a salvage treatment case. Regulatory services are not well established in developing countries, necessitating extra documentation, establishing new policies and rules, working with government agencies to get approvals. This was a new concept of treatment to many stakeholders. Therefore, dummy seeds were ordered to remove any potential obstacle before ordering actual radioactive seeds for treatment. Also, dry runs were conducted to ensure all parties were aware entire process of treatment. Challenges related to logistics and custom clearances of radioactive seeds were resolved by communication with concerned airline team and organizing shipment to be delivered during working hours.

Conclusions: The LDR brachytherapy treatment was successfully launched in Oman. This abstract provides a glimpse of some of the challenges that were faced and how it was resolved in a country where this program was not already established.

190

IN VIVO DOSIMETRY FOR SUPERFICIAL HIGH DOSE RATE BRACHYTHERAPY WITH OPTICALLY STIMULATED LUMINESCENCE DOSIMETERS: A COMPARISON STUDY WITH METAL-OXIDE-SEMICONDUCTOR FIELD-EFFECT TRANSISTORS

Alana Lopes, Eric Sabondjian, Alejandra Rangel
Trillium Health Partners, Mississauga, ON

Purpose: To calibrate and commission optically-stimulated luminescence dosimeters (OSLDs) for in vivo measurements in contact based treatments for superficial high dose rate (HDR) brachytherapy in place of metal-oxide-semiconductor field-effect transistors (MOSFETs).

Materials and Methods: Five dosimetric characteristics were tested using Landauer nanoDot^TM OSLDs. To evaluate dose linearity, single OSLDs were placed in a fixed location while the dwell time varied. For dose rate dependence, the dwell time was held constant and a single OSLD was placed at varying source-to-OSLD distances. Next, a group of OSLDs were readout 34 consecutive times to test readout depletion while OSLDs were optically annealed using a mercury lamp light source for 34.7 hours. Angular dependence was measured using a solid water phantom with a circular hole machined into the centre for OSLD rotation. End-to-end tests were performed using a Freiburg flap and Valencia applicator in two separate cases for pacemaker and lens patients respectively. OSLD measurements were compared to both MOSFETs and the expected treatment planning system (TPS) dose.

Results: A supralinear response of OSLDs was observed for doses above 275 cGy. OSLDs were found to be independent of dose rate and exhibited minimal readout depletion with 0.05% reduction in signal per readout. OSLDs were successfully optically annealed to 0.01% of their original signal after 24 hours of illumination while angular dependence was found to only be significant in edge-on scenarios where a reduction in signal was as much as 16%. Measured doses were compared to those of the TPS and found to be in agreement for pacemaker patients to within a measurement uncertainty of ±5%. For lens patients, OSLDs were found to be the more accurate dosimetric system with a maximum disagreement with the TPS being 0.09%.

Conclusions: OSLDs can successfully be used in place of MOSFETs for in vivo dosimetry for superficial HDR brachytherapy.

191

THREE DIMENSIONAL VARIATIONS & THEIR EFFECTS ON EQUIVALENT DOSE IN 2 GRAY FRACTIONS (EQD2) FOR THE ORGANS AT RISK DURING IMAGE-GUIDED BRACHYTHERAPY

Agha Muhammad Hammad Khan, Mahmoud Al Fishaway, Furhan Altaf, Ana Paula E Galerani Lopes, Tauseef Ali, Sara Tajammul, Mohsina Vallengara, Jamsari Khalid, Iqbal Abdullah AlAmri, Zahid Almandhari, Nadeem Pervez
Sultan Qaboos Comprehensive Cancer Care and Research Centre (SQCCCRC), Muscat, OM

Purpose: To evaluate three dimensional variations & their effects on Equivalent Dose in 2Gy Fractions (EQD2) for the organs at risk (OARs) during image-guided brachytherapy (IGBT).

Materials and Methods: From November 2021 to September 2022, retrospective data were collected from 13 consecutive patients with gynecological malignancies. After rectal and bladder protocols preparation and implant procedure, a planning CT scan and MRI scan were performed in all fractions. CT and MRI scans were fused with rigid registration focusing on implant applicator. All OARs contours were independently contoured on CT and MRI images, which were also peer-reviewed. Patient's demographic information, applicator type, and the interval between the CT and MRI were recorded.

Results: Between the CT and MRI images, a mean of 28 minutes was recorded. 88% of patients' bladder volumes increased by an average of 38% while in 58% of patients, sigmoid volume increased by an average of 5.6%. In 91% of patients, volume of rectum decreased by an average of 14%. During the analysis, on average, the centre of the bladder and rectum moved 0.4 & 0. 1 cm shift away from direction from target. The average Dose to 2cc (D2cc) in the bladder increased by 2.3%, while it decreased by 1.3% & 2.8% in rectum & sigmoid respectively. EQD2 of bladder, rectum and sigmoid changed by 1.2% (CT 71.4 Gy, versus MRI 72.2 Gy), 0.3% (CT 69.8 Gy, versus MRI 69.5 Gy) & 0.2% (CT 55.6 Gy, versus MRI 55.9 Gy), that did not violate the D2cc for EQD2 cutoff as suggested by EMBRACE studies.

Conclusions: Our institute's time-dependent analysis of IGBT pretreatment CT and MRI scans revealed OAR motion between images. OARs deviated from the target due to these modifications, resulting in D2cc variations that did not translate significant values in terms of EQD2 calculation suggested by EMBRACE cutoffs.

192

INVESTIGATION OF THE DOSE PROPERTIES AND SOURCE TO SOURCE VARIABILITIES IN XOFT SOURCE MODEL S7500

Azin Esmaelbeigi[1], Jonathan Kalinowski[1], Te Vuong[2], Shirin A. Enger[1,2]
[1]*McGill University, Montréal, QC*
[2]*Jewish General Hospital, Montréal, QC*

Purpose: In order to overcome the uncertainty caused by the source to source variability in output of the Xoft electronic brachytherapy source, the aim of this study was to develop and optimize a Monte Carlo dose calculations software for characterization of the source and investigation of its dosimetry.

Materials and Methods: A Monte Carlo dose calculation package based on the Geant4 toolkit was developed. The source geometry, and elemental composition of the Xoft source was modeled based on the manufacturer specifications. Source to source discrepancies were investigated. Uniform bremsstrahlung splitting was used to increase the efficiency of the bremsstrahlung production. The spectrum of the source was calculated with and without the bremsstrahlung splitting and compared with the NIST measurements in 178 cm from the source origin in air. The beam quality for the produced spectrum in terms of half value layer (HVL) and air kerma rate were calculated 2.5 cm from the source. Furthermore, calculation of the TG-43 parameters is ongoing.

Results: A photon splitting factor of n=100 gives rise to the same spectrum as NIST measurements and previously simulated data without photon splitting. The calculated air kerma rate in air was 3.08 Gy/min +1%. The beam HVL, which is 0.43 mm Al, and in agreement with published data. Due to the discrepancy of geometry and material composition in certain components of the source, there is a source to source variability in the generated spectra and dosimetric properties.

Conclusions: A Monte Carlo package for dosimetry of electronic brachytherapy was developed and its performance was optimized. A large number of simulations are performed. Moreover, for each new source for clinical use, measurements with a CdTe x-ray and gamma-ray spectrometer will be performed, so as to have a robust pipeline of quality assurance for our Xoft sources that relies on both simulations and measurements.

193

APPLICATION OF A NOVEL MONTE CARLO BASED METHOD TO DETERMINE THE EMBEDDED DISTRIBUTIONS OF ALPHA-EMITTERS FROM THEIR MEASURED ALPHA SPECTRA IN DIFFUSING ALPHA-EMITTERS RADIATION THERAPY (DART)

Julien Mondor[1,2], Jean-François Carrier[1,3,2], Yuji Kamio[2,3]
[1]*Université de Montréal, Montréal, QC*
[2]*Centre de Recherche du Centre Hospitalier de l'Université de Montréal (crCHUM), Montréal, QC*
[3]*Centre Hospitalier de l'Université de Montréal, Montréal, QC*

Purpose: This work presents a novel method using Monte Carlo simulations to model the embedded alpha-emitters distributions of ^{224}Ra, ^{220}Rn and ^{212}Bi in DaRT brachytherapy seeds.

Materials and Methods: A complete alpha-spectrometry setup was modelled using GAMOS, a GEANT4-based framework including its PIPS (Particle-implanted passivated silicon) detector and measurement chamber. A constant partial pressure of 5 mbar was used under continuous air flow to evacuate diffusing ^{220}Rn gas. A DaRT stainless-steel cylindrical seed was modelled and positioned on a sample tray to generate simulated alpha spectra. The PIPS detector response function was determined by comparing simulated ^{224}Ra alpha spectrum with experimental alpha spectrometry data taken before the thermal treatment used to embed the ^{224}Ra during seed production. Simulations involving thin cylindrical layers of ^{224}Ra positioned at various depths up to 25 nm under the seed's surface were made to generate a library of simulated alpha spectra. This library was then used to determine the intraseed distribution of each alpha-emitters of interest pre- and post-baking by minimizing differences between simulated and experimental alpha spectrometry data.

Results: Alpha spectra from more complex multi-layer sources can be simulated by weighting and summing each of its library layers spectrum after convolution with the PIPS detector's response function. Optimization weights revealing the intraseed distribution of ^{224}Ra, ^{220}Rn and ^{212}Bi were obtained following a chi-square minimization process. Significant presence of ^{212}Bi in pre-baking spectrometry data suggest the electrostatic collection of short-lived ^{212}Pb contaminant alongside ^{224}Ra during seed production. In this work, differences between generated and measured alpha spectra for each alpha-emitters were less than 5%. The entire workflow was repeated (n=5) to evaluate statistical uncertainties on the determined intraseed distribution.

Conclusions: In this work, a novel Monte Carlo based method was successfully applied to determine the intraseed distributions of alpha-emitters in DaRT brachytherapy using their measured alpha spectra. This work can be used to produce more detailed and accurate DaRT brachytherapy seed models for Monte Carlo simulations.

194

CHARACTERIZATION OF NOVEL 3D-PRINTED METAL SHIELDING FOR BRACHYTHERAPY APPLICATORS

K. Maiti McGrath[1,2], Krista Chytyk-Praznik[1,2], Amanda Cherpak[1,2]
[1]*Dalhousie University, Halifax, NS*
[2]*Nova Scotia Health, Halifax, NS*

Purpose: To characterize 3D-printed stainless steel metal samples in the presence of an Iridium-192 source for organ-at-risk sparing in gynecologic brachytherapy.

Materials and Methods: Samples of 3D-printed stainless steel (5.5 x 5.5 cm^2, thickness ranging from 1-5 mm) were embedded in a solid water phantom at varying distances from source catheters. An Ir-192 brachytherapy source was passed through the phantom and resulting dose was measured using EBT3 Gafchromic film. Film was first positioned in the sagittal plane 2 cm away from the catheters, with the metal directly below the film and then with the metal halfway between the film and the catheter (1 cm separation). A plan was created and delivered to give a uniform dose at the film plane. The second setup allowed for measurement of a depth dose curve in solid water by positioning the film in the transverse plane directly above the metal samples.

Results: The planar dose passing through the metal samples, thickness 1 mm - 5 mm, decreased compared to solid water by 3.8%, 8.4%, 12.2%, 16.0%, and 22.0% respectively. These were measured with the metal midway between the film and the catheter plane. Dose enhancement on the order of 5% was noted when metal was directly adjacent to the film. The average decrease in depth dose from a single dwell position ranged from 1.8% to 15.6%.

Conclusions: The 3D-printed metal samples show potential for use in 3D-printed personalized shielding. A maximum reduction in dose of 22.0% compared to solid water was measured 2 cm from the source using the 5 mm sample. An outer layer of solid water can reduce dose enhancement due to increased scatter near the metal. Greater thicknesses would be needed for further dose reduction to OARs and will be investigated in future work.

195

ALPHA PARTICLE DOSE MODELING IN DART BRACHYTHERAPY: SENSITIVITY OF DIFFUSION-LEAKAGE PARAMETERS, SEED GEOMETRY AND INTER-SEED EFFECTS

Patrick Chevé[1], Paul Charbonneau[1], Jean-François Carrier[1], Yuji Kamio[2]
[1]*Université de Montréal, Montréal, QC*
[2]*Centre hospitalier de l'Université de Montréal, Montréal, QC*

Purpose: The Diffusion-Leakage (DL) model allows to calculate doses in Diffusing alpha-emitters Radiation Therapy (DaRT). The first objective of this work is to present how the variations, over clinically relevant ranges for various tumour types, of the DL parameters related to the desorption, diffusion and leakage processes affect the position of the clinically significant alpha particle 10 Gy isodose. The second objective is to present the effects of different modeling approximations such as the source geometry (hollow or solid cylinder), the source cross section representation (circular or "pixelized") and dose superposition for multiple sources.

Materials and Methods: A finite volume approach was used to develop numerical schemes of increasing complexity that were used to simulate the DL model in 1D, 2D and 3D. These schemes were coded in Python and the Ra-224 source activity was set to 3 µCi/cm. 1D simulations in cylindrical coordinates were used to study sensitivity of various parameters (desorption, diffusion, leakage) while 2D simulations in cylindrical and Cartesian coordinates were used to assess various modeling approximations.

Results: For the simulation parameters considered, the combined variations of the diffusion lengths of Rn-220, Pb-212 and Bi-212 are shown to affect the position of the alpha particle 10 Gy isodose about four times more than the variation of the leakage probabilities and about ten times more than the variation of the desorption probabilities. The effect on the position of the alpha particle 10 Gy isodose is negligible (a displacement less than 0.1 mm) when approximating a hollow source by a solid source or when approximating the circular cross section of the source by a "pixelized" one. For clinically realistic inter-source spacings, the maximum relative error is less than 10^{-4} when superposing several single-source dose maps to build multiple-sources dose maps.

Conclusions: In this work, a code based on a finite volume approach was successfully developed to model the alpha particle dose in DaRT and study its sensitivity to variations on DL model parameters. This code could be used to simulate any specific tumour/tissue types by integrating their respective experimental data as they become available.

196

3D PRINTED MODEL FOR SURFACE MOULD PREPARATION ON A DOWN SYNDROME BRACHYTHERAPY PATIENT

Iqbal Al Amri, Rohit Inippully, Mahmood AL Fishawy, Nirmal

Babu, Hajir Al Siyabi, Mohammed Al Ghafri
Sultan Qaboos Comprehensive Cancer Center, Muscat, OM

Purpose: A down-syndrome patient was intended for adjuvant radiotherapy for Dermato-fibrosarcoma protuberans. The lesion was on the parietal region of the head of the patient. Given the lesion proximity to the brain, curvature of the lesion and also complications of anesthesia for down-syndrome patient, brachytherapy was intended for treatment. Anesthesia complications for down syndrome patients are airway infections, atlanto-occipital dislocation and bradycardia. Instead of sedating the patient for a long time for preparation of a mould applicator, a 3D-printed model of the patient's head was used to prepare the applicator on.

Materials and Methods: A thermoplastic mask was prepared initially on the patient 3D printed model. Since the 3D printed head model had the location of the delineated tumour, catheter placement was very convenient. The area above the tumour was cut out from the thermoplastic mask and replaced by dental wax sheets of 2 mm to provide material for attenuation. 11 applicator mould probes (catheters) from Varian mould applicator set were placed 1 cm apart from each other on dental wax sheets 2 mm on each side. This sandwiched catheter set was placed above the dental wax on the thermoplastic mask. Each probe was marked from 1 to 11 from the posterior side.

Results: 3D-printed model enabled sufficient time and relaxed environment for applicator preparation. The fitting of the applicator prepared on the 3D printed head model was suitable on the patient. Minor air gaps were removed using ultrasound gel.

Conclusions: The standard dosage for Dermatofibrosarcoma protuberans is 50-66 Gy given in 25-33 fractions through External Beam Radiation therapy. We were able to achieve the same Equivalent Dose of 53.7 Gy in 5 sessions of brachytherapy, significantly reducing the anesthesia sessions and the risk associated with anesthesia for the down syndrome patient. Only down side of 3D printing would be time required to prepare the model, which was 22 hours in this case.

197

MONTE CARLO DOSE MODELLING OF EMBEDDED BETA/GAMMA EMISSIONS FROM DART ALPHA-EMITTERS BRACHYTHERAPY SEEDS USING GEANT4

Julien Mondor[1,2], Yuji Kamio[2,3], Patrick Chevé[1,2], Jean-François Carrier[1,3,2]
[1]*Université de Montréal, Montréal, QC*
[2]*Centre de Recherche du Centre Hospitalier de l'Université de Montréal (crCHUM), Montréal, QC*
[3]*Centre Hospitalier de l'Université de Montréal, Montréal, QC*

Purpose: This work presents dosimetric calculations of the dose distribution of embedded beta-emitters and isomeric transition emissions (gammas & internal conversion electrons) coming from diffusing alpha-emitters radiation therapy (DaRT) seeds.

Materials and Methods: A DaRT brachytherapy seed of 1 cm was modelled using GAMOS, a GEANT4-based framework using a stainless-steel cylindrical geometry. Desorption probabilities of ^{220}Rn and ^{212}Pb were 0.38 and 0.5 respectively. An initial ^{224}Ra activity of 20 Bq (9 million histories) was simulated explicitly and extrapolated to a clinically relevant activity of 74 kBq. 2D dose distributions deposited by the upper right quadrant of the seed was scored in a 2 x 2 x 2 cm^3 soft tissue-equivalent phantom with 0.1 mm voxels. Using the cylindrical symmetry of the seed, a mean 2D dose distribution (r, z) was obtained by averaging 360 dose distributions sampled from θ = 0° to 179° using a bilinear interpolation.

Results: The appearance of the resulting isodoses were improved by smoothing them with a gaussian filter (σ = 4). A comparison was made against the dose distribution from the main diffusing alpha-emitters. Diffusing alpha-emitters contribute more significantly to the absorbed dose in the immediate vicinity of the seed with 100 Gy (versus 10 Gy for embedded beta/gamma emissions) at a distance of r = 2.0 mm. However, their contributions become similar at a distance of r = 3 mm (~5 Gy) and embedded beta/gamma emissions contribute more significantly to the dose further away with the 1 Gy isodose reaching a distance of r = 5.2 mm (versus r = 3.8 mm for alpha-emitters) and 0.1 Gy at r = 8.2 mm.

Conclusions: In this work, we report dosimetric calculations of the dose distribution from embedded beta-emitters and their secondary emissions (gammas and IC electrons) coming from DaRT brachytherapy seeds. The total beta/gamma dose could be evaluated by summing the contribution from embedded emitters evaluated in this work to the contribution from diffusing emitters.

198

EVALUATING ONLINE YOUTUBE RESOURCES FOR CERVICAL CANCER BRACHYTHERAPY

Sarah Keyes[1], Brandon Chai[2], Paris-Ann Ingledew[2]
[1]*University of British Columbia, Vancouver, BC*
[2]*British Columbia Cancer, Vancouver, BC*

Purpose: Cervical cancer remains the third most common cancer in females aged 25-44 years, with brachytherapy an important modality of treatment. Patients often rely on the internet to seek cervical cancer information; however, few studies have evaluated the quality of these resources. The aim of this study is to describe and evaluate the current landscape of YouTube videos available to patients on cervical cancer brachytherapy.

Materials and Methods: Using a clear-cache Chrome browser in incognito mode, YouTube was searched using "cervical cancer brachytherapy", "cervical cancer radiation brachytherapy", and "cervical cancer brachytherapy treatment" on January 30, 2023. Videos were sorted by relevance and the first 50 videos from each search was collected. Videos were excluded if they were not in English (either audio or in-video subtext) or >1 hour in duration. Duplicates were removed. Videos were aggregately ranked and evaluated for general parameters, source information, and content. Two coders evaluated the first 10 videos to ensure consistency. Descriptive analyses were applied.

Results: Of 150, 47 unique videos were included in the analysis. Videos were published between November 2, 2009 and January 27, 2023, with 53.2% of videos published within the past three years as of February 2023. Median length was four minutes 42 seconds. Median view, like, and comment counts were 8150, 43, and three, respectively. Over half of videos (55.3%) were published from the USA. Videos were most commonly published by a healthcare facility/organization (36.2%), or else a commercial (21.3%) or personal (17.0%) account. Most videos were presented by a physician (53.2%), unknown (27.7%), or patient (19.1%), often as an interview (42.6%). Videos largely targeted patients (66.0%) compared to healthcare professionals/students (34.0%). Around half generally discussed the spectrum of treatments for cervical cancer including surgery, chemotherapy, and radiation therapy (53.2%), as well as described brachytherapy (48.9%) and its use in treating cervical cancer (46.8%). Commonly, videos discussed logistics of brachytherapy treatments (36.2%), treatment applicators (34.0%), and brachytherapy advantages and disadvantages (27.7% each). Few explained the procedure (19.1%) or described side effects (12.8%). Only 12.8% were for commercial purposes, and 4.3% contained grossly misleading/inaccurate information.

Conclusions: This study provides an overview of the videos available to patients on cervical cancer brachytherapy. Videos generally presented a balanced overview of the treatments for cervical cancer, including brachytherapy. However, few videos included pertinent patient-relevant information such as brachytherapy side effects. This may inform physicians of the limitations of online videos and guide the development of additional patient educational resources. Further research should appraise other online resources for cervical cancer radiation therapy.

199

IMPLEMENTATION AND EARLY EXPERIENCE OF BREAST INTRAOPERATIVE ELECTRON BEAM RADIATION THERAPY

Dominique Guillet[1,2], Karim Zerouali[1,2], Thi Trinh Thuc Vu[1,2], Renée Larouche[1,2], Rami Younan[1,2], David Roberge[1,2]
[1]*Université de Montréal, Montréal, QC*
[2]*Centre Hospitalier de l'Université de Montréal, Montréal, QC*

Purpose: A mobile linear accelerator, the Mobetron (IntraOp, CA), is the first dedicated intraoperative radiotherapy (IOeRT) Linac with electron beams installed in Canada. The promise of IOeRT is to allow direct irradiation of the tumour bed at the time of resection while healthy tissues are moved out of the way or protected from the radiation with an internal shield. Extensive collaboration between multiple departments (radiation oncology, radiation protection, sterilization and surgery) as well as teamwork among different professionals (anesthetists, nurses, medical physicists, radiation oncologists, surgeons, technologists, etc.) were necessary to build a successful IOeRT program.

Materials and Methods: Medical physicists were responsible for commissioning and radiation surveys of the dedicated shielded operating room (OR). New accessories were locally developed using 3D printing. The clinical process was drafted and tested by the multidisciplinary team. Dry-runs in the OR with their staff were done to identify the necessary modifications to the standard surgical procedure as well as ensure proper OR staff training for radiation safety. Further quality control was obtained by performing in vivo measurements during treatment. An international multi-centre prospective study was joined to standardize the early breast IOeRT practice and compare the initial results to established centres.

Results: Locally acquired output factors and percent depth doses compared well with available data. The in vivo measurements confirmed proper cone and shield positioning within the patients. Since February 2020, 28 breast patients have benefited from IOeRT treatments with positive follow-up and without adverse outcome, mostly receiving definitive treatments and for a few patients, boosts. Furthermore, starting in February 2023, the technique has been extended to digestive intraoperative radiotherapy (DIRT), which necessitated new clinical processes drafted by the multidisciplinary team.

Conclusions: A strong multidisciplinary collaboration is necessary to a successful implementation of IOeRT in the clinic. This collaborative effort must be maintained to improve and innovate upon the technique.

200

A CANADIAN BREAST RADIOTHERAPY PRACTICE SURVEY

Cheryl Duzenli[1,2], Tania Karan[1], Maria Corsten[3], Lisa Glass[4], Thalat Monajemi[5], Samantha Lloyd[2,3], Robynn Ferris[1], Marija Popovic[6]
[1]*British Columbia Cancer, Vancouver, BC*
[2]*University of British Columbia, Vancouver, BC*
[3]*Eastern Health, St. John's, NL*
[4]*University of Saskatchewan, Regina, SK*
[5]*Dalhousie University, Halifax, NS*
[6]*McGill University, Montréal, QC*

Purpose: To understand variations in breast radiotherapy practice across Canada.

Materials and Methods: Twenty-nine Canadian Cancer Treatment centres responded to the survey between November 2022 and January 2023 (response rate of 60%). All 10 provinces were represented. Radical breast RT comprised up to 40% of the total RT workload per centre, with a median of 20%. Clinic size varied significantly with 15 centres having ≤4 linacs, 11 centres having 5-9 linacs and four centres having 10-16 linacs. The 50Gy/25 fraction regimen was used 7% of the time, 26Gy/5 fractions 26% of the time , 40Gy/15 fractions 27% of the time and 42.5Gy/16 fractions 30% of the time. For special techniques, five centres perform breast brachytherapy and two centres perform IORT. The majority of centres offer partial breast to the surgical cavity using external beam RT. Prone setup is used at 10 centres. Three centres perform simultaneous integrated boost and 11 centres use VMAT for selected breast +/- regional nodal irradiation (RNI). All centres offer DIBH for left breast cases. For the 40Gy/15 fraction whole breast prescription, planning dose constraints for mean heart dose range from <1Gy to <5Gy and mean lung dose constraints range from <2Gy to <20Gy. A variety of other dose volume dose constraints is used for lung and heart for different prescriptions.

Results: Twenty-nine Canadian Cancer Treatment centres responded to the survey between November 2022 and January 2023 (response rate of 60%). All 10 provinces were represented. Radical breast RT comprised up to 40% of the total RT workload per centre, with a median of 20%. Clinic size varied significantly with 15 centres having ≤4 linacs, 11 centres having 5-9 linacs and four centres having 10-16 linacs. The 50Gy/25 fraction regimen was used 7% of the time, 26Gy/5 fractions 26% of the time, 40Gy/15 fractions 27% of the time and 42.5Gy/16 fractions 30% of the time. For special techniques, five centres perform breast brachytherapy and two centres perform IORT. The majority of centres offer partial breast to the surgical cavity using external beam RT. Prone setup is used at 10 centres. Three centres perform simultaneous integrated boost and 11 centres use VMAT for selected breast +/- regional nodal irradiation (RNI). All centres offer DIBH for left breast cases. For the 40Gy/15 fraction whole breast prescription, planning dose constraints for mean heart dose range from <1Gy to <5Gy and mean lung dose constraints range from <2Gy to <20Gy. A variety of other dose volume dose constraints is used for lung and heart for different prescriptions.

Conclusions: This survey has revealed consistent trends in hypofractionated dose prescriptions for whole breast RT across Canada. Significant variation is seen in the use of VMAT and prone breast positioning. DIBH utilization is consistent while treatment planning dose constraints for heart and lung vary significantly. Further exchange of information on breast RT practice across Canada is underway.

201

A RADIATION ONCOLOGIST'S EXPERIENCE TREATING MALIGNANT GLIOMA WITH TUMOUR TREATING FIELDS IN CANADA

David Roberge
University of Montréal, Montréal, QC

Purpose: The FDA approved tumour treating fields (TTField) in 2011. Through a special access program of Health Canada a limited number of TTField treatments have been provided prior to regulatory approval.

Materials and Methods: This work describes a single physician's experience with TTField. Cases where access was provided as an extension of prior research use were excluded. With ethics review board approval, charts were retrospectively reviewed.

Survival times were calculated using the Kaplan-Meier method for adjuvant patients (actual survival in recurrent cases).

Results: From 2013-2022, 42 cases were identified (one patient with post-EF14 use was excluded). Fifty-seven percent were from Quebec, 24% from Ontario and the rest from either Alberta or British Colombia. TTField was prescribed as an adjuvant following chemo-radiation in 28 cases and for recurrent disease in 14. Median age was 48 (range 18-75). Seventy-four percent of patients were male. Median KPS was 73%. 95% were classified as glioblastoma by the criteria used at the time of diagnosis. Where known, 44% had methylation of the MGMT promoter. Adjuvant treatment started a median of 1.4 months following radiotherapy. Recurrent patients had had a median of two prior lines of treatment (range 1-9). Two young adults discontinued treatment after less than one week but otherwise patients tolerated the device until treatment was recommended to be discontinued. Median OS for adjuvant patients was 15.4 months, 5.2 months for recurrent patients. For adjuvant patients, median time on treatment was nine months.

Conclusions: It was possible to offer TTField over a wide geographic area with support from device support specialists. Treatment may be more easily integrated into care with the development of a larger network of prescribers following regulatory approval.

202

SAFETY AND EFFICACY OF FRACTIONATED STEREOTACTIC RADIATION THERAPY FOR PITUITARY ADENOMAS

Aveline Marie Ylanan[1,2], Alan Nichol[3,2], Roy Ma[3,2], Michael McKenzie[3,2], Fred Hsu[1,2], Sheikh Nisar Ahmed[1,2], Arthur Cheung[4,2], Ryojo Akagami[3,2], Peter Gooderham[3,2], Michelle Johnson[2], Ermias Gete[3,2], Isabelle Vallieres[2,5], Waseem Sharieff[1,2]
[1]*British Columbia Cancer, Abbotsford, BC*
[2]*University of British Columbia, Vancouver, BC*
[3]*British Columbia Cancer, Vancouver, BC*
[4]*British Columbia Cancer, Surrey, BC*
[5]*British Columbia Cancer, Victoria, BC*

Purpose: To determine the clinical outcomes of patients with pituitary adenomas treated with fractionated stereotactic radiation therapy (FSRT).

Materials and Methods: This is a retrospective case series of patients treated for pituitary adenoma with FSRT between January 1, 1998 and December 31, 2016. Cases were identified through a population-based registry. Patient charts and radiation treatment plans were reviewed to abstract patient and disease characteristics, and treatment details. Local control was defined as the absence of growth on follow-up imaging. Biochemical control was defined as the normalization of elevated hormone levels without suppressive medications. Data were analyzed with descriptive statistics, linear regression models and Kaplan Meier curves.

Results: There were 201 patients treated with FSRT, of whom 193 (96%) had prior surgery. Eighty-six percent of patients were treated using 1.8 Gy daily fractions to a median dose of 50.4 Gy. Radiation was delivered either using fixed conformal beams (68.8%) or arcs (31.2%). The median follow-up period was 10.1 years. Local control was 96.5%. Of 50 patients with secreting adenomas, 36% had biochemical control. There were 27 deaths; none due to tumour progression or treatment related complications. Late effects included hypopituitarism (28.4%), decline in vision (2.0%), and secondary malignancy (1.5%). No patient had radionecrosis or seizures following FSRT.

Conclusions: Our experience suggests that FSRT is a safe and effective treatment for pituitary adenomas.

203

18F-DOPA PET SCAN MAPPED WITH RADIOTHERAPY DOSIMETRY FOR THE MANAGEMENT OF TUMOUR RECURRENCE VERSUS RADIATION NECROSIS IN HIGH GRADE GLIOMAS: AN INSTITUTIONAL EXPERIENCE

Asmara Waheed, Jay Easaw, Kelvin Young, Egiroh Omene, Albert Murtha, Aswin Abraham, John Amanie, Lindsay Rowe, Samir Patel, Ravi Bhargava, Daniel Thut, Freimut Juengling, Helene Daly, Hans-Sonke Jans, Wilson Roa
University of Alberta, Edmonton, AB

Purpose: Patients with High grade glioma (HGG) who underwent chemoradiation usually have routine Magnetic Resonance Imaging (MRI) every two to three months for surveillance. Quite often, the treatment related changes including radiation necrosis (RN) and pseudo-progression (PP) are indistinguishable from tumour recurrence (TR), which can cause significant dilemma to the treating physician. The main aim of this study is to investigate the utility of Fluoro-dihydroxyphenylalanine Positron Emission Tomography (^{18}F -DOPA PET) scan mapped with radiotherapy planning dosimetry in differentiating true progression from RN and PP during follow up, and the potential application in further treatment management.

Materials and Methods: We retrospectively reviewed ten accrued HGG patients over a duration of 12 months, who were initially treated with concurrent chemoradiation and found to have clinical and/or MRI changes suggesting TR or RN on follow up. Each patient underwent a ^{18}F-DOPA PET scan and the images were mapped with the corresponding CT and MRI radiotherapy plan. We then analyzed the overlap of fused images with the contours of primary tumour and target volumes. Descriptive analysis was used to identify TR and RN, and patterns of correlation with dosimetry.

Results: ^{18}F-DOPA PET scan identified TR in eight patients and RN in two patients. Majority of scans identified progression based on PET metabolic uptake. Tumour progression was identified inside the PTV target volume in four patients. Tumour progression outside the high dose volume was identified in one patient and at marginal borders of targets in three patients. We found the mirror symmetry of PET finding inside the brain, baseline extent of tumour, and uptake changes over time useful in recognizing a differentiating pattern when compared with the initial planning scan. Also, utility of ^{18}F-DOPA PET scan may go beyond identification of necrosis in Radiation Oncology. It can reveal early metabolic uptake in irradiated area upon recurrence and identify potential re-treatment opportunities upon mapping of low-dose areas.

Conclusions: ^{18}F-DOPA PET scan has significant utility for future CNS practice in Radiation Oncology, indicating not just necrosis from prior radiotherapy, but identifying early tumour progression, its location and opportunity for re-treatment based on the mapped dosimetry.

204

DEVELOPMENT OF A DECISION AID FOR PATIENT WITH EXTENSIVE BRAIN METASTASES

Tatiana Conrad[1], David Shultz[2], Derek Tsang[2], Tiffany Tam[3], Luluel Khan[4], Cassandra Carey[1]
[1]*Southlake Regional Health Centre, Newmarket, ON*
[2]*Princess Margaret Cancer Centre, Toronto, ON*
[3]*Royal Victoria Regional Health Centre, Barrie, ON*
[4]*Credit Valley Cancer Centre, Mississauga, ON*

Purpose: Brain metastases (BrM) management has become a significant component of cancer care and involves complex decision making, specifically for patients with extensive (≥ 5) lesions. Research shows that health outcomes and care satisfaction are both improved when patients are involved in decision-making.

This study will be the first of its kind in this patient population, and aims to develop a decision-aid (DA) which will serve two purposes: (1) to better inform patients on risks and benefits of stereotactic radiosurgery versus whole brain radiotherapy in the face of multiple metastases and (2) to assist patients in highlighting their own values leading to more optimal shared decision-making.

Materials and Methods: Preparation Phase: A literature review was conducted to identify current evidence and recommendations on the management of BrM. The review was supplemented with input about care team and patient needs from an advisory group of key players and patient representatives from four cancer centres. Development Phase: A decision-aid has been developed by core team members and includes information about: i) condition/ decision, alternative options, outcomes and their probabilities; ii) patient-values worksheet and iii) narrative excerpts from other patient experiences. Evaluation Phase: Satisfaction ratings will be provided by 30 patients using a 5-point Likert scale. Ten patients will participate in a 45-minute interview to determine their thought process and role of the DA in their decision-making. Data will be analyzed using descriptive statistics and qualitative thematic content analysis.

Results: A DA for patients with extensive BrM was developed. It integrates key evidence on outcomes and toxicities for treatment options, together with information gained from patient priorities when facing a treatment decision. The evaluation component is forthcoming.

Conclusions: This DA can facilitate shared decision making between clinicians and patients with extensive BrM. The DA was developed in accordance with consensus guidelines.

205

MODERATE HYPOFRACTIONATED RE-IRRADIATION FOR RECURRENT GLIOBLASTOMA MULTIFORME

Danny Jazmati, Edwin Boelke, Yechan Flaig, Jan Haussmann, Wilfried Budach, Stefanie Corradini, Amir Rezazadeh, Balint Tamaskovics, Christiane Matuschek
Heinrich Heine University, Dusseldorf, DE

Purpose: Due to improvements in the technical delivery of irradiation, radiotherapy is becoming increasingly relevant in the multimodality treatment of patients with relapsed glioblastoma. The aim of this study is to retrospectively evaluate the efficacy and tolerability of hypofractionated irradiation with 40 Gy in 15 fractions in an interdisciplinary approach consisting of re-induction chemotherapy with temozolomide and surgery with and without carmustine implant.

Materials and Methods: Patients with histologically confirmed glioblastoma who received re-irradiation in our institution were eligible for retrospective data analysis. Data on patient characteristics, therapy, outcome and tolerability were collected and analyzed. Side effects were classified according to CTCAE.

Results: Fifty-five patients were eligible for the study. Most patients received surgery and re-induction chemotherapy including temozolomide. One patient experienced a higher grade radiotherapy-related complication (cerebral edema CTCAE°IV). A shunt infection occurred in another. The median progression-free and overall survival was six and 10 months, respectively. The interval between first radiation and recurrence, the use of surgery and age were significant predictors of better overall survival. There were no higher-grade toxicities. Radiotherapy-induced imaging chances occurred in six patients. One clinically manifest radionecrosis in one patient. One patient developed a secondary haematological tumour.

Conclusions: Overall, our data can demonstrate the tolerability of hypofractionated re-irradiation with 15 X 2.06Gy as part of an intensive multimodal therapy concept. More studies are necessary to improve the survival rates for patients with relapsed Glioblastoma.

206

SHARING MONO-INSTITUTIONAL EXPERIENCE OF TREATING PANCREATIC CANCER WITH STEREOTACTIC BODY RADIATION THERAPY (SBRT) AS AN ADJUVANT THERAPY FOR NON-OPERATIVE PATIENTS OR SALVAGING LOCAL FAILURE

Asmara Waheed, Aswin Abraham, Shannah Murland, Diane Severin, Kent Powell, Arun Elangovan, Nawaid Usmani, Keith Tankel, Kim Paulson, Xiaofu Zhu, Clarence Wong, Eugene Yip, Sunita Ghosh, Amr Heikal, Ben Burke, Kurian Joseph
University of Alberta, Edmonton, AB

Purpose: Stereotactic body radiotherapy (SBRT) is an evolving treatment for the local management of pancreatic cancer (PC). SBRT is offered as an adjuvant therapy for non-operative patients or for salvaging local failure. The main purpose of this study is to report our initial experience in terms of local control (LC) and toxicity for PC patients treated with SBRT.

Materials and Methods: We conducted a retrospective review of patients treated with SBRT. Patients were identified after a multidisciplinary rounds discussion. Treatment was delivered on Truebeam using abdominal compression (AC) or end expiratory breath hold (EEBH) technique for motion management with image guidance using implanted fiducial markers. Target delineation was done using departmental protocol & uniform Planning Target Volume (PTV) margin of 5 mm was generated in all cases. The median prescribed dose was 35Gy (30-50Gy), delivered in 5 fractions. Toxicities were recorded using Common Terminology Criteria for Adverse Events (CTCAE) v5.0 during radiotherapy (RT) and at three, six, nine and 12 months follow up. Survival was estimated using Kaplan-Meier method.

Results: Between April 2017 and August 2022, 15 patients with PC were offered SBRT. The main indication was palliation for local control; while in two patients, SBRT was delivered for oligo-metastatic disease, in two other patients as neoadjuvant therapy post-chemotherapy for conversion into resectable disease and in one patient as salvage for local failure after surgery. Patients were given an average of 10 cycles of induction chemotherapy. FOLFIRINOX was given to 40% patients while other patients received gemcitabine, nab-paclitaxel and FOLFIRI. The median age of the patients was 70 years (range: 47-85). The median follow-up from date of diagnosis was 17.4 months (range: 3.4-74). The overall survival (OS) was 100% at one year and 76% at two years. The progression-free survival (PFS) was 65.6% at six months, 54.7% at nine months and 41% at one year. The median survival was 28.18 months and median PFS was 11.2 months. The one-year and six-month local control rates were 50.8 % and 71% respectively. The median values for treated target volumes were 75.1 cm^3 for PTV, 28.6 cm^3 for gross tumour volume (GTV) and 24.8 cm^3 for internal target volume (ITV). We found the median treatment time utilized for delivering SBRT using AC technique was 275 sec, which is approximately half of the time required for SBRT treatment using EEBH technique, which was 526 sec. No radiation related toxicities were reported during RT and at three and six months follow up. Two patients developed GI/II gastrointestinal (GI) bleeding due to disease progression at six and nine months respectively during follow up while one patient developed lower GI bleed at six months. Total three deaths were reported, two patients died of progression while one patient was died of other reasons.

Conclusions: We are successful in implementing SBRT program at our centre. EEBH was found to be the preferred motion management technique despite longer treatment times. SBRT appears to be a promising treatment option to achieve LC with limited acute toxicities. Future studies involving dose escalation are planned as part of a clinical trial.

207

TOXICITY AND CLINICAL OUTCOMES TO ABDOMINAL RADIOTHERAPY USING 5 FRACTIONS FOR NON-SURGICAL PATIENTS

Rie Asso[1], Fabio Cury[2], Carolyn Freeman[1], Neil Kopek[1]
[1]McGill University Health Centre, Montréal, QC
[2]McGill University, Montréal, QC

Purpose: Surgery is the standard treatment for several primary abdominal tumours, including pancreatic and retroperitoneal sarcomas. Abdominal radiotherapy is often considered, either consolidative or as a non-surgical alternative when resection is not possible. Hypofractionated radiation therapy (HFRT) offers logistical advantages in terms of both patient convenience but also ease of integration within a multimodality treatment strategy that seeks to minimize delays and interruptions in systemic therapy. In addition, there is a potential radiobiological advantage with respect to overcoming relative radioresistance. Applying HFRT to abdominal tumours, however, could be limited by the tolerance of normal surrounding organs. To analyze toxicity and clinical outcomes in patients treated with five fraction HFRT for non-surgical pancreatic tumours and retroperitoneal sarcomas.

Materials and Methods: This is a single institution retrospective review of pancreatic and sarcoma patients treated between 2011 and 2022 with five fractions HFRT to doses between 25 to 30Gy. Cases treated with exclusively palliative intent were excluded, as cases where the HFRT was part of a pre-operative strategy. Patients who were previously resected and/or received chemotherapy were included. Descriptive statistics were used to analyze demographic and disease characteristics. NCI Common Terminology Criteria for Adverse Events version 5.0 were used for toxicity grading. Kaplan-Meier method estimated the clinical outcomes.

Results: Forty-nine cases, nine with sarcoma and 40 with pancreas cancer confirmed by pathology, were reviewed. The mean age was 68 years [range: 32-93]. The most common prescription dose was 30Gy (N=25) in five fractions typically delivered on non-consecutive days. The majority of cases received previous chemotherapy (79%), and more than one-quarter (28.5%) had previous surgery for the primary disease. The mean size of the tumours was 4.7 cm and 43 had a single lesion. During planning, a 4DCT was done to assess for respiratory motion and generate an ITV. Among the 49 patients, 75.5% presented acute side effects. The most common acute side effect was fatigue (42.8%), followed by nausea (24.5%), and abdominal pain (22.4%), all low grade with one case of Grade 3 acute abdominal pain. Chronic side effects were observed in 15 patients, abdominal pain being the most frequent. Bowel perforation (n=2) and cholangitis (n=3) were observed in the context of disease progression. At the time of analysis, 81.6% (n=40) of patients had died. Seven patients had no follow-up. Local control (Figure 1)/ metastases free survival and OS (Figure 3) at six months and one year: 62.8%/36.4%/61.4% and 42.5%/19.4%/38.3%, respectively. The median overall survival was nine months.

Conclusions: HFRT in five fractions for abdominal tumours appears to be well tolerated with encouraging rates of local control in this cohort of non-surgical candidates.

208

SINGLE-INSTITUTION OUTCOMES OF CYBERKNIFE SBRT IN RENAL CELL CARCINOMA

Osbert Zalay, Janice Doody, Julia Malone, Shawn Malone
The Ottawa Hospital, Ottawa, ON

Purpose: The standard of care for localized renal cell carcinoma (RCC) is surgical resection with total nephrectomy for Stage T1b (>4 cm) or higher tumours, or partial nephrectomy for smaller tumours. Stereotactic Body Radiotherapy (SBRT) is available for patients who are medically inoperable and for those with a solitary kidney, in order to preserve renal function. Although no level A evidence exists for the use of SBRT in RCC, recent studies including a meta-analysis (Correa et al., 2019) and updated reporting from the International Radiosurgery Oncology Consortium for Kidney (IROCK), suggest that SBRT in this setting is both effective and safe. Here we present our single-institution experience.

Materials and Methods: We performed a retrospective review of patients with localized RCC treated at the Ottawa Hospital between 2011 and 2020 with curative-intent SBRT using the Cyberknife radiosurgery system. Image guidance relied on fiducials being placed within the kidney to track tumour motion with Synchrony™ (Accuray). The planning target volume was the gross tumour volume plus a 5 mm margin. Eight patients were treated to 39 Gy in 3 fractions. Five patients were treated with 35-40 Gy in 5 fractions in order to respect small bowel tolerance. Clinical and imaging follow-up was performed every six months for two years, then annually afterwards. We looked at survival, recurrences and toxicity, and used Kaplan-Meier analysis to obtain actuarial estimate of relapse risk with time.

Results: Ten of the 13 patients were medically inoperable, two had solitary kidney and one patient had an unresectable local relapse with direct invasion of the vertebral column (non-metastatic). The mean age of patients was 81 years (range 65-90 years). Mean tumour size was 36 cc (range 11-79 cc) and mean PTV was 64 cc (range 29-136 cc). Two patients developed nausea and/or emesis, two patients suffered from fatigue and the one patient who had local invasion of the bony spine experienced a pain flare. A delayed SBRT fracture occurred in the patient with local relapse, 1 patient had a modest decline in renal function as measured by creatinine clearance. There was no incidence of late bowel toxicity. Local failure occurred in one patient. One patient developed metastatic disease. There were no deaths from RCC.

Conclusions: Our retrospective centre-specific experience demonstrates that SBRT is an effective treatment for localized RCC, with minimal toxicity and durable tumour control, consistent with reported outcomes from studies performed elsewhere.

209

CHANGE OF THE NEUTROPHIL TO LYMPHOCYTE RATIO DURING TREATMENT: A POTENTIAL PROGNOSTIC BIOMARKER IN METASTATIC PROSTATE CANCER TREATED WITH RADIUM-223 DICHLORIDE

Cédric Charrois-Durand, Kevin Kaulanjan, Johanna Dahan, Fred Saad, Guila Delouya, Edouard Auclin, Daniel Taussky
University of Montréal, Montréal, QC

Purpose: The neutrophil to lymphocyte ratio (NLR) at baseline has been shown to have prognostic value in metastatic prostate cancer. Little is known about the importance of a change in the NLR during treatment in patients treated with Radium-223 (^{223}Ra). We investigated the prognostic value of the NLR at baseline and during therapy in patients with metastatic prostate cancer treated with ^{223}Ra.

Materials and Methods: We reviewed all patients treated with ^{223}Ra in our centre. Patients were stratified according to NLR ≤5 and >5 at baseline and at 12 weeks of therapy. Overall survival (OS) was estimated by the Kaplan-Meier method and compared with the Log Rank test. The association between NLR measured at baseline and at 12 weeks and OS were evaluated using univariate and mulivariable Cox models.

Results: A total of 149 patients treated with ^{223}Ra were evaluated. OS was significantly longer in patients that had an NLR ≤5 (versus >5) at baseline (14.5 months [95% CI 10.2–16.4] versus 8.5 months [95% CI 6.8–10.5], p<0.0001) and at 12 weeks (15.0 months [95% CI 12.7–21.4] versus 9.5 months [95% CI 8.3–18.4), p=0.03). Patients with a baseline NLR ≤5 that remained ≤5 at 12 weeks of treatment had significantly longer median survivals (16.0 months [95% CI 14.8–25.5]) compared to patients whose NLR was ≤5 at baseline that converted at 12 weeks to >5 (9.1 months [95% CI 7.1–NR]), p=0.001.

Conclusions: In the present study, NLR at baseline and after 12 weeks of ^{223}Ra therapy were found to be of prognostic value. Those findings needs to be validated in larger prospective cohorts.

210

CONTOUR AGREEMENT? ACCURACY? WHAT ABOUT A DOSIMETRIC PERSPECTIVE ON WHEN MILLIMETERS MATTER IN CERVIX EXTERNAL BEAM RADIOTHERAPY?

Geetha Menon[1,2], Brenda Rose[1], Patricia Oliva[2], Fleur Huang[1,2]
[1]*Cross Cancer Institute, Edmonton, AB*
[2]*University of Alberta, Edmonton, AB*

Purpose: Inter- and intra-observer contouring variability has been well studied in cervical external beam radiotherapy (EBRT), with main interest being the target volumes. Organ at risk (OAR) contouring accuracy is an area of emerging study as autocontouring algorithms and streamlining efforts evolve. Systematic variability in OAR segmentation may exist but the dosimetric impact is not well-characterized. We explored to what extent millimeter-changes in OAR contours might alter dose-volume metrics in locally advanced cervical cancer (LACC) EBRT.

Materials and Methods: EBRT plans for LACC, contoured (by a single observer) and planned as per the EMBRACE-II protocol, were included. CT-delineated OAR volumes were taken as ground truth (GT). Bladder (BL), rectum (RC), sigmoid (SG), and bowel (BW) were systematically expanded or contracted (±1, 2, 3 mm, from outer edge); components outside PTV45 but inside the 30 Gy and 40 Gy isodose clouds (IDL), respectively, were isolated. A similar method was applied to components inside PTV45 (modulating the OAR edge that lies within PTV45). For all OAR and intermediate structures, dose-volume metrics (shown as median [range]) and relative anatomic information were extracted. Descriptive statistics were applied.

Results: Ten VMAT plans (patients treated 11/2018 - 12/2021) were selected, all prescribed 45 Gy in 25 fx. Half had simultaneous integrated boost (SIB) to pelvic (55 Gy) and/or para-aortic (PA; 57.5 Gy) involved nodes. PTV45 (1727.3 [1125.0 – 2256.5] cm^3) D95 was 95.8 [95.0 – 99.1]% and plan conformality index was 1.0 [0.9 – 1.4]. Except for rectum V40 (78.6 [65.9 – 100.0]%), planning constraints were met for all GT OARs (V30/V40 Gy for bladder 79.9/56.5%, bowel 286/107.9 cm^3 (no PA) and 613.2/245.1 cm^3 (with PA), sigmoid Dmax 100.6%, rectum V30 94.7%). Nearly 1/3 of GT bladder was inside the 30Gy-IDL, compared to 10.0 – 16.7% for other OARs. As expected, smaller GT OAR fractions lay within the 40Gy-IDL (1.9 – 7.1%). GT OARs were all partly inside PTV45, but to different degrees: rectum 72.3% > sigmoid 59.0% > bladder 50.5% > bowel 7.3%. Compared to RC and SG, volume changes were smaller within 30Gy-IDL (and 40Gy-IDL): -13.8 – +24.3 (-16.5 – +11.8) and -20.6 – +18.9 (-17.0 – +24.5)%, for BL and BW components, respectively, for ±3 mm contour modulation. RC volume within the 30Gy-IDL, for a ±1 mm variation, spanned -30.3 – +71.2% (±2 mm: -47.0 – +115.2%; ±3 mm: -57.6 – 137.1%). Proportional changes showed a broad range, although absolute volumes were small for these variances (RC 12.9/6.3cc and SG 27.8/6.3cc within the 30Gy-/40Gy-IDLs for a ±3 mm change). Corresponding dose differences within the 30Gy-/40Gy-IDLs were <1% for all OARs except RC: 3.2/4.4% for ±3 mm contour variation. OAR volume change within PTV45, which was greatest for SG (149.9%) and SB (114.7%) for a ±3 mm change in contour, also impacted dose (5.7% and 6.2% difference in Dmax, respectively); proximity to PA nodal SIB was a contributing factor.

Conclusions: In this EBRT planning exercise, systematic over- or under-contouring of OARs showed dose variances that could approach levels that may be of clinical significance. The practical implications require further study, including in MRI settings.

211

CAN THE G8 OBJECTIVELY IDENTIFY HNC SBRT CANDIDATES?

Christina Mallouk[1], Adam Mutsaers[2], Mohammed Aldohan[2], Ahmed Abugharib[2], Irene Karam[2], Andrew Bayley[2], Liying Zhang[2], Madette Galapin[2], Kevin Higgins[2], Danny Enepekides[2], Ian Poon[2], Antoine Eskander[2]
[1]*University of Ottawa, Ottawa, ON*
[2]*University of Toronto, Toronto, ON*

Purpose: Stereotactic body radiotherapy (SBRT) has been increasingly utilized in head and neck cancer (HNC) for patients who have been identified as unfit for conventional, radical treatment using subjective physician assessment and holistic multidisciplinary discussions. An objective measurement involving a combination of TNM staging and the use of the validated oncologic Geriatric 8 (G8) scale is hypothesized to be useful in standardizing the process by which patients are deemed unfit for radical treatment and therefore are considered candidates for SBRT.

Materials and Methods: This retrospective analysis included patients with squamous cell carcinoma (SCC) of the HN who received SBRT at a large Canadian cancer program. Patient factors including age, BMI, degree of weight loss, food intake, etc. were abstracted retrospectively from electronic medical records to formulate a G8 score for each patient. This value, along with the TNM stage, was analyzed against a validated cut-off to classify the patient as UNFIT (UF) or FIT (F) (UF when G8 <11 if T0-3 and/or N0-2 OR ≤14 if T4 and/or N3). The number of UF and F patients were then quantified and compared against the number of subjectively unfit patients as a measure of accuracy. The demographics and clinical characteristics of the UF and F groups were also compared using Wilcoxon rank-sum nonparametric test and Fisher's exact test. To search for significant predictive factors related to the binary outcome of UF versus F, a multivariate logistic regression model was performed using variables such as gender, M stage, primary tumour site (PS), maximum tumour diameter (MD), radiation dose, year of last fraction, and the presence of symptoms, caregivers, and recent hospitalizations.

Results: One hundred eighteen patients with a median age of 85 (54-102), a median radiation dose of 45 Gy (30-50 Gy), and a median maximum tumour diameter of 40 mm (4-100 mm). Eighty-two of the patients (69.5%) had an M-stage of M0, 24 (20.3%) an M-stage of MX, and 11 (9.3%) an M-stage of M1. PSs included skin (35.6%), oral cavity (28.0%), nodal (22.0%), and pharynx (11.0%). Eighty-one (68.6%) patients were classified as UF and 37 (31.4%) as F. On multivariate analysis, MD was found to be significantly positively correlated to the outcome of UF versus F (p=0.0196). PS was also found to be significantly correlated to the outcome

(p=0.0140), with oral cavity tumours having a stronger correlation than skin, pharynx, or nodal tumours.

Conclusions: The majority of subjectively unfit patients were categorized as UF with the G8 scale, suggesting that this method may be an accurate objective measure, although variables such as MD and PS seem to significantly affect this result and should be considered both in future studies and when evaluating patients for SBRT consideration.

212

ASSOCIATION OF TUMOUR VOLUME WITH SURVIVAL IN T3 SUPRAGLOTTIC CANCERS MANAGED WITH RADIOTHERAPY

Nauman Malik[1], Michael Hier[2,3], Grégoire Morand[2,3], Rui Fu[4], Nicolin Hainc[5], Shao Hui (Sophie) Huang[4], Eugene Yu[4], Stephanie Johnson-Obaseki[6], Jonathan Whelan[6], John Lysack[7], Wayne Matthews[7], Adam Globerman[8], Paul Kerr[8], Pejman Maralani[9,4], Irene Karam[9,4], Antoine Eskander[4,9]
[1]*University of California, San Francisco, CA*
[2]*McGill University, Montréal, QC*
[3]*Lady Davis Institute for Medical Research, Jewish General Hospital, Montréal, QC*
[4]*University of Toronto, Toronto, ON*
[5]*University of Zurich, Zurich, CH*
[6]*University of Ottawa, Ottawa, ON*
[7]*University of Calgary, Calgary, AB*
[8]*University of Manitoba, Winnipeg, MB*
[9]*Sunnybrook Health Sciences Centre, Toronto, ON*

Purpose: Prior retrospective evidence has suggested higher tumour volume (TV) is associated with worse outcomes in T3 larynx cancers managed with radiotherapy, however these were single centre reports and included patients treated before intensity modulated radiotherapy (IMRT) era. The purpose of this study was to investigate the association of TV and outcomes in T3 supraglottic cancers managed with radiotherapy.

Materials and Methods: This was a retrospective study involving seven Canadian cancer centres as part of the Canadian Head & Neck Collaborative Research Initiative. Patients diagnosed with American Joint Committee on Cancer (AJCC 7th ed) cT3 N0 M0 supraglottic carcinoma from 2002 - 2018 and treated with curative intent radiotherapy were included. IMRT use and availability of diagnostic imaging to abstract TV were required. Expert neuroradiologists used a standardized operating protocol to measure and report TV across all centres. Primary outcomes were overall survival (OS) and disease-free survival (DFS); secondary outcomes were laryngectomy free survival and onset of late Grade ≥3 toxicity as per CTCAE 5.0, > 6 months after treatment. A restricted cubic spline analysis with five knots and linearity of hazard was tested. Kaplan-Meier estimates were used for OS and DFS, and Cox proportional hazards for survival hazard ratios.

Results: Two hundred thirty-nine patients met inclusion criteria, 176 (73.6%) males with mean (standard deviation, SD) age 65.21 (9.43) years. 90 patients (38%) were N0, 32 (13%) were N1, 3 (1%) were N2a, 60 (25%) were N2b, 47 (20%) were N2c, and 7 (3%) were N3. 151 (64%) of patients received concurrent systemic therapy. Mean (SD) tumour volume was 11.37 (12.11) cm^3, and median volume was 7.80 cm^3 (interquartile range [IQR] 4.56 – 14.47 cm^3) With a median follow-up of 2.76 (IQR 1.29-4.44) years, two-year OS was 72.7% (95% confidence interval [CI] 66.9 – 78.9%), two-year DFS was 53.6% (95 %CI 47.4 – 60.6%). The linearity assumption of hazard could not be rejected for both OS and DFS (p>0.05), and volume was analyzed as a continuous variable. In multivariable analyses, larger TV was associated with worse OS (HR per 1cm^3 increase 1.01, 95% CI: 1.00-1.02, p<0.01) and DFS (HR per cm^3 increase 1.01, 95% CI, 1.00 – 1.02, p=0.02), and receiving systemic therapy was associated with improved OS (HR 0.36, 95% CI 0.23 – 0.57, p<0.01). Two-year cumulative incidence of laryngectomy was 14.4% (95% CI 9.5 – 19.4%), while two-year late Grade ≥3 toxicity was 18.4% (95% CI 13.3 – 23.5%).

Conclusions: Higher TV in T3 supraglottic cancers managed with IMRT is associated with worse overall survival and disease-free survival with no clear threshold seen, and concurrent systemic therapy improved overall survival. Patients with large TV and poor baseline laryngeal function should be considered for upfront laryngectomy and risk-adapted adjuvant therapy.

213

MODERNIZATION OF NASAL PROTHESIS FABRICATION THROUGH THE USE OF THE BLENDER API, 3D SCANNING AND PRINTING

Daniel Markel[1], Eric Dufresne[2], Karim Zerouali[2], Stephane Bedwani[1]
[1]*Université de Montréal, Montréal, QC*
[2]*Centre Hospitalier de l'Université de Montréal' Montréal, QC*

Purpose: To improve the efficiency, functionality and cost of nasal prosthesis production for cancer patients who have received a full or partial surgical resection of the nose. The main objective of this work is to digitize the entire workflow for nasal prosthesis creation by incorporating automation, 3D scanning and printing.

Materials and Methods: An industrial handheld 3D scanner (Artec, Luxembourg) is used to provide high resolution facial scans (0.1 mm) of the patient, specifically the nasal cavity and surrounding area. This has the advantage of minimizing geometric distortions compared to an analogue casting process. Using Zbrush (Pixologic, Los Angeles, CA, USA), the nose is sculpted digitally in 3D with the assistance of photographs taken prior to the surgery. Using the nose model and facial scan, an in-house Python script using the Blender API (Blender Foundation, Amsterdam, The Netherlands) fully automates the creation of a mold using a series of morphological procedures and rules. This includes the generation of both male and female pieces along with an insert to maintain breathing channels and a synthetic septum in order to mimic the functionality and feel of a real nose. The molds are then 3D printed and filled with silicon mixed with dyes in order to match the patients' skin tone. Additional aesthetic flourishes are then added manually such as the addition of synthetic hair and dyes to create a realistic texture.

Results: The new workflow is able to reduce the nasal prosthesis production time from a manually intensive two days to six hours excluding printing time. This time and material savings between the two processes translates to an approximate cost reduction of $545 per prosthetic or 40% of the conventional cost of production. As of this writing, four patients have had prostheses created from the new semi-automatic pipeline.

Conclusions: The incorporation of 3D scanning/printing and the Blender API have allowed the semi-automatization of nasal prosthesis fabrication, reducing the time and cost while maintaining if not improving the quality of the prothesis. Digitization of the process improves fidelity compared to analogue plaster molds and allows molds and the prosthesis to be easily reprinted and recast at a future date, which is not always possible with plaster molds should they become damaged over time. Some challenges remain to fully account for the variability of patient morphology which can cause failures in the mold generation script.

214

FILLING THE GAP: IMPROVING COMMUNICATION BETWEEN THE DENTISTRY AND RADIOTHERAPY DEPARTMENTS

Madette Galapin[1], Melanie Gilbert[2,3], Andrew Bayley[1,3], Irene

Karam[1,3], Francois Gallant[1], Lee Chin[1,3], Hari Zafiriadis[1], Kevin Nazareth[1], Darby Erler[1,3], Ian Poon[1,3]
[1]Sunnybrook-Odette Cancer Centre, Toronto, ON
[2]Sunnybrook Health Sciences Centre, Toronto, ON
[3]University of Toronto, Toronto, ON

Purpose: Patients with head and neck cancer (HNC) should have a consultation with a dentist experienced in radiotherapy (XRT) side effects prior to the start of XRT, ideally before simulation (sim). In our institution, patients frequently had their sim and dental consultation on the same day resulting in confusion as to whether to proceed with or delay sim. Additionally, some patients who had dental extractions (DEs) after sim required a repeat sim (resim) due to a change in the resting jaw position, which subsequently delayed the start of XRT. The aim of this quality improvement (QI) initiative was to prevent unnecessary resims and delays to starting XRT for HNC patients by improving the communication between the Departments of Dentistry and Radiotherapy.

Materials and Methods: An email communication template was developed collaboratively between the Departments of Dentistry and Radiotherapy. The template included information on: the date of planned DEs; which teeth were to be extracted; whether the DEs would cause a change to the resting jaw position; and the suggested number of days for healing. From October 2020 – October 2021, 70 HNC patients seen in consultation with Dentistry required DEs. Emails were sent by the dentist to the Clinical Specialist Radiation Therapist (CSRT) for triaging. A collaborative decision with the Radiation Oncologist (RO) was made to: delay sim or start of XRT; proceed with XRT with mandatory review of first day verification images by the RO and/or CSRT; include an oral assessment by the RO during sim; order a resim; or proceed without intervention.

Results: Of the 70 patients triaged by the CSRT, 32 (46%) required an intervention. The HNC medical physicist evaluated the dosimetry of seven cases where DEs were done after sim and found that only three showed insignificant increases to max doses when the high dose volume was adjacent to the extraction, and none had any significant dose increases to adjacent organs at risk. A decision tree was developed collaboratively with the HNC Radiation Site Group that identified five clinical scenarios for HNC patients who require DEs and the possible decisions required by the ROs. A change to practice was implemented in which the sim radiation therapists (RTTs) were made responsible for triaging the Dentistry team's email communications.

Conclusions: The new channel of communication between the two Departments allow RTTs and ROs to appropriately identify which patients need an intervention to prevent unnecessary resims or delays in starting XRT. This QI initiative also increased awareness amongst the RTTs on the impact of DEs, promoted professional autonomy, and strengthened collaborative decision making. Challenges involved the execution of the referral pathway since referrals for Dentistry and sim were sent at the same time, which increased the likelihood of DEs occurring after sim. A future QI initiative will be undertaken to improve the referral pathway.

215
SURVIVAL OUTCOMES OF EXTENSIVE STAGE SMALL CELL LUNG CANCER PATIENTS TREATED WITH CONSOLIDATIVE THORACIC RADIOTHERAPY AT A TERTIARY CANCER CENTRE

Vijithan Sugumar, Rohan Salunkhe, Xiang Y. Ye, Luna Zhan, Alexander Sun, Andrea Bezjak, John Cho, Srinivas Raman, Andrew J. Hope, Meredith E. Giuliani, Natasha B. Leighl, Adrian G. Sacher, Frances A. Shepherd, Penelope Bradbury, Geoffrey Liu, Benjamin H. Lok
University of Toronto, Toronto, ON

Purpose: Most small cell lung cancer cases present as Stage IV (M1) or extensive stage (ES-SCLC), which are defined as tumour extending outside the hemithorax without a tolerable radiation portal. The CREST trial demonstrated improved local control with a modest overall survival (OS) benefit at the two-year secondary end point of 14% survival with consolidative thoracic radiotherapy (CTRT) compared to 3% without CTRT. Low toxicity rates were also observed. This study reports our institutional ES-SCLC experience for patients treated with CTRT.

Materials and Methods: A retrospective review was conducted on ES-SCLC patients treated with CTRT at our institution between 2014 and 2019. CTRT was defined as ≥30Gy of thoracic radiotherapy. OS and tolerability of treatment were assessed in this population. Chemotherapy details were also captured. OS rate was determined using the Kaplan-Meier method and the time from start of CTRT to last date of follow-up or death. CTRT tolerability was determined using incidence and grade of esophagitis and radiation pneumonitis as per CTCAE v5.

Results: We identified 100 ES-SCLC patients treated with any thoracic RT at our institute, of which 45 received thoracic RT for palliative intent or with <30Gy. The remaining 55 patients received ≥30Gy CTRT and were included for analysis. The median age was 65.1 years (range 46.6-86.9) and 36 (65%) were male. The median follow-up for this sample was 0.8 (range 0.03-4.2) years. Median chemotherapy cycles were 6 (range 1-6), most receiving ≥4 cycles (87%) and completing chemotherapy prior to CTRT initiation (91%) with a minority concurrently receiving chemotherapy and CTRT (9%). Platinum chemotherapy was the most common (96%) with 2 patients receiving etoposide alone (4%). The most common CTRT regimens were 30Gy in 10 fractions (80%) followed by 40Gy in 15 fractions (9%) and 45Gy in 30 twice-daily fractions (7%). Most patients (67%) were treated with IMRT/VMAT technique, while the remaining (33%) patients were treated with 3DCRT. The median survival time was 1.3 years with 1- and 2-year OS of 57.2% (CI 44.0 – 74.3%) and 26.1% (CI 12.9 – 52.7%), respectively. CTRT was well tolerated with no Grade 4+ toxicities. The most common toxicity was esophagitis with 21 patients (39%), of which 15 were G1 (28%) and six were G2 (11%). Radiation pneumonitis was present in five patients (9.2%) with one G1 (2%), three G2 (6%), and one G3 (2%) cases.

Conclusions: Consolidative TRT for ES-SCLC in this institutional series was at least as good as the reported CREST outcome with modest acute toxicities in this cohort. Disease burden at diagnosis, chemotherapy response, patterns of failure, and subsequent therapies will be further investigated.

216
IMPACT OF INTRA-FRACTION MOTION CORRECTION ON TARGET AND OAR DOSIMETRY IN SINGLE FRACTION LUNG STEREOTACTIC ABLATIVE RADIATION THERAPY

Clara Fallone, Alasdair Syme
Dalhousie University, Halifax, NS

Purpose: This research assesses the impact of intra-fraction motion correction on target and OAR dosimetry in single-fraction lung stereotactic ablative radiation therapy (SABR).

Materials and Methods: Thirteen NSCLC patients were treated with linac-based free-breathing single-fraction lung SABR. Cone-beam CT images were acquired surrounding each treatment arc and following any position changes. Images were matched to the reference CT simulation image and differences between the actual patient position and the reference position were obtained for three orthogonal directions. The movement of each patient in the treatment planning system was modelled given the omission (Case 1) or application (Case 2) of intra-fraction motion correction.

Arc isocentres in each plan were specified to represent the calculated patient deviation for each modelled case and plans were forward-calculated using the original monitor units. OAR and target metrics were computed and compared for the original treatment plan and the modelled motion cases. The % isodose value that covered the full volume of the CTV was also determined for the treatment plan and modelled cases.

Results: As expected, modelling the impact of motion on the dose distribution yielded inferior target and OAR dosimetry compared to the original treatment plan. Not performing intra-fraction motion corrections yielded a 40% increase in the number of failed dosimetric objectives compared to completing corrections. Intra-fraction motion correction yielded fewer failed objectives in nine of 13 patients and an equivalent number in the remaining patients. Furthermore, the PTV volume covered by the 90% isodose line was 13% higher on average with intra-fraction motion correction. Larger minimum dose values (14% on average) were observed in the PTV when corrections were applied. In 12 of 13 patients (>90%), intra-fraction motion corrections led to >90% isodose line CTV coverage. This finding suggests that PTV margin reduction can be considered if intra-fraction motion corrections are applied, based on van Herk margin guidelines.

Conclusions: Intra-fraction motion correction yields improved target and OAR dosimetry in single-fraction lung SABR.

217
TOXICITY OF PATIENTS WITH ULTRA-CENTRAL THORACIC TUMOURS TREATED WITH STEREOTACTIC BODY RADIOTHERAPY WITH DOSE OF 50Gy IN 5 FRACTIONS

Rie Asso, Neil Kopek, Marie Duclos, Bassam Abdulkarim, Tanner Connel, Paul Ramia, Asma Saidi, Sergio Faria
McGill University Health Centre, Montréal, QC

Purpose: The ideal regimen for stereotactic body radiotherapy (SBRT) in ultra-central lung tumours is still to be defined, mostly due to the risk of unacceptable or fatal toxicity. There is not much information on outcomes after SBRT for this group of patients. We summarize here our experience with ultra-central lung cancer patients treated with the dose of 50 Gy delivered in 5 fractions.

Materials and Methods: This study is a retrospective review of all cases of ultra-central thoracic tumours treated with SBRT with the dose of 50Gy in 5 fractions, delivered every other day at our institution. In all cases, as we defined ultra-central lung tumour, the PTV overlapped or touched one or more of the following structures: bronchial tree, trachea, great vessels, heart, and esophagus. Metastatic and primary lung lesions were included. The volumes of treatment were defined by 4D-CT to consider breathing motion. Normal organ constraints followed the recommendations of the RTO 0813 trial as follows: Spinal cord: max 30Gy. Lung right or lung left: V13Gy[cc] < 1500. Esophagus: Max: 52Gy and nonadjacent esophagus: V27.5Gy[cc] < 5. Heart: V32Gy[cc] < 15; max 52Gy. Great vessels: Max 52Gy and non-adjacent great vessels V47Gy[cc] < 10. Trachea plus bronchus: Max 52Gy and non-adjacent V18Gy[cc] < 4. Follow-up, at the discretion of the treating MD, included periodic CT scans of the thorax after SBRT and assessment of radiation-induced toxicity scored with CTCv3.0.

Results: Between December 2015 and February 2022, 86 patients were eligible for this review. Median follow-up was 17 months (range: 1-76 months); the median age was 74 years (range: 37-98 years). Histology was as follows: 50 patients had biopsy proved NSCLC, 16 had no biopsy, and 20 had metastatic non-lung primaries. Overlapped structures were as follows: with great vessels in 46 cases, heart in 20 cases, trachea/branchial tree in 18 cases, and esophagus in two cases. In 16 patients the overlap was present in more than one structure. Overall, 68.6% did not report acute toxicity. The most common acute side effects were fatigue (15.1%), coughing (8.1%), shortness of breath (6.9%), esophagitis (2.3%), and dysphagia (1.1%). No Grade 3 or more significant toxicity was described. As acute side effects, many patients had exacerbations of the previous condition, such as shortness of breath (16 patients) or coughing (four patients) during follow-up. Pneumonitis was found as a late side effect in four cases. One patient had empyema associated with a fistula in the non-irradiated lung, where the patient had previous surgery, but in the irradiated lung, no severe complication was detected. There were no deaths attributed to the SBRT treatment. 67.5% of 86 patients were alive at the time of the review; 87.2% had local control, and 65.1% had metastases-free survival.

Conclusions: In this cohort of patients, no death or even severe acute or chronic toxicity was attributed to SBRT. SBRT seems safe for ultra-central lesions using the regimen of 50Gy in 5 fractions with the constraints of the RTOG 0813 trial.

218
MANAGEMENT OF VERY EARLY SMALL CELL LUNG CANCER: A CANADIAN SURVEY STUDY

Bayan Malakouti-Nejad, Sara Moore, Paul Wheatley-Price, David Tiberi
The Ottawa Hospital, Ottawa, ON

Purpose: Concurrent chemoradiotherapy (CRT) is the gold standard in management of limited-stage small cell lung cancer (LS-SCLC). Local therapy with surgery or stereotactic radiotherapy (SBRT), followed by adjuvant chemotherapy may be appropriate in patients with very early (T1-T2, N0) disease. This study aimed to determine practice patterns for very early LS-SCLC among lung cancer specialists in Canada.

Materials and Methods: A survey was developed and distributed to Canadian medical and radiation oncologists specializing in lung cancer. The survey consisted of three sections: (1) physician demographics, (2) general practice approach, and (3) preferred approach for three clinical scenarios: (1) a peripheral T1 lesion; (2) a central T1 lesion; (3) a peripheral T2 lesion). Responses were analyzed to detect differences in management across cases and among physician groups.

Results: A total of 77 physicians participated. In Case 1, when the patient was eligible for surgery, most respondents (73%) chose surgery with adjuvant chemotherapy as their preferred management, with only 19% choosing CRT. CRT was selected by a higher proportion in Case 2 (48%) and Case 3 (61%) ($p<0.05$). If medically operable, most chose CRT over SBRT and adjuvant chemotherapy in all cases. CRT was significantly more popular in Case 2 (84%) and Case 3 (86%) than in Case 1 (55%) ($p<0.05$). Subgroup analysis showed physicians from Western Canadian were more likely to choose CRT, those from Ontario were more likely to offer SBRT, and those who have spent longer in practice were more likely to choose CRT over local therapy.

Conclusions: There is significant variation in practice patterns for management of very early LS-SCLC in Canada. CRT remains the most popular strategy in most cases, with surgery and adjuvant chemotherapy preferred for small peripheral lesions. Larger and more central tumours are more likely to be managed with CRT. Variation in practice is correlated to region and physician experience.

219
A DIGITAL WORKFLOW TO CREATE PATIENT-SPECIFIC RADIATION ORAL SHIELDS FOR ORTHOVOLTAGE

Renée Larouche[1,2], Charles Martel[1,2], Martin Lebeau[1], Andrée Jutras[1], David Roberge[1,2], Stéphane Bedwani[1,3]
[1]Centre Hospitalier de l'Université de Montréal, Montréal, QC
[2]Université de Montréal, Montréal, QC
[3]Centre de Recherche du Centre Hospitalier de l'Université de Montréal (crCHUM), Montréal, QC

Purpose: Integrating 3D technologies in the clinic allows new workflows to emerge and improve patient care. A specific workflow was developed to replace our handmade oral shields used in orthovoltage radiation therapy.

Materials and Methods: The new workflow requires the patient to have one additional appointment before his orthovoltage treatments to produce one or more dental impressions. Each impression is later digitally reconstructed using a 3D optical scanner. A custom oral shield is then designed from the reconstruction. The device is subsequently produced using a stereolithography 3D printer with a biocompatible resin. A 1-mm lead sheet is then shaped on the device and covered by a thin layer of the same biocompatible resin that is cured by UV light. The assembled device is finally sterilized in the autoclave. Attenuation and backscatter measurements were also conducted on a similar flat shield device before clinical implementation.

Results: The custom radiation oral shields fit well and protected the teeth and gums. Once in place, they didn't move. Patient comfort was improved by wetting the custom shields before insertion in their mouth. The installation was fast and did not require any adjustment, which simplified the technologist's task and reduced the patient's presence time. The custom radiation oral shield attenuated 99.5% of the incident beam and backscatter dose enhancement factor measurements showed an increase of only 0.1%.

Conclusions: We observed benefits to use 3D printed shields for patients receiving orthovoltage. Benefits include ease of installation, a custom shield with smooth edges that was easy to position, improved sanitary protocol, good attenuation properties and with very low backscatter contamination. Further advancement in orthovoltage will integrate optical 3D scanning and 3D printing to facilitate the making of patient-specific shields for different anatomical regions.

220
UNCOVERING THE ARMPIT OF AXILLARY SBRT

Adam Mutsaers, Jason Savio Fernandes, George Li, Saher Ali, Hanbo Chen, Gregory Czarnota, Irene Karam, Daniel Palhares, Ian Poon, Hany Soliman, Danny Vesprini, Patrick Cheung, Arjun Sahgal, Alexander V Louie
University of Toronto, Toronto, ON

Purpose: The growing use of stereotactic body radiotherapy (SBRT) in metastatic cancer has led to applications in new and unique anatomic locations, highlighting the importance of effective, safe, reproducible treatment delivery. The objective of this study was to review our institutional SBRT experience for axillary metastases (AM), focusing on outcomes, safety and process.

Materials and Methods: In this ethics approved single-institution retrospective review, patients treated with SBRT to AM from 2014-2022 had tumour, treatment planning, and dosimetric variables abstracted. Toxicity was assessed per Common Terminology for Adverse Events V5.0. Cumulative incidence functions were used to estimate the incidence of local failure (LF), with death as competing risk. Kaplan-Meier method was used to estimate progression-free (PFS) and overall survival (OS).

Results: We analyzed 37 patients with 39 AM who received SBRT. Patients were predominantly female (60%), Eastern Cooperative Oncology Group performance status 0-1 (62%), and elderly (median age: 72), with a median follow-up of 14.6 months. Common primary sites included breast (n=16, 43%), skin (n=7, 19%), and lung (n=5, 14%). Treatment indication included oligoprogression (n=18, 46%), oligometastases (n=14, 36%) and symptomatic progression (n=7, 18%). A minority had prior overlapping radiation (n=7, 18%) or regional surgery (n=4, 11%), while most had prior systemic therapy (n=26, 70%). Significant heterogeneity in simulation, planning and treatment was identified. Immobilization included 5-point thermoplastic mask (n=12, 32%), Vacloc (n=12, 32%) arms-up thorax bag (n=11, 30%). 4-D CT scans were obtained in 46%, MR simulation in 21%, and intravenous contrast in 10%. Median dose was 40Gy (interquartile range (IQR): 35-40) in 5 fractions, (BED_{10}=72Gy), over a median of 12 days (IQR: 9-14). Seventeen cases (44%) utilized a low-dose elective volume to cover remaining axilla; 14% used a high dose clinical target volume. Median planning target volume margin was 5mm (range: 3-10mm), and plans were generated with five different dose constraint protocols. At first radiographic assessment, 87% had partial or complete response, with a single progression. Of symptomatic patients (n=14), 57% had complete symptom resolution and 21% had improvement. One and two-year LF rate were 19% and 31%, respectively. Median OS was 21.0 months (95% [Confidence Interval (CI)] 17.3-not reached) and median PFS was 7.0 months (95% [CI] 4.3-11.3). Acute and late toxicities were uncommon, with two Grade 3 events (one plexopathy in a case with tumour involving brachial plexus, one skin ulceration) identified, and no Grade 4/5.

Conclusions: In this series of AM SBRT, low rates of toxicity, and good rates of LF and symptom improvement were observed. As treatment was delivered with a variety of individual treatment differences, an institutional protocol is under development to standardize technique, optimize efficiency and improve evaluability.

221
SURVEY ON THE STRUCTURE OF INPATIENT CARE PROVIDED BY RADIATION ONCOLOGISTS IN CANADA

Daniel Tesolin, Ege Babadagli, Michael Sun, Bayan Malakouti-Nejad, Jason Pantarotto, Marc Gaudet, Robert MacRae
University of Ottawa, Ottawa, ON

Purpose: There is variation in Canada regarding structure, size, and management of Radiation Oncology inpatient services. With the increasing complexity and specialization of radiotherapy practice, comparative data is required to guide decision-makers in this field to adequately design Radiation Oncology inpatient services.

Materials and Methods: A 27-item ethics approved survey was developed and distributed to Radiation Oncologists acting as Physician Leads for Radiation Oncology departments in academic and community cancer centres across Canada. The survey was distributed to 49 Physician Leads between June 2022 and January 2023. Descriptive statistics were used to evaluate the responses.

Results: The response rate was 59% (29/49). The respondents were distributed across seven different provinces. Of the centres, 38% (11/29) had a Royal College accredited residency training program, 66% (19/29) were community sites, and 55% (16/29) had a dedicated inpatient service. The number of inpatient beds per centre ranged from 0 to 20, with a median of 6. The number of linear accelerators per centre ranged from two to 12, with a median of five. The number of Radiation Oncologists employed per centre ranged from two to 22, with a median of 10. The number of consults seen by each centre per year ranged from 750 to 5000, with a median of 2520. The inpatient care model was evenly distributed with 55% (16/29) of centres acting as a consulting service either having no inpatients or inpatients admitted

under a hospitalist service, while 45% (13/29) of centres admitting their own inpatients with or without General Practitioners in Oncology, Nurse Practitioners or Physician Assistants to assist. Only 7% (two of 29) of centres where Radiation Oncologists acted as consultants-only had a residency training program. Only 21% (six of 29) of respondents believed Radiation Oncologists should admit patients as the most responsible physician and 50% (three of six) of those respondents indicated that admission should only be under a strict set of criteria. Most respondents, 79% (23/29), preferred to remain as a consultation service only, citing expertise and patient care concerns.

Conclusions: There is variability in the structure, size, and scope of practice of Radiation Oncology inpatient services across Canada. Overall, respondents believe that the scope of inpatient practice should be specifically tailored to suit the clinical expertise of Radiation Oncologists. This data may have implications for shaping inpatient practice in the future.

222

NEW ASPECTS REGARDING MARKERS FOR THE CLINICAL COURSE IN THE BLOOD OF PATIENTS WITH SARS-COV-2 INFECTION. A TOOL TO PROTECT OUR ONCOLOGY PATIENTS

Danny Jazmati, Edwin Boelke, Johannes Fischer, Yechan Flaig, Wilfried Budach, Amir Rezazadeh, Jan Haussmann, Balint Tamaskovics, Christiane Matuschek
Heinrich Heine University, Dusseldorf, DE

Purpose: SARS-CoV-2 is still a chalenge for our oncology patients. During radiochemotherapy some patients are not able to develop protective antibodies after vaccination against SARS-CoV-2. These patients are at more risk to develop Covid-19. A few investiations have detected a correlation between HLA variants and differential COVID-19 outcomes and have demonstrated that HLA genotypes are associated with differential immune responses against SARS-CoV-2, especially in severe ill patients. We wanted to find out which of our oncology patients are of high risk for a severe clinical outcome and if we could detect them with blood samples.

Materials and Methods: Next generation sequencing based-HLA typing was performed in 303 female and 231 male non-hospitalized North Rhine Westphalian patients infected with SARS-CoV2 during the first and second wave. For HLA-Class I we obtained results from 528 patients, and for HLA-Class-II from 531. In those patients, who became ill between March 2020 and January 2021, the 22 most common HLA class I (HLA-A, -B, -C) or HLA class II (HLA –DRB1/3/4, -DQA1, -DQB1) haplotypes were determined. The identified HLA haplotypes as well as the presence of a CCR5 32D mutation and number of O and A blood group alleles were associated to disease severity and duration of the disease.

Results: The influence of the HLA haplotypes on disease severity and duration was more pronounced than the influence of age, sex, or AB0 blood group. These association were sex dependent. The presence of mutated CCR5 resulted in a longer recovery period in males.

Conclusions: Certain HLA haplotypes are associated with a more severe clinical outcome. Therefore HLA testing could be an option to detect patients who are at risk for a more severe clinical outcome.

223

EVIDENCE TO GUIDE DAY-TO-DAY PRACTICE OF CONE-BEAM COMPUTER TOMOGRAPHY RE-IMAGING

Marzena Kastyak-Ibrahim[1,2], Bryan Kim[1,2], Joanna Foster[1], Amanda Jacques[1], Jean-david Jutras[1,2], Fiona Lochray[1], Lisa Barbera[1,2]
[1]*Tom Baker Cancer Centre, Calgary, AB*
[2]*University of Calgary, Calgary, AB*

Purpose: Cone-beam Computer Tomography (CBCT) imaging is an integral part of patient positioning prior to the delivery of radiation treatment. At our institution, when shifts applied from initial CBCT exceed the set tolerance specific to each tumour site, CBCT is repeated to ensure that the target is in the planned position. There are both benefits and costs associated with CBCT reimaging which directly impacts day-to-day clinical practice. A better understanding of the need to re-image is of interest to all professionals involved in the patient treatment. This study is part of a larger project aimed at evaluating our existing clinical practice of re-imaging, the reasons for re-imaging and determining the cases where the benefit of re-imaging is evident. The purpose of this preliminary study was to determine the frequency of CBCT re-imaging as dictated by site-specific protocols used in the clinic and to evaluate whether additional shifts were still required after re-imaging.

Materials and Methods: This is a prospective cross-sectional study. Over a two-week period, every patient requiring repeat CBCT was captured manually. We only included re-imaging cases where applied shifts exceeded our institutional tolerances for translational and rotational corrections. Repeat imaging related to bowel and bladder issues, as well as other set-up issues were excluded. Information collected included magnitude of couch shifts and rotations applied after CBCT re-imaging as well as tumour group.

Results: 1,945 fractions were delivered during the two-week observation window. Of these over 10% required re-imaging. More than 80% of the fractions during which re-imaging occurred were from patients with head and neck and brain cancer (the distribution between the two groups was even; the brain group did not include stereotactic radiosurgery patients). Almost two-thirds of re-imaging cases resulted from rotational corrections exceeding tolerance, while 21% and 16% of cases were due to the translation only corrections and translational combined with rotational corrections, respectively. On average, the absolute value of all the translational shifts (vertical, longitudinal, and latitudinal) applied after re-imaging was smaller than 0.2 cm and rotations shifts (Pitch, Roll, and Rotation) were smaller than 0.5°.

Conclusions: We conclude that CBCT re-imaging is common, seen most often in patients with head and neck or brain cancer. This preliminary work will lead to site-specific evaluations starting with brain and head and neck to find ways to further improve our clinical practice, while fostering interprofessional collaboration.

224

NEW ASPECTS REGARDING PERCUTANEOUS FRACTIONATED RADIOTHERAPY OF THE GROIN TO ELIMINATE LYMPHATIC FISTULAS AFTER VASCULAR SURGERY

Danny Jazmati, Edwin Bölke, Wilfried Budach, Jan Haussmann, Yechan Flaig, Balint Tamaskovics, Amir Rezazadeh, Christiane Matuschek
Heinrich Heine University, Dusseldorf, DE

Purpose: Vascular surgery of the inguinal area can be complicated by persistent lymphatic fistulas. Rapid and effective treatment is essential to prevent infection, sepsis, bleeding, and possible leg amputation. Current data on irradiation of lymphatic fistulas lacks of recommendation on the appropriate individual and total dose, the time of irradiation, and the target volume. Presumably, a dose of 0.3-0.5 to 1-12 Gy should be sufficient for the purpose. Currently, radiotherapy is a “can” recommendation, with a level 4 low evidence and a Grade C recommendation, according to

the DEGRO S2 guideline. As part of a pilot study, we analyzed the impact and limitations of low-dose radiation therapy in the treatment of inguinal lymphatic fistulas.

Materials and Methods: As part of an internal quality control project, patients irradiated in the groin area after vascular surgery arterial occlusive disease (AOD) III-IV, repair of pseudo aneurysm or lymph node dissection due to melanoma were selected, and an exploratory analysis on retrospectively collected data was performed.

Results: Twelve patients (10 men and two women) aged 62.83 ± 12.14 years underwent open vascular reconstruction surgery for Stage II (n= 2), III (n=1), and IV (n=7) arterial occlusive disease (AOD), lymph node dissection for melanoma (n=1) or repair of a pseudoaneurysm (n=1). Surgical vascular access was obtained through the groin and was associated with a persistent lymphatic fistula, secreting more than 50 ml/day. Patients were irradiated five times a week up to a maximum of 10 fractions for the duration of the radiation period. 0.4 Gy per fraction were applied in the first seven cases, while five patients were treated with a de-escalated dose of 0.3 Gy. The lymphatic fistula resolved in every patient, without higher grade complications.

Conclusions: Low-dose irradiation of the groin as a treatment option for persistent lymphatic fistula after inguinal vascular surgery is a possible therapeutic option to prevent wound infection and possible lower extremity amputation.

225

FUNCTIONAL AND TOXICITY OUTCOMES OF RADIATION THERAPY FOR DUPUYTREN'S CONTRACTURE

Justin Oh, Yi Peng Wang, Susan Hiniker
Stanford University, Stanford, CA

Purpose: The purpose of the study was to assess the patient function and satisfaction outcomes and to describe the incidence and nature of toxicty after radiotherapy for Dupuytren's contracture.

Materials and Methods: Patients who were treated for Dupuytren's contracture with radiation between 2019 - 2022 at a single institution were identified. Demographic, clinical, and treatment characteristics were collected. Validated Southhampton Dupuytren's Scoring Scheme (SDSS) survey and toxicity questionnaires were administered to the patients to assess the functional outcome and the rate and type of side effects. Kruskal Wallis test will be performed to identify factors associated with functional or toxicity outcomes.

Results: Twenty-seven patients were identified and consented to the surveys. There were no Grade 3 or higher acute or late side effects. Further data and analysis are pending.

Conclusions: Radiation treatment for Dupuytren's contracture is well tolerated with no incidence of Grade 3 or higher toxicity. Further conclusion about functional and satisfaction outcomes are pending.

226

OUTCOMES OF PEDIATRIC AND ADOLESCENT PATIENTS WITH METASTATIC SARCOMA TREATED WITH SURGICAL RESECTION OR STEREOTACTIC ABLATIVE RADIATION THERAPY

Justin Oh, Paulina Gutkin, Yi Peng Wang, Sarah Donaldson, Robert Steffner, Matias Bruzoni, Raffi Avedian, Sheri Spunt, Allison Pribnow, Susan Hiniker
Stanford University, Stanford, CA

Purpose: To determine the local recurrence (LR) and complication rates for surgical resection and SABR for metastatic sites in pediatric and adolescent patients with sarcomas.

Materials and Methods: A single institution retrospective-review of pediatric and adolescent patients (less than age 25) diagnosed with new or recurrent metastatic sarcoma and treated with SABR or surgery between 2009 – 2020 was conducted. Intracranial metastases were excluded. LR, defined as tumour recurrence at surgical site or within the planning target volume of SABR was determined for each treatment course. Local failure free survival (LFFS), defined as time from treatment course to either death or LR, was assessed by Kaplan Meier. Toxicity ≥ Grade 2 as per the National Cancer Institute Common Terminology Criteria for Adverse Events Version 5 (NCI-CTCAE) was recorded. Logistic regression analysis to assess factors associated with local failure is pending.

Results: Seventeen patients with median age of 18 years (range 2 – 23) were included. One hundred sixty-eight metastatic lesions were treated with 32 courses of radiotherapy and 35 resections. Median follow-up from surgery and SABR was 1.9 years and 1.2 years respectively. Median number of MDT was three per patient. Seven (41%) patients had osteosarcoma, four (24%) had synovial sarcoma, two (12%) had small round blue cell sarcoma, and the rest had other types. Median equivalent dose in 2Gy fraction for SABR was 88Gy (a/B = 3, range 54 – 140 Gy). The most common site treated by SABR was bone (23 of 32 courses) and by surgery was lung (32 of 35 resections). There were eight (23%) LRs in surgery and 6 (19%) LRs in SABR subset. Two-year LFFS was 56±10% and 57±12.8% for the surgery and SABR subsets respectively (Figure 1, log rank p=0.69). Osteosarcoma histology was associated with poorest LFFS on univariate analysis (HR = 14, 95% confidence interval 2.1 – 62, p=0.004). Median OS from the time of diagnosis and MDT was 7.2 and 2.2 years respectively. One SABR treatment was associated with a Grade 2 pain flare, and another was associated with a potential Grade 3 contained gastric perforation requiring surgery. One surgical resection was associated with Grade 3 wound dehiscence requiring a repeat surgery. There was no other Grade 2 or higher complications recorded.

Conclusions: Surgical resection or SABR may be safe and effective in providing local control for pediatric and adolescent patients with metastatic sarcoma. Further analysis with a larger cohort and longer follow-up to identify factors associated with LR and histology-specific therapy is pending.

227

PLANNING FOR THE RIGHT CARE AT THE RIGHT TIME: DEVELOPMENT AND IMPLEMENTATION OF AN AUTOMATED RESUSCITATION STATUS TOOL

Natalie Rozanec[1,2], Cynthia Heron[1], Edwin Chan[1], Shaziya Malam[1], John San Miguel[1], Jennifer Daley-Morris[1], Charles Cho[1,2,3], Peter Anglin[1], James Loudon[1,2]
[1]Southlake Regional Health Centre, Newmarket, ON
[2]University of Toronto, Toronto, ON
[3]Princess Margaret Cancer Centre, Toronto, ON

Purpose: Patients receiving cancer care make several visits to hospitals and cancer centres throughout their cancer journey. Over the last few years, there has been significant effort across Canada to promote advocacy and awareness of patients' goals of care (GoC). Several tools are available to communicate these wishes to first responders in the community, however, most of these tools provide specific orders for paramedics and firefighters, and are not meant to direct other healthcare personnel. This initiative reports on the design and implementation of an automated communication tool to document and display orders for the resuscitation status (RS) of outpatients receiving care at a regional cancer centre.

Materials and Methods: An inter-professional working group was formed, which included a patient/family advisor, representatives from medical and radiation oncology, as well as palliative care. Consensus was reached to align RS options (Full Resuscitation, Critical Care, Medical Care, Comfort Care) with those used by the inpatient team to ensure consistency across the organization and facilitate clinical handovers. A 'Resuscitation Status' order was added to the Mosaiq™ electronic medical record (EMR) orders menu for prescribers to select. This prompts an 'RS' pop-up window for staff, who then select the appropriate RS category, indicate whether supporting documentation was provided, document who provided consent as well as who was present for the discussion. It also provides a place to enter the names and contact information for multiple substitute decision makers and powers of attorney. Approving this order auto-generates a RS document into the patient's EMR which is automatically tagged for viewing in the 'GoC/RS' EMR tab. An accompanying RS policy and procedure was also drafted and sent for full consultation.

Results: The RS form, policy and procedure were reviewed and approved by the Radiation Medicine, Medical Oncology and Palliative Care Clinical Service Teams. Full clinical implementation was rolled out on December 1, 2022. The RS process is now in use by all outpatient cancer clinics.

Conclusions: Development and implementation of a cancer centre-wide process to document the RS of patients has allowed for improved communication among staff and more frequent conversations about RS with patients. Documentation and auto-generation of the RS form is fast, taking less than one minute to complete. In the event of an emergency, one click on the patient's 'GoC/RS' tab provides staff with fast and easy access to the most recent RS order set to ensure patients are receiving the right care at the right time.

228

IMPROVING THE CANCER CENTRE WORK EXPERIENCE: ONE SIZE DOES NOT FIT ALL

Rajiv Samant[1], Ege Babadagli[1], Selena Laprade[1], Gordon Locke[1], Angela McNeil[2], Joanne Meng[1], Julie Renaud[2], Elisabeth Cisa-Paré[3], Jessica Chan[4], Jiheon Song[5]
[1]*University of Ottawa, Ottawa, ON*
[2]*The Ottawa Hospital, Ottawa, ON*
[3]*Northern Ontario School of Medicine, Ottawa, ON*
[4]*University of British Columbia, Vancouver, BC*
[5]*University of Toronto, Toronto, ON*

Purpose: Working at a cancer centre can be immensely rewarding, yet it is also highly demanding and associated with significant stressors. Therefore, it is important to develop approaches that will make it easier for oncology healthcare professionals to feel more satisfied with their work experience and allow them to provide the best care possible.

Materials and Methods: An ethics approved staff satisfaction survey was developed in-house to gain insights regarding workplace experience among all staff at our regional cancer centre. It was delivered via an online format, with both multiple choice and free text sections. We summarized the most common themes from the staff responses for qualitative review.

Results: In total, 478 individuals completed the online survey. This represented the majority of the cancer centre staff, with 75.1% women, 23.2% men and 1.7% preferring not to say. The median age range was 41-50 years, with 76.8% either married or in common-law relationships. Most (64.3%) had worked at the cancer centre for at least five years, with almost half (47.1%) having worked for 10 or more years. The breakdown according to healthcare professional type was as follows: 21% nurses, 20% radiation therapists, 18% physicians, 13% clerical staff, 6% pharmacy, 5% clinical research, 4% administrative assistants, 4% physics, 4% managers and 5% other types of staff. Almost all (97.4%) generally enjoyed their work and found working with cancer patients rewarding (93.3%). There was definite evidence of work-related stress; 18.6% stated it was "very much" and 62.1% "a little bit". In terms of their workload, 61.3% stated it was "very busy" and 10% stated it was "excessively busy". The dislikes and workplace challenges varied according to staff role and the most common ones were as follows: unsupportive work environment for radiation therapists and clerical staff; technology problems for physicians; excessive workload for pharmacy and managers; no future prospects for physics; and a combination of unsupportive work environment and workload for nurses, clinical trials staff and administrative assistants. Similarly, suggestions for improvement also varied depending on staff role and included the following: making technology more user-friendly, greater flexibility in work schedules, reducing workload, more supportive work environment, better communication within the cancer centre, improving teamwork and acknowledging individual staff contributions.

Conclusions: Clearly, cancer centre staff enjoy their work and find it rewarding, but there continue to be significant challenges, and these vary according to one's role. Therefore, it appears that a generic approach for all is not ideal, and strategies that are more focused and individualized need to be developed to improve the workplace experience.

229

SURVEY ON RESIDENT PERCEPTIONS OF RADIATION ONCOLOGY INPATIENT CARE IN CANADA

Michael Sun, Bayan Malakouti-Nejad, Daniel Tesolin, Ege Babadagli, Graham Cook, Marc Gaudet, Robert MacRae
The Ottawa Hospital Cancer Centre, Ottawa, ON

Purpose: Management of inpatients is an often-overlooked component of Radiation Oncology practice, and there is variance in the structure of inpatient care at academic centres across Canada. This has implications for residency training programs, as residents at different institutions will have varying degrees of exposure to and emphasis on inpatient care. We sought to determine how inpatient Radiation Oncology is structured across Canada, its impact on residency programs, and how residents perceive inpatient practice fitting into their training.

Materials and Methods: A survey was developed and distributed to Radiation Oncology residents across Canada. The survey elicited information regarding inpatient service structure, residents' perception thereof, and its impact on their training. Data and selected narrative responses were reported.

Results: A total of 43 residents participated, with respondents from all 13 residency programs. Eleven programs have a dedicated inpatient service, ten of which rely on residents for weekend and/or overnight ward coverage. Resident perceptions were split, with 27.5% (11/40) reporting that inpatient service enhances their training, while 35% feel that it detracts from their learning. Additionally, 47.5% (19/40) report feeling stressed and 65% (26/40) report feeling overworked due to their inpatient responsibilities. Most residents (65.9%, 27/41) feel that Radiation Oncology should function solely as a consultation service as opposed to an admitting service.

Conclusions: This study suggests that while the structure of inpatient Radiation Oncology service varies across academic centres in Canada, they tend to rely heavily on residents for after-hours coverage. Residents' perceptions of inpatient management also vary, though many feel stressed or overworked and feel that inpatient care detracts from their training. These findings may

help inform how residency programs can be modified to better suit the needs of trainees and elucidate the role that inpatient care should play in Radiation Oncology in the future.

230
THE IMPACT OF A STUDENT-LED RADIATION ONCOLOGY INTEREST GROUP ON MEDICAL LEARNER INTEREST AND ACCESS TO THE SPECIALTY
Benson Wan, Ian J. Gerard, Piotr Pater, Tanner Connell, Joanne Alfieri
McGill University, Montréal, QC

Purpose: In many Canadian medical school curricula, radiation oncology (RO) topics are limited, often mentioned as an adjunct to surgery or chemotherapy. Furthermore, RO exposure in clerkship is frequently limited to elective rotations. Thus, leaners receive scant exposure to RO, possibly impacting global oncology awareness, access, and interest. To address this, the RO interest group (ROIG) was founded by a group of medical students in December 2020. The ROIG facilitates a broad range of events, including didactic lectures on introductory RO topics, technical medical physics workshops, panel discussions, and departmental tours with equipment demos. With growing interest, we hypothesized that the ROIG had an impact on both strengthening pre-existing interest and on fostering new interest in RO.

Materials and Methods: To evaluate the impact of the ROIG, a survey was distributed to attendees via e-mail and social media. Ten quantitative five-point Likert-scale questions addressed the following: the role of the ROIG as a facilitator or barrier to accessing RO, a change in interest in RO, the impact on interest in comparison to medical school curricula, changes in participants' desire to pursue electives or residency in RO, and likelihood to recommend the group to peers. Qualitative free-form questions recorded favourite and least favourite events, suggestions, and commentary. A long-term follow-up questionnaire will follow ROIG's impact on graduating trainees.

Results: Twenty-four of 114 attendees completed the survey (21%). All participants stated that the ROIG was a facilitator to accessing RO (100%), and most disagreed on ROIG being a barrier (96%). Participants indicated that the ROIG increased their interest in RO (71%) and did not decrease their interest (83%). Ninety-six percent of participants would recommend the ROIG to peers. Most respondents stated that the ROIG facilitated interest better than current medical school curricula (75%), which was felt to be insufficient in introducing RO (88%). ROIG had no clear impact on students' likelihood to pursue RO electives, to apply to RO residency, or to contact faculty to learn more. The physics lectures and career panels were the favourite events, and there was no common least favourite event. Suggestions for future events included networking events, a lecture on artificial intelligence, patient panel discussion, and formal shadowing. Six graduating students agreed to complete the follow-up questionnaire.

Conclusions: The ROIG was founded to address gaps in RO exposure in medical school. Feedback suggests the group facilitated access to RO, led to increased interest in RO, and will be recommended to peers. Currently, ROIG has not influenced students' decisions to pursue electives or further training in RO. Future work includes implementing new events, expanding the ROIG to other universities, and analyzing follow-up survey data. Moving forward, interest groups may play an important role in promoting awareness, access, and interest of niche specialties such as RO.

231
CHARACTERISTICS ASSESSMENT OF ONLINE YOUTUBE VIDEOS ON RADIOTHERAPY FOR BREAST CANCER
Brandon Chai[1], Paris-Ann Ingledew[2]
[1]*University of British Columbia, Vancouver, BC*
[2]*British Columbia Cancer, Vancouver, BC*

Purpose: Radiotherapy (RT) is an important component of breast cancer management but is underutilized due to barriers such as the lack of proper education. YouTube is commonly used for obtaining health information, yet the quality of information can be variable. This study systematically evaluates the characteristics of educational YouTube videos on RT for breast cancer.

Materials and Methods: A total of 200 YouTube videos were identified by recording the first 50 videos of four searches. Duplicates were removed, videos were rank ordered and screened against pre-determined inclusion criteria, then the first 50 videos were reviewed using a video assessment tool. Two independent reviewers were used to ensure consistency in rating.

Results: The USA (66%) or UK (20%) were the most common locations of publication. Publishers were frequently affiliated with health care facilities (48%) or non-profits (30%). The interview using a physician (68%) or patient (26%) was the most common media type, and B-roll footage with narration (48%) was the second most common. Most videos were targeted towards patients (96%), had comments (56%) and subtitles available (96%). The most common themes identified were Explaining RT (54%), Acute Side Effects (40%) and Patient Care Experience (32%).

Conclusions: This review is useful to inform the future development of video resources for health education in this topic for breast cancer patients. Though parameters were variable and inconsistently followed best practice guidelines, YouTube remains as a potentially important tool for the dissemination of health information.

232
ABDOMINAL SCHWANNOMA MIMICKING LYMPH NODE METASTASIS IN RECTAL CANCER
Enxhi Kotrri, Derek Jonker, Rebecca Auer, Gordon Locke
University of Ottawa, Ottawa, ON

Purpose: Schwannomas are rare benign tumours that are often asymptomatic and identified incidentally on imaging studies. The purpose of this case report is to present a case in which a schwannoma was found incidentally to be mimicking lymph node metastasis in a patient with rectal cancer, which changed the patient's management.

Materials and Methods: Patient provided consent for write-up of case report and data was extracted via electronic medical records. A thorough literature review was done on schwannomas and similar cases of schwannomas mimicking other pathologies.

Results: This is a case of a 69-year-old male who was found to have a rectal adenocarcinoma on colonoscopy after presenting with a change in bowel habits and rectal bleeding. Staging investigations showed the rectal adenocarcinoma in the mid-rectum, and also identified a necrotic retroperitoneal lymph node suspicious for metastatic disease. His rectal cancer was staged as a cT3bN0M1, and the initial treatment recommended was total neoadjuvant therapy entailing radiotherapy of 25Gy/5fx and six cycles of CAPOX chemotherapy, followed by definitive surgical excision shortly thereafter, as per the RAPIDO trial. As management would be significantly changed by lymph node involvement, patient underwent a CT-guided core needle biopsy of the suspicious lymph node, which revealed a schwannoma and reclassified the rectal cancer as a clinical cT3BN0. He underwent treatment of

his rectal cancer consisting of radiotherapy of 25Gy/5fx, followed by definitive surgical management 12 weeks later. He remained systemically well following treatment, and is now undergoing oncologic surveillance for the rectal cancer and schwannoma.

Conclusions: Overall, this case highlights how the incidental discovery of a schwannoma that was mimicking lymph node metastasis changed the patient's management plan after being identified on biopsy, including recommendation against systemic therapy, thereby allowing him to receive the most optimal treatment for his disease.

233
INTERACTIVE LINEAR ACCELERATOR MODELS FOR MEDICAL EDUCATION
Parminder Basran
Cornell University, Ithaca, NY

Purpose: Interactive models and gamification in medical education can improve learning outcomes, enhance practical skills, and prepare trainees for the challenges of real life. Gamification forms include simulations, virtual reality constructs, board games, role-playing and multi-player games, and puzzles. We aim to explore methods by which complex electro-mechanical componentry can be visualized and gamified in modern high-energy linear accelerators.

Materials and Methods: Lego© and additive manufacturing were used to design and construct two different types of medical linear accelerator componentry to deconstruct and demystify their inner workings. In coordination with a design team, two virtual models of a linear accelerator using Lego© and a 3D printed 3D puzzle of a medical linear accelerator were created.

Results: For our Lego© models, a simple model of a medical linear accelerator with a moveable gantry, couch, portal, and kV imaging panels at approximately 1/40th scale was constructed. A 1/10th scale of the linear accelerator head was also created with moveable targets, flattening filters, light-field sources, collimators, and multi-leaf collimators. Users can physically manipulate each component and appreciate physical effects such as rounded MLC leaf-edges, inter- and intra-leaf leakage, and light-field to radiation field congruence. The 3D printed linac deconstructs major elements of the medical linear accelerator, such as the waveguide, klystron, and bending magnet, that users can assemble.

Conclusions: These educational tools offer novel ways to learn complex electro-mechanical equipment encountered in radiation oncology, enhance problem-solving, supplement traditional learning approaches, and foster motivation and engagement. There remains great potential in these medical education approaches, particularly in radiation oncology.

234
PATIENTS AS PARTNERS IN UNDERGRADUATE ALLIED HEALTH CURRICULUM: HOW ARE THEY INVOLVED?
Cynthia Palmaria, Amanda Bolderston, Susan Fawcett
University of Alberta, Edmonton, AB

Purpose: Patient involvement in radiation therapy educational programs is thought to enhance student skill development. There is little research in the radiation therapy field in this area. This scoping review thus examined literature on the practices and benefits of integrating patients/service users in the wider field of allied health student education.

Materials and Methods: Electronic databases MEDLINE, EMBASE and CINAHL were searched for English-language articles on patient involvement in allied health educational programs. Date range was 2011 to present. Clinical placement educational activities were excluded. A Microsoft Excel form was developed to extract data on (i) country of origin (ii) population and methods (iii) educational intervention type (iv) training for patients/service users and (v) key findings. Three reviewers independently screened and extracted relevant data. Any disagreement was discussed and resolved by consensus. Data were synthesized through a thematic narrative approach.

Results: The initial search yielded 93 articles. After review 24 were selected based on planned and active involvement of service users in the curriculum. Allied health professions included respiratory therapy, physiotherapy, occupational therapy, speech and language pathology and radiation therapists. The studies were mainly undergraduate (24) with one graduate program. Most research engaged patients in curriculum delivery (19) and student assessment (five). These collaborations emphasized positive outcomes on student skills development (20) and patient empowerment (two). While six articles recommended patient training and two role clarification, two specified more studies are needed. Finally, two papers suggested aftercare for students subsequent to patient interaction.

Conclusions: Evidence suggested collaboration between education programs and patients enhances student skills and improvement of healthcare delivery. Both patients and students shared insights on the benefits of patient integration into the students' learning experiences. The insights from this study will be used to further develop a survey that examines current global practice in radiation therapy programs.

235
ASSESSMENT OF LUNG CANCER YOUTUBE VIDEOS FOR PATIENT EDUCATION
Brandon Chai[1], Paris-Ann Ingledew[2]
[1]*University of British Columbia, Vancouver, BC*
[2]*British Columbia Cancer, Vancouver, BC*

Purpose: The internet is essential for obtaining information about lung cancer, which is the leading contributor to global cancer deaths. YouTube is a video-streaming platform that is popular amongst health consumers; however, the quality of videos is variable, and few studies have evaluated their role in lung cancer education. This study uses a systematic approach to assess the lung cancer YouTube videos for patient education.

Materials and Methods: Using the search term "lung cancer", the first 50 YouTube videos were recorded after applying exclusion criteria and removing duplicates. A video assessment tool was used to evaluate the videos in three domains: general parameters, source parameters and video content. A modified DISCERN tool was used to assess video reliability. Two independent reviewers evaluated the videos and discrepancies were resolved via consensus.

Results: Under half the videos were published within three years. Mean video length was six minutes and 12 seconds. Video publishers were commonly from the USA (70%); were affiliated with a health care facility/ organization (30%), non-profit (26%) or commercial organization (30%); had a physician presenter (46%); were targeted towards patients (68%); and had subtitles (96%). Seventy four percent of videos supported optimal learning by including effective audio and visual channels. Lung cancer epidemiology, risk factors and definitions (nature of the disease and classification) were amongst the most common topics covered. Prognostic and diagnostic information were covered less than expected.

Conclusions: This study describes the landscape of YouTube videos for lung cancer. It informs the development of future lung cancer videos and guides healthcare providers when recommending educational resources to their patients.

236

IMPORTANCE OF LEADERSHIP SKILL DEVELOPMENT AMONG HEALTH CARE PROFESSIONALS IN LMIC

Agha Muhammad Hammad Khan[1], Tooba Ali[2], Agha Muhammad Hassaan Khan[3], Maria Tariq[2], Bilal Mahar Qureshi[2], Nasir Ali[2], Sehrish Abrar[2], Asim Hafiz[2], Ahmed Nadeem Abbasi[2]
[1]Sultan Qaboos Comprehensive Cancer Care and Research Centre (SQCCCRC), Seeb, OM
[2]The Aga Khan University, Karachi, PK
[3]Institute of Business Management, Karachi, PK

Purpose: This study aims to evaluate the impact of leadership skill development sessions on postgraduate resident training and radiation oncology faculty's professional development and to highlight the need of including these concepts in training programs in LMIC.

Materials and Methods: Workshops were conducted from January 2022 to August 2022 at a tertiary care hospital, Section of Radiation Oncology with the collaboration of Business School leads with the aim to conduct sessions on attributes of leadership skills development. After obtaining approval from the institutional ethical review committee, the 10 workshops' impact was evaluated. These included: caring for the carers', emotional intelligence, entrepreneurial mindset, communication skills, problem-solving skills, change management, mentoring the mentors, strategic visioning, ideation and conflict resolution. Pre-workshop and post-workshop responses were recorded via a Google form, to assess understanding and the need for learning leadership skills from the attending participants.

Results: Our study participants included 75% residents, 28% consultants and 2% allied professionals. The participants' response rate was 98%. A total of 88% of study participants agreed that their understanding of a particular trait for leadership skill development improved after attending the session. 95% agreed that these sessions improved their practical approach while 93% marked to include these leadership skills trait programs in the study curriculum. A significant fraction of participants (78%), who initially disagreed with this concept of incorporating leadership skill development in the radiation oncology residency curriculum changed their minds after attending these workshops.

Conclusions: Leadership skills have been incorporated as part of the study curriculum in various leading radiation oncology residency programs worldwide. As it is an integral component of professional growth which eventually translates into improved patient care and drives positive change in healthcare setup. Therefore we are in dire need of training managerial skills in the post-graduate curriculum to develop future leaders

237

TEACHING PROFESSIONAL ETHICS IN MEDICAL PHYSICS GRADUATE PROGRAM

Marija Popovic[1], Ives R. Levesque[1], Cassandra Stambaugh[2], Wang Dongxu[3]
[1]McGill University, Montréal, QC
[2]Tufts Medical Center, Boston, MA
[3]Memorial Sloan Kettering Cancer Center, New York, US

Purpose: The topic of professional ethics is part of core curriculum set by CAMPEP standards for graduate programs in Medical Physics but, at this time, no published accounts of teaching practices exist. We have developed a workshop for graduate students based on case study of peer-reviewed, published cases developed by AAPM Medical Physics Leadership Academy (MPLA) to teach skills in ethical reasoning and professional conduct outlined in Code of Ethics of both COMP and AAPM.

Materials and Methods: In 2020, the MPLA Committee of AAPM published four peer-reviewed cases. The cases are narratives of workplace challenges and interpersonal situations that can be used to help develop the necessary skills to improve patient care and advance the profession. The developed teaching approach involves preparatory reading of cases and review of AAPM Code of ethics, small-group discussions and facilitator-led review. The workshop was attended by 32 graduate students. Student assessment involved pre- and post-workshop multiple choice exams. Student feedback consisted of free-form answers to 10 questions. The overall student opinion was deduced by analyzing common words used by students.

Results: The effectiveness of the workshop design was evaluated through student and instructor feedback. Students reacted very favourably, indicating that the workshop contributed to achieving the objective 'to understand the professional ethics issues related to work of a medical physicist'. There was also overwhelmingly positive opinion on the question regarding the overall workshop structure. Suggestions for improvement revolved around the breadth of preparatory material, which some students considered onerous.

Conclusions: We present a strategy for teaching professionalism and ethics in graduate medical physics program curriculum. The goal of the workshop was to provide students with a method to systematically manage dilemmas that arise in the everyday practice of medical physics. The method may be used by other institutions seeking to formalize teaching of professional ethics at the graduate level.

238

IMPLEMENTING DEMENTIA-FRIENDLY CARE APPROACH FOR CANCER PATIENTS LIVING WITH DEMENTIA

Shelley Canning[1], Jagbir Kaur[2], Michael McKenzie[2], Genevieve St-Martin[2], Lillian Hung[3], Nicole Percival[4], Jasleen Brar[1], Rachel Wan[3], Lynn Jackson[5], Sara Makortoff[5],
[1]University of the Fraser Valley, Abbotsford, BC
[2]British Columbia Cancer, Vancouver, BC
[3]University of British Columbia, Vancouver, BC
[4]Fraser Health Authority, Mission, BC
[5]N/A, BC

Purpose: The purpose of this study is to address the inequity of care outcomes for patients living with dementia through exploring current challenges and barriers, and proposing a dementia-friendly approach to cancer care. There is growing recognition that the number of cancer patients living with dementia is increasing. Within this small but growing area of scholarship, these patients have been found to experience poor outcomes; they receive less cancer screening, staging, and curative treatment than patients without dementia, thus they are typically diagnosed at later stage cancers with lower survival rates. The cancer journey is also difficult for their caregivers who play central roles in navigating care systems and communicating with the cancer care team. And, although they are experts in cancer, care providers often lack confidence and knowledge regarding dementia-care.

Materials and Methods: This is a three-year interdisciplinary study funded by the Alzheimer's Society of Canada and set in a provincial cancer centre. We are conducting qualitative applied health research drawing on a focused ethnography methodology

underpinned by a person-centred philosophy. Phase one explores the cancer care experiences of patients living with dementia, their caregivers, and their care providers; a total of 55 participants are being interviewed from these groups. Data is also being gathered through participant observation as patients and caregivers navigate the care environment during treatment and follow up visits across cancer centre sites. Phase one findings will inform the development of a dementia-friendly cancer care education module and recommendations for practice in phase two.

Results: In this presentation we will share the early findings from phase one of our study. Early caregiver and patient data emphasizes pragmatic challenges related to "navigating memory issues" when patients don't remember their diagnoses and the reason for clinic visits, and the need to "prepare for every eventuality" during appointments. Early care provider data points to the challenges of successfully "sharing the diagnosis" of dementia within the care team and "navigating unpredictable responses".

Conclusions: Phase one data underpins the importance for both additional dementia aware education for caner care providers, and recommendations for dementia-friendly policies and processes to better tailor cancer care for patients living with dementia ensuring equity.

239

LEARN ONCOLOGY THROUGH SOCIAL MEDIA: IS IT POSSIBLE?

Saveen Sidhoo[1], Stella Kang[2], Paris-Ann Ingledew[3]
[1]*University of Alberta, Edmonton, AB*
[2]*Dalhousie University, Halifax, NS*
[3]*University of British Columbia, Vancouver, BC*

Purpose: Social media (SM) use has increased within education, allowing for global transfer of knowledge within the reach of a button. While slow to adapt in healthcare, this trend has become more prevalent as a generation of physicians enter practice who grew up with SM. This is especially highlighted during the pandemic, where medical schools suddenly adapted a virtual learning platform to uphold training requirements but follow social distancing. Platforms such as Twitter (Twtter), Instagram (IG), podcasts and YouTube (YT), offer unique communication tools for various educational purposes; thus presenting a moment for educators to accommodate many learning styles. LearnOncology (LO) is a free e-resource intended to support students and healthcare providers to improve oncology education. The website is currently used in 169+ countries and attracts 500 users/month including students, residents, physicians, and other allied health. The site consists of online modules, virtual patients, an oncology app, YT videos and most recently, podcasts. In 2021, we integrated IG and Twtter into the LO offerings with the aim to increase educational reach of the site and incorporate unique educational opportunities. Here, we describe the purposeful integration of SM to improve educational offerings and interaction of learners with a medical education (MedEd) website. We report on the iterative inclusion of best practices in integration of SM and impact on engagement.

Materials and Methods: Review of literature indentified a number of studies analyzing best practices in SM to engage learners for MedEd. A variety of interventions were identified to improve the reach of SM platforms. Iteratively, these interventions were implemented including daily quizzes, and links to literature or new online content. Analytics from the platforms were collected. The number of likes, followers, accounts reached and engaged, and impressions/views were recorded from June 2022 and February 2023. Trend analysis assessed engagement over time.

Results: At the start of the project, there were 79 posts on both Twttr and IG. Fourteen additional posts were produced. With interventions incorporated, followers on IG increased 32.4% from 17 to 225, and 83.0% on Twttr from 53 to 97. On IG, number of likes averaged at 7 (range: 3-15), and number of impressions 492 (range: 0-2345). On Twttr, number of likes averaged at three (range: 0-10), and number of impressions 431 (range: 50-2225). Highest trafficked posts related to podcasts. Posts with collaborators garnered the most traffic.

Conclusions: Incorporation of SM into MedEd is evolving. Here, we identified key principles to incorporate SM into MedEd websites. With integration of these principles, we demonstrate a progressive and expanded reach of this MedEd site. Lessons here may be applied to a range of medical educators as they develop new online learning tools.

240

USING 18F PSMA-1007 PET AND MULTIPARAMETRIC MRI WITH PROSTATE SBRT TO ESCALATE THE DOSE TO DOMINANT INTRAPROSTATIC LESIONS - ARGOS-CLIMBER: INTERIM RESULTS OF A PHASE I/II CLINICAL TRIAL

Aneesh Dhar[1,2], Glenn Bauman[1,2], Lucas Mendez[1,2], Hatim Fakir[1,2], David Laidley[1,2], Zahra Kassam[1,2], Wei Liu[3], TingYim Lee[4,1], Aaron Ward[1], Jonathan Thiessen[4], Anders Celinski[2], Melanie Davidson[5], Jane Bayani[6], Matt Mulligan[2], Linada Berryhill[2], John Conyngham[2], Wee Loon Ong[5] , Andrew Loblaw[5,7]
[1]*Western University, London, ON*
[2]*London Health Sciences Centre, London, ON*
[3]*British Columbia Cancer, Vancouver, BC*
[4]*Lawson Health Research Institute, London, ON*
[5]*Sunnybrook-Odette Cancer Centre, Toronto, ON*
[6]*Ontario Institute for Cancer Research, Toronto, ON*
[7]*University of Toronto, Toronto, ON*

Purpose: Most recurrences after primary prostate cancer radiation therapy originate from dominant intraprostatic lesions (DILs). Prostate multiparametric Magnetic Resonance Imaging (mpMRI) to target DILs during radiation planning has been shown to improve clinical outcomes for patients in the FLAME trial. 18-Fluorine Prostate Specific Membrane Antigen-1007 (18F PSMA-1007) Positron Emission Tomography (PET) can also target DILs and offers the further opportunities for targeted dose escalation.

Materials and Methods: ARGOS-CLIMBER is a prospective phase I/II trial enrolling 50 patients with unfavourable intermediate or high-risk disease across two Ontario centres. A hybrid PET/MR scanner was used to acquire co-registered 18F PSMA-1007 PET and mpMRI images prior to stereotactic body radiation therapy (SBRT). The images were rigidly fused with the computed tomography (CT) simulation scans. All patients received intra-prostatic fiducial markers. All DILs were delineated on mpMRI and PET images: on mpMRI, DILs were delineated in areas with low T2 signal and restricted diffusion, and included all lesions with a score of 4 or 5 on the Prostate Image Reporting And Data System (PIRADS v2.1); on 18F PSMA-1007 PET, DILs were delineated automatically by using a Standardized Uptake Value (SUV) threshold of 20-40% of the maximum SUV in the prostate, then this volume was manually edited to the anatomy of the DIL on mpMRI or CT. Final DIL volumes were the union of PET and mpMRI volumes. Planning targets were as follows: whole prostate 35Gy/5; seminal vesicles and elective nodal regions 25Gy/5; imaging involved nodes 35Gy/5; DILs up to 50Gy/5, while respecting organ at risk constraints. Patients were treated every other day with cone beam CT guidance and 6-18 months of adjuvant androgen deprivation. The primary outcome is chronic (six month) toxicity. Secondary outcomes include acute (six week) toxicity, quality of life metrics and cancer control outcomes including biopsy clearance at two years. PET, mpMRI and biologic biomarkers at six months and two years post treatment are exploratory endpoints.

Results: Between May 2022 and January 2023, 20 patients have been enrolled, with 18 patients having completed treatment. There were 29 and 34 DILs detected on mpMRI and 18F PSMA-1007 PET, respectively, with a median (range) of 2 (0 – 4) MR DILs and 1 (0 – 4) PET DILs per patient. The median (IQR) size of the MR and PET DILs was 14 mm (9 – 20 mm) and 11 mm (9 – 31 mm). The median (IQR) maximum dose delivered to the combined DIL was 46.9 Gy (45.5 – 48.0 Gy), and the median (IQR) D99% to this volume was 42.4 Gy (40.8 – 45.5 Gy). No patients experienced Grade 3+ acute toxicity thus far.

Conclusions: Dose escalation to multi-modality imaging defined DILs on ARGOS/CLIMBER has been feasible with acceptable acute toxicity. Accrual completion is expected by Q2 2023, with the six-month primary endpoint of GI/GU toxicity available by Q4 2023.

241

REDUCTION OF METAL ARTIFACTS IN 7T MRI FOR PRE-CLINICAL DIFFUSING ALPHA-EMITTING RADIATION THERAPY RECTAL STUDIES

Mélodie Cyr, Behnaz Behmand, Naim Chabaytah, Joud Babik, Shirin A. Enger
McGill University, Montréal, QC

Purpose: In brachytherapy, radioactive seeds are place directly inside a solid tumour which ensures a conformal dose to the tumour, while sparing healthy surrounding tissue. Recently, a novel 224-Ra based interstitial treatment modality relying on diffusing alpha-emitting radiation therapy (DaRT) has been introduced to treat solid tumours. Temporary or permanently implantable seeds impregnated with small activity of 224Ra are placed inside tumours. Short-lived alpha-particle emitting atoms are released in the decay chain of 224Ra. Although the range of alpha particles released in the decay process is a couple of cell diameters, these atoms diffuse inside the tumour contributing to a high-dose region up to 5 mm around the seed. However, the distance that these alpha-emitting atoms travel from the seed (diffusion length) is not well known for several cancer types. The currently used diffusion lengths are based on pre-clinical studies through subcutaneous animal models and a few orthotopic models. In this study, a feasibility study using tumours grown in the rectum of the mice through an orthotopic intra-rectal injection of colorectal adenocarcinoma cells, was studied as well as an intra-rectal injection of inert DaRT seeds. Through this study, an optimization of MR images was completed to reduce metal induced artefacts.

Materials and Methods: In this orthotopic model, HT-29 colorectal adenocarcinoma cells ($1x10^6$ cells/25 µl in Matrigel) were injected using a 28G needle in the submucosal layer of the intestinal wall of 10 NSG male mice. The tumours growth and localization were monitored using a 7T Magnetic Resonance Imaging (MRI) machine with RARE-acquisition sequence. Once the tumours were ~5-7 mm in diameter, they were injected with inert DaRT seeds (5 mm long x 0.3 mm diameter) using a 21G applicator (Alpha TAU Medical, Israel). The mice underwent final imaging to determine the placement of the seeds within the tumours. The metal artifact reduction was completed by using a 50 ml gelatin phantom and carcasses with seeds. The sequence parameters were tested to reduce the metal artifacts.

Results: The orthotopic intra-rectal injection resulted in an 80% tumour success rate. Two mice were excluded from the seed injection due to tumour size and location. The mice underwent imaging post cell injection. The seeds were injected through an intra-rectal method and were placed roughly within the centre of the tumours. The final imaging confirmed that 75% of the seeds were still in the mice a week after the injection. The MRI optimization confirmed that the relaxation time of five seconds, echo-time of 25.6 ms, resonance frequency bandwidth of 50 kHZ and slice thickness of 0.27 mm was required to reduce the metal artifacts.

Conclusions: The feasibility study of an orthotopic model of colorectal adenocarcinoma, as well as inert DaRT seeds, were successful. This model can be used for further animal studies to investigate the diffusion lengths of active DaRT seeds. The systemic approach of using DaRT and determining the diffusion lengths of the daughter radionuclides will help to optimize cancer patients' treatment plans.

242

INVESTIGATING THE APPLICATIONS OF GLIAL ACTIVATION IMAGING USING [18F]-FEPPA PET FOLLOWING CRANIAL IRRADIATION TO GUIDE RADIOTHERAPY TREATMENTS

Sawyer Badiuk[1], Lise Desjardins[2], Matthew Fox[1,2], Paula Foster[1,3], Jonathan Thiessen[1,2], Jeff Chen[1], Eugene Wong[1,2,4]
[1]*Western University, London, ONN*
[2]*Lawson Health Research Institute, London, ON*
[3]*Robarts Research Institute, London, ON*
[4]*London Regional Cancer Program, London, ON*

Purpose: To investigate the neuroinflammation reaction of the brain following cranial irradiation using glial activation PET imaging with the novel radiotracer [^{18}F]-FEPPA for a murine model.

Materials and Methods: To evaluate radiation induced glial activation, half-brain irradiation will be performed on non-tumour bearing immunocompetent mice (BALB/c) (N = 30) using a micro-CT/RT system with sham (n=6), 4 Gy (n=12) and 16 Gy (n=12). Dynamic [^{18}F]-FEPPA PET scans will be acquired for 90 minutes at 48 hours, two weeks and four weeks after irradiation to quantify level and duration of glial activation. PET kinetic analysis will be completed to evaluate the time activity curves and volume of distribution (Vt). Standard uptake value (SUV) will also be employed in our analyses. Immunohistochemistry identifying glial activation will be completed by staining activated microglia and translocator proteins (TSPO) which is the specific ligand of [^{18}F]-FEPPA.

Results: A pilot study our group completed validated that [^{18}F]-FEPPA is a suitable radiotracer to image glial activation in the brain following irradiation. Preliminary results demonstrated that partial brain irradiation induces global inflammation and that glial activation is dependent upon dose and length of time post-irradiation.

Conclusions: This study will map the spatiotemporal dose-response of the brain when partially irradiated with different levels of dose. It will provide data to understand how the brain, specifically glial cells respond to irradiation and the resulting duration and amount of inflammation. Following this, whole brain irradiation will be investigated to provide a comprehensive understanding of radiation, subsequent glial activation which may have implications to late cognitive function.

243

DOSE REDUCTION IN QUANTITATIVE IODINE IMAGING WITH PHOTON-COUNTING CT

Pierre-Antoine Rodesch, Devon Richtsmeier, Magdalena Bazalova-Carter
[1]*University of Victoria, Victoria, BC*

Purpose: Computed tomography (CT) acquisitions are performed for adult patients at 120 kV, but lower tube voltages can reduce the dose while preserving image quality in monoenergetic CT images. Currently, multienergy (or spectral) CT is performed with dual-energy (DE) measurements using energy integrating detectors. However, DE-CT configurations limit the minimal voltage to 120 kV in spectral mode, preventing the production

of spectral images in low-voltage dose-saving protocols. On the other hand, CT scanners equipped with a photon-counting detector (PCD) can reconstruct mono- and multienergy images in the same acquisition. The goal of this work was to investigate whether PCD-CT can perform accurate spectral imaging with a low energy spectrum of 80 or 100 kV, resulting in dose reduction. Specifically, we have quantified iodine concentrations for images acquired at 80, 100, and 120 kV.

Materials and Methods: Vials filled with varying concentrations of iohexol (2.5, 3.5, 4.9 and 9.3 mg I/ml) were placed in a 10 cm diameter polyethylene phantom to reproduce the contrast of a clinical CT angiography task. Acquisitions were performed with a table-top PCD-CT scanner featuring a prototype CZT detector with a 330-µm pixel pitch providing six energy bins (Thresholds: 35/41/47/53/59/65 keV). The x-ray tube current was set to 1.04 mA, 0.69 mA and 0.5 mA to provide a constant dose at 80 kV, 100 kV and 120 kV, respectively. A monoenergetic image and water\iodine material decomposition (MD) maps were reconstructed for each tube voltage. For the MD, a semi-empirical forward model was defined and tuned through calibration measurements. The calibration basis was composed of 20 combinations of known water lengths and iodine concentrations. The model was used as an input for a projection-based MD algorithm, reconstructing water and iodine maps. The error on iodine concentrations was evaluated in the iodine maps and the vial contrast-to-noise ratios (CNRs) were measured in both monoenergetic images and iodine maps.

Results: Compared to the 120 kV monoenergetic image, CNR increases of 8.1% and 17.4% were measured at 100 kV and 80 kV, respectively. The mean concentration error in iodine maps was 0.25 mg/ml at 80 kV, 0.15 mg/ml at 100 kV, and 0.18 mg/ml at 120 kV. With respect to the 120 kV iodine map, the CNR in 100 kV iodine map improved by 0.9% and was reduced by 16% at 80 kV. At a constant radiation dose, the CNR improved while reducing the tube voltage in the monoenergetic image. PCD-CT can provide accurate iodine spectral images at 80 and 100 kV with an error inferior to 1 mg/ml. However, while the CNR was maintained at 100 kV compared to the 120 kV iodine map, it was reduced at 80 kV.

Conclusions: PCD-CT can provide accurate spectral iodine images at 80 and 100 kV tube voltages while improving CNR in the monoenergetic image. However, care should be taken in selecting the appropriate tube current, as tube voltages that are too low can increase the noise in PCD-CT spectral images. PCDs would enable the provision of accurate iodine quantification in low-voltage dose-saving protocols, which is not possible with current clinical DE-CTs.

244

RESOLVING THE 2.1 PPM ALLYLIC FATTY ACID RESONANCE WITH MAGNETIC RESONANCE SPECTROSCOPY AT 3 T

Nathaniel Bly, Atiyah Yahya
University of Alberta, Edmonton, AB

Purpose: Magnetic Resonance Spectroscopy (MRS) is a non-invasive means of estimating fat composition in vivo. The allylic resonance at ≈2.1 ppm arises from methylene protons that neighbour double bonded carbons, thereby providing information about fat unsaturation. However, at clinical field strengths, the allylic peak suffers overlap from the ≈2.3 ppm resonance which results from the protons in a position to the carbonyl group. The purpose of this work is to investigate the fatty acid spectral response as a function of Point RESolved (STEAM) echo time (TE) at 3 T to determine values that resolve the two resonances from each other by J-coupling evolution of the protons. PRESS and STEAM are two commonly employed in-vivo MRS sequences.

Materials and Methods: Spectra were acquired with a 3 T Philips MRI scanner from peanut oil using STEAM (mixing time, TM = 20 ms) and PRESS (TE_1 = 17 ms). Echo times were varied in steps of 10 ms from 20 ms – 250 ms and 40 ms – 250 ms, for STEAM and PRESS, respectively. Spectra were acquired as 2048 complex data points sampled at 2000 Hz from a 15 x 15 x 15 mm^3 voxel with a repetition time of three seconds and 32 signal averages. In-vivo spectra were acquired from a 8 x 8 x 8 mm^3 positioned in the tibial bone marrow of the right leg of a male volunteer. Echo times that resolved the 2.1 and 2.3 ppm resonances in the oil spectra were selected and used in-vivo. All other spectral parameters were the same as for the phantom acquisitions.

Results: The oil spectra were processed and assessed; echo times that resolved the 2.1 and 2.3 ppm resonances were selected. A few TE values resolved the two resonances but it was found that PRESS with a total TE of 70 ms and 90 ms and STEAM (TM = 20 ms) with TE values of 90 and 100 ms resolved the two resonances while yielding relatively higher signal for the two resonances compared to other TE values.

Conclusions: The selected PRESS and STEAM TE values enable the allylic fatty acid resonance at approximately 2.1 ppm to be resolved from the neighbouring fatty acid resonance at about 2.3 ppm, at 3 T. All selected TE values result in adequate signal from both resonances for quantification. The PRESS spectra are better resolved and yield a higher signal yield than that obtained with STEAM. However, the STEAM spectra do not exhibit any negative side lobes. In addition, STEAM (TM = 20 ms) with a TE of 100 ms has been previously demonstrated to be suitable for resolving the fat olefinic resonances from that of water at 3 T and therefore would be suitable for quantifying multiple resonances.

245

APPARENT DIFFUSION COEFFICIENT REPEATABILITY AND REPRODUCIBILITY WITHIN THE PROSTATE FOR MR-GUIDED ADAPTIVE RADIATION THERAPY

Nitara Fernando[1], Tony Tadic[2], Winnie Li[2], Tirth Patel[2], Jerusha Padayachee[3], Anna T Santiago[4], Jennifer Dang[2], Peter Chung[2], Enrique Gutierrez[2], Catherine Coolens[2], Ed Taylor[2], Jeff D Winter[2]
[1]*Western University, London, ON*
[2]*Princess Margaret Cancer Centre, Toronto, ON*
[3]*Auckland City Hospital, Auckland, NZ*
[4]*University Health Network, Toronto, ON*

Purpose: MR-guided biological-based adaptive radiation therapy offers the ability to adapt the dose at each fraction based on both the daily anatomy as well as MR biomarker changes within the target. With the introduction of the magnetic resonance linear accelerator (MR-linac), it is possible to longitudinally assess apparent diffusion coefficient (ADC) changes within prostate at each fraction. It is critical to establish the accuracy of ADC value-tracking over multiple fractions to enable ADC-driven dose adaptation. The purpose of this work is to report the repeatability and reproducibility of ADC values across treatment using deformable registration to account for interfraction translations, rotations, and deformations of the prostate.

Materials and Methods: To evaluate within-fraction repeatability, we collected twice-per-fraction repeat ADC measurements during three consecutive fractions in 20 patients with prostate-only radiation therapy treated on a 1.5 T MR-linac. Clinical target volume (CTV) regions-of-interest (ROIs) were prospectively delineated on T2-weighted MR, and we retrospectively contoured the gross tumour volume (GTV) and peripheral zone (PZ). The contours on the T2-weighted MR were rigidly copied to the multiple ADC maps for each fraction. An automated script generated hybrid intensity- and structure-based deformable image registrations between the T2w images from successive fractions and we

applied the deformed vector fields to deformably register the corresponding ADC maps. We extracted individual voxel, mean and 10th-percentile ADC values from each contour and calculated repeatability and reproducibility using the intraclass correlation coefficients (ICC) and percent repeatability coefficient (%RC) within and between fractions.

Results: Visual inspection confirmed (near sub-voxel) accuracy of the DIR throughout the prostate for all patients and fractions. Excellent ADC repeatability and reproducibility existed for all ROIs (ICC > 0.86) within and between fractions for mean and 10th percentile values. Only good repeatability and reproducibility existed for individual voxels for all ROIs (ICC > 0.542). Similarly, low %RC within-fraction (4.2 – 17.9%) for mean and 10th percentile ADC values existed, with greater %RC between fractions (10.2 - 36.8%). Our results suggest mean ADC values are more repeatable than 10th percentile ADC as assessed by ICC and %RC. Additionally, %RC and ICC results correlated with ROI volume, with greatest precision observed for CTV and least for GTV. Larger ROIs (CTV and PZ) may have better repeatability and reproducibility due to the greater number of voxels being sampled.

Conclusions: Results of this study suggest excellent repeatability and reproducibility for mean and 10th percentile ADC values in the prostate CTV as well as GTV and non-GTV peripheral zone. This work establishes accuracy for deformable voxel-level ADC value tracking for future implementation of biologically based adaptive RT.

246

CHARACTERIZING THE HU CONSTANCY OF THE VARIAN ETHOS HYPERSIGHT CBCT AND COMPARING IT TO CONVENTIONAL SYSTEMS

Clara Fallone[1,2], Lee MacDonald[1,2], Amanda Cherpak[1,2], James Robar[1,2]
[1]*Nova Scotia Health Authority, Halifax, NS*
[2]*Dalhousie University, Halifax, NS*

Purpose: To characterize the HU constancy of the Varian Ethos HyperSight CBCT and compare it to conventional systems.

Materials and Methods: Hounsfield unit (HU) to relative electron density (RED) curves were generated for each of HyperSight CBCT and conventional FBCT (GE Optima CT580RT) and CBCT (Varian TrueBeam) using the Sun Nuclear Advanced Electron Density (AED) phantom. For each image, the mean CT value and standard deviation of each insert was quantified. A HU to RED curve was constructed from the expected (manufacturer) insert RED and the measured CT numbers. Separate linear functions were fit to the data for HU ≤ 0 and for HU > 0. Calculated RED values for each insert were obtained from the HU to RED curves. These calculated RED values were compared to the expected RED values; average and maximum absolute % differences were computed and compared. The impact of using imaging blade collimation was also investigated for HyperSight. Images were acquired for various HyperSight protocols using a) the phantom with extensions and blade collimation, b) the phantom without extensions and without blade collimation, and c) the phantom without extensions and with blade collimation. HU accuracy in each case was assessed using the same methodology described above.

Results: HyperSight and GE FBCT yielded comparable error magnitude between calculated and expected RED values, whereas Truebeam CBCT yielded larger errors. For all Ethos protocols tested, the HU-RED curves agreed within measured error. However, the HU-RED curves acquired without collimation were more variable from those acquired with collimation. Calculated RED values from scans without collimation displayed larger differences with expected RED values; however maximum deviations were all below 4.2%. Using phantom extensions did not appear to affect results.

Conclusions: HyperSight shows superior HU constancy to Truebeam CBCT and comparable constancy to GE FBCT. Omitting imaging blade collimation potentially degraded HU constancy results; however results agreed within error.

247

THE EFFECT OF CT ACQUISITION PARAMETERS ON EXTRACTED RADIOMIC FEATURES USING COMPUTATIONAL PHANTOMS

Jaryd Christie, Mohamed Abdelrazek, Stewart Gaede, Sarah Mattonen
Western University, London, ON

Purpose: To assess the effect of the tube current (mAs), slice thickness and reconstruction kernel on quantitative computed tomography (CT) radiomic features using the extended cardiac-torso (XCAT) computational phantoms and the x-ray-based cancer imaging simulation toolkit (XCIST) package.

Materials and Methods: An XCAT male computational phantom was used to model real patients. A lung tumour volume was extracted from a dataset of non-small cell lung cancer (NSCLC) patients and inserted and into the lungs of the computational phantom. The XCIST package was used to acquire CT scans on the phantom using 18 different acquisition protocols composed of all combinations of: three different tube currents (30, 150, and 300 mAs), three slice thicknesses (1, 2.5 and 5 mm), and two reconstruction kernels (lung and standard). The CT scanner was modelled to characterize a third-generation 64-detector-row-scanner; LightSpeed VCT (GE Healthcare, Madison, WI). The lung tumour was segmented using a semi-automatic segmentation algorithm. Pyradiomics was used to extract first-order and texture radiomic features from the segmented region on both the original and wavelet-filtered image, resulting in 838 radiomic features (bin width 25 HU, resampled to 1 mm^3). Features were extracted twice, both with and without the image normalization function within Pyradiomics. The intraclass correlation coefficient (ICC) was used to assess the stability of each feature between acquisition protocols with an ICC of 0.80 suggesting good feature stability. An F-test was performed to assess which features showed a statistically significant deviation from having an ICC of 0.80 ($p<0.05$).

Results: Radiomic features were most impacted by slice thickness, with only 34% of the extracted features demonstrating good stability. Features were less affected by changes in tube current and reconstruction kernel with 70% and 84% of the features demonstrating stability, respectively. When changing the reconstruction kernel, features extracted from the original image were more stable (87% stable) compared to features extracted on the wavelet-filtered images (69% stable). On the contrary, changes in tube current most affected the gray-level dependence matrix (GLDM) and gray-level run length matrix (GLRLM) features with less than 40% of the features showing good stability. Changes in slice thickness resulted in as low as 11% of first-order features showing stability. These results remained similar when normalization was added.

Conclusions: Our findings suggest changes in the acquisition parameters can have a significant effect on radiomic features. This study demonstrates the utility of XCAT phantoms for evaluating the stability of radiomic features and provides a valuable resource for the radiomics community. The use of XCAT phantoms can help to ensure the reliability and validity of radiomic features and can facilitate the development of more robust and accurate predictive models for patient outcomes.

248

COMPARISON OF INSPIRATION AND EXPIRATION DENSITY-BASED CT MEASUREMENTS WITH CT TEXTURE-BASED RADIOMICS IN PREDICTING COPD SYMPTOMS

Meghan Koo[1], Kalysta Makimoto[1], Wan Tan[2], Jim Hogg[2], Jean Bourbeau[3], Miranda Kirby[1]
[1]*Toronto Metropolitan University, Toronto, ON*
[2]*University of British Columbia, Vancouver, BC*
[3]*McGill University Health Centre, Montréal, QC*

Purpose: Established computed tomography (CT) biomarkers, such as density-based CT measurements, are pathologically validated in chronic obstructive pulmonary disease (COPD) and measure disease extent but do not fully capture the complex structural changes that occur in the lung. Texture-based CT radiomics is a novel technique that extracts measurements based on the spatial information of the grey-levels within CT images. The aim of this study is to investigate the association between texture-radiomics on inspiration and expiration CT with COPD symptoms, and compare these emerging features to established density-based CT measurements.

Materials and Methods: Canadian-Cohort-Obstructive-Lung-Disease (CanCOLD) study participants performed full-inspiratory and full-expiratory CT imaging. Baseline COPD symptoms were assessed using St. George's Respiratory Questionnaire (SGRQ) and COPD Assessment Test (CAT). Low attenuation below -950HU (LAA_{950}) on inspiration images quantified percentage of CT emphysema. LAA_{856} on expiration images quantified percentage of CT gas trapping. 101 radiomics measurements from six texture-radiomics sets were extracted from inspiration and expiration images respectively using MATLAB. LASSO regression was performed on the inspiration and expiration radiomics values, and coefficients were summed, to generate a RadScore for inspiration ($RadScore_{Insp}$) and expiration ($RadScore_{Exp}$) for each subject. Binary logistic regression (BLR) determined associations of symptom scores with CT measurements adjusted by covariates: age, sex, race, BMI, pack-years, smoking status, CT model, comorbidities (Asthma; Tuberculosis; Heart Disease, Systemic Hypertension or Diabetes), use of respiratory medications (bronchodilator, inhaled steroid, oral steroid), CT_{Insp} lung volume/total lung capacity, CT_{Exp} lung volume/residual volume.

Results: A total of 873 participants were investigated (n=330 no-COPD, n=543 COPD). There were significant differences between the groups for female sex (no-COPD=46.7%; COPD=38.1%; p=0.01) and age (no-COPD=66±10yrs; COPD=67±10yrs; p=0.04), but not for Caucasian race (no-COPD=94.8%; COPD=96.3%; p=0.56) or BMI (no-COPD=27.8±5kg/m^2; COPD=27.2±5kg/m^2; p=0.08). In a BLR model to predict CAT Score with all 4 CT measurements included, LAA_{950} was not significant (p>0.05), whereas LAA_{856} and both RadScores were statistically significant (p<0.02), with RadScoreExp having the highest Odds Ratio (OR=1.119). In the binary logistic model to predict SGRQ with all CT measurements included, LAA_{950} was not significant (p>0.05), whereas LAA_{856} and both RadScores are statistically significant (p<0.01), with RadScoreExp having the highest Odds Ratio (OR=1.186).

Conclusions: These findings demonstrate that texture-based radiomics derived from inspiration and expiration CT images provide independent prognostic information that is associated with respiratory symptoms when compared to established density-based measurements.

249

MICROWAVE-BASED BREAST IMAGING: EXISTING EVIDENCE, CHALLENGES, AND FUTURE PATHS

Tyson Reimer1, Stephen Pistorius[2]
[1]*University of Manitoba, Winnipeg, MB*
[2]*CancerCare Manitoba Research Institute, Winnipeg, MB*

Purpose: Microwave-based breast imaging is an emerging research field that uses low-power microwave-frequency electromagnetic radiation for diagnosis. A significant contrast in the microwave properties of malignant and healthy breast tissues has motivated investigations into this modality, but various limitations still need to be addressed. Several research groups have developed pre-clinical imaging systems to pursue this goal, and preliminary estimates of the diagnostic performance of the modality have been reported. This presentation will review the progress toward using microwave-based imaging for breast cancer detection.

Materials and Methods: A scoping review was performed to examine all published conference and journal articles that evaluated the performance of microwave-based breast cancer detection in either phantom or patient data. Studies were identified using the Scopus search engine with search terms: "breast" AND ("microwave" OR "radar") AND ("imaging" OR "detection" OR "sensing"). One hundred and eighty-five articles were identified for inclusion in this review.

Results: Sensitivity estimates ranged from 63-100%, and specificity estimates ranged from 20-65% in image-based breast cancer detection. Twelve articles reported estimates of the diagnostic performance of image-based cancer detection, with the most extensive study using data from 225 patients. Eleven of the twelve studies estimated the diagnostic sensitivity, while only four estimated the specificity (two of which used phantom data). Additionally, image quality analysis has focused entirely on image contrast, and only one in four articles presenting image-based tumour detection results presented any images of healthy breasts. This emphasis has led to research efforts largely developing high-contrast image reconstruction methods without sufficient consideration of image accuracy in the context of healthy breast reconstructions, leading to little investigation into the modality's specificity. Within the limited number of articles presenting healthy breast reconstructions, a hot-spot artifact is observed. This artifact consists of a localized region of relatively high-intensity responses, but its impacts on image quality and diagnostic specificity have not been explored in the literature.

Conclusions: Despite a growing number of clinical trials into the effectiveness of microwave-based breast cancer detection, further investigations into the specificity of the modality are needed before larger clinical trials are performed. Existing evidence demonstrates promising sensitivity of these systems, but current specificity estimates are not as encouraging. Insufficient attention has been devoted to the specificity of the modality, and future work in microwave breast imaging must address all aspects of diagnostic performance. Image artifacts and accuracy must also be further explored due to the potential connection between the low specificity estimates and the common hot-spot artifact.

250

DOES DIAGNOSTIC MRI BEFORE RADIOTHERAPY FOR PROSTATE CANCER CAUSE A WILL ROGERS PHENOMENON?

Johanna Dahan
Université de Montréal, Montréal, QC

Purpose: Pre-treatment diagnostic MRI is used in prostate cancer detection and staging; however little is known about its potential for radiotherapy treatment decision, or its prognostic value. We investigated the impact of the MRI in treatment decision to detect an eventual shift in treatment option which could cause a Will Rogers phenomenon. This is a mathematical paradox that results from moving an element from one set to another raising the average values of both sets.

Materials and Methods: We analyzed 1280 patients treated by either external-beam radiotherapy (EBRT) or brachytherapy as sole treatment or as a boost from 2014-2022. A diagnostic MRI

had to be done ≤12 months before treatment. PIRADS score, index lesion diameter and the presence of capsule contact and extra-prostatic extension were analyzed. Distribution of radiological and clinical features between treatment-groups were estimated using a chi-squared test.

Results: Three hundred and fourteen patients (24.5%) had a diagnostic MRI before treatment. An MRI was more frequent (p=0.017) in patients treated with EBRT (32.0%) than with a brachytherapy-boost (24.0%) or seed brachytherapy as monotherapy (22.5%). A PIRADS 5 lesion was seen in 32.4%, PIRADS 4 in 52.4% and PIRADS 3 were reported in only 8%. Organ-confined disease without any contact with the capsule was found in 51%. A clinically significant number of 22% patients with CAPRA≤ 3 disease presented with lesions ³15 mm. A lesion ≥ 20 mm was present in only 55 of patients treated with seed brachytherapy but 30-33% of patients treated with different modalities. Compared to EBRT and brachytherapy boost, patients treated with seed brachytherapy were more likely (p=0.012) to have organ confined disease without capsular contact (58%) versus 39% treated with brachytherapy boost and 52% treated with EBRT. Of the 39 patients who had a recurrence, only five had an MRI: 4 had a lesion of ≥ 20 mm and 3 had seminal vesicle invasion. Patients who didn't have a diagnostic MRI didn't have worse biochemical recurrence-free survival than patients who had an MRI (p=0.35).

Conclusions: More than twenty percent of patients with CAPRA ≤ 3 presented a lesion ³15 mm (PIRADS 5) on MRI. Patients with larger cancer on MRI seem to be directed away from LDR therapy and biochemical recurrence didn't differ whether patients had an MRI or not: a possible Will Rogers phenomenon.

251

PROSTATE SPECIFIC MEMBRANE ANTIGEN POSITRON EMISSION TOMOGRAPHY FOR PATIENTS WITH RECURRENT PROSTATE CANCER (PREP) - A PROSPECTIVE, MULTICENTRE REGISTRY

Aneesh Dhar[1], Glenn Bauman[1,2], Lucas Mendez[2,1], Girish Kulkarni[3,4], Antonio Finelli[3,4], Alejandro Berlin[3,4], Peter Chung[3,4], Andrew Bayley[3,5], Hans Chung[3,5], Laurence Klotz[5,3], Robert Wolfson[5,3], Himu Lukka[6,7], Katherine Zukotynski[7,6], Anil Kapoor[8,6], Bobby Shayegan[8,6], Joseph Chin[2,1], Catherine Hildebrand[2], Irina Rachinsky[2,1], Eugene Leung[9,10], Luke Lavallee[9,10], Chris Morash[10,9], David Tiberi[10,9], Marlon Hagerty[11], Kevin Ramchandar[11], Jonathan Boekhoud[11], Walid Shahrour[11], Deanna Langer[12], Pamela MacCrostie[12], Victor Mak[12], Ur Metser[3,4]

[1]Western University, London, ON
[2]London Health Sciences Centre, London, ON
[3]University of Toronto, Toronto, ON
[4]University Health Network, Toronto, ON
[5]Sunnybrook Health Sciences Centre, Toronto, ON
[6]McMaster University, Hamilton, ON
[7]Hamilton Health Sciences, Hamilton, ON
[8]St. Joseph's Health Care, Hamilton, ON
[9]The Ottawa Hospital, Ottawa, ON
[10]University of Ottawa, Ottawa, ON
[11]Thunder Bay Regional Health Sciences Centre, Thunder Bay, ON
[12]Cancer Care Ontario (Ontario Health), Toronto, ON

Purpose: Prostate Specific Membrane Antigen (PSMA) Positron Emission Tomography/Computed Tomography (PET/CT) can have positive findings for patients with prostate cancer, even when conventional imaging (CI) is negative.

Materials and Methods: PREP is a prospective registry open at five Ontario centres. Enrollment is according to six clinical cohorts: (1) Node positive disease or persistently detectable prostate specific antigen (PSA) post-radical prostatectomy (RP); (2) biochemical failure (BCF) after initial RP; (3) BCF after initial RP and adjuvant or salvage radiation therapy (RT); 4) BCF after RP and salvage ADT; (5) BCF after prior PSMA PET lesion-directed therapy; and (6) BCF (per Phoenix definition) after definitive RT. All PSMA PET/CTs used 18F DCFPyL as a radiotracer. CI was required for all patients initially (PREP1), but this has been modified (PREP 2) to require CI only when PSA is greater than 10 ng/mL. The primary endpoint is overall detection rate, with secondary endpoints including detection rate by clinical cohort, patterns of recurrence and change in planned management based on PSMA PET/CT results.

Results: From December 2018 to March 2022, 3967 PSMA PET/CT studies were completed; 348 (12%) were repeat scans. Median age (Interquartile range (IQR)) for all cohorts was 71 (66–76) years. For cohorts 2, 3 and 6 (BCF after local therapy), the median PSA (IQR) was 0.33 (0.2–0.93) ng/mL, 1.0 (0.45–2.57) ng/mL, and 4.4 (3.1–7.5) ng/mL. For these cohorts, the overall detection rate was 49, 72 and 90%, with limited (pelvic only or oligometastatic) disease detected in 45, 61, and 71% of scans and extensive metastatic disease detected in 4, 11, and 19% of scans. When grouped by initial PSA, the overall, limited disease and extensive disease detection rates in all six cohorts were the following: for PSA less than 0.1 ng/mL, 12, 12, and 0%; PSA between 0.1–0.3 ng/mL, 38, 37, and 1%; PSA between 0.3–0.5 ng/mL, 55, 52, and 3%; PSA between 0.5–1.0 ng/mL, 67, 62, and 5%; and for PSA greater than 1.0 ng/mL, 88, 68, and 20%. In all cohorts, when PSA was less than 10 ng/mL, the overall detection rates, with or without CI, were similar (64 versus 70%), as were changes in management (59 versus 50%). For cohorts 2, 3, and 6, the PSMA PET/CT changed management in more than half of cases: 26, 32, and 32% of cases changed management to local salvage; 11, 18, and 25% changed management to systemic therapy; and 6, 6, and 6% changed management to observation.

Conclusions: PREP is a multicentre registry of patients with recurrent prostate cancer who received PSMA PET/CT. The detection rate increased with increasing PSA levels; half of scans with PSA greater than 0.3 ng/mL had positive findings. The omission of CI in patients with PSA less than 10 ng/mL did not dramatically change patterns of disease detection or management change. A change in management were seen in most men after PSMA PET/CT.

252

SIGNAL TO NOISE VARIABILITY OF PHASED ARRAY COIL ELEMENTS USED IN A RADIATION ONCOLOGY DEDICATED MRI SIMULATOR

Alyaa Elzibak[1,2], Brige Chugh[1,2], Alex Karotki[1], Stephen Breen[1,2]
[1]Odette Cancer Centre, Sunnybrook Health Sciences Centre, Toronto, ON
[2]University of Toronto, Toronto, ON

Purpose: MRI simulators are becoming more prevalent in radiation oncology departments and a number of quality control (QC) documents have been published. Recommendations of radiofrequency (RF) coil QC range from monthly to quarterly or annual testing, depending on coil type, utilization and resources. This study analyses signal-to-noise ratio (SNR) for each element of our phased array coils, for a radiation oncology dedicated MRI simulator.

Materials and Methods: QC was completed using a 1.5T MRI simulator (Ingenia 1.5T, Philips Systems) and five phased array coils. Data from 75 elements was collected on a monthly basis over three years. Coils included: two anterior coils (16 elements each), a posterior coil (12 elements), a head coil (15 elements), and a head and neck coil (16 elements). Testing was completed using vendor-provided phantoms, methodology and automatic

analysis procedure. For each coil element, the minimum and coefficient of variation (CV) of the SNR values acquired during the three years was tabulated.

Results: The SNR consistently exceeded the vendor's specification (vendor tolerances ranged from 56 – 116) for each of the 75 elements. The CV ranged from 1.4% – 7.8%; flexible coils showed more elements with higher CV compared to rigid coils (63% of the flexible coil elements showed CV > 3% compared to 14% of the elements in rigid coils).

Conclusions: AAPM TG-284 report states that flexible coils are more likely to be susceptible to damage and element failure given their non-rigid design and frequent use, justifying recommendations of monthly testing of the elements. Although coil failures were not noted in our data, more elements of the flexible coils showed CV >3% compared to the rigid coils. Potential contributions of set-up variability were not investigated.

253

FINDING REPRODUCIBLE AND INFORMATIVE RADIOMIC FEATURES ASSOCIATED TO CLINICAL ENDPOINTS AND TO IMMUNOHISTOCHEMISTRY BIOMARKERS FROM CT IMAGING DATA IN AN IMMUNOTHERAPY-TREATED NSCLC COHORT

Leyla Ebrahimpour[1], Yannick Lemaréchal[1], Michèle Orain[1], Philippe Joubert[1], Fabien Lamaze[1], Philippe Després[1], Venkata Manem[2]
[1]*Université Laval, Quebec City, QC*
[2]*Université du Québec à Trois-Rivières, Quebec City, QC*

Purpose: The objective of this study is to find reproducible and predictive radiomic features from Computed Tomography (CT) images that are correlated to clinical endpoints and immunohistochemistry (IHC) biomarkers in an immunotherapy-treated non-small cell lung cancer (NSCLC) cohort.

Materials and Methods: A retrospective study of NSCLC patients receiving immunotherapy was undertaken. The dataset includes 164 patients that have CT-scans and survival endpoints, while 34 of them have IHC data as well. For all of the patients, we extracted 1,224 and 441 radiomic features using two IBSI-compliant pipelines, Pyradiomics and RaCat respectively. They were grouped into shape-, intensity-, and textural-based categories. The intraclass comparison between features across these two pipelines was assessed by the Pearson, Spearman, F-test, and Mutual Information estimators and corrected for false positives using the False Discovery Rate (FDR) method. To assess the influence of the clustering of pixels based on their intensity (defined as the gray-level discretization), on the robustness of features, we computed their association with two survival endpoints (Overall Survival (OS) and progression-free Survival (PFS)) and with eight IHC markers (CD3, CD4, CD8, CD56, CD163, Lag3, PD1, and TIM) considering two different bin counts and bin width for a sub-group of 34 Samples.

Results: Our results showed that first-order radiomic features were amongst the most reproducible features. Importantly, our findings conveyed that while the values of radiomic features were strongly pipeline-dependent, the textural radiomic features that were associated to the clinical parameters and IHC markers were strongly dependent to the type of discretization too. When changing the bin width or bin count, only 20% of the overall texture-based radiomic features have a lower rank differential change (less than 50) in the target prediction ranking score. Whereas, this value is 100% for the shape-based features and 90% for the intensity-based features.

Conclusions: Through this work, we highlighted a significant heterogeneity between radiomic pipelines as well as the impact of gray-level discretization on the discovery of immunotherapy biomarkers in NSCLC patients. Based on this, it is crucial to harmonize the radiomics processing methods to develop clinically robust predictive models in future studies.

254

LOW-TESLA MRI IMAGING EFFECTIVELY REDUCES HARDWARE ARTIFACTS IN PATIENTS WITH METAL IMPLANTS

Abdulaziz Alghamdi, Soon Huh, Adam Holtzman, Danny Indelicato, Jiyeon Park
University of Florida, Jacksonville, FL

Purpose: Hardware artifacts in MRI scans of patients with metal implants can cause signal voids and incomplete visualization of the spine, leading to misinterpretation of findings. Optimization of imaging parameters and hardware suppression techniques such as SEMAC have been used to minimize these artifacts. However, this study investigated the effectiveness of low-Tesla MRI imaging as an alternative to dedicated hardware suppression techniques for reducing hardware artifacts in patients with metal implants.

Materials and Methods: Eleven patients, including seven with thoracic, two with cervical, and two with lumbar hardware implantation of note Two of these patients had residual tumours that were not captured by diagnostic imaging, underwent low-Tesla MRI scans to investigate hardware artifacts. The study analyzed the effects of various imaging parameters on hardware artifact reduction. The study utilized 0.23T MRI to decrease susceptibility artifacts caused by metal implants, and implemented B-FFE3 D pulse sequences that were optimized using a bone phantom consisting of titanium screws and aluminum plates submerged in a water phantom. The imaging parameters were adjusted to decrease susceptibility artifacts, particularly Ring artifacts caused by pedicle screws, resulting in optimized TR of 8.8mSec, TE of TR/2, FOV of 200cm, Matrix of 200 to 240, slice thickness of 3 to 4 mm, flip angles of 60, and a scan time of less than four minutes. These parameters were determined by following the general guidelines in Artifact Reduction Technique (ARF).

Results: Optimizing imaging parameters resulted in a significant reduction of hardware artifacts, improving the image quality of the spinal cord and gross residual tumour, which was confirmed by the treating radiation oncologist.

Conclusions: In conclusion, this study highlights the effectiveness of low-Tesla MRI imaging with optimized imaging parameters in reducing hardware artifacts in patients with metal implants. The findings suggest that this imaging modality should be preferred for obtaining accurate and improved image quality for spinal cord and residual tumour visualization, thereby aiding better target delination and treatment planning.

255

LOGISTIC DOSE DISTANCE MODEL TO PREDICT MOIST DESQUAMATION IN BREAST RADIOTHERAPY

Aria Malhotra[1], Emilie Carpentier[1], Sheri Grahame[2], Alan Nichol[1,2], Elisa Chan[1,2], Cheryl Duzenli[1,2]
[1]*University of British Columbia, Vancouver, BC*
[2]*British Columbia Cancer, Vancouver, BC*

Purpose: A metric is developed to improve understanding of skin radiobiology and to predict the presence and location of moist desquamation (MD), based on measured dose and skin assessments of a patient population at high risk of developing radiotherapy induced skin reactions.

Materials and Methods: Twenty breast patients participated in a pilot study of a novel carbon fibre breast support device. During treatment, the dose distribution was measured using film in the inframammary fold region. The skin was assessed for MD by staff and patients at regular intervals. With two different dose fractionations used in the pilot study, all doses were corrected with $EQD2_{11}$ to account for biological effects of fractionation. The classification of MD in this study was based on a combination of staff assessments and patient reported outcomes. A logistic model was modified and developed to predict MD, accounting for the spatial distribution of measured skin dose. Two adjustable parameters define the slope and the inflection point of the function and a normalization value sets the threshold for MD. Parameters were tested by applying the metric on the 20 patient skin dose distributions.

Results: Six of 20 patients have reports of MD in this study. There were statistically significant differences in the metric between patients who did and did not develop MD with the parameters set to a slope of 5 and an inflection point of 10mm – 30mm. The model indicated specific regions expected to develop MD, correctly classifying all 6 reported cases of MD and 12 of 14 (86%) cases not reporting MD. Pixel clusters with an average contiguous surface area of 14 cm^2 having dose > 43Gy ($EQD2_{11}$) were flagged for MD.

Conclusions: This dose-distance metric has been shown to predict specific regions of skin expected to develop MD in breast radiotherapy. Expanded testing of this model is underway.

256

PATIENT-SPECIFIC PRE-TREATMENT NUCLEI SIZE DISTRIBUTION IS OF SIGNIFICANCE FOR POST RADIATION THERAPY LOCOREGIONAL RECURRENCE AND SURVIVAL OUTCOMES

Yujing Zou[1], Magali Lecavalier-Barsoum[1], Manuela Pelmus [1], Farhad Maleki [2], Shirin A. Enger[1]
[1]McGill University, Montréal, QC
[2]University of Calgary, Calgary, AB

Purpose: Microdosimetry studies showed varying nuclei / cell target size distribution receiving radiation may result in differing specific energy deposited among tissues, therefore influencing patient-specific dose response. In this study, we investigated the significance of pre-treatment nuclei / cell distributions for their post radiation therapy recurrence and survival outcomes for gynecological cancer patients.

Materials and Methods: Fifty-one gynecological (i.e., cervix, vaginal, and vulva) cancer patients (median age at diagnosis = 60 years) with a median follow-up time of 26.4 months were included into the current study retrospectively. All patients had undergone a combination of external beam radiation therapy (RT), brachytherapy, concurrent chemotherapy. The post RT outcomes of interest were locoregional recurrence, distant metastasis, and survival. Clinical variables (i.e., age at diagnosis, radiological and clinical stage at diagnosis, cancer type, histology, and p16 status) were collected. Patient-specific nuclei size and cell spacing (collectively referred to as "target size") distributions from cancerous and non-tumoural regions of diagnostic pre-treatment hematoxylin and eosin-stained digital histopathology whole slide images were automatically extracted. Independent Welch's t tests between each target size pair (i.e., a cancerous region quantity against a non-tumoural region quantity) were computed. For each clinical endpoint, a Mann-Whitney U test was implemented to investigate whether a target size feature for a given binary outcome is significantly different from those with the opposite outcome, for each of the extracted target size features.

Results: The median of total treatment time was 43 days, while the follow-up period of locoregional recurrence, distant metastasis, and survival were 8.20 months, 9.51 months, and 19.33 months, respectively. The Welch's t tests showed that each target size pair were all significantly different from each other except for cancerous and non-tumoural cell spacing distribution mean. Mann–Whitney U tests revealed a significant difference between patient-specific cancerous nuclei size distribution mean for patients with and without post RT locoregional recurrence (w-statistic = 82.0, p=0.018) and survival (w-statistic = 102.0, p=0.007). Furthermore, the nuclei size distribution mean across patients that developed post RT locoregional recurrence is smaller than those that did not, the same result was revealed for those who survived as opposed to deceased. However, no significant difference was found for each target size feature given opposite distant metastasis outcomes.

Conclusions: We showed that patient-specific pre-treatment cancerous nuclei target size matters in relation to post radiation therapy locoregional recurrence and survival outcomes in gynecological cancer patients.

257

THREE-DIMENSIONAL ULTRASOUND FUSION OF TRANS-ABDOMINAL AND TRANS-RECTAL IMAGES FOR VISUALIZATION OF GYNECOLOGICAL HIGH DOSE-RATE BRACHYTHERAPY APPLICATORS

Tiana Trumpour[1], Jamiel Nasser[4], Carla du Toit[2], Claire Park[1], Jessica Rodgers[3], Lucas Mendez[1], Kathleen Surry[1], Aaron Fenster[1]
[1]Western University, London, ON
[2]Robarts Research Institute, London, ON
[3]University of Manitoba, Winnipeg, MB
[4]University of Waterloo, Waterloo, ON

Purpose: High dose-rate brachytherapy is a common radiotherapy method for treating gynecological cancer, in which specialized intracavitary applicators, interstitial needles, or a hybrid combination are placed locally nearby the tumour to provide conformal radiation doses. Accurate placement of the applicator and needles is necessary to ensure accurate dose escalation and acceptable treatment outcomes. Our previous work investigated the use of combining three-dimensional (3D) trans-abdominal ultrasound (TAUS) and 3D trans-rectal ultrasound (TRUS) images to provide visualization of the applicator, needles, and surrounding pelvic anatomy. While our methods were successful for a single applicator type, we propose a more comprehensive fusion technique and an investigation of additional applicators for a robust proof-of-concept.

Materials and Methods: A phantom study was performed using a custom tri-modal imaging phantom that included internal anatomical structures and either a ring-and-tandem hybrid Vienna applicator with interstitial needles or an intracavitary tandem-and-ovoids Fletcher applicator. Fiducial points used to evaluate the registration were needle tips (N=4) in the Vienna phantom and brass fiducial spheres (N=4) in the Fletcher phantom. We acquired both 3D TAUS and 3D TRUS images of each phantom using our in-house developed mechatronic imaging system, which can accommodate any conventional US transducer. A 3D rendering of each of the applicators was created and subsequently overlaid on the 3D US images using the shadows and reflections present in each imaging view. Rigid registration of the two 3D US images was performed using the applicator models as landmarks, with successive image fusion being performed using an optimized 3D voxel combination algorithm. Target registration error (TRE) and fiducial localization error (FLE) of the fiducial points were evaluated to assess the registration accuracy of the 3D TAUS-TRUS fusion. The final fused 3D US image was compared with gold-standard

magnetic resonance (MR) and computed tomography (CT) images of the same phantoms.

Results: Qualitative analysis by a trained observer determined that full visualization of the applicators, needle tips, and surrounding phantom anatomy was obtained using the fused 3D US images. Registration of the Vienna applicator resulted in a mean TRE and FLE of 2.8 ± 0.2 mm and 0.7 ± 0.3 mm, respectively, while the Fletcher applicator phantom showed a mean TRE and FLE of 5.6 ± 0.2 mm and 0.5 ± 0.3 mm, respectively. Comparisons of anatomical segmentations between the fused 3D US image and the corresponding CT and MR images will be quantified.

Conclusions: Our results indicate that our 3D TAUS-TRUS fusion technique is generalizable to diverse gynecological brachytherapy applicators with acceptable visualization of the region of interest. This technique shows potential as an improved intra-operative image guidance method as well as shows the possibility for 3D US-based dose planning.

258

SET UP TIME AND REPRODUCIBILITY FOR PATIENTS WITH LARGE OR PENDULOUS BREASTS IN SUPINE BREAST RADIOTHERAPY

Michelle Medina[1], Amy Frederick[2], Cheryl Duzenli[1,2]
[1]*University of British Columbia, Vancouver, BC*
[2]*British Columbia Cancer, Vancouver, BC*

Purpose: Previous studies have reported reduced patient set up reproducibility, increased radiation-related toxicities, and worse cosmetic outcomes for patients with large and/or pendulous breasts undergoing supine breast radiotherapy. The Carbon-fibre Adjustable Reusable Accessory (CARA) for breast support is a novel immobilization device designed to address these issues. The purpose of this study is to compare patient setup time and reproducibility between patients treated with and without CARA.

Materials and Methods: A total of 27 breast cancer patients with inframammary folds or lateral ptosis participating in a pilot study had kV imaging data available for retrospective review. Of these, 18 were immobilized with CARA and nine were immobilized according to current standard of care. Patient set up consisted of the alignment of skin marks with the treatment room lasers followed by an isocentre shift. The set up verification protocol required a minimum of orthogonal kV imaging during the first 3 treatment fractions and weekly thereafter. Setup reproducibility was measured using the couch shifts applied in the anterior-posterior (AP), superior-inferior (SI), and left-right (LR) directions according to the online match between orthogonal kV images and reference digitally reconstructed radiographs. Averages and standard deviations (SDs) of the absolute shifts and setup times were calculated for each patient over their treatment course. The distributions of couch shifts in each cardinal direction and the average time required to complete patient setup were compared between the two cohorts using two-tailed Wilcoxon Rank Sum Tests. A p-value ≤ 0.05 was considered statistically significant.

Results: The median (range) average absolute couch shifts in the AP, SI, and LR directions were 0.22 cm (0.11 - 0.50 cm), 0.37 cm (0.13 - 0.75 cm), and 0.58 cm (0.24 - 1.2 cm) for patients immobilized with CARA and 0.20 cm (0.09 - 0.43 cm), 0.46 cm (0.21 - 0.87 cm), and 0.50 cm (0.21 - 2.28 cm) for patients immobilized according to the current standard of care. The standard deviations of absolute couch shifts in the AP, SI, and LR directions were also comparable between the two groups. The median (range) average patient setup time was 5.57 min (2.87 - 14.08 min) for patients immobilized with CARA and 7.70 min (3.00 – 15.18 min) without CARA. There were no statistically significant differences in patient setup time or reproducibility among patients immobilized with and without CARA.

Conclusions: Patient set up time and reproducibility were comparable among patients immobilized with and without CARA but these results are limited by the small sample size in this study and novelty of the device. A more rigorous analysis will be performed as part of a phase III randomized controlled trial evaluating CARA.

259

DEVELOPMENT OF A COST-EFFICIENT SCINTILLATION-FIBER DETECTOR FOR USE IN AUTOMATED SYNTHESIS OF POSITRON EMISSION TOMOGRAPHY RADIOTRACERS

Hailey SH Ahn[1], Liam Carroll[1], Robert Hopewell[2], I-Huang Tsai[2], Shirin A Enger[3]
[1]*McGill University, Montréal, QC*
[2]*Montreal Neurological Institute, Montréal, QC*
[3]*Jewish General Hospital, Montréal, QC*

Purpose: Radiolabelling is a critical step in positron emission tomography (PET) radiotracer production, involving complex multistep chemical reactions. Nowadays, the process is broken down into a series of automated unit operations to improve its efficiency and accuracy. Within the automated synthesis module, several radiation detectors are placed in at key locations to ensure that the correct reactions are taking place. These detectors however cost thousands of dollars per channel, motivating the development of a cost-efficient alternative. The objective of this work was to develop a multichannel detector using low-cost scintillating fibers and silicon photomultipliers (SiPMs) to allow monitoring of the transfer of radioactivity throughout the process.

Materials and Methods: The detector is constructed using plastic scintillating fibers (Saint-Gobain, BCF-12), optical fibers (Eska), a 6x6 mm^2 SiPM (Onsemi, microfc-60035-smt), and inexpensive electronic circuitry (Axani, 2017). The scintillating fibers act as the sensitive volume of the detector, and are placed next to the reaction vials and cartridges to detect emitted annihilation photons. They are coupled to an optical fiber to guide photons to the SiPM, producing detectable signal. Monte Carlo simulations with the Geant4 toolkit were performed to optimize the detector construction and increase detection efficiency. Three configurations were simulated, each with 100 million 511 keV annihilation photons, isotropically-emitting from a water filled glass vial with 1 cm radius and 3 cm height. The three scintillation fiber constructions were: 1) single fiber placed 1 mm from the vial, 2) single fiber surrounded by 1 cm of bolus (fiber 1.1 cm from the vial), and 3) 4x4 fiber bundle, with each fiber 1 cm in length and 1 mm in diameter. Energy deposited per event was scored and used to predict the expected voltage from the SiPM given the total light collection efficiency (Beddar, 2003).

Results: The sensitive volume of the low-cost detector is small and compact, making it ideal for placement inside the chemistry modules. From the deposited energy per event calculated with the Monte Carlo method, the maximum SiPM voltage pulse height for the three detector constructions were estimated to be 1.064, 1.051, and 1.591 mV, respectively. Despite significant electronic noise due to the inexpensive electronics ($\sigma \sim 1$ mV), the 16-fiber bundle design was found to produce detectable pulses that could be used to provide a rough estimate of the activity in each compartment. The total cost of the detector is approximately USD $200 per channel, reducing the cost by 85-95% compared to commercially available detectors.

Conclusions: The scintillation fiber detector provides a cost-efficient solution to troubleshoot the automated synthesis of PET radiotracers. By optimizing the configuration of plastic scintillating fibers, the detector can be used to detect annihilation photons and measure activity, allowing for early detection of faulty reaction steps, ultimately reducing radiotracer production costs and preventing delays in patient scans.

260

INCORPORATING DNA REPAIR MECHANISMS INTO A MONTE CARLO MODEL OF DNA DAMAGE BY NEUTRONS

Nicolas Desjardins, John Kildea
[1]*McGill University, Montréal, QC*

Purpose: The risk associated with the stochastic effects of neutron irradiation is known to be strongly energy dependent. Over the past decade, several studies have used Monte Carlo simulations to estimate the relative biological effectiveness (RBE) of neutrons for various types of DNA damage in order to understand its energy dependence at the fundamental level. However, none of these studies implemented DNA repair simulations in their pipeline. In this project, we investigated the effects of adding repair mechanisms to Monte Carlo-based RBE estimates of DNA damage by neutrons.

Materials and Methods: Our group had previously carried out condensed history (CH) simulations to profile the energy spectra and relative dose contribution of the secondary particles produced by neutron interactions in tissue. In this project, we used the results of our CH simulations to simulate the irradiation of TOPAS-nBio's DNA model by a flat spectrum of neutrons ranging from 1 eV to 10 MeV, as well as reference X-rays at 250 keV. Induced DNA damage was recorded using the standard DNA damage data (SDD) format. DNA repair was simulated using the DNA Mechanistic Repair Simulator (DaMaRiS) framework.

Results: At the time of writing, only non-homologous end joining has been implemented. Our preliminary estimates of the RBE of neutrons to cause misrepairs is higher than our estimate for the RBE of neutrons to cause double-strand breaks pre-repair. However, our preliminary estimates for the RBE of neutron to cause mis-repairs is still much lower than the NCRP's radiation quality factor Q and the ICRP's radiation weighting factor w_R.

Conclusions: Our preliminary results incorporating DNA damage suggest that the quantity of misrepair caused by neutrons has a more significant energy dependence than the quantity of double-strand breaks alone. For now, our results are still preliminary, and validation work is ongoing.

261

A 3D STAR SHOT TO DETERMINE AXES OF ROTATION

Robert Corns, Kaida Yang, Mason Ross, Shiva Bhandari, Makunda Aryal, Peter Ciaccio
East Carolina University, Greenville, NC

Purpose: Star shots are a method to determine the location of the gantry, collimator, and couch axes of rotation. Presented is a technique to extend this traditional 2D method to 3D, allowing the user to relate each axis relative to the others.

Materials and Methods: A film is wrapped around a cylinder and the cylinder is aligned to the isocentre and gantry axis. Slits exposures are taken through an mlc gap for gantry, collimator and couch rotations. The radiation slit approximates a plane and the resulting exposures are modeled as cylindrical sections. Each exposure will have an entrance and exit. Unwrapping the film reveals linear and sinewave patterns. Locations of exposed pixels on the film relate to the gantry's z-axis and arc-length s along the cylinder. The collimator forms two local star shot patterns, one at the entrance and one at the exit. Treating each as a 2D star shots, their radiation centres can be found. Map these centres back on to the cylinder and they will be on opposites sides of the cylinder. Joining the entrance and exit centres makes a line representing the collimator's axis of rotation in 3D. The same logic applies to the couch axis of rotation. The logic for the gantry axis differs because it forms a virtual star shot in the centre of the cylinder. The gantry exposures make vertical lines on the film. Map these back on the cylinder and take and axial slice. The film shows where entrance and exit exposures are around the circumference of the cylinder. Joining an entrance to its exit draws a line through the centre of the cylinder and collectively all these lines form a virtual star shot. This can be treated as a 2D star shot and its radiation centre found. Do this exercise at each end of the cylinder. Joining the centres from each end forms a 3D line that represents the gantry's axis of rotation. With all three axes represented in 3D, statistics on how close they are to each are made. Essentially a point P in space is picked and the distance from P to each axis computed. The largest of these three distances is scored. The optimization moves P around until this largest distance is as small as possible. This algorithm was implemented using MatLab. The steps involved are: binarizing the image to exposed or unexposed pixels; fitting curves to the exposed pixels coordinates; finding the radiation centres and joining them in 3D to form a rotation axis, and; find the smallest sphere nearest to all three axes.

Results: A typical result was the sphere' centre P = (-0.25, 0.042, 0.19) mm and the distance from P to the gantry axis = 0.2543 mm, from P to the couch axis = 0.2543 mm and from P to the collimator axis = 0.2353 mm.

Conclusions: A 3D star shot technique was presented that is capable of accurately and precisely of determining the relative positions of gantry, collimator, and couch axes of rotation in 3D. The method encodes the 3D information by wrapping a film around a cylinder.

262

A FRAMEWORK FOR DESIGNING GLASS VESSELS USED IN WATER CALORIMETRY

Mark D'Souza[1], James Renaud[2], Arman Sarfehnia[3]
[1]*Toronto Metropolitan University, Toronto, ON*
[2]*National Research Council of Canada, Ottawa, ON*
[3]*Sunnybrook Health Sciences Centre, Toronto, ON*

Purpose: In a water calorimeter (WC), absolute dose-to-water at a point (quantity of interest in radiotherapy) is measured directly by an accurate determination of radiation-induced temperature rise. To avoid heat defect, i.e. exo/endothermic reactions with water impurities, the temperature sensors are contained within a glass vessel (GV) filled with high-purity water. To account for heat transfer (such as conduction and convection) that can change the measured temperature rise, a heat transfer (k_{ht}) correction is applied. In this study, we use Finite Element Method (FEM) analysis to study the sensitivity of k_{ht} to several of its main contributors, i.e. several GV-related parameters. This way, we develop a framework to guide the process for designing modality-specific parallel-plate GV.

Materials and Methods: k_{ht} was numerically determined by simulating the GV in a WC under a realistic and an ideal condition (where in the former case, heat transfer was modeled while it was nulled in the ideal scenario). To determine simulation robustness, FEM studies to observe the effects of different boundary conditions (isothermal versus adiabatic) as well as the geometry of the WC were analyzed. Following this, a parallel-plate GV inside a WC was modeled. A WC glass temperature sensor was also modeled within the vessel and placed at AAPM TG51 defined reference depth. The magnitude and variation of k_{ht} as a function of GV dimensions/ thickness/position for several different energies (6 MV, 6 MeV, 9 MeV, 18 MeV) were determined.

Results: FEM analysis showed that as long as the WC dimensions were larger than the radiation field size, k_{ht} varied by less than 0.01 %. The effects of a fixed temperature boundary versus a

thermally insulated boundary differed by 0.1 %. As the sensors were moved away from the front GV surface, k_{ht} dropped by 25% for all energies up to a distance of around 8 mm, beyond which there was a much lower variation in k_{ht}. An equal front and back GV thickness resulted in the smallest and most stable k_{ht} for all but the lowest electron beam energy modeled. For the 6 MeV beam, k_{ht} was smallest and most stable between different GV positions when the front and back vessel thicknesses were respectively set to 0.70 mm and 1.30 mm.

Conclusions: A FEM framework was developed to help design WC GVs. Our process showed FEM simulations are robust and minimally affected by boundary conditions and WC dimensions as long as the WC dimensions are at least 1 cm larger than the radiation field size. Our framework showed that the thicknesses of the front/back windows as well as the position of the sensors with respect to these play an important role on k_{ht}. Unequal GV window thicknesses may produce k_{ht} corrections that are small in magnitude and vary minimally as the GV position changes in specific applications such as a 6 MeV beam. This shows that the proposed framework can be used to identify if unique vessel designs exist for other clinical beams.

263

THE MINIMUM ACCEPTABLE BLADDER VOLUME IN PROSTATE CANCER RADIATION THERAPY WITH VMAT DELIVERY TECHNIQUE

Congwu Cui, Holly Campbell
Saint John Regional Hospital, Horizon Health Network, Saint John, NB

Purpose: It is often difficult to maintain the consistency of bladder filling in prostate cancer radiation therapy. This work is to retrospectively study the dosimetric effect of the bladder volume variation between simulation and treatment and therefore to optimize the bladder preparation protocol.

Materials and Methods: The bladders of 37 patients treated for prostate cancer with the 36.25Gy/5fx VMAT SBRT technique were contoured on the simulation CT, MRI and CBCT images. The bladder volumes are in range of 55-800cc with differences of -82%~295% between simulation and treatment. The dose assessment metrics of V18.1Gy, V28Gy, V38Gy, V39.5Gy (bladder) and Dmax, V18.3Gy, V36.25Gy, V32.62Gy, V18.12Gy (bladder wall) were assessed against the bladder volumes in simulation and treatment.

Results: The absolute volume metrics and Dmax of bladder and bladder wall are not correlated to the bladder volume although the relative volume metrics do decrease with the bladder volume increase. If the bladder volume is >200cc, all the relative volume metrics are within the constraints. The absolute volume metrics of V38Gy of 7% and V39.5Gy of 14% of the patients exceed constraints when bladder filling is different from that in simulation while V38Gy of only one patient and V39.5Gy of only two patients exceed constraint if bladder volume >200cc.

Conclusions: The absolute volume dose assessment metrics of bladder and bladder wall are not correlated to the bladder volume. If bladder volume is >200cc, all the relative volume metrics of the patients in this study are within constraints. If the bladder dose of the initial plan is within constraints or deemed acceptable by a radiation oncologist and the bladder is >200cc on the treatment day, no further bladder preparation is needed for the treatment. A simple method is proposed to estimate the bladder volume based on CBCT image. The bladder preparation procedure can be potentially simplified and therefore reduce patient waiting time due to bladder filling variation.

264

MONITORING OF THE LONG-TERM PERFORMANCE OF a-Si 1200 ELECTRONIC PORTAL IMAGING DEVICE

Ivan Kutuzov, Boyd McCurdy, Ryan Rivest, Eric Van Uytven
University of Manitoba, Winnipeg, MC

Purpose: The electronic portal imaging device (EPID) can be used for machine or patient-specific quality assurance (QA), and for in vivo dosimetry. To be able to rely on EPID measurements in the clinic, the users must be confident in long-term stability of detector response. The aim of this study was to evaluate EPID performance as a dosimeter over an extended period of time.

Materials and Methods: Weekly measurements of an a-Si 1200 EPID dose response were carried out over a 24-month period with a clinically-used TrueBeam linear accelerator. All available beam energies were monitored, including 6MV, 10MV, 23MV, 6FFF, and 10FFF. EPID calibration fields (dark field and flood field) were also measured to assess their long-term reproducibility. Weekly measurements of the EPID response against absolute dosimeters, including an ion chamber and ion chamber array, positioned on beam central axis, were also carried out to evaluate EPID response variability over the period of observation. Measurements of the secondary absolute dosimeters were used as baselines, and the ratios of EPID readings to these measurements were analyzed using standard deviation. The Pearson correlation coefficient was used to evaluate correlation between EPID and ion chamber/array measurements. Short-term stability of the EPID response was evaluated using a series of consecutive measurements, made on the same day, and compared to its long-term stability. The pixel sensitivity matrix or PSM (i.e. the variation in individual pixel gains) was determined several times throughout the monitoring period and analyzed for long-term constancy.

Results: The variation of dark field signal calculated over the entire observation period did not exceed 0.16%. The calculated variation of flood field signal over the period of observation ranged from 0.43% to 0.46%, depending on the beam energy. The flood field measurements showed strong correlation between different beam energies, with a minimum correlation coefficient of 0.94. This suggest that the long-term machine output variation was he main cause of the observed changes in measured signal. Weekly EPID measurements showed moderate correlation with the ion chamber and chamber array measurements, with the correlation coefficients ranging from 0.61 to 0.72. The ratio of EPID to secondary dosimeter measurements showed standard deviations from 0.26% to 0.55% in the long term, while short term measurements showed standard deviations from 0.04% to 0.07% for EPID and 0.02% to 0.06% for secondary dosimeters. The pixel sensitivity matrix did not demonstrate significant changes over the observation period - over 94% of pixels showed differences below 1%, and 100% of pixels showed difference below 2%.

Conclusions: The dosimetric performance of an a-Si 1200 EPID was evaluated over a two-year period using multiple metrics. The results of the evaluation confirm high detector stability and high reproducibility of the investigated model of EPID detector and reinforce earlier studies found in literature.

265

MULTI-POINTS CALORIMETER USING FIBER BRAGG GRATINGS FOR SMALL FIELD DOSIMETRY IN RADIOTHERAPY

Marie-Anne Lebel-Cormier[1], Tommy Boilard[2], Martin Bernier[2], Luc Beaulieu[3]
[1]CHU de Québec - Université Laval et CRCHU de Québec, Quebec City, QC
[2]Université Laval, [3]CHU de Québec - Université Laval et CRCHU de Québec, Quebec City, QC

Purpose: The interest of using fiber Bragg gratings (FBGs) dosimeters in radiotherapy (RT) lies in their i) submillimeter detection volume, ii) customizable spatial resolution, iii) multi-points dose measurement, iv) real-time data acquisition and v) insensitivity to Cherenkov light. These characteristics could prove very useful especially for high data points density small field dosimetry since no standard is available yet for this particular type of dosimetry. We developed a multi-points FBGs dosimeter customized for small field RT dosimetry with a spatial resolution of 1 mm and a detection volume of 0.005 mm^3 per data point.

Materials and Methods: Thirty co-located 1 mm-long FBGs (adding up to a 3 cm long detector), uniformly spanning from 1505 nm to 1605 nm, are written through the coating of a standard 80 m diameter polyimide-coated silica fiber with the femtosecond scanning phase-mask technique and a custom e-beam phase mask. The detector is embedded in a plastic cylinder having a 0.63 cm (1/4") diameter and 30 cm length, which will experience thermal expansion due to radiation energy deposition thereby stretching the FBGs and changing the Bragg wavelength. Irradiations were performed with a Varian TrueBeam linear accelerator. For every irradiation, 2000 MU are delivered at 600 MU/min and the dose to the detector is calculated with the TPS (Ray Station). Fields of 10 x 10 cm^2 or 15 x 15 cm^2 are used respectively for photons and electrons irradiations. For the energy dependency, the build-up distance (d) used is 1.5 cm for 6 MV, 6 MeV, 9 MeV and 3.5 cm for 18 MV, 12 MeV, 18 MeV. For the output factor and dose profile measurements, a build-up distance (d) of 10.0 cm is used for fields ranging from 2 x 2 cm^2 to 30 x 30 cm^2.

Results: The dose profile of a 2 x 2 cm^2 6 MV beam was measured with a mean and a maximum relative difference of 1.8% and 6.4% (excluding the penumbra region). The output factor for a 6 MV beam is also measured and the measurements are in general agreement with the expected values within the experimental uncertainty for every measurement except for the 2 x 2 cm^2 field. A relative difference under 7% was obtained excluding the 2 x 2 cm^2 field which has a 15% gap. The detector response to different energy of photons and electrons beams is within 5% of the mean response (0.068 ± 0.002 pm/Gy).

Conclusions: We developed a small field calorimeter for RT using FBGs, which, to our knowledge, has never been done before. This detector allows dose profile and output factor measurements, and is energy independent within a range of 5%. In order to minimize the uncertainty on the dose measurements, an interrogator having a higher spectral resolution could be used. This type of detector could prove really useful for small field dosimetry, but also potentially for MRI-LINAC and FLASH since silica fibers are highly resistant to radiation and are already used for high dose range in the nuclear field. For this prototype, we used a PMMA coating, but other types of plastic could also be suitable to better match water density and limit small field particle fluence perturbation.

266 WITHDRAWN

267
CHARACTERIZATION OF CHANGES IN SCINTILLATION SPECTRUM OF PLASTIC SCINTILLATOR DOSIMETERS AFTER RADIATION DAMAGE UNDER ULTRA-HIGH DOSE RATE 200 MEV ELECTRONS AT CLEAR

Cloé Giguère[1,2], Alexander Hart[3], Nolan Esplen[3], John Bateman[4,5], Pierre Korysko[5], Wilfrid Farabolini[5], Magdalena Bazalova-Carter[3], Luc Beaulieu[1,2]
[1]*Université Laval, Quebec City, QC*
[2]*CHU de Québec-Université Laval, Quebec City, QC*
[3]*University of Victoria, Victoria, BC*
[4]*University of Oxford, Geneva, CH*
[5]*CERN, Geneva, CH*

Purpose: To characterize the short and long-term effects of radiation damage on the scintillation spectrum of plastic scintillator dosimeters (PSDs) exposed to Very High Energy Electron (VHEE) beams operating under Ultra-High Dose Rate (UHDR) conditions at the CERN Linear Electron Accelerator for Research (CLEAR) facility.

Materials and Methods: Two PSDs were connected by a clear fiber to the Hyperscint RP-100 (Medscint Quebec, Canada) scintillation dosimetry system. The two scintillators investigated were the polystyrene based scintillating fiber BCF12, with an emission peak at 435 nm and a polyvinyltoluene based proprietary Medscint scintillator with an emission peak at 425 nm. The PSDs were deliberately damaged by irradiation with a 200 MeV electron beam at CLEAR using a dose rate of ~18 Gy/train with a train frequency of 0.83 Hz until a total dose of ~2.5 kGy was reached. The irradiations were repeated multiple times and output linearity measurements were taken in between. For these, PSD output was measured from ~4 to 60 Gy/train (~$6x10^7$ to $9x10^8$ Gy/s for a 66 ns train length) with three single trains delivered per charge value. In total, doses-to-water of 26.2 kGy and 13.8 kGy were delivered to the BCF12 and Medscint PSDs respectively. The spectra with background subtracted were normalized by their area under the curve or their maximum value and compared to the initial spectra obtained beforehand using a kV photon beam.

Results: Gradual spectral changes consisting of flattening at the peak of the spectrum and broadening towards longer, greener wavelengths as well as a decrease of scintillator output with increasing total absorbed dose were seen for both PSDs. In addition, their spectral peak positions were shifted by +3 nm (± 2 nm) after the final irradiation. A decrease in the normalized peak height of about 24% and 22% was measured for BCF12 and Medscint PSDs at 26.2 kGy and 13.8 kGy, respectively. At half maximum, the final spectra were broadened towards longer wavelengths by about 35% for BCF12 and 24% for Medscint compared to the initial spectra. No short-term recovery of these spectral changes was observed after either 15 minutes or 17 hours rest. However, the BCF12 PSD output did recover up to 99.6% of its output after 15 minutes rest at 18 kGy total delivered dose.

Conclusions: The characterization of spectral changes in BCF12 and Medscint PSDs leads to a better understanding of the effects of radiation damage in PSDs. The lack of short-term spectral recovery observed suggests irreparable damage to both scintillators. This work is a critical step toward the use of plastic scintillators for dosimetry in extreme radiotherapy conditions, such as in UHDR VHEE beams.

268
SHOULD WE IMPLEMENT TRS 483 RECOMMEDNDED CORRECTION FACTORS FOR CYBERKNIFE CONES OUTPUT IN VARIOUS DETECTOR TYPES

Iqbal AL AMRI, Mahmood AL Fishawy, Mohammed Ali Gourmani, Nirmal Babu
Sultan Qaboos Comprehensive Cancer Center, Muscat, OM

Purpose: The small field dosimetry measurement is one of the critical parts in treatment requirements, especially in the era of SRS and SBRT.TRS 483 recommended detector-based correction factor (CF) for the output factor measurements, this study aimed to compare the measurements of CyberKnife output factors for fixed and iris collimators, with and without applying CF and comparing to composite data provided by Accuray.

Materials and Methods: PTW 60019 CVD detector, PTW 60018 unshielded diode, and Sun Nuclear Edge detectors are used in these output factor measurements for 24 Fixed and Iris cones (5 mm to 60 mm) of Cyberknife S7.

Results: The study results divided into three groups according to cone size, group A: (20 to 60 mm) cones, group B: (10 to 15 mm) cones, group C: (5 and 7.5 mm) cones, and comparing our result relative to composite data from Accuray.The study data of fixed cones without applying CF shows an average variance percentage of (0.12%, 0.49%, and 1.63%) with maximum of (0.3%, 1.31%, and 4.52%) for A, B, and C groups respectively. Furthermore, when applying CF, results present an average variance percentage of (0.13%, 0.99%, and 3.42%) with maximum of (0.52%, 1.39%, and 6.91%) for A, B, and C groups respectively.On the other hand, for iris without applying CF, the result shows an average variance percentage of (0.2%, 0.8%, 1.6%) with maximum of (0.49%, 1.64%, 2.95%) for A, B, and C groups respectively. Moreover, when applying CF, the study displays an average variance percentage of (0.23%, 0.6%, and 2.58%) with maximum of (0.49%, 0.95%, 5.38%) for A, B, and C group respectively.

Conclusions: This study showed that the variance percentage between measured and composite data from Accuray is less when not applying the CF, especially for small fixed and iris Cyberknife cones.

269

IMPLEMENTATION AND VALIDATION OF NON-UNIFORM MAGNETIC FIELDS INTO PENELOPE/PENEASY

Jacob Groeneveld[1,2], Fletcher Barrett[1], Charles Kirkby[1,2]
[1]*University of Calgary, Calgary, AB*
[2]*Jack Ady Cancer Centre, Lethbridge, AB*

Purpose: PENELOPE provides a means of simulating the transport of charged particles in the presence of external electromagnetic fields. The user must hard-code the magnetic field and recompile the source code. In this work, we develop the means of introducing non-uniform magnetic fields without recompilation and validate this implementation.

Materials and Methods: We edited the underlying FORTRAN subroutines in the Monte Carlo code to handle non-uniform magnetic fields. A text file defines an arbitrary magnetic field volume into a 3D grid. A trilinear interpolation scheme enables the code to obtain the precise magnetic field vector at any arbitrary point within the grid, corresponding to the particle location at each step in the Monte Carlo simulation. For validation, test electrons with energies of 6, 12, and 18 MeV were transported through a heterogeneous magnetic field gradient directed perpendicular to the incident velocity vector that varied in magnitude from -1 T to 1 T over 4 cm. Simulation results were compared to a numerical solution using 4th-order Runge-Kutta (**RK4**) methods applied to electrons transported through the same magnetic field.

Results: In general, the methods produced qualitatively similar tracks. Compared to the RK4 methods, the uncertainty relative to the mean step length of 25 microns was 0.4 %, 0.1 %, and 0.1% for 6, 12, and 18 MeV, respectively. Over the entire trajectory, through a downstream distance of 4 cm, track lengths from RK4 techniques and PENELOPE differed by 100 microns on average for the magnetic field test configuration.

Conclusions: PENELOPE simulations using non-uniform magnetic fields were consistent with the trajectories of electrons simulated with RK4 techniques. We can now introduce a non-uniform magnetic field into further studies involving PENELOPE.

270

APPLICATION OF 3D POLYMER GEL DOSIMETRY (PGD) TO COMMISSION A VIRTUAL CONE TECHNIQUE FOR STEREOTACTIC RADIOSURGERY OF TRIGEMINAL NEURALGIA

Tenzin Kunkyab[1], Michael Lamey[2], Andrew Jirasek[1], Toney Teke[2], Benjamin Mou[2], Derek Hyde[2]
[1]*The University of British Columbia, Kelowna, BC*
[2]*British Columbia Cancer, Kelowna, BC*

Purpose: A virtual cone technique was commissioned for stereotactic radiosurgery (SRS) using a high-definition multi-leaf collimator (HDMLC) to produce a small spherical dose distribution for the treatment of trigeminal neuralgia. The purpose of the study is to investigate if a 3D polymer gel dosimeter (PGD) and on-board Cone-beam CT (CBCT) readout can be used to verify the geometric precision and the dosimetry of this innovative technique.

Materials and Methods: We developed an in-house executable Varian Eclipse script based on the original work from the University of Alabama at Birmingham. The treatment plan includes 10 gantry arcs at couch angles 0°, 36°, 72°, 288°, and 324°, with 2 arcs per couch angle using collimator angles 45° and 135°. The Varian HDMLC was used to plan and deliver a dose distribution with 50% isodose spheroid diameters of 5.2 mm or less, for a prescription dose of 80 Gy to Dmax. To verify the dose delivery, we used a NIPAM-based gel dosimeter and EBT3 film. Film measurements with two orientations (coronal and sagittal) were used for the virtual cone plan. Due to the exposure range of the film and the gel, the maximum point dose was scaled such that the planned dose was 29.2 Gy for gel and 32 Gy for EBT3 film.

Results: For 50% isodose dose width, Eclipse plan gave a calculated diameter of 6.13 mm, 6.20 mm, 5.34 mm, EBT3 film with 5.60 mm, 5.81 mm, 5.64 mm and with PGD, the diameters of the sphere were 6.07 mm, 6.20 mm, 5.50 mm.

Conclusions: The largest deviation between gel and plan versus EBT3 is in the sagittal plane, which differed by 0.53 mm. The coronal and transverse measurements were close to or less than 0.4 mm between the gel and EBT3 film. However, the measurements of PGD are consistent with the treatment plan within 0.2 mm.

271

GRID THERAPY WITH VERY-HIGH ENERGY ELECTRONS

Nathan Clements[1], Nolan Esplen[1], Magdalena Bazalova-Carter[1], Pierre Korysko[2], Joseph Bateman[2], Wilfrid Farabolini[3], Manjit Dosanjh[2], Roberto Corsini[3]
[1]*University of Victoria, Victoria, BC*
[2]*University of Oxford, Geneva, CH*
[3]*CERN, Geneva, CH*

Purpose: The goal of this work was to evaluate the feasibility of very-high energy electron (VHEE) GRID therapy. Firstly, using Monte Carlo (MC) software to simulate treatment of a pediatric glioblastoma (GBM). Secondly, by conducting the first experimental VHEE GRID irradiations.

Materials and Methods: VHEE GRID and open beam radiotherapy treatment of a pediatric GBM at ultra-high dose rates (UHDRs) and energies of 150 and 250 MeV were simulated using TOPAS MC software. Dose volume histograms (DVHs) and mean dose rates were used to compare multi-directional VHEE open beam and GRID treatments to a clinical 6 MV VMAT plan. In each VHEE simulation, twelve sources were placed isometrically around the tumour isocentre. For GRID treatments, a GRID-patterned tungsten collimator (0.5 mm hole widths and 1.1 mm septas) was placed between the source and the patient. The GRID treatments were evaluated by considering the peak-to-valley dose ratio (PVDR) since a higher PVDR has been linked to greater normal tissue sparing. GRID experiments were performed on the CLEAR VHEE beamline at CERN. Film dosimetry was used to investigate dose distributions and assess the feasibility of VHEE GRID treatments. Films were placed in 0.5 cm or 1 cm intervals in a water phantom at depths between 13 mm and 63 mm. At energies of 140 and

200 MeV, films were irradiated at UHDRs with and without a 3D-printed tungsten GRID-patterned collimator (0.5 mm hole widths and 1.1 mm septas) spatially-fractionating the beam. In addition, an MC model of the CLEAR beam was built in TOPAS and will be validated using the film measurements.

Results: Simulated VHEE GRID presented a surface (5 mm depth) PVDR of (38 ± 3) and a depth of convergence of 37 mm at 150 MeV and a surface PVDR of (34 ± 3) with a depth of convergence of 53 mm at 250 MeV. For a pediatric GBM case, VHEE treatments without GRID-fractionation produced 25% and 22% lower volume-averaged doses to OARs compared to the 6 MV VMAT plan and eight of nine and nine of nine of the patient structures were exposed to volume-averaged dose rates >40 Gy/s for the 150 MeV and 250 MeV plans, respectively. The 150 and 250 MeV GRID treatments produced 17% and 38% higher volume-averaged doses to OARs with three of nine patient structures with volume-averaged dose rates of >40 Gy/s. Experimental GRID irradiations produced a PVDR of (2.22 ± 0.06) at 13 mm depth with a depth of convergence of 41 mm at 200 MeV, and a PVDR of (1.61 ± 0.02) at 13 mm depth with a depth of convergence of 31 mm at 140 MeV. Central peak instantaneous dose rates at all depths were >90 MGy/s and >130 MGy/s for the 200 and 140 MeV GRID dose distributions, respectively.

Conclusions: Through MC simulation, we have demonstrated that VHEE sources are capable of UHDR SFRT treatments that can produce acceptable dose metrics while eliciting the potential for normal tissue sparing. Through film dosimetry on the CLEAR beamline, we have established proof-of-principle and a measurement-validated MC model for optimizing VHEE GRID.

272

CLINICAL IMPLEMENTATION AND PRELIMINARY PATIENT OUTCOMES OF FLATTENING FILTER FREE IRRADIATION AT AN EXTENDED DISTANCE FOR TOTAL BODY IRRADIATION (FIRE-TBI)

Rebecca Frederick[1,2], Alana Hudson[1,2], Alexander Balogh[1,2], Jeffrey Cao[1,2], Andrew Daly[1,3], Adam Blais[1,2], Greg Pierce[1,4]
[1]*University of Calgary, Calgary, AB*
[2]*Tom Baker Cancer Centre, Calgary, AB*
[3]*Foothills Medical Centre, Calgary, AB*
[4]*Varian Medical Systems, Palo Alto, CA*

Purpose: To evaluate in vivo time savings and any changes in patient outcome when implementing a total body irradiation (TBI) technique using flattening filter free (FFF) beams at a higher dose rate.

Materials and Methods: FIRE-TBI (Flattening filter free IRradiation at an Extended distance for Total Body Irradiation) is an extension of our institution's current extended source-to-skin distance (SSD) sweeping arc VMAT TBI technique. Patients lie supine and prone on a custom couch for an anteroposterior-posteroanterior delivery. The linear accelerator gantry arcs back and forth over the patient eight times for each orientation. Treatment planning is facilitated by automated beam placement using the Eclipse Scripting Application Programming Interface (ESAPI). The application sets field isocentre placement, arc length, and multileaf collimator leaf positions for initial dose calculation. Inverse optimization improves dose homogeneity and provides shielding for the lungs. The maximum dose rate of 1400 monitor units (MU)/min is used. Thirteen patients eligible for TBI consented to participate in a prospective comparative study between March and December 2022. Six patients were randomized to 6 MV FFF FIRE-TBI and seven patients to the standard 6 MV TBI technique. The dose prescription for all patients was 4Gy/2 fractions b.i.d with at least six hours between fractions. We statistically compared dosimetric parameters and stopwatch measured treatment times between arms. Acute outcomes related to patient safety were reviewed to ensure that FIRE-TBI had no adverse effect on treatment efficacy. These included stomatitis, patient-controlled analgesia (PCA) use related to stomatitis, and non-infectious pneumonitis at three- and six-months post-transplant.

Results: All FIRE-TBI plans met our criteria for clinical acceptability. The median 'Body retracted 5 mm from skin' D2% and mean lung dose for FIRE-TBI were 110.7% and 101.7% and for standard TBI were 113.3% and 103.9% respectively (p=0.02). Median total treatment times were 104.0 min for FIRE-TBI and 118.7 min for standard TBI (p=0.01), representing approximately 15 min of time savings over both fractions. All 13 patients experienced Grade 3 stomatitis. There were no significant differences in the duration of severe stomatitis between treatment arms. The median total PCA morphine milligram equivalent doses were 963.7 mg for the standard TBI technique, and 142.0 mg for the FIRE-TBI technique (p=0.03). While this trend is interesting, given the small sample size no firm conclusions can be drawn. With a median follow up of 7 months, no cases of non-infectious pneumonitis have been identified. No severe adverse events potentially related to radiation occurred in the FIRE-TBI arm.

Conclusions: We have successfully implemented FIRE-TBI at our institution, leading to significantly shorter treatment times and high patient and staff satisfaction. Six patients have been treated with no change in severe TBI-related toxicities.

273

IMPACT OF RANGE UNCERTAINTIES ON ROBUST MIXED ELECTRON-PHOTON BEAM RADIATION THERAPY

Veng Jean Heng[1], Monica Serban[2], Marc-André Renaud[3], Jan Seuntjens[2]
[1]*McGill University, Montréal, QC*
[2]*Princess Margaret Cancer Centre, Toronto, ON*
[3]*Gray Oncology Solutions, Montréal, QC*

Purpose: Mixed electron-photon Beam Radiation Therapy (MBRT) is an emerging external beam treatment technique that combines both photons and electrons on conventional treatment machines. Previous studies have established the importance of robustly accounting for setup uncertainties in MBRT plans. In analogy to proton therapy the present study investigates the impact of range uncertainties on MBRT dose distributions.

Materials and Methods: To evaluate the impact of range uncertainties, MBRT plans were generated on Brems, an in-house web-based treatment planning system, for two patients: a post-mastectomy breast cancer and a pre-operative chest wall sarcoma. For each plan, photon beamlets were calculated using an in-house collapsed cone convolution superposition algorithm. A pre-calculated Monte Carlo method was devised to efficiently generate electron beamlets. In addition to a nominal, non-perturbed scenario, beamlets were calculated in eight perturbed scenarios: six setup scenarios where the phantom isocentre is shifted ±5 mm in each Cartesean direction, and two range scenarios where the patient's CT numbers are scaled by ±3.5% prior to conversion to physical densities. Using a stochastic programming approach, the beamlets were robustly optimized with a column generation algorithm to generate a robust MBRT plan. For both plans, doses were recalculated by Monte Carlo for final dose evaluation in all robust scenarios and normalized such that 95% of the CTV received 50 Gy, averaged over all scenarios.

Results: For both patients, the CTV's DVH in the range scenarios represented smaller deviation from the nominal scenario's DVH than the setup scenarios. In the post-mastectomy case, the CTV's V50Gy was reduced by 1.8% in the worst range scenario while it was degraded by 4.7% in the worst setup scenario. However,

range scenarios were observed to have a larger impact to the lung dose in the post-mastectomy case. The worst deviation from the nominal scenario's V20Gy to the ipsilateral lung was found to be 2.2% and 2.4% for the worst range and setup scenario, respectively. This was not the case for the pre-operative patient where deviations in range scenarios (0.13%) were found to be negligible compared to setup scenarios (2.5%). This difference in observation could be due to the significantly higher electron contribution to the dose in the post-mastectomy plan. The ratio of electron to total MUs was 90.8% and 62.3% in the post-mastectomy and pre-operative plan, respectively.

Conclusions: The impact of range uncertainties on plan quality of MBRT plans was assessed on two patients. Although the CTV's DVH was not found to be significantly deteriorated in the variable range scenarios in comparison to variable setup scenarios, range uncertainties may have a larger impact in heterogeneous regions like the lung. The importance of accounting for range uncertainties may differ across plans according to the relative electron usage and patient geometry. These findings remain to be confirmed on more patients and treatment sites.

274
AN EXPLORATION OF ANNULAR PARALLEL PLATE WAVEGUIDES FOR ELECTRIC FIELD GENERATION IN A DIELECTRIC WALL ACCELERATOR

Morgan Maher[1], Christopher Lund[1], Julien Bancheri[1], David Cooke[1], Jan Seuntjens[2,3]
[1]*McGill University, Montréal, QC*
[2]*Princess Margaret Cancer Centre, Toronto, ON*
[3]*University of Toronto, Toronto, ON*

Purpose: This work is part of a Canadian initiative to re-examine the feasibility of Dielectric Wall Accelerator (DWA) technology, which could provide a compact (~3 m) and affordable alternative to existing proton therapy accelerators. DWAs operate by synchronizing the delivery of short-lived (~1 ns) strong (~100 MV/m) electric field pulses with the trajectory of charged particles through the accelerator. Annular parallel plate waveguides (PPWG) are proposed here as a means of generating the accelerating fields, as they (1) eliminate documented problems in the literature associated with magnetic interference between adjacent field generators, (2) are compatible with switching technology able to withstand high electric field stress, (3) allow for the generation of time-varying accelerating fields (which are necessary for longitudinal beam stability), and (4) provide passive amplification of the electrical input thus lowering stress on upstream circuits while supplying stronger accelerating fields. However, this passive amplification depends on the properties of the PPWG and is non-uniform in the frequency domain, leading to pulse distortion. This work aims to computationally characterize the geometric and material dependency of these distortions in order to optimize the annular PPWG design for a DWA.

Materials and Methods: A 2D axisymmetric model of annular PPWGs was constructed in COMSOL Multiphysics using the RF interface. A multi-parametric sweep of the inner radius (r_{in}), outer radius (r_{out}), and relative permittivity (ε_r) was implemented, where for each study the PPWG was excited at r_{out} using a Gaussian input pulse with a 20 GHz bandwidth. The output pulse for each study was extracted at r_{in} and the frequency response was analyzed.

Results: All simulated PPWGs exhibited non-uniform amplification across the bandwidth studied, with amplification factors increasing to a plateau at higher frequencies. Decreasing r_{in}, increasing r_{out}, and increasing ε_r all increased amplification of the signal. Changes to r_{in} were found to have a disproportionate effect at higher frequencies (>5 GHz), changes to r_{out} had a near uniform effect across all frequencies studied, and changes in ε_r disproportionately affected lower frequencies (<5 GHz).

Conclusions: These data show the impact of geometric and material properties on pulse amplification. Maximizing this amplification requires: (1) minimizing r_{in}, where the lower bound is determined by the transverse spread of the particle beam, (2) maximizing r_{out}, where the upper bound is limited by cost, weight, and size constraints of the overall accelerator, and (3) maximizing ε_r, where constraints are related to breakdown voltage, cost, and availability of suitable waveguide materials. Furthermore, the distinct impact of each parameter on the frequency response means that the design of the PPWG will affect the time profile of any transmitted pulse. These data thus play an important role in pulse design by providing a bridge between upstream circuitry and studies of beam stability.

275
PLANNING STRATEGIES FOR DYNAMIC TUMOUR TRACKING TREATMENTS

Emilie Carpentier[1], Marie-Laure Camborde[2], Tania Karan[2], Alanah Bergman[2], Tony Mestrovic[2]
[1]*University of British Columbia, Vancouver, BC*
[2]*British Columbia Cancer, Vancouver, BC*

Purpose: Dynamic tumour tracking (DTT) is a motion management technique where a radiation beam follows a moving tumour in real time. Improperly modelling DTT beam motion leaves an organ at risk (OAR) vulnerable to exceeding its dose limit. This work investigates two planning strategies for DTT plans optimized on a single breathing phase, the "Boolean OAR Method" and the "Aperture Sorting Method," to determine if they can successfully spare an OAR while maintaining sufficient target coverage.

Materials and Methods: A step-and-shoot intensity modulated radiation therapy (sIMRT) treatment plan was optimized on the exhale phase for ten previously treated liver stereotactic ablative radiotherapy patients. The "Boolean OAR Method" creates a union of an OAR's contours from two breathing phases (exhale and inhale) on the exhale phase and protects this boolean OAR during plan optimization. The "Aperture Sorting Method" assigns apertures to the breathing phase where it contributes the least to an OAR's maximum dose. These strategies were compared to determine which is more effective at sparing an OAR while maintaining target coverage.

Results: All ten OARs exceeded their dose limits on the original plan 4D dose distributions and average target coverage was $V_{100\%}$ = 91.3%±2.9% (ranging from 85.1% to 94.8%). The "Boolean OAR Method" was unable to spare three of the ten OARs, and mean target coverage decreased to $V_{100\%}$ = 87.1%±3.8% (ranging from 80.7% to 93.7%). The "Aperture Sorting Method" failed to spare one OAR. The mean target coverage remained high at $V_{100\%}$ = 91.7%±2.8% (ranging from 84.9% to 94.5%).

Conclusions: 4D planning strategies are simple to implement and can improve OAR sparing during DTT treatments. The "Boolean OAR Method" is quick but comes at the cost of reduced target coverage and OAR sparing is not guaranteed. The "Aperture Sorting Method" requires more time to implement, however it results in improved OAR sparing and target coverage.

276
CHARACTERIZATION OF MLC LATENCY FOR NON-INVASIVE INTRAFRACTIONAL TUMOUR-TRACKED RADIOTHERAPY (NIFTERT) ON ALBERTA LINAC-MR

Benjamin Schultz, Satyapal Rathee, Gino Fallone, Jihyun Yun
University of Alberta, Edmonton, AB

Purpose: To develop a method for measuring the mechanical latency of the multileaf collimator (MLC) on Alberta Linac-MR at various gantry angles. This latency, combined with the image processing and image acquisition latencies, form the overall system latency at which nifteRT must predict target position for successful implementation of real-time MRI-guided MLC tracking; an approach with proven potential to reduce margins for mobile tumours.

Materials and Methods: We programmed a QUASAR MRI^{4D} motion phantom to emulate 1-D sinusoidal tumour motion. In-house developed software and hardware is used to receive 1-D positional data from the phantom. To track the moving phantom in real-time, MLC position is changed every 50 ms. Latency is taken as the time lag between set (i.e. phantom motion) and reached positions of MLC leaves. Currently, the reached position of the MLC leaves are provided by the MLC emulator, which was developed by the MLC manufacturer. This emulator closely resembles the firmware/hardware implementation of the physical MLC on the Alberta Linac-MR. Both the set and reached positions of the leaves are recorded in our software every 50 ms, which communicates directly with the phantom and emulator systems. The set and reached positions of MLC, as a function of time, are fitted to sinusoidal functions, and the time lag between the fitted functions is taken as the latency.

Results: Our preliminary results showed latencies of 126 ± 5 ms using the MLC emulator in combination with the QUASAR motion phantom. The uncertainty comes from the standard deviation between the latencies repeating the experiment using the same waveform. Our result is similar to previous work by Glitzner et al. (Phys. Med. Biol. 64(15) (2019)) where the MLC latency on the Elekta Unity Linac-MR was measured as 141 ms.

Conclusions: This work measured the latency of MLC motion in Alberta Linac-MR at ~ 130 ms when using an MLC emulator. Future works will measure the latency of the physical MLC using the Alberta Linac-MR at various gantry angles, while using various thoracoabdominal tumour trajectories representing realistic tumour motions during respiration.

277

AN INVESTIGATION INTO THE BENEFIT OF USING A HIGHER THRESHOLD OF CORRECTIBLE ROTATIONS IN CYBERKNIFE TREATMENTS

Meaghen Shiha[1], Emily Heath[1], Eric Vandervoort[2,3,1]
[1]*Carleton University, Ottawa, ON*
[2]*The Ottawa Hospital, Ottawa, ON*
[3]*University of Ottawa, Ottawa, ON*

Purpose: To investigate the clinical benefit and feasibility of delivering treatments with a higher threshold of correctible rotations when treating abdominal tumours with the CyberKnife robotic radiosurgery system.

Materials and Methods: A retrospective study of 70 patients treated with the CyberKnife system with Synchrony respiratory motion compensation was performed to examine the benefit of using the prostate beam path which allows for the correction of larger target rotations than the standard full path. Log files of the patient treatment courses were analyzed to quantify the rotations of the target throughout treatment. For each patient treated, the percentage of rotations corrected during treatment with the lower threshold was compared to the number that could have been corrected using the prostate path. The accuracy of the delivered dose and motion tracking accuracy for dynamic phantoms was evaluated. The prostate path was then used prospectively for three patient treatments with abdominal tumours. Standard and prostate path treatment plans were also compared.

Results: When examining the data from the 70 patients only 30% of accurately calculated target rotations were corrected, on average, for each patient treatment using the standard path threshold. Re-analysis of these patients showed that the use of the prostate path could correct 47% of the target rotations. Phantom measurements using the prostate path agree at 2%/2mm levels with rotational corrections at maximum thresholds. Standard and prostate path treatment plans were similar in terms of target coverage, dose to healthy organs and dose fall-off.

Conclusions: For the retrospective study, 17% more rotational corrections could have been achieved using the prostate path for abdominal targets. Of the three patients treated with the prostate path, rotational corrections could not be employed for one treatment course for reasons unrelated to the path used. The other two had on average, 53% of their accurately calculated rotations corrected.

278

EVALUATION OF PATIENT-SPECIFIC QUALITY CONTROL (QC) FOR MARKERLESS DYNAMIC TUMOUR TRACKING (MDTT) DELIVERIES

Marie-Laure Camborde, Tania Karan, Ronald Horwood, Ante Mestrovic, Alanah Bergman
British Columbia Cancer, Vancouver, BC

Purpose: To report on the patient-specific QC for MDTT for liver and lung tumours treated using the dome-of-liver/diaphragm as a surrogate for the target position and compare to the QC of conventional fiducial-based tracking.

Materials and Methods: Vero4DRT (Brainlab) is a linear accelerator that has a gimbal-mounted waveguide and collimation system allowing the radiation beam to perform dynamic tumour tracking based on a patient's respiratory motion. A correlation model is built between an external IR marker placed on the chest and an internal structure, which may be implanted fiducial surrogates or in the case of MDTT, an anatomic landmark.
During treatment an orthogonal kV image pair is taken every second. The auto detected internal structure position versus the predicted position is recorded in treatment log files. Five IMRT tracking plans were delivered to two commercial motion phantoms with in-house additions for patient-specific tracking QC. For point dose measurements, a 0.6cc farmer chamber was placed inside the Brainlab dynamic tracking phantom which contains fiducials for fiducial-based tracking delivery and an anatomic landmark for MDTT. For 2D dose distribution measurements, a gafchromic film insert for the Quasar Respiratory Motion Phantom was constructed. The phantom contains both fiducials and has a liver-dome shape at one end to facilitate MDTT. Both motion platforms were interfaced with software that enabled patient-specific respiratory motion traces acquired during a 4DCT scan. Each plan was delivered three times on each phantom: (1) in static mode, (2) during fiducial-based tracking, and (3) during MDTT. Chamber measurements taken during static and tracked delivery were compared to the average chamber dose from the Raystation treatment planning software (TPS). Film distributions measured during tracked deliveries were compared to the static film distribution using gamma analysis with FILMQA PRO software. Finally, dynamic tracking treatment statistics, extracted from log files, were compared between fiducial and markerless tracking deliveries.

Results: All chamber measurements resulted in dose differences <2.5% compared with the TPS. Dose differences between fiducial-based and MDTT were 0.26% on average (range 0.03-0.62%). For film dose map analysis, gamma pass rates were >95% for all plans for all tracking methods. The average gamma pass rate for 3%/3mm was 99.4% (fiducial-based) versus 98.4% (markerless).

For 2%/2 mm, the average gamma pass rate was 96.4% (fiducial-based tracking) versus 95.6% (MDTT). Dynamic treatment statistics from logs files reported an average 3D absolute deviation from predicted position of 0.52 mm (±0.24) for fiducial tracking and 1.19 mm (±0.50) for MDTT.

Conclusions: Both fiducial-based and MDTT plans meet passing criteria for patient-specific QC. 3D absolute deviation of detected versus predicted position are larger for MDTT compared to fiducial tracking, however no significant impact on dose delivery was measured.

279

RESULT OF A NATIONAL SURVEY: TIME FOR CANADA TO JOIN THE GLOBAL RESEARCH ON BORON NEUTRON CAPTURE THERAPY?

Ming Pan[1], Retage Al-Bader[1], John Agapito[2]
[1]*Western University, London, ON*
[2]*University of Windsor, Windsor, ON*

Purpose: Canada recently closed its major neutron source, NRU reactor in Chalk River. A replacement prototype compact accelerator-based neutron source (CANS) has been planned for proposed research including BNCT. We applied for Canada Foundation for Innovation 2023 Innovation Fund (CFI #42891) to develop accelerator-based Boron Neutron Capture Therapy (AB-BNCT) in an acute care hospital. A national survey was conducted among Canadian radiation oncologists (RO) and medical physicists (MP) to identify the challenges we might face.

Materials and Methods: After REB approval, the survey was distributed by two national professional organizations, i.e. Canadian Association of Radiation Oncology and Canadian Organization of Medical Physicists. It has 17 questions in three domains: eligibility, demographics, and specific knowledge of BNCT. Eligibility is limited to RO with an independent/academic license, board-certified MP, or residents in a formal residency-training program. It is voluntary, anonymous, and without compensation. The results were analyzed using descriptive statistics.

Results: We collected 118 valid responses from all ten provinces: the majority from Ontario (45.7%) and Quebec (18.6%) that have 61% of the Canadian population. There are 70 RO (59.3%) and 48 MP (40.7%), including seven RO and two MP residents. Gender, age group, and years of practice are well representing the current Canadian radiation oncology workforce (e.g. 72% male, 40.7% in age group 35-45 years, and 30.5% had 10-20 year independent practice). Most RO/MP know BNCT's indications or rationale (60.2%). However, only 1.4% RO referred, observed, or participated in BNCT, versus 0%, 2.1%, and 2.1% in MP, respectively. Many do not know the reasons of early BNCT's failure (44.1%). Others blame lack of clinical trials and limited neutron sources (42.4%); nuclear reactors not suited to perform clinical procedures (34.7%); no modern treatment planning system (34.7%); lack of precision in measuring boron concentration in vivo (28.8%); no effective boron compounds (24.6%); or presence of undesired radiation in neutron beam (16.9%). Only 29.7%, 8% and 5% correctly identified Japan as the first country to approve routine AB-BNCT for recurrent head and neck cancer in 2020, knew about 20 AB-BNCT facilities globally, and were aware of 20 countries attending IAEA's BNCT meeting to update its technical guidance document on BNCT (IAEA-TECDOC-1223) in 2020, respectively. BNCT was recommended for the four common indications by 15.7%-18.6% of RO, i.e. large unresectable glioblastoma multiforme, malignant meningioma, head and neck cancer that recurred/progressed after maximal dose chemoradiation, or large unresectable localized malignant melanoma that recurred/progressed after multiple surgeries. The majority (87.3%) agreed that Canada definitely should (63.6%) or possibly should (23.7%) join BNCT preclinical/clinical research and 88.1% of RO/MP either definitely would (55.9%) or possibly would (32.2%) refer a cancer patient to a Canadian BNCT centre after such facility becomes available.

Conclusions: Most RO/MP support Canada to join BNCT global research. However, the limited knowledge and lack of experience remains a challenge. Further educational sessions on BNCT development and CFI funding to build the first AB-BNCT facility are needed to realize this innovative cancer treatment in Canada.

280

CLINICAL IMPLEMENTATION OF INTRAOPERATIVE RADIOTHERAPY: 10-YEAR EXPERIENCE AT MUHC

Marija Popovic[1], Monica Serban[2], Michael Evans[1], William Parker[1], Jan Seuntjens[2]
[1]*McGill University, Montréal, QC*
[2]*University of Toronto, Toronto, ON*

Purpose: We present strategies and challenges of clinical implementation of intraoperatiove radiotherapy (IORT) in a large radiotherapy program. IORT has been used at McGill University Health Centre (MUHC) since November 2013. Herein, we detail the clinical implementation of IORT program for breast cancer. We present methods developed to standardize treatment delivery and prevent errors in IORT.

Materials and Methods: A IORT program was developed and implemented at MUHC in November 2013 with Zeiss INTRABEAM. Several key steps comprised the clinical implementation. Extensive radiation surveys and radiation protection planning were required to ensure safe use. This was complemented by radiation safety training of all OR staff. Essential protocols and processes were developed in a multidisciplinary setting, involving radiation and surgical oncologists, nurses, patient liaisons and medical physicists. To avoid needless sterilization of applicators, a methodology to size the tumour bed was developed. Failure modes were explored, and contingencies in staffing were planned to ensure adequate clinical coverage and levels of training.

Results: A workflow starts with radiation therapy liaison who, through patient's electronic chart and tasks, informs physicists and radiation oncologist of the patient's scheduled surgery time. This triggers physicists to complete patient-specific testing of the equipment and supplies ahead of the planned procedure. Pre-defined quality checklists serve to verify the required steps are performed before and during the procedure. Upon treatment completion, treatment records are transferred to patient's radiotherapy electronic chart for long-term keeping. Workflows and procedures from 2013 were revised with the relocation of the surgical suite to the new hospital site in 2015. Continuing education training for operating room staff ensued, both on operating procedures and radiation safety aspects of IORT. To date, the methodology was used to treat 61 early-stage breast cancer patients successfully.

Conclusions: We present strategies to overcome risks and challenges in the IORT implementation process. Detailed clinical processes and protocols of our IORT program have been developed over 10 years of robust experience. The presented methodology be made available to institutions interested in implementing an IORT program.

281

THE USE OF IMPLANTED CARDIAC LEADS OR AN ANATOMICAL SURROGATE FOR RESPIRATORY TRACKING IN CARDIAC RADIOSURGERY

Jakob Marshall[1], Alanah Bergman[2], Tania Karan[2], Marc Deyell[1], Devin Schellenberg[3], Richard Thompson[4], Steven Thomas[2]

[1]University of British Columbia, Vancouver, BC
[2]British Columbia Cancer, Vancouver, BC
[3]British Columbia Cancer, Surrey, BC
[4]University of Alberta, Edmonton, AB

Purpose: To quantify the motion correlation between multiple implanted cardiac leads and the diaphragm using dual orthogonal x-ray fluoroscopy. To assess suitability of different cardiac leads as a surrogate for respiratory motion in cardiac radiosurgery (CaRS).

Materials and Methods: The motion of multiple cardiac leads and the diaphragm was tracked using bi-planar fluoroscopy for two patients previously considered for CaRS. Two image sets were analyzed for each patient: free breathing and abdominal compression. Fluoroscopy images were acquired at a frequency of 5 Hz for 15-20 seconds. The position of all implanted cardiac leads (patient A: 4 leads, patient B: 3 leads) was tracked in 3D and the diaphragm was tracked in 1D. Respiratory motion of the cardiac leads was extracted using a low pass filter. Correlation coefficients were determined for each combination of the cardiac leads or diaphragm to determine whether they are effective motion surrogates. For cardiac leads, correlation was calculated using each anatomical coordinate (left, posterior, superior) or the total motion, taken as the magnitude of the 3D vector displacement. The use of a temporal lag (<1s) between motion signals was also explored. Principal component analysis was performed independently for each lead to explore (i) the ability to describe the motion in terms of a single coordinate axis and (ii) the potential for better correlation coefficients while considering motion along a single coordinate axis.

Results: Lead motion, in terms of any single anatomical coordinate or the total motion, was insufficient to correlate the motion between all combinations of leads within a dataset without a temporal lag. Correlation strength was increased by using a small time lag to eliminate any phase shift between motion profiles. Correlations between total motion of each lead was >0.6 for free breathing and >0.45 for abdominal compression across both patients but weaker correlations were observed between the leads and diaphragm. The first principal component for each lead was primarily directed in the superior-inferior direction and described the majority of the motion variance. The motion along the first principal component between different leads and/or the diaphragm showed consistently strong correlations ≥0.7 except for the atrial pacing lead in patient B under abdominal compression. Over 67% of the correlations were >0.9 suggesting very strong associations between the motions.

Conclusions: Our preliminary results suggest that respiratory motion of cardiac leads are moderately to strongly correlated amongst one another and the diaphragm under both abdominal compression and free breathing conditions. This could result in the ability to use the motion of a cardiac lead or the diaphragm for respiratory-correlated dynamic tracking in CaRS.

282
SPLENDEURS ET MISERES WITH KNOWLEDGE-BASED PLANNING FOR PROSTATE STEREOTACTIC ABLATIVE BODY RADIOTHERAPY

Dominique Fortin[1], Abraham Alexander[2]
[1]British Columbia Cancer, Victoria, BC
[2]University of British Columbia, Vancouver, BC

Purpose: Knowledge-Based Planning (KBP) has recently been introduced at out clinic to help guide the planning of prostate stereotactic ablative body radiotherapy (SABR) by estimating a priori the achievable dose objectives for the sparing of organs at risk on a per-patient basis. An audit of radiotherapy (RT) treatments planned before and after the clinical release of KBP was conducted to investigate changes in plan quality and variability, and to verify the proper usage of KBP.

Materials and Methods: Data were extracted from the RT database for 135 prostate SABR patients treated at our centre between January 2021 and January 2023: 67 patients planned before and 68 after the clinical release of KBP. The RT plans for the first cohort were re-optimized to train and validate the KBP model. Dose metrics considered in assessing the quality of plans were: CTV $D_{95\%}$; PTV $D_{95\%}$; bladder V_{37Gy}, V_{36Gy}, V_{33Gy}, V_{18Gy}; and rectum V_{36Gy}, V_{33Gy}, V_{29Gy} and V_{18Gy}. The metrics were ranked to determine the 5, 25, 50, 75 and 95 percentile values for all 3 plan sets: pre-KBP, training, and post-KBP. Paired or unpaired Student's T-tests were performed to compare the pre-KBP versus training, and pre-KBP versus post-KBP datasets, respectively.

Results: Five patients in the post-KBP cohort were found to be planned without KBP and were excluded from the dosimetric comparisons. No statistically significant differences were found between pre-KBP and post-KBP plans in terms of the CTV $_{D95\%}$, rectum V_{36Gy} and V_{33Gy}, and for all bladder metrics. A small yet significant 1% increase in the PTV $D_{95\%}$ was observed for the post-KBP cohort. The average rectum V_{18Gy} (V_{29Gy}) was reduced by 50% (30%) in the post-KBP cohort, consistent with improvements achieved in the training dataset. Except for the V_{36Gy}, the variance of all rectum metrics were reduced post-KBP by factors of 2-11, while a two-fold increase in variance was found for the bladder V_{33Gy} and V_{36Gy}, despite expectation to the contrary based on the training dataset.

Conclusions: KBP has eased the RT planning process for prostate SABR at our clinic. An audit revealed improved and generally reduced variability in quality when KBP was used properly. Over-reliance on the KBP estimates may have caused a slight increase in the variance of some bladder metrics.

283
THE EFFECT OF REAL-TIME IMAGING DOSE ON OAR CONSTRAINTS IN LUNG SBRT

Ruwan Abeywardhana[1], R. Lee MacDonald1[1,2], Mike Sattarivand[1,2]
[1]Nova Scotia Cancer Centre, Halifax, NS
[2]Dalhousie University, Halifax, NS

Purpose: Imaging dose from image guidance is typically ignored in the treatment planning process. Real-time imaging during treatment may add considerable dose to organs at risk (OARs). The purpose of this study is to quantify the effect of dose from real-time tumour monitoring using ExacTrac kV image guidance on OAR constraints in lung stereotactic body radiation therapy (SBRT).

Materials and Methods: We analyzed 24 lung SBRT patients who were treated with a volumetric arc therapy (VMAT) technique with prescription of 48 Gy in 4 fractions. Imaging doses from all four SBRT fractions were calculated retrospectively assuming patients went through real-time tumour monitoring during their actual VMAT treatment times. Patients' contour structures and CT data were exported from the treatment planning system and patient specific 3D imaging dose distribution was calculated in a validated Monte-Carlo model of ExacTrac imaging system using DOSEXYZnrc. Treatment dose was added to the imaging dose and dose volume histograms (DVHs) and D2% (dose received by 2% volume) were calculated for all structures using an in-house Matlab software. Seventeen OAR constraints were analyzed on lungs, trachea, esophagus, large bronchus, heart, aorta, and spinal cord.

Results: The highest D2% from imaging dose alone were for bone and skin which received 206 and 96 cGy respectively (i.e.,

4.3% and 2.0% of the prescription dose respectively). Seven patients had one or more fail constraints with treatment dose alone with a total of 12 fails in those patients. Adding imaging dose increased the OAR constraints in the range zero to 27% (mean 0.55%, six cases >5%) compared to treatment dose alone. Addition of imaging dose did not change pass/fail results of any OAR constraints in all patients.

Conclusions: Patient-specific imaging dose was quantified for real-time ExacTrac kV image guidance system. Additional imaging dose was within 5% recommended value by the AAPM Task Group 180. ExacTrac real-time imaging dose increased the OAR doses but did not alter the OAR constraints in SBRT patient with 4 fractions. Further studies are required for cases with larger number of fractions where imaging dose is increased.

284

IMPACT OF NOVEL RECONSTRUCTION AND METAL ARTIFACT REDUCTION ALGORITHMS ON METAL ELECTRON DENSITY CURVE FOR KVCT SIMULATOR

Robert Stodilka[1], Brandon Disher[1], Matt Mulligan[1], Homeira Mosalaei[1], Hatem Mehrez[2], Stewart Gaede[1]
[1]Western University, London, ON
[2]N/A, Markham, ON

Purpose: Radiotherapy therapy planning requires CT Number (CT#) conversion to electron density for all materials in patients. This conversion is challenging for metal prostheses made of high atomic number materials, which produce streaking / beam-hardening artifacts and large variability in CT numbers. The purpose of this work was to (1) characterize CT# variability for a wide range of metals; (2) evaluate the impact of novel reconstruction and metal artifact reduction algorithms on CT# variability; (3) and determine how to uniquely identify metals to facilitate density "overrides" in radiotherapy planning.

Materials and Methods: Six metal samples (densities 2.70-8.96 g/cm^3 and electron density relative to water 2.34-7.36) were cut into solid rods (diameter 25.4 mm and length 76.2 mm) and suspended in a water tank. 120 kVp Helical kVCT scans (Aquilion Exceed LB, Canon Medical Systems Corporation, Otawara, Japan) were acquired and reconstructed using manufacturer's Adaptive Iterative Dose Reduction (AIDR) and deep-learning (Advanced Intelligent Clear IQ Engine, AiCE) techniques, with and without Single Energy Metal-Artifact-Reduction (SEMAR) algorithm and 16-bit dynamic range. MVCT scans (Tomotherapy, Accuray Inc, Sunnyvale, USA) were also acquired and reconstructed using filtered-back projection and used as reference standard. For each reconstruction: distribution of metals' CT# were analyzed spatially and histographically. CT#s were compared against relative electron density, and coefficient of determination was evaluated. The impact of image reconstruction and SEMAR on CT# were also assessed.

Results: For all metals with densities ≥ 4.51 g/cm^3 (titanium), transaxial kVCT profiles showed cupping artifacts caused by beam hardening. Cupping severity increased with metal density, even reducing CT# at object boundaries. Linear regression between metals' peak CT# and electron density demonstrated a high coefficient of determination r^2>0.95 for all reconstructions. However, for high density metals ≥ 7.93g/cm^3 (stainless steel), histogram analysis revealed that sparingly few voxels were linearly correlated with electron density due to the severity of cupping. The impact of reconstruction algorithm and SEMAR on metal CT# was insignificant, with variation less than 1.7% and 5.4%, respectively; and without improving correlation between CT# and electron density. MVCT reconstructions showed no cupping artifact and CT# correlation to electron density had an r^2 of 0.998.

Conclusions: At 120 kVp, metals with densities ≤ 7.93 g/cm^3 can be differentiated based on CT Number, despite significant beam-hardening artifacts. Metals with greater densities cannot be differentiated. Neither image reconstruction nor single energy metal-artifact-reduction algorithms remedy this challenge.

285

OPTIMIZING THE DELIVERABILITY OF BINARY COLLIMATION-BASED SRS TREATMENT TECHNIQUE FOR MULTIPLE METASTASES WITH MULTIPLE PRESCRIPTIONS

Eva Lee, Lee MacDonald, Christopher Thomas, Alasdair Syme
Dalhousie University, Halifax, NS

Purpose: Novel treatment technique, CODA-iABC, for multi-metastases cranial SRS/SRT has been shown to be superior to VMAT with respect to OAR dose sparing and MU efficiency [1]. Dynamic gantry, couch, and collimator trajectories are modeled using an idealized MLC binary target collimation approach at each control point, whereas plan deliveries must adhere to the physical limitations of the mechanical systems involved (e.g., MLC leaf speed). This work focuses on optimizing the delivery of the CODA-iABC plans on a Varian TrueBeam accelerator considering both dosimetric fidelity and treatment efficiency as variables.

Materials and Methods: Seven plans were studied, each consisting of a full gantry arc and two 180° couch arcs. A transition window (TW) between control points (CPs) defines the fraction of a CP dedicated to the transition of binary MLC. The size of the TW is marked by two additional motion points (MP) around a CP, where the transition of binary MLC motion starts at the first MP and completes at the next MP. Plans were delivered with six TW widths: 20%, 40%, 60%, 80%, 100% (continuous arc delivery), and 0% (step-and-shoot delivery). A seventh method used a variable TW. Delivery accuracy was evaluated with an Octavius detector. The total beam-on-time was manually recorded.

Results: In the fixed TW method, gamma passing rate and beam-on time decreased as a function of TW width. The degradation of gamma pass rates as a function of TW had variability across the patient population, while the reduction in treatment time was consistent. In the variable TW method, plan delivery time was substantially improved (1.25 minutes faster) while maintaining high dose delivery accuracy. The average gamma pass rate and delivery time are 98% and 9 minutes for plans delivered with the variable TW method.

Conclusions: This work demonstrates the feasibility of delivering high-quality CODA-iABC plans in the current clinical setting, in which dynamic trajectories were used with periodic binary target collimation. The variable TW method was found to be more suitable for the dynamic delivery of CODA-iABC plans than the fixed TW method.

References:

[1] Lee, E., MacDonald, R. L., Thomas, C. G., Ward, L., & Syme, A. (2022). Intra-arc binary collimation with dynamic axes trajectory optimization for the SRS treatment of multiple metastases with multiple prescriptions. Medical physics, 49(7), 4305–4321. https://doi.org/10.1002/mp.15689

286

ASSESSING THE CONTROL POINT-SPECIFIC DOSIMETRIC IMPACT OF POPULATION-BASED INFRAFRACTIONAL MOTION IN CRANIAL RADIOSURGERY OF MULTIPLE METASTASES WITH A SINGLE ISOCENTRE

Cody Church[1], R. Lee MacDonald[2]
[1]N/A, Halifax, NS
[2]Nova Scotia Health, Halifax, NS

Purpose: Patient motion during radiosurgery can lead to the deterioration of plan quality when treating multiple metastases with a single isocentre [Guckenberger, 2012]. This was investigated for two treatment techniques: VMAT and a dynamic conformal arc technique referred to herein as intra-arc binary collimation (iABC) [Lee, 2022] to assess their respective robustness to motion.

Materials and Methods: Seven patients were selected for this study and their respective arc geometries were previously described [Lee, 2022]. To simulate motion, traces along each orthogonal axis were sampled from the population statistics of previously treated fractions in a thermoplastic mask (n=1,446) [MacDonald, 2020]. Field-specific dose matrices for these patients were shifted using these randomly sampled traces and was repeated for 100 iterations. For each control point, the sum of all mean dosimetric errors in each region of interest (ROI) was scored. For one patient, the sensitivity of dosimetric degradation was assessed with respect to the control point-specific directionality of motion by examining the reduction of $V_{99\%.}$

Results: The tenth percentile of control points which resulted in both the smallest and largest dosimetric errors were on average larger with VMAT than iABC (p=0.02). Between the subset of control points (large versus small), VMAT exhibited larger control point-specific mean errors than iABC (0.0692 versus 0.0229 cGy). For patient seven, when motion traces with identical magnitude but direction specified to maximize coverage losses versus those that minimize coverages losses were applied in reconstruction, the difference in $V_{99\%}$ was 14.74% for VMAT and 5.00% for iABC.

Conclusions: The dosimetric robustness for complex treatment plans (VMAT) appeared lower in the studied cases, and the magnitude of degradation is in part due to the directionality of intrafraction motion on a control point-specific basis. Analysis of this type may assist in defining intra-fraction motion tolerances on a patient, treatment plan, and control-point specific basis.

287

IMPACT OF ABDOMINAL COMPRESSION ON HEART AND STOMACH RESPIRATORY MOTION FOR STEREOTACTIC ARRHYTHMIA RADIOABLATION

Daniel Cecchi, Hali Morrison, Nicolas Ploquin
University of Calgary, Calgary, AB

Purpose: Abdominal compression (AC) is a common radiotherapy motion management technique which can be extremely uncomfortable for patients. The goal of this work is to compare heart, heart substructures, and stomach motion with AC compared to free-breathing (FB) for stereotactic arrhythmia radioablation (STAR) patients.

Materials and Methods: 4D computed tomography (4DCT) scans of previous lung SBRT (n=18), liver SBRT (n=18), and STAR patients (n=2) were acquired. Lung patients were imaged with FB, liver patients with AC, and STAR patients imaged with both techniques. The following structures were contoured on each phase of the 4DCT: heart, left-ventricle (LV), LV components (LVCs) (anterior, apical, inferior, lateral, septal), and stomach. We compared centroid motion differences between FB and AC scans in magnitude and in range of motion (ROM) for the left/right (LR), ant/post (AP), and sup/inf (SI) directions. Treatment volume overlap with stomach was also evaluated by calculating the minimum distance between LVCs and the stomach. Statistical analysis was performed using a Mann-Whitney U-test with significance a = 0.05 between all FB and AC sets.

Results: Median reported values are for all delineated cardiac structures where applicable given comparable observed motion. Over the total patient dataset, no significant difference was observed in centroid magnitude motion between FB and AC patients for all cardiac structures (med. FB: 8.3mm, AC: 7.7 mm; p>0.11). Cardiac structure ROM showed no statistical difference in the LR (med. FB: 4.7 mm, AC: 4.4 mm; p>0.55), AP (med. FB: 6.0 mm, AC: 5.1 mm; p>0.55), and SI (med. FB: 7.9 mm, AC: 7.3 mm; p>0.15) direction. Effect of AC compared to FB on STAR patients varied between patients. Stomach ROM was significantly reduced in the AP direction (med. FB: 4.5 mm, AC: 2.6 mm; p<0.004) with AC though was not affected in LR (med. FB: 3.0 mm, AC: 2.1 mm; p>0.23) or SI (med. FB: 7.7 mm, AC: 7.2 mm; p>0.56). Unlike for cardiac structures, stomach ROM was reduced in both STAR patients. Minimum distances between LVCs and stomach were within 10 mm for the apical, inferior, and lateral components for >80%, >65%, and >90% of FB and AC scans, respectively, on at least one phase of the respiratory cycle. AC did not have an effetc on the magnitude of this distance between FB and AC patients (p>0.12).

Conclusions: AC exhibits a non-uniform effect on cardiac structure motion between patients, though does not significantly affect motion differences overall. In addition, AC does not appear to help reduce dose to the stomach over the total patient dataset.

288

CLINICAL INTEGRATION OF MULTIJET FUSION 3D PRINTING-BASED BOLUS FOR VMAT CHEST WALL PATIENTS

Tami Joseph[1], James Clancey[1], Jennifer Hurley[1], Allison Sibley[2], Malgorzata D'Souza[2], Elizabeth Orton[2], Amanda Cherpak[1], Thalat Monajemi[1]
[1]*Nova Scotia Health, Halifax, NS*
[2]*Adaptiiv Medical Technologies, Halifax, NS*

Purpose: This work aims to qualify highly flexible Adaptiiv On Demand (AOD) MultiJet Fusion (MJF) 3D printing-based Moulded Silicone Bolus (3DM-SIL) for use within a clinical workflow for VMAT chest wall (CHWL) and breast and compare it with semi-rigid AOD MJF 3D printed thermoplastic polyurethane bolus (3D-TPU). Indications for use, properties and tolerances for planning, QA and on-treatment set-up considerations are investigated and described.

Materials and Methods: For an anthropomorphic phantom, 5 mm custom-shaped boluses were produced using 3D-TPU and 3DM-SIL. Feedback was collected from a treating RTT to assess physical fit and setup of both boluses. Manufacturer and clinical CT-based QA was performed to assess density consistency, thickness, shape accuracy relative to the intended design. Dose measurements were made using OSLDs placed on the phantom bolus to confirm the appropriate CT HU value for 3D-TPU and 3DM-SIL. A plan comparison study was conducted to determine the planning workflow for the boluses and the effect on dose distribution. Positioning accuracy and air gaps were assessed via CBCT data.

Results: RTT feedback indicated that 3DM-SIL is an acceptable alternative to 3D-TPU for irregular post-mastectomy surface geometry and/or for DIBH. CT-based QA indicates 3DM-SIL and 3D-TPU density consistency within +/- 50 HU and clinically acceptable thickness and shape accuracy. Manufacturer QA shows +/- 5 % mass accuracy and ≤ 5 mm spatial shape accuracy for 3DM-SIL and +/- 0.02 g/cc density accuracy and ≤ 3 mm spatial shape accuracy for 3D-TPU. OSLD results confirm 150 CT HU density accurately represents 3DM-SIL and 0 HU accurately represents 3D-TPU. Plan comparison shows that, based on skin and PTV minimum dose, the difference between assuming water-equivalency and 150 HU remains within 1 %. Positioning accuracy and air gaps are comparable between 3D-TPU versus 3DM-SIL.

Conclusions: The main indications for use of custom-shaped 3D printing-based bolus for VMAT chest wall patients are those with highly irregular post-mastectomy surface geometry and those treated with DIBH. This study qualifies 3DM-SIL as a viable and useful alternative to 3D-TPU.

289
DEFORMABLE IMAGE REGISTRATION-BASED DOSE ACCUMULATION FOR LUNG REIRRADIATION CASES
Marco Di Francesco[1], Marija Popovic[2], Monica Serban[3]
[1]*Hôpital Maisonneuve-Rosemont, Montréal, QC*
[2]*McGill University, Montréal, QC*
[3]*University of Toronto, Toronto, ON*

Purpose: Deformable image registration (DIR) is a tool that has a potential to improve dose accumulation in the re-irradiation setting. While DIR algorithms are commonly available in modern treatment planning systems, their limitations remain a roadblock in their full integration into the clinical routine. The goal of this project was to commission the commercially available DIR algorithm specifically for use in lung re-irradiation.

Materials and Methods: We developed a process of obtaining DIRs which meet tolerances specified by the AAPM TG-132 report for a digital phantom. The methodology was applied to 21 clinical cases, and a patient-specific QA process was established. Deformations were performed using structure-guiding feature on anatomical landmark point structures for regions of interest encompassed by the 10% isodose lines. The resulting dose sums were compared to current departmental standard.

Results: The methodology developed here satisfies TG-132-recommended tolerances in the digital phantom and in 48% of clinical cases. In 38% of clinical cases at least one metric exceeded the tolerance. Fourteen percent of cases could not be fully verified due to complex anatomical displacements. DIR-based sum plans were compared to the current standard practice that utilizes rigid image deformation. Notable differences in cumulative dose between the two methods were observed in the heart, carina, and great vessels. In total, nine clinical cases had at least one organ where the dose difference between DIR and standard methods exceeded 10Gy. A significantly lower lung dose was observed in DIR-based dose summation for the critical volume receiving less than 12.5Gy (CV12.5Gy), D_mean mean dose, and volume receiving over 20Gy (V20Gy) parameters, with p-values of 0.01, 0.001, and <0.001, respectively.

Conclusions: The commissioned DIR can adequately deform lung scans, and with appropriately defined regions of interest and landmark point guidance, it can be reliably used in the clinic. The proposed DIR-based methodology used with a commercially available DIR-algoritm can benefit lung cancer patients as an accurate alternative to the current standards of dose accumulation.

290
PLAN TRANSFORMATION MADE EASY
Stashu Kozlowski[1,2], Michael Jensen[1], Raxa Sankreacha[1,2], Hossein Afsharpour[1,2]
[1]*Trillium Health Partners, Mississauga, ON*
[2]*University of Toronto, Toronto, ON*

WITHDRAWN

Purpose: [illegible] Field-In-Field plans [illegible] replanning. Transformation is the process by which an Eclipse treatment plan with Standard (SD) MLCs is changed to become deliverable on a High Definition (HD) MLC Varian unit. Contrary to replanning, transformation is fast and enables a radiotherapy clinic to transfer between linacs to avoid patient cancellation. We previously reported on a method to overcome this technical barrier when moving patients between Varian units equipped with different MLC types (1). That technique required user manipulation of data outside of Eclipse making it prone to human error (2). We recently developed a script that performs plan transformation within Eclipse. The purpose of this report is to describe our script and to discuss dosimetric impacts as a result of this type of transformation.

Materials and Methods: An in-house Eclipse API script has been developed to perform plan transformation directly inside Eclipse Version 15.6 in a single click. This method is quick and doesn't require any manipulation outside of Eclipse. The script is able to handle SD to HD MLC transformation for FiF plans without the need to replan. Each transformed segment is an exact geometric replication of the segment before transformation but with HD MLC instead of SD MLC. Breast treatments represent the largest number of FiF plans in our clinic. Five breast tangent plans were selected and put through the transformation process. All these patients had initially been planned for a SD MLC linac and met collimation criteria prior to transformation. DVH parameters were extracted and analyzed.

Results: Our script was able to transform plans in a quick and efficient manner. Transformation of FiF plans with this script is almost instantaneous. The transformed plans differed slightly before and after transformation due to the inherent dosimetric differences between SD and HD MLCs. However, the impact on coverage was limited. The impact of these differences are clinically insignificant given that we limit the number of transformed fractions to one third of the total fraction number.

Conclusions: Use of Eclipse API is a feasible option to automate plan transformation. It allows us to keep the entire process internal to Eclipse. By doing so, this process helps us reduce mistakes and accelerates plan transformation to allow more flexibility in transfers between linacs during machine break down.

References:
1. Afsharpour H, Nielsen M, Jensen M, et al. A feasibility study of "plan transformation": A novel workaround enabling patient transfer between different Varian machines; Phys. Med. 2021.
2. Yang R, Lamey M, Bartha L, Johnston M, Warburton A, Gillund D, Becker N; Automated conversion of Millennium-120 VMAT plans to HDMLC geometry: Software development and treatment of first patients; J. Appl. Clin. Med. Phys. 2022.

291
CHANGES IN BODY CONTOUR DURING TREATMENT AND THEIR EFFECTS ON VMAT PELVIC PLANS
Eric Sabondjian[1], Michael Jensen[1], Mithunan Modchalingam[1], Charmainne Cruje[1]
[1]*Trillium Health Partners, Toronto, ON*

Purpose: With recent increased plan complexities requiring the need for VMAT techniques we are noticing an increased rate of re-CT simulations and re-plans. Combined with increased patient volumes there is even greater workload on Treatment Planners, Radiation Therapists, Physicists, and Radiation Oncologists. Therefore, reducing the rate of potentially unnecessary re-plans will benefit the entire clinic. One of the factors contributing to re-CT simulations and re-plans occurs when the patient's body contour has changed at some point during treatment through either weight gain, weight loss, or patient comfort with their positioning. These changes are most apparent in pelvic patients. This study looked at quantifying the change in target coverage and organ at risk doses caused by changes in the body contour.

Materials and Methods: A preliminary study was conducted using five randomly selected pelvic patients which include both Simultaneous In-Field Boost and non-boost plans. The body

contour was modified to simulate both weight gain and weight loss as follows: +/- 3 cm or 5 cm for 1/6th of the arc, +/- 1 cm or 3 cm for 1/3rd of the arc, and +/- 1 cm or 2 cm for half of the arc. Planning Target Volumes for primary and nodal coverages were analyzed as well as rectal doses for organ at risk (OAR) analysis, and maximum dose points.

Results: As expected for weight gain simulations, the target and OAR doses were lower, and the contrary was observed when weight loss was simulated. On average the largest dose differences were seen when contour changes were over 1 cm for at least 1/3rd of the arc, and were on average 5%. The larger differences measured in contour changes observed with 1/6th of the arc were for weight loss simulations and were due to the body contour going inside of the PTV.

Conclusions: VMAT plans in general are quite forgiving due to the amount of angles used in the delivery of the plan. Measuring changes of ~5% in target coverage and OAR doses for contour changes of greater than 1 cm for 1/3rd of the arc or more does not necessarily equate to a re-plan. The number of fractions remaining and location of hot spots will play a factor.

292

STATIC COUCH NON-COPLANAR ARC SELETION OPTIMIZATION FOR LUNG SBRT TREATMENT PLANNING

John Lincoln, Lee MacDonald, Alasdair Syme, Christopher G. Thomas
Dalhousie University, Halifax, NS

Purpose: Non-coplanar arc geometry optimizations that take advantage of beam's eye view (BEV) geometric overlap information have been proven to reduce dose to healthy organs at risk (OARs). Recently, a metric called mean arc distance (MAD) has been developed that quantifies the arc geometry sampling of 4 π space. The purpose of this research is to combine improved BEV overlap information with MAD to generate static couch lung stereotactic body radiotherapy (SBRT) treatment plans deliverable on a C-arm linear accelerator.

Materials and Methods: An algorithm utilizing the Moller-Trumbore ray-triangle intersection method was employed to compute a cost surrogate for dose to overlapping OARs using distances interpolated onto a PDD. Cost was combined with MAD for 100,000 random combinations of arc trajectories. A novel pathfinding algorithm for arc selection was performed, balancing the contributions of MAD and overlap cost for the final trajectory. This methodology was evaluated for 10 lung SBRT patients. Cases were also planned with arcs from a clinical treatment template protocol for dosimetric and plan quality comparison. Results were evaluated using dose constraints in the context of RTOG0915.

Results: Five of six OARs had maximum dose reductions when planned with the novel trajectory optimization algorithm. Significant maximum dose reductions were found for esophagus (8.48 ± 1.40 Gy, p=0.0019) and trachea (5.75 ± 2.63 Gy, p=0.048). Mean dose to contralateral lung was also significantly reduced (0.57 ± 0.09 Gy, p = 0.0019). There were two significant increases in OAR doses: mean dose to ipsilateral lung (0.46 ± 0.15, p=0.019) and V5% to ipsilateral lung (5.75 ± 2.63, p=0.048). Paddick conformity index increased by 0.05 ± 0.03 (p=0.15), remaining below a limit of 1.2 for both techniques.

Conclusions: Static couch non-coplanar optimization yielded maximum dose reductions to OARs while maintaining target conformity for lung SBRT.

293

PROSTATE STEREOTACTIC BODY RADIOTHERAPY TREATMENT PLANNING AND IMAGE GUIDANCE: INITIAL EXPERIENCE FROM TWO INSTITUTIONS

Derek Liu, Nelson Leong, Varun Thakur, Julius Pekar, Ali El-Gayed
Saskatchewan Cancer Agency, Saskatoon, SK

Purpose: Two institutions within a Canadian province began offering prostate Stereotactic Body Radiotherapy (SBRT) in 2019, providing an effective and convenient treatment option for localized prostate cancer. The study presents our experience with planning dosimetry and image guidance, with attention to inter- and intra- fraction motion.

Materials and Methods: Twenty-four patients (17+7) received prostate SBRT treatment between 2019 and 2022, prescribed to 36.25 Gy in 5 fractions every other day. Standard prep for both institutions consisted of polyethylene glycol 3350 one week prior and drinking 500 mL water one hour prior. Patients were immobilized using knee rest +/- vacuum bag, based on institution. A 5 mm PTV expansion was applied to the prostate and proximal seminal vesicle target, with delineation aided by magnetic resonance imaging. Fiducial-based image guidance consisted of initial, verification and post-treatment imaging. CBCT image matches were reviewed by an experienced Radiation Oncologist. Interfraction motion was calculated as the shift from the prostate match to the bony pelvis. Intrafraction motion was calculated as the post-treatment CBCT shift away from the treatment position and was distinguished between patient pelvis motion and prostate motion relative to pelvis.

Results: Target coverage of 100% dose to 98% PTV volume was achieved with mean conformity index of 1.11, with the exception of one case to balance coverage with OAR constraint. Median rectum D10% was 31 Gy and median bladder D50% was 1.2 Gy. The median interfraction motion of the prostate relative to the bony anatomy was 1.8, 2.1 and 0.1 mm (AP, SI, lateral) and was systematic for individual patients. 12% and 5% of the treatment sessions exceeded 5 and 7 mm respectively, with potential implications if additional nearby targets are involved. Nineteen percent of verification CBCT matches exceeded 2 mm, requiring repeat verification as per institutional procedure. Of the repeated scans, only one continued to exceed 2 mm. In comparison, post-treatment shifts exceeded 2 and 4 mm for 7% and 4% of sessions, suggesting an initial patient settling time consistent with observations from other stereotactic sites. Planning margins sufficiently accounted for intrafraction motion. However, small differences due to immobilization were observed. For knee rest alone, total motion was largest in the lateral direction (0.9 ± 1.0 mm) mostly due to pelvis motion. For knee rest and vacuum bag, the largest motion was in the AP (1.1 ± 1.3 mm) and SI (1.2 ± 1.5 mm) directions due to prostate and pelvis motions.

Conclusions: We have evaluated our prostate SBRT treatments to date and gained valuable experience to guide future program expansion. Despite the limited sample size, the results are pointing to the value of verification CBCT and the comparable yet differential performance of immobilization devices. Further data collection will increase the sensitivity of the analysis.

294

STRATEGIES TO MANAGE RADIATION THERAPY WAIT TIME "READY-TO-TREAT TO START OF TREATMENT" PERFORMANCE IN ONTARIO

James Loudon[1,2], Tara MacDonald[3], Laurie Stillwaugh[4], Richard Singh[5], Dennis Vergel de Dios[6], Sandi Sodhi[6], Melissa Diffey[7], Tammy Mathurin[8], Brandee Pidgeon[9], Rob Blanchette[3], Melisa King[10], Kit Tam[11], Jackson Chan[8], Steve Russell[12], Lorella

Divanbeigi[13], Yat Tsang[13], Christine Black[14], Laura D'Alimonte[15], Mellissa Linke[16], Margaret Hart[17], Brian Liszewski[2,17], Eric Gutierrez[17]
[1]*Southlake Regional Health Centre, Newmarket, ON*
[2]*University of Toronto, Toronto, ON*
[3]*London Health Sciences Centre, London, ON*
[4]*Health Sciences North, London, ON*
[5]*Niagara Health, St. Catharines, ON*
[6]*Trillium Health Partners, Toronto, ON*
[7]*The Ottawa Hospital, Ottawa, ON*
[8]*Hamilton Health Sciences, Hamilton, ON*
[9]*Royal Victoria Regional Health Centre, Barrie, ON*
[10]*Grand River Regional Cancer Centre, Kitchener, ON*
[11]*Kingston Health Sciences Centre, Kingston, ON*
[12]*Sunnybrook Health Sciences Centre, Toronto, ON*
[13]*University Health Network, Toronto, ON*
[14]*Lakeridge Health, Oshawa, ON*
[15]*Windsor Regional Hospital, Windsor, ON*
[16]*Thunder Bay Regional Health Sciences Centre, Thunder Bay, ON*
[17]*Ontario Health (Cancer Care Ontario), Toronto, ON*

Purpose: The radiation therapy wait time metric, "ready-to-treat to start of treatment", is a key performance indicator in Ontario that refers to the date when any planned delay is over and the patient is ready to begin treatment from a social, personal, and medical perspective. It is important to minimize wait times for patients and this initiative provides insight into the strategies used by Ontario Cancer Centres to address the ready-to-treat to start of treatment performance metric.

Materials and Methods: A survey was completed by representatives at each Ontario Cancer Centre to determine factors contributing to treatment plan delays, treatment start delays, and technique or disease site-specific delays. Local strategies to minimize delays were identified.

Results: Fifteen surveys were completed, representing all cancer centres in Ontario. The top factors contributing to a treatment plan delay were: waiting for diagnostic tests, coordinating with other cancer treatments, and waiting for information from another cancer centre (previous treatment), reported by 80%, 67%, and 60% of cancer centres respectively. The top factors contributing treatment start delays were: contour delays, statutory holidays, and plan approval delays, reported by 100%, 80%, and 73% of cancer centres respectively. Strategies used by cancer centres to manage wait times included: (1) extending operational hours (67%), (2) planned overtime (67%), (3) weekend treatments (47%), (4) using internal reports (87%), (5) scheduling CT simulation the same day as the consult (73%), (6) placing a "hold" appointment for new starts (47%), and (7) setting more stringent internal wait time targets (40%). Delays were attributed to specialty techniques or disease sites at 67% of cancer centres.

Conclusions: Various strategies were used to manage radiation therapy ready-to-treat to start of treatment wait times across Ontario. Results of this initiative will be used to create a resource document of strategies that cancer centres may refer to when addressing wait time performance.

295

INFLUENCE OF SOCIO-ECONOMIC STATUS ON RADIOTHERAPY ADVERSE EVENTS

Philip Wong[1], Thanansayan Dhivagaran[2], Ronald Cheung[1], Emma Ito[1], Kitty Chan[1], Nathaniel So[1], Harald Keller[1], Frederick Cheung[1], Edward Rubinstein[3], Zhihui Amy Liu[1], Richard Tsang[1]
[1]*University of Toronto, Toronto, ON*
[2]*McMaster University, Hamilton, ON*
[3]*University Health Network, Toronto, ON*

Purpose: Socio-economic status (SES) are known to influence cancer patient outcomes. The purpose of this study is to evaluate whether SES affected the short-term clinical experience of patients treated with radiotherapy (RT) during the pandemic.

Materials and Methods: This was a single institution, retrospective cohort quality improvement study. The primary endpoint consisted of adverse events (AEs) defined as an unplanned admission to a drop-in radiation-nursing clinic (RNC) or the institution's emergency department (ED) within 90 days of a radiation course. Adult cancer patients who received external beam RT from April 1, 2019, to March 31, 2022 were included. Patients were classified into two periods: treated prior to the pandemic (pre-COVID), and during the pandemic (COVID-era), with a cut off date of March 31, 2020. SES, age, RT intent (curative, palliative, SBRT), regimen (conventional fractionation and hypofractionation), disease site, and sex were included as co-variables. SES was obtained by matching a patient's postal code with a provincial data tool with four distinct dimensions: (1) residential instability, (2) material deprivation, (3) ethnic concentration, and (4) dependency. For each SES dimension, a score of 1-5 (best-worst) is assigned to individuals. A backward stepwise multivariable logistic regression analysis was performed to analyze the variables and identify the factors that were significantly associated ($p<0.05$) with increased risk of AEs. Institutional ethics review board exemption was obtained.

Results: Across the three-year period, 15,715 patients (5,499 pre-COVID and 10,216 COVID-era patients) were identified and included in the analyses, and 5,756 AEs were observed. The analyses revealed that patient age ($p<0.001$), disease site ($p<0.001$), treatment intent ($p<0.001$) and treatment regimen ($p=0.005$) were associated with the risk of developing AEs. AEs risk was correlated with the treatment period (pre-COVID versus COVIDera) ($p<0.001$) and material deprivation ($p=0.027$). Adjusting for the other variables, patients who were least materially deprived were at lower risk (Odds Ratio (OR)=0.88, 95%CI [0.78-0.98]) of developing AEs than patients who were most materially deprived. Patient sex ($p>0.1$), residential instability ($p=0.069$), ethnic concentration ($p>0.5$) and dependency ($p>0.5$) were not associated with AEs risk. Patients with more (SES score 1-4 versus 5) residential instability ($p<0.001$; OR=0.82, 95%CI [0.74-0.90]) and less (SES score 1 versus 2-5) material deprivations ($p=0.006$; OR=0.76, 95%CI [0.66-0.88]) were at reduced the risk of ED visits. SES was not associated with RNC visits.

Conclusions: In a universal health care system, SES (residential instability and material deprivation) were associated with the increased risk of ED within 90 days of RT. Proactive care and virtual monitoring during the 90-day period after RT in high-risk patients may reduce ED visits. ED visits beyond our tertiary institution are being gathered to address this study limitation.

296

A POPULATION-BASED ANALYSIS OF THE MANAGEMENT OF SYMPTOMS OF DEPRESSION AMONG PATIENTS WITH STAGE IV NON-SMALL CELL LUNG CANCER IN ONTARIO, CANADA

Vivian Tan[1], Michael Tjong[2], Wing Chan[3], Michael Yan[2], Victoria Delibasic[3], Gail Darling[2], Laura Davis[4], Mark Doherty[2], Julie Hallet[2], Biniam Kidane[5], Alyson Mahar[6], Nicole Mittmann[7], Ambika Parmar[2], Frances Wright[2], Hendrick Tan[8], Natalie Coburn[2], Alexander Louie[2]
[1]*Western University, London, ON*
[2]*University of Toronto, Toronto, ON*
[3]*ICES, Toronto, ON*
[4]*McGill University, Montréal, QC*
[5]*University of Manitoba, Winnipeg, MB*
[6]*Queen's University, Kingston, ON*
[7]*Canadian Agency for Drugs and Technology in Health, Ottawa, ON*
[8]*GenesisCare, Perth, AU*

Purpose: Patients with lung cancer can experience significant psychological morbidities including depression. The purpose of the study was to characterize the patterns and factors associated with interventions for symptoms of depression in Stage IV non-small cell lung cancer (NSCLC).

Materials and Methods: We conducted a population-based cohort study using health services administrative data in Ontario, Canada of patients diagnosed with NSCLC from January 2007 to September 2018. Symptoms of moderate to severe depression was defined by reporting at least one Edmonton Symptom Assessment System (ESAS) score ≥2 following diagnosis. Patient factors included age, sex, comorbidity burden, residence, and income quintile. Interventions included psychiatry/psychology assessment, social work referral and anti-depressant therapy (for patients ≥65 years of age with drug coverage through the Ontario Drug Benefit program). Multivariable modified Poisson regression models were used to examine the association between patient factors and intervention use.

Results: A total of 13,159 patients with Stage IV NSCLC lung cancer was included in the study. Symptoms of moderate to severe depression was prevalent with 71.4% (n=9,397) of patients who reported ESAS ≥2 at least once. There was low utilization of psychiatry/psychology assessments (6.6%) and social work referrals (15.8%) in the cohort. For patients ≥65 years of age, 20.8% of patients were prescribed anti-depressant medications. Patients who reported moderate to severe depression were more likely to receive psychiatry assessment/ psychology referral (7.8% versus 3.5%; standardized difference [SD] 19%), social work referral (17.4% versus 11.9%; SD 16%) and anti-depressant prescriptions (23.1% versus 14.9%; SD 21%) as compared to those with none or mild depression symptoms. In multivariable analyses, older patients were less likely to receive psychiatry/psychology assessment, social work referral and anti-depressant prescriptions. Females were more likely to obtain a psychiatry/psychology assessment or social work referral than males. In addition, patients from non-major urban or rural residences were less likely to receive psychiatry/psychology assessment or social work referral, however patients from rural residences were more likely to be prescribed anti-depressants.

Conclusions: There is a high prevalence of moderate to severe depression symptoms in Stage IV NSCLC. Although the proportion receiving public interventions is low, patients with moderate to severe depression symptoms were more likely to receive intervention. We identify patient populations who are less likely to receive interventions that will help inform resource planning.

297

POPULATION ANALYSIS OF SABR/SRS FOR THE TREATMENT OF METASTATIC CANCER IN A JURISDICTION OF 15 MILLION PEOPLE

Jason Pantarotto[1], Eric Gutierrez[2], Julie Kraus[2], Brian Liszewski[2], Timothy Hanna[3]
[1]*University of Ottawa, Ottawa, ON*
[2]*Ontario Health (Cancer Care Ontario), Toronto, ON*
[3]*Cancer Research Institute at Queen's University, Kingston, ON*

Purpose: Stereotactic Ablative Radiotherapy (SABR) or Stereotactic Radiosurgery (SRS) for oligometastatic cancer or oligoprogression of metastatic cancer is supported by an expanding body of evidence in the literature. The degree of uptake of these techniques, supplanting traditional and potentially less resource-intensive techniques in this patient population, would be of interest to clinicians and administrators alike.

Materials and Methods: A review of provincial data for Ontario, Canada (population ~ 15 million) was performed to quantify the use of SABR/SRS to metastases either in the brain or elsewhere in the body. Data was obtained from a new (April 2022) activity-based hospital funding model, responsible for ALL radiation treatment remuneration at all facilities across the province (i.e., single payer system). Funding is triggered when a patient is treated as per 1 or more of the ~270 provincial radiation protocols, defined as a "protocol instance". Protocols were developed by clinicians across Ontario according to a consensus-based iterative process, considering provincial, national and international guidelines and/or evidence-based practice. Prerequisite information for remuneration included (but was not limited to): patient demographics, identification of whether a primary tumour or metastasis(es) was treated, protocol, radiation technique, dose/fractionation, and encounter dates. Submission of data was performed by the 17 hospitals who provide radiation services and logic checked centrally by the provincial cancer agency following submission. Validation of data is performed by ongoing iterative processes.

Results: From April 1 to November 30, 2022, a total of 31,916 radiation protocol instances were funded for 27,298 patients. Of these, 4,156 (13%) were SABR/SRS protocols. When only treatment to metastases were considered, the total number of SABR/SRS protocol instances was 3,024 (9.5% of total) and 29.4% of the total number of protocol instances delivered to metastases (10,271). The 3024 consisted of 1567 protocol instances to brain metastases (51.8%) and 1457 protocol instances elsewhere in the body, most often to lung (13.2%), spine (11.5%), non-spine bone (7.6%) and liver (5.8%), with a further 10.0% to unspecified extra-cranial metastases. Data for all 17 Ontario treatment facilities revealed a range of SABR/SRS usage from 1.8 to 59.8% of all protocol instances to metastases (median 23.2%, IQ range 16.9%).

Conclusions: On review of recently submitted data, nearly one-third of all radiation treatments to metastases in Ontario are delivered using a SABR/SRS technique. There is wide regional variation in the use of these techniques. Reasons for this variation require further investigation.

298

IMPACT OF HEALTHCARE ACCESS DURING COVID-19 SHUTDOWN IN ANAL CANCER DIAGNOSIS

Amandeep Taggar[1,2], Kevin Martell[3], Jasmine Dhaliwal[1], Paveen Mann[1], Kelvin Chan[1], Shun Wong[1]
[1]*Sunnybrook-Odette Cancer Centre, Toronto, ON*
[2]*University of Toronto, Toronto, ON*
[3]*Tom Baker Cancer Centre, Calgary, AB*

Purpose: COVID-19 pandemic shutdown caused a significant disruption in healthcare services, leading to a reduction in routine check-ups and a shift towards virtual care. This resulted in many patients delaying or avoiding seeking medical attention for symptoms, which can lead to delay in diagnosis, especially for conditions such as anal cancer that require a physical examination. Anecdotally, many physicians have reported that patients have been presenting with larger tumours and being diagnosed with advanced stages compared to before the pandemic. We wanted to test the hypothesis that the pandemic has indeed resulted in late diagnosis, leading to advanced stage of anal cancer at presentation.

Materials and Methods: This is a single institution audit of all patients with histological diagnosis of anal squamous cell carcinoma referred to a large academic centre from 2018-2022. We determined patient demographics and tumour and treatment characteristics for patients presenting during the two years immediately prior to COVID shutdown (pre-COVID years 1 and 2: January 1, 2018 – March 31, 2020), the year of shutdown (year 3: April 1, 2020 – March 31, 2021), the year after shutdown was lifted with restrictions (year 4: April 1, 2021 – March 31, 2022) and fully open year (year 5: April 1, 2022 – December 31, 2022).

Patients with adenocarcinoma histology or those referred due to local or recurrent disease were excluded. Descriptive statistics were used to describe the data. Kruskal-Wallace, Fisher-Freeman-Halton and Chi-square tests were used to compare tumour sizes, metastasis rate and treatment intent.

Results: One hundred and fifty-five (n= 35, 30, 26, 36 and 28 in pre-COVID shutdown years 1 and 2 and COVID years 3-5, respectively) anal cancer patients were seen between 2018 and 2022. There were 112 female and 33 male patients. Median age at presentation was 66 years (Range: 42-98). Median tumour size at the time of diagnosis was 4.10cm, (IQR: 2.70-5.40), 4.00cm (IQR: 3.20-4.60), 4.70cm (IQR: 3.00-4.84), 5.30cm (IQR: 3.33-5.24) and 4.60cm (IQR: 2.60-6.15) for year 1, year 2, year 3, year 4 and year 5, respectively (p=.20). During the two pre-COVID years, one out of 65 (1.5%) patients presented with distant metastasis (common iliac nodes only) compared to 11 of 90 (12.2%) during the COVID years (p=.01). During post COVID shutdown period (years 3 to 5), a higher proportion of patients (10/80, 12.5%) were treated with palliative radiotherapy, compared to none (0%) in pre-COVID period (years 1 and 2), (p=.02).

Conclusions: This data suggests that COVID-19 shutdown negatively impacted the presentation of anal cancer patients. There was a trend towards larger tumours at the time of presentation and a significantly higher number of patients presenting with metastatic disease. This could be due to lack of routine check-ups and avoidance of medical attention for symptoms during COVID-19 shutdown. A larger population wide inquiry is necessary to understand the full impact of delayed medical attention on anal cancer diagnosis and treatment outcomes.

299

POPULATION-BASED DIFFERENCES IN CANCER INCIDENCE BETWEEN IMMIGRANTS AND NON-IMMIGRANTS IN CANADA FROM 1992-2015

Hadassah Abraham[1], Larine Sluggett[1], Dezene Huber[1], Robert Olson[2]
[1]*N/A, Prince George, BC*
[2]*University of British Columbia, Vancouver, BC*

Purpose: The purpose of this study was to investigate if there are differences in cancer incidence between immigrants and non-immigrants in Canada.

Materials and Methods: In this retrospective study, a linked-database approach was employed using Statistics Canada data. The Canadian Cancer Registry and Canadian Vital Statistics Database were linked with the 1991 Census cohort and the cohort was followed from 1992-2015 for cancer incidence. Excluded persons included Census non-respondents, institutional residents, those living on reserves and those less than 25 years of age. Sampling and bootstrap weights were used to ensure the sample represented the Canadian population and for statistical analyses. Total unweighted and weighted sample was 2,585,160 and 17,002,560, respectively which provided adequate power to answer the research question. Multivariate logistic regression and cox regression models included age, sex, household income, marital status, highest degree of education, knowledge of Canada's official languages (English or French), immigrant status and region of birth. Subcategories of immigrants were created based on time spent in Canada (0-4, 5-9, 10-19, 20+ years).

Results: Raw data showed that 16.8% of immigrants and 15.9% of non-immigrants had cancer. After adjusting, logistic regression analyses showed that immigrants had lower odds of any cancer diagnoses in comparison with non-immigrants (OR=0.92, 95% CI [0.92,0.93], p<.001), as well as lung (OR=0.74, 95% CI [0.72-0.75], p<.001); breast (OR=0.96, 95% CI [0.94-0.98], p=.001; colorectal (OR=0.93, 95% CI [0.91-0.95], p<.001) and head and neck cancer (OR=0.85, 95% CI [0.81-0.90], p<.001). However, immigrants had higher odds of stomach cancer and non-cervix gynecological cancers (OR=1.39, 95% CI [1.32-1.46]; OR=1.06, 95% CI [1.02-1.10]), respectively. Hazard ratios were lower for immigrants in comparison to the Canadian-born but increased based on time spent in Canada (0-4 years: 0.77, 95% CI [0.71-0.84], p<.001; 5-9 years: 0.82, 95% CI [0.75-0.89], p<.001; 10-19 years: 0.90, 95% CI [0.82-0.98], p=.011).

Conclusions: This study demonstrates a significant difference in cancer incidence between immigrants and non-immigrants. These results support current research in the observation of a 'healthy immigrant effect' (HIE) which convey that immigrants have better health outcomes than their native-born counterparts, with the effect decreasing over time spent in the host country. Since we controlled for demographic and socio-economic factors, we propose other factors to be contributing to the HIE such as individual-level health behaviours including smoking, diet and access to screening services. While it points to a HIE, we propose this phenomenon to be more complex due to the possibility of under-reporting of cases or differences in health behaviours, warranting further studies in this area.

300

STEREOTACTIC RADIOTHERAPY FOR THE RE-TREATMENT OF PELVIC AND PARA-AORTIC DISEASE IN GYNECOLOGIC CANCERS

Samreen Javed Chaudry, Anand Swaminath, Kara Schnarr, Elysia Donovan, Julianna Sienna
McMaster University, Hamilton, ON

Purpose: The safety and effectiveness of stereotactic body radiotherapy (SBRT) in the re-treatment of recurrent gynecological malignancies has not been well established. This study reports a single- institutional experience in re-irradiation of the pelvis and para-aortic region for relapses of gynecologic malignancies using SBRT.

Materials and Methods: A retrospective chart review was conducted of all gynecologic cancer patients receiving SBRT to a region of overlap with a previous radiotherapy field between 2010 and 2020. Clinical charts and radiotherapy plans were reviewed. The rates of Grade 3 or higher toxicity, cumumlative doses to abdominopelvic organs at risk, with conversion to BED as well as local control and distant failure were determined.

Results: A total of fifteen patients met criteria for inclusion. Median age at diagnosis was 53.5 years (range 38-72). Five patients were diagnosed with ovarian carcinoma (33%), three with cervical cancer (20%) and seven with uterine cancer (47%). The median time between initial radiotherapy and SBRT was three years (range 1-14 years). Seven patients received chemotherapy prior to SBRT. Patients received SBRT for pelvic (n=7), para-aortic (n=2), combined pelvic and para-aortic (n=5), and inguinal nodal (n=1) recurrences. The median prescription dose was 30Gy (range 25-25Gy) in five fractions. Median cumulative BED doses for organs at risk included small bowel : 89Gy (α/β=4, range 30-121Gy), large bowel 74 Gy (α/β=5, range 14-111Gy), sigmoid 63 Gy (α/β=5, range 14-166Gy), sacral nerves 73Gy (α/β= 3, range 52 -170Gy), bladder 62Gy (α/β=5, range 33 -122Gy), rectum 79 Gy(α/β=2.5, range 40-100Gy), and kidney 64.3Gy (α/β=2). After a median follow-up of 29 months (range 4-129 months), no severe (≥Grade 3) acute/late genitourinary or low gastrointestinal toxicity was observed. Two (13.3%) patients had local recurrence at median of 22 months, and nine (60%) patients failed distantly at median of eight months. At last follow-up four patients were alive and disease free (26.7%), five alive with disease (33.3%) and six died of disease (40%).

Conclusions: This study suggests that re-irradiation with SBRT for gynecologic malignancies provides excellent, durable local control with acceptable toxicity. Failure predominantly occurs distantly, however there may be a small cohort of patients who remain well without distant failure. Further evaluation of dose tolerances for SBRT re-irradiation and corresponding toxicity risk, as well as optimal combination with systemic therapies is warranted in a larger prospective cohort of patients.

301

RADIOTHERAPY CAPABILITIES, POPULATION, AVERAGE INCOME, AND HEALTH INSURANCE STATUS AS PREDICTORS OF CANCER MORTALITY AT THE COUNTY LEVEL IN THE UNITED STATES

Matthew Beckett[1], May Abdel-Wahab[2], Luc Goethals[2], Ryan Kraus[3], Kseniya Denysenko[2], Maria Fernanda Barone Mussalem Gentile[2], Yaroslav Pynda[2]
[1]*University of Ottawa, Ottawa, ON*
[2]*International Atomic Energy Agency, Ottawa, ON*
[3]*University of Utah, Salt Lake City, UT*

Purpose: Sufficient radiotherapy capacity at the country level is commonly seen in high income countries and is an essential factor in access to high quality cancer care. However, universal access is not always possible due to other factors beyond the commonly used parameter of machines per million population. This study aims to assess the barriers cancer patients in a high income country face in accessing radiotherapy, and how this impacts cancer mortality.

Materials and Methods: This cross-sectional study utilized United States county level oncologic and demographic data obtained from Centers for Disease Control and Prevention and the International Atomic Energy Agency Directory of Radiotherapy Centres. Radiotherapy facilities in the United States were mapped using Geographic Information Systems software. Univariate analysis was used to identify whether distance to a radiotherapy center or various socioeconomic factors were predictive of all-cancer mortality-to-incidence ratios. Variables that were deemed to be significant ($p \leq 0.05$) on univariate analysis were then included in a step-wise backwards elimination method of multiple regression analysis.

Results: Among the United States counties studied, 31.3% of counties have at least one radiotherapy facility and 8.3% have five or more radiotherapy facilities. Median linear distance from a county's centroid to the nearest radiotherapy centre was 36 Km and the median county all-cancer mortality to incidence ratio (MIR) was 0.37. The ratio of radiotherapy centres, linear accelerators and brachy therapy units per 1 million people were significantly associated with all-cancer MIR ($p<0.05$). Greater distance to radiotherapy facilities, lower county population, lower average income per county, and higher proportion of patients without health insurance were statistically significant predictors of increased all-cancer MIR (R-squared: 0.2113, $F=94.22$, $p<0.001$).

Conclusions: This analysis used unique high-quality datasets to identify significant barriers to radiotherapy access that correspond to higher cancer mortality at the county level. Geographic access, personal income, and insurance status all contribute to these concerning disparities. Efforts and novel strategies to address and minimize these barriers are needed to ensure access to care and improve oncologic outcomes.

302

HEALTH CARE SYSTEM FACTORS ASSOCIATED WITH RECEIPT OF TREATMENT AND WITH TREATMENT INTENT IN STAGE III NON-SMALL CELL LUNG CANCER: A POPULATION-BASED STUDY IN ONTARIO

Stephane Thibodeau[1], Paul Nguyen[1], Andrew Robinson[1], Fabio Ynoe de Moraes[1], Jason Pantarotto[2], Timothy Hanna[1]
[1]*Queen's University, Kingston, ON*
[2]*University of Ottawa, Ottawa, ON*

Purpose: Stage III non-small cell lung cancer (NSCLC) is a heterogeneous disease entity, portending a spectrum of anatomic extent, health status, and treatment approaches. Receipt of treatment and treatment intent should be independent of health system factors when care quality is optimal. We investigated whether modifiable health care system-level factors are associated with receipt of treatment and treatment intent in Stage III NSCLC.

Materials and Methods: This was a population-based, retrospective cohort study with health administrative data from Ontario, Canada, 2010-2018 for those aged ≥20 years, with AJCC 7 or 8 Stage III NSCLC. We explored system factors associated with NSCLC treatment: region of residence, diagnostic interval, advanced radiation (e.g. IMRT, VMAT) and systemic therapy treatment volumes, and travel distance. The relative risk (RR) of (1) any treatment versus no treatment (i.e., no surgery, radiation or systemic therapy of any intent), and (2) palliative versus non-palliative treatment was determined, using multivariable stepwise Poisson regression models. We adjusted for patient, disease and treatment factors, including age, sex, income quintile, stage subgroup, comorbidity and histology.

Results: We identified 7,093 people with Stage III NSCLC between 2010 and 2018. There were differences in patient and disease/treatment factors between groups. For example, major factors associated with no receipt of any treatment include advanced age (adjusted RR [95% confidence interval]: 75-79 versus 20-64, 0.95 [0.92-0.98]; 80+ versus 20-64, 0.83 [0.80-0.87]), greater Elixhauser comorbidity score (RR: 1-2 versus 0, 0.95 [0.92-0.98]; 3+ versus 0, 0.88 [0.84-0.92]), dementia (RR: 0.78 [0.70-0.87]), palliative care consultation (RR: 0.92 [0.89-0.94]) and geriatric consultation (RR: 0.82 [0.71-0.95]) (all $p<0.05$). After adjustment for these factors, there were no system factors associated with receipt of treatment versus no treatment. For those that received treatment, major patient and disease/treatment factors associated with palliative intent were similar to factors associated with no treatment, but included histology and stage sub-group. The major system factor associated with palliative intent treatment amongst those treated was region of residence (RR: Region ranges from 0.88 to 1.67, $p<0.001$). When the analysis was stratified by era (2010-2012 versus 2013-2015 versus 2016-2018), there was an increase in non-palliative treatment and use of advanced radiotherapy techniques and immunotherapy over time, but regional variation of intent was similar.

Conclusions: Region of residence emerged as the major factor associated with choice of treatment intent for Stage III NSCLC after adjusting for patient, disease and treatment factors. This variation remained, even as advances in radiotherapy and systemic therapy were adopted. Our study suggests possible opportunities to improve care outcomes by addressing unexplained regional variation in care.

303

SCALING UP CHEMORADIATION SERVICES IN UGANDA: OPPORTUNITIES AND CHALLENGES FOR THE ROAD TO CARE PROGRAM

Ndinawe John Bosco[1], Joda Kuk[2], Kanyike Daniel[3], Kara Schnarr[2]
[1]*Road to Care, Mbarara, UG*
[2]*McMaster University, Hamilton, ON*
[3]*Makerere University, Kampala, UG*

Purpose: In Uganda, 6,959 women are diagnosed with cervical cancer annually; 4,607 die from the disease. The high case fatality rate (66%) is partly due to the geographic scarcity of radiotherapy

treatment facilities limiting access to curative-intent treatment. Between 1995 - 2016, Uganda had one cobalt-60 external beam radiotherapy machine, located in Kampala. In 2016, this sole radiotherapy machine broke down, leaving the country with no radiotherapy capacity for two years. During these two years (2016-2018), various stakeholders including the Uganda Cancer Institute (UCI), Road to Care (RTC), the Ministry of Health and Hospice Africa Uganda (HAU) developed an initiative to refer cervical cancer patients to the Aga Khan University Hospital in Nairobi, Kenya for chemoradiation. Road to care funded and supported a cohort of 35 Stage II cervical cancer patients to go for treatment in Nairobi, while the situation in Uganda was being addressed. To address the lack of radiotherapy services, the UCI constructed a 6-bunker facility, and to date has acquired three external beam treatment machines (two cobalt-60 units and one TrueBeam linear accelerator) and one cobalt-HDR brachytherapy unit. In 2016, the old cobalt-60 unit with its decayed source was only able to treat 30 patients per month. In 2023, with the three new external beam radiotherapy machines, the UCI is able to treat 150 patients per month. To accomplish this workload, the UCI now has nine radiation therapists on staff. With this growth in treatment capacity, RTC, a Canadian charity whose aim is to address the geographic barriers to accessing radiotherapy treatment, has also scaled up to increase the number of patients from rural areas of Uganda who can access care.

Materials and Methods: The RTC care pathway functions in collaboration with multiple Ugandan partner organizations. HAU and Kigezi Healthcare Foundation facilitate the work up of Stage II-III cervical cancer patients, provide pretreatment education, and refer patients to the UCI for chemoradiation and brachytherapy. Radical treatment usually requires patients to stay in Kampala for two months. The majority of patients from outside of Kampala experience difficulty in finding appropriate accommodations for the duration of treatment. In response, in RTC opened two radiotherapy hostels within 1km of the UCI with the capacity to host 40 patients and their caregivers at a time.

Results: To scale up of radiotherapy services in Uganda, the UCI has dramatically increased the number of radiotherapy machines and radiation therapists. In order to see that this capacity increase also benefits patients living in rural regions of Uganda, RTC has also scaled up services and accommodations. RTC currently facilitates the treatment of 102 patients annually.

Conclusions: The availability of radiotherapy treatment in Uganda is improving through immense local initiative, and Road to Care, a Canadian-supported care-pathway will continue to work alongside Ugandan partners to facilitate access to this life-saving treatment.

304
THE CHANGING LANDSCAPE OF RADIATION THERAPY: IMPLICATIONS FOR FUTURE PLANNING
James Loudon, Ivan Yeung, Charles Cho, Woodrow Wells
University of Toronto, Toronto, ON

Purpose: During the COVID-19 pandemic, stage migration has led to patients presenting later with more advanced cancers requiring complex treatment. Hypofractionation of radiation therapy treatments was also implemented as a strategy to reduce the number of patient visits to cancer centres. This initiative reports a regional cancer centre's experience of how radiation therapy activity has changed since the COVID-19 pandemic.

Materials and Methods: The number of CT simulations, treatment plans, and fractions were extracted from the MosaiQ oncology information system for fiscal year (FY)s 2019-20 to FY2022-23. FY2019-20 represents pre-pandemic activity and FY2020-21 represents the first pandemic year. FY2022-23 was estimated by straight-line projection of eight months year-to-date. The trend by type of treatment plan was also evaluated.

Results: For FY2020-21, fractions, CT simulations, and treatment plans decreased by 20.6%, 4.6%, and 6.8% respectively, compared to FY2019-20. Activity volumes continued to recover and in FY2022-23, fractions trended 9.5% below pre-pandemic activity. However, CT simulations, and treatment plans trended 8.3% and 1.5% higher, compared to FY2019-20. Evaluation by plan type also identified an increased use of more complex treatment plans, VMAT and stereotactic, which trended 45.8% and 34.3% higher. For FY2022-23, VMAT and stereotactic plans represented 37.6% and 3.7% of the total treatment plans.

Conclusions: Radiation therapy activity has shifted upstream compared to pre-pandemic activity. The increased use of more complex treatment plans suggests increased patient complexity. However, future research is needed to further understand the impact of stage migration and complexity of treatment planning. In planning for the future, the trend observed has implications for how radiation therapy health human resources are allocated to better align with the distribution of activity. Specifically, this generates greater intensity of activity in treatment planning, including quality review to ensure safe delivery and optimal patient experience.

305
ALL THAT GLITTERS IS NOT GOLD: EXAMINING COST EFFECTIVENESS ANALYSES IN RADIATION ONCOLOGY
Adam Mutsaers[1], Vivian Tan[2], Andrew N. Youssef[2], Gabriel Boldt[2], David Palma[2], Melody Qu[2], Greg Zaric[2], Alexander V. Louie[1]
[1]*University of Toronto, Toronto, ON*
[2]*Western University, London, ON*

Purpose: Cost effectiveness analyses (CEA) provide data for health policy decisions in resource constrained environments. These are important in Radiation Oncology as infrastructure and delivery costs increase and indications expand. The purpose of this study was to systematically review methodologic quality and trends in CEAs involving radiotherapy (RT).

Materials and Methods: A systematic review was performed on cost effectiveness/utility studies involving RT, querying PubMed and Embase from inception to September 2020. Non-English, reviews, abstracts and cost-only studies were excluded. Independent reviewers screened and abstracted study demographics, economic parameters and methodological details.

Results: After screening 1652 abstracts, 214 met criteria. The first publication was in 1995, and more than half (n=113, 53%) were published after 2014. Author institutions were from North America (n=128, 60%), Europe (n=49, 23%) and Asia (n=30, 14%) with most reporting in US$ (n=143, 67%). A majority utilized a decision model (n=164, 77%), healthcare payer perspective (n=171, 80%) and a finite time horizon (n=108, 50%). Publications spanned 96 unique journals, most commonly Int J Radiat Oncol Biol Phys (n=35, 16%). Treatment intent was curative in 171 studies. Disease sites included breast (n=34, 16%), genitourinary (n=31, 14%), and gastrointestinal (n=31, 14%). RT was mostly used as primary treatment (n=144, 67%), followed by adjuvant (n=70, 33%) and neoadjuvant (n=10, 5%). Emerging topics included stereotactic RT (n=45, 21%), immunotherapy (n=6, 3%), oligometastasis (n=4, 2%), and heavy particles (n=23, 11%). RT was compared to other RT (n=136, 64%), surgery (n=43, 20%), drugs (n=14, 7%) and observation (n=31, 17%). Incomplete reporting was common. Missing elements included analysis perspective (n=13, 6%), time horizon (n=38, 18%), discounting of utilities (n=71, 33%) or costs (n=54, 25%), and willingness-to-pay threshold (n=59, 28%). Furthermore, 27

studies did not perform sensitivity analyses, 36 did not evaluate incremental cost-effectiveness ratio and only 60 explicitly utilized recognized reporting guidelines. Conflict of interest statements were found in 63%, with sponsor statements in 59%; 25% were industry sponsors. Outcome parameters were obtained from primary (author institution/trial data) sources in 33%, including randomized trials (RCTs) (n=20, 9%), retrospective data (n=20, 9%) and population data (n=9, 4%). The remainder utilized secondary sources including RCTs (n=71, 33%), retrospective data (n=35, 16%) or meta-analyses (n=11, 5%). Outcomes included quality adjusted life years (n=158, 74%), life-years (n=30, 14%) or toxicity (n=26,12%). 31% utilized author generated utilities; of literature derived only 49% were matched to disease and clinical context.

Conclusions: While CEAs are increasingly common in RT, reporting and methodologic rigour must improve. Greater use of published guidelines will improve data quality for decision makers.

306

WHICH CRITERIA SHOULD WE USE TO DETERMINE AN ADEQUATE NUMBER OF LINEAR ACCELERATORS IN EMERGING ECONOMY COUNTRIES?

Zahid Al Mandhari, Ana Paula Galerani Lopes
Sultan Qaboos Comprehensive Cancer Care and Research Centre (SQCCCRC), Muscat, OM

Purpose: In the age of limited resources, knowing the number of linear accelerators (LINACS) is paramount for designing and planning comprehensive coverage for a given population. In Oman, we have a stable population with minimal rates of immigration/emigration. The current needs of LINACS are met so we have a unique opportunity to test some of these guidelines. The results should help emerging economies use a similar approach in estimating their needs. This study was conducted to estimate the demand for radiotherapy services in Oman, using the most common methods and recommendations available in the literature.

Materials and Methods: The following calculation methods were analyzed: COCIR - targets a density of seven radiotherapy units/million persons; ESTRO/QUARTS - one LINAC per 400 patients/year or one LINAC per 180,000 persons; and IAEA method that utilizes a combination of cancer incidence, number fractions per cancer type, and machine workload. Population demographics with cancer incidence were extracted from the latest Oman Cancer Registry data, 2019. For the density of LINAC, we used the 2019 population of 4.603 million. Workload considered 4 fractions/hour, 8-hour shift, 248 working days. Calculations included the total number of cancer cases, average number of fractions/year, machine workload, rate of patients receiving radiotherapy per cancer type, the optimal number of fractions per treatment course, reirradiation rate, and radiotherapy utilization rate per cancer type.

Results: Based on the 10 most frequent cancer incidence (1,437 cases), the total number of fractions/years was 22,920. The workload of machines was 7,936 fractions/year. Calculations included total cancer incidence (2,039) and an average of fractions/patients based on the average of fractions per cancer site. The total number of fractions was 27,715. The reirradiation ratio increased by 25% in the number of fractions and resulted in a total of 34,644 fractions. For the COCIR, ESTRO/QUARTS, and IAEA recommendations, the range was 2.8 to 32 of LINACS for adequate coverage in Oman (respectively 32; 4 to 25; and 2.8).

Conclusions: The analysis of the recommended guidelines for calculating the required number of LINACS in Oman showed a wide range. While in practice we know currently the number of LINACS required for our population is five, for emerging economies the ESTRO/QUARTS recommendations of one LINAC per 400 patients/year, or the IAEA calculation methods are the closest approximation to the actual needs.

307

THE EFFECTIVENESS AND SAFETY OF STEREOTACTIC BODY RADIATION THERAPY IN THE TREATMENT OF OLIGOPROGRESSIVE BREAST CANCER: A SYSTEMATIC REVIEW

Sherif Ramadan[1], Bernie Yan[2], Katarzyna Jerzak[3], Alexander Louie[3], Elysia Donovan[2]
[1]*Western University, London, ON*
[2]*McMaster University, Hamilton, ON*
[3]*University of Toronto, Toronto, ON*

Purpose: Oligoprogressive breast cancer is a term used to describe patients who have metastatic disease progression at a limited number of sites while on systemic therapy. In breast cancer, patients are commonly treated with endocrine, targeted or chemotherapies, and stereotactic body radiotherapy (SBRT) has emerged as a metastasis-directed therapy to treat oligoprogressive sites. This can subsequently allow patients to stay on their current line of systemic treatment for a longer duration of time. This study systematically reviewed the efficacy and safety of SBRT in oligoprogressive breast cancer.

Materials and Methods: A literature search was conducted in the MEDLINE database for relevant research articles. Inclusion criteria were studies that mentioned synonyms of SBRT and oligoprogressive breast cancer. Studies were excluded if they were not original research articles, exclusively discussed oligometastatic disease, or did not use SBRT for breast cancer. Data extracted included, patient demographics, disease characteristics, breast tumour subtype, metastatic sites treated, and SBRT dose. Key outcomes of interest were toxicity, local control, progression, and overall survival.

Results: From 863 references, five retrospective single-centre cohort studies were identified for data extraction. All studies included patients with both oligometastatic and oligoprogressive disease. Across the five studies a total of 112 oligoprogressive breast cancer patients were identified. Patient ages ranged from 22-84, with a median age of 55 years old. Most patients had hormone-receptor positive, and Her2 negative disease, and a small proportion of patients were Her2 positive. Moreover, patients had received between one and four lines of systemic therapy. The three most common areas of oligometastases were bone, lung, and liver respectively. SBRT doses varied from 24-60 Gy in 1-10 fractions based on the location and size of the lesions. There were 40 total toxicity events reported, with 62.5% (n=25) Grade 1-2 events and 37.5% (n=15) Grade 3-5 events. The majority of Grade 3-5 toxicities were hematological and noted when patients were concurrently receiving CDK4/6 inhibitors. PFS and OS varied significantly across included studies, ranging from 17-57% and 62-91% respectively. Patients with oligometastatic disease were noted to have higher rates of PFS and OS than patients with oligoprogressive disease.

Conclusions: There are limited data on SBRT usage for patients with oligoprogressive breast cancer. Toxicity and survival data varied significantly in the five studies. This demonstrates the heterogeneity of this clinical entity, particularly given the fact that the majority of patients studied had favourable hormonal disease status. More prospective and randomized trials to evaluate the utility of SBRT for oligoprogressive metastatic breast cancer are needed.

308
SAFETY INCIDENTS AND NEAR-MISS EVENTS IN PEDIATRIC RADIOTHERAPY
Matthew Volpini, Katie Lekx-Toniolo, Lesley Buckley
The Ottawa Hospital, Ottawa, ON

Purpose: The Ottawa Hospital's Radiation Oncology Program maintains an Incident Learning System (ILS) as one part of a quality assurance program that ensures safe and effective radiotherapy treatment. The ILS tracks safety incidents and near-misses from all major domains of radiation medicine including treatment simulation, planning, delivery, and patient care. Common root causes for such safety incidents and near-misses include lapses in communication, errors in treatment planning/delivery, and technical difficulties. Previous studies suggest that ILS submission rates are higher for pediatric cases compared to adults. Despite this, there is a paucity of data exploring patient-, disease-, and treatment-specific factors associated with this trend.

Materials and Methods: In this project, we analyzed ILS submissions that involve children and adolescents age ≤20 years old from January 2014 to December 2022. Each submission was analyzed for the nature of the safety incident or near-miss, including origin domain and root cause. We also completed incident and clinical review to identify patient-, disease-, or treatment-related factors that may have contributed to the ILS submission.

Results: From January 2014 to December 2022, pediatric patients accounted for 0.6% of the total number of treatment plans initiated at our centre, but 1.3% of the total ILS submissions from the same time period, suggesting a higher rate of pediatric ILS submissions relative to adults. There were a total of 26 pediatric safety incidents and near-misses. Thirteen of these (50%) were related to documentation errors and poor communication. Two patients (8%) had ILS submissions during physician cross-coverage. Three patients (12%) required general anesthesia as part of their treatment. Four patients (16%) were reported to have significant pain requiring analgesia during treatment.

Conclusions: At our centre, we observed a higher rate of pediatric ILS submissions compared to adults. Clinical review identified clinical and radiotherapy treatment variables associated with the impetus for ILS submission. These variables may serve as potential targets for quality improvement initiatives to reduce the rate of ILS-worthy events in pediatric treatments.

309
PROSPECTIVE CLINICAL TRIALS OF NOVEL SYSTEMIC THERAPIES IN ADVANCED NON-SMALL CELL LUNG CANCER-WHAT ABOUT RADIOTHERAPY?
Kara Ruicci[1], Adam Mutsaers[2], David Palma[3], Ambika Parmar[2], Alexander Louie[2]
[1]*University of Toronto, Toronto, ON*
[2]*Sunnybrook-Odette Cancer Centre, Toronto, ON*
[3]*London Health Sciences Centre, London, ON*

Purpose: Novel systemic therapies (NSTs), including immunotherapies and targeted therapies, are growing in use and efficacy for advanced, recurrent and metastatic non-small cell lung cancer (NSCLC). Despite these successes, radiotherapy (RT) is frequently used alongside systemic treatment for palliation, or with ablative intent for oligometastases. As guidance regarding the delivery of RT alongside NSTs varies by protocol, the objective of this study was to evaluate protocol specifications concerning pre- and peri-trial RT to inform safety.

Materials and Methods: The clinicaltrials.gov database was queried for completed phase II-IV NST trials examining advanced, recurrent and metastatic NSCLC from inception to January 2023. Trial records were independently reviewed by two investigators, with discrepancies settled by a third or by consensus. Trial information including study design, primary endpoint, agents used and specifications regarding use of pre- and peri-trial RT (timeframe, washout period, dose and target) was extracted and synthesized with descriptive statistics.

Results: Of 721 identified trials, 112 met inclusion criteria, including 58,351 unique patients. Studies were predominantly multi-institutional (n=92, 82%), multinational (n=62, 55%), industry sponsored (n=89, 79%), open label (n=81, 72%) and used a randomized parallel assignment design (n=84, 75%). Primary endpoints included progression-free survival (n=50, 45%), response rate (n=31, 28%), overall survival (n=27, 24%) and toxicity (n=4, 3%). Phase III studies were most common (n=57, 51%), followed by Phase II (n=51, 45%) and Phase IV (n=4, 4%) studies. Immunotherapy trials comprised 30% (n=34) of the studies, while 70% (n=78) examined targeted therapies. A minimum 28-day pre-trial recovery period for non-palliative RT was most common (n=40, 36%). Per protocol guidance of RT during study drug administration was less common; in 45% (n=50) of trials palliative dose RT was allowed if clinically indicated. Few trials (n=10, 9%) directly outlined the allowable total dose, technique or field size in either the pre- or peri-trial periods.

Conclusions: Although the use of both NSTs and RT for the treatment of advanced NSCLC is common, recent published clinical trials do not optimally provide guidance on the concurrent delivery of RT within the context of study drugs. Future prospective NST trials would benefit from more consistent guidance with respect to pre- and peri-trial RT, whether for palliation or ablative intent.

310
EXTREMITY DOSE ESTIMATES IN HDR STUCK SOURCE EMERGENCIES WITH UNKNOWN SOURCE POSITIONS
Krista Chytyk-Praznik, Kathleen MacLean, Michel Ladouceur, Alasdair Syme
Dalhousie University, Halifax, NS

Purpose: To parameterize dose estimates to the extremity of a physician responding to an HDR stuck source emergency in which the exact spatial relationship between the source and the extremity cannot be known with confidence.

Materials and Methods: A previously designed HDR emergency response simulator was used to model the effect of source proximity. The simulator consisted of a detailed motion capture system that recorded comprehensive spatial information, with optically tracked reflective markers representing the source and anatomical regions on the participant during the trials. Raw tracking data was used to calculate the distance between the source and a given anatomical region until the responder's hand was at its closest to the source marker. At that point, the distance between the hand and source was locked and an array of distances representing plausible hand-source separations (3 – 100 mm) was used to calculate doses until the source was deposited in the emergency safe. The resulting doses to the hands were calculated and compared to our previously reported data.

Results: Extremity dose calculated for the experienced responder with the smallest hand-source separation (3 mm) reached up to 6 Gy (0.013 Gy in the original trial). In the case of a novice responder, who took over 5X as long to place the source in the safe as the experienced responder, up to 88 Gy was delivered with a 3 mm distance to the source (0.1 Gy in the original trial). At the 100 mm distance, the doses drop to about 0.005 Gy and 0.085 Gy for the experienced and novice responders, respectively.

Conclusions: High doses to extremities are possible during a stuck source scenario when the source to hand distance is only a few millimeters. With the exact location of the source unknown, doses

can be reduced by limiting the period of exposure – which can be achieved through the routine practice of emergency procedures.

311

DEVELOPMENT AND TESTING OF A SYMPTOM COMPLEXITY ALGORITHM USING ESAS-R CANCER

Lisa Barbera[1,2], Claire Link[2], Siwei Qi[2], Linda Watson[1,2]
[1]*University of Calgary, Calgary, AB*
[2]*CancerCare Alberta, Calgary, AB*

Purpose: Since 2019 the ambulatory cancer program in Alberta has used a validated algorithm to assign a symptom complexity score to completed Patient-Reported Outcomes (PROs) measures. The algorithm used the number and severity (0-10) of symptoms reported on the Edmonton Symptom Assessment System-Revised (ESAS-r) to assign a complexity score of low, moderate or high. Pain could trigger high complexity independently if rated 7 or higher. The cancer program recently began using a new measure (ESAS-r Cancer), in turn creating the need to modify the algorithm. The purpose of this study was to develop and test a modified algorithm based on ESAS-r Cancer, using the original algorithm as the gold standard.

Materials and Methods: Paper copies of ESAS-r and ESAS-r Cancer were mailed to 1600 randomly sampled cancer patients. Complexity scores were assigned to each ESAS-r using the original algorithm. To enable broader utility of the new algorithm, even in settings with limited technology, a sum score methodology was utilized instead of the multiple criteria options of the original algorithm. To achieve this we calculated sum scores for each ESAS-r, testing different weighting for pain scores to account for the importance of this symptom in the previous algorithm. Using pain weights of 1-5 we tested the scores against the original algorithm scores to find the optimal pain weight. We then calculated sum scores for each ESAS-r Cancer using the optimal pain weight and obtained different cutoffs for each complexity level by using different metrics: Youden's J, Closest Top Left Corner and Kolmogorov-Smirnov (K-S). Finally, we calculated the accuracy index of the new cutoffs against the gold standard.

Results: Four hundred and sixty-four patients (29% response rate) completed the ESAS-r and ESAS-r Cancer. The ROC curve of pain weighted by three showed the largest AUC (0.968), indicating the complexity scores most closely matched those assigned by the original algorithm. We then calculated sum scores for ESAS-r Cancer utilizing this weighting for pain (x3) to determine cutoff points. Three possible cutoff scores for high complexity were determined: 55 using Youden's J, 65 using Closest Top Left Corner and 37 using K-S. We repeated the same analysis for low complexity, with cutoffs of 30, 30 and 24, respectively. The cutoff scores with the highest accuracy were 65 (high) and 30 (low), determined using Closest Top Left Corner (accuracy of 93.8%, versus 88% with Youden's J and 72.7% with K-S.).

Conclusions: We modified and tested a new algorithm to define symptom complexity using ESAS-r Cancer. This algorithm is now in use in Alberta's cancer program and helps guide patient care, condensing a large amount of PROs information into an easily interpretable summary score. The simplicity of the algorithm calculation will allow easy computation in centres using paper or electronic platforms. This algorithm facilitates interdisciplinary collaboration as individual symptom complexity can be used by all care teams to determine how to tailor care for a patient.

312

EXAMINING THE EFFICACY AND SAFETY PROFILE OF PALLIATIVE RADIOTHERAPY USING 30 GY IN 5 FRACTIONS

Zhang Hao (Jim) Li[1,2], Timothy Kong[1,2], Emma Dunne[1,2], Mitchell Chung Chiu Liu[1,2], Jee Suk Chang[1,2], Tina Wanting Zhang[1,2], Matthew Chan[1,2], Ronan McDermott[1,2]
[1]*University of British Columbia, Vancouver, BC*
[2]*British Columbia Cancer, Vancouver, BC*

Purpose: Higher biological equivalent doses of radiotherapy (RT) can improve symptom palliation and local control in select tumour sites. However, not all patients meet criteria for treatment with stereotactic ablative radiotherapy (SABR). Furthermore, SABR is a resource intensive technique which may limit its use in many centres. The 30 Gray in 5 fractions regimen (30/5) stems from a modification of 5-fraction SABR regimens. It is a conformal, homogenous hypo-fractionated regimen that delivers higher dose than conventional palliative RT while still respecting the normal tissue constraints for 5-fraction SABR. It uses streamlined contouring and planning with less stringent requirements for immobilization and image guidance, compared to what is required for SABR. This study evaluates the clinical outcomes of patients receiving 30/5.

Materials and Methods: A single institution retrospective review of clinical and treatment data was performed for patients who received 30/5 from October 2020 to August 2022. Local control (LC) was calculated for all treatment courses. Distant metastasis-free survival (DMFS), progression-free survival (PFS), and overall survival (OS) were calculated for all patients. Survival analyses were analyzed by the Kaplan-Meier method and curves compared by log-rank test. Univariate and multivariate analyses were performed using cox-regression analysis.

Results: A total of 77 patients and 92 courses of 30/5 were available for analysis. The most common primary tumour was lung (44%), followed by gastrointestinal (GI; 20%), breast (10%), and genitourinary (10%). The median age of patients was 64 years (range: 37-93). The median tumour size treated was 11.4 cm^3 (range: 0.3 - 210.9 cm^3). Treatment sites included lung (31%), lymph nodes (22%), non-spine bone (20%), and spine (15%). At median follow-up of 10.1 months, 25 deaths occurred. Median LC after receiving 30/5 was 18.5 months (95% CI: 15.7-21.3 months), median DMFS was 6.6 months (95% CI: 4.6-8.6 months), median PFS was 6.4 months (95% CI: 4.9-8.0 months), and median OS was 18.1 months (95% CI: 13.1-23.1 months). Median time to initiating, restarting, or changing systemic therapy was 12.8 mo (95% CI: 7.6-18.0 months). Radiosensitive (lung, prostate, breast, gyne, and head/neck) tumours had better LC than radioresistant (GI, renal cell, sarcoma, melanoma) tumours (median 20.9 versus 12.1 months, $p<0.02$). Six Grade 2 toxicities occurred (6.5% of all treatments). No Grade 3 or higher toxicities occurred.

Conclusions: The 30/5 regimen is a safe, well-tolerated, and resource efficient regimen with effective local control. This may serve as a practical alternative for patients who require palliative RT but not optimal candidates for SABR. As expected, radiosensitive tumours had better local control than radioresistant tumours. Future research can further explore the safety, efficacy, and indications of 30/5 as a palliative RT option.

313

HIGH SYMPTOM BURDEN IN PATIENTS RECEIVING RADIOTHERAPY AND FACTORS ASSOCIATED WITH BEING OFFERED AN INTERVENTION

Allison Rau[1], Linda Watson[2,1], Demetra Yannitsos[1], Petra Grendarova[1], Siwei Qi[2], Lisa Barbera[1]
[1]*University of Calgary, Calgary, AB*
[2]*Alberta Health Services, Calgary, AB*

Purpose: Symptom scales such as the Edmonton Symptom Assessment System (ESAS) are routinely administered during radiation oncology visits to elicit symptom burden and help guide

management. Our goal was to identify factors that influence whether patients with high symptom complexity scores were intervened on.

Materials and Methods: We completed a retrospective chart audit of adult cancer patients who had at least one radiotherapy appointment at our institution between October 1, 2019, and April 1, 2020. Using the provincial registry and Electronic Medical Records we identified all patients with a high symptom complexity score. Symptom complexity scores are assigned based on the self-reported severity of ESAS symptoms and the number of concerns indicated by the patient at a single visit. High symptom complexity scores are classified as any symptom scored 10 (10 being most severe); pain scored 7 to 9; 3-5 symptoms scored between 7 to 9; and 6+ symptoms scored between 4 to 6. The ESAS symptom scored the highest or identified by the patient as highest priority was selected as the main symptom. Data was also collected on cancer type, treatment intent, and if an intervention was offered on the main symptom. Demographic data and symptom outcomes were summarized using descriptive statistics. The primary outcome of whether an intervention was offered for the main symptom was analyzed using a multivariable logistic regression model.

Results: A total of 200 patients were included. Average age across all tumour groups was 61.7 years, with 106 (53.0%) females. Overall, pain (43.0%) was reported most frequently as the main symptom, followed by tiredness (12.5%) and anxiety (11.0%). In total, 150 (75.0%) patients were offered an intervention for the main symptom. Multivariable regression showed factors associated with being offered an intervention were: symptom score of 9 (OR 9.56, 95% CI 1.64-62.84) and score 10 (OR 7.90, 95% CI 1.69-38.18) compared to symptom score of ≤6; palliative intent radiation treatment compared to curative intent (OR 3.87, 96% CI 1.46-11.06); and first review appointment compared to consultation (OR 1.93, 95% CI 0.68-5.82). Compared to tiredness, symptoms associated with being offered an intervention included: pain (OR 22.57, 95% CI 6.47-91.14), nausea (OR 15.69, 95% CI 1.51-412.4), shortness of breath (OR 7.97, 95% CI 1.20-63.74), and anxiety (OR 6.69, 95% CI 1.58-31.64).

Conclusions: Our study reveals that patients are more likely to be offered an intervention if they are experiencing main symptoms of pain, nausea, shortness of breath, or anxiety. Patients with high symptom scores, receiving palliative intent radiation, or at their first radiation review visit are also more likely to be offered an intervention. Twenty-five percent of patients were not offered an intervention. This knowledge will guide clinical care and symptom management practices within the radiation oncology department.

314

A PRACTICAL METHOD FOR QUALITY ASSURANCE OF THE TIME DELAY ASSOCIATED WITH A MOTION MANAGEMENT SYSTEM USING A QUASAR™ PHANTOM

Amanda Swan[1], Greg Pierce[2]
[1]*Cross Cancer Institute, Edmonton, AB*
[2]*University of Calgary, Calgary, AB*

Purpose: Varian Medical System's Respiratory Gating for Scanners (RGSC) system is an advanced motion management system that tracks a surface marker block throughout the respiratory cycle as a surrogate for internal tumour motion. A user can set a portion of the respiratory trace during which the beam is to turn on. Inherent in both the imaging and treatment beam is a time delay, representing the delay between when the system detects that the marker block is within the appropriate gating window and when the beam turns on. It is important to characterize this delay and ensure it is within a specified range to confirm that the uncertainty is in line with the associated target margins used. If the time delay is larger than expected, this can lead to possible geometric misses. The American Association of Physicists in Medicine's Task Group 142 report on quality assurance (QA) of medical accelerators recommends the inclusion of testing of the system time delay. We propose a method for performing this QA using a commercial phantom.

Materials and Methods: The QUASAR™ Respiratory Motion Phantom was used in conjunction with custom ceramic (kV imaging) and steel (MV imaging) ball inserts. A CT scan with the ball at the equilibrium position was obtained, and the ball insert was contoured. Using a sinusoidal trajectory, the ball motion was modelled, and the position based on an expected time delay of 0.1s was contoured. Tolerance and action contours were also created from the sinusoidal trajectory as an expansion of the expected position. The phantom was set up and aligned using a Varian TrueBeam linear accelerator, and both kV and MV images were acquired at both beam on and beam off. The position of the ball was evaluated relative to the contours.

Results: Both the kV and MV time delays were found to be within the expected range using this method. A breathing rate of 60 breaths per minute and an amplitude of 2 cm were found to provide an adequately sensitive test for observing the system time delay. The method was found to be efficient to perform.

Conclusions: This method of testing the kV and MV beam time delays on a linear accelerator was found to be simple and effective and would serve as a useful annual QA test.

315

OZONE HEALTH AND SAFETY CONSIDERATIONS FOR FLASH RADIOTHERAPY

Amy Frederick[1], Andrew K.H. Robertson[1], Gurpreet K. Sandhu[2], Sheila MacMahon[1], M. Peter Petric[1]
[1]*British Columbia Cancer, Vancouver, BC*
[2]*British Columbia Cancer, Surrey, BC*

Purpose: Medical linear accelerators (LINACs) can produce ozone by the ionization and subsequent recombination of oxygen gas. Ozone is a potential health hazard for staff and patients because it can cause a range of acute and chronic health problems depending on the concentration and duration of exposure. Health Canada recommends a maximum exposure limit of 20 ppb averaged over eight hours. Previous studies have reported ozone concentrations < 15 ppb during LINAC x-ray and electron irradiation but FLASH radiotherapy beams could yield higher concentrations. The purpose of this study was to compare ozone concentrations produced in the LINAC vault during non-FLASH and FLASH radiotherapy.

Materials and Methods: All measurements were performed in a vault equipped with a TrueBeam LINAC (Varian Medical Systems). The vault dimensions are 6.50 x 6.43 x 2.77 m^3 and the air exchange rate is approximately 12 air changes per hour. A portable air quality monitor (Aeroqual series 500) was used to measure ozone concentration (detectable range: 1 – 500 ppb, sampling frequency: 60 s) at the vault entrance. For reference, the daily variation in ozone concentration during patient treatments was measured over the course of a typical workday. To produce 10 MeV FLASH electron beams, the LINAC was operated in 10 MV flattening filter-free (FFF) photon mode with the target and ion chamber retracted and the flattening filter replaced with an electron scattering foil. Ozone concentrations were measured for 10 MeV FLASH electron beams as well as 15 MV and 10 MV FFF non-FLASH photon beams; gantry angles of 0^o and 270^o; field sizes of 10 x 10, 20 x 20, and 40 x 40 cm^2; dose rates of 0.1 – 50.0 Gy/s at isocentre; and with/without scattering material in the field.

Results: During the reference measurements, 22 radiotherapy treatments (1.8 – 7.5 Gy/fraction) were delivered over eight hours and resulted in an average (range) ozone concentration of 3 ppb (0 – 12 ppb). Dose levels (< 50 Gy) and setup geometries (i.e., scattering material in field) relevant for clinical treatments or research irradiations did not produce detectable ozone concentrations for all beams tested. The average (range) ozone concentrations measured during simulated radiation surveys were 7 ppb (0 – 41 ppb) for FLASH electron beams and 2 ppb (0 – 8 ppb) for non-FLASH photon beams. The ozone concentration increased with dose rate, beam-on time, and the volume of air irradiated. Ozone concentration decayed approximately exponentially with a half life of 1 – 3 minutes following its peak post-irradiation.

Conclusions: All ozone concentrations were safe and below the maximum exposure limit recommended by Health Canada. Increased ventilation or limitations on room entry may be used to further reduce staff ozone exposure during FLASH radiotherapy radiation surveys and commissioning.

316

RADIATION TREATMENT CONSIDERATIONS FOR PATIENTS WITH IMPLANTED MEDICAL DEVICES

Brian Liszewski[1,3], Michelle Nielsen[1,2]
[1]*Ontario Health (Cancer Care Ontario), Toronto, ON*
[2]*Sunnybrook Health Sciences Centre, Toronto, ON*
[3]*University of Toronto, Toronto, ON*

Purpose: Advances in medical technology are driving the integration of implanted medical devices in the management of chronic health conditions, including but not limited cardiac implantable electronic devices (CIED), glucose monitors, cochlear implants, and deep brain stimulators. This has led to developing considerations with respect to radiation exposure to multiple types of implant device over a course of treatment. Although cancer programs may have local implanted device policies variation in guidance and the devices considered exist. This initiative sought to take a provincial approach to establish recommendations when developing implanted device policies.

Materials and Methods: Following an incident that resulted in the malfunction of an implanted cardiac device policies were collected from all regional cancer programs within the province. A thematic analysis was performed specifically focusing on pre-, during and post-treatment considerations as well as stakeholders engagement along the care pathway. A summary of identified themes was used to develop the recommendation document.

Results: Ten domains were identified to be considered in the development of institution-specific policies and procedures for implanted devices, including requirements; responsibility for identification; documentation responsibility and locations; engagement of relevant stakeholders (e.g. cardiology), imaging/planning considerations; beam energy and dose constraints, on treatment monitoring and additional considerations (e.g. MR simulation etc.)

Conclusions: The purpose of this document is to heighten awareness within the clinical community of existing and emerging implanted devices, provide considerations for minimizing possible negative effects on patient care and avoid potential corruption or malfunction of implanted medical devices during or after exposure to radiation.

317

EFFECTS OF PALLIATIVE ESOPHAGEAL EBRT IN PATIENTS WITH STENT FOR ESOPHAGEAL CANCER: BRITISH COLUMBIA PATTERN OF PRACTICE SURVEY AND RETROSPECTIVE COHORT STUDY

Emily Adams[1], Héloïse Lavoie-Gagnon[2], Farhana Islam[1], Michael Humer[3,4], Theodora Koulis[3,5], Benjamin Mou[3,6],David Kim[3,6], Siavash Atrchian[3,6]
[1]*University of Toronto, Toronto, ON*
[2]*Centre hospitalier Universitaire de Sherbrooke, Sherbrooke, QC*
[3]*University of British Columbia, Vancouver, BC*
[4]*Kelowna General Hospital, Kelowna, BC*
[5]*British Columbia Cancer, Victoria, BC*
[6]*British Columbia Cancer, Kelowna, BC*

Purpose: Self-expandable metallic stents (SEMS) provide immediate but nondurable dysphagia relief in esophageal cancer, while external beam radiotherapy (EBRT) provides lasting dysphagia relief after a delayed onset. While the combination of SEMS and EBRT provides a promising palliation option for esophageal cancer, there is a lack of consensus among physicians and the literature on its safety and efficacy. We investigate British Columbia (BC) pattern of practice and local patient outcomes regarding EBRT during SEMS placement in patients with incurable esophageal cancer.

Materials and Methods: We surveyed BC radiation oncologists on if, when, how and why they would offer EBRT to palliate esophageal cancer patients with a stent in place. We also conducted a single-centre retrospective chart review from January 2010 to July 2020 to compare stent-related complications and survival in patients with incurable esophageal cancer treated with SEMS alone or SEMS + EBRT.

Results: Nineteen of 22 survey respondents reported that they would consider treating a patient with an existing SEMS with palliative EBRT for esophageal cancer. In our chart review, 66 patients were included in the SEMS alone group and 26 in the SEMS + EBRT group. Patients in the SEMS + EBRT group survived significantly longer than those treated with SEMS alone, with a median overall survival of 163.5 days (95% CI [65, 302]) and 65 days (95% CI [36, 105]), respectively. Patients who did not receive radiation showed 3.05 (95% CI [-4.67, -1.44]) fewer number of stent-related complications and 9.05 (95% CI [3.11, 26.27]) times greater odds of experiencing more severe complications compared to patients who received esophageal radiation.

Conclusions: Most BC radiation oncologists would consider palliative EBRT in esophageal cancer patients with an existing SEMS. This combined treatment option demonstrates prolonged survival compared to stenting alone. SEMS monotherapy, however, is associated with fewer, more severe stent-related complications. Further prospective studies are needed to confirm these findings.

318

OPTIMIZATION OF WORKUP PATHWAYS TO DECREASE RADIOTHERAPY WAIT TIMES AND IMPROVING PATIENT EXPERIENCE: A SINGLE CENTRE STUDY

Abdulmajeed Dayyat[1], Kwamena Beecham[1], Ashraf Mahmoud-Ahmad[1], Aimee Brenna[2], Helmut Hollenhorst[1], Amanda Caissie[1]
[1]*Dalhousie University, Halifax, NS*
[2]*Nova Scotia Health, Halifax, NS*

Purpose: Wait times are challenging for certain radiotherapy (RT) centres, and benchmarking is challenging, given the different standards used. Beyond the standards of referral to consult and consult to treatment, certain centres have established a "ready-to-treat" (RTT) definition to address the reality of patients requiring further investigations from consult to enable a treatment plan. In this single RT centre study, a Timely Access and Patient Support (TAPS) model of care has been implemented aiming to improve access to care and, ultimately, patient outcomes.

Materials and Methods: This comparative cohort study was conducted in a single mid-size RT centre serving mainly rural communities as part of a larger multi-centre academic institution. In collaboration with a Radiation Oncologist (RO), the TAPS clinic is run by a Nurse Practitioner who provides patient assessment and submits requisitions to ensure the patient has support services and is RTT by the time of RO consult. All newly suspected/diagnosed adult cancer patients referred to the centre with a triage priority of ≥2 weeks were eligible. Non-metastatic breast and prostate cancers were excluded. Retrospective and prospective data were collected from patient medical records, and descriptive statistical analysis was performed. Pre- and post-TAPS clinic comparison was made for wait times and patient-reported outcomes (PROs) using the Edmonton Symptom Assessment System-revised.

Results: During the first six months of the study, 66 eligible patients were assessed in the TAPS clinic, prompting 177 orders including referrals (52%) (top 3: social worker 30%, dietitian 20%, and cancer patient navigator 11%), investigations (27%) (top 3: CT 21%, MRI 19%, and biopsy 25%), and interventions (21%). The most common cancers were thoracic (33%), GI (23%) and head and neck (14%). The mean wait time from referral to TAPS consult was five days compared to 15 days for pre-TAPS patients to be seen in RO consult. The mean wait time from referral to RTT was 33 days versus 40 days in the post- versus pre-TAPS setting. Seventy-one percent of post-TAPS patients were RTT at RO consult compared with 43% pre-TAPS. Post-TAPS patients reported less fatigue and anxiety and better overall well-being during CT simulation compared to pre-TAPS patients.

Conclusions: Preliminary data of TAPS clinic implementation has shown the potential to positively impact RTT times and PROs for psychosocial distress by the time of RT planning. This data also sheds light on the topic of wait time definitions, the investigations required before RTT and the potential role of physician extenders within the health care team to facilitate accelerated workup of malignancies. While TAPS study data will help to inform local cancer care program operations, it is also considered relevant to the broader RT community and professional RT societies addressing standards related to RT access.

319

RAPID AUTOMATED EXTRACTION OF DOSE-VOLUME HISTOGRAM DATA FOR ARBITRARY PATIENT COHORTS

Logan Montgomery[1], Tim Olding[1,2], Kurtis Dekker[1,2]
[1]*Cancer Centre of Southeastern Ontario, Kingston, ON*
[2]*Queen's University, Kingston, ON*

Purpose: Retrospective analysis of bulk dose-volume histogram (DVH) data can aid in quantifying practice drift and/or inform future changes in practice. However, manual extraction of DVH data is not feasible for large patient cohorts. The Eclipse™ Scripting Application Programming Interface (ESAPI) allows users to extract these data from the Eclipse treatment planning system database without requiring export of any DICOM data. We have used ESAPI to develop a simple software tool that allows users without programming experience to efficiently extract bulk DVH data for any arbitrary patient cohort. This tool is now being used to analyze a variety of patient cohorts of clinical interest in our centre.

Materials and Methods: The software was developed using the C# programming language and ESAPI. Users must provide two main inputs into the program: a patient cohort and the DVH data of interest. The patient cohort is provided as a CSV file that can be obtained via an SQL query, for example. DVH data of interest are specified for an arbitrary number of structures via an Excel sheet, which contains a variety of additional software settings. Intersection volumes between overlapping structures can also be requested, in order to aid in analysis. During software execution, the Eclipse database is accessed one patient at a time and results are output to a CSV file. The software includes robust handling of free-text fields such as structure names and interactively allows users to resolve niche cases.

Results: We stress tested the software and verified that it had no detrimental impact on the performance of our clinical system. The output was validated through spot checks by opening patient plans in the Eclipse treatment planning system and manually measuring the data of interest. Data retrieval takes up to a few seconds per patient, depending on the amount of data requested. We have used this software to analyze a variety of data, including a statistical comparison of heart and lung dose metrics for over 1500 breast cancer patients treated in deep inspiration breath hold versus those in free breathing. These data are currently being used to inform internal review of treatment techniques and DVH criteria.

Conclusions: We have developed an efficient and user-friendly software tool to extract bulk DVH data from the Eclipse treatment planning system database, for any arbitrary patient cohort. This tool facilitates efficient extraction of DVH data of clinical interest for the purposes of quality control and quality improvement.

320

MONITORING CT DOSES IN DIAGNOSTIC RADIOLOGY THROUGH A DASHBOARD

Pierre-Luc Asselin[1], Yannick Lemaréchal[2], Gabriel Couture[1], Samuel Ouellet[1], Jonathan Boivin[2], Philippe Després[1]
[1]*Université Laval, Quebec City, QC*
[2]*CHU de Québec-Université Laval, Quebec City, QC*

Computed Tomography is the principal contributor to ionizing radiation exposure of medical origin for the Canadian population. The Canadian Computed Tomography Survey by Health Canada provides guidance in the safe use of radiation-emitting devices, notably by proposing Diagnostic Reference Levels (DRLs) for typical CT exams (e.g. head, chest, abdomen). DRLs can be measured, but this remains a periodic one-off procedure that, although part of a quality assurance program, might fail to capture the reality of clinical activities. There is a need to monitor more closely and continuously the use of ionizing radiation in CT, as demanded for instance by provincial authorities in Québec.

Purpose: To develop a dashboard to monitor both Weighted Dose Index (CTDIw) and Dose Length Product (DLPs) of CT examinations in a large institution to provide visualization and analytic tools to managers and technical personnel. FAIR principles guidelines are implemented within the data workflow.

Materials and Methods: The dashboard was developed with the OpenSearch suite (a fork of the Elastic suite). Data were collected from the Picture Archiving and Communication System (PACS) of the institution, de-identified and securely stored within OpenSearch indexes. Dashboard functionalities include reporting by anatomical region examined, unit, protocol, patient sex or any information contained in DICOM headers.

Results: The dashboard provides an overview of radiation usage in CT, give rise to opportunities to study clinical practice trends and ease the identification of outliers to improve heath care. The technology used was found to be well adapted to the analysis of massive datasets without interfering with clinical activities. First analysis of available dosimetric data are under way.

Conclusions: A dashboard fed by secure data pipelines was developed to aggregate and visualize dosimetric data from clinical CT studies. Next steps include the development of alerts

for events (e.g. high dose, repeated exams) and the integration of data from other centres to generate a personalized report on cumulative dose from CT studies.

321
COMPARISON OF PATIENT-SPECIFIC QUALITY ASSURANCE RESULTS FROM A DELIVER-LOG BASED CALCULATION SYSTEM AND DOSE RECONSTRUCTION IN PATIENT ANATOMY BASED ON PHANTOM MEASUREMENTS

Gordon Chan[1], Orest Ostapiak[1,2], Tom Chow[1], Baochang Liu[1], Marcin Wierzbicki[1,2]
[1]*Juravinski Cancer Centre, Hamilton, ON*
[2]*McMaster University, Hamilton, ON*

Purpose: To compare the patient-specific quality assurance dosimetric results obtained using delivery-log based calculations and phantom-based measurements with dose reconstruction in patient anatomy.

Materials and Methods: Seventeen clinically approved SBRT plans calculated in Varian Eclipse using 6FFF energy were delivered on two beam-matched TrueBeam STx linacs. For each plan, a measurement was made with a Delta^4 Phantom+, and the dose in patient anatomy was reconstructed using the Delta^{4DVH} Anatomy TMM algorithm. The delivery-log data was sent to MobiusFX to calculate the patient dose distribution using a collapsed cone convolution method. The beam data used in the TMM algorithm had been characterized against the in-house measured data, while the beam model in MobiusFX was commissioned by the vendor based on a set of reference beam data.

Results: For both MobiusFX and Delta^{4DVH}, the modelled beam profiles and PDDs for a set of field sizes ranging from 4x4 cm^2 to 20x20 cm^2 were found to be within 2% of their respective reference data. For each plan, the mean PTV dose calculated by MobiusFX, Delta^{4DVH} and Eclipse was compared. The ratio of mean PTV dose in MobiusFX/Delta^{4DVH} ranged from -7.0% to 5.0%, with a mean of 0.6%. Fifteen of 17 plans had dose ratios MobiusFX/Eclipse and Delta^{4DVH}/Eclipse within 3% of unity. The remaining two plans had ratios of 3.2% (MobiusFX/Eclipse) and 4.8% (Delta^{4DVH}/Eclipse). A negative correlation was also observed between MobiusFX/Eclipse and Delta^{4DVH}/Eclipse with a Pearson correlation coefficient of -0.83.

Conclusions: The mean PTV dose in patient anatomy calculated by MobiusFX, Delta^{4DVH} and Eclipse were compared in 17 SBRT clinical plans. In 88% of the plans, both MobiusFX and Delta^{4DVH} calculated PTV mean dose values are within 3% of Eclipse planned dose. The negative correlation observed between MobiusFX/Eclipse and Delta^{4DVH}/Eclipse suggests an investigation into the tuning of the MobiusFX dosimetry leaf gap may be warranted.

322
PATIENT EXPERIENCE IN A RADIATION THERAPY DEPARTMENT PRE- AND DURING THE COVID-19 PANDEMIC

Lisa Barbera[1,2], Demetra Yannitsos[1], Petra Grendarova[1]
[1]*University of Calgary, Calgary, AB*
[2]*Tom Baker Cancer Centre, Calgary, AB*

Purpose: Measuring patient experience over time promotes continual high-quality care and quality improvement (QI). The purpose of this study was to investigate current patient experience in the radiation department (during the Covid-19 pandemic), and to compare results to previous data collected in 2019. This work is part of the Person-centred Radiation Oncology Service Enhancement (PROSE) program, a multi-year QI initiative aimed at improving patient experience in the radiation department of a tertiary cancer centre.

Materials and Methods: We collected patient experience data using the Your Voice Matters (YVM) questionnaire. This captures information on the patient's last visit including arrival and departure experiences, and interactions with healthcare providers. Recruitment occurred between April and June 2022. Consecutive patients were approached in the radiation department waiting areas to complete the YVM regarding their consultation or radiation treatment appointment. The proportion of patients with positive experience scores were calculated for 2022 results. Unadjusted results were compared between 2019 and 2022. Adjusted analysis included logistic regression modelling to evaluate factors associated with an overall positive experience. Content analysis was completed for current qualitative data.

Results: Of the 472 patients approached, 400 completed the YVM: 200 regarding their consultation and 200 regarding their latest radiation treatment appointment. The most favourable experiences included polite reception staff, feeling respected and listened to. Compared to 2019, there was no significant difference in overall experience scores. Results demonstrated improvements in wait times past scheduled appointment times for consultations ($p<0.01$) and treatments ($p<0.01$). Results demonstrated deterioration in friends/family included in care during consultations ($p=0.03$) and treatments ($p=0.02$). Despite improvements, wait times as well as contacting the clinic remain areas requiring improvements. In 2022, factors associated with a positive experience included being a patient with breast cancer (OR=5.5; 95%CI:1.23,39.2) compared to lung. The content analysis of patient comments revealed the largest number expressing positive experiences, especially during treatments.

Conclusions: Patients at our institution continued to have positive experiences over time, despite the ongoing COVID-19 pandemic. Improvements were most evident with wait times. Other items such as contacting the clinic remain areas for improvement.

323
AUTOMATED LOW CONTRAST DETECTION FOR ACR MRI PHANTOM QUALITY ASSURANCE

Joseph Madamesila, Ali Golestani
University of Calgary, Calgary, AB

Purpose: To create an algorithm for low contrast detection in the American College of Radiation (ACR) magnetic resonance imaging (MRI) phantom during quality assurance.

Materials and Methods: The low contrast module consists of four slices, each with 10 sets of three disks arranged in a circular spoke pattern. Each spoke is considered a pass if all three disks are visible (after window adjustment by the user) with a maximum of 40 points possible. We developed a Python code to perform low contrast detectability with no human intervention. The inner low contrast module is first separated from the rest of the phantom. Lines are generated from the centre at specific angles. For each angle the image intensity is sampled to create a profile. This is repeated to find the location of all 10 spokes. Each profile is fine-tuned by minor angle adjustments to address possible misalignment in phantom positioning. Accuracy is calculated for each spoke by multiplying a template defined by the specifications of the contrast disks in the phantom with its corresponding profile. The average number is compared with a threshold to decide pass or fail. Five MRI datasets were taken during quality assurance and analyzed manually by conventional measurement. A Rose model-based algorithm for low contrast, which simulates the performance of the human eye on an absolute scale, was also compared. Results were compared with our proposed algorithm.

Results: Spoke pass rates generally agreed with human quality assurance measurements, showing point differences of 2.7±4.2.

Results also compared more favourably than the Rose model (visibility threshold of 0.20), which showed point differences of 4.7±4.3 using the same dataset. Average algorithm run time was 4.3 seconds per dataset.

Conclusions: We presented a novel algorithm for automatically analyzing the ACR phantom low contrast module. Future work will consist of refining the algorithm and integration into our clinic's quality assurance program.

324

AN INVESTIGATIONAL STUDY OF UNACCEPTABLE MONITOR UNITS IN STEREOTACTIC ABLATION RADIOTHERAPY (SABR) VOLUMETRIC MODULATED ARC THERAPY (VMAT) TREATMENT PLANS

Gurpreet K. Sandhu, Fred Cao
British Columbia Cancer, Surrey, BC

Purpose: Stereotactic Ablative Radiotherapy (SABR) is a technique used to deliver highly precise radiation therapy in small number of high dose fractions. SABR treatment (using IMRT/VMAT techniques) is delivered precisely and efficiently, while patient is immobilized using dedicated site-specific immobilization devices. Aim of this study is to investigate an erratic and unpredictable behaviour of a treatment planning system (TPS), which generate unnecessary alarmingly high monitor units (MUs) for SABR VMAT plans.

Materials and Methods: Thirty-nine patients with eight different treatment sites (18 liver, three lung, three spine, one brain, five head and neck, seven prostate/pelvis, one gynecological and one shoulder) were selected for this study. Three of these plans were IMRT and 36 were VMAT; 14 treatment plans were with standard prescriptions and 25 were SABR prescriptions. Total 210 treatment plans were generated using Eclipse treatment planning system (version 10.0, Varian Medical Systems, Inc, Palo Alto, CA™). Plan optimization and dose calculations were performed with the progressive resolution optimizer (PRO) algorithm versions PO13.6 and PO15.6 and Anisotropic Analytic Algorithm (AAA). For every plan, all the optimizing parameters and plan objectives were kept same except changing the calculation optimizer. These plans were generated to deliver on Varian TrueBeam treatment units. Plans were compared for plan quality (PTV coverage, OAR doses and QA passing rate) and total number of MUs to deliver the treatment.

Results: PO15.6 produced an inconsistent, unpredictable and alarmingly high MUs. For six out 18 liver SABR VMAT plans, for similar quality plans using PO15.6 optimizer resulted in >13% increase (with a maximum increase up to 72.6%) in MUs as compared to PO13.6. For all other treatment sites (SABR/non-SABR; VMAT/IMRT) increase in MUs with PO15.6 was <13% as compared to PO13.6. This MUs increase found to be unnecessary, with no contribution to the quality improvement of treatment plan. We didn't find any logical justification for this erratic behaviour of PO15.6 optimizer, due to its nonreproducible nature.

Conclusions: An unnecessary increase in MUs can result in an increase in patient's time on treatment table and chances of patient movement, and hence increase chances of mistreatment. Unnecessary MUs increase can also leads to an increase in out of field dose to patient and increase chances of secondary cancers. Additionally, increase in MUs can increase the machine workload and waste of treatment units' valuable time and resources. This unacceptable behaviour of TPS can negatively impact the goal of SABR treatment by increasing the treatment time, reducing treatment efficiency and efficacy, and increasing out of field dose. Efforts and strategies should be implemented to remove any undesired MUs, while creating the quality treatment plans. At our institution, we discontinue the use of the PO15.6 optimizer for SABR treatment planning.

325

COMPARISON OF SET-UP ERRORS BETWEEN BREAST AND THORAX ALL-IN-ONE SOLUTION AND BREAST BOARD IN BREAST CANCER PATIENTS

Aya Hassabelrasol, Agha Muhammed Hammad, Jamsari Khalid, Zahid Al Mandhari
Sultan Qaboos Comprehensive Cancer Care and Research Centre (SQCCCRC), Muscat, OM

Purpose: To compare the set-up errors between Breast and Thorax All-in-one solution and Breast board in breast cancer patients using values acquired from CBCT images.

Materials and Methods: Data was collected retrospectively from ARIA system of 40 patients with breast cancer. Anterior MV and lateral KV pairs and Cone-beam CT-scan (CBCT) images were used for online set-up correction as per departmental protocol. For study purposes, 387 CBCT exposures has been analyzed All data were filled in Excel sheet with translational and rotational shifts. Systematic errors (Σ) and Random errors (σ) has been noted.

Results: The systematic (Σ) translational errors for AIO and breast board were 0.00684 mm and -.03229 mm, respectively, and rotational Σ errors were 0.12042° and 0.39128°, respectively. Whereas the random (σ) translational errors for AIO and breast board were 0.294 mm and 1.979 mm respectively, and rotational σ errors were 0.7296° and 0.7296°, respectively.

Conclusions: The comparison of the set-up using AIO and breast board for breast cases showed that the systematic and random errors are less when using AIO. A prospective randomized study required to confirm these findings and under consideration.

326

OUTCOMES OF HYPOFRACTIONATED RADIOTHERAPY WITH INDUCTION OR SEQUENTIAL CHEMOTHERAPY FOR UNRESECTABLE STAGE III NON-SMALL CELL LUNG CANCER: SINGLE INSTITUTION EXPERIENCE

Ian J. Gerard, Neelabh Rastogi, Jayson Paragas, Tanner Connel, Bassam Abdulkarim, Marie Duclos, Sergio Faria, Neil Kopek
McGill University, Montréal, QC

Purpose: The standard of care for unresectable Stage III non-small cell lung cancer (NSCLC) patients not candidates for concurrent chemotherapy (CT) and radiotherapy (RT) is not well established. Hypofractionated RT (hRT) can be used after CT induction, or, as a bridge to sequential CT to offer a curative intent treatment regimen. Tumour and nodal proximity to mediastinal structures plays an important role regarding the degree of safe hypofractionation. There is limited published evidence related the benefits of hRT combined with induction or sequential CT among this group of patients. We analyzed the outcomes of Stage III NSCLC receiving a hRT regimen of 52.5 Gy in 15 fractions alone, or with either induction or sequential CT.

Materials and Methods: In this retrospective review, patients with Stage III NSCLC receiving hRT 52.5 Gy in 15 fractions between 2008-2020 were included for analysis. Patients were separated into three cohorts: (1) hRT alone, (2) induction CT followed by hRT, and (3) hRT followed by sequential CT. Overall survival (OS) and radiation toxicity (CTCAE v5.0) were analyzed for all three cohorts. Patients for whom sequential chemotherapy was planned, but not delivered, were included in cohort 2 through intention-to-treat analysis. The OS at two years was statistically evaluated using a log-rank test with alpha set at 0.05.

Results: Eighty-three patients met criteria for analysis with 35, 30, and 18 patients respectively in cohorts 1, 2, and 3. Median age at treatment was 75 (43-91) with 53% of patients being men and 43%

women. Tumour histology varied between adenocarcinoma (43%), squamous cell carcinoma (44%), and others (13%). The median/two-year OS for cohorts 1, 2, and 3 was eight months/19%, 25 months/50%, and 17 months/72% respectively. OS between any chemotherapy and no chemotherapy was statistically significant ($p=6.1x10^{-7}$) while the timing of chemotherapy did not reach statistical significance (p= 0.15). RT was overall well tolerated with Grade 1-2 fatigue being the most common side effect (81%), one patient had Grade 3 pneumonitis, and one patient had a rib fracture.

Conclusions: Among patients with Stage III NSCLCs, moderately hRT of 52.5 Gy in 15 fractions, with either induction or sequential CT appears to provide a survival advantage compared to hRT alone, with an acceptable side-effect profile. The two-year OS reported here is similar to other published hRT regimens (SOCCAR trial 50 Gy in 20 fractions) and conventional fractionation (RTOG0617). Conclusions are limited by the retrospective nature of the study, and the introduction of immunotherapy (IO) for Stage III NSCLC in 2019 in Canada. Future work will focus on evaluating dosimetry, the impact of IO, and, patients not included in this analysis that also received this regimen (oligometastasis, locoregional failure, other stages).

327

CONVENTIONALLY FRACTIONATED VERSUS HYPOFRACTIONATED RADIOTHERAPY FOR TREATMENT OF UNRESECTABLE PANCREATIC CANCER: LOCAL CONTROL AND SURVIVAL OUTCOMES IN A RETROSPECTIVE SINGLE-INSTITUTIONAL ANALYSIS

Daniel Tesolin, Vimoj Nair
University of Ottawa, Ottawa, ON

Purpose: Unresectable pancreatic cancer (UPC) is associated with dismal survival outcomes, with a reported median survival of 8-12 months. The role of radiotherapy (RT) and the choice of optimal fractionation remains unclear. Our objective was analyzing the outcomes associated with local radiotherapy as well as determine the best radiotherapeutic approach to treat these patients.

Materials and Methods: From a database of 209 radiation plans of patients treated for pancreatic cancer in a single institution between August 2007 to August 2021, patients with UPC were selected for this REB approved retrospective study.

Results: From the 209 plans, 136 unique patients were identified who had RT for UPC. The mean age of the cohort was 67.6 years, 10% were >80 years and 37% were female. Median follow-up was 9.3 months. Fifty-four patients had distant metastases at the time of RT and were analyzed separately. Outcomes where analyzed based on whether patients received Conventionally fractionated RT (CFRT) (defined as >15 fractions) (n=23 (17%)), Hypofractionated RT (HypoRT) (defined as ≤15 fractions and EQD2<40Gy for $\alpha/\beta=3$) (n=40 (29%)) and those treated with Stereotactic Body RT (SBRT) (defined as ≤5 fractions and EQD2≥40Gy for $\alpha/\beta=3$) (n=19 (14%)). The mean overall survival (OS) and freedom from progression (FFP) in the SBRT cohort was 17.2 and 7.4 months respectively, in the CFRT cohort was 22.6 and 9.9 months respectively and in the HypoRT cohort was 11.4 and 4.9 months respectively. All CFRT patients received chemotherapy. Mean OS was drastically lower in SBRT and HypoRT patients who did not receive any chemotherapy (11.9 and 3.4 months respectively). Patients with metastatic disease at presentation and receiving HypoRT had mean OS of 13.4 months. The average EQD2 for the cohorts were 45.4 Gy, 49.2 Gy and 30.3 Gy for CFRT, SBRT and HypoRT respectively.

Conclusions: Our study demonstrates that CFRT with concurrent chemotherapy offers better therapeutic outcomes in patients with UPC compared to HypoRT. The role of dose escalated SBRT needs to be explored as an equal alternative.

328

TOXICITIES ASSOCIATED WITH RADIOTHERAPY FOR PROSTATE CANCER PATIENTS TREATED WITH VMAT

Catherine McKenna[1,2], Johnson Darko[1,2], Ernest Osei[1,2]
[1]*Grand River Regional Cancer Centre, Kitchener, ON*
[2]*University of Waterloo, Waterloo, ON*

Purpose: Toxicities resulting from radiotherapy (XRT) can be detrimental to patient's quality of life (QoL). There is also an increased risk of secondary cancers from XRT. Prostate cancer patients treated with XRT have an increased risk for colorectal cancer. Our aim is to evaluate the toxicity profiles for prostate cancer patients receiving VMAT XRT. We predicted that patients with prostate only (PRT) are at a higher risk of toxicities compared to those with treatment to whole pelvis (WPRT) due to greater area of irradiation near organs at risk.

Materials and Methods: We extracted and analyzed toxicity and dosimetric data of 538 patients treated between 2013 and 2015 at our cancer centre. The clinical data was collected for the period during radiation treatment and up to two years of follow-up. Toxicities recorded were classified using the RTOG Toxicity Criteria Scale and categorized by region of impact: genitourinary (GU), gastrointestinal (GI), rectal, and other. "Other" toxicities were defined as those detrimental to patient QoL but could not be attributed to any specific anatomical regions, such as fatigue or depression. The highest-grade toxicity available for each type was used in the analysis for this study. Patients were stratified into PRT or WPRT for either a total dose of 66Gy for salvage or post-op irradiation; or 78Gy as primary treatment. Mean ± standard deviations and t-test were used to compare patient characteristics. A univariate binary logistic regression was also used to determine the odds ratios of reporting toxicity between cohorts.

Results: There were no significant differences in anatomical structures between all the patient cohorts (p>0.05) except for rectum where WPRT-78Gy patients had significantly larger volume compared to PRT-78Gy patients (p=0.023). Patients with treatment to the pelvis, irrespective of prescribed dose, had significantly higher dose to the rectum (p<0.001) and bladder (p<0.001) compared to patients with treatment to only the prostate. WPRT-78Gy patients were at higher odds for reporting rectal (OR = 3.058), GI (OR = 2.945) toxicities during treatment, and GU (OR = 2.044) toxicities following treatment, compared to PRT-78Gy patients. WPRT-66Gy patients were at lower odds for reporting during treatment GU (OR = 0.266) toxicity, but at higher odds for reporting late GI (OR = 3.205) toxicities, compared to PRT-66Gy patients.

Conclusions: When 78Gy XRT-VMAT is the primary treatment, patients receiving treatment to the whole pelvis were at a higher risk of rectal and GI toxicities compared to patients with treatment to only the prostate due to the increased dose to the OARs. In patients treated to 66Gy with salvage or post-op XRT, the whole pelvis treated patients were at a higher risk of GI toxicities following their treatment compared to prostate only.

Correction to Abstract #164 from 2022 CARO ASM

164

INTERRUPTION OF CARE: AN IMPORTANT QUALITY METRIC IN CHEMO-RADIATION FOR LOCALLY ADVANCED HEAD AND NECK SQUAMOUS CELL CANCERS (LASCCHN) IN SUB-SAHARAN AFRICA

Chinelo onwualu-Chigbo[1], Nwamaka Lasebikan[1], Chudi Obuba[1],Kenneth Nwankwo[1], Ikechukwu Chukwuocha[1], Vitalis Okwor[1], Jhingram Anuja[2], Rebecca KS Wong[3]
[1]University of Nigeria Teaching Hospital, Enugu, NG
[2]The University of Texas MD Anderson Cancer Center, Houston, TX
[3]University of Toronto, Toronto, ON

Purpose: Implementation of evidence-based, guideline recommended treatment such as concurrent chemoradiotherapy (CRT) for LASCCHN does not always equate to timely completion of care for patients in LMIC. The objective of this report is to identify reasons for treatment interruption and its effect.

Materials and Methods: A prospective study to document patient reported outcomes during treatment for patients with LASCCHN recommended to receive concurrent CRT was open to accrual. Our institutional treatment protocol is 0-3 courses of iCT (Paclitaxel 175mg/m2,Cisplatin 100mg/m2 q3w) followed by CRT (60Gy in 30fr, IV Cisplatin 40mg/m2 wkly). Study inclusion criteria were: LASCCHN, ECOG 0-1, recommended for radical CRT. A phone administered questionnaire, designed to enquire about treatment delays and patient impact was implemented as part of our follow-up. The outcome measures were duration of concurrent chemo-radiation treatment, disease progression; need to transfer care and patient perception on delay.

Results: Between November 2020 and November 2021, 30 patients were enrolled and attempt was made to contact all. Seven patients (35%) have died and 13 patients (or their caregivers) participated in the follow-up interviews and formed the basis for the current report. All patients received iCT. In 11/13 (85%) patients, there was a 2-4 week delay in commencing CRT. Reasons were: financial constraints (three), social (one), CT-related delays (two) and RT machine downtime (five). The mean duration of CRT was 9.8 weeks (SD2.4). While all patients completed 60 Gy, none completed this in 6w. The duration of CRT was >6to≤8w: 3; 8to≤10w: 5; and >10w: 5. The reasons for CRT interruptions were machine breakdown (seven), financial (five), toxicity (one). No patient transferred care to other institutions. Eight patients developed new symptoms during treatment interruption. Eleven of 13 recalled being dissatisfied (anger, disappointment, worry) with the delay.

Conclusions: Despite availability of CRT for treating locally advanced SCCHN, there are systemic challenges in timely treatment completion. Solutions to mitigate these are urgently needed.


caro acro
Canadian Association of Radiation Oncology
Association canadienne de radio-oncologie
JOIN US FOR
CARO ASM 2024 IN VANCOUVER!
SAVE THE DATE:
September 11-14, 2024
Sheraton Wall Centre, Vancouver, BC
www.caro-acro.ca


COMP
Canadian Organization of Medical Physicists
OCPM
Organisation canadienne des physiciens médicaux
REGINA
SAVE THE DATE
COMP ASM
June 5-7, 2024
DELTA
HOTELS
MARRIOTT